AD-A125 167 AERODYNAMICALLY EFFICIENT GRADIENT REFRACTIVE INDEX MISSILE SEEKER LENS(U) NAVAL POSTGRADUATE SCHOOL MONTEREY CA H M CARR OCT 82 NPS67-82-012 1/6

UNCLASSIFIED F/G 16/4 NL

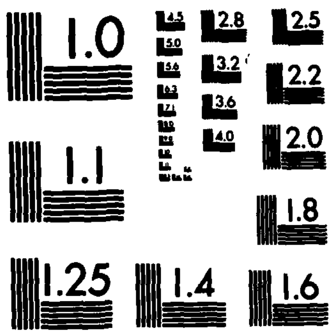

MICROCOPY RESOLUTION TEST CHART
NATIONAL BUREAU OF STANDARDS-1963-A

NPS67-82-012

2

NAVAL POSTGRADUATE SCHOOL
Monterey, California

AD A125167

THESIS

AERODYNAMICALLY EFFICIENT
GRADIENT REFRACTIVE INDEX
MISSILE SEEKER LENS

by

Herbert M. Carr III

October 1982

Thesis Advisor: A. E. Fuhs

Approved for public release; distribution unlimited.

Prepared for: Defense Advanced Research Projects Agency
1400 Wilson Boulevard
Arlington, VA 22209

UNCLASSIFIED

SECURITY CLASSIFICATION OF THIS PAGE (When Data Entered)

REPORT DOCUMENTATION PAGE		READ INSTRUCTIONS BEFORE COMPLETING FORM
1. REPORT NUMBER NPS67-82-012	2. GOVT ACCESSION NO. AD-A123467	3. RECIPIENT'S CATALOG NUMBER
4. TITLE (and Subtitle) Aerodynamically Efficient Gradient Refractive Index Missile Seeker Lens		5. TYPE OF REPORT & PERIOD COVERED Master's Thesis; October, 1982
		6. PERFORMING ORG. REPORT NUMBER
7. AUTHOR(s) Herbert M. Carr III		8. CONTRACT OR GRANT NUMBER(s) DARPA ORDER 4035
9. PERFORMING ORGANIZATION NAME AND ADDRESS Naval Postgraduate School Monterey, California 93940		10. PROGRAM ELEMENT, PROJECT, TASK AREA & WORK UNIT NUMBERS
11. CONTROLLING OFFICE NAME AND ADDRESS Naval Postgraduate School Monterey, California 93940		12. REPORT DATE October, 1982
		13. NUMBER OF PAGES 483
14. MONITORING AGENCY NAME & ADDRESS(if different from Controlling Office) LTC. Rene Larriva Defense Advanced Research Projects Agency 1400 Wilson Blvd. Arlington, VA 22209		15. SECURITY CLASS. (of this report) Unclassified
		15a. DECLASSIFICATION/DOWNGRADING SCHEDULE

16. DISTRIBUTION STATEMENT (of this Report)

Approved for public release; distribution unlimited.

17. DISTRIBUTION STATEMENT (of the abstract entered in Block 20, if different from Report)

18. SUPPLEMENTARY NOTES

19. KEY WORDS (Continue on reverse side if necessary and identify by block number)

Missile Sensors
Missile Aerodynamics
Projectile Aerodynamics
Gradient Refractive Index
Lens Design
Conical Optics
Conical Lens
Guided Projectile

20. ABSTRACT (Continue on reverse side if necessary and identify by block number)

This thesis explores the use of a pointed seeker lens designed using a spherically symmetric gradient refractive index (GRIN). The design helps to solve the current design conflict between optical quality and aerodynamic drag inherent in hemispherical seeker lenses. Equations for lens design and the evaluation of off-axis lens performance have been developed for both a homogeneous version and a GRIN version of the pointed

DD FORM 1473, 1 JAN 73 EDITION OF 1 NOV 65 IS OBSOLETE

S/N 0102-014-6601

UNCLASSIFIED

SECURITY CLASSIFICATION OF THIS PAGE (When Data Entered)

#20 - ABSTRACT - (CONTINUED)

seeker lens. The homogeneous lens is used as a comparison and a check for the GRIN lens. A FORTRAN program (GISL) has been written and employed to evaluate and compare both the homogeneous lens and many different configurations of possible GRIN lens designs. Results indicate that the GRIN lens has highly superior off-axis imaging performance as compared to the homogeneous lens. The best results were obtained for the GRIN lens with a fifty percent, positive, spherically symmetric gradient index with center of symmetry interior to the lens. Only very slightly inferior performance was observed with a five percent version of the same lens; such a lens possible can be manufactured today. GRIN lens performance also indicates that for objects off-axis by more than 17.2 degrees a large scale, multiple element sensor array may be required; with such a sensor array, objects off-axis by more than 37.2 degrees may require mirror elements to compensate for image movement.

Approved for public release; distribution unlimited.

Aerodynamically Efficient Gradient Refractive Index Missile Seeker Lens

by

Herbert M. Carr III
Captain, United States Army
B.S., University of Texas, 1971

Submitted in partial fulfillment of the requirements for the degree of

MASTER OF SCIENCE IN ENGINEERING SCIENCE

from the

NAVAL POSTGRADUATE SCHOOL
October 1982

Author: ______________________

Approved by: ______________________
Thesis Advisor

____
Chairman, Department of Aeronautics

____
Dean of Science and Engineering

ABSTRACT

This thesis explores the use of a pointed seeker lens designed using a spherically symmetric gradient refractive index (GRIN). The design helps to solve the current design conflict between optical quality and aerodynamic drag inherent in hemispherical seeker lenses. Equations for lens design and the evaluation of off-axis lens performance have been developed for both a homogeneous version and a GRIN version of the pointed seeker lens. The homogeneous lens is used as a comparison and a check for the GRIN lens. A FORTRAN program (GISL) has been written and employed to evaluate and compare both the homogeneous lens and many different configurations of possible GRIN lens designs. Results indicate that the GRIN lens has highly superior off-axis imaging performance as compared to the homogeneous lens. The best results were obtained for the GRIN lens with a fifty percent, positive, spherically symmetric gradient index with center of symmetry interior to the lens. Only very slightly inferior performance was observed with a five percent version of the same lens; such a lens possibly can be manufactured today. GRIN lens performance also indicates that for objects off-axis by more than 17.2 degrees a large scale, multiple element sensor array may be required; with such a sensor array, objects off-axis by more than 37.2 degrees may require mirror elements to compensate for image movement.

TABLE OF CONTENTS

LIST OF TABLES

LIST OF FIGURES

LIST OF SYMBOLS

Symbol in Equations	FORTRAN Symbol	Equation Number Where First Introduced	Definition	Units
a	A	113	Parameter of gradient index function	Nondimensional
a		41	Defined by Equation 44	
A		24	Defined by Equation 25	
A		137	Defined by Equation 138	
A_1		161	Defined by Equation 164	
A_2		160	Defined by Equation 161	
A_3		169	Defined by Equation 170	
A_5		179	Defined by Equation 184	
A_6		178	Defined by Equation 181	
AB	AB	30	Line segment from A to B, from nose to apex of cone	Nondimensional
b	B	113	Parameter of gradient index function	Nondimensional
b		41	Defined by Equation 45	
B		24,137	Defined by Equation 26	
B_1		161	Defined by Equation 165	
B_2		160	Defined by Equation 162	
B_5		179	Defined by Equation 185	
B_6		178	Defined by Equation 182	
BF	BF	2	Line segement from B to F, focal length	Nondimensional
c		41	Defined by Equation 46	

c		24	Defined by Equation 27	
C		137	Defined by Equation 139	
C_1		161	Defined by Equation 166	
C_2		160	Defined by Equation 163	
C_6		178	Defined by Equation 183	
d		41	Defined by Equation 47	
d	ERROR	142	Error parameter in meridian plane ray intercept with outside surface	Nondimensional
D	D2	72	Geometrical length of skew ray in homogeneous lens	Nondimensional
D'	D3	95	Geometrical length of skew ray from cone to image plane	Nondimensional
DYDXN(J)	DYDXN(J)	20	Slope of normal to outside surface in the meridian plane at the Jth point	Nondimensional
DYDXT(J)	DYDXT(J)	21	Slope of outside surface tangent in the meridian plane at the Jth point	Nondimensional
$DYDXN_{PIM}$		51	Slope of normal to outside surface in the meridian plane. Interpolated value	Nondimensional
e	E	108	Spherical GRIN scalar invariant	Nondimensional
e		41	Defined by Equation 48	
$f(x,y,z)$			General function of x, y, and z	
f_x		82	Partial derivative of function f with respect to x	

f_y		82	Partial derivative of function f with respect to y	
f_z		82	Partial derivative of function f with respect to z	
i		186	Summation index	
$\hat{i}$		53	Unit vector in the x direction	
I	I	3	Number of angular increments in lens design algorithm	
I_A			Fraction of absorbed radiant energy during transmission through the lens	Nondimensional
I_1	I1	17	Angle of incidence with respect to local normal at outside surface	Radians
I_1'	I1P	16	Angle of refraction with respect to the local normal at the outside surface	Radians
I_2	I2	12	Angle of incidence with respect to the local normal at the inside surface	Radians
I_2'	I2P	10	Angle of refraction with respect to the local normal at the inside surface	Radians
I_R		102	Fraction of reflected radiant energy at the surface interface	Nondimensional
I_T	NTNCTY	102	Fraction of transmitted radiant energy at the interface	Nondimensional
I_i	NTNCTY(G)	190	Intensity element of intensity summation	Nondimensional

I_{av}	XMAVE	190	Average value of ray intensity	Nondimensional
$\hat{j}$		53	Unit vector in the x-direction	
J	J	4	Ray Number index	
k	LK	63	Direction cosine, x-direction, of outside surface normal	
k'	LKP	83	Direction cosine, z--direction, of inside surface normal	
$\hat{k}$		55	Unit vector in y-direction	
K	CK	58	x-direction cosine of ray exterior to lens surface	
K'	CKP	63	x-direction cosine of ray inside the lens	
K"	CKPP	92	x-direction cosine of the ray after refraction by the lens	
l	LL	64	y-direction cosine of outside surface normal	
l'	LLP	84	y-direction cosine of inside surface normal	
L	CL	58	y-direction cosine of the ray external to the lens	
L'	CLP	64	y-direction cosine of the ray internal to the lens	
L"	CLPP	93	y-direction cosine of the ray after diffraction by the lens	

l_0		122	Generalized z-direction cosine of the initial ray direction in GRIN	
m	LM	65	z-direction cosine of outside surface normal	
m		38	Generalized slope of a line segment	
m'	LMP	85	z-direction cosine of inside surface normal	
M	CM	58	z-direction cosine of ray external to the lens	
M'	CMP	65	z-direction cosine of ray internal to the lens	
M"	CMPP	94	z-direction cosine of ray after refraction by the lens	
n		108	Generalized local value of the gradient refractive index	Nondimensional
n_0		109	Generalized value of the gradient index at the initial intercept point	Nondimensional
n_2	N2	125	Local lens interior value of the GRIN	Nondimensional
N		186	Generalized nth value of summation index	
N_1	N1	1	Homogeneous index of refraction of medium 1, exterior to lens	Nondimensional
N_2	N2	1	Homogeneous index of refraction of medium 2, interior to lens	Nondimensional
N_3	N3	12	Homogeneous index of refraction of medium 3, behind the lens	Nondimensional
$\bar{N}'$		55	Normal vector at the point of intersection at the outside surface	

$\bar{N}_m$		53	Normal vector in the meridian plane corresponding to $\bar{N}'$	
$\hat{N}_i$		80	Generalized surface normal unit vector	
N_{ti}		104	Ratio of indices of refraction at an interface	Nondimensional
$\hat{N}_{po}$		148	Unit normal vector to plane of skew ray	
N_{pox}	NPOX	149	Defined by Equation 150	
N_{poy}	NPOY	149	Defined by equation 151	
N_{poz}	NPOZ	149	Defined by Equation 152	
OB	OSYMB	126	Line segment from the center of symmetry of the GRIN function, O_s, to B, the origin	Nondimensional
O_s		112	Location of the GRIN center of symmetry on the lens axis	Nondimensional
P_0		120	Generalized initial x-direction cosine of the GRIN ray	
P_1		76	Defined by Equation 77	
P_2		76	Defined by Equation 78	
P_3		76	Defined by Equation 79	
PAR1	PAR1	40	Defined by Equation 41	
PAR2	PAR2	40	Defined by Equation 42	
PAR3	PAR3	40	Defined by Equation 43	
q_0		121	Generalized y-direction cosine of initial GRIN ray direction	
Q		5	Perpendicular distance between ray and line parallel to ray through the origin at B in Figure 3	Nondimensional

QP		37	Line segment defined by Figure 5	Nondimensional
QP'		37	Line segment defined by Figure 5	Nondimensional
r	RAD	108	Radial coordinate in GRIN from O_s	Nondimensional
r_0	R0	108	Initial value of r at ray intercept point	Nondimensional
$\hat{r}_0$		146	Unit vector in direction from O_s to intercept point on outside surface	
r_{ox}	R0X	151	x-direction cosine of $\hat{r}_0$	
r_{oy}	ROY	150	y-direction cosine of $\hat{r}_0$	
r_{oz}	ROZ	150	z-direction cosine of $\hat{r}_0$	
$\hat{r}_{iH}$		156	Unit vector from O_s to point of homogeneous intercept on inside surface	
r_g	RADH	160	Geometrical radius from O_s to cone during iteration for the inside surface intercept	Nondimensional
r_{PI}	RAD	174	Radius to inside surface intercept as found by interation	Nondimensional
r_{11}		103	Reflection coefficient for parallel E vector	Nondimensional
r		104	Reflection coefficient for perpendicular E vector	Nondimensional
R	R	2	Maximum inside radius of cone measured from the lens axis	Meters
R	RAD	33	Radius of circle in the y-z plane	Nondimensional
$\hat{R}$		57	Unit vector in the ray direction	

$\bar{R}'$		62	Vector in the direction of refracted ray	
R_z	RZERO	113	Maximum possible radius in GRIN	Nondimensional
S	S	51	Line segment in the meridian plane; see Figure 5	Nondimensional
ST	ST	51	Inclusive line segment in the meridian plane; see Figure 5	Nondimensional
T	T	14	Edge thickness of the lens	Nondimensional
U	U	17	Direction of the ray with respect to the lens axis in the meridian plane	Radians
U'	UP	13	Direction of the ray inside the lens with respect to the lens axis in the meridian plane	Radians
U"	UDP	4	Angle between ray and lens axis at the focal point in the meridian plane	Radians
v		115	Integration variable	Nondimensional
x		22	General x-coordinate along lens axis	Nondimensional
x'		30	General x-coordinate in the grid plane (tilted)	Nondimensional
$\lvert x \rvert$		2	Absolute value of any quantity x	
x_0	XO	40	x-coordinate of outside surface skew ray intercept	Nondimensional
x_i	XI	69	x-coordinate of inside surface intercept	Nondimensional

x_{im}	XIM	95	x-coordinate in the image plane (Spot Diagram)	Nondimensional
x_{1H}	X1H	130	First x-coordinate of imaginary homogeneous intercept in GRIN design	Nondimensional
x_p	XP	135	x-coordinate of the first intermediate point on the GRIN ray during iteration in the design algorithm	Nondimensional
x'_{1H}	X1HP	141	Second x-coordinate of imaginary homogeneous intercept in GRIN design	Nondimensional
$x_p'''\cdots$	XP	143	Successive values of x_p during iteration	Nondimensional
x_{PIM}		52	x-coordinate of ray intercept in meridian plane	Nondimensional
$X_1(J)$	X1(J)	14	x-coordinate of the Jth ray on the outside surface in the meridian plane	Nondimensional
$X_2(J)$	X2(J)	5	x-coordinate of the Jth ray on the inside surface in the meridian plane	Nondimensional
y		22	General y-coordinate (vertical)	Nondimensional
y'		31	y-coordinate in the tilted grid plane	Nondimensional
y_0	Y0	49	y-coordinate of outside surface skew ray intercept	Nondimensional
y_i	YI	170	y-coordinate of inside surface skew ray intercept	Nondimensional

y_{im}	YIM	96	y-coordinate of the skew ray in the image plane (Spot Diagram)	Nondimensional
y_{1H}	Y1H	131	First y-coordinate of imaginary HIN intercept in GRIN design (iteration)	Nondimensional
y'_{1H}	Y1HP	137	Second y-coordinate of imaginary HIN intercept in GRIN design (iteration)	Nondimensional
y_p	YP	136	x-coordinate of the first intermediate point on the GRIN ray during iteration in the design algorithm	Nondimensional
$y_p^{''' \cdots}$	YP	144	Successive values of y_p during iteration	Nondimensional
y_c	YCENTR	186	y-coordinate of the image centroid in the Spot Diagram	Nondimensional
Y_i	YIM(G)	186	Individual y-coordinates of image plane ray intercept	Nondimensional
$y_1(J)$	Y1(J)	15	y-coordinate of the Jth ray on the outside surface in the meridian plane	Nondimensional
$y_2(J)$	J2(J)	5	y-coordinate of the ray on the inside surface in the meridian plane	Nondimensional
z		32	General z-coordinate (horizontal)	Nondimensional
z'		32	z-coordinate in the grid plane (tilted)	Nondimensional
z_0	ZO	50	z-coordinate of the skew ray on the outside surface	Nondimensional
z_i	ZI	71	z-coordinate of the skew ray on the inside surface (cone)	Nondimensional

z_{im}	ZIM	97	z-coordinate of the skew ray in the image plane (Spot Diagram)	Nondimensional
α	ALPHA	2	Cone half-angle	Radians
α_p	ALFAP	30	Grid plane tilt angle with respect to the lens axis	Radians/Degrees
β	BETA	2	Total angle between lens axis and the point of maximum radius of the cone; measured at the focal point	Radians
γ	GAMMA	29	Nose half-angle (opaque region)	Radians
δ		120	Defined by Equation 124	
$\Delta U''$	DLUDP	3	Angle between successive rays at the focal point	Radians
Δx		52	Incremental change in x; see Figure 5	
Δy		52	Incremental change in y; see Figure 5	
ε	EPSILON	109	Sign function (± 1)	
ζ	ZETA	134	Angle between instantaneous GRIN ray direction and the lens axis in the meridian plane	Radians
η		120	Defined by Equation 123	
θ		108	Generalized angular coordinate of GRIN ray in the plane of the ray	Radians
θ_1		1	Generalized angle of incidence with respect to the local normal	Radians
θ_2		1	Generalized angle of refraction with respect to the local normal	Radians
θ_0	THETA0	108	Reference (at surface intercept) in GRIN	Radians

θ_H	THETAH	125	Iteration trial value of θ	Radians
θ_T		125	Total angular GRIN coordinate	Radians
θ_p	THETAP	173	Trial values of θ during iteration	Radians
θ'_p	XNEW	173	Revised trial value of θ during iteration	Radians
μ		54	Angle between meridian plane and the point of intersection on the outside surface	Radians
π	PI	13	Proportionality factor between the circumference and the diameter of a circle; 3.14159...	Radians
σ_r	RMSRAD	189	Spot size; RMS radius of image	Nondimensional
σ_y	SIGMAY	188	Standard deviation of y-coordinates of rays in the Spot Diagram	Nondimensional
σ_z	SIGMAZ	187	z-standard deviation of rays in the Spot Diagram	Nondimensional
ϕ	PHI	57	Angle between skew ray and the outside surface with respect to the surface normal	Radians
ϕ'	PHIP	61	Refraction angle between skew ray and the outside surface normal	Radians
ϕ_i	PHII	90	Angle of skew ray intercept with respect to the inside surface normal	Radians
ϕ'_i	PHIIP	91	Refraction angle of skew ray with respect to the inside surface normal	Radians

ψ	PSI	118	Angle between skew ray direction and radial direction from O_s	Radians
ψ_0	PSI0	109	Initial value of angle ψ at point of intercept at outside surface	Radians

ACKNOWLEDGEMENTS

The author would like to express his sincere appreciation to Distinguished Professor Allen E. Fuhs for his invaluable guidance, friendship, and time away from sabbatical. Without him this thesis would not have been possible.

The author would also like to thank Dr. Oded Amichai for his friendship and his assistance in many areas most notably in the intricacies of the IBM 3033.

I. INTRODUCTION

Historically, the design of tactical missiles employing passive or semiactive infrared (IR) seekers has involved a difficult compromise between aerodynamic requirements and optical or seeker requirements. Whereas aerodynamically the missile nose region should be sharp in order to reduce drag, optically it should be hemispherically shaped for image quality and as large as possible to increase aperture and therefore acquisition or tracking range. Some IR homing missiles designed for very short range anti-armor missions have totally ignored nose drag in order to optimize seeker performance while other designs for longer range missiles requiring high cruise velocities and greater aerodynamic efficiency have used the blunted ogive as a compromise. There have not been any IR designs which have ignored optics in favor of aerodynamics; nor has there been employed a pointed seeker lens with the desired optical qualities.

In order to increase the performance of optically guided missiles beyond the current state of development, the conflict between aerodynamic requirements and optical restrictions must be resolved. Significant improvement in missile performance by increasing thrust is not likely due to the highly advanced state of propulsion today. One way to resolve the aerodynamics-optics problem is to design a pointed lens which has, if not

imaging quality, enough optical performance to allow the reduction of tracking data.

The lens must be in the general shape of a cone or ogive with half angle compatible with the design free stream Mach number in order to maintain an attached shock wave. Such a spike-shaped lens might also be used in the diffuser portion of an optically guided ramjet with nose inlet to conserve stagnation pressure. A diffuser-lens may benefit by a semi-isentropic spike shaped lens.

Poor optical performance due to the pointed shape of sharp lenses has precluded their use. Gradient Refractive Index (GRIN) materials, however, permit the lens designer the freedom to spatially vary the lens index of refraction to compensate for a traditionally poor optical shape. Although the use of GRIN has seen widespread use in fiber optics technology, it has been used infrequently in lens applications until recently. Lens designers are discovering that multiple-element photographic objectives may be redesigned using a two-element gradient lens [1]. It should be noted, however, that such GRIN lens have not yet been successfully fabricated even though large index changes in glass have been accomplished by the diffusion of doped electropolarizable ions [2]. Extensive research is being conducted in the creation of ever larger and more precise gradients. A total change in refractive index of approximately five percent is currently attainable.

At the Naval Postgraduate School, Frazier [3], Terrell [4], and Amichai [5] have studied GRIN as applied to the sharp lens problem. The brief introduction by Frazier was followed by Terrell who designed a sharp lens having a conical outside surface and a variable inner surface using a homogeneous index (HIN) and then also briefly touched on the GRIN application. Amichai extended Terrell's lens to the GRIN case and included preliminary results from this thesis in a computer routine intended as a framework for lens optimization by following researchers.

This thesis investigates the design and off-axis performance (skew rays) of a GRIN seeker lens having a variable outer surface and a fixed right circular cone as an inside surface. The variable outside surface is determined by the character of the spherical gradient employed and varies from a pseudo ogive to an approximate isentropic spike as shown in Figure 1. First, the theory of the HIN lens is developed, followed by the design of a homogeneous lens intended both as a comparison and a check for the GRIN lens theory and the design which follows. Lens performance parameters are discussed and results presented for both the HIN and GRIN lenses.

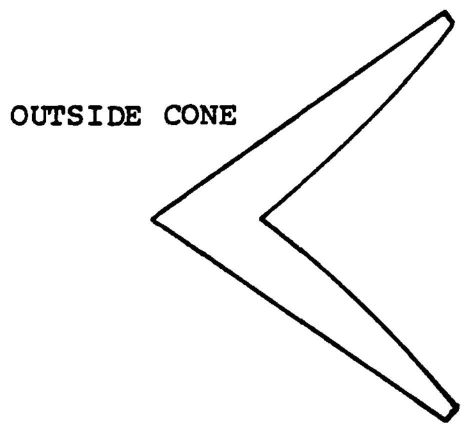

(a) Terrell's Lens With Conical Outer Surface

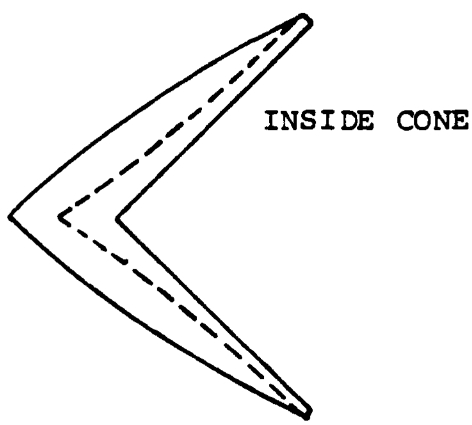

(b) Lens Shapes In This Thesis With Conical Inner Surface.

Figure 1. Lens Shapes

II. THE HOMOGENEOUS LENS

A. THEORY

Snell's law is the cornerstone of contemporary lens design in homogeneous optical materials. In the HIN case Snell's law is used in the familiar form

$$N_1 \sin \theta_1 = N_2 \sin \theta_2 \tag{1}$$

where N_i is the index of refraction of the material corresponding to surface intercept angle θ_i, with respect to the surface normal, at the interface between surfaces. Lens geometry and the relative values of N_i determine the resultant optical behavior.

B. ASSUMPTIONS AND SIGN CONVENTION

In order to simplify the design and analysis of the seeker lens problem, certain assumptions have been introduced. Although energy loss upon transmission through the lens at each surface is calculated, it is assumed that the light is monochromatic radiation, time dependent electric and magnetic fields. Light impinging upon the lens is assumed to have a planar wave front as if propagating from an object at infinity. The presence of a shock wave attached to the lens is ignored as are any other regions of expansion or compression in the flow field about the lens [6]. Furthermore, the index of refraction of the free stream is assumed

to be equal to that of the interior space behind the lens even though computer routines were written with the flexibility to process unequal values.

The sign convention used is a right handed system with spatial coordinates positive to the right, up, and out of the page as seen by the reader. All angles are assumed positive counterclockwise from point of reference unless otherwise noted. All linear dimensions are implicitly non-dimensionalized with respect to the maximum radius of the right circular cone forming the inside surface of the lens.

C. HIN LENS DESIGN

The lens design procedure consists of calculating both the loci of points forming the outside surface and the slope of the surface at each point in the meridian plane. It is convenient to approach the problem by placing a point source of light at the design focal point F and calculating successive refracted ray paths U' using Snell's law at points D_i on the inside surface in Figure 2. Points E_i are formed by the intercept of the refracted ray and the slope of the outside surface as extended from the previous point E_{i-1}. The tangent to the surface which will refract the ray in the desired direction, U, may again be found from Snell's law. The accuracy of the calculated surface increases as the spacing between points decreases or as angle $\Delta U''$ becomes very small. The final ray is parallel to the lens axis and point D_n corresponds to point B, which is the origin. The area

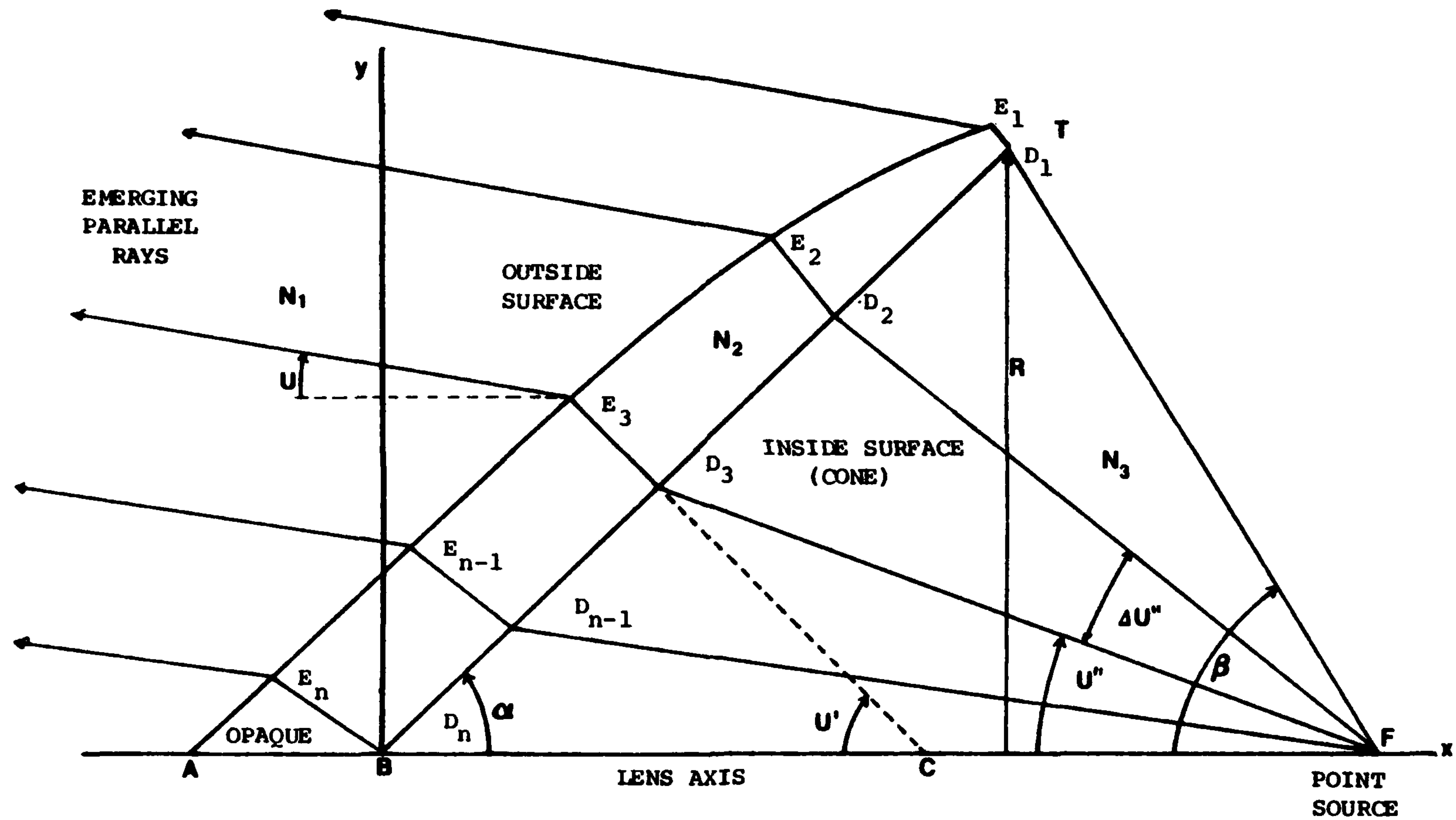

Figure 2. Conceptual Drawing and Coordinate System of Outer Surface Solution

formed by the triangle ABE_n is opaque to prevent rays from scattering through the opposite side of the lens.

A particular lens is begun by specifying the focal length BF, the cone half-angle α, the indices of refraction N_1, N_2, and N_3, the cone radius at the edge R, the ray direction angle U, and the total number of rays to be traced. The thickness, T, of the lens at the edge (E_1D_1) must also be specified in order to define which of the family of possible outer surfaces will be calculated. In general, angle U will be taken to be zero in order to investigate objects on-axis at infinity. R will always be set equal to one and to nondimensionalize all linear dimensions every length is implicitly expressed as a ratio with respect to R. The angle β at the focal point is measured from the lens axis to D_1 and is expressed as

$$\tan|\beta| = \frac{R}{(BF - R\cdot\text{cotan}\ \alpha)} \qquad (2)$$

Thus, if I+1 is the total number of rays to be traced, then

$$\Delta U'' = \beta/I \qquad (3)$$

and

$$U'' = \beta - J\cdot\Delta U'' \qquad (4)$$

where J is the ray number. To begin tne lens design the

coordiantes $x_2(J), y_2(J)$ of point D_J must be found. Here the subscript 2 refers to the inside surface where $x_1(J)$, $y_1(J)$ are the coordinates of E_J on the outside surface.

Following Kingslake [7], Q in Figure 3 may be expressed as

$$Q = BF \sin U'' = x_2(J) \sin U'' + y_2(J) \cos U'' \quad (5)$$

But,

$$y_2(J) \cdot = x_2(J) \tan \alpha \quad (6)$$

so that

$$BF \sin U'' = x_2(J)[\sin U'' + \tan \alpha \cos U''] \quad (7)$$

Now, $x_2(J)$ and $y_2(J)$ are

$$x_2(J) = \frac{BF \sin U''}{[\sin U'' + \tan \alpha \cos U'']} \quad (8)$$

$$y_2(J) = \frac{BF \ \ in U'' \tan \alpha}{[\sin U'' + \tan \alpha \cos U'']} \quad (9)$$

Looking now to find the incident angle I_2' which the ray forms with the inside surface at D_J it can be seen that

$$\tan (\alpha + I_2') = \frac{BF - x_2(J)}{y_2(J)} \quad (10)$$

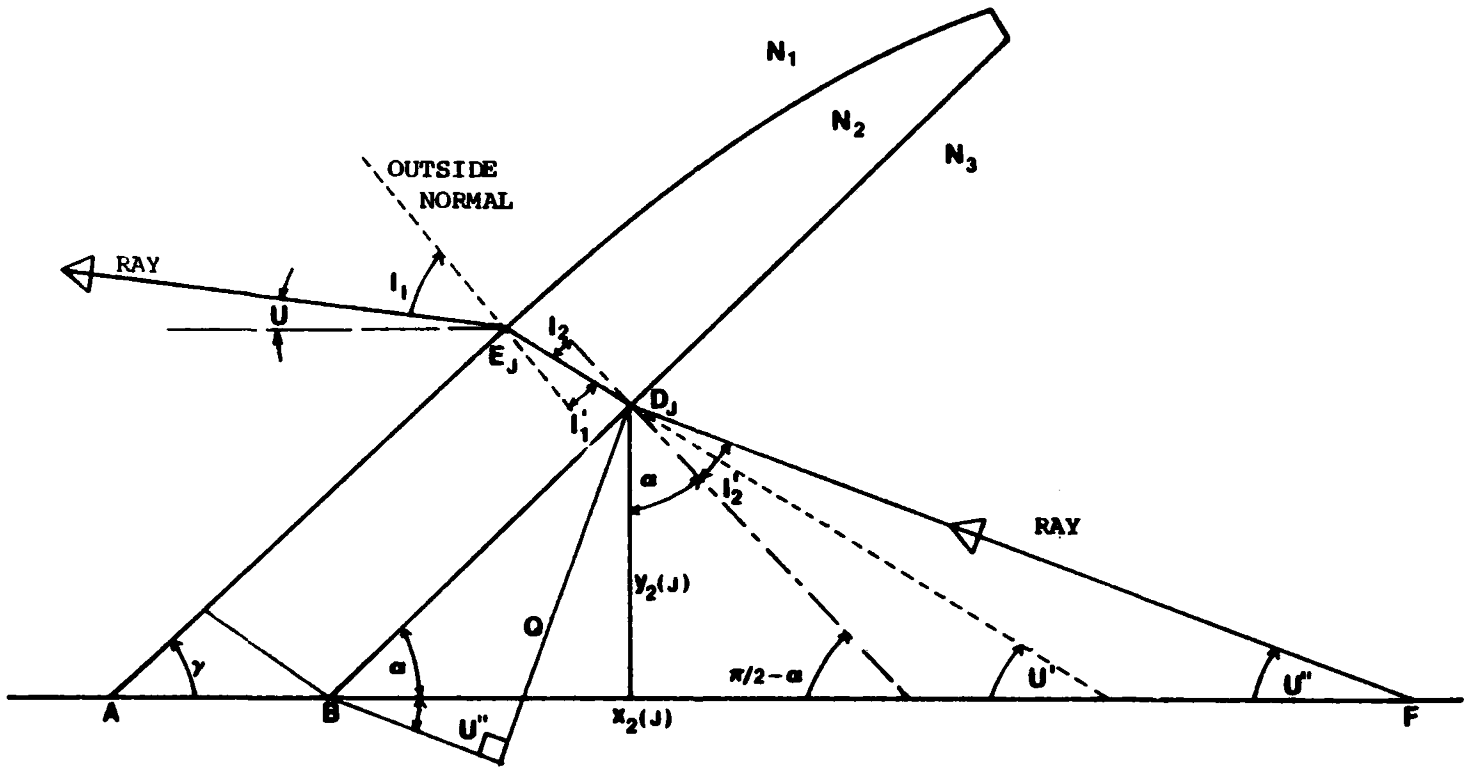

Figure 3. Ray Trace Geometry

Substituting into Equation (1), Snell's law, the refraction angle I_2 can now be written as

$$I_2 = \sin^{-1}[(\frac{N_3}{N_2}) \sin I_2'] \qquad (12)$$

The path of the ray inside the lens may now be expressed in the form of the angle U' where

$$U' = (\frac{\pi}{2} - \alpha) - I_2 \qquad (13)$$

To this stage all rays are treated the same. Now, however, a differentiation must be made between the outermost ray which defines the edge of the lens and all other subsequent rays.

For the outermost ray the thickness, T, of the lens at the edge can be specified which yields $x_1(1)$ and $y_1(1)$ immediately:

$$x_1(1) = x_2(1) - T \cos U' \qquad (14)$$

$$y_1(1) = y_2(1) + T \cos U' \qquad (15)$$

At point E_1 we may write Equation (1) again to obtain

$$I_1' = \sin^{-1}[(\frac{N_1}{N_2}) \sin I_1] \qquad (16)$$

where angles I_1 and I_1' are the incident and refracted angles at the outside surface and are not yet known. Angles I_1 and I_1' may be found by first noting that

$$U + I_1 = U' + I_1' \tag{17}$$

then substituting Equation (16) into (17) and rearranging terms to obtain

$$I_1 = U' - U + \sin^{-1}[(\frac{N_1}{N_2})\sin I_1] \tag{18}$$

It can be shown after some algebraic manipulation that Equation (18) may be solved for the angle I_1 in the form

$$I_1 = \sin^{-1}\{\frac{\sin^2(U' - U)}{[\cos(U'-U) - N_1/N_2]^2 + \sin^2(U' - U)}\}^{1/2} \tag{19}$$

Angle I_1' may be found, if desired, by substitution of Equation (19) into Equation (16). Of more importance, however, is the determination of the slope of the outer surface and the surface normal. Now that angle I_1 is known these slopes may be written as

$$\mathrm{DYDXN(J)} = \frac{dy}{dx}\Big|_{normal} = -\tan(U + I_1) \tag{20}$$

and

$$DYDXT(J) = \left.\frac{dy}{dx}\right|_{\substack{surface\\ tangent}} = \cot an(U + L_1) \tag{21}$$

Equations (20) and (21) may be evaluated by using Equation (19) for I_1.

Now that all the parameters are known for the first ray, the remainder of the points E_J and the respective slopes may be found. Each successive ray is traced as before by Equations (4) through (13). Equations (14) and (15), however, may not now be used since the lens thickness along the ray can not be specified. Instead, the intersection of the ray and the surface slope from the previous ray is used to define the new point E_{J+1}. The intersection is found by first writing the equations of lines representing the ray and the surface tangent. For the ray:

$$y = -x \tan U' + y_2(J) + x_2(J) \tan(U') \tag{22}$$

For the surface tangent:

$$y = x \cot(I_1 + U) + y_1(J-1) - x_1(J-1) \cot(I_1 + U) \tag{23}$$

Equations (22) and (23) are solved simultaneously to yield the coordinates of E_J which are

$$y_1(J) = \{\frac{A + B}{C}\} \tag{24}$$

where:

$$A = \cot(I_1+U)\ \cot(U')\,[y_2(J)+x_2(J)\tan(U')] \tag{25}$$

$$B = y_1(J-1) - x_1(J-1)\ \cot(I_1 + U) \tag{26}$$

$$C = 1 + \cot(I_1 + U)\ \cot(U') \tag{27}$$

and

$$x_1(J) = \cot(U')\,[-y_1(J)+y_2(J)+x_2(J)\tan(U')] \tag{28}$$

Now Equations (19), (20), and (21) are used to calculate I_1 and the slopes at E_J. Therefore, the remainder of the lens surface may be generated. The opaque region at the surface is formed by extending the slope of the surface at E_K to intersect the lens axis. Here, K refers to the last ray. The nose half-angle, γ, thus formed is given by

$$\tan \gamma = \left.\frac{dy}{dx}\right|_{\text{surface},\ E_K} \tag{29}$$

D. SKEW RAYS

A skew ray is one that begins from an off-axis object point and enters the lens either in front of or behind the meridian plane ($z = 0$). For every skew ray, there is a corresponding mirror image skew ray on the opposite side of the meridian plane so that two skew rays are traced at the

expense of only one calculation. These two skew rays intersect at the same diapoint.

Large numbers of skew rays are traced through a lens in order to study lens performance at different obliquities. The procedure is to superimpose a grid over the lens aperture and to trace rays through the intersections of the grid, through the lens and onto the image plane. An image plane spot diagram and an energy density plot are then constructed for study.

To accomplish this, the aperture grid has been attached to the nose (opaque region) of the seeker lens at station A; see Figure 3. The plane of the aperture grid is tilted relative to the lens by a variable angle. A transformation between the grid coordinates and the lens coordinates has been derived to connect skew rays from grid to intercept with the outside surface of the lens. Referring to Figure 4, it can easily be seen that

$$x' = [x + AB]\cos \alpha_p - y \sin \alpha_p \qquad (30)$$

$$y' = [x + AB]\sin \alpha_p + y \cos \alpha_p \qquad (31)$$

$$z' = z \qquad (32)$$

where α_p is the tilt of the grid plane, AB is the length of the opaque nose portion on the x-axis. Both z and z' are positive out of the page.

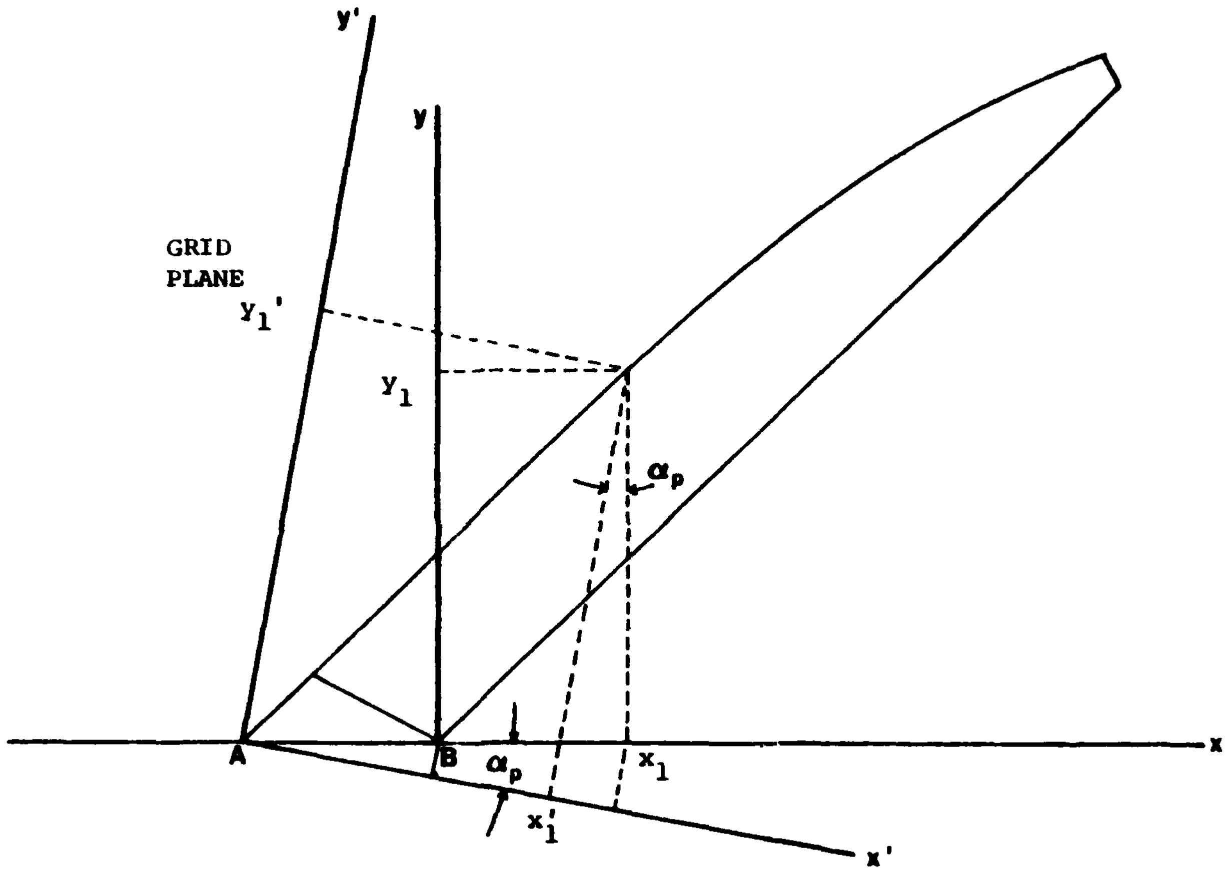

Figure 4. Coordinate Transformation (z and z' are out of the page)

The three dimensional lens outer surface is generated by rotating the array of outer surface coordinates in the meridian plane through 2π about the lens axis. Each pair of coordinates $x_1(J), y_1(J)$ thus describe a circle in the y-z plane of the lens. This circle transforms, however, to an ellipse in the grid plane given by the equation

$$y' = [x + AB] \sin \alpha_p \pm \sqrt{R^2 - z'^2} \cos \alpha_p \tag{33}$$

where R is the radius of the circle in the x-y plane. R may be expressed by the familiar equation of a circle

$$R^2 = y^2 + z^2 \tag{34}$$

in the y-z plane of the lens, or by solving Equation (33) for R in the grid plane

$$R^2 = z'^2 + \left(\frac{y'}{\cos \alpha_p} - (x + AB) \tan \alpha_p\right)^2 \tag{35}$$

With the aid of the foregoing groundwork, the x,y,z coordinates of the ray intercept with the outer surface may be found. To see how this is accomplished, first refer to Figure 5. The skew ray will pass outside the circle formed by rotating some point $x_1(J), y_1(J)$ and inside the next circle formed by rotating $x_1(J-1), y_1(J-1)$. In so doing the skew ray will

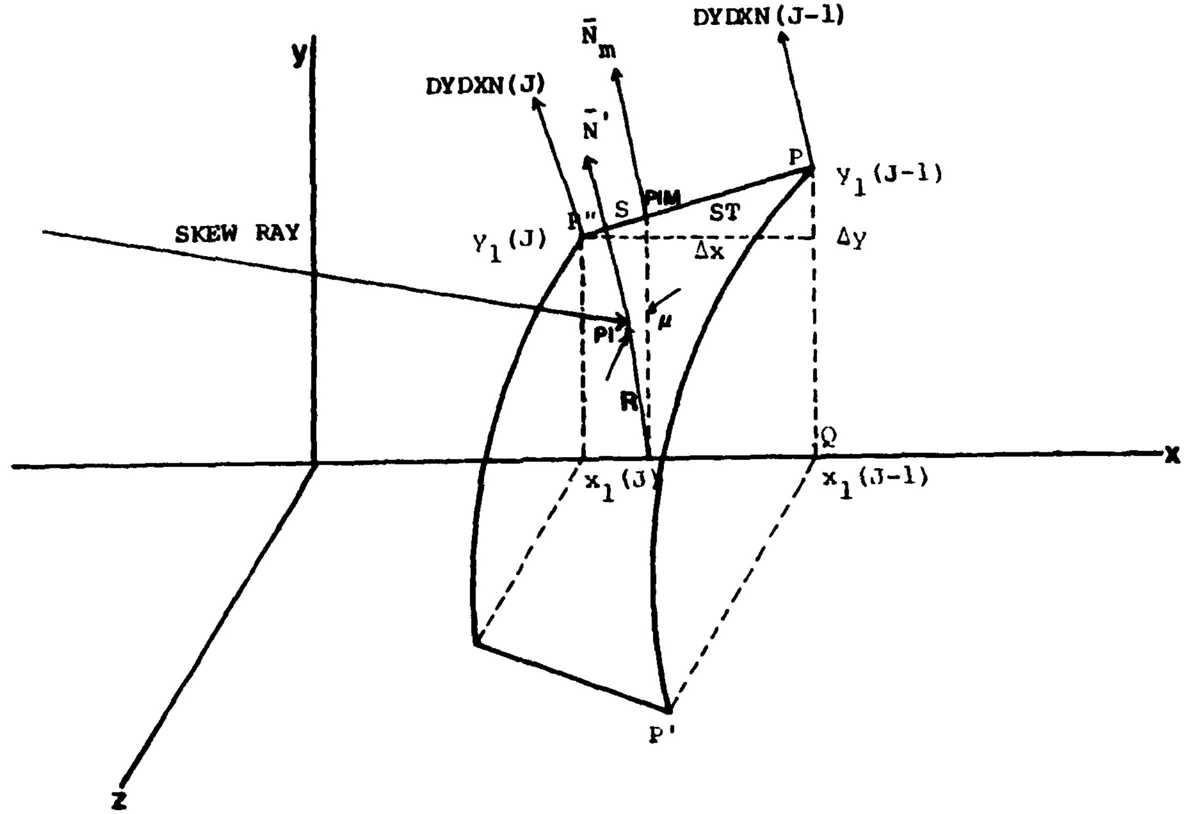

Figure 5. Geometry of Skew Ray Intercept With Outside Surface. X, Y Plane is the Meridian Plane. $\bar{N}_m$ is the Surface Normal in the Meridian Plane; $\bar{N}'$ the Surface Normal at the Point of Intercept, PI.

intercept an imaginary cone formed by the two circles.[1] Now, the y',z' of the skew ray in the grid plane and a trial value $x_1(J)$ from the array of surface points are substituted into Equation (35) and a value for R is calculated. If R is greater than $y_1(J)$ but less than $y_1(J-1)$ than the appropriate circles have been found. If not, another trial value of $x_1(J)$ is picked. In practice the $x_1(J)$ corresponding to

$$y_1(J) = z' \tag{36}$$

is chosen as the first trial value and subsequent trial values are $x_1(J-1)$, $x_1(J-2)$ and so forth.

The equation of the cone passing through the two circles may be derived by again referring to Figure 5 and noting that

$$QP = QP' = \sqrt{y^2 + z^2} = R \tag{37a}$$

$$QP = y = m[x - x_1(J)] + y_1(J) \tag{37b}$$

where the slope m is given by

---

[1]Recall that a straight line between points E_J was used to form the outer surface in the meridian plane. These approximations are valid only if the spacing between points or circles is very small.

$$m = \frac{y_1(J-1) - y_1(J)}{x_1(J-1) - x_1(J)} \tag{38}$$

and therefore

$$R^2 = \{[\frac{y_1(J-1) - y_1(J)}{x_1(J-1) - x_1(J)}][X - X(j)] + y_1(J)\}^2 \tag{39}$$

By equating Equation (39) to Equation (35) and solving for x, the expression for the x-coordinate, x_0, of the outside surface ray intercept may be found. After some algebra, this reduces to the complicated relationship

$$x_0 = \frac{PAR1}{PAR2} \pm \sqrt{\frac{PAR1}{PAR2} - \frac{PAR3}{PAR2}} \tag{40}$$

where:

$$PAR1 = ab + ce - b^2AB - c^2d \tag{41}$$

$$PAR2 = b^2 - c^2 \tag{42}$$

$$PAR3 = a^2 + b^2(AB)^2 - 2abAB + z' - (e-cd)^2 \tag{43}$$

and where

$$a = y'/\cos \alpha_p \tag{44}$$

$$b = \tan \alpha_p \tag{45}$$

$$c = \left[\frac{y_1(J-1) - y_1(J)}{x_1(J-1) - x_1(J)}\right] \quad (46)$$

$$d = x_1(J) \quad (47)$$

$$e = y_1(J) \quad (48)$$

It has been found that the plus sign in Equation (40) gives the correct values until PAR1/PAR2 becomes greater than $x_1(1)$ at which time the negative sign must be used. It now follows from Equations (31), (32) and (40) that the y_0 and z_0 coordinates of the intercept are

$$y_0 = \frac{y'}{\cos \alpha_p} - (x_0 + AB) \tan \alpha_p \quad (49)$$

and

$$z_0 = z' \quad (50)$$

The next step in tracing the skew ray is to ascertain the direction cosines of the ray inside the lens after refraction at the outside surface. This is accomplished in a series of steps beginning with the determination of the angle ϕ which the skew ray makes with the normal to the surface at the point of intercept. Angle ϕ may be found by taking the scalar product of the direction cosines of the

skew ray and the surface normal. Thus to find ϕ, the surface normal must first be obtained.

As might be surmised by the reader, the direction cosines of the surface normal can be found by taking the gradient of Equation (39) with Equation (37) substituted for R. Several orders of magnitude may be gained in accuracy, however, if the normal $\bar{N}_m$ is found by interpolation in the meridian plane and then rotated to the point of intercept by angle μ as in Figure 5. This interpolation procedure involves multiplying the ratio S/ST with the difference between DYDXN(J) and DYDXN(J-1) and adding the product to DYDXN(J).

$$DYDXN_{PIM} = \frac{S}{ST}(DYDXN(J-1) - DYDXN(J)) + DYDXN(J) \qquad (51)$$

where subscript PIM refers to point of intersection, meridian. Values of the slopes of the normals in the meridian plane, DYDXN(J), are given by Equation (20) and S and ST are the linear separation of points P", PIM and P", P respectively. S/ST is given by

$$\frac{S}{ST} = \frac{[(R - y_1(J))^2 + (x_{PIM} - x_1(J))^2]^{1/2}}{(\Delta x^2 + \Delta y^2)^{1/2}} \qquad (52)$$

Therefore, the normal vector, $\bar{N}_m$, in the meridian plane is

$$\bar{N}_m = (\frac{1}{DYDXN_{PIM}})\hat{i} + \hat{j} \qquad (53)$$

and since

$$\tan \mu = \frac{z'}{y_0} = \frac{z_0}{y_0} \tag{54}$$

the normal vector at the point of intersection on the outside surface becomes

$$\overline{N}' = \left(\frac{1}{DYDXN_{PIM}}\right)\hat{i} + \cos\left(\tan^{-1} \frac{z_0}{y_0}\right)\hat{j} + \sin\left(\tan^{-1} \frac{z_0}{y_0}\right)\hat{k} \tag{55}$$

and

$$|\overline{N}'| = [DYDXN_{PIM}{}^{-2} + 1]^{1/2} \tag{56}$$

Now the scalar product of the skew ray vector, $\hat{R}$, and surface normal, $\overline{N}'$, may be performed to find ϕ. Since the acute angle between these vectors is required, the dot product must be written

$$\hat{R} \cdot \overline{N}' = |\overline{N}'| \cos(\pi - \phi) \tag{57}$$

Substituting Equation (55) for $\overline{N}'$ and noting that

$$\hat{R} = K\hat{i} + L\hat{j} + M\hat{k} = \cos \alpha_p \hat{i} - \sin \alpha_p \hat{j} \tag{58}$$

the left side of Equation (56) may be expanded to

$$\hat{R} \cdot \overline{N}' = \frac{\cos \alpha_p}{DYDXN_{PIM}} - \sin \alpha_p \cos\left(\tan^{-1} \frac{z_0}{y_0}\right) \tag{59}$$

Solving Equation (56) for the angle ϕ and introducing Equation (58), the expression for angle ϕ becomes

$$\phi = \pi - \cos^{-1}\left\{\frac{\dfrac{\cos \alpha_p}{DYDXN_{PIM}} - \sin \alpha_p \cos(\tan^{-1} \dfrac{z_0}{y_0})}{[DYDXN_{PIM}^{-2} + \cos^2(\tan^{-1} \dfrac{z_0}{y_0}) + \sin^{-2}(\tan^{-1} \dfrac{z_0}{y_0})]^{1/2}}\right\} \tag{60}$$

Now that the acute angle, ϕ, between the ray and the outside surface normal is known, ϕ', the angle between the refracted ray inside the lens and the surface normal may be found using Snell's law.

$$\phi' = \sin^{-1}(\frac{N_1}{N_2} \sin \phi) \tag{61}$$

The next step is to ascertain the direction cosines K', L', M' of the refracted ray inside the lens. Following Kingslake [7], Figure 6 shows the optical vector relationship between $\overline{R}$, the skew ray, $\overline{R}'$, the refracted skew ray, $\overline{N}'$, the surface normal, and the indices of refraction of the two media. Algebraically this relationship is written as

$$N_2\overline{R}' = N_1\overline{R} + (N_2 \cos \phi' - N_1 \cos \phi)\overline{N}' \tag{62}$$

By resolving Equation (61) into component form, the direction cosines of $\overline{R}'$ may be found. After rearranging, K', L', and M' become

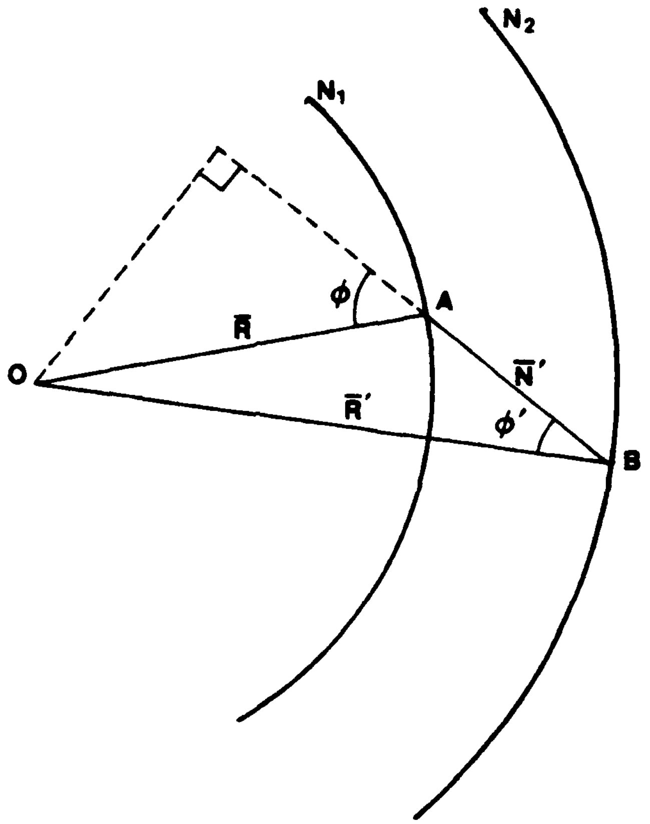

Figure 6. Kingslake's Skew Ray Diffraction Diagram

$$K' = \frac{N_1}{N_2} K + (\cos \phi' - \frac{N_1}{N_2} \cos \phi) k \tag{63}$$

$$L' = \frac{N_1}{N_2} L + (\cos \phi' - \frac{N_1}{N_2} \cos \phi) \ell \tag{64}$$

$$M' = \frac{N_1}{N_2} M + (\cos \phi' - \frac{N_1}{N_2} \cos \phi) m \tag{65}$$

where K, L, and M are given by Equation (57) and k, ℓ, m are

$$k = \frac{DYDXN_{PIM}^{-1}}{|\overline{N}'|} \tag{66}$$

$$\ell = \frac{\cos(\tan^{-1} \frac{z_0}{y_0})}{|\overline{N}'|} \tag{67}$$

$$m = \frac{\sin(\tan^{-1} \frac{z_0}{y_0})}{|\overline{N}'|} \tag{68}$$

Again, $|\overline{N}'|$ in Equations (66) through (68) is expressed by Equation (56).

At this stage in the process of tracing the skew ray, the coordinates of the external ray intercept x_0, y_0, z_0 are known as are the direction cosines K', L', M' of the skew ray inside the lens. The next step is, of course, to find the ray intercept with the inside surface (cone) and the direction of the ray subsequent to refraction. The intermediate steps are similar to, if not identical with,

the foregoing. One major difference, however, is that the inside conical surface may be expressed analytically and the intercept coordinates x_i, y_i, z_i may be found exactly without approximation. Proceeding, it can be seen that if x_i, y_i, z_i were already known, Equations (63), (64), and (65) could be rewritten as

$$K' = \frac{x_i - x_0}{D} \tag{69}$$

$$L' = \frac{y_i - y_0}{D} \tag{70}$$

$$M' = \frac{z_i - z_0}{D} \tag{71}$$

where D is the distance between surface intercept points. Upon rearranging:

$$x_i = DK' + x_0 \tag{72}$$

$$y_i = DL' + y_0 \tag{73}$$

$$z_i = DM' + z_0 \tag{74}$$

Furthermore, there exists a relationship between x_i, y_i, and z_i which is given by the expression for the inside conical surface:

$$y_i^2 + z_i^2 - x_i^2 \tan^2 \alpha = 0 \tag{75}$$

where α is the half-angle of the cone. Substituting Equations (72), (73), and (74) into Equation (75) and solving for D, it is seen that

$$D = \frac{-P_1}{P_2} \pm \frac{\sqrt{P_1^2 - P_2 P_3}}{P_2} \tag{76}$$

where

$$P_1 = L'y_0 + M'z_0 - K'x_0 \tan^2 \alpha \tag{77}$$

$$P_2 = L'^2 + M'^2 - K'^2 \tan^2 \alpha \tag{78}$$

and

$$P_3 = y_0^2 + z_0^2 - x_0^2 \tan^2 \alpha \tag{79}$$

Correct values for D are obtained by using the minus sign in Equation (76). Now that D is known, values for K', L', M', x_0, y_0, and z_0 are substituted into Equations (72), (73), and (74) to yield the coordinates of the inside surface intercept point.

In the case of the inside surface, the gradient may be used to obtain the surface normal at the point of intercept since this surface has been expressed analytically. If Equation (75) is denoted by f(x,y,z) then

$$\hat{N}_i = \left. \frac{\nabla f}{|\nabla f|} \right|_{x_i, y_i, z_i} \tag{80}$$

where $\hat{N}_i$ is the unit vector in the direction of the surface normal at the point of intercept. Here,

$$\bar{\nabla} f = \frac{\partial f}{\partial x} \hat{i} + \frac{\partial f}{\partial y} \hat{j} + \frac{\partial f}{\partial z} \hat{k} \tag{81}$$

or alternately,

$$\bar{\nabla} f = f_x \hat{i} + f_y \hat{j} + f_z \hat{k} \tag{82}$$

Thus, the direction cosines of the normal k', ℓ', m' may be expressed as

$$k' = \frac{f_x}{|\bar{\nabla} f|} \tag{83}$$

$$\ell' = \frac{f_y}{|\bar{\nabla} f|} \tag{84}$$

$$m' = \frac{f_z}{|\bar{\nabla} f|} \tag{85}$$

where:

$$f_x = -2x_i \tan^2\alpha \tag{86}$$

$$f_y = 2y_i \tag{87}$$

$$f_z = 2z_i \tag{88}$$

and

$$|\overline{\nabla} f| = 2[x_i^2 \tan^4 \alpha + y_i^2 + z_i^2]^{1/2} \tag{89}$$

Now that the two unit vectors $\hat{R}'$ and $\hat{N}'$ are known the incident acute angle of the skew ray with the inside surface, ϕ_i, may be ascertained by again taking the scalar product as in Equation (57). Thus,

$$\phi_i = \pi - \cos^{-1}[K'k' + L'\ell' + M'm'] \tag{90}$$

and using Equation (1) again

$$\phi_i' = \sin^{-1}[\frac{N_2}{N_3} \sin \phi_i] \tag{91}$$

where ϕ_i' is the acute angle between the skew ray and the surface normal after refraction at the inside surface. Direction cosines K", L", M" of the skew ray after refraction are found analogously to K', L', and M' in Equations (63), (64) and (65). Here, however, N_2, N_3, K', L', M', Φ_i, Φ_i', and k', ℓ', m' are substituted for N_1, N_2, K, L, M, Φ, Φ', and k, ℓ, m respectively. Thus

$$K'' = \frac{N_2}{N_3} K' + (\cos \phi_i' - \frac{N_2}{N_3} \cos \phi_i) k' \tag{92}$$

$$L'' = \frac{N_2}{N_3} L' + (\cos \phi_i' - \frac{N_2}{N_3} \cos \phi_i) \ell' \tag{93}$$

and

$$M'' = \frac{N_2}{N_3} M' + (\cos \phi_i' - \frac{N_2}{N_3} \cos \phi_i) m' \qquad (94)$$

Finally, the skew ray intercept with the image plane may be found. The image plane is treated as another surface along the path of the skew ray, and the intercept coordinates x_{im}, y_{im}, z_{im} are easy to find. Equations (72), (73) and (74) may be used again in the form

$$x_{im} = D'K'' + x_i \qquad (95)$$

$$y_{im} = D'L'' + y_i \qquad (96)$$

$$z_{im} = D'M'' + z_i \qquad (97)$$

where D', in this instance, is the linear separation between coordinates x_i, y_i, z_i at the inside surface and x_{im}, y_{im}, z_{im} of the image plane. Furthermore,

$$x_{im} = BF \qquad (98)$$

is the equation of the image plane. It follows that

$$D' = \frac{(BF - x_i)}{K''} \qquad (99)$$

after substitution of Equation (98) into Equation (95). Therefore,

$$y_{im} = [\frac{BF - x_i}{K''}]L'' + y_i \qquad (100)$$

and

$$z_{im} = [\frac{BF - x_i}{K''}]M'' + z_i \qquad (101)$$

Hence, the skew ray has been traced onto the image plane at the focal point of the lens. The y_{im} coordinate of the corresponding mirror image skew ray is the same as Equation (100). The z_{im} coordinate, however, is the negative of Equation (101) since the mirror image ray is behind (when viewed along the z-axis) the meridian plane. After tracing a complete set of skew rays through the lens a spot diagram may be plotted. Clearly, the number of rays to be traced depends entirely upon the incremental size of the aperture grid chosen. According to Kingslake [7], at least 100 rays must be traced to give a fair approximation of the actual image. In addition to the spot diagram, an energy density plot may now be constructed by counting the number of rays within progressively larger radii from the image centroid and then plotting the number of rays as a function of radius. Here, each ray is assumed to contain a unit, nondimensional, an amount of radiant energy for convenience.

E. RADIANT ENERGY LOSS

In reality, each ray loses intensity upon transmission at each interface. Of the total amount of energy contained in each ray, a fraction I_T will be transmitted, a fraction I_R will be reflected, and a fraction I_A will be absorbed by the medium into which the ray is propagating. Since it has been assumed that absorption is negligible, it must be true that

$$I_T + I_R = 1 \tag{102}$$

Furthermore, the relative amounts of transmitted and reflected electromagnetic energy may be calculated by the well-known Fresnel Equations which state the dependency of I_T and I_R upon the angle of incidence and the indices of refraction at the interface. That I_T and I_R are further dependent upon the orientation of the electric vector with respect to the geometry of ray incidence is fundamental to the boundary conditions which govern the form of the Fresnel relations as derived in Hecht-Zajac [8]. Since this thesis examines lens response to monochromatic radiation, the indices of refraction are not considered as a function of wavelength; further, the electric vector orientation is assumed to be rapidly and randomly changing with time. By time averaging field components, it may be seen that the reflectance is

$$I_R = \frac{1}{2}(r_\perp^2 + r_\parallel^2) \tag{103}$$

where

$$r_{\perp} = \frac{\cos \phi - (N_{ti}^2 - \sin^2 \phi)^{1/2}}{\cos \phi + (N_{ti}^2 - \sin^2 \phi)^{1/2}} \tag{104}$$

and

$$r_{\parallel} = \frac{N_{ti}^2 \cos \phi - (N_{ti}^2 - \sin^2 \phi_i)^{1/2}}{N_{ti}^2 \cos \phi + (N_{ti}^2 - \sin^2 \phi)^{1/2}} \tag{105}$$

Here, N_{ti} is the ratio of the index of refraction of the transmission side of the interface to the index of refraction of the incident side. From Equation (102) it now follows that the transmittance through the interface is

$$I_t = 1 - I_R \tag{106}$$

The total transmittance through the lens is simply the product of I_t at the outside surface with that of the inside surface where ϕ_i is substituted for ϕ in Equations (104) and (105).

Total internal reflection of the ray may occur at the inside surface if the incident angle becomes too large. Following Reference (7), this occurs when angle ϕ_i is equal to or greater than $\pi/2$. Thus, Snell's law becomes

$$\sin \phi_i = \frac{N_3}{N_2} \tag{107}$$

and any ray with ϕ_i equal to or greater than this will be

totally internally reflected. In this thesis such rays are labeled "failed rays" since they fail to intersect the image plane. If N_2 is 1.5 and N_3 is 1.0, the incident angle for total internal reflection is 41.81°, or greater.

F. OPTICAL PATH LENGTH (OPL)

The optical path length of a skew ray is an analytical tool with which the researcher may ascertain the phase of a ray at the end of the path. By so doing, the image diffraction pattern may be constructed which shows the addition or subtraction of amplitude depending upon relative phase. Since each ray must begin with the same phase, monochromatic radiation is used for diffraction experiments. OPL is included here only as a matter of interest. The calculation of optical path length is simply the sum of the geometrical path segments of a ray multiplied by the corresponding index of refraction of the medium for that segment.

III. THE GRIN LENS

A. THEORY

This thesis assumes a spherically symmetric, inhomogeneous, isentropic medium in which the refractive index varies from point to point but is independent of direction at each point. The refractive index is a function of the coordinates of the points of the region being considered. The problem of describing the resulting curved paths of rays in such GRIN materials has been solved long ago in the form of a single second order vectorial differential equation. Marchand [9] has shown that the solution to the differential equation in the case of spherical gradients can be written in polar coordinates in the plane of the ray as

$$\theta = \theta_0 + e \int_{r_0}^{r} \frac{dr}{r[n^2 r^2 - e^2]^{1/2}} \qquad (108)$$

Here r_0 and θ_0 are values of r and θ at a convenient reference point on the ray and $|e|$ is a scalar constant along the ray given by

$$e = \varepsilon\, n_0\, r_0 \sin \psi_0 \qquad (109)$$

Referring to Figure 7, r is measured from the center of symmetry of the index function; angles θ and θ_0 are measured

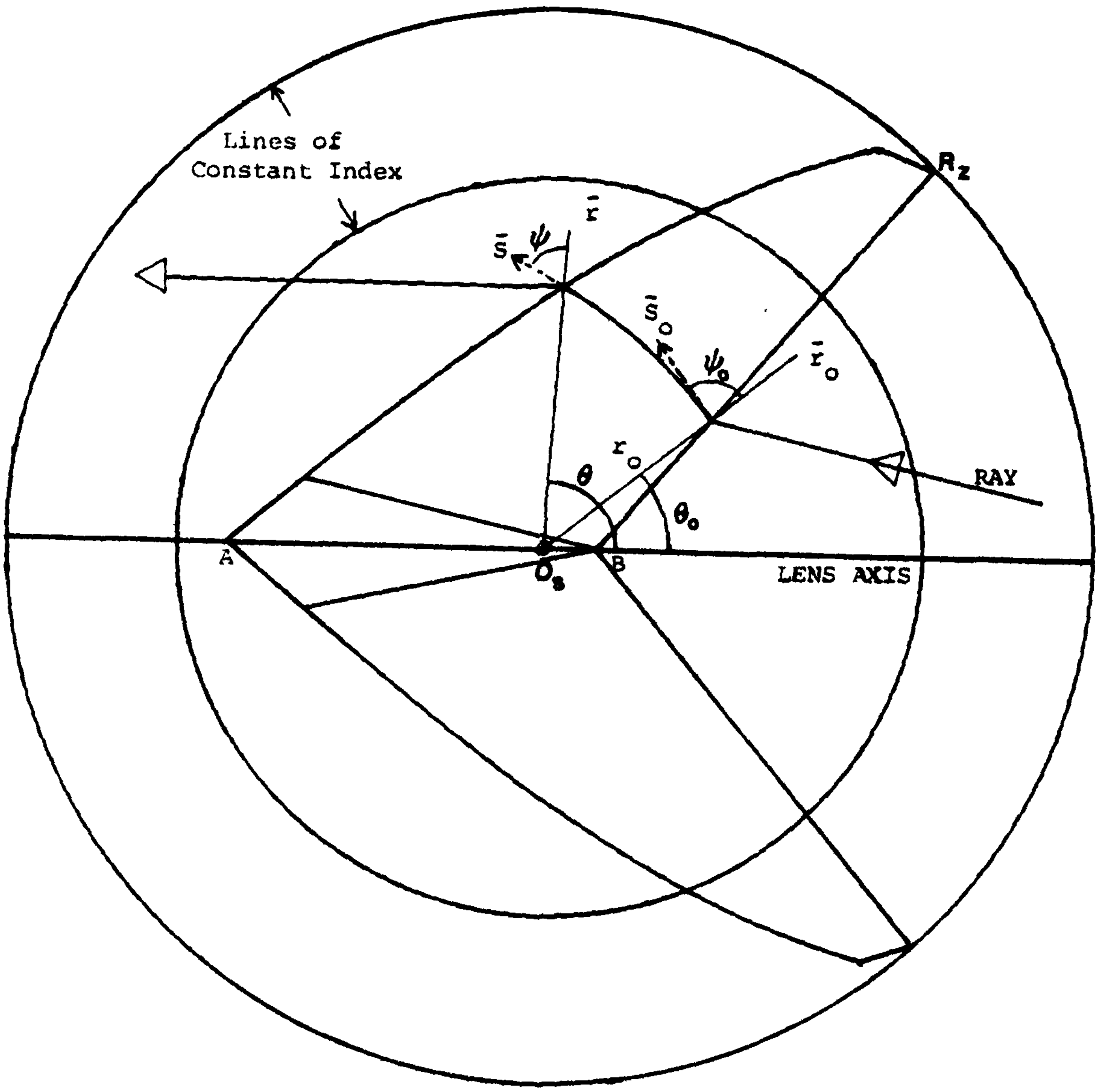

Figure 7. Grin Lens Geometry

counterclockwise from the lens axis; angles ψ and ψ_0 are measured counterclockwise from the radius vector to the instantaneous ray direction vector. ε is the sign function expressed as

$$\varepsilon = \operatorname{sgn} |\psi_0| = \pm 1 \tag{110}$$

where

$$|\psi_0| \gtrless \pi/2 \tag{111}$$

In Equation (109), n_0 refers to the index function n evaluated at r_0. The form of n has been chosen as

$$n = n(O_s, r) \tag{112}$$

where O_s denotes the position of the center of symmetry on the lens axis (shown in Figure 7) and r is the radial coordinate from O_s to the point in question. This form allows the study of the effects on lens performance as O_s is changed.

More specifically, in order to allow the analytical integration of Equation (108), the expression used for $n(O_s, r)$ is a generalized version of that employed by Luneburg as described by Marchand [9]. Here

$$n = [a + b(\frac{r}{R_Z})^2]^{1/2} \tag{113}$$

whereas Luneburg used specific values for a and b. Generalizing the index function enables the strength, or percent change of the gradient to be varied as well as the algebraic sign of the gradient. If the parameter b is negative, a decreasing parabolic gradient results; conversely a positive b yields an increasing parabolic gradient. By visualizing a plane wave front passing through a spherical gradient, it may be seen that the negative gradient results in light rays bending forward at the center, as shown in Figure 7, whereas a positive gradient has the opposite effect. This principle was used by Wood, as related by Marchand [9], in constructing simple lenses having plane faces and a radial index. The Wood lens acted as a converging or diverging lens depending upon the sign of the gradient used.

Additionally, it must be noted that if the parameter b is equal to zero, Equation (113) reduces to

$$n = \sqrt{a} \tag{114}$$

which is a HIN lens having constant index of refraction. This fact has facilitated the correlation of GRIN and HIN computer trace algorithms.

Equation (108) may be integrated by a change of variable using the relation

$$v = \left(\frac{r_0}{r}\right)^2 \tag{115}$$

which leads to the solution

$$\theta = \theta_0 - \frac{\varepsilon}{2}\left\{\sin^{-1}\left[\frac{2e^2/r^2 - a}{\sqrt{a^2 + 4be^2/R_Z^2}}\right] - \sin^{-1}\left[\frac{2e^2/r_0^2 - a}{\sqrt{a^2 + 4be^2/R_Z^2}}\right]\right\} \tag{116}$$

Equation (116) gives θ as a function of r. This equation can be easily solved for r as a function of θ in the form

$$r = \frac{\sqrt{2}\ |e|}{\left\{a+\sqrt{a^2+\frac{4be^2}{R_Z^2}}\sin\left[-2\varepsilon(\theta-\theta_0)+\sin^{-1}\left[\frac{2e^2/r_0^2 - a}{\sqrt{a^2+4be^2/R_Z^2}}\right]\right]\right\}^{1/2}} \tag{117}$$

The instantaneous direction of the ray at any point r,θ may be ascertained by using the invariance of e. Hence,

$$e = \varepsilon n r \sin\psi = \varepsilon n_0 r_0 \sin\psi_0 \tag{118}$$

and

$$\psi = \sin^{-1}\left[\frac{n_0 r_0 \sin\psi_0}{nr}\right] \tag{119}$$

Furthermore, the orientation of the plane of the ray may be easily deduced since every ray in a spherical medium is a plane curve lying in a plane through the center of symmetry.

Using this fact, Marchand [9] has shown that a suitable conversion from coordinates r and θ in the plane of the ray to global Cartesian coordinates may be written in the form

$$x = r(\delta \frac{x_0}{r_0} + \eta\ p_0) \tag{120}$$

$$y = r(\delta \frac{y_0}{r_0} + \eta\ q_0) \tag{121}$$

$$z = r(\delta \frac{z_0}{r_0} + \eta\ \ell_0) \tag{122}$$

Here p_0, q_0, ℓ_0 are the initial direction cosines of the ray at r_0,θ_0; x_0, y_0, and z_0 are the Cartesian coordinates corresponding to r_0,θ_0. The parameters δ and η are given by Marchand as

$$\eta = \sin\theta/\sin\psi_0 \tag{123}$$

$$\delta = \cos\theta - \eta\cos\psi_0 \tag{124}$$

It should be noted that Equation (117) may become singular for certain rays where ψ or ψ_0 become very close to zero or π. This singularity may be more easily seen in Equation (123) where η becomes indeterminate as both θ and ψ_0 approach zero and/or π. In practice these conditions occur when O_s is located either far out in object space, coincident with B, or on the image side of the lens; see Figure 8. Positioning

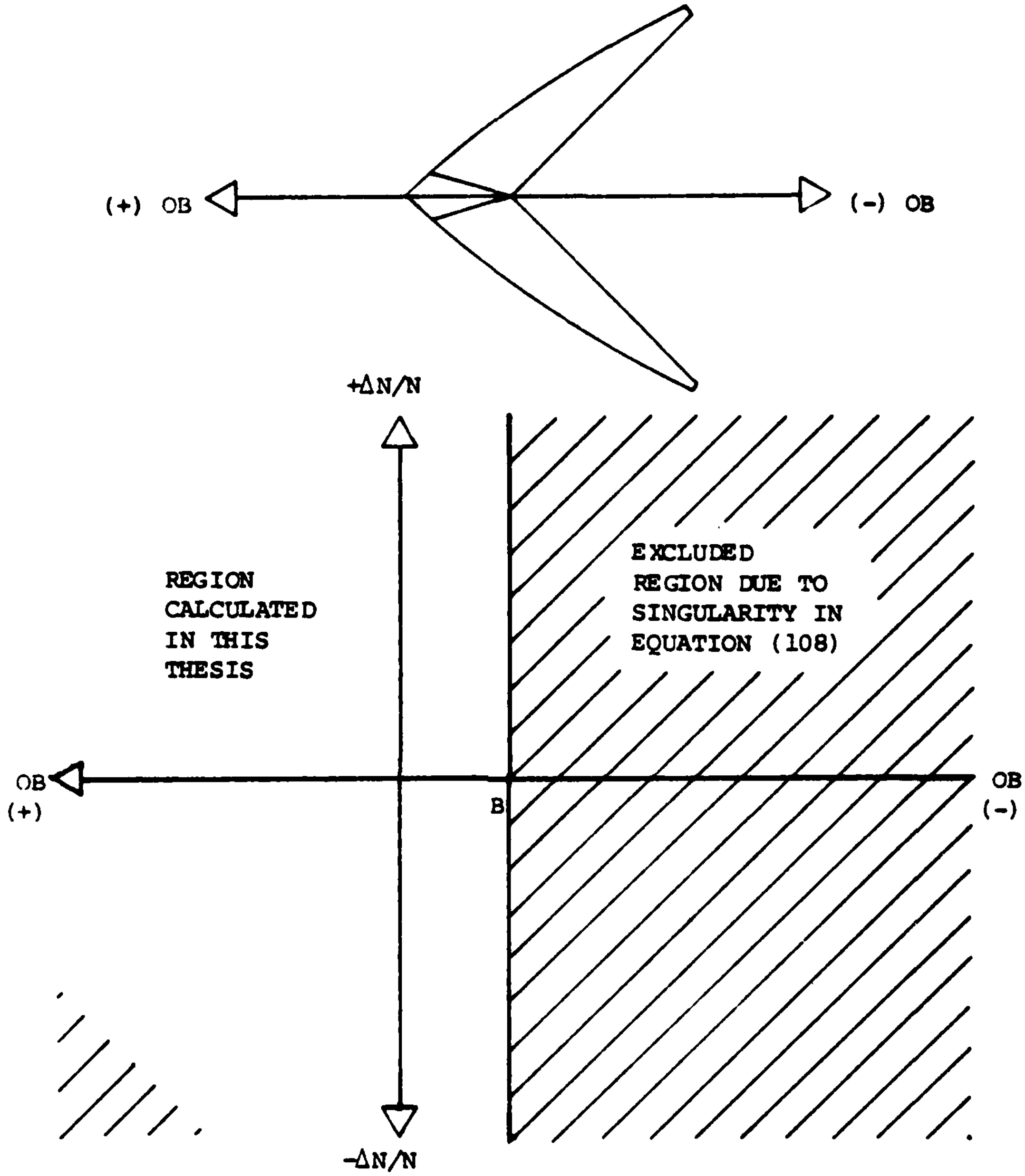

Figure 8. Excluded Regions for Center of Symmetry Due to Singularities

the center of symmetry at these locations has therefore been avoided.

B. ASSUMPTIONS

The aforementioned assumptions for the HIN case also apply here. Additionally, it must be assumed, as depicted in Figure 7, that the GRIN lens could or soon may be fabricated from a sphere of dielectric material with the required spherically symmetric parabolic gradient.

C. GRIN LENS DESIGN PARAMETERS

In the HIN lens, the available design parameters are basic. These include: F, R, T, α, U, and N_2. Parameters available for varying the design of the GRIN lens, however, include those of the HIN case but expand the index of refraction variable N_2 into O_s, a, +b, and -b. These additional lens design parameters greatly expand the lens designer's power to bend radiant energy to his will.

D. GRIN LENS DESIGN

The GRIN lens design procedure, although paralleling that of the HIN case, is somewhat more complicated in that the rays are now curved and the index of refraction varies. Accordingly, the same design process is used but with more intermediate calculations required.

The additional calculations arise since the intercept of the GRIN ray with the surface tangent cannot be solved in closed form, and an iterative solution must be used.

The reader will note that Equation (117) will yield r if $(\theta-\theta_0)$ is known. Hence the iterative procedure is to "guess" $(\theta-\theta_0)$ based on the HIN coordinates x_{1H},y_{1H} which are calculated as in the homogeneous lens. Thus

$$\theta_H = \theta_T - \theta_0 \tag{125}$$

in Figure 9 is used in Equation (117) to find point p. The tangent to the ray path at point p is now extended to intercept the surface tangent again using the homogeneous intercept relations to find x'_{1H},y'_{1H}. The prime superscripts indicate successive iteration values. The distance d is employed as a measure of the error of point p. If d is not within an acceptable margin then θ'_H is calculated based on x'_{1H},y'_{1H} and the procedure repeated to find p' in Figure 9. If d' is not within allowable error then the iteration continues until it is acceptable. In practice, this iteration procedure has proved to be extremely rapid, rarely requiring more than three iterative steps before converging. Slight modifications, however, must be introduced to handle a positive gradient. Furthermore, if O_s is located outside the lens proper, a decreasing angular increment must be subtracted from θ_H to ensure that each radial vector r_H, r'_H, ... intersects the ray during iteration. These modifications to the intercept iteration procedure are recorded in the program listing for program GISL (for Gradient Index Seeker Lens). Refer to Appendices A, B, and C for a full description of GISL.

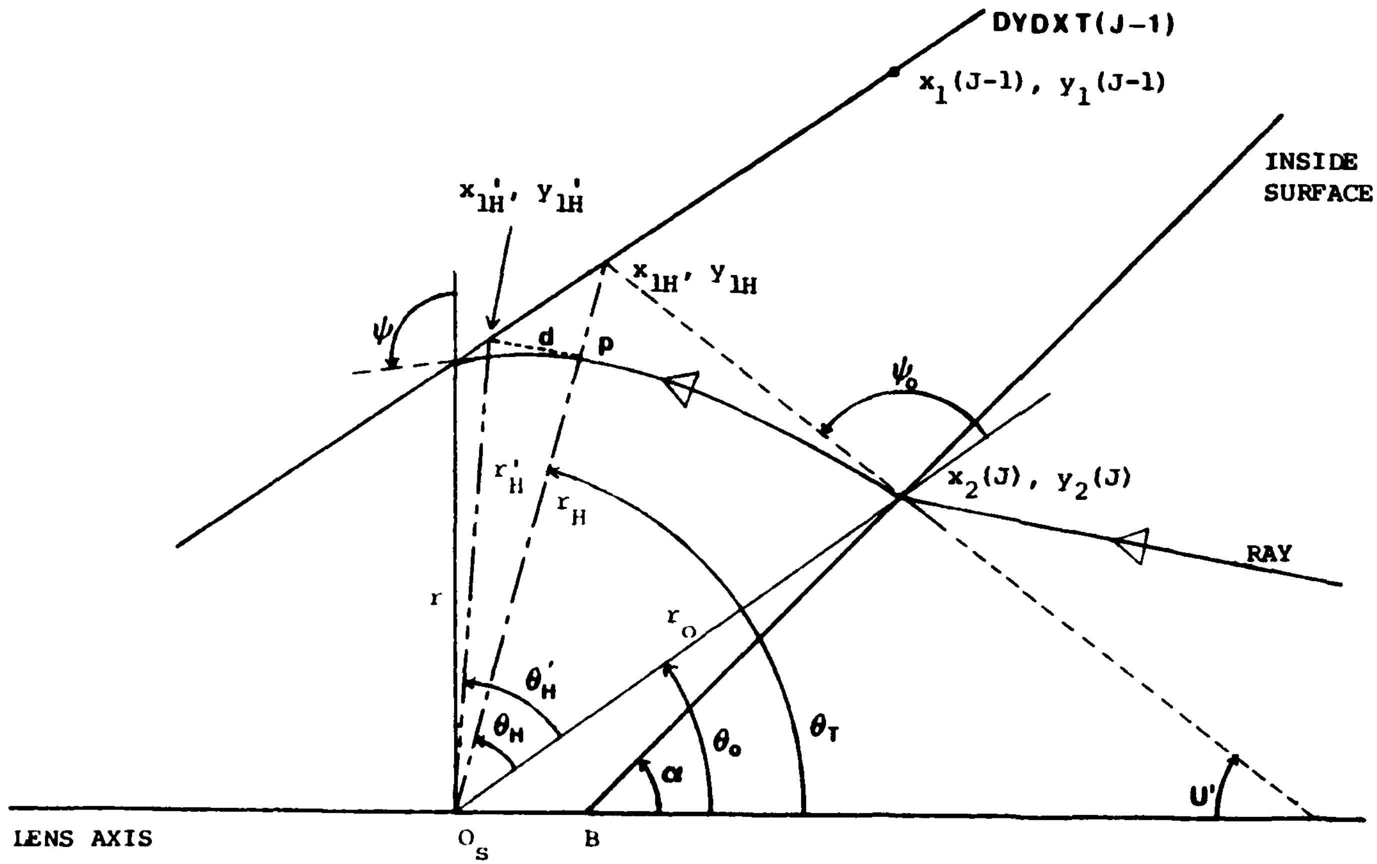

Figure 9. Grin Ray Intercept Geometry

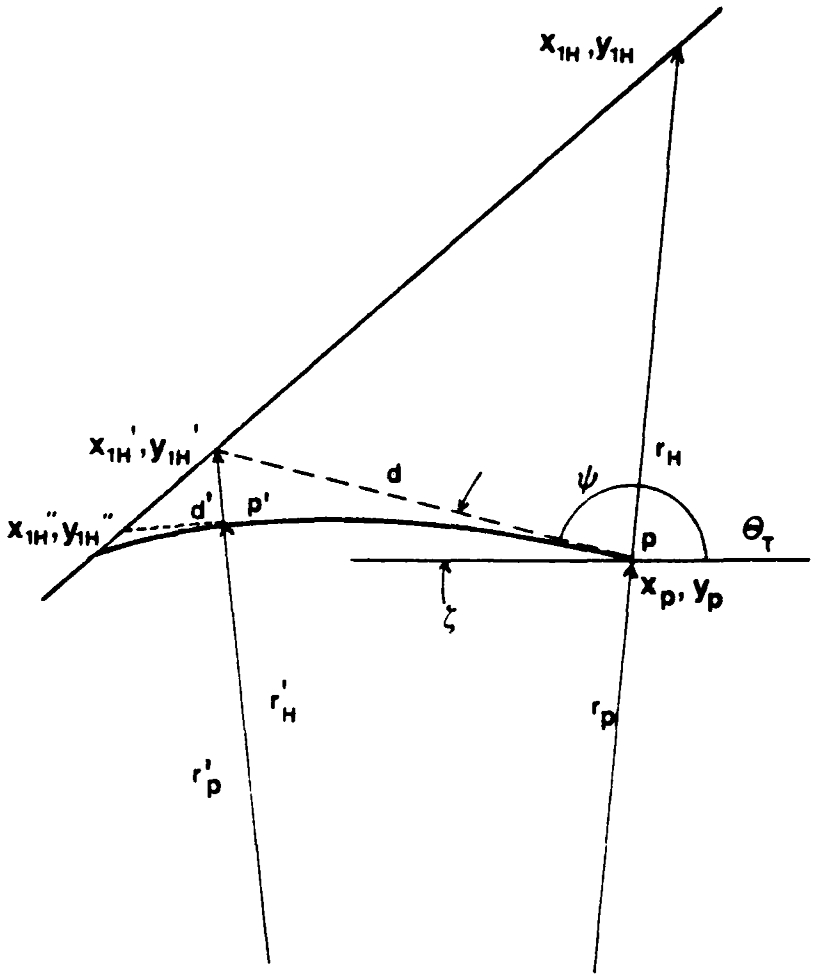

Figure 10. Expanded View, Intercept Geometry

With the overall iterative intercept procedure now being clear, the mathematical details of the GRIN lens design follow. Referring again to Figure 9, the GRIN ray is traced as in the HIN design procedure to obtain the coordinates $x_2(J), y_2(J)$ on the inside surface in the meridian plane. Now, before Snell's law can be used, the index of refraction must be found at these coordinates. Using Equation (113)

$$n_2 = [a + b(\frac{r_0}{R_Z})^2]^{1/2} \tag{125}$$

where

$$r_0 = \sqrt{(x_2(J) + OB)^2 + y_2(J)^2} \tag{126}$$

and where

$$R_Z = \sqrt{(x_2(1) + OB)^2 + y_2(1)^2} \tag{127}$$

Furthermore, by inspection it can be easily seen that

$$\psi_0 = \pi - U' - \theta_0 \tag{128}$$

U' is identical to the HIN case[1] and

---

[1]Here Equation (125) must be substituted for N_2 in [illegible]ation (12).

$$\theta_0 = \tan^{-1}\left[\frac{y_2(J)}{y_2(J) + OB}\right] \tag{129}$$

In Equations (126) through (129) OB is the line segment from O_s to B and is defined as a positive quantity to the left of B for algebraic ease of manipulation. By substitution into Equation (109) the scalar constant, e, of the ray can now be found. Furthermore, since angle U' is now known coordinates x_{1H}, y_{1H} may be calculated using Equations (14) and (15) or Equations (24) through (28).

For the first ray defining the edge of the lens, Equations (14) and (15) are employed, and, since no iteration is required, angle $(\theta_T - \theta_0)$ is used in Equation (117) to find r immediately. Here

$$\cos\theta_T = \frac{x_{1H} + OB}{r_H} \tag{130}$$

and

$$r_H = \sqrt{(x_{1H} + OB)^2 + y_{1H}^2} \tag{131}$$

Thus

$$x_1(1) = r\cos\theta_T - OB \tag{132}$$

and

$$y_1(1) = r \sin \theta_T \tag{133}$$

are the coordinates of the first point on the outside surface. Since e is known, Equation (119) is employed to find the angle ψ. Angle ζ in Figure 10 is employed to translate ψ into the ray direction with respect to the lens axis by the relation

$$\zeta = \pi - (\psi + \theta_T) \tag{134}$$

Therefore, by substituting ζ for U' in Equations (19), (20), and (21), DYDXN(1) and DYDXT(1) may be found. Here again, N_2 in Equation (19) must be replaced by n_2 as given by Equation (113) evaluated at $x_1(1), y_1(1)$.

Now that the first point on the outside surface is known, along with the surface tangent, the remainder of the K number of rays may be processed to yield the balance of the outside surface. Each subsequent intercept between ray and tangent must be iterated. Thus, unlike the first ray, once x_{1H}, y_{1H}, r_H, r_p, ψ, and ζ are known, x_{1H}' and y_{1H}' are ascertained by the substitution of the coordinates of point p for $x_2(J), y_2(J)$ in Equations (24) through (28) with U' replaced by ζ. The coordinates of point p are

$$x_p = r_p \cos \theta_T - OB \tag{135}$$

$$y_p = r_p \sin \theta_T \tag{136}$$

Therefore

$$y_{1H}' = \{\frac{A + B}{C}\} \qquad (137)$$

where

$$A = \cot(I_1 + U) \cot \zeta [y_p + x_p \tan \zeta] \qquad (138$$

$$B = y_1(J-1) - x_1(J-1) \cot[I_1 + U] \qquad (26)$$

$$C = 1 + \cot(I_1 + U) \cot \zeta \qquad (139)$$

and

$$I_1 = \sin^{-1} \left\{ \frac{\sin^2(\zeta-U)}{[\cos(\zeta-U) - N_1/n_2]^2 + \sin^2(\zeta-U)} \right\} \qquad (140)$$

Note that n_2 in Equation (140) is found from Equation (113) evaluated at r_p.

Additionally,

$$x_{1H}' = \cot \zeta [-y_{1H}' + y_p + x_p \tan \zeta] \qquad (141)$$

Now the error, d, may be evaluated as

$$d = \sqrt{(x_p - x_{1H}')^2 + (y_{1H}' - y_p)^2} \qquad (142)$$

Here d is compared to 1×10^{-5}. If d is larger than this value then the entire procedure is repeated by substituting x_{1H}', y_{1H}' for x_{1H}, y_{1H} and so forth. Once the error criteria are satisfied

$$x_1(J) = x_p \tag{143}$$

$$y_1(J) = y_p \tag{144}$$

and the next ray is processed. Correlation between GRIN (with b set equal to zero) and HIN design procedures run with identical parameters has shown agreement to the fifth and sixth decimal places.

E. SKEW RAYS IN GRIN

GRIN skew rays are handled analogously to the homogeneous case with the same coordinate transformation from grid plane to global coordinates being required. It is only after the initial directions cosines of the GRIN skew ray K', L', M' are found that the differences between GRIN and HIN appear. The only exception to this being the use of Equation (113) in Snell's law for refraction at the interface. Since the GRIN skew rays display curvature in a plane through O_s, K', L', and M' are constantly changing until intercept with the inside conical surface. Therefore, not only must the plane of the skew ray be analytically described, but the final values of K', L', M' must be found. Due to the nature of

GRIN rays, the procedure for finding the ray intercept with the conical inside surface is different from both the HIN case and the iteration procedure employed in the meridian plane due to the multiplicity of the geometry encountered. The Newton-Raphson iteration routine has been found to be ideal for this purpose.

To begin, the magnitude and direction of the initial radius vector $\bar{r}_0$ from O_s for x_0, y_0, z_0 must be ascertained. The magnitude is given by

$$r_0 = [(x_0 + OB)^2 + y_0^2 + z_0^2]^{1/2} \tag{145}$$

Therefore the unit vector in the direction of the intercept is

$$\hat{r}_0 = \frac{x_0 + OB}{r_0}\hat{i} + \frac{y_0}{r_0}\hat{j} + \frac{z_0}{r_0}\hat{k} \tag{146}$$

The plane of the ray may be fully described by the vector normal to the plane. Two vectors, $\hat{r}_0$ and $\hat{R}$ lie in the plane of the ray. $\hat{R}$ is the unit vector in the initial direction of the ray after refraction and described using direction cosines as

$$\hat{R} = K'\hat{i} + L'\hat{j} + M'\hat{k} \tag{147}$$

Thus, the plane of the ray may be described by the cross product

$$\hat{N}_{p_0} = \hat{r}_0 \times \hat{R} \qquad (148)$$

or

$$\hat{N}_{p_0} = N_{p_{0x}} \hat{i} + N_{p_{0y}} \hat{j} + N_{p_{0z}} \hat{k} \qquad (149)$$

where

$$N_{p_{0x}} = r_{0y} M' - r_{0z} L' \qquad (150)$$

$$N_{p_{0y}} = r_{0z} K' - r_{0x} M' \qquad (151)$$

and

$$N_{p_{0z}} = r_{0x} L' - r_{0y} K' \qquad (152)$$

In Equations (150), (151), and (152) r_{0x}, r_{0y}, and r_{0z} refer to the x, y, and z components of $\hat{r}_0$ in Equation (146). Furthermore, the angle ψ_0 between $\hat{r}_0$ and $\hat{R}$ may be found from the dot product as

$$\psi_0 = \cos^{-1}[r_{0x} K' + r_{0y} L' + r_{0z} M'] \qquad (153)$$

Now the scalar invariant e may be found. Substituting known values into Equation (109):

$$e = \varepsilon[a + b(\frac{r_0}{R_Z})^2]^{1/2} r_0 \sin \psi_0 \qquad (154)$$

where R_Z is unchanged from that found during previous calculations for the lens shape by Equation (127).

With the foregoing groundwork established, the intercept of the ray with the inside surface may be calculated. The Newton-Raphson iteration scheme requires the calculation of the radius vector from O_s to the cone by geometrical methods and the radius to the ray by GRIN theory. The difference between the two radii is then divided by the difference between the derivatives of the two functions. The resulting quantity is subtracted from the trial angle, θ_p, in the plane of the ray, to give a new trial angle θ_p'. The process is continued until the difference between radii is less than 1×10^{-5}. The first trial angle is measured to a reference HIN intercept as if the material were homogeneous since the actual GRIN ray curves only slightly. The coordinates of this HIN intercept point are designated x_{iH}, y_{iH}, z_{iH} and are derived using the HIN equations as before. To obtain the first trial angle, the scalar product between $\hat{r}_0$ and $\hat{r}_{iH}$ is used. Here

$$r_{iH} = [(x_{iH} + OB)^2 + y_{iH}^2 + z_{iH}^2]^{1/2} \qquad (155)$$

and

$$\hat{r}_{iH} = \frac{x_{iH} + OB}{r_{iH}} \hat{i} + \frac{y_{iH}}{r_{iH}} \hat{j} + \frac{z_{iH}}{r_{iH}} \hat{k} \tag{156}$$

Thus,

$$\theta_p = \cos^{-1}[r_{0x} r_{iHx} + r_{0y} r_{iHy} + r_{0z} r_{iHz}] \tag{157}$$

where r_{iHx}, r_{iHy}, and r_{iHz} are the x, y, and z components of r_{iH}, respectively.

In Equation (117) θ_p is substituted for $(\theta-\theta_0)$ to yield r as required by the iteration procedure. The geometrical radius, r_g, is not so easily acquired. First, note that the equation of the plane of the ray inside the lens is given by

$$N_{p0x}(x-x_0) + N_{p0y}(y-y_0) + N_{p0z}(z-z_0) = 0 \tag{158}$$

Secondly, the equation of the conical surface is given by Equation (75). The combination of the plane of the ray and the cone yield the loci of possible intercept points on the inside surface. In Cartesian coordinates, the sum of Equations (75) and (158) is

$$x(N_{p0x} - x\tan^2\ ] + y[N_{p0y} + y] + z[N_{p0z} + z] - N_{p0x}x_0$$

$$- N_{p0y}y_0 - N_{p0z}z_0 = 0 \tag{159}$$

Equation (159) must be transformed into coordinates r and θ_p

in the plane of the ray. The transformation is made possible using Equations (120) through (124). Upon substitution, and after solving for r_g, Equation (159) becomes

$$r_g = \frac{-B_2}{2A_2} \pm \sqrt{\frac{B_2^2}{4A_2^2} + \frac{C_2}{A_2}} \tag{160}$$

where

$$A_2 = B_1^2 + C_1^2 - A_1^2 \tan^2\alpha \tag{161}$$

$$B_2 = B_1 N_{poy} + C_1 N_{poz} + A_1 N_{pox} + 2A_1 \, OB \tan^2\alpha \tag{162}$$

$$C_2 = OBN_{pox} + OB^2 \tan^2\alpha + N_{pox} x_0 + N_{poy} y_0$$

$$+ N_{poz} z_0 \tag{163}$$

and

$$A_1 = \frac{\delta}{r_0}(x_0 + OB) + \eta K' \tag{164}$$

$$B_1 = \frac{\delta y_0}{r_0} + \eta L' \tag{165}$$

$$C_1 = \frac{\delta z_0}{r_0} + \eta M' \tag{166}$$

Here, δ and η are found from

$$\eta = \sin \theta_p / \sin \psi_0 \tag{167}$$

and

$$\delta = \cos \theta_p - \cos \psi_0 \tag{168}$$

which follow from Equations (123) and (124). The plus sign in Equation (160) yields the correct values. Now that r of the ray and r_g of the surface are known, the derivatives of r and r_g with respect to θ at θ_p must be found. It can be shown that for the ray

$$\left.\frac{dr}{d\theta}\right|_{\theta_p} = \frac{\varepsilon r^3}{2e^2} \cos[-2\,\varepsilon\,\theta_p + \sin^{-1}(A_3)] \tag{169}$$

where

$$A_3 = \frac{2e^2/r_0^2 - a}{\sqrt{a^2 + 4be^2/R_Z^2}} \tag{170}$$

The derivative of r_g is somewhat more complicated. With persistence, however, it can be shown that

$$\frac{dr_g}{d\theta} = -\frac{1}{2A_2^2}[A_2 \frac{dB_2}{d\theta} - B_2 \frac{dA_2}{d\theta}] + \frac{1}{2}[\frac{B_2^2}{4A_2^2} + \frac{C_2}{A_2}]^{-1/2} [C_3] \tag{171}$$

where A_2, B_2, and C_2 are given by Equations (161) through (168) and

$$C_3 = [\frac{1}{2A_2^4}(A_2^2 B_2 \frac{dB_2}{d\theta} - B_2^2 A_2 \frac{dA_2}{d\theta}) - \frac{C_2}{A_2^2} \frac{dA_2}{d\theta}] \tag{172}$$

Therefore, the r and θ_p to the intercept are found by iteration of revised trial values

$$\theta_p' = \theta_p - \frac{(r - r_g)}{(\frac{dr}{d\theta} - \frac{dr_g}{d\theta})} \tag{173}$$

In practice the quotient of differences in Equation (173) is reduced by a factor of 1.3 to slow convergence and provide stability. The number of iterations, however, rarely exceeds five.

Values for r and θ_p are now transformed into Cartesian coordinates x_i, y_i, z_i by substitution into Equations (120) through (124). Next, the values of the direction cosines K', L', and M' at the intercept are needed. The angle ψ between the radius vector and the tangent to the ray at intercept may first be deduced from the scalar invariant, e. Hence

$$\psi = \sin^{-1}(\frac{e}{n_2 r_{PI}}) \tag{174}$$

Where e is known, n_2 is evaluated at r_{PI}; r_{PI} is the radius to the intercept as found by the iteration above. Three constraints on the direction cosines may be written. These are:

1) The scalar product of the radius vector, $\hat{r}_{PI}$, and the instantaneous ray direction vector, $\hat{R}$, at intercept.

2) The scalar product of the normal to the plane of the ray $\hat{N}_{p0}$ and $\hat{R}$.

3) The sum of the squares of the direction cosines must sum to unity.

Mathematically, the above constraints are written as

$$\frac{(x_i + OB)}{r_{PI}} K' + \frac{y_i}{r_{PI}} L' + \frac{z_i}{r_{PI}} M' = \cos \psi \tag{175}$$

$$N_{P0x}K' + N_{p0y}L' + N_{p0z}M' = 0 \tag{176}$$

$$K'^2 + L'^2 + M'^2 = 1 \tag{177}$$

To find K', L', and M', Equations (175), (176) and (177) are solved simultaneously. It can be shown that the solution leads to

$$M' = \frac{-B_6}{2A_6} \pm \sqrt{\frac{B_6^2}{4A_6^2} - \frac{C_6}{A_6}} \tag{178}$$

$$L' = A_5 - B_5M' \tag{179}$$

$$K' = (1 - L'^2 - M'^2)^{1/2} \tag{180}$$

where

$$A_6 = [1 + (\frac{N_{P0z}}{N_{p0x}})^2]B_5^2 - \frac{2\,N_{p0y}\,N_{p0z}}{N_{p0x}^2} B_5$$
$$+ (\frac{N_{p0z}}{N_{p0x}})^2 + 1 \tag{181}$$

$$B_6 = \frac{2\,N_{p0y}\,N_{p0z}}{N_{p0x}} A_5 -]\,[1 + (\frac{N_{p0z}}{N_{p0x}})^2]A_5B_5 \qquad (182)$$

$$C_6 = [1 + (\frac{N_{p0z}}{N_{p0x}})^2]A_5^2 - 1 \qquad (183)$$

and

$$A_5 = \frac{N_{p0x}\cos\psi}{N_{p0x}B_4 - N_{p0y}A_4} \qquad (184)$$

$$B_5 = \frac{N_{p0x}C_4 - N_{p0z}A_4}{N_{p0x}B_4 - N_{p0y}A_4} \qquad (185)$$

Furthermore, in Equations (184) and (185), A_4, B_4, and C_4 are the coefficients of K', L' and M' in Equation (175).

Now that the direction cosines of the ray are known at the point of intersection with the inside surface, the index of refraction, n_2, is computed by substituting r_{PI} into Equation (113). The remainder of the skew ray trace to the image plane is identical to the homogeneous procedure.

AD-A125 167 AERODYNAMICALLY EFFICIENT GRADIENT REFRACTIVE INDEX MISSILE SEEKER LENS(U) NAVAL POSTGRADUATE SCHOOL MONTEREY CA H M CARR OCT 82 NPS67-82-012 2/6

UNCLASSIFIED F/G 16/4 NL

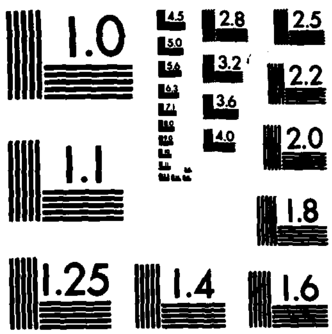

MICROCOPY RESOLUTION TEST CHART
NATIONAL BUREAU OF STANDARDS-1963-A

$$B_6 = \frac{2\,N_{p0y}\,N_{p0z}}{N_{p0x}}\,A_5 -]\,[1 + (\frac{N_{p0z}}{N_{p0x}})^2]A_5B_5 \qquad (182)$$

$$C_6 = [1 + (\frac{N_{p0z}}{N_{p0x}})^2]A_5^2 - 1 \qquad (183)$$

and

$$A_5 = \frac{N_{p0x}\cos\psi}{N_{p0x}B_4 - N_{p0y}A_4} \qquad (184)$$

$$B_5 = \frac{N_{p0x}C_4 - N_{p0z}A_4}{N_{p0x}B_4 - N_{p0y}A_4} \qquad (185)$$

Furthermore, in Equations (184) and (185), A_4, B_4, and C_4 are the coefficients of K', L' and M' in Equation (175).

Now that the direction cosines of the ray are known at the point of intersection with the inside surface, the index of refraction, n_2, is computed by substituting r_{PI} into Equation (113). The remainder of the skew ray trace to the image plane is identical to the homogeneous procedure.

IV. LENS PERFORMANCE PARAMETERS

The function of the seeker lens is to focus electromagnetic energy either reflected from or emitted by the target onto a detector. Angular displacement of the target with respect to the missile body axes as well as target angular rate information are both desired outputs from the seeker. Hence, it is not only important just to be able to detect the target by focusing energy into a spot on the detector, it is equally important that this spot be as small as possible to enable the precise position of the spot on the detector to be discerned.

The ability of a lens to focus an object to a small spot does not guarantee the quality of the image. For a FLIR optical system extensive effort is expended to obtain an image with minimum aberration [10]. Seeker optics, however, are generally non-imaging devices where the pressure of the different aberrations does not detract from the function of the seeker as long as a tight image is maintained [11].

Accordingly, the most important parameter by which seeker lens performance is judged is that of spot size at different obliquities. Since the image found at the focal point is not necessarily circular nor equally dense, the standard deviation in the y and z directions with respect to image centroid is used to define spot size.

Therefore, once the coordinate pairs of all the skew rays have been calculated in the image plane, the first step in

the analysis of lens performance is to calculate the image centroid [12]. If the spot diagram is composed of N rays, the centroid location, y_c is

$$y_c = \frac{1}{N} \sum_{i=1}^{N} Y_i \tag{186}$$

Since there is symmetry about the x-y plane, the z coordinate of the centroid will always be zero.

The next step in finding the spot size is to find the standard deviations of the spot diagram in the y and z directions. This is accomplished by summing the squares of the differences of the intercept coordinates with respect to the centroid and then dividing by the number of rays. The standard deviations then, are given by

$$\sigma_z^2 = \frac{1}{N} \sum_{i=1}^{N} Z_i^2 \tag{187}$$

and

$$\sigma_y^2 = \frac{1}{N} \sum_{i=1}^{N} (Y_i - y_c)^2 \tag{188}$$

The spot size, σ_r, is now defined by

$$\sigma_r = \sqrt{\sigma_z^2 + \sigma_y^2} \tag{189}$$

Of further interest in appraising lens performance is the energy density of the image as a function of radius from the centroid. In nondimensional form, this is simply the number of rays in the spot diagram within a succession of circles of increasing size overlaid about the centroid. Here, each ray is assumed to carry a unit amount of radiant energy. This type of plot facilitates the comparison of different lens designs by detailing the distribution of energy within each image. Clearly, it is desirable to have as much energy as possible concentrated very close to the image centroid. Between two lenses with equal spot sizes, the preferred lens has more energy concentrated within a smaller radius.

Every ray, however, does not deliver an equal amount of energy to the focal plane. It is prudent, therefore, to include as a performance parameter the average ray intensity. Again, for N rays, the intensity I of each ray is summed and normalized by N to yield

$$I_{av} = \frac{1}{N} \sum_{i=1}^{N} I_i \qquad (190)$$

Finally, each lens design is checked for "failed rays". The reader will recall that these rays fail to intercept the image plane due to total internal reflection, total external reflection, or failure to intercept the inside surface within the bounds of the lens. Hence, a lens design with fewer "failed rays" or no "failed rays" at all is a preferred lens.

Although there are many other performance criteria by which lenses are compared, the foregoing parameters are more than sufficient to judge the merit of preliminary seeker lens designs. It should be noted, however, that notwithstanding the fact that the image centroid and standard deviations were used as stepping stones to obtain image spot size, they have significant meaning of their own. The standard deviations σ_y and σ_z inform the lens designer as to the horizontal and vertical spread of the image. Image centroid location, y_c, at increasing obliquities is of obvious importance since excessive displacement will cause the image to miss the detector entirely and would dictate the necessity for a second lens element to dampen the movement. Furthermore, since Line of Sight (LOS) measurement accuracy to the target is highly dependent upon the linearity of y_c as a function of the lens tilt angle, lens designs which exhibit a greater degree of such linear behavior are the preferred designs.

To summarize, it is sufficient to note that although spot size is the most important of the performance parameters, every other parameter has a significant impact on the performance of a particular lens.

V. RESULTS FOR THE HOMOGENEOUS LENS

The performance of the homogeneous lens is presented primarily as a comparison with which to compare the performance of the GRIN lens. Here, the relationship of spot size to increasing lens obliquity and lens thickness are presented as well as the image centroid movement as a function of obliquity. Additionally, the reader is introduced to the four basic computer plots used to display the results: lens shape, object plane with superimposed skew ray grid, image plane or spot diagram, and energy density. These plots were generated on the VERSATEC Plotter using arrays of data points produced by program GISL on the IBM 3033 mainframe computer.

To begin, Figure 11 shows the homogeneous lens shape. The first of the four basic plots, the lens shape plot, presents the lens side view in the meridian plane. The outer surface (curved) and the inner surface (cone) are constructed by connecting the points $x_1(J)$, $y_1(H)$ and $x_2(J)$,$y_2(J)$, respectively, by straight lines. At the apex of the lens about the lens axis is a trapezoidal region which represents the opaque nose area. In the legend are listed the lens design parameters and the significant calculated dimensions of the lens. Since all linear dimensions are implicitly normalized with respect to the maximum inside radius, R, the lens may be scaled up or down by multiplying each dimension by a factor of R_{new}/R. Beginning at the top, the parameters listed in the legend are explained in Table 1.

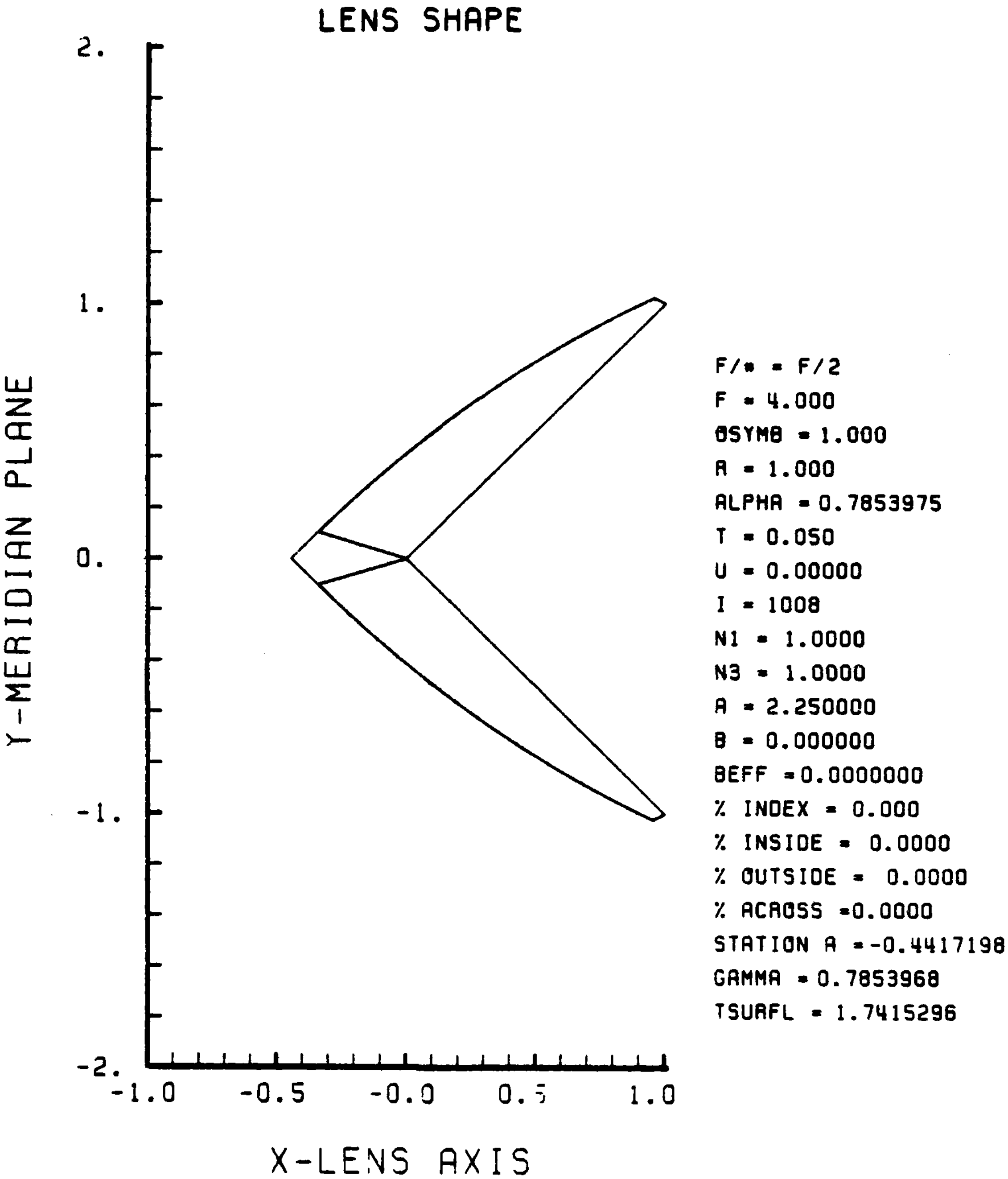

Figure 11. Homogeneous Lens Shape for N_2 = 1.5

TABLE 1

Explanation of Lens Shape Plot Legend

PARAMETER	TYPE OF PARAMETER	MEANING
F/#	DESIGN	F number. F/# = F/2R
F	DESIGN	Focal length from B.*
OSYMB	DESIGN	OB. Line segment O_s to B (positive to left).* Immaterial in HIN
R	DESIGN	Maximum radius of cone*
ALPHA	DESIGN	α--cone half-angle,* radians
T	DESIGN	Edge thickness*
U	DESIGN	Incident ray offset angle (design)*, radians
I	DESIGN	Number of iterations. I+1 = number of rays
N_1	DESIGN	Free stream index of refraction
N_3	DESIGN	Index of refraction of interior lens cavity
A	DESIGN	a in $n_2(r) = \sqrt{a + b(r^2/R_Z^2}$, gradient refractive index function. $N_2 = \sqrt{a}$ in HIN.
B	DESIGN	b in $n_2(r)$. Zero in HIN
B_{EFF}	CALCULATED	b effective = b/R_Z^2
% Index	DESIGN	Percent change in $n_2(r)$ from r = 0 to r = R_Z
% Inside	CALCULATED	Percent change in $n_2(r)$ along inside surface from lens axis to edge
% Outside	CALCULATED	Percent change in $n_2(r)$ along outside surface from opaque region to edge

Table 1 (Continued)

PARAMETER	TYPE OF PARAMETER	MEANING*
% Across	CALCULATED	Percent change in $n_2(r)$ across lens from lens axis to outside surface at the thickest point
STATION A	CALCULATED	x-coordinate at nose of lens*
GAMMA	CALCULATED	γ--nose half-angle of opaque nose region,* radians
TSURFL	CALCULATED	Total outside surface length from Station A to the edge

*Refer to Figure 2 for clarification

The HIN lens shape has a convex outer surface with maximum thickness on axis of almost ten times the edge thickness. Although the lens has a good aerodynamic shape resembling an ogive, the outer surface is not a circular arc nor can a single analytical function be fitted to the array of points describing the surface. Note that the nose half-angle, γ, is almost identical to the cone half-angle, α.

All lenses have been designed with a cone half-angle of 45° which is approximately the maximum angle for which aerodynamically efficient lens shapes may be designed, considering a free stream Mach Number not to exceed three. Without exception, overall lens performance is more severely degraded as angle α is reduced.

Table 2 explains the legend of Figure 12, which is the second basic plot. Here the lens is depicted as seen from the skew ray grid plane. The lens tilt angle, α_p, causes the equally spaced (in J) circles descriging the surface of the lens to appear as ellipses. In Figure 12, the grid spacing has been reduced from 0.1, which is normally used, to 0.3 to allow identification of individual rays for correlation with the image plane spot diagram. Although the small number of rays used is not sufficient to given an accurate definition of spot size, the number is sufficient to describe where rays in the object plane are being focused in the image plane by the HIN lens. The skew rays in Figure 12 have been numbered in the order in which they were processed. Actually, only rays 1 through 19 were actually traced; 20 through 33 are

TABLE 2

Explanation of OBJECT PLANE Plot Legend

PARAMETER	TYPE OF PARAMETER	MEANING
ALFAP	Analysis	α_p. Lens tilt angle, radians
Rays	Analysis	Total number of rays processed
Failed Rays	Analysis	Total number of rays failing to pass through the lens*

*Failed Rays are indicated on the plot by a diamond superimposed on the grid location of the ray.

mirror image skew rays. Ray 30 corresponds to ray 14, for example, Here, the lens has been tilted by 0.4 radians, or 22.9 degrees, and 33 rays have been processed of which none have failed to intercept the image plane. The staircase pattern has been added in this case in order to show the resulting distortion present in the image plane (Figure 13).

The Spot Diagram in Figure 13 is an example of the third basic computer plot; see Table 3. Unlike most Spot Diagrams, this example has the individual rays numbered for comparison with Figure 12; also the resulting distorted staircase pattern is sketched. By cross-referencing individual rays between Figures 12 and 13, it is possible to recognize where certain areas of the lens are focusing rays in the image plane. Rays 1, 4, 20, and 22 about the opaque nose region form a coma tail which contributes most of the image spread. Rays 33,

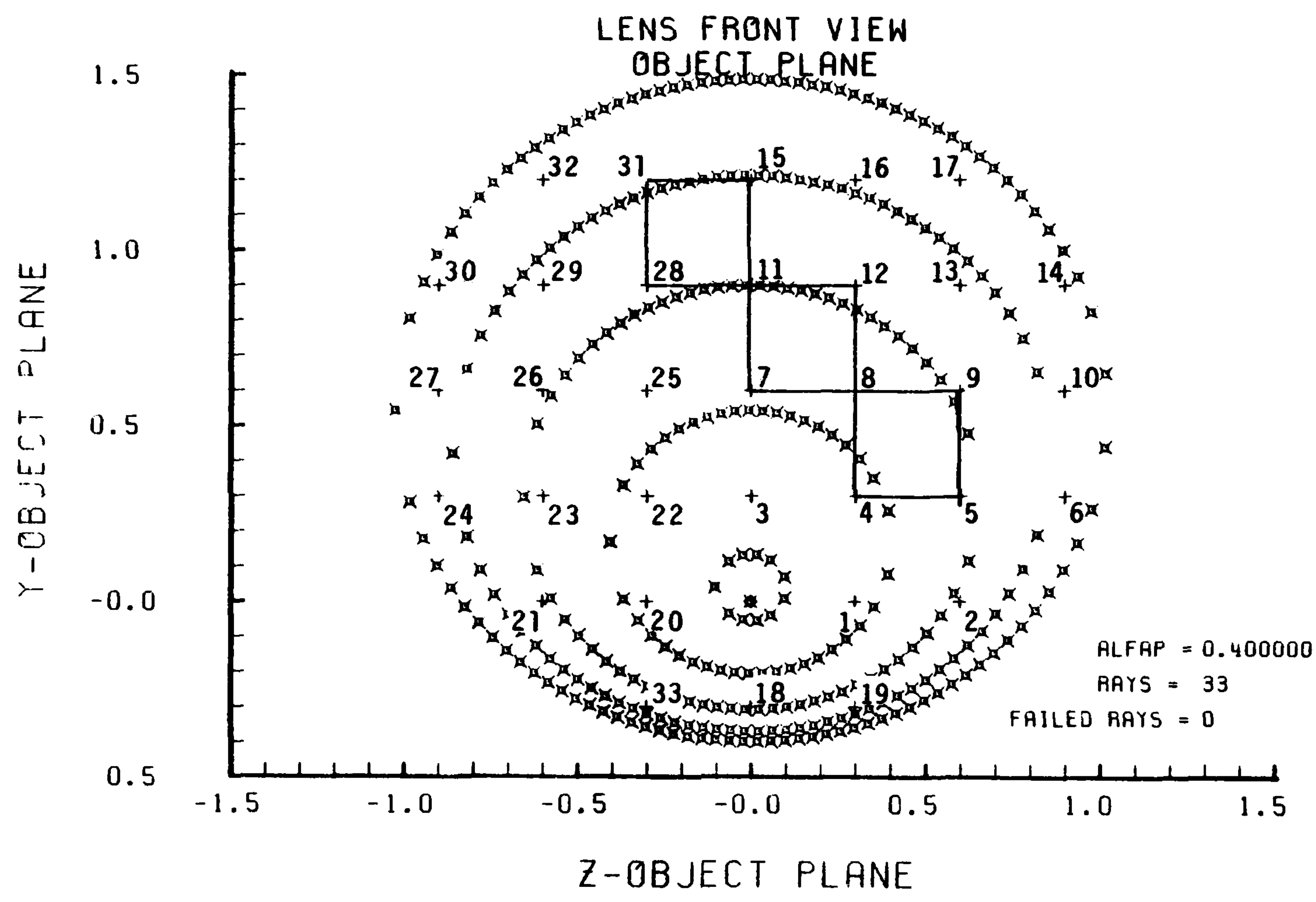

Figure 12. Example Object Plane

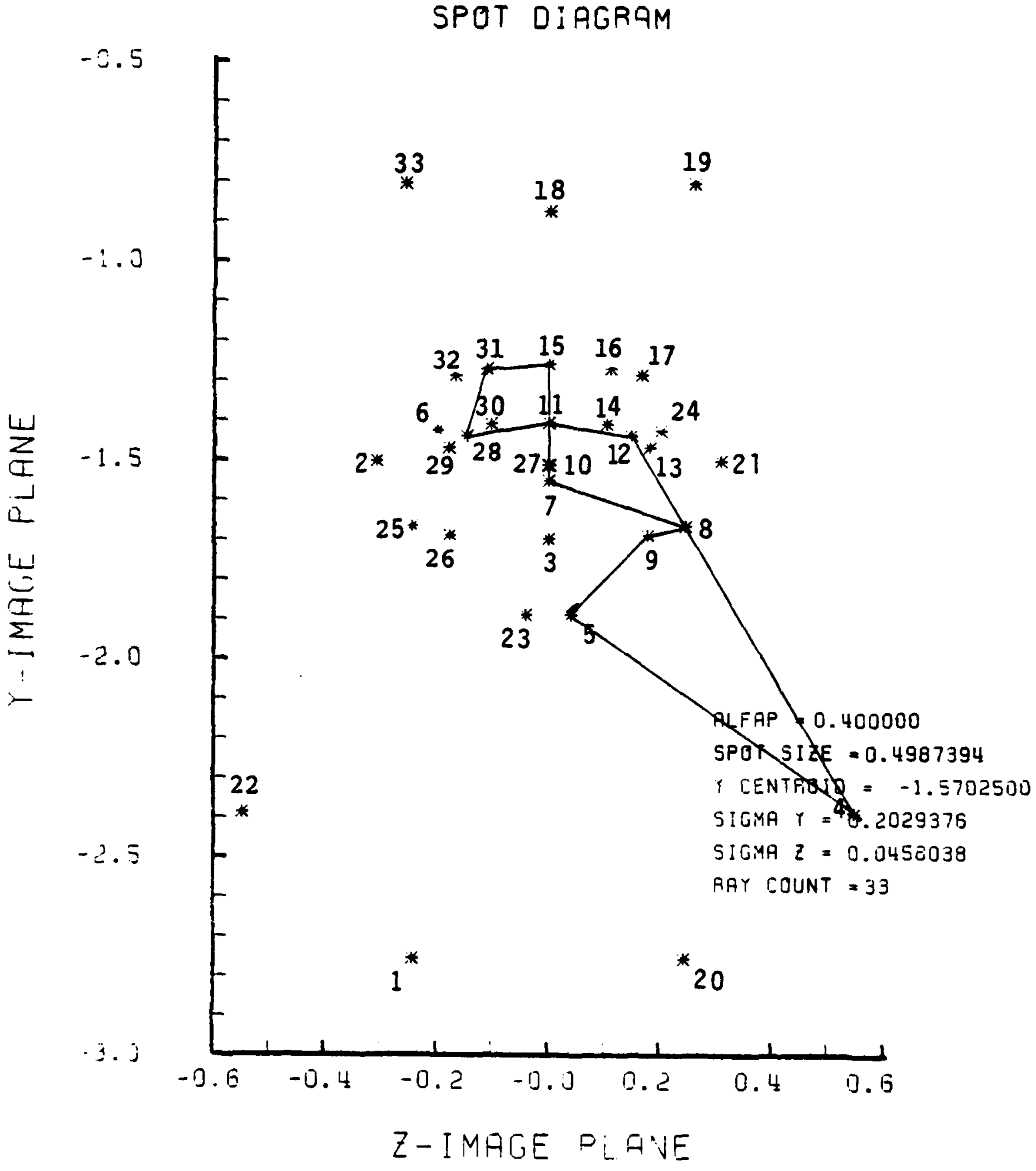

Figure 13. Spot Diagram for HIN Lens Design Shown in Figure 11

TABLE 3

Explanation of Spot Diagram Legend

PARAMETER	TYPE OF PARAMETER	MEANING
ALFAP	Analysis	α_p, lens tilt angle, radians
SPOT SIZE	Performance	σ_r, see Equation (189)
Y-CENTROID	Performance	y_c, y-coordinate of image centroid; see Equation (186)
SIGMA Y	Performance	σ_y, y-standard deviation; see Equation (188)
SIGMA Z	Performance	σ_z, z-standard deviation; see Equation (187)
RAY COUNT	Performance	Number of rays striking the image plane

18, and 19 from the bottom portion of the homogeneous lens are imaged at the top and are widely separated from the core of the image. In general, the regions of the lens which have been found to contribute the bulk of the widely spaced rays are the immediate nose region and the lower portion of the lens.

Furthermore, the distortion present in the image of the staircase pattern clearly shows that regions closest to the nose yield the greatest distortion. Horizontal lines are switched end for end and tilted approximately 45 degrees.

The upper portion of the lens performs the best. Rays 3, 7, 11, and 15 in the meridian plane are focused on the y_{IM} axis in a fairly tight region; rays 10, 14, 17, 27, 30,

and 32 about the upper periphery in the object plane are all focused within the image core.

Table 3 explains the legend of the spot diagram. It is seen that the standard deviation in the y-direction is approximately five times that of the z-direction. This elongation of the image is not readily evident in the spot diagram since the ordinate and abscissa have not been plotted with equal increments. This results from the great disparity between Spot Diagrams of the various lens designs studied. It is important, therefore, for the reader to take careful note of the relative sizes of the y_{IM} and z_{IM} axes.

Of primary importance is the spot size in Figure 13. The value for spot size is adversely affected by the poorest performing regions of the lens. Were it not for these errant rays, the spot size would be considerably smaller. The image intensity pattern is benefitted, however, by the fact that the rays spread the farthest from the centroid contribute significantly less energy per ray than those being focused in the core of the image. Table 4 lists the relative intensities of the primary skew rays plotted in Figure 13. It is seen that the high intercept angles experienced by the rays closest to the bottom of the lens and, to a lesser extent, those near the nose, result in higher reflectivity and lower transmission through the lens.

In the legend of Figure 14, the average of ray intensity is given. The Spot Diagram Energy Density distribution may be seen at a glance. The fraction of energy (number of rays)

TABLE 4

Skew Ray Intensities of HIN Lens

a) Numberical Order

Ray	Intensity	Ray	Intensity
1	0.746	11	0.919
2	0.789	12	0.918
3	0.921	13	0.910
4	0.892	14	0.887
5	0.877	15	0.918
6	0.811	16	0.916
7	0.920	17	0.910
8	0.917	18	0.640
9	0.904	19	0.576
10	0.870		

b) In order of Descending Intensity

Intensity	Ray(s)	Intensity	Ray(s)
0.921	3	0.887	14
0.920	7	0.877	5
0.919	11	0.870	10
0.918	12,15	0.811	6
0.917	8	0.789	2
0.916	16	0.746	1
0.910	13,17	0.640	18
0.904	9	0.576	19
0.892	4		

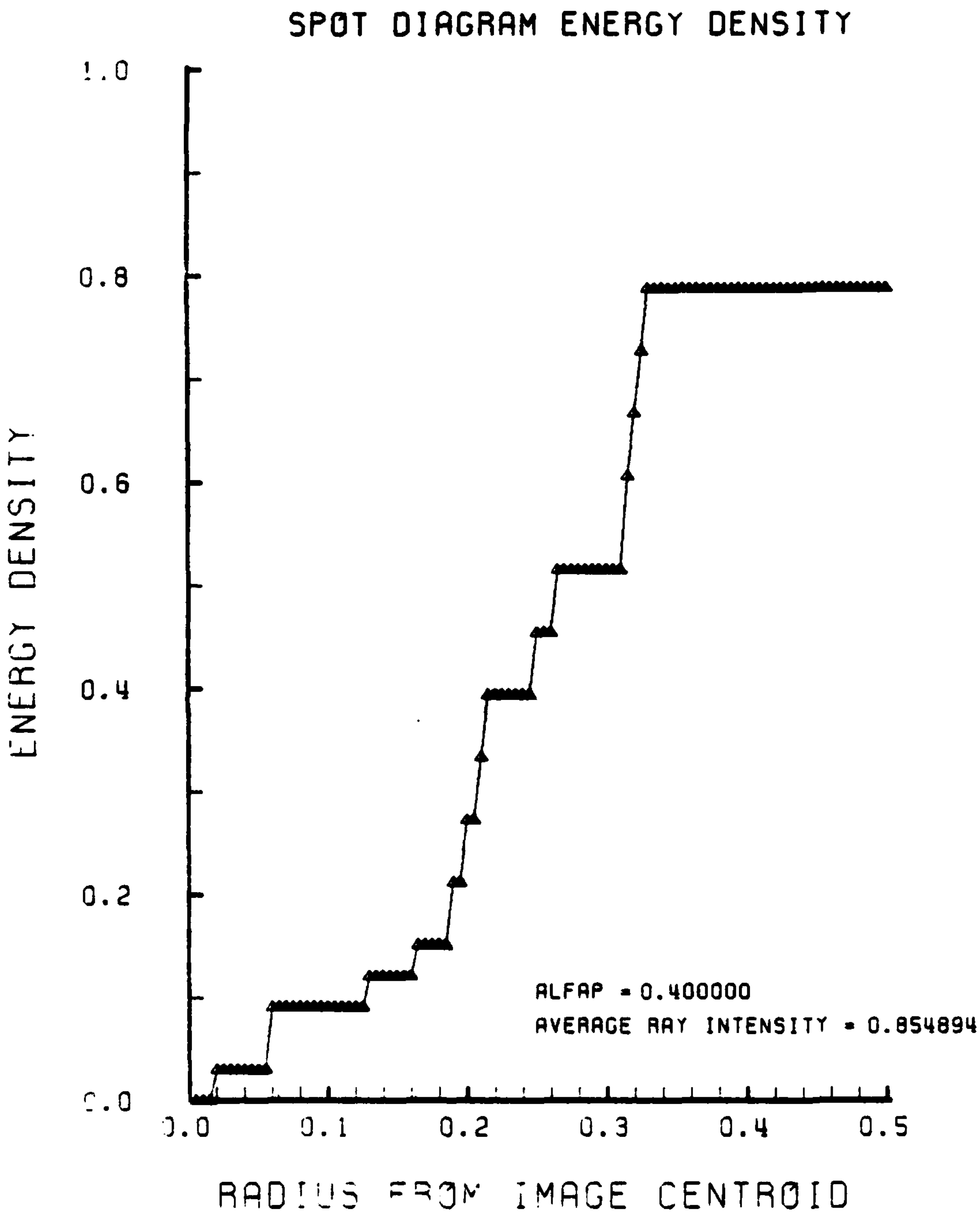

Figure 14. Nondimensional Encircled Energy Plot for HIN Lens Design of Figure 11

shown as a function of radius from the Spot Diagram centroid is normalized with respect to the total number of rays traces (Rays, in Figure 12) regardless of whether all of the rays successfully intercepted the image plane. Thus the fourth basic plot may be used in conjunction with the Spot Diagram to further define the image concentration with respect to the centroid.

The response of the HIN lens to increasing tilt angles is given in Figures D-1 through D-23 where the index of refraction of the lens has been set at 1.5. Whereas the spot size at $\alpha_p = 0.0$ is very small, that at $\alpha_p = 0.7$ radians is quite large at 67% of the lens radius. Figures 15 and 16 summarize spot size and centroid locations for the lens. Spot size growth, although somewhat irregular at the higher angles, is pronounced. Furthermore, the centroid movement is seen to be an approximately linear function of α_p until $\alpha_p \cong 0.3$ and easily exceeds the radial dimension of the lens at higher tilt angles.

Figure 17 shows that the HIN lens may be slightly improved by increasing the edge thickness, T, by a small amount. The lens may be otherwise tuned to improve performance at certain tilt angles by designing the lens with U slightly greater than zero. These performance improvements are practically insignificant, however, and neither lens tuning by the parameter U nor T produce improvement across the spectrum of tilt angles. Instead, an improvement at one α_p usually has resulted in a degradation at others.

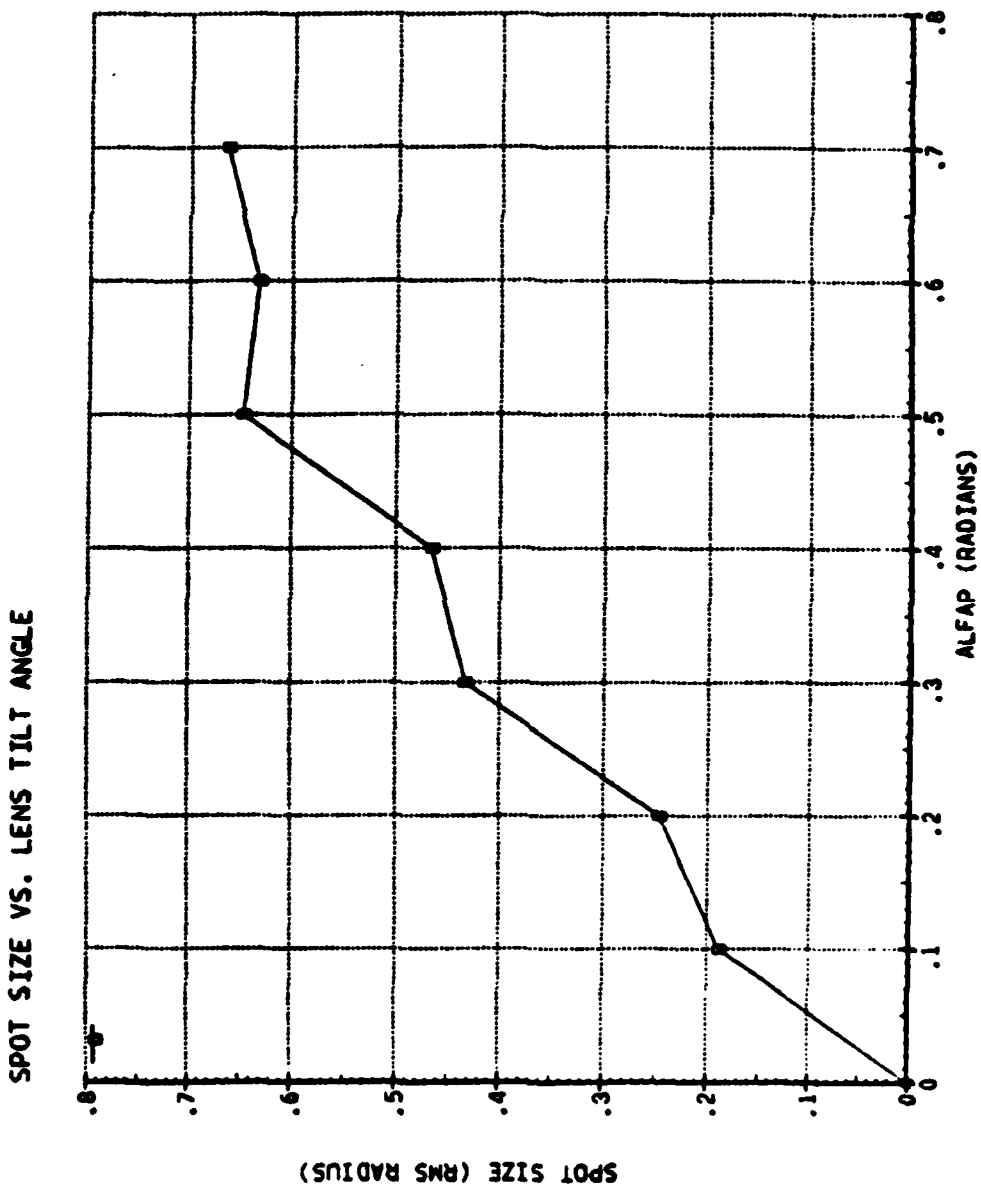

Figure 15. HIN Lens Spot Size versus α_p for $N_2 = 1.5$

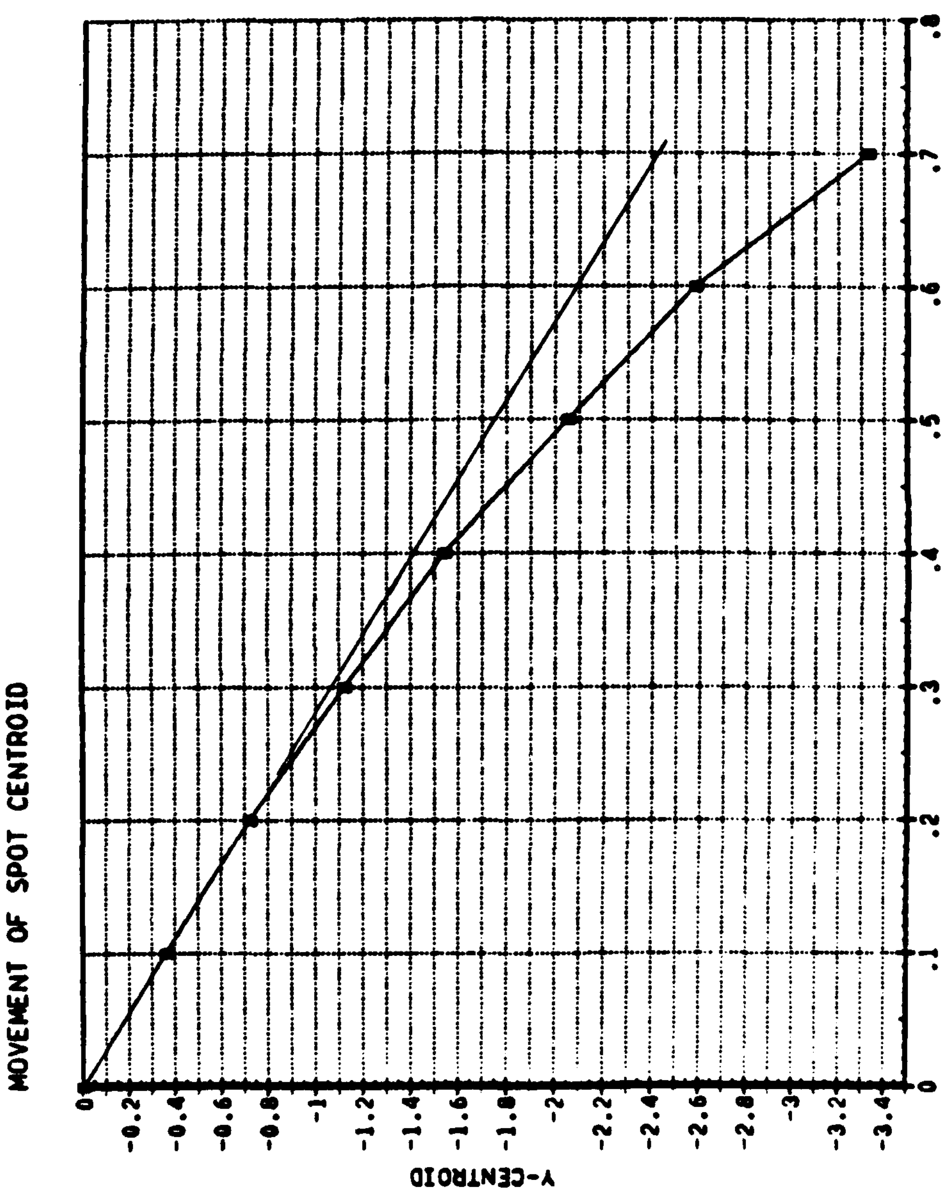

Figure 16. HIN Lens Centroid Movement versus α_p at $N_2 = 1.5$

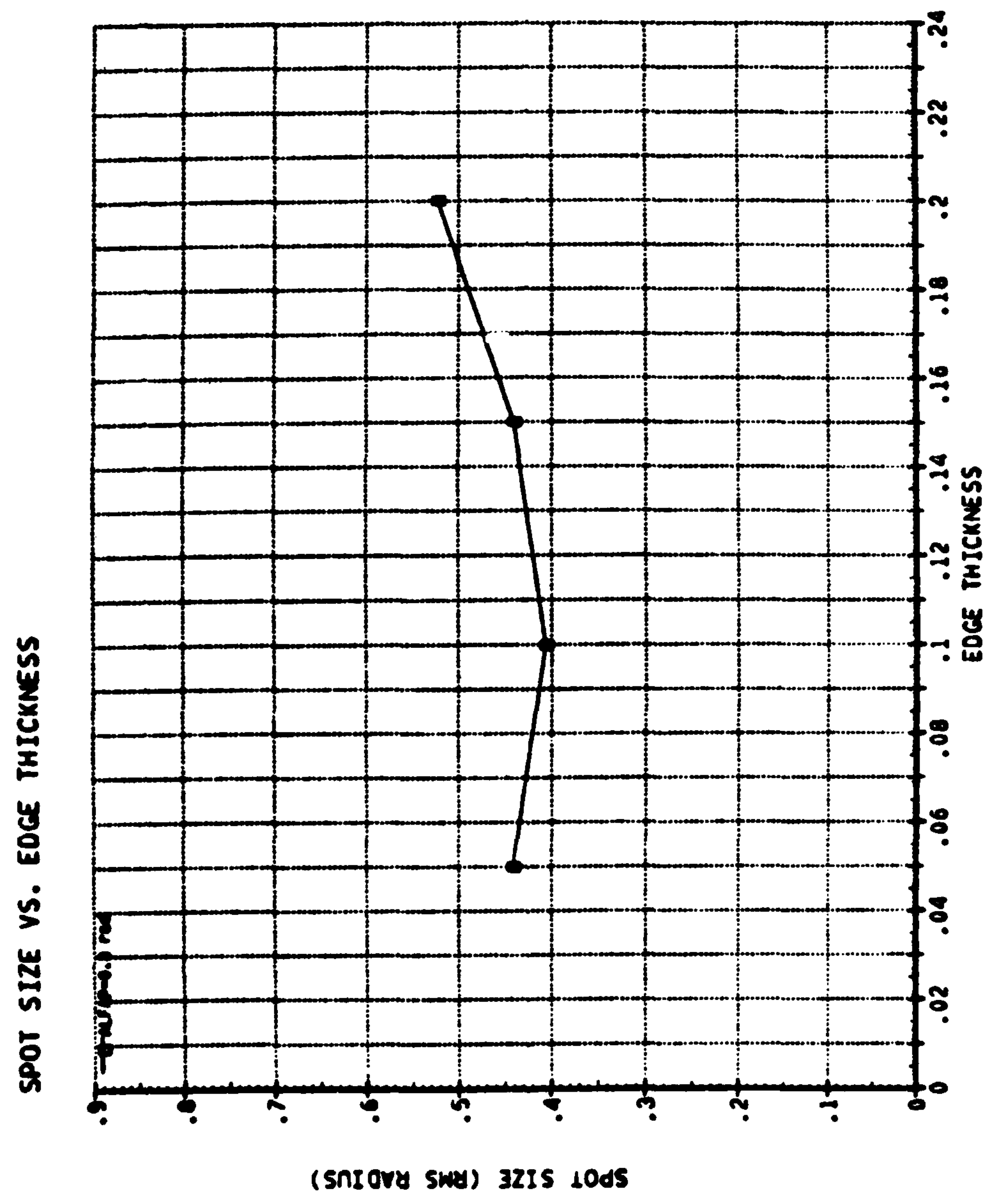

Figure 17. HIN Lens Spot Size versus Edge Thickness at α_p = 0.3 Radians and N_2 = 1.5

Finally, the homogeneous lens is shown with index of refraction of three at the intermediate tilt angle of 0.3 radians in Figures D-24 through D-27. The lens shape required to accommodate the higher index of refraction is seen to be thinner and displays less outside surface curvature than the HIN lens with $N_2 = 1.5$. Spot size is significantly reduced. Since infrared lenses such as germanium generally have fairly high refractive indices, improved lens performance at these higher values is encouraging.

VI. GRIN LENS RESULTS

The performance of the GRIN lens is similar in many respects to the homogeneous lens. The relationship between characteristic regions of the GRIN lens, such as the lower lens portion, and where these regions image bundles of rays is identical to the HIN lens as depicted in Figures 11 and 12. The growth of spot size with increasing α_p and the respective movement of image centroid typical of the homogeneous lens is clearly displayed by the GRIN lens as well.

The measure of the superiority of the GRIN lens, therefore, lies in the successful correction or improvement of the deficiencies seen in the HIN lens. Here, the reduction of spot size is of primary concern.

As a modest example of the ability of the gradient refractive index to reduce spot size, the GRIN lens design shown in Figure 18 is examined. This lens is very similar in shape to the homogeneous lens with $N_2 = 1.5$. Note, however, that unlike the HIN lens, the nose half-angle, γ, is slightly larger than that of the cone, indicating more outside surface curvature. The object plane for this lens, at $\alpha_p = 0.4$, is shown in Figure 19. Here, the error in focusing rays present in the image plane has been superimposed over the grid plane. y_{IM} coordinate error contours (with respect to the centroid) are shown in the left half of the plane and z_{IM} contours in the right. These contours vividly show that the largest

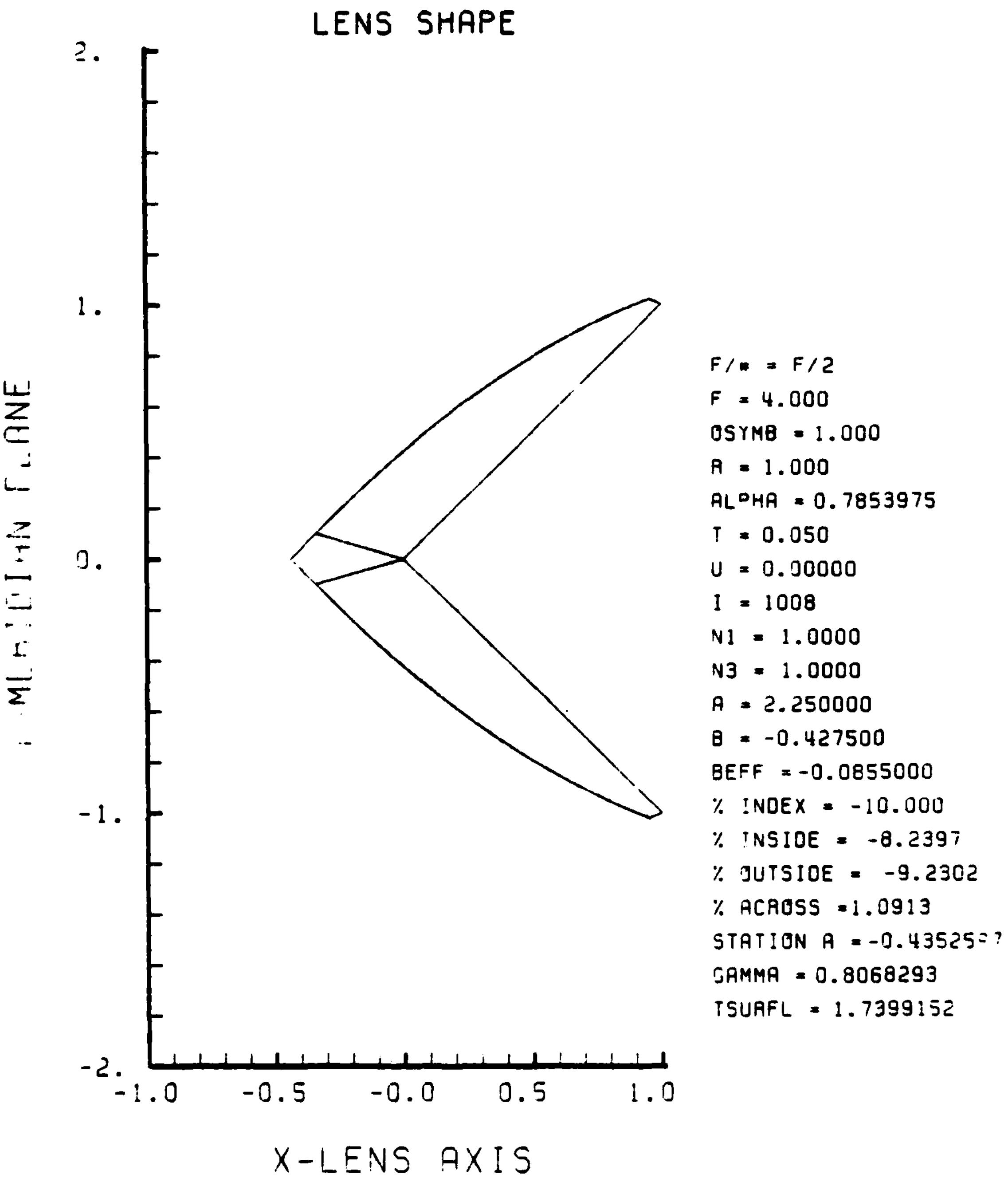

Figure 18. Example GRIN Lens Design with 10% Negative Gradient at OB = 1.0

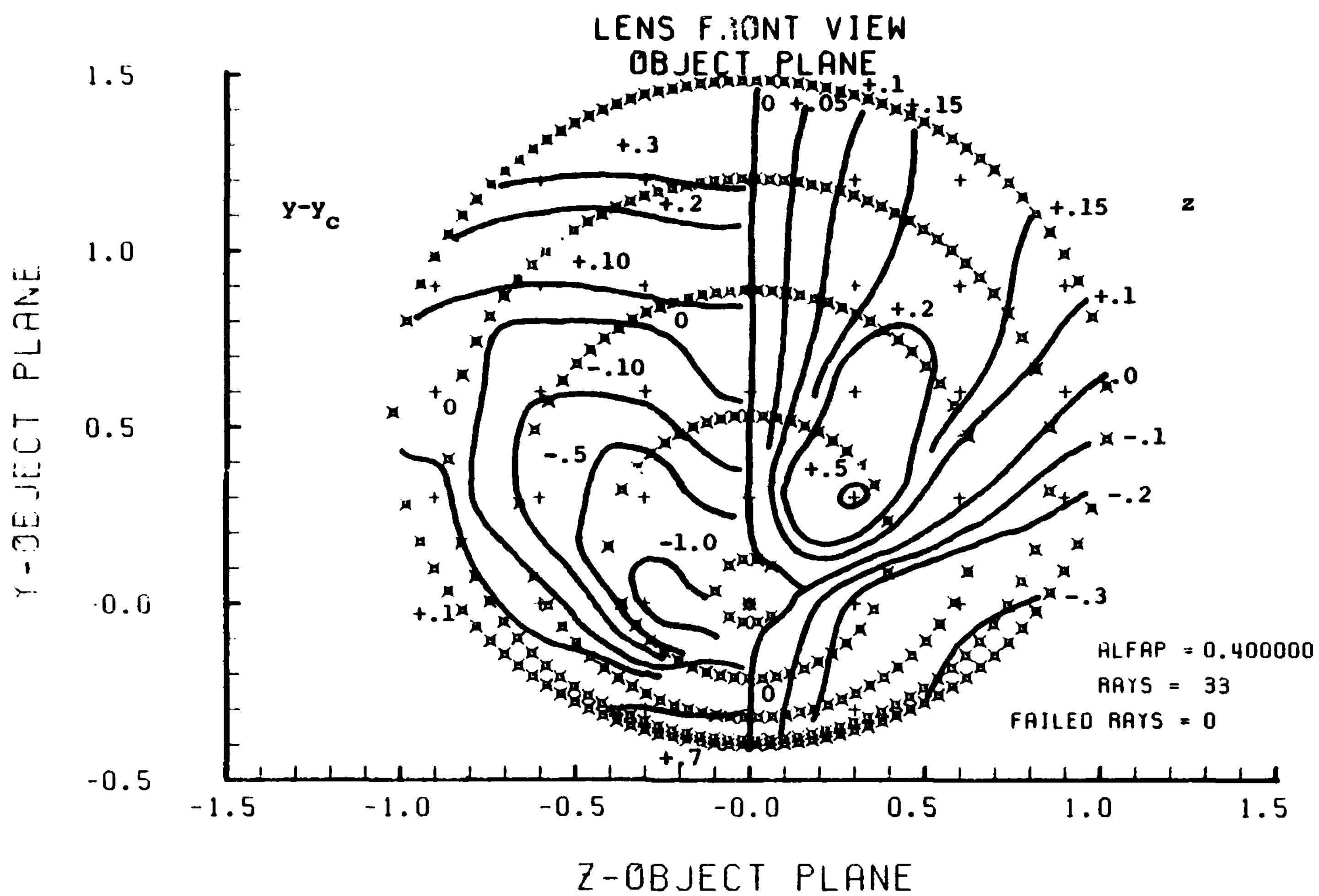

Figure 19. Example GRIN Lens Object Plane. Contours in the Left Half Depict the Difference Between the y Coordinate in the Image Plane and Image Centroid. The Right Hand Contour Shows the Corresponding z Displacement in the Image Plane.

errors in both y and z stem from the nose and bottom of the lens. The best performance is contributed by the upper central region. The reader will note that negative errors in z occur below the $y_0 = 0$ plane of the lens and that negative errors in y straddle the $y_0 = 0$ plane.

The corresponding intensity contours are displayed in Figure 20. Of significance here is that regions which perform relatively well in y and z error also perform well in transmitting energy. Regions of the lens which are characterized by relatively high angles of incidence, therefore, perform the poorest and have the most to gain from better combinations of gradient index and O_S

The Spot Diagram, Figure 21, displays an image pattern virtually identical with the HIN lens in Figure 11. The GRIN spot size, σ_r, however, is slightly smaller by approximately 2% and both σ_y and σ_z are correspondingly smaller which indicates superior performance by the GRIN version. Image centroid for the GRIN is displaced further than that for HIN. The average intensity transmitted by the GRIN lens compares favorably at 0.88 as opposed to the average intensity of the HIN at 0.85. Further evidence of superiority of the GRIN lens is seen in the form of a steeper slope to the Encircled Energy Plot (Figure 22) than that of the HIN lens in Figure 13.

Although the example GRIN design displays marginal superiority, some GRIN designs do not. In particular, it

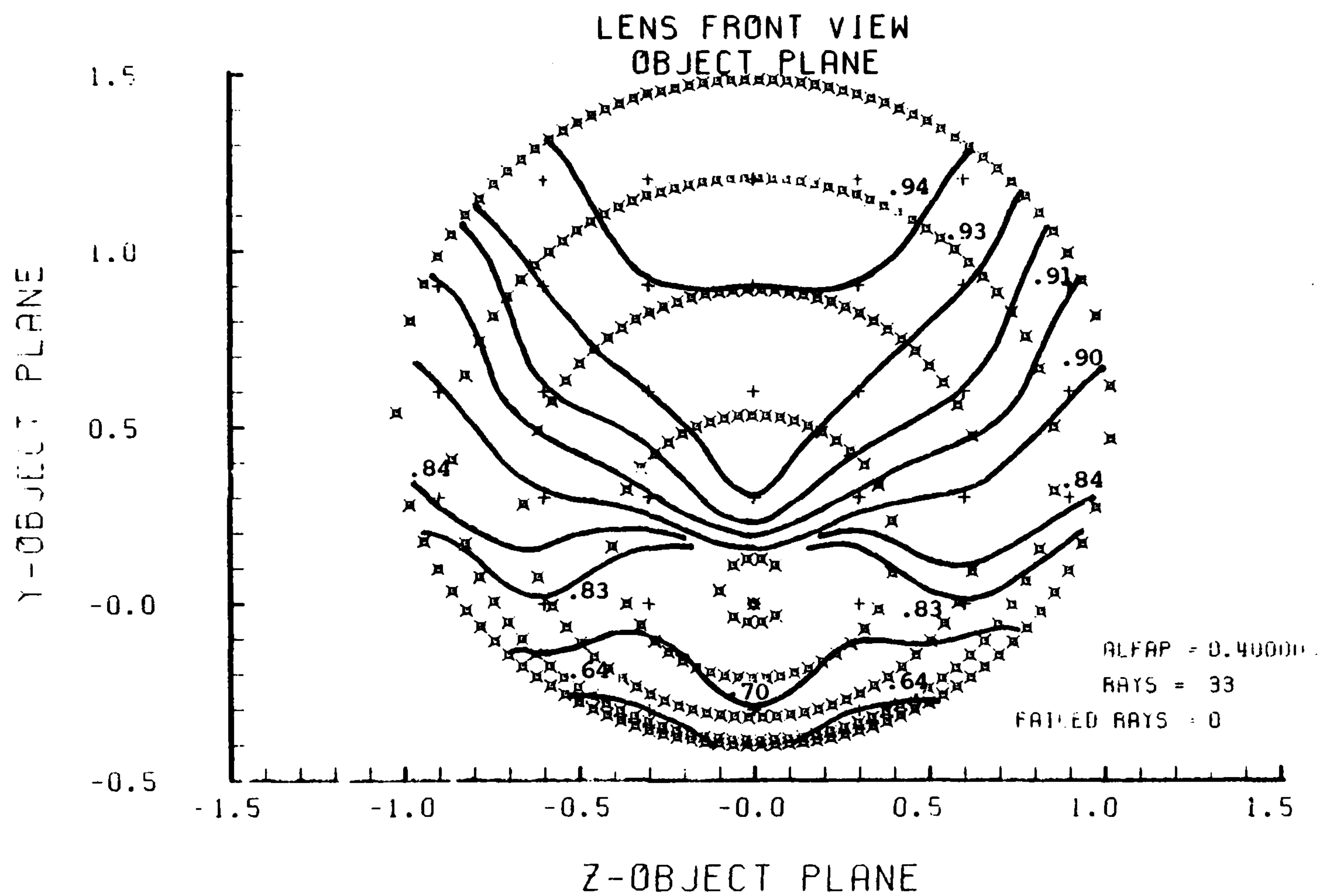

Figure 20. Intensity Contours of the Example GRIN Lens Shown in Figure 45

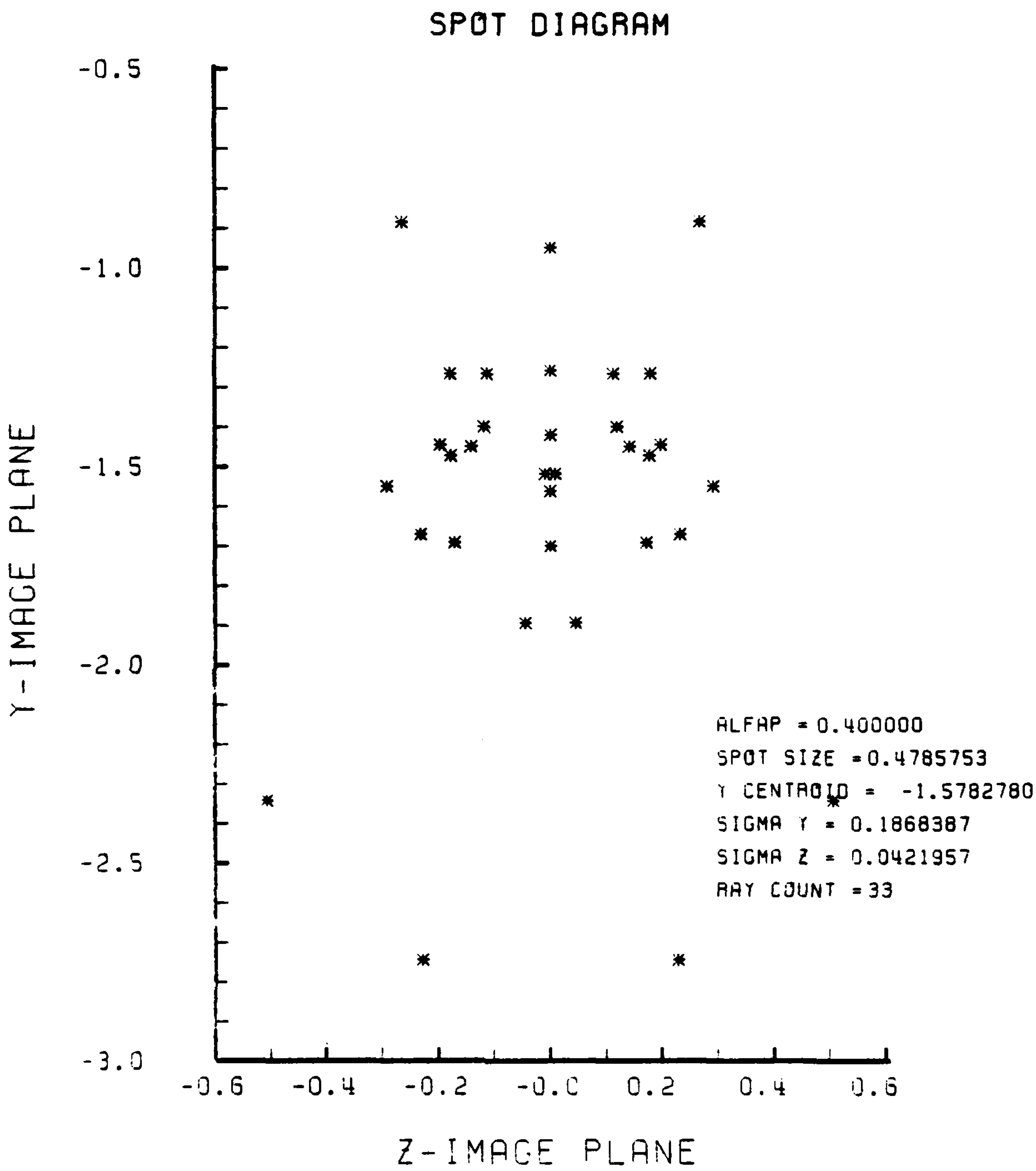

Figure 21. Example GRIN Spot Diagram at $\alpha_p = 0.4$ Radians for GRIN Lens Design Shown in Figure 18

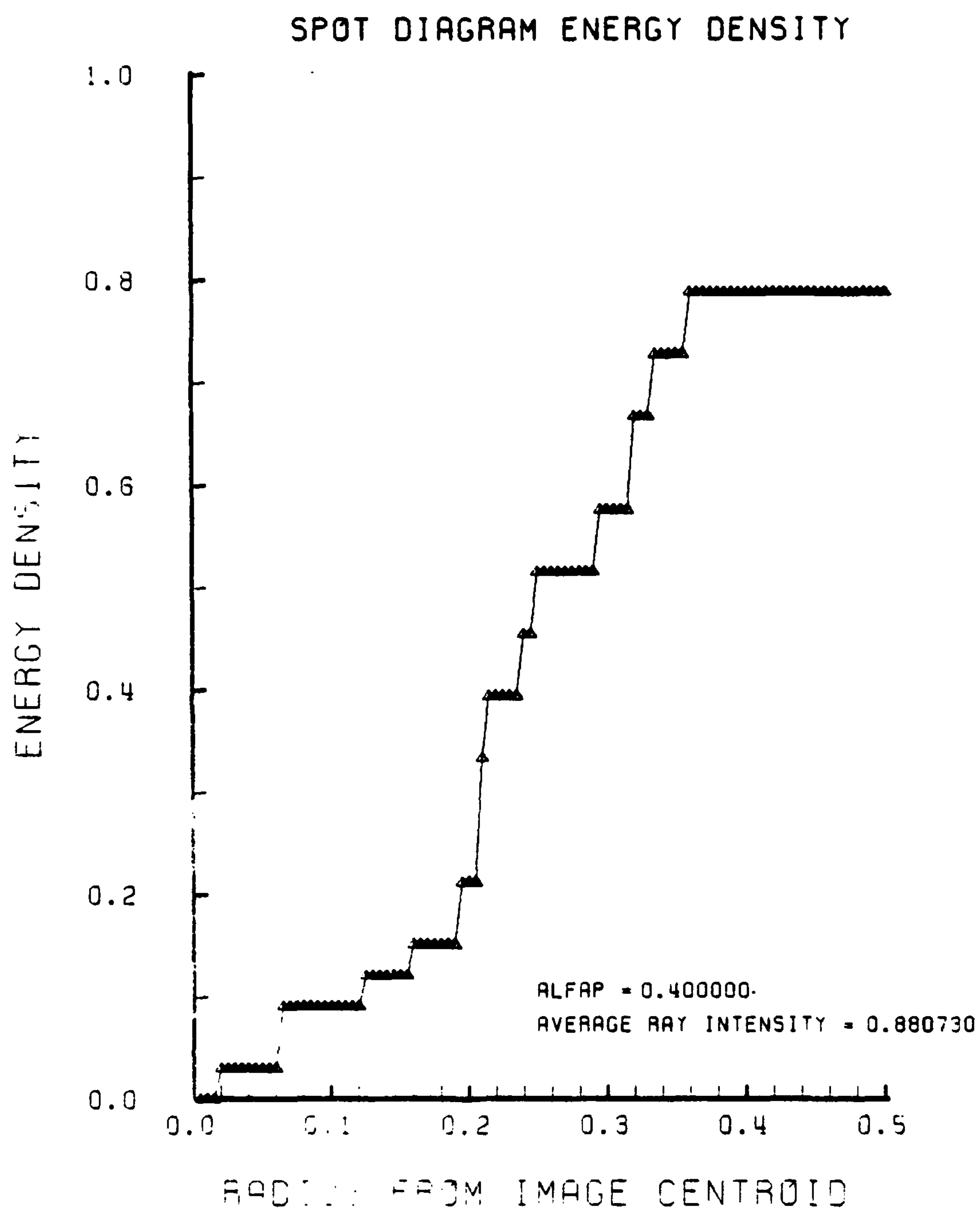

Figure 22. Example GRIN Encircled Energy Plot Corresponding to Figure 21

has been found that as the center of symmetry of the index function, O_s, is moved further away from the interior of the GRIN lens, performance deteriorates.

Two series of GRIN lens designs have been examined at the intermediate tilt angle of 0.3 radians in order to define the spectrum of lens performance. Both design series explore the GRIN lens for O_S inside, outside, and far outside the interior of the lens. The first series, Figures E-1 through E-92, are GRIN designs in the "low range" of refractive index with the index parameter "a" set at 2.25. This first set is compared to the HIN lens with $N_2 = \sqrt{a} = 1.5$. The second, or "high range" series is for $a = 9.0$, as compared to the HIN at $N_2 = 3.0$, and are displayed in Figures F-1 to F-128. Both the high and low range lenses exploit gradient changes of 5, 10, 25, and 50 percent both positive and negative, where possible. A negative 50% gradient in the low range is, of course, not possible since an index of below 1.0 would result. The center of symmetry was not located at $x \geq 0$ due to the aforementioned singularity encountered at very small angles.

The lens shapes of the GRIN designs shown vary widely. The outside surface may be either convex or concave and exhibits a thinner profile at higher values of refractive index. Although all of the resultant GRIN lens shapes are superior aerodynamically to the hemispherical seeker lenses currently in use, the convex version of the lens has more

obvious applications for a Sidewinder type tactical missile, whereas the concave lens shape is more applicable to the diffuser of a ramjet with nose inlet.

Object plane diagrams show that for lens designs exhibiting smaller spot size, fewer or none of the skew rays failed. This fact underscores the success of GRIN in controlling image deterioration contributed by the nose region of the lenses. Although the lower lens and nose regions still create the largest of the image spread, the extent is reduced.

Figures 23 and 24 are contour diagrams summarizing spot size performance of GRIN lens designs in the low and high range respectively. From these diagrams, it can be seen immediately that the best performance is obtained from lenses having the center of symmetry inside the lens. From this fact, it may be deduced that large changes in refractive index are desired along the surface of the lens rather than across. Except for isolated regions at -5%, increasing gradients produce smaller spot sizes. The positive gradient in the high range, however, has an almost constant spot size from +5% to +50% where an improvement of only 0.6% is seen. In both the low and high ranges the positive gradient at 50% and at OB = 0.05 has proved to be the best performing combination. Again, as in the HIN lens the high range exhibits the smaller spot size.

The best GRIN lens is now further examined over the range of obliquities up to 0.8 radians. Furthermore, since it has

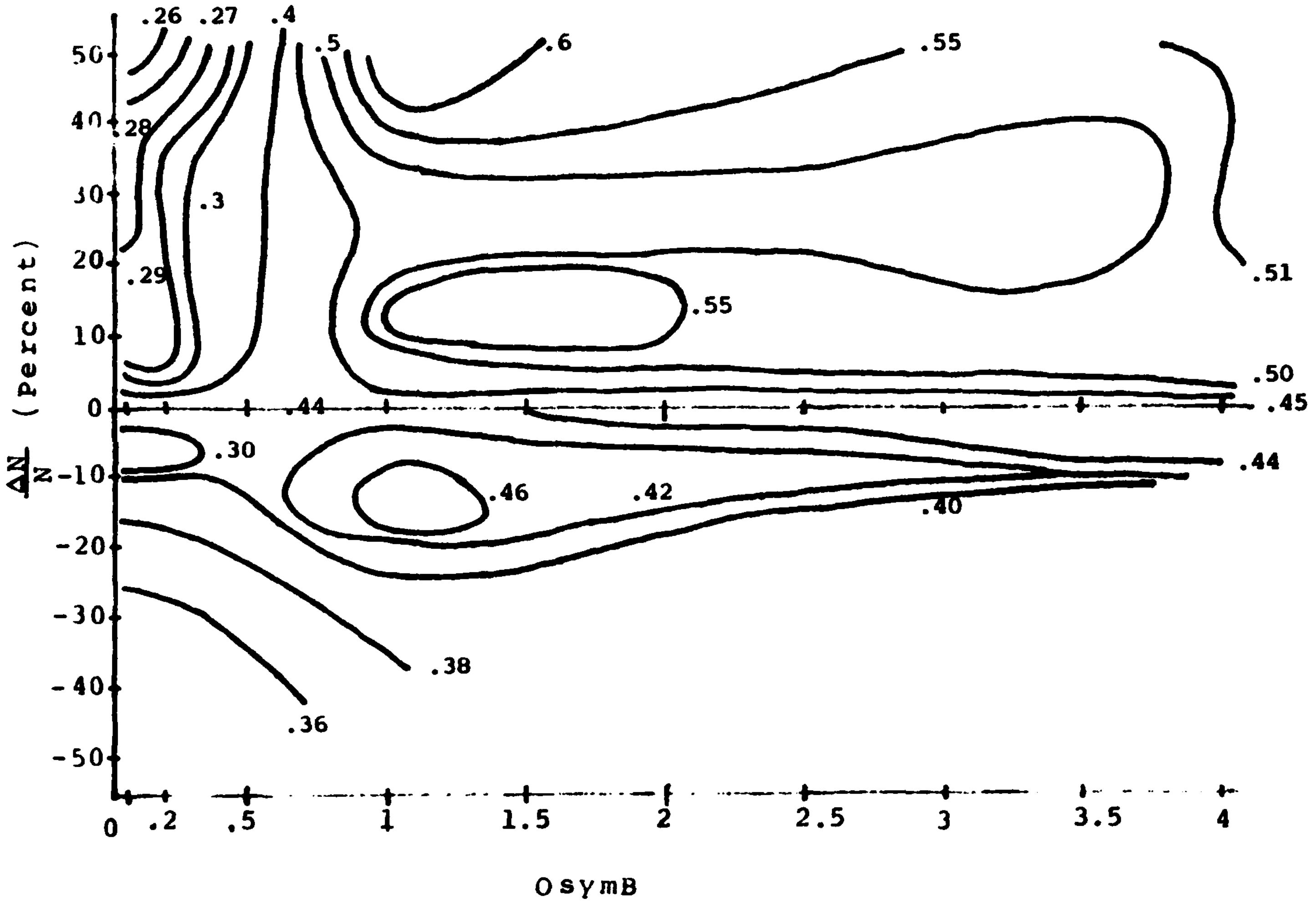

Figure 23. Contour Plot Summary of GRIN Lens Spot Size Performance for α_p = 0.3 radians, a = 2.25

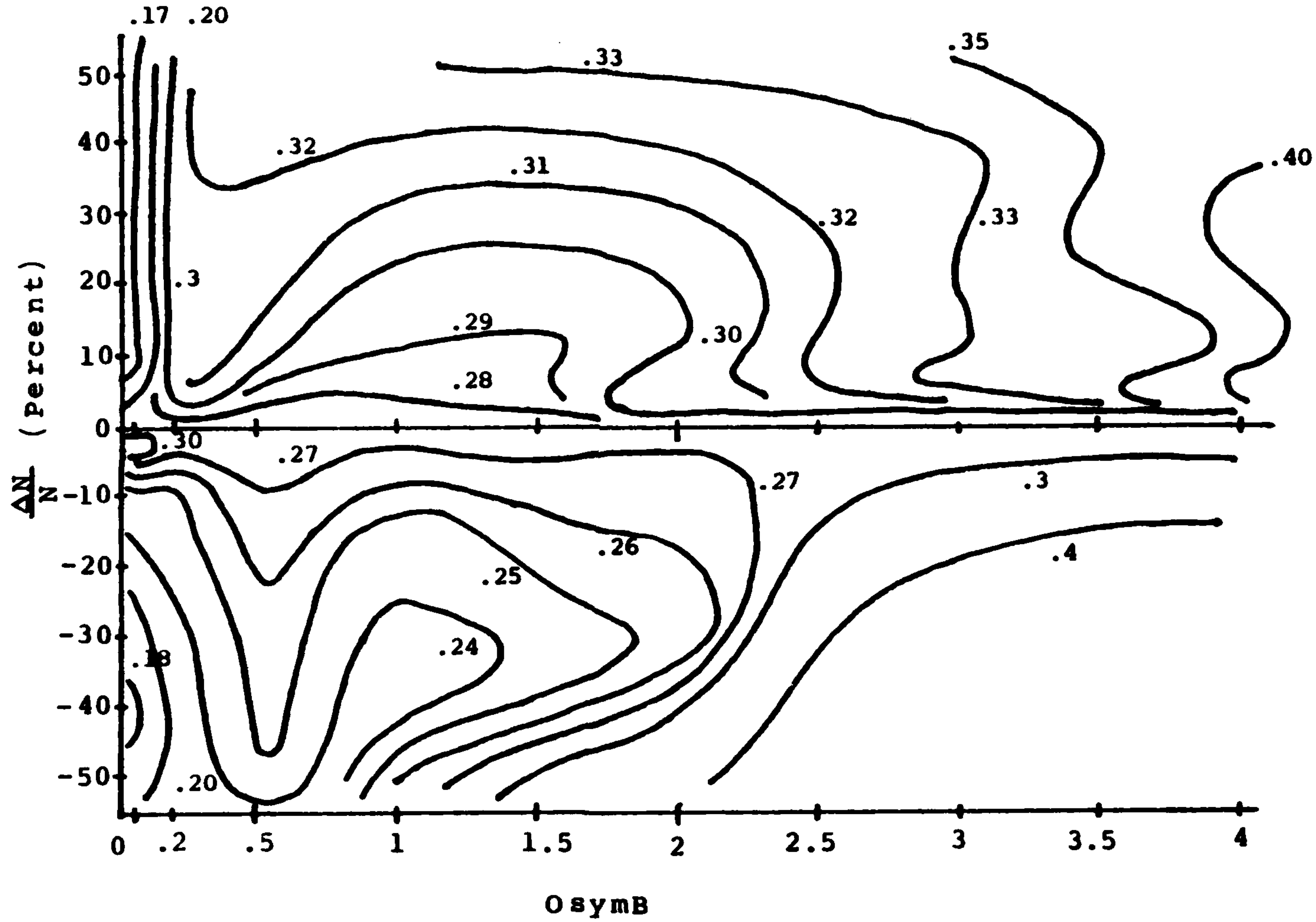

Figure 24. Contour Plot Summarizing GRIN Lens Spot Size Performance at α_p = 0.3 radians, a = 9.0

been determined that placing the focal point at $x = 2.0$, improves spot size performance at lower values of α_p, another series of plots is given for F/1. With the focal point at $x = 1.5$, severe degradation results; for $F = 3.0$ only modest differences with F/2 are evident. Appendices G and H show the performance of the "best" GRIN lens at F/1 and F/2.

Here it may be fully recognized that the resulting behavior of a "good" gradient refractive index seeker lens is far superior to that of the HIN lens for $\alpha_p \leq 0.6$ radians; see Table 5. The reader will note that there are no failed rays even at 0.8 radians (45.8 degrees). Although centroid movement at F/2 is slightly greater than the HIN lens, by changing to F/1, this can be corrected; see Figure 25. The F/1 version, moreover, displays a range of spot sizes significantly smaller than that for the F/2 lens below $\alpha_p \cong 0.54$ radians or the HIN lens below 0.68 radians; see Figure 26. That the lens displays more desirable performance with a shorter focal length is a surprising but highly desired result. Since seeker optics systems are volumn limited, any reduction in the lens focal length is beneficial to the final design and packaging requirements.

It is significant for the reader to note that centroid movement beyond a value of ±1.0 exceeds the physical dimensions of the lens radius. If the interior of the lens mount is of similar dimension, it follows that the requirement for y_{CENTR} to be less than ±1.0 restricts the F/1 lens to approximately 0.65 radians of tilt whereas the F/2 lens is further restricted to less than 0.3 radians. The superior performance

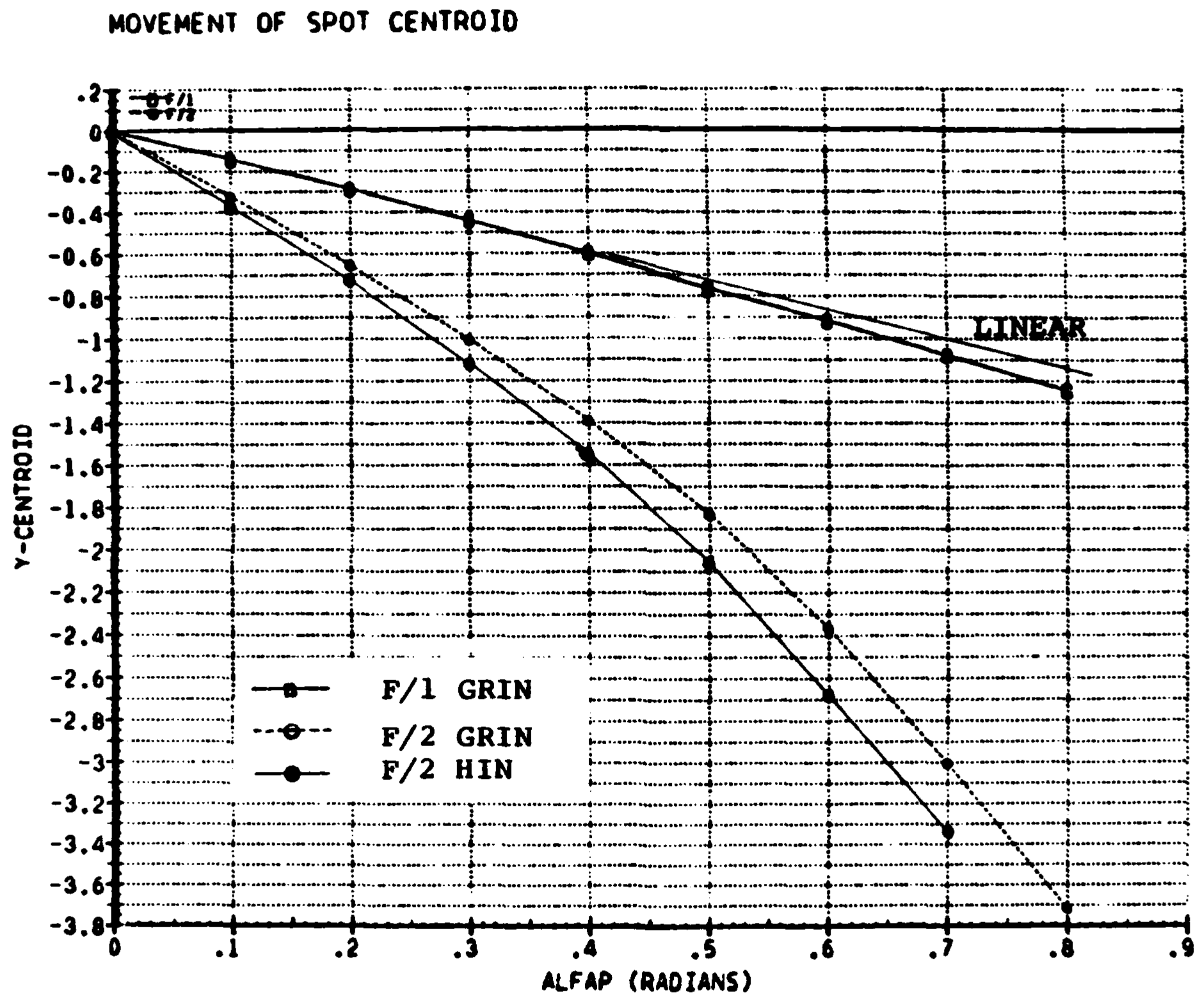

Figure 25. "Best" GRIN Lens Centroid Moment for F/Numbers of F/1 and F/2

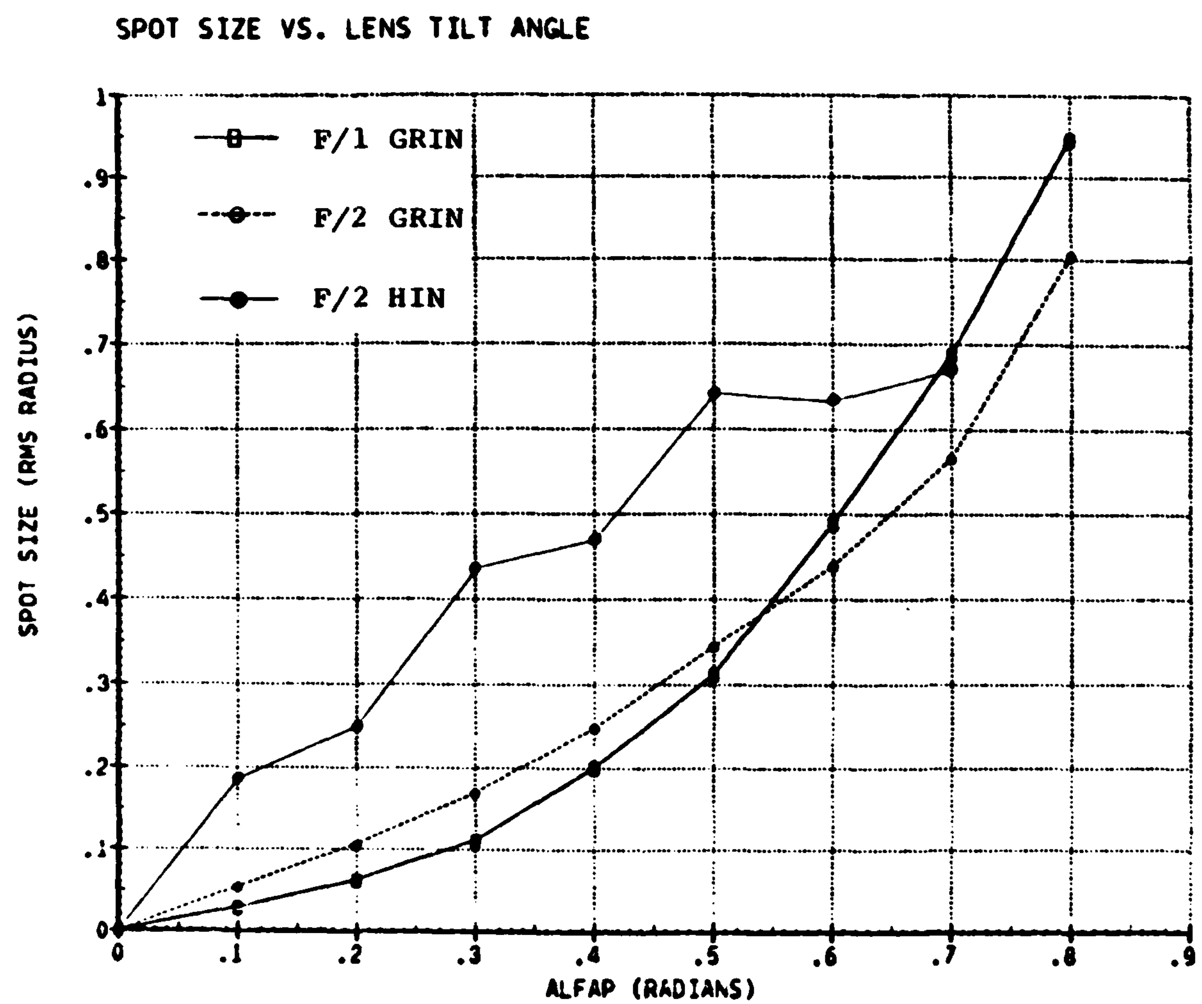

Figure 26. "Best" GRIN Lens Spot Size Performance for F/Numbers of F/1 and F/2

TABLE 5

Comparison of HIN and GRIN Lens Designs

Performance Parameter or Feature	HIN	GRIN*
Shape of Outer Surface	Convex	Concave
Fraction of Failed Rays at α_p = 0.7 radians	0.143	0.0
Linearity of Centroid Motion; α_p for $\Delta y/y$ deviation of 10%	0.4 radians	0.8 radians
Spot Size for α_p		
α_p = 0.1 radians	0.190	0.029
α_p = 0.2 radians	0.247	0.063
α_p = 0.3 radians	0.442	0.112
α_p = 0.4 radians	0.466	0.201
α_p = 0.5 radians	0.637	0.313
α_p = 0.6 radians	0.632	0.490
α_p = 0.7 radians	0.667	0.688
α_p = 0.8 radians	N/A	0.947
Spot radius for 80% of energy @ α_p = 0.4 radians	Does not attain 80% within 0.50	0.28
Average relative intensity of skew rays @ α_p = 0.4 radians	0.82	0.44

*"Best" GRIN lens with 50% positive gradient, O_S = 0.05, in the F/1 configuration.

of the F/2 lens above 0.54 radians is, therefore, unusable. Attempts to improve upon this performance by increasing the edge thickness, T, or by slightly adjusting the parameter U, as with the homogeneous lens only produced uniformly degraded performance in every respect.

Although the "best" GRIN lens resulted from a positive 50% gradient change in refractive index, it has been noted that this configuration was only slightly better than the same lens with a positive 5% change. Furthermore, since refractive index gradients of five percent or better have already been produced, it is entirely feasible that if the precise parabolic change could be controlled, this lens could be produced today.

Despite the obvious success of GRIN in controlling spot size growth and image centroid movement, a penalty in the form of reduced ray intensity has been paid. That increasing spot size performance is tempered by a loss of intensity may be seen by comparing "good" GRIN encircled energy plots with that of the HIN lens. Note that the HIN lens with $N_2 = 3.0$ also loses ~ 50% to intensity; see Figure 44. This loss in intensity is partially offset, however, by the GRIN lens with an increased number of rays transmitted and by the reduced spot size.

One drawback to the use of the GRIN lens as a self sufficient, single element lens is still that of the relative sizes of image and detector. Hence, even though GRIN has

significantly reduced spot size below $\alpha_p \cong 0.6$, that size is still significant at tilt angles above 0.3 radians. In order to use the lens without a secondary focusing element or mirror arrangement, a large composite sensor array would be required.

VII. CONCLUSION

Gradient refractive index materials may be employed to design a pointed seeker lens which exhibits optical performance far superior to that obtainable with conventional homogeneous optical material. A fifty percent, positive, parabolic gradient index with center of symmetry interior to the lens was found to yield the best performance although a five percent version of the same lens was only very slightly inferior; this lens may possibly be fabricated today.

For objects off-axis by more than 0.3 radians (~17.2 degrees) a secondary lens element may be required unless a large scale multiple element sensor array is employed. With such arrays, objects off-axis by more than 0.65 radians (37.2 degrees) may require Cassegrainian or other mirror elements to compensate image movement.

VIII. RECOMMENDATIONS FOR FUTURE WORK

This thesis investigated a spherically symmetric GRIN seeker lens with inside conical surface. Future studies should investigate:

a) The elimination of the singularity problem by modification of the theoretical equations for GRIN using numerical techniques. See Reference 13.

b) The optimization of the GRIN lens with both inside and outside curvature.

c) The effect on lens performance due to an attached shock wave.

d) The effect on lens performance when the object is no longer in the far field and wave front curvature must be taken into account.

e) The performance of the lens using wavelengths corresponding to atmospheric windows.

f) The effect of a radially symmetric gradient index on lens performance.

g) The feasibility of adding an anamorphic gradient-index lens located on the missile body to increase off-axis tracking/acquisition capability to 90° and beyond. See Figure 1 of Reference 14.

APPENDIX A

COMPUTER LOGIC FLOW DIAGRAM FOR PROGRAM GISL

This appendix together with Appendices B and C describe the FORTRAN program GISL. GISL may be used to design either a homogeneous (B = 0), or a GRIN lens to the user's specifications by changing the design parameter where indicated by comments in the input section of the program. Additional software required to run GISL and plot the results are not described since these system-dependent procedures do not apply elsewhere.

The flow diagrams which follow provide the reader with the information necessary to follow the fundamental logic of the main program and subroutines of GISL. Not shown is Subroutine DIRECT which has been derived from Subroutine DIRECT as described by Amichai [5] with only slight modifications.

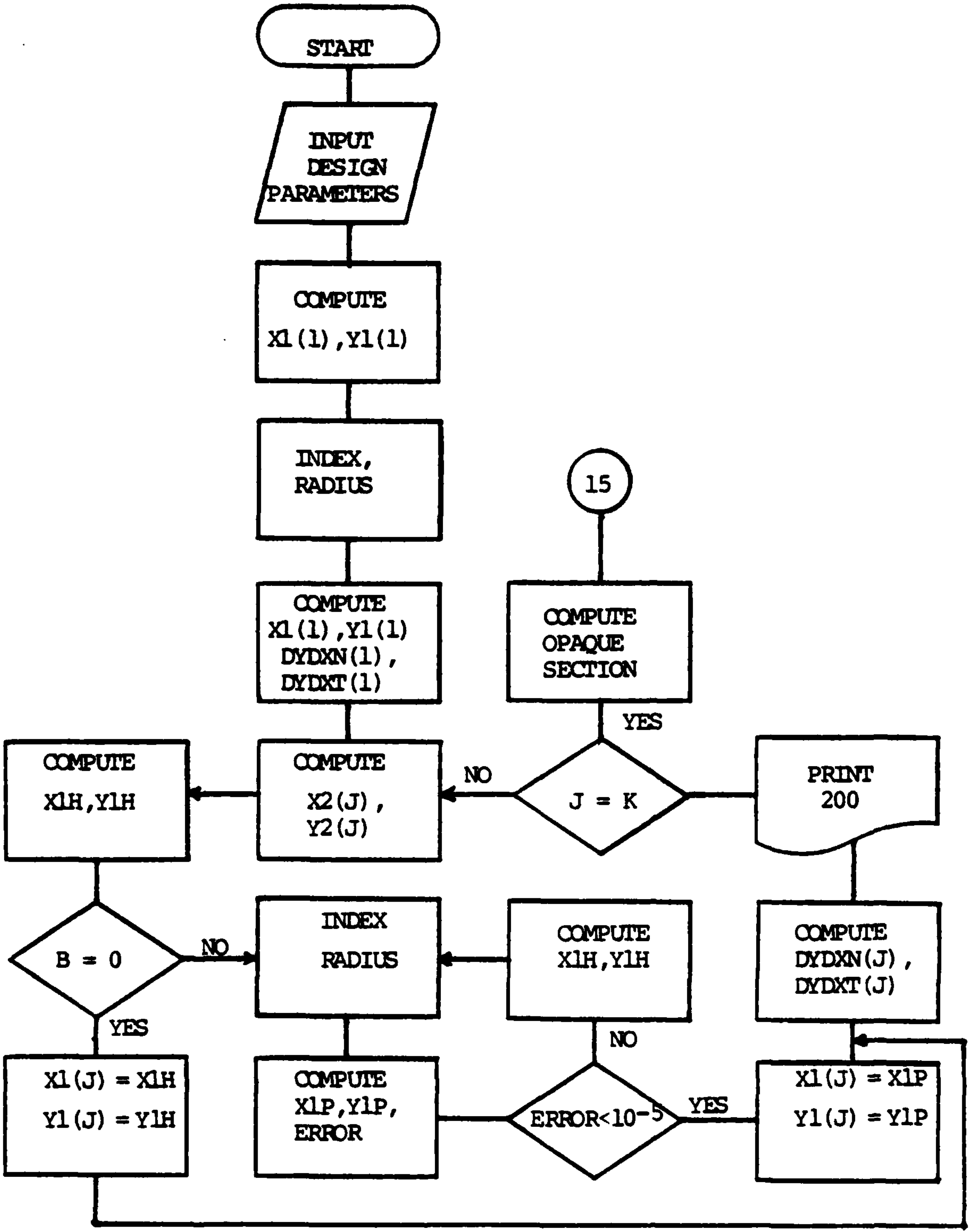
START
INPUT DESIGN PARAMETERS
COMPUTE X1(1),Y1(1)
INDEX, RADIUS
COMPUTE X1(1),Y1(1) DYDXN(1), DYDXT(1)
15
COMPUTE OPAQUE SECTION
YES
COMPUTE X1H,Y1H
COMPUTE X2(J), Y2(J)
NO
J = K
PRINT 200
B = 0
NO
INDEX RADIUS
COMPUTE X1H,Y1H
COMPUTE DYDXN(J), DYDXT(J)
YES
NO
X1(J) = X1H
Y1(J) = Y1H
COMPUTE X1P,Y1P, ERROR
ERROR<10-5
YES
X1(J) = X1P
Y1(J) = Y1P

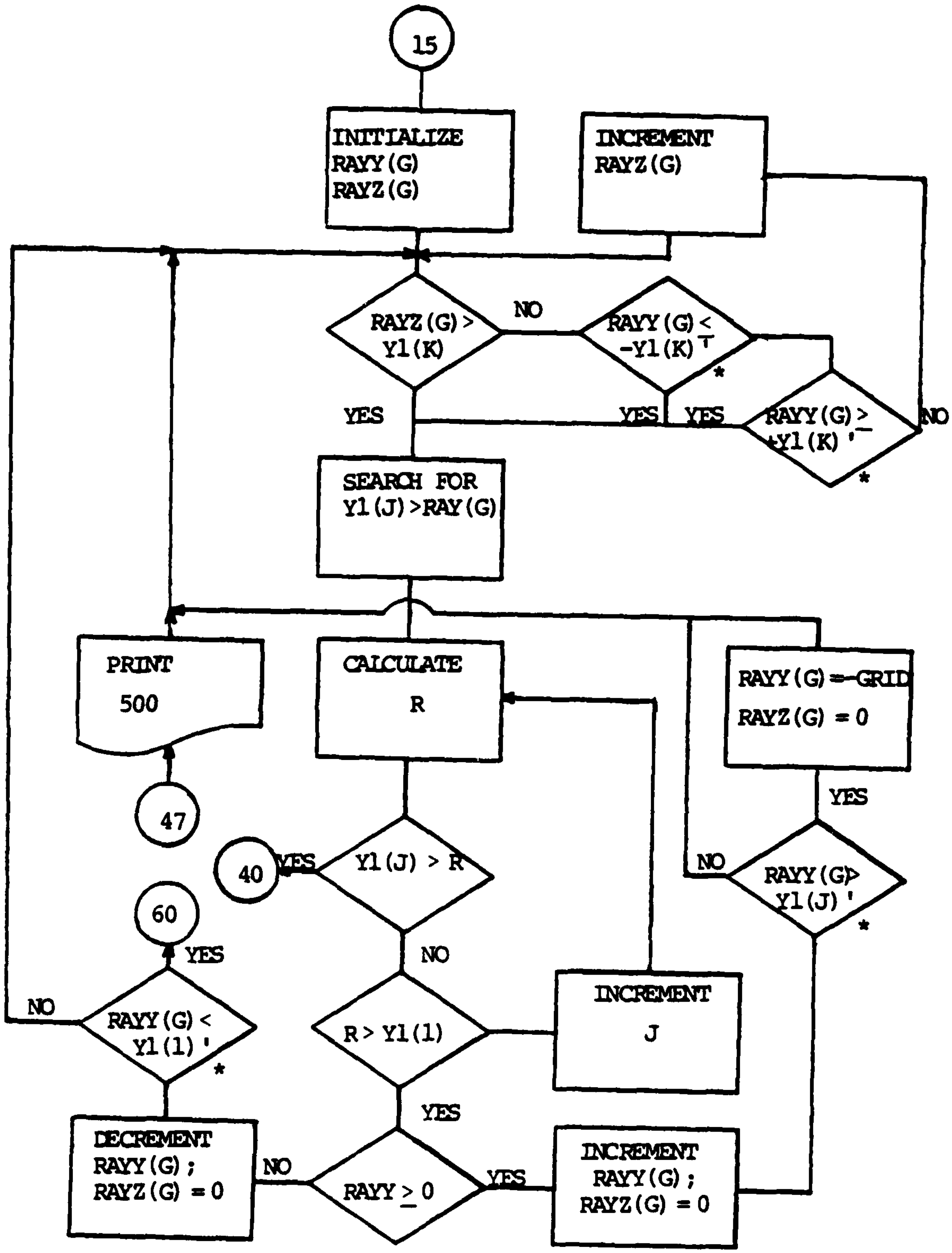

*Here, the prime indicates Y-coordinate as transformed into the grid plane.

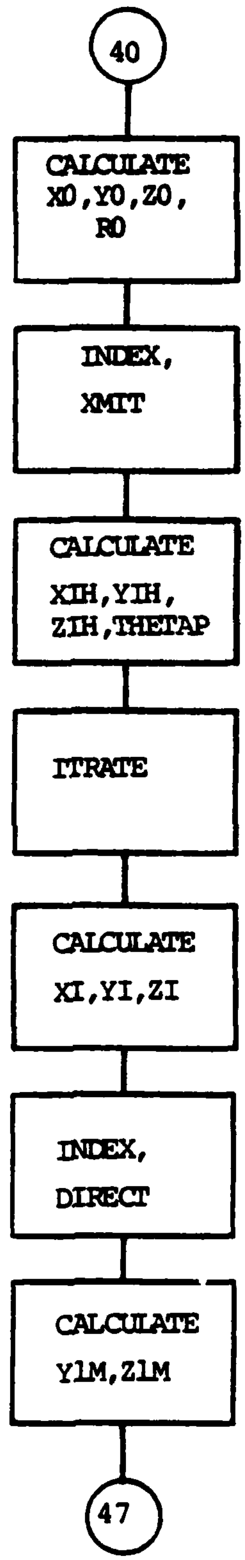
40
CALCULATE
X0,Y0,Z0,
R0
INDEX,
XMIT
CALCULATE
XIH,YIH,
ZIH,THETAP
ITRATE
CALCULATE
XI,YI,ZI
INDEX,
DIRECT
CALCULATE
Y1M,Z1M
47

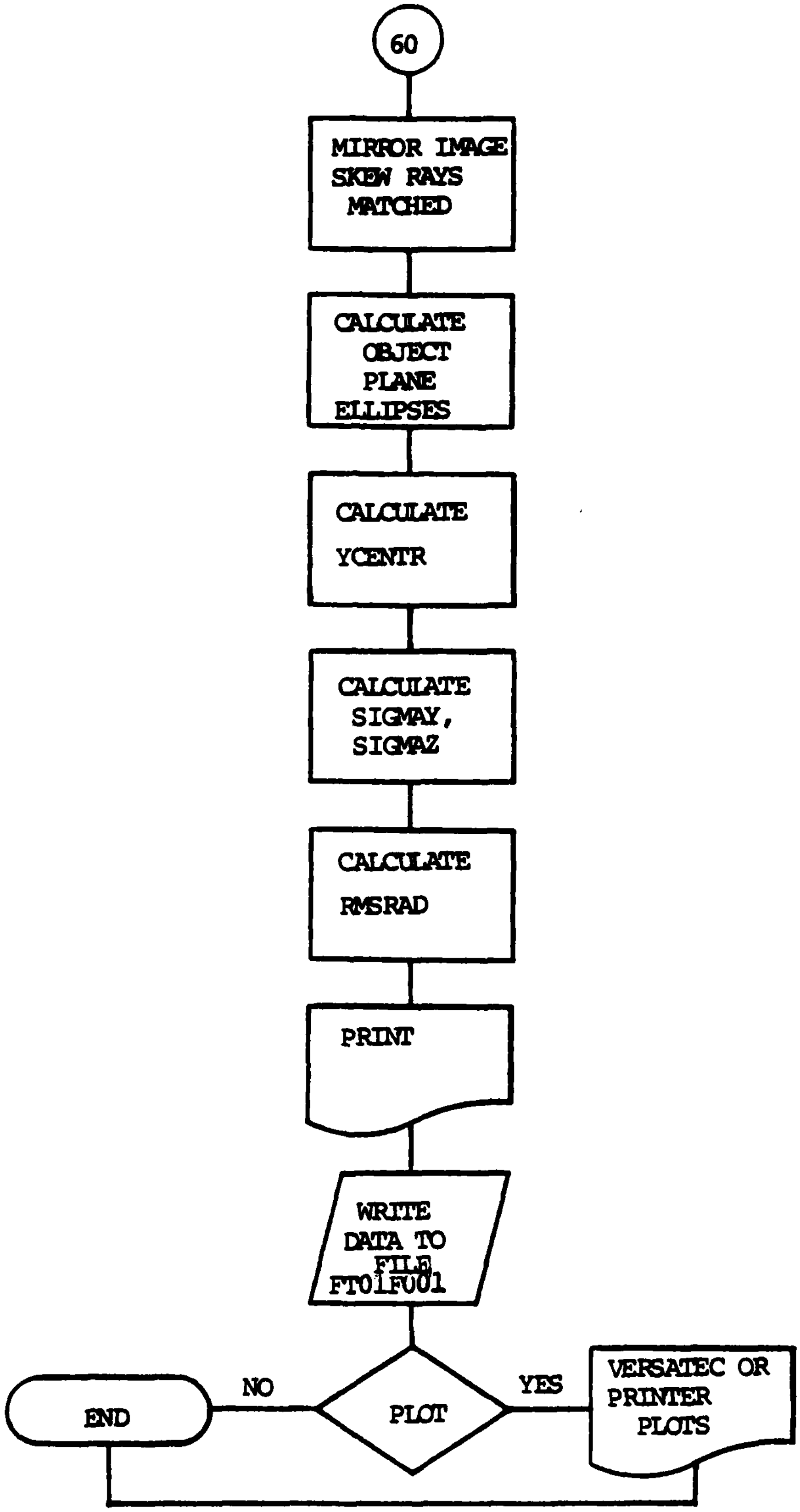
60
MIRROR IMAGE
SKEW RAYS
MATCHED
CALCULATE
OBJECT
PLANE
ELLIPSES
CALCULATE
YCENTR
CALCULATE
SIGMAY,
SIGMAZ
CALCULATE
RMSRAD
PRINT
WRITE
DATA TO
FILE
FT01F001
PLOT
NO
YES
END
VERSATEC OR
PRINTER
PLOTS

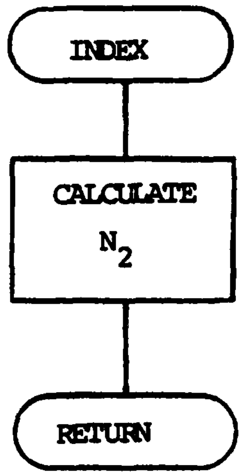
INDEX
CALCULATE
N_2
RETURN

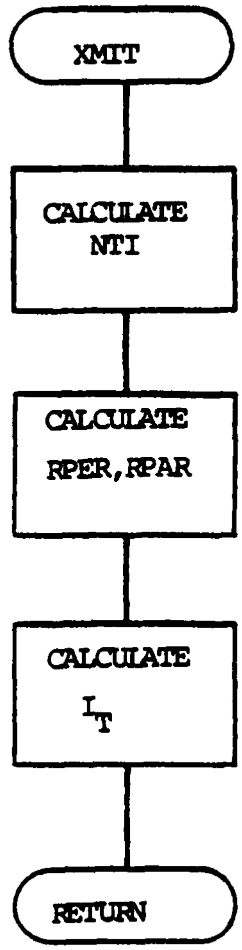
XMIT
CALCULATE
NTI
CALCULATE
RPER, RPAR
CALCULATE
I_T
RETURN

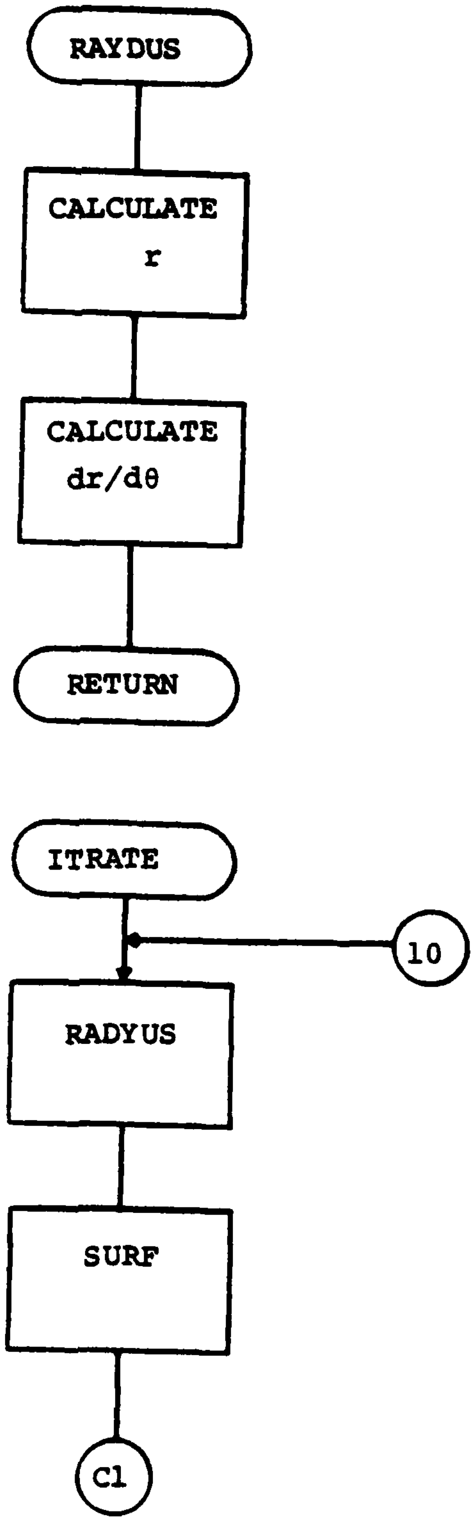
RAYDUS
CALCULATE
r
CALCULATE
dr/dθ
RETURN
ITRATE
10
RADYUS
SURF
C1

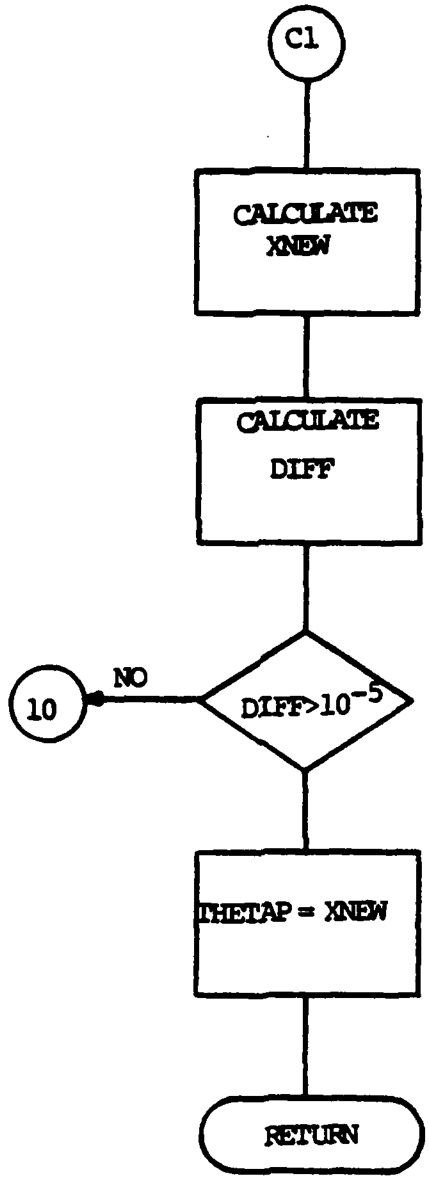
C1
CALCULATE XNEW
CALCULATE DIFF
NO
10
DIFF>10^-5
THETAP = XNEW
RETURN

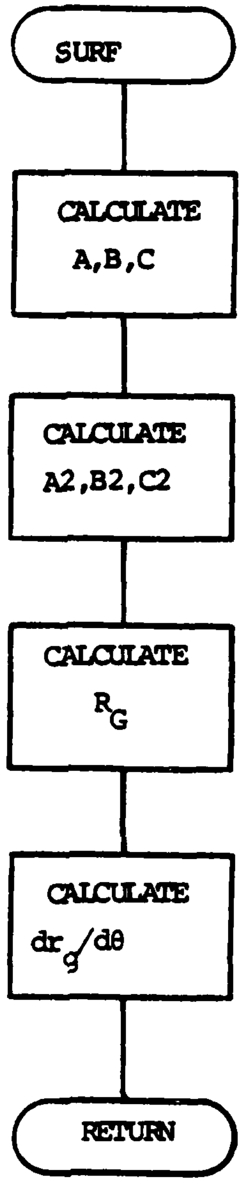
SURF
CALCULATE
A,B,C
CALCULATE
A2,B2,C2
CALCULATE
R_G
CALCULATE
$dr_g/d\theta$
RETURN

APPENDIX B

LISTING OF FORTRAN PROGRAM GISL

```
C
C     ******************************************************************
C     *                                                                *
C     *              GRADIENT INDEX SEEKER LENS                        *
C     *                                                                *
C     ******************************************************************
C
C
C
      INTEGER I,J,K,L,G,H,M,N,P,FLAG(1000),Q,RAYS,S,DRAYS,ELLNUM,
     1NUMBR,COORD,ENUM,NUMB,IANGLE,THICK,GG,HH,COUNT,SHAPE,GGT,
     1COOR(500),NUMBT,VARY,ELLIPS,SQURAY,THKNES,TRIP,FILTER,COORT,
     1FACE
      REAL BF,UDP(1010),ALPHA,U,BETA,R,DLUDP,F,I2P(1010),ED,
     1I2(1010),ARSIN,COTAN,SIN,COS,TAN,ATAN,SQRT,ARCOS,
     1UP(1010),I1(1010),X1(1010),Y1(1010),X2(1010),Y2(1010),
     1DYDXN(1010),DYDXT(1010),I1P(1010),GAMMA,AB,ONP,
     1N1,N2,N3,T,ALFAP,GRID,RAYY(1000),RAYZ(1000),CENI,TORBI,BOTI,TOPI,
     1RADIUS,CEN,TOP,BOT,TORB,DELTAX,DELTAY,SP,ST,RATIO,DYDXNP,LK,LL
      REAL CL,NPI,NPJ,NPK,THETA,PHI,PHIP,AO,BO,CO,DO,EO,PAR1,
     1PAR2,XO,YO,ZO,NUM,CKP,CLP,CMP,NUM1,NUM2,NUM3,NUM4,D2,XI,YI,ZI,
     1NUM5,CKPP,CLPP,CMPP,D3,OPL(1000),D1,NUM6,NUM7,NTNCTY(1000),
     1YIM(1000),ZIM(1000),ELL,ELY(7,1000),ELZ(7,1000),ELZZ,LM,CK,ZOYO,
     1PAR3,NUM8,LKP,LLP,LMP,THETAI,XDIAPT(1000),YDIAPT(1000),SUM1,
     1SUM2,SUM3,SIGMAZ(10,500),SIGMAY(10,500),RMSRAD(10,500)
      REAL ROC(300),SUM4(300),FRACTN(300),SDRAD(1000),YCENTR(20,500),
     1RO,PI,THETAE,EPSLON,PI2,PSIO,E,A,B,OSYMB,THETAO,RAD,PSI,PSIP,X1H,
     1Y1H,Z1H,THETAH(50),X1P,Y1P,ZETA,X1HP,Y1HP,ERROR,N20,XP,YP,ZP,RH,
     1RCY,ROZ,NPOX,NPOY,NPOZ,NPO,D2T,OPHX,OPHY,OPHZ,OSYMPH,THETAP,
     1RZERO,ABS,TCRIT,ROX,EONR,X1PP,A1,B1,C1
      REAL Y1PP,ZETAP,BASE,BAS1,BEFF,ROOC,N2X21,N2X1K,N2X2K,
     1PRCNTE,PRCNTT,PRCNTO,SURFL,TSURFL,SLINCR,ARKCOS,CHEKRO,CALIBR,
     1KKLLMM,CKKP,CLLP,CMMP,THTAP,BETAO,ALFAO,RDOTG,RDOTS,RADH,
     1SIGN,DIFFOR,XMAVE,XMAVET
      COMMON A,B,E,RZERO,EPSLON,PI2,J
      COMMON/DIR/A1,B1,C1,NPOX,NPOY,NPOZ,PSIP
      COMMON/SUR/PSIO,XO,OSYMB,YO,ZO,RO,CKKP,CLLP,CMMP,N20,ALPHA
      COMMON/XM/N1,N3
C
C
C     OUTPUT OPTIONS:
C
C     CAUTION. OUTPUT OPTIONS MUST BE CHOSEN WITH CARE TO AVOID
C     EXCESSIVE PRINTING AND VOLUMOUS OUTPUT. OPTIONS "VARY" AND
C     "THKNES" WILL MULTIPLY THE PAGES OF OUTPUT. IN GENERAL
C     NO MORE THAN ONE SUCH REPEAT PARAMETER SHOULD BE USED
C     IN THE SAME RUN.
C
```

```
C     TO HAVE LENS SHAPE DATA PRINTED SET "SHAPE" TO 1. OTHERWISE       GIS00520
C     SET "SHAPE"=0.                                                    GIS00530
      SHAPE=1                                                           GIS00540
C                                                                       GIS00550
C     TO HAVE SKEW RAY AND MIRROR IMAGE SKEW RAY DATA PRINTED SET       GIS00560
C     "SQURAY" TO 1. ELSE SET "SQURAY" TO 0. (INTEGER)                  GIS00570
      SQURAY=1                                                          GIS00580
C                                                                       GIS00590
C     TO HAVE ELLIPSE SHAPE DATA PRINTED SET "ELLIPS" TO 1. OTHERWISE   GIS00600
C     SET "ELLIPS"=0.                                                   GIS00610
      ELLIPS=0                                                          GIS00620
C                                                                       GIS00630
C    INPUT KNOWNS FOR GLP LENS SHAPE:                                   GIS00640
C                                                                       GIS00650
C     FOCAL LENGTH:                                                     GIS00660
      F=4.0                                                             GIS00670
C     INSIDE SURFACE CONE HALF-ANGLE:                                   GIS00680
      ALPHA=0.7853982                                                   GIS00690
C     INCIDENT RAY OFFSET ANGLE:                                        GIS00700
      U=0.000000                                                        GIS00710
C     NUMBER OF ITERATIONS (MUST BE AN EVEN INTEGER GT 750)             GIS00720
      I=100                                                             GIS00730
C     MAXIMUM RADIUS OF INSIDE SURFACE CONE:                            GIS00740
      R=1.0                                                             GIS00750
C     THICKNESS OF LENS AT THE EDGE:                                    GIS00760
      T=0.05                                                            GIS00770
C     OR, IF IT IS DESIRED TO HAVE THE THICKNESS BE CHANGED FROM T=0.05 GIS00780
C     TO T=0.55 BY A 0.05 STEP INCREMENT, SET "THKNES" TO 1. ELSE ENSUREGIS00790
C     THAT "THKNES"=0. (INTEGER)                                        GIS00800
      THKNES=0                                                          GIS00810
C                                                                       GIS00820
C     INDICES OF REFRACTION                                             GIS00830
      N1=1.0                                                            GIS00840
C     THE FOLLOWING ARE CONSTANTS A & B FOR N2(R). SEE SUBR INDEX.      GIS00850
C     NOTE THAT IF B=0.0, N2(R) NO LONGER VARIES AS A FUNCTION OF R     GIS00860
C     WHICH CORRESPONDS TO THE HOMOGENEOUS LENS WITH N2=SQRT(A).        GIS00870
      A=9.00                                                            GIS00880
      B=+11.25                                                          GIS00890
C     THE FOLLOWING IS THE DISTANCE FROM 0,0 TO THE CENTER OF           GIS00900
C     SYMMETRY OF THE GRADIENT INDEX ALONG THE X-AXIS. THE              GIS00910
C     POSITIVE SENSE IMPLIES THAT OSYM IS TO THE LEFT OF 0,0.           GIS00920
C     CONVERSELY, THE NEGATIVE SENSE IMPLIES THAT OSYM IS TO            GIS00930
C     THE RIGHT OF 0,0.                                                 GIS00940
      OSYMB=+0.05                                                       GIS00950
      N3=1.0                                                            GIS00960
      BETA=ATAN(R/(F-R*COTAN(ALPHA)))                                   GIS00970
      PI=3.141592653589793                                              GIS00980
      PI2=PI/2.0                                                        GIS00990
```

```
C
C     INPUT KNOWNS FOR TRACE RAY:
C
C        INCLINATION OF OBJECT PLANE (RADIANS)
         ALFAP=0.4
C        CR IF IT IS DESIRED TO HAVE ALFAP VARY BETWEEN 0.0 AND 0.7:
C        SET VARY = 1, OTHERWISE SET VARY = 0
         VARY = 0
C        SIZE OF GRID INCREMENT:
         GRID=0.3
         ELLNUM=4
C        NUMBER OF ELLIPSES = ENUM. ELLNUM MUST BE EVEN AND
C        I/ELLNUM MUST BE AN INTEGER WITH NO REMAINDER
         ENUM=ELLNUM+1
C        ELL IS THE Z COORDINATE INCREMENT FOR ELLIPSE PLOTS
         ELL=GRID/7.5
C
C
C
C     ALGCRITHM GLM LENS SHAPE (SEE INPUT ABOVE)
C
C
C        AT THIS POINT, IF "THKNES" IS 1, THE REMAINDER CF THE PRCGRAM
C        WILL BE REPEATED FOR T=0.05 TO T=0.55 BY A 0.05 INCREMENT STEP.
         IF(THKNES .EQ. 1) T=0.05
           GO TO 3
      2  CONTINUE
         T=T+0.05
      3  CCNTINUE
         DLUDP=BETA/I
         BF=F/R
         WRITE(6,1900)
         IF(SHAPE .EC. 1) WRITE(6,100) ALPHA,BETA,R,U,I,T,N1,
        1N3,BF,DLUDP
C     START AT THE EDGE _ 1ST RAY
         FILTER=0
         J=1
         UDP(J)=BETA
         X2(J)=(BF*SIN(UDP(J)))/(SIN(UDP(J))+(TAN(ALPHA))*COS(UDP(J)))
         Y2(J)=(X2(J))*TAN(ALPHA)
         I2P(J)=-ALPHA+ATAN((BF-X2(J))/Y2(J))
         RO=SQRT((X2(J)+OSYMB)**2+Y2(J)**2)
         RZERO=RO
         IF(OSYMB .LT. 0.0) RZERO=2.0*RO
         CALL INDEX(RO,N20)
         I2(J)=ARSIN((N3/N20)*SIN(I2P(J)))
         UP(J)=PI2-ALPHA-I2(J)
         BASE=X2(J)+CSYMB
```

```
      IF(BASE .EQ. 0.0) OSYMB=1.0000001*OSYMB
      BASE=X2(J)+OSYMB
      THETAO=ATAN(Y2(J)/BASE)
      IF(BASE .LT. 0.0) THETAO=PI+THETAO
      ED=T/R
      X1H=X2(J)-ED*COS(UP(J))
      Y1H=Y2(J)+ED*SIN(UP(J))
      BAS1=X1H+OSYMB
      IF(BAS1 .EQ. 0.0)OSYMB=1.0000001*OSYMB
      BAS1=X1H+OSYMB
      THETAE=ATAN(Y1H/BAS1)-THETAO
      IF(BAS1 .LT. 0.0) THETAE=PI+THETAE
      PSIO=PI-UP(J)-THETAO
      EPSLON=1.0
      IF(PSIO .GT. PI2) EPSLON=-1.0
      E=EPSLON*N2O*RO*SIN(PSIO)
      CALL SWITCH(RO,TCRIT)
      CALL RADYUS(RO,THETAE,RAD,RDOTG,FILTER)
      IF(FILTER .EQ. 1)WRITE(6,1800)
      IF(FILTER .EQ. 1)GC TO 82
      X1(J)=RAD*COS(THETAE+THETAO)-OSYMB
      Y1(J)=RAD*SIN(THETAE+THETAO)
      CALL INDEX(RAD,N2)
C     HERE TAKE PI-PSI  INSTEAD OF PSI AS IN THE TEXT SINCE 'ARSIN'
C     RETURNS AN ANGLE  ALWAYS LE PI2:
      PSI=PI-ARSIN(E/(EPSLON*N2*RAD))
      IF(THETAE .GE. TCRIT)PSI=PI-PSI
      IF(EPSLON .GT. 0)PSI=PI-PSI
      ZETA=PI-PSI-THETAE-THETAO
      I1(J)=ARSIN(SQRT(((SIN(ZETA-U))**2)/((COS(ZETA-U)-(N1/N2))**2+
     1(SIN(ZETA-U))**2)))
      I1P(J)=ARSIN((N1/N2)*SIN(I1(J)))
      DYDXN(J)=-TAN(I1(J)+U)
      DYDXT(J)=COTAN(I1(J)+U)
      IF(SHAPE .EQ. 0) GO TO 5
      WRITE(6,200) J,X1(J),Y1(J),X2(J),Y2(J),UDP(J),I2P(J),I2(J),UP(J),
     1I1P(J),I1(J),DYDXT(J)
    5 CONTINUE
C    END OF TRACE FOR 1ST RAY
      K=I+1
      SURFL=0.0
      DO 10 J=2,K
         L=J-1
         UDP(J)=BETA-(L)*DLUDP
         X2(J)=(BF*SIN(UDP(J)))/(SIN(UDP(J))+(TAN(ALPHA))*COS(UDP(J)))
         Y2(J)=(X2(J))*TAN(ALPHA)
         RO=SQRT((X2(J)+OSYMB)**2+Y2(J)**2)
         IF(J .EQ. K) ROOO=RO
```

```
      I2P(J)=-ALPHA+ATAN((BF-X2(J))/Y2(J))                             GIS01960
      CALL INDEX(RO,N20)                                                GIS01970
      I2(J)=ARSIN((N3/N20)*SIN(I2P(J)))                                 GIS01980
      UP(J)=PI2-ALPHA-I2(J)                                             GIS01990
      THETAO=ARCOS((X2(J)+OSYMB)/RO)                                    GIS02000
      PSIO=PI-UP(J)-THETAO                                              GIS02010
      EPSLON=1.0                                                        GIS02020
      IF(PSIO .GT. PI2) EPSLON=-1.0                                     GIS02030
      E=EPSLON*N20*RO*SIN(PSIO)                                         GIS02040
      Y1H=((COTAN(I1(L)+U))*(COTAN(UP(J)))*(Y2(J)+                      GIS02050
     1X2(J)*TAN(UP(J)))+Y1(L)-X1(L)*COTAN(I1(L)+U))/(1.0+               GIS02060
     1(COTAN(I1(L)+U))*COTAN(UP(J)))                                    GIS02070
      X1H=(COTAN(UP(J)))*(-Y1H+Y2(J)+X2(J)*TAN(UP(J)))                  GIS02080
      IF(B .EQ. 0.0) GO TO 8                                            GIS02090
      IF(PSIO .LE. 0.05 .AND. PSIO .GE. -0.15) GO TO 8                  GIS02100
      TRIP=0                                                            GIS02110
      ZETAP=3.14                                                        GIS02120
      X1PP=X1H                                                          GIS02130
      Y1PP=Y1H                                                          GIS02140
      IF(B .GT. 0.0 .AND. PSIO .GT. 0.0) X1H=X1(L)                      GIS02150
      IF(B .GT. 0.0 .AND. PSIO .GT. 0.0) Y1H=Y1(L)                      GIS02160
    6 CONTINUE                                                          GIS02170
      RH=SQRT((X1H+OSYMB)**2+Y1H**2)                                    GIS02180
      ARKCOS=ARCOS((X1H+OSYMB)/RH)                                      GIS02190
      TRIP=TRIP+1                                                       GIS02200
      THETAH(TRIP)=ARKCOS-THETAO                                        GIS02210
      IF(OSYMB .GT. 0.4) THETAH(TRIP)=THETAH(TRIP)*(1.0-.1+.020*TRIP)GIS02220
      THTHT=THETAH(TRIP)                                                GIS02230
      IF(B.GT.0.0 .AND. TRIP.GT.1 .AND. PSIO .GT. 0.0) THETAH(TRIP)= GIS02240
     1THETAH(TRIP-1)+(THETAH(TRIP)-THETAH(TRIP-1))/(3.5-0.0416*TRIP) GIS02250
      IF(B .GT. 0.0 .AND. PSIO .LT. 0.0) THETAH(TRIP)=THETAH(TRIP)*  GIS02260
     1(1.0-0.01/TRIP)                                                   GIS02270
      CALL SWITCH(RO,TCRIT)                                             GIS02280
      CALL RADYUS(RO,THETAH(TRIP),RAD,RDOTG,FILTER)                     GIS02290
      IF(FILTER .EQ. 1) WRITE(6,1800)                                   GIS02300
      IF(FILTER .EQ. 1) GO TO 82                                        GIS02310
      X1P=RAD*COS(THETAH(TRIP)+THETAO)-OSYMB                            GIS02320
      Y1P=RAD*SIN(THETAH(TRIP)+THETAO)                                  GIS02330
      CALL INDEX(RAD,N2)                                                GIS02340
C     WE TAKE PI-PSIP VICE PSIP BECAUSE OF THE CHARACTER OF             GIS02350
C     THE 'ARSIN' FUNCTION IN FORTRAN.                                  GIS02360
      EONR=E/(EPSLON*N2*RAD)                                            GIS02370
      IF(EONR .GT. 1.0) WRITE(6,9978)EONR                               GIS02380
 9978 FORMAT(10X,'EONR =',F19.16)                                       GIS02390
      IF(EONR .GT. 1.0)EONR=1.0                                         GIS02400
      PSIP=PI-ARSIN(EONR)                                               GIS02410
      IF(THETAH(TRIP).GE.TCRIT.OR.PSIO.LT.PI2.AND.PSIO.GT.-PI2)PSIP= GIS02420
     1PI-PSIP                                                           GIS02430
```

```
      ZETA=PI-PSIP-THETAH(TRIP)-THETAO                                  GISO2440
      IF(B .LE. 0 .AND. ZETA .GT. ZETAP) X1P=X1PP                       GISO2450
      IF(B .LE. 0 .AND. ZETA .GT. ZETAP) Y1P=Y1PP                       GISO2460
      IF(B .LE. 0 .AND. ZETA .GT. ZETAP) GO TO 7                        GISO2470
      IF(X1P .EQ. X1PP .AND. Y1P .EQ. Y1PP) GO TO 7                     GISO2480
      ZETAP=ZETA                                                        GISO2490
      X1PP=X1P                                                          GISO2500
      Y1PP=Y1P                                                          GISO2510
      Y1HP=((COTAN(I1(L)+U))*(COTAN(ZETA))*(Y1P+                        GISO2520
     1X1P*TAN(ZETA))+Y1(L)-X1(L)*COTAN(I1(L)+U))/(1.0+                  GISO2530
     1(COTAN(I1(L)+U))*COTAN(ZETA))                                     GISO2540
      X1HP=(COTAN(ZETA))*(-Y1HP+Y1P+X1P*TAN(ZETA))                      GISO2550
      ERROR=SQRT((X1HP-X1P)**2+(Y1HP-Y1P)**2)                           GISO2560
      IF(ERROR .LE. 0.0000100) GO TC 7                                  GISO2570
      X1H=X1HP                                                          GISO2580
      Y1H=Y1HP                                                          GISO2590
      GO TO 6                                                           GISO2600
    7 CONTINUE                                                          GISO2610
      X1(J)=X1P                                                         GISO2620
      Y1(J)=Y1P                                                         GISO2630
      GO TO 9                                                           GISO2640
    8 CONTINUE                                                          GISO2650
      X1(J)=X1H                                                         GISO2660
      Y1(J)=Y1H                                                         GISO2670
      ZETA=UP(J)                                                        GISO2680
    9 CONTINUE                                                          GISO2690
      IF(Y1(J) .LE. 0.0) GO TO 11                                       GISO2700
      I1(J)=ARSIN(SQRT((SIN(ZETA-U))**2/((COS(ZETA-U)-(N1/N2))**2+      GISO2710
     1(SIN(ZETA-U))**2)))                                               GISO2720
      I1P(J)=ARSIN((N1/N2)*SIN(I1(J)))                                  GISO2730
      DYDXN(J)=(-TAN(I1(J)+U))                                          GISO2740
      DYDXT(J)=COTAN(I1(J)+U)                                           GISO2750
      SLINCR=SQRT((X1(J)-X1(L))**2+(Y1(L)-Y1(J))**2)                    GISO2760
      SURFL=SURFL+SLINCR                                                GISO2770
      IF(SHAPE .EQ. 0) GO TO 10                                         GISO2780
      WRITE(6,200)J,X1(J),Y1(J),X2(J),Y2(J),UDP(J),I2P(J),I2(J),        GISO2790
     1UP(J),I1P(J),I1(J),DYDXT(J)                                       GISO2800
   10 CONTINUE                                                          GISO2810
      GO TO 12                                                          GISO2820
C                                                                       GISO2830
C     END OF TRACE FOR RAY (I+1)                                        GISO2840
C     OPAQUE NOSE SECTION FOLLOWS                                       GISO2850
C                                                                       GISO2860
   11 CONTINUE                                                          GISO2870
      K=J-1                                                             GISO2880
   12 CONTINUE                                                          GISO2890
      AB=(-X1(K))+(Y1(K))/DYDXT(K)                                      GISO2900
      STATNA=-AB                                                        GISO2910
```

```
      GAMMA=ATAN(DYDXT(K))                                              GIS02920
      CNP=(Y1(K))/SIN(GAMMA)                                            GIS02930
      TSURFL=ONP+SURFL                                                  GIS02940
      WRITE(6,300) GAMMA,STATNA,ONP,SURFL,TSURFL                        GIS02950
C                                                                       GIS02960
C    LENS INDEX OF REFRACTION DATA -- N2(R) --                          GIS02970
C                                                                       GIS02980
      BEFF=B/(RZERO**2)                                                 GIS02990
      N2X21=SQRT(A+BEFF*RZERO**2)                                       GIS03000
      IF(OSYMB .LT. 0.0)N2X21=SQRT(A+BEFF*((RZERO/2.0)**2))             GIS03010
      CALL INDEX(RAD,N2X1K)                                             GIS03020
      CALL INDEX(ROOO,N2X2K)                                            GIS03030
      PRCNTE=-((N2X2K-N2X21)/N2X2K)*100.0                               GIS03040
      PRCNTT=-((N2X2K-N2X1K)/N2X2K)*100.0                               GIS03050
      PRCNTO=-((N2X1K-N2X21)/N2X1K)*100.0                               GIS03060
      WRITE(6,170C)A,BEFF,OSYMB,PRCNTE,PRCNTT,PRCNTO                    GIS03070
C    END GLM LENS SHAPE                                                 GIS03080
C                                                                       GIS03090
C    ALGCRITHM TRACE RAY (SEE INPUTS;X1(J),Y1(J),DYDXN(J),X2(J))        GIS03100
C                                                                       GIS03110
C     IF VARY IS "1" TRACE RAY WILL BE REPEATED FOR ALFAP = 0.0 TO C.7  GIS03120
      IF(VARY .EQ. 0) GO TO 15                                          GIS03130
      ALFAP=0.0                                                         GIS03140
      GO TO 15                                                          GIS03150
   14 ALFAP=ALFAP+0.1                                                   GIS03160
   15 CONTINUE                                                          GIS03170
      G=1                                                               GIS03180
      CCUNT=0                                                           GIS03190
      RAYY(G)=0.0                                                       GIS03200
      RAYZ(G)=0.0                                                       GIS03210
      NTNCTY(G)=1.0                                                     GIS03220
      XMAVET=0.0                                                        GIS03230
      XMAVE=0.0                                                         GIS03240
      IF(SQURAY .EQ. 1) WRITE(6,400) ALFAP,GRID                         GIS03250
   20 CONTINUE                                                          GIS03260
      IF(RAYZ(G) .GE. Y1(K)) GO TO 30                                   GIS03270
        CENI=(AB+X1(K))*SIN(ALFAP)                                      GIS03280
        TORBI=SQRT(Y1(K)**2-RAYZ(G)**2)                                 GIS03290
        BOTI=CENI-TORBI                                                 GIS03300
        IF(RAYY(G) .LE. BOTI) GO TO 30                                  GIS03310
          TOPI=CENI+TORBI                                               GIS03320
          IF(RAYY(G) .GE. TOPI) GO TO 30                                GIS03330
            RAYZ(G)=RAYZ(G)+GRID                                        GIS03340
            GO TO 20                                                    GIS03350
   30 CONTINUE                                                          GIS03360
C  SEARCH FOR Y1(J) JUST GT RAYZ(G); RETRIEVE X1(J)                     GIS03370
      M=K/2                                                             GIS03380
      IF(Y1(M) .LT. RAYZ(G)) GO TO 32                                   GIS03390
```

```
      IF(RAYY(G) .GT. 1.15) GO TO 32                                    GIS03400
        N=K-1                                                           GIS03410
   31 CONTINUE                                                          GIS03420
      IF(Y1(N) .GT. RAYZ(G)) GO TO 36                                   GIS03430
        N=N-1                                                           GIS03440
        IF(N .EQ. 0) GO TO 34                                           GIS03450
        GO TO 31                                                        GIS03460
   32 CONTINUE                                                          GIS03470
      N=M                                                               GIS03480
   33 CONTINUE                                                          GIS03490
      IF(Y1(N) .GT. RAYZ(G)) GO TO 36                                   GIS03500
        N=N-1                                                           GIS03510
        IF(N .EQ. 0) GO TO 34                                           GIS03520
          GO TO 33                                                      GIS03530
   34 CONTINUE                                                          GIS03540
      RAYZ(G)=0.0                                                       GIS03550
      IF(RAYY(G) .LT. 0.0) GO TO 35                                     GIS03560
        RAYY(G)=RAYY(G)+GRID                                            GIS03570
        GO TO 20                                                        GIS03580
   35 CONTINUE                                                          GIS03590
      RAYY(G)=RAYY(G)-GRID                                              GIS03600
      GO TO 20                                                          GIS03610
   36 CONTINUE                                                          GIS03620
      RADIUS=SQRT(RAYZ(G)**2+((RAYY(G)/COS(ALFAP))-(X1(N)+AB)*          GIS03630
     1TAN(ALFAP))**2)                                                   GIS03640
      IF(Y1(N) .GT. RADIUS) GO TO 40                                    GIS03650
        IF(RADIUS .GT.Y1(1)) GO TO 37                                   GIS03660
        N=N-1                                                           GIS03670
        GC TO 36                                                        GIS03680
   37 CONTINUE                                                          GIS03690
      N=N-1                                                             GIS03700
      IF(N .GT. 0) GO TC 36                                             GIS03710
      CEN=(X1(1)+AB)*SIN(ALFAP)                                         GIS03720
      TORB=Y1(1)*COS(ALFAP)                                             GIS03730
      RAYZ(G)=0.0                                                       GIS03740
      IF(RAYY(G) .GE. 0.0) GO TO 38                                     GIS03750
        RAYY(G)=RAYY(G)-GRIC                                            GIS03760
        BOT=CEN-TORB                                                    GIS03770
C       CHECK FOR BOTTOM EDGE OF LENS, GO TO MIRROR IMAGE RAYS          GIS03780
        IF(RAYY(G) .LT. BOT) GO TO 60                                   GIS03790
          GO TO 2C                                                      GIS03800
   38 CONTINUE                                                          GIS03810
      RAYY(G)=RAYY(G)+GRID                                              GIS03820
      TOP=CEN+TORB                                                      GIS03830
      IF(RAYY(G) .GT. TOP) GO TO 39                                     GIS03840
        GO TO 20                                                        GIS03850
   39 CONTINUE                                                          GIS03860
      RAYY(G)=-GRID                                                     GIS03870
```

```
      GO TO 20                                                          GIS03880
   40 CCNTINUE                                                          GIS03890
      P=N+1                                                             GIS03900
C     CALCULATE INTERCEPT POINT ON OUTER SURFACE                        GIS03910
      AC=RAYY(G)/COS(ALFAP)                                             GIS03920
      BO=TAN(ALFAP)                                                     GIS03930
      CO=(Y1(N)-Y1(P))/(X1(N)-X1(P))                                    GIS03940
      DO=X1(P)                                                          GIS03950
      EO=Y1(P)                                                          GIS03960
      PAR1=(AO*BO+CO*EO-(CO**2)*DO-AB*(BO**2))                          GIS03970
      PAR2=(BO**2-CO**2)                                                GIS03980
      PAR3=(AO**2+AB*(BO**2)*AB-2.0*AO*BO*AB+                           GIS03990
     1RAYZ(G)**2-(EO-CO*DO)**2)                                         GIS04000
      XO=(PAR1/PAR2)+SQRT((PAR1/PAR2)**2-PAR3/PAR2)                     GIS04010
      IF((PAR1/PAR2).GT.X1(1))XO=XO-2.0*SQRT((PAR1/PAR2)**2-PAR3/PAR2)  GIS04020
      YO=(RAYY(G)/COS(ALFAP))-(XO+AB)*TAN(ALFAP)                        GIS04030
      ZO=RAYZ(G)                                                        GIS04040
C     CALCULATE THE DIRECTION COSINES OF OUTSIDE SURFACE NORMAL         GIS04050
      DELTAX=X1(N)-X1(P)                                                GIS04060
      DELTAY=Y1(N)-Y1(P)                                                GIS04070
      SP=SQRT((RADIUS-Y1(P))**2+(XO-X1(P))**2)                          GIS04080
      ST=SQRT(DELTAX**2+DELTAY**2)                                      GIS04090
      RATIO=SP/ST                                                       GIS04100
      DYDXNP=RATIC*(DYDXN(N)-DYDXN(P))+CYDXN(P)                         GIS04110
      NPI=1.0/DYDXNP                                                    GIS04120
      IF(YO .EQ. 0.0) GO TO 41                                          GIS04130
        ZOYC=(ZO/YO)                                                    GIS04140
        IF(ZOYO .GE. 8235000) GO TO 41                                  GIS04150
        IF(ZOYO .LE. -8235000) GO TO 42                                 GIS04160
          NPJ=COS(ATAN(ZO/YO))                                          GIS04170
          NPK=SIN(ATAN(ZO/YO))                                          GIS04180
          GO TO 43                                                      GIS04190
   41 CONTINUE                                                          GIS04200
      NPJ=0.0                                                           GIS04210
      NPK=1.0                                                           GIS04220
      GO TO 43                                                          GIS04230
   42 CCNTINUE                                                          GIS04240
      NPJ=0.0                                                           GIS04250
      NPK=-1.0                                                          GIS04260
   43 CONTINUE                                                          GIS04270
C     DIRECTION COSINES OF EXTERNAL RAY                                 GIS04280
      CK=COS(ALFAP)                                                     GIS04290
      CL=-SIN(ALFAP)                                                    GIS04300
C     DIRECTION COSINES OF OUTSIDE SURFACE NORMAL                       GIS04310
      LK=NPI/(SQRT(NPI**2+NPJ**2+NPK**2))                               GIS04320
      LL=(NPJ*LK)/NPI                                                   GIS04330
      LM=(NPK*LK)/NPI                                                   GIS04340
      IF(YO .LT. 0.0) GC TO 44                                          GIS04350
```

```
      GO TO 45
   44 CONTINUE
      LL=-LL
      LM=-LM
   45 CCNTINUE
      THETA=ARCOS(CK*LK+CL*LL)
C     ANGLES OF INCIDENCE AND REFRACTION OUTSIDE SURFACE
      PHI=PI-THETA
      RO=SQRT((XO+OSYMB)**2+YO**2+ZO**2)
      CALL INDEX(RO,N2O)
      PHIP=ARSIN((N1/N2O)*SIN(PHI))
C     CALCULATION OF TRANSMITED INTENSITY AT OUTSIDE SURFACE
      FACE=1
      CALL XMIT(PHI,N2O,XMTNC,FACE)
      IF(FACE .EQ. 3) GO TO 53
      NUM=COS(PHIP)-(N1/N2O)*COS(PHI)
C     INITIAL DIRECTION COSINES OF INTERNAL REFRACTED RAY
      CKP=(N1/N2O)*CK-NUM*LK
      CLP=(N1/N2O)*CL-NUM*LL
      CMP=-NUM*LM
      CKKP=CKP
      CLLP=CLP
      CMMP=CMP
C     INTERNAL RAY LENGTH AND INSIDE SURFACE INTERCEPT
      ROX=(XO+OSYMB)/RO
      ROY=YO/RO
      ROZ=ZO/RO
      NPOX=ROY*CMP-ROZ*CLP
      NPOY=ROZ*CKP-ROX*CMP
      NPOZ=ROX*CLP-ROY*CKP
      NPO=SQRT(NPOX**2+NPOY**2+NPOZ**2)
      NPOX=NPOX/NPO
      NPOY=NPOY/NPO
      NPOZ=NPOZ/NPO
      PSIO=ARCOS(ROX*CKP+ROY*CLP+ROZ*CMP)
      EPSLON=1.0
      IF(PSIO .GE. PI2) EPSLON=-1.0
      E=EPSLON*N2C*RO*SIN(PSIO)
      NUM1=(CLP*YO+CMP*ZO-CKP*XO*(TAN(ALPHA)**2))
      NUM2=(CLP**2+CMP**2-(CKP**2)*(TAN(ALPHA)**2))
      NUM3=(YO**2+ZO**2-(XO**2)*(TAN(ALPHA)**2))
      NUM4=NUM1**2-NUM2*NUM3
C     CHECK FOR INTERCEPT WITH INSIDE SURFACE
      IF(NUM4 .LT. 0.0) GO TO 50
        D2=-NUM1/NUM2-SQRT(NUM4)/NUM2
          XIH=D2*CKP+XO
          YIH=D2*CLP+YO
          ZIH=C2*CMP+ZO
```

```
      IF(ZIH .LT. 0.0) GO TO 50                                          GIS04840
      IF(PSIO .GE. (PI-0.05)) GO TO 455                                  GIS04850
      OSYMPH=SQRT((CSYMB+XIH)**2+YIH**2+ZIH**2)                          GIS04860
      OPHX=(OSYMB+XIH)/OSYMPH                                            GIS04870
      OPHY=YIH/OSYMPH                                                    GIS04880
      OPHZ=ZIH/OSYMPH                                                    GIS04890
      THETAP=ARCOS(ROX*OPHX+ROY*OPHY+ROZ*OPHZ)                           GIS04900
      XINT=XO+CSYMPH*CKP                                                 GIS04910
      XINTD=-OSYMB-XINT                                                  GIS04920
      IF(OSYMB .LT. 0.0 .AND. XINTD .GT. 0.0) THETAP=-THETAP             GIS04930
      SIGN=+1.0                                                          GIS04940
      IF(THETAP .LT. 0.0) SIGN=-1.0                                      GIS04950
      IF(THETAP .LT. 0.0) PSIO=-PSIO                                     GIS04960
      CALL SURF(THETAP,RADD,RDOT,SIGN,FILTER)                            GIS04970
      IF(RADD .LT. 0.0) SIGN=-SIGN                                       GIS04980
      CALL ITRATE(SIGN,THETAP,RAD,THTAP,FILTER)                          GIS04990
      IF(PSIO.GT.PI2.AND.OSYMB.LT.0.0.AND.FILTER.EQ.2)GO TO 455          GIS05000
      IF(FILTER .EQ. 2 .OR. FILTER .EQ. 1) GO TO 51                      GIS05010
      IF(FILTER .EQ. 3) GO TO 50                                         GIS05020
      BETAO=SIN(THTAP)/SIN(PSIO)                                         GIS05030
      ALFAO=COS(THTAP)-BETAO*COS(PSIO)                                   GIS05040
      XI=RAD*(ALFAO*((XO+OSYMB)/RO)+BETAO*CKKP)-OSYMB                    GIS05050
      YI=RAD*(ALFAO*(YO/RO)+BETAO*CLLP)                                  GIS05060
      ZI=RAD*(ALFAO*(ZO/RO)+BETAO*CMMP)                                  GIS05070
      CALL INDEX(RAD,N2)                                                 GIS05080
      CALL SWITCH((RO),TCRIT)                                            GIS05090
      EONR=E/(EPSLON*N2*RAD)                                             GIS05100
      IF(EONR .GT. 1.0) WRITE(6,9978)EONR                                GIS05110
      IF(EONR .GT. 1.0) EONR=1.0                                         GIS05120
      PSIP=ARSIN(EONR)                                                   GIS05130
      IF(PSIO .LT. 0.0 .AND. (ABS(PSIO-PSIP)) .GT. PI2)PSIP=PI-PSIP GIS05140
      IF(PSIO .LT. 0.0) PSIP=-PSIP                                       GIS05150
      IF(THTAP .GT. 0.6 .AND. TCRIT .GT. THTAP)PSIP=PI-PSIP              GIS05160
      A1=(XI+CSYMB)/RAD                                                  GIS05170
      B1=YI/RAD                                                          GIS05180
      C1=ZI/RAD                                                          GIS05190
      CALL CIRECT(CKP,CLP,CMP)                                           GIS05200
      GO TO 456                                                          GIS05210
  455 CONTINUE                                                           GIS05220
      XI=XIH                                                             GIS05230
      YI=YIH                                                             GIS05240
      ZI=ZIH                                                             GIS05250
  456 CONTINUE                                                           GIS05260
      IF(XI .LT. 0.0 .OR. XI .GT. X2(1)) GO TO 51                        GIS05270
      NUM5=SQRT((XI**2)*(TAN(ALPHA)**4)+YI**2+ZI**2)                     GIS05280
C     DIRECTICN COSINES OF INSIDE NCRMAL                                 GIS05290
      LKP=-XI*(TAN(ALPHA)**2)/NUM5                                       GIS05300
      LLP=YI/NUM5                                                        GIS05310
```

```
      LMP=ZI/NUM5
      KKLLMM=CKP*LKF+CLP*LLP+CMP*LMP
      IF(KKLLMM .GE. 1.0)THETAI=0.0
      IF(KKLLMM .LE. -1.0)THETAI=PI
      IF((ABS(KKLLMM)) .GE. 1.0) GO TO 457
      THETAI=ARCOS((CKP*LKP)+(CLP*LLP)+(CMP*LMP))
  457 CONTINUE
C     ANGLES OF INCIDENCE AND TOTAL INTERNAL REFLECTION
C     AT THE INSIDE SURFACE:
      PHII=PI-THETAI
      TIRA=ARSIN(N3/N2)
C     CHECK FOR TOTAL INTERNAL REFLECTION:
      IF(PHII .GE. TIRA) GO TO 52
        PHIIP=ARSIN((N2/N3)*SIN(PHII))
C       CALCULATION OF TRANSMITTED INTENSITY AT INSIDE SURFACE
        FACE=2
        CALL XMIT(PHII,N2,XMTNCP,FACE)
        NTNCTY(G)=XMTNC*XMTNCP
        XMAVET=XMAVET+NTNCTY(G)
        XMAVE=XMAVET/(G*1.0)
        NUM8=COS(PHIIP)-(N2/N3)*COS(PHII)
C       DIRECTION COSINES OF INSIDE EXTERNAL REFRACTED RAY
        CKPP=(N2/N3)*CKP-NUM8*LKP
        CLPP=(N2/N3)*CLP-NUM8*LLP
        CMPP=(N2/N3)*CMP-NUM8*LMP
C       LENGTH OF INSIDE EXTERNAL REFRACTED RAY
        D3=(BF-XI)/CKPP
        NUM6=((XO+AB)*CK+YO*CL)
        NUM7=((XO+AB)*(-CL)+YO*CK)
C       LENGTH OF OUTSIDE INCIDENT RAY
        D1=SQRT((XO-NUM6)**2+(YO-NUM7)**2)
C       TOTAL OPTICAL PATHLENGTH:
        OPL(G)=N1*D1+N2*D2+N3*D3
C       INTERSECTION WITH THE IMAGE PLANE:
        YIM(G)=((BF-XI)/CKPP)*CLPP+YI
        ZIM(G)=((BF-XI)/CKPP)*CMPP+ZI
        IF(CMPP .LT. 0.000000000001 .AND. CMPP .GT. -0.000000000001)
     1    GO TO 46
          XDIAPT(G)=(-ZIM(G)/CMPP)*CKPP+AB
          YDIAPT(G)=(-ZIM(G)/CMPP)*CLPP+YIM(G)
          GO TO 47
   46 CONTINUE
        XDIAPT(G)=99999.
        YDIAPT(G)=99999.
   47 CONTINUE
        IF(SQURAY .EQ. 1) WRITE(6,500)G,RAYY(G),RAYZ(G),XO,YO,XI,
     1  YI,ZI,OPL(G),YIM(G),ZIM(G),NTNCTY(G),XDIAPT(G),YDIAPT(G)
        FLAG(G)=0
```

```
   49 CONTINUE                                                          GIS05800
      H=G                                                               GIS05810
      G=H+1                                                             GIS05820
      NTNCTY(G)=1.0                                                     GIS05830
      RAYY(G)=RAYY(H)                                                   GIS05840
      RAYZ(G)=RAYZ(H)+GRID                                              GIS05850
      IF(FLAG(H) .EQ. 0) COUNT=COUNT+1                                  GIS05860
      GO TO 30                                                          GIS05870
C     END OF RAY TRACE                                                  GIS05880
   50 CONTINUE                                                          GIS05890
      NTNCTY(G)=0.0                                                     GIS05900
      FLAG(G)=1                                                         GIS05910
      IF(SQURAY .EQ. 1) WRITE(6,600)G,RAYY(G),RAYZ(G)                   GIS05920
      GO TO 49                                                          GIS05930
   51 CONTINUE                                                          GIS05940
      NTNCTY(G)=0.0                                                     GIS05950
      FLAG(G)=2                                                         GIS05960
      IF(SQURAY .EQ. 1) WRITE(6,700)G,RAYY(G),RAYZ(G)                   GIS05970
      GO TO 49                                                          GIS05980
   52 CONTINUE                                                          GIS05990
      NTNCTY(G)=0.0                                                     GIS06000
      FLAG(G)=3                                                         GIS06010
      IF(SQURAY .EQ. 1) WRITE(6,800)G,RAYY(G),RAYZ(G)                   GIS06020
      GO TO 49                                                          GIS06030
   53 CONTINUE                                                          GIS06040
      NTNCTY(G)=0.0                                                     GIS06050
      FLAG(G)=4                                                         GIS06060
      IF(SQURAY .EQ. 1) WRITE(6,802) G,RAYY(G),RAYZ(G)                  GIS06070
      GO TO 49                                                          GIS06080
C                                                                       GIS06090
C     MIRROR IMAGE RAY MATCHING FOLLOWS                                 GIS06100
C                                                                       GIS06110
   60 CONTINUE                                                          GIS06120
      IF(SQURAY .EQ.1) WRITE(6,401)                                     GIS06130
      Q=G-1                                                             GIS06140
      S=G-Q                                                             GIS06150
   61 CONTINUE                                                          GIS06160
      IF(RAYZ(S) .EQ. 0.0) S=S+1                                        GIS06170
        IF(S .GT. Q) GO TO 70                                           GIS06180
          FLAG(G)=FLAG(S)                                               GIS06190
          IF(FLAG(G) .EQ. 0) COUNT=COUNT+1                              GIS06200
          RAYY(G)=RAYY(S)                                               GIS06210
          RAYZ(G)=-RAYZ(S)                                              GIS06220
          IF(FLAG(S) .GE. 1) GO TO 63                                   GIS06230
            XDIAPT(G)=XDIAPT(S)                                         GIS06240
            YDIAPT(G)=YDIAPT(S)                                         GIS06250
            YIM(G)=YIM(S)                                               GIS06260
            ZIM(G)=-ZIM(S)                                              GIS06270
```

```
      OPL(G)=OPL(S)
      NTNCTY(G)=NTNCTY(S)
      IF(SQURAY .EQ. 1) WRITE(6,501)G,S,RAYY(G),RAYZ(G),OPL(G),
     1YIM(G),ZIM(G),NTNCTY(G)
   62 CCNTINUE
      S=S+1
      G=G+1
      GO TO 61
   63 CONTINUE
      IF(FLAG(S) .GE. 2) GO TO 64
        IF(SQURAY .EQ. 1) WRITE(6,601)G,S,RAYY(G),RAYZ(G)
        GO TO 62
   64 CCNTINUE
      IF(FLAG(S) .GE. 3) GO TO 65
        IF(SQURAY .EQ. 1) WRITE(6,701)G,S,RAYY(G),RAYZ(G)
        GO TO 62
   65 CONTINUE
      IF(FLAG(S) .EQ. 4) GO TO 67
      IF(SQURAY .EQ. 1)  WRITE(6,801)G,S,RAYY(G),RAYZ(G)
      GO TO 62
   67 CCNTINUE
      IF(SQURAY .EQ. 1)WRITE(6,803)G,S,RAYY(G),RAYZ(G)
      GO TO 62
   7C CCNTINUE
      RAYS=G-1
      DRAYS=RAYS-C
      IF(SQURAY .EQ. 1)  WRITE(6,900)RAYS,DRAYS,COUNT
C
C     GENERATE OBJECT PLANE ELLIPSES:
C
      IF(ELLIPS .EQ. 1)  WRITE(6,1000)ENUM
      NLMBR=1
      NUMB=1
   71 CCNTINUE
      CCORD=1
      ELZ(NUMB,COORD)=-Y1(NUMBR)
   72 CONTINUE
      ELY(NUMB,COORD)=(X1(NLMBR)+AB)*SIN(ALFAP)+SQRT((Y1(NUMBR))**2-
     1(ELZ(NUMB,COORD))**2)*COS(ALFAP)
      ELZZ=ELZ(NUMB,COORD)
      IF(ELLIPS .EQ. 1)  WRITE(6,1100)NUMBR,COORD,ELY(NUMB,COORD),
     1ELZ(NUMB,COCRD)
      COORD=COORD+1
      ELZ(NUMB,COORD)=ELZZ+ELL
      IF(ELZ(NUMB,COORD) .GE. Y1(NUMBR)) GO TO 73
        GO TO 72
   73 CONTINUE
      ELZZ=ELZ(NUMB,COORD)
```

```
   74 CONTINUE
      ELZ(NUMB,COORD)=ELZZ-ELL
      IF(ELZ(NUMB,COORD) .LE. -Y1(NUMBR)) GO TO 75
      ELY(NUMB,COORD)=(X1(NUMBR)+AB)*SIN(ALFAP)-SQRT((Y1(NUMBR))**2-
     1(ELZ(NUMB,CCORD))**2)*COS(ALFAP)
      ELZZ=ELZ(NUMB,COORD)
      IF(ELLIPS .EQ. 1) WRITE(6,1100)NUMBR,COORD,ELY(NUMB,COORD),
     1ELZ(NUMB,COCRD)
      COOR(NUMB)=COORD
      CCORD=COORD+1
      GO TO 74
   75 CONTINUE
      NUMBR=NUMBR+(K-1)/ELLNUM
      NUMB=NUMB+1
      IF(NUMBR .GT. K) GO TO 76
      GO TO 71
   76 CONTINUE
      IF(ELLIPS .EQ. 1) WRITE(6,1200)
      NUMBT=NUMB-1
C
C     IMAGE PLANE SPOT DIAGRAM STATISTICAL ANALYSIS:
C
      SUM1=0.0
      DO 77 G=1,RAYS
        IF(FLAG(G) .GT. 0) GO TO 77
          SUM1=YIM(G)+SUM1
   77 CONTINUE
C     REFERENCE EACH ITERATION TO INCIDENT ANGLE & THICKNESS BY:
      IANGLE=ALFAP*10+1
      THICK=(T/R)*100
C     CENTROID OF SPOT:
      YCENTR(IANGLE,THICK)=SUM1/COUNT
C     STANDARD DEVIATIONS:
      SUM2=0.0
      SUM3=0.0
      DO 78 G=1,RAYS
        IF(FLAG(G) .GT. 0) GO TO 78
        SUM2=ZIM(G)**2+SUM2
        SUM3=(YCENTR(IANGLE,THICK)-YIM(G))**2+SUM3
   78 CONTINUE
      SIGMAZ(IANGLE,THICK)=SUM2/COUNT
      SIGMAY(IANGLE,THICK)=SUM3/COUNT
C     ROOT MEAN SQUARE SPCT SIZE:
      RMSRAD(IANGLE,THICK)=SQRT(SIGMAZ(IANGLE,THICK)+SIGMAY(IANGLE,
     1THICK))
      WRITE(6,1300) T,U,ALFAP,R,YCENTR(IANGLE,THICK),
     1SIGMAY(IANGLE,THICK),SIGMAZ(IANGLE,THICK),RMSRAD(IANGLE,THICK)
C
```

```
C      SPOT DIAGRAM ENERGY DENSITY VS. RADIUS FROM CENTROIC:
C
       DO 79 G=1,RAYS
         IF(FLAG(G) .GT. 0) GO TO 79
         SDRAD(G)=SQRT((YCENTR(IANGLE,THICK)-YIM(G))**2+ZIM(G)**2)
   79  CONTINUE
       GG=1
       ROC(GG)=0.005
       SUM4(GG)=0.0
   80  CCNTINUE
       DO 81 G=1,RAYS
         IF(FLAG(G) .GT. 0) GO TO 81
         IF(SDRAC(G) .LE. ROC(GG)) SUM4(GG)=1+SUM4(GG)
   81  CONTINUE
       FRACTN(GG)=SUM4(GG)/RAYS
       WRITE(6,1400) GG,ROC(GG),FRACTN(GG)
       HH=GG
       GG=GG+1
       ROC(GG)=RCC(HH)+0.005
       SUM4(GG)=0.0
       IF(ROC(GG) .GT. 0.5) GO TO 82
       GC TO 80
   82  CONTINUE
       GGT=GG-1
       IF(VARY .EQ. 1 .AND. ALFAP .LT. 0.65) GC TC 14
       WRITE(6,1500)
       IF(T .LT. 0.5 .AND. THKNES .EQ. 1) GO TO 2
       WRITE(6,1600)
C
C
C      PLOT OUTPUT
C
C      WRITE OUTPUT FOR PLOT INTO FILE FT01F001
C
C
       WRITE(1,83)F,ALPHA,U,I,R,T,N1,N2,N3,ALFAP,GRID,STATNA,GAMMA,RAYS,
      1COUNT,K,GGT,IANGLE,THICK,OSYMB,TSURFL,BEFF,PRCNTO,PRCNTE,PRCNTT,
      1XMAVE,A,B
   83  FORMAT(' ',3F9.7,I4,4F9.7/' ',3F9.7,F9.5,F9.7/' ',6I4,4F11.7/1X,
      15F11.7)
       DO 85 J=1,K
          WRITE(1,84)X1(J),Y1(J),X2(J),Y2(J)
   84     FORMAT(' ',4F10.7)
   85  CONTINUE
       DC 88 G=1,RAYS
          WRITE(1,86)RAYY(G),RAYZ(G),FLAG(G)
   86     FORMAT(' ',2F10.7,3X,I1)
          IF(FLAG(C) .GT. 0) GO TO 88
```

```
      WRITE(1,87)YIM(G),ZIM(G)                                          GIS07720
87       FORMAT(' ',2F10.7)                                             GIS07730
88 CONTINUE                                                             GIS07740
   DO 90 GG=1,GGT                                                       GIS07750
      WRITE(1,89)ROC (GG),FRACTN(GG)                                    GIS07760
89    FORMAT(' ',F10.7,2X,F10.7)                                        GIS07770
90 CONTINUE                                                             GIS07780
   WRITE(1,91)YCENTR(IANGLE,THICK),SIGMAY(IANGLE,THICK),                GIS07790
  1SIGMAZ(IANGLE,THICK),RMSRAD(IANGLE,THICK),NUMBT                      GIS07800
91 FCRMAT(' ',4F10.7,I4)                                                GIS07810
   DO 96 NUMB=1,NUMBT                                                   GIS07820
      WRITE(1,92)COOR(NUMB)                                             GIS07830
92    FORMAT(' ',I3)                                                    GIS07840
      COORT=COCR(NUMB)                                                  GIS07850
      DO 95 COORD=1,COORT                                               GIS07860
         WRITE(1,94)ELY(NUMB,COORD),ELZ(NUMB,COORD)                     GIS07870
94       FORMAT(' ',F11.8,3X,F11.8)                                     GIS07880
95    CONTINUE                                                          GIS07890
96 CONTINUE                                                             GIS07900
   WRITE(1,97)                                                          GIS07910
97 FCRMAT(' ','/*')                                                     GIS07920
   WRITE(6,98)                                                          GIS07930
98 FORMAT(' ','TO OBTAIN PLOTS FROM THE PLOTTER OR THE PRINTER,'/' ',GIS07940
  1'ISSUE THE FOLLOWING COMMAND: '/' ',8X,'FOR PRINTER PLOTS',          GIS07950
  1T36,'ENTER "CHARTS PRINTER"'/' ',8X,'FOR PLCTTER GRAPHS',T36,        GIS07960
  1'ENTER "CHARTS PLCTTER"')                                            GIS07970
   WRITE(6,99)                                                          GIS07980
99 FORMAT(' ','END OF PROGRAM')                                         GIS07990
   STOP                                                                 GIS08000
10C FORMAT('1',' LENS PARAMETERS:'///5X,'ALPHA = ',F9.7,2X,             GIS08010
  1'BETA = ',F9.7,2X,'RADIUS = ',F7.5//5X,'INCIDENT ANGLE = ',          GIS08020
  1F9.6,2X,'ITERATIONS = ',I5//5X,'EDGE THICKNESS = ',F9.7,2X,          GIS08030
  1'INDICES OF REFRACTION: N1 = ',F7.5//5X,'N3 = ',                     GIS08040
  1F7.5,2X,'FOCAL LENGTH FROM STATION ZERO = ',F7.5,2X,                 GIS08050
  1'DELTA UDP = ',F7.5///                                               GIS08060
  11X,'  J        X1          Y1          X2          Y2          UDP         I2PGIS08070
  1        I2'//25X,'UP          I1P         I1        DYDXT'//)        GIS08080
200 FORMAT(1X,I4,7F10.7/20X,4F10.7/)                                    GIS08090
300 FORMAT('0'/1X,'NOSE SECTION DATA:'//2X,'NOSE HALF ANGLE = ',        GIS08100
  1F7.5,2X,'STATION A = ',F9.5/2X,'OPAQUE SURFACE LENGTH = ',F7.5/2X,GIS08110
  1'TRANSPARENT SURFACE LENGTH =',F7.5/2X,'TOTAL LENS SURFACE LENGTH GIS08120
  1=',F7.5///)                                                          GIS08130
400 FOPMAT('1','SKEW RAY TRACE PARAMETERS:'///5X,'ALFAP= ',F9.7,2X,     GIS08140
  1'GRID= ',F9.7,2X,'SEE LENS PARAMETERS ABOVE.'///2X,'RAY       RAYY   GIS08150
  1     RAYZ        X0          Y0          XI          YI          ZI'//14X,'0GIS08160
  1PL         YIM         ZIM         NTNCTY      XDIAPT      YDIAPT'///)GIS08170
50C FORMAT(1X,I4,7F10.7/8X,F13.9,3F10.7,2E13.3/)                        GIS08180
60C FORMAT(1X,I4,2F10.7,' NO INTERCEPT WITH 2NC SURFACE'/)              GIS08190
```

```
700 FORMAT(1X,I4,2F10.7,' INTERCEPT CUTSIDE BOUNDARY OF 2ND SURFACE'/)GISO8200
800 FCRMAT(1X,I4,2F10.7,2X,'TOTAL INTERNAL REFLECTION AT 2ND SURFACE'/GISO8210
   1)                                                                 GISO8220
401 FORMAT('1'/////'MIRROR IMAGE SKEW RAYS FOLLOW'///1X,'IMAGE'/2X,'RAGISO8230
   1Y  RAY   RAYY        RAYZ          OPL          YIM        ZIM      NTNCTGISO8240
   1Y'//)                                                             GISO8250
501 FORMAT(I4,1X,I4,2F10.7,F13.9,3F10.7/)                             GISO8260
601 FORMAT(I4,1X,I4,2F10.7,' NO INTERCEPT WITH 2ND SURFACE'/)         GISO8270
701 FORMAT(I4,1X,I4,2F10.7,' INTERCEPT OUTSIDE OF BOUNDARY OF 2ND SURFGISO8280
   1ACE'/)                                                            GISO8290
801 FORMAT(I4,1X,I4,2F10.7,' TOTAL INTERNAL REFLECTION'/)             GISO8300
802 FORMAT(1X,I4,2F10.7,2X,'TOTAL EXTERNAL REFLECTION'/)              GISO8310
803 FCRMAT(I4,1X,I4,2F10.7,'TOTAL EXTERNAL REFLECTION'/)              GISO8320
900 FORMAT(1X,'END OF SKEW RAY TRACE.'//3X,'TOTAL NUMBER OF RAYS TRACEGISO8330
   1D = ',I4/3X,'TOTAL NUMBER OF MIRROR IMAGE RAYS = ',I4/3X,'TOTAL NUGISO8340
   1MBER OF RAYS STRIKING IMAGE PLANE = ',I4///)                      GISO8350
1000 FORMAT('1','TWO DIMENSIONAL PRCJECTION OF 3-DIM LENS'///3X,'GENERAGISO8360
   1TED ELLIPSES ARE REFERENCED TO THE CORRESPONDING JTH COORD'/3X,'INGISO8370
   1THE MERIDIAN PLANE AS COMPUTED IN THE ABOVE'/3X,'GLM LENS SHAPEAL GISO8380
   1GORITHM. INSIDE/OUTSIDE ELLIPSES DEFINE THE '/3X,'LIMITS OF THE TRGISO8390
   1ANSPARENT/OPAQUE PARTS.'/3X,'THE NUMBER OF ELLIPSES =  ',I3//1X,' GISO8400
   1 J   COORD     ELY          ELZ'//)                               GISO8410
1100 FORMAT(1X,I4,3X,I4,2F10.7)                                       GISO8420
1200 FORMAT(1X/'CALCULATION CF ELLIPSE COORDINATES COMPLETE.')        GISO8430
1300 FORMAT('1'////'IMAGE PLANE SPOT DIAGRAM ANALYSIS:'///1X,'THICKNESSGISO8440
   1 =',F9.7,'  U =',F9.7,'  ALFAP =',F9.7,'  R =',F9.7//1X,'CENTROID:GISO8450
   1 ZCENTR = 0.0,  YCENTR = ',F10.7//1X,'STANDARD DEVIATIONS:  SIGMAYGISO8460
   1 = ',F10.7,2X,'SIGMAZ = ',F10.7//1X,'RMS SPOT SIZE: RMSRAD = ',   GISO8470
   1F10.7///1X,'SPOT DIAGRAM ENERGY DENSITY VS. RADIUS FROM CENTROID:'GISO8480
   1//1X,' GG      RADIUS     FRACTION'//)                            GISO8490
1400 FORMAT(I4,2F11.7)                                                GISO8500
1500 FORMAT(1X/'SPOT DIAGRAM CALCULATIONS COMPLETE.'////)             GISO8510
1600 FORMAT(1X/'END OF PROGRAM'////)                                  GISO8520
1700 FORMAT(1X,'LENS INDEX OF REFRACTION DATA'/2X,'THE INDEX GRADIENT IGISO8530
   1S: N2(R) = SQRT((',F4.2,')+(',F6.3,')*R**2)'/2X,'WITH THE CENTER OGISO8540
   1F SYMMETRY LOCATED AT ',F7.3/2X,'(MINUS IMPLIES THE CSYM IS ON THEGISO8550
   1 IMAGE SIDE).'/2X,'PERCENT CHANGE OF THE LENS INDEX GRADIENT:'/   GISO8560
   14X,'INSIDE SURFACE FRCM CENTER TC EDGE :',F10.5/4X,'INSIDE SURFACEGISO8570
   1 TO OUTSIDE SURFACE AT THICKEST POINT :',F10.5/4X,'OUTSIDE SURFACEGISO8580
   1 FROM CENTER TO EDGE :',F10.5////)                                GISO8590
1800 FORMAT(1X,'IMAGINARY RADIUS DUE TC IMPRCPER A TO B RATIO IN N2(R) GISO8600
   1FCR THIS RAY')                                                    GISO8610
1900 FORMAT(1X,'*****************************************************GISO8620
   1***************'/1X,'*',68X,'*'/1X,'*',25X,'GISL TABULAR OUTPUT',2GISO8630
   14X,'*'/1X,'*',68X,'*'/1X,'****************************************GISO8640
   1*****************************'///)                                GISO8650
     END                                                              GISO8660
C                                                                     GISO8670
```

```
C                                                                       GIS08680
C     SUBROUTINE INDEX CALCULATES THE INDEX OF REFRACTION AS A FUNCTION GIS08690
C      OF RADIUS FROM THE CENTER OF SYMMETRY. THE VALUES OF THE INDEX   GIS08700
C      CONSTANTS A AND B ARE USER INPUTS.                               GIS08710
C                                                                       GIS08720
       SUBROUTINE INDEX(R,N)                                            GIS08730
       REAL R,N,A,B,RZERO,E,EPSLON,SQRT                                 GIS08740
       COMMON A,B,E,RZERC,EPSLON,PI2,J                                  GIS08750
       N=SQRT(A+B*(R/RZERO)**2)                                         GIS08760
       RETURN                                                           GIS08770
       END                                                              GIS08780
C                                                                       GIS08790
C                                                                       GIS08800
C     SUBROUTINE TRANSMIT CALCULATES THE TRANSMITTED INTENSITY OF       GIS08810
C      EACH RAY AT BOTH THE OUTSIDE AND INSIDE SURFACES USING THE       GIS08820
C      FRESNEL EQUATIONS .                                              GIS08830
C                                                                       GIS08840
       SUBROUTINE XMIT(PHI,N2,XM1,FACE)                                 GIS08850
       REAL PHI,N3,XM1,NTI,N1,N2,SQRT,COS                               GIS08860
       INTEGER FACE                                                     GIS08870
       COMMON/XM/N1,N3                                                  GIS08880
C                                                                       GIS08890
       NTI=N2/N1                                                        GIS08900
       IF(FACE .EQ. 2) NTI=N3/N2                                        GIS08910
       VALUE=NTI**2-(SIN(PHI)**2)                                       GIS08920
       IF(VALUE .LT. 0.0) GO TO 10                                      GIS08930
       SQ=SQRT(VALUE)                                                   GIS08940
       COSP=COS(PHI)                                                    GIS08950
       RPER=(COSP-SQ)/(COSP+SQ)                                         GIS08960
       RPAR=((NTI**2)*COSP-SQ)/((NTI**2)*COSP+SQ)                       GIS08970
       XM1=1.0-0.5*(RPER**2+RPAR**2)                                    GIS08980
       RETURN                                                           GIS08990
    10 CONTINUE                                                         GIS09000
       FACE=3                                                           GIS09010
       RETURN                                                           GIS09020
       END                                                              GIS09030
C                                                                       GIS09040
C                                                                       GIS09050
C     SUBROUTINE RADYUS CALCULATES THE RADIAL DIMENSION FROM THE CENTER GIS09060
C      OF SYMMETRY TO THE RAY AT THE ANGLE SPECIFIED.                   GIS09070
C      RADYUS ALSO FINDS D(R)/D(THETA) FOR SUBR ITRATE.                 GIS09080
C                                                                       GIS09090
       SUBROUTINE RADYUS(RC,ANGLE,R,DRDTHG,FILTER)                      GIS09100
       REAL ANGLE,R,E,RAT,A,B,EPSLON,ARCSYN,FRACTN,RO,SQRT,COS,SIN,ARSIN GIS09110
       INTEGER J,FILTER                                                 GIS09120
       COMMON A,B,E,RZERC,EPSLON,PI2,J                                  GIS09130
       RAT=SQRT(A**2+4.*B*(E**2)/RZERO**2)                              GIS09140
       ARCSYN=ARSIN((2.0*(E/RO)**2-A)/RAT)                              GIS09150
```

```
      IF(ANGLE .LT. 0.0) ARCSYN=2*PI2-ARCSYN
      FRACTN=SIN(-EPSLON*2.0*ANGLE+ARCSYN)
      IF((A+RAT*FRACTN) .LE. 0.0) GO TO 10
      R=SQRT(2.0)*ABS(E)/SQRT(A+RAT*FRACTN)
      IF(FRACTN .LE. (-0.989)) GO TO 10
      DRDTHG=((EPSLON*R**3)/(2.0*E**2))*COS(-2.0*EPSLON*ANGLE+ARCSYN)
   10 CONTINUE
      FILTER=0
      IF(FRACTN .LE. (-0.989))FILTER=2
      IF((A+RAT*FRACTN) .LT. 0.0) FILTER=1
      RETURN
      END
C
C
C    SUBROUTINE SWITCH CALCULATES THE POINT ON THE RAY WHERE
C     D(R)/D(THETA) IS ZERO. THIS ENABLES THE MAIN ROUTINE TO
C     DETERMINE WHETHER PSIP SHOULD BE EVALUATED IN THE 1ST OR 2ND
C     QUADRANT.
C
      SUBROUTINE SWITCH(RC,THTACR)
      REAL THTACR,RAT,E,EPSLON,A2B,PI2,RO,SQRT,ARSIN
      COMMON A,B,E,RZERO,EPSLON,PI2,J
      RAT=SQRT(A**2+4.*B*(E**2)/RZERO**2)
      THTACR=0.5*(PI2-ARSIN((2.0*(E**2/RO**2)-A)/RAT))
C     IF(THTACR .LT. 0.0) THTACR=THTACR+2.0*PI2
      RETURN
      END
C
C
C     SUBROUTINE SURF CALCULATES BOTH THE RADIUS TO THE
C    LOCUS OF THE INTERCEPT OF THE RAY PLANE AND THE IN-
C    SIDE SURFACE AND THE DERIVATIVE OF THE RADIUS WRT THETA
C    GIVEN THE ANGLE THETA. SURF IS DESIGNED PRIMARILY
C    FOR USE WITH SUBROUTINE ITRATE.
C
      SUBROUTINE SURF(THETA,R,RDOT,SIGN,FILTER)
      COMMON/SUR/PSIO,XC,OSYMB,YO,ZO,RO,CKKP,CLLP,CMMP,N2O,ALPHA
      COMMON/DIR/A1,B1,C1,NPOX,NPOY,NPOZ,PSIP
      REAL N2O,OSYMB,NPCX,NPOY,NPOZ,SIN,COS,TAN,COTAN,SQRT,ATAN
      INTEGER FILTER
C
      ALFA=COS(THETA)-SIN(THETA)*COTAN(PSIO)
      BETA=SIN(THETA)/SIN(PSIO)
      A=ALFA*(XO+CSYMB)/RO+BETA*CKKP
      B=ALFA*YO/RO+BETA*CLLP
      C=ALFA*ZO/RO+BETA*CMMP
      A2=B**2+C**2-(A**2)*(TAN(ALPHA)**2)
      B2=B*NPOY+C*NPOZ+A*NPOX+2.0*A*OSYMB*(TAN(ALPHA)**2)
```

```
      C2=CSYMB*NPOX+(CSYMB*TAN(ALPHA))**2+NPOX*XO+NPOY*YO+NPOZ*ZO        GIS09640
      SQUARE=0.25*(B2/A2)**2+C2/A2                                        GIS09650
      IF(SQUARE .LT. 0.0) FILTER=3                                        GIS09660
      IF(FILTER .EQ. 3) RETURN                                            GIS09670
      R=-B2/(2.0*A2)+SIGN*SQRT(SQUARE)                                    GIS09680
C     CALCULATE DR/DTHETA                                                 GIS09690
      DAL=-SIN(THETA)-COS(THETA)*COTAN(PSIO)                              GIS09700
      DBE=COS(THETA)/SIN(PSIO)                                            GIS09710
      DA=DAL*(XC+CSYMB)/RO+DBE*CKKP                                       GIS09720
      DB=DAL*YO/RO+DBE*CLLP                                               GIS09730
      DC=DAL*ZO/RO+DBE*CMMP                                               GIS09740
      DA2=2.0*B*DB+2.0*C*DC-2.0*A*DA*(TAN(ALPHA)**2)                      GIS09750
      DB2=DB*NPOY+DC*NPOZ+DA*NPOX+2.0*DA*CSYMB*(TAN(ALPHA)**2)            GIS09760
      A3=-0.5*(A2*DB2-B2*DA2)/(A2**2)                                     GIS09770
      B3=SIGN/(2.0*SQRT(0.25*(B2/A2)**2+C2/A2))                           GIS09780
      C3=0.25*((A2**2)*2.0*B2*DB2-(B2**2)*2.0*A2*DA2)/(A2**4)-            GIS09790
     1C2*DA2/(A2**2)                                                      GIS09800
      RDOT=A3+B3*C3                                                       GIS09810
      RETURN                                                              GIS09820
      END                                                                 GIS09830
C                                                                         GIS09840
C                                                                         GIS09850
C    SUBROUTINE DIRECT CALCULATES THE VECTOR DIRECTION COSINES OF         GIS09860
C     A SKEW RAY AT THE POINT OF INTERCEPT WITH THE INSIDE SURFACE.       GIS09870
C                                                                         GIS09880
      SUBROUTINE DIRECT(CKP,CLP,CMP)                                      GIS09890
      COMMON/DIR/RRX,RRY,RRZ,NPFX,NPFY,NPFZ,PSIR                          GIS09900
      REAL RRX,RRY,RRZ,NPFX,NPFY,NPFZ,PSIR,CKP,CLP,CMP,COS,SQRT           GIS09910
      EPS=1.0E-06                                                         GIS09920
      SIGN=+1.0                                                           GIS09930
      IF((ABS(NPFX)) .GT. EPS) GO TO 50                                   GIS09940
      IF((ABS(NPFY)) .GT. EPS) GO TO 30                                   GIS09950
      IF((ABS(RRY)) .LT. EPS) GO TO 25                                    GIS09960
        CMP=0.0                                                           GIS09970
      APP=1.0+(RRX/RRY)**2                                                GIS09980
      BPP=COS(PSIR)*RRX/RRY**2                                            GIS09990
      CPP=(COS(PSIR)/RRY)**2-1.0                                          GIS10000
        CKP=BPP/APP+SIGN*SQRT(BPP**2-APP*CPP)/APP                         GIS10010
        CLP=(COS(PSIR)-RRX*CKP)/RRY                                       GIS10020
        RETURN                                                            GIS10030
   25 CONTINUE                                                            GIS10040
        CMP=0.0                                                           GIS10050
        CKP=COS(PSIR)/RRX                                                 GIS10060
        CLP=SIGN*SQRT(1.0-CKP**2)                                         GIS10070
        RETURN                                                            GIS10080
   30 CONTINUE                                                            GIS10090
      IF((ABS(NPFZ)) .GT. EPS) GO TO 40                                   GIS10100
      IF((ABS(RRZ)) .LT. EPS) GO TO 35                                    GIS10110
```

```
      CLP=0.0                                                          GIS10120
     APP=1.0+(RRX/RRZ)**2                                              GIS10130
     BPP=COS(PSIR)*RRX/RRZ**2                                          GIS10140
     CPP=(COS(PSIR)/RRZ)**2-1.0                                        GIS10150
      CKP=BPP/APP+SQRT(BPP**2-APP*CPP)/APP                             GIS10160
      CMP=(COS(PSIR)-RRX*CKP)/RRZ                                      GIS10170
      RETURN                                                           GIS10180
  35 CONTINUE                                                          GIS10190
      CLP=0.0                                                          GIS10200
      CKP=COS(PSIR)/RRX                                                GIS10210
      CMP=SIGN*SQRT(1.0-CKP**2)                                        GIS10220
      RETURN                                                           GIS10230
  4C CONTINUE                                                          GIS10240
     IF((ABS(RRX)) .GT. EPS) GO TO 45                                  GIS10250
      CLP=COS(PSIR)/(RRY-NPFY/NPFZ*RRZ)                                GIS10260
      CMP=-NPFY/NPFZ*CLP                                               GIS10270
      CKP=SIGN*SQRT(1.0-CLP**2-CMP**2)                                 GIS10280
      RETURN                                                           GIS10290
  45 CONTINUE                                                          GIS10300
     IF((ABS(RRY-NPFY/NPFZ*RRZ)) .GT. EPS) GO TO 47                    GIS10310
      CKP=COS(PSIR)/RRX                                                GIS10320
      CLP=SIGN*SQRT((1.0-CKP**2)/(1.0+(NPFY/NPFZ)**2))                 GIS10330
      CMP=-NPFY/NPFZ*CLP                                               GIS10340
      RETURN                                                           GIS10350
  47 CONTINUE                                                          GIS10360
     SIGN=-1.0                                                         GIS10370
     IF(RRY .LT. 0.0 .OR. RRX .LT. 0.0) SIGN=+1.0                      GIS10380
     IF(RRY .LT. 0.0 .AND. RRX .LT. 0.0) SIGN=-1.0                     GIS10390
     APP=((RRY-NPFY/NPFZ*RRZ)/RRX)**2+1.0+(NPFY/NPFZ)**2               GIS10400
     BPP=2.0*COS(PSIR)/(RRX**2)*(RRY-NPFY/NPFZ*RRZ)                    GIS10410
     CPP=(COS(PSIR)/RRX)**2-1.0                                        GIS10420
      CLP=BPP/(2.0*APP)+SIGN*SQRT(BPP**2-4.0*APP*CPP)/(2.0*APP)        GIS10430
      CMP=-NPFY/NPFZ*CLP                                               GIS10440
      CKP=(COS(PSIR)-(RRY-NPFY/NPFZ*RRZ)*CLP)/RRX                      GIS10450
      RETURN                                                           GIS10460
  50 CONTINUE                                                          GIS10470
     SIGN=-1.0                                                         GIS10480
     IF(RRY .LT. 0.0)SIGN=+1.0                                         GIS10490
     IF(RRY .LT. 0.0 .AND. NPFZ .LT. 0.0) SIGN=-1.0                    GIS10500
     AA=NPFX*RRY-NPFY*RRX                                              GIS10510
     BB=NPFX*RRZ-NPFZ*RRX                                              GIS10520
     CC=NPFX*COS(PSIR)                                                 GIS10530
     IF((ABS(BB)) .GT. EPS)GO TO 60                                    GIS10540
      CLP=CC/AA                                                        GIS10550
     APP=(NPFZ/NPFX)**2+1.0                                            GIS10560
     BPP=NPFY*NPFZ/NPFX**2*CLP                                         GIS10570
     CPP=((NPFY/NPFX)**2+1.0)*CLP**2-1.0                               GIS10580
      CMP=-BPP/APP+SIGN*SQRT(BPP**2-APP*CPP)/APP                       GIS10590
```

```
      CKP=(-NPFY*CLP-NPFZ*CMP)/NPFX
      RETURN
   60 CONTINUE
      IF(BB .GT. 0.0) SIGN=-1.0
      AF=(NPFY/NPFX)**2+1.0
      BP=(NPFZ/NPFX)**2+1.0
      CP=2.0*NPFY*NPFZ/NPFX**2
      AFP=AP+BP*(AA/BB)**2-CP*AA/BB
      BPP=2.0*AA*CC*BP/BB**2-CP*CC/BB
      CFP=BP*(CC/BB)**2-1.0
        CLP=BPP/(2.0*APP)+SIGN*SQRT(BPP**2-4.0*APP*CPP)/(2.0*APP)
        CMP=CC/BB-AA/BB*CLP
        CKP=(-NPFY*CLP-NPFZ*CMP)/NPFX
        RETURN
      END
C
C
C     SUBROUTINE ITRATE PERFORMS ITERATION TO FIND R AND THETAP
C    OF THE INTERCEPT OF THE GRIN SKEW-RAY AND THE INSIDE CONICAL
C    SURFACE USING THE NEWTON-RAPHSON ITERATION PROCEDURE.
C
      SUBROUTINE ITRATE(SIGN,THETA,R,THETAP,FILTER)
      COMMON A,B,E,RZERO,EPSLON,PI2,J
      COMMON/DIR/A1,B1,C1,NPOX,NPOY,NPOZ,PSIP
      COMMON/SUR/PSIO,XO,OSYMB,YO,ZO,RO,CKKP,CLLP,CMMP,N2O,ALPHA
      INTEGER LOOP,FILTER
C
      LOOP=0
   10 CONTINUE
      CALL RADYUS(RO,THETA,RADG,RDOTG,FILTER)
      IF(FILTER .EQ. 1)RETURN
      IF(FILTER .EQ. 2)RETURN
      CALL SURF(THETA,RADH,RDOTS,SIGN,FILTER)
      IF(FILTER .EQ. 3)RETURN
      FX=RADG-RADH
      FXDOT=RDOTG-RDOTS
      XNEW=THETA-(FX/FXDOT)/1.3
      DIFF=ABS(THETA-XNEW)
      IF(DIFF .GT. 0.00001) GO TO 20
      THETAP=THETA
      R=RADG
      RETURN
   20 CONTINUE
      IF(LOOP .GE. 90) GO TO 30
      LOOP=LOOP+1
      THETA=XNEW
      GO TO 10
   30 CONTINUE
```

```
      IF(LOOP .GE. 90) FILTER=3                                         GIS11080
      WRITE(6,6410)                                                     GIS11090
 6410 FORMAT(/1X,'SOLUTICN NOT FOUND')                                  GIS11100
      RETURN                                                            GIS11110
      END                                                               GIS11120
```

APPENDIX C

SAMPLE TABULAR OUTPUT FROM PROGRAM GISL

```
************************************************************
*                                                          *
*                   GISL TABULAR OUTPUT                    *
*                                                          *
************************************************************
```

1 LENS PARAMETERS:

ALPHA = 0.7853982 BETA = 0.3217505 RADIUS = 1.00000

INCIDENT ANGLE = 0.0 ITERATIONS = 100

EDGE THICKNESS = 0.0500000 INDICES OF REFRACTION: N1 = 1.00000

N3 = 1.00000 FOCAL LENGTH FROM STATION ZERO = 4.00000 DELTA UDP = 0.00322

J	X1	Y1	X2	Y2	UDP	I2P	I2
			UP	I1P	I1	DYDXT	
1	0.9616396	1.0320053	1.0000000	0.9999998	0.3217505	0.4636472	0.0995450
			0.6858528	0.1720029	0.8769178	0.8318774	
2	0.9527428	1.0245905	0.9919431	0.9919429	0.3185330	0.4668649	0.1006271
			0.6847707	0.1727901	0.8770413	0.8316687	
3	0.9438142	1.0171518	0.9838600	0.9838598	0.3153155	0.4700826	0.1017177
			0.6836802	0.1735849	0.8771699	0.8314511	
4	0.9348540	1.0096884	0.9757503	0.9757501	0.3120980	0.4732993	0.1028165
			0.6825813	0.1743850	0.8772871	0.8312529	
5	0.9258599	1.0022020	0.9676142	0.9676141	0.3088804	0.4765170	0.1039242
			0.6814736	0.1751921	0.8774052	0.8310531	
6	0.9168330	0.9946885	0.9594508	0.9594507	0.3056630	0.4797347	0.1050406
			0.6803573	0.1760102	0.8775480	0.8308118	
7	0.9077742	0.9871492	0.9512604	0.9512602	0.3024455	0.4829524	0.1061657
			0.6792321	0.1768308	0.8776608	0.8306212	
8	0.8986831	0.9795850	0.9430425	0.9430423	0.2992280	0.4861692	0.1072993
			0.6780985	0.1776611	0.8777914	0.8304005	

9	0.8895560	0.9719930	0.9347960	0.9347959	0.2960104	0.4893869	0.1084422	0.6769556	0.1784965	0.8779076	0.8302040
10	0.8803961	0.9643753	0.9265221	0.9265219	0.2927930	0.4926046	0.1095940	0.6758038	0.1793403	0.8780314	0.8299952
11	0.8712009	0.9567289	0.9182188	0.9182186	0.2895755	0.4958213	0.1107548	0.6746430	0.1801909	0.8781521	0.8297914
12	0.8619708	0.9490560	0.9098864	0.9098862	0.2863579	0.4990390	0.1119250	0.6734728	0.1810462	0.8782556	0.8296165
13	0.8527024	0.9413573	0.9015246	0.9015244	0.2831404	0.5022567	0.1131043	0.6722935	0.1819105	0.8783699	0.8294234
14	0.8433996	0.9336274	0.8931330	0.8931329	0.2759229	0.5054744	0.1142931	0.6711047	0.1827840	0.8784947	0.8292129
15	0.8340593	0.9258732	0.8847126	0.8847124	0.2767054	0.5086921	0.1154910	0.6699068	0.1836621	0.8786031	0.8290300
16	0.8246826	0.9180898	0.8762615	0.8762614	0.2734879	0.5119098	0.1166985	0.6686993	0.1845482	0.8787155	0.8288405
17	0.8152681	0.9102768	0.8677794	0.8677792	0.2702704	0.5151275	0.1179156	0.6674823	0.1854381	0.8788039	0.8286913
18	0.8058172	0.9024346	0.8592664	0.8592662	0.2670529	0.5183452	0.1191421	0.6662558	0.1863384	0.8789114	0.8285100
19	0.7963278	0.8945618	0.8507230	0.8507228	0.2638354	0.5215619	0.1203781	0.6650197	0.1872448	0.8790098	0.8283439
20	0.7867995	0.8866592	0.8421465	0.8421463	0.2606179	0.5247796	0.1216241	0.6637738	0.1881607	0.8791218	0.8281551
21	0.7772329	0.8787258	0.8335392	0.8335391	0.2574005	0.5279973	0.1228797	0.6625181	0.1890816	0.8792174	0.8279940
22	0.7676280	0.8707618	0.8248989	0.8248987	0.2541829	0.5312141	0.1241450	0.6612529	0.1900077	0.8792992	0.8278561
23	0.7579840	0.8627660	0.8162262	0.8162261	0.2509654	0.5344318	0.1254203	0.6599776	0.1909401	0.8793746	0.8277292
24	0.7482984	0.8547372	0.8075203	0.8075202	0.2477480	0.5376495	0.1267056	0.6586922	0.1918799	0.8794488	0.8276040

25	0.7385736	0.8466769	0.7987810	0.7987808	0.2445304	0.5408671	0.1280009	0.6573970	0.1928259	0.8795164	0.8274904
26	0.7288064	0.8385835	0.7900075	0.7900074	0.2413129	0.5440839	0.1293058	0.6560920	0.1937829	0.8796067	0.8273380
27	0.7189997	0.8304576	0.7811996	0.7811995	0.2380954	0.5473016	0.1306210	0.6547768	0.1947386	0.8796439	0.8272754
28	0.7091515	0.8222976	0.7723581	0.7723579	0.2348779	0.5505193	0.1319463	0.6534515	0.1957040	0.8796960	0.8271877
29	0.6992603	0.8141024	0.7634806	0.7634804	0.2316604	0.5537370	0.1332816	0.6521162	0.1966770	0.8797513	0.8270944
30	0.6893276	0.8058743	0.7545682	0.7545680	0.2284429	0.5569547	0.1346271	0.6507707	0.1976526	0.8797790	0.8270478
31	0.6793501	0.7976097	0.7456194	0.7456192	0.2252254	0.5601724	0.1359826	0.6494152	0.1986350	0.8798047	0.8270046
32	0.6693305	0.7893112	0.7366352	0.7366350	0.2220079	0.5633891	0.1373481	0.6480498	0.1996242	0.8798310	0.8269601
33	0.6592678	0.7809767	0.7276143	0.7276142	0.2187904	0.5666068	0.1387237	0.6466741	0.2006130	0.8798138	0.8269892
34	0.6491598	0.7726042	0.7185560	0.7185559	0.2155729	0.5698245	0.1401095	0.6452883	0.2016122	0.8798180	0.8269823
35	0.6390076	0.7641952	0.7094607	0.7094606	0.2123554	0.5730422	0.1415054	0.6438924	0.2026151	0.8798057	0.8270029
36	0.6288099	0.7557480	0.7003270	0.7003269	0.2091379	0.5762599	0.1429113	0.6424865	0.2036191	0.8797619	0.8270767
37	0.6185674	0.7472628	0.6911556	0.6911554	0.2059204	0.5794767	0.1443270	0.6410708	0.2046333	0.8797413	0.8271113
38	0.6082788	0.7387393	0.6819450	0.6819448	0.2027029	0.5826944	0.1457528	0.6396450	0.2056431	0.8796603	0.8272479
39	0.5979443	0.7301762	0.6726955	0.6726953	0.1994854	0.5859120	0.1471885	0.6382093	0.2066600	0.8795860	0.8273730
40	0.5875602	0.7215751	0.6634064	0.6634063	0.1962678	0.5891297	0.1486340	0.6367638	0.2076797	0.8794951	0.8275260

41	0.5771319	0.7129317	0.6540776	0.6540775	0.1930503	0.5923465	0.1500890	0.6353088	0.2087043	0.8794014	0.8276839
42	0.5666530	0.7042491	0.6447080	0.6447079	0.1898329	0.5955642	0.1515539	0.6338440	0.2097281	0.8792736	0.8278992
43	0.5561299	0.6955217	0.6352974	0.6352973	0.1866153	0.5987819	0.1530283	0.6323695	0.2107540	0.8791294	0.8281425
44	0.5455577	0.6867517	0.6258453	0.6258451	0.1833978	0.6019996	0.1545120	0.6308858	0.2117817	0.8789694	0.8284122
45	0.5349353	0.6779414	0.6163516	0.6163515	0.1801803	0.6052173	0.1560050	0.6293928	0.2128095	0.8787854	0.8287225
46	0.5242630	0.6690865	0.6068150	0.6068149	0.1769629	0.6084350	0.1575071	0.6278907	0.2138370	0.8785779	0.8290725
47	0.5135422	0.6601877	0.5972365	0.5972363	0.1737453	0.6116517	0.1590179	0.6263800	0.2148613	0.8783325	0.8294867
48	0.5027711	0.6512430	0.5876139	0.5876138	0.1705278	0.6148694	0.1605376	0.6248602	0.2158903	0.8780947	0.8298882
49	0.4919505	0.6422523	0.5779477	0.5779476	0.1673103	0.6180871	0.1620658	0.6233320	0.2169136	0.8778104	0.8303685
50	0.4810801	0.6332145	0.5682372	0.5682371	0.1640928	0.6213048	0.1636023	0.6217955	0.2179340	0.8774970	0.8308981
51	0.4701589	0.6241291	0.5584818	0.5584816	0.1608753	0.6245225	0.1651468	0.6202511	0.2189507	0.8771533	0.8314793
52	0.4591874	0.6149944	0.5486809	0.5486808	0.1576578	0.6277393	0.1666989	0.6186990	0.2199641	0.8767840	0.8321041
53	0.4481649	0.6058107	0.5388345	0.5388344	0.1544403	0.6309569	0.1682587	0.6171392	0.2209763	0.8764024	0.8327499
54	0.4370912	0.5965770	0.5289415	0.5289414	0.1512228	0.6341746	0.1698255	0.6155723	0.2219762	0.8759543	0.8335092
55	0.4259651	0.5872923	0.5190016	0.5190015	0.1480053	0.6373923	0.1713992	0.6139987	0.2229703	0.8754758	0.8343204
56	0.4147875	0.5779552	0.5090140	0.5090139	0.1447878	0.6406100	0.1729792	0.6124186	0.2239618	0.8749874	0.8351490

57	0.4035584	0.5685652	0.4989785	0.4989784	0.1415703	0.6438268	0.1745651	0.6108327	0.2249327	0.8744001	0.8361464
58	0.3922781	0.5591206	0.4888944	0.4888943	0.1383528	0.6470445	0.1761568	0.6092411	0.2259064	0.8738380	0.8371021
59	0.3809454	0.5496220	0.4787614	0.4787613	0.1351352	0.6502622	0.1777536	0.6076442	0.2268587	0.8731809	0.8382204
60	0.3695607	0.5400661	0.4685786	0.4685785	0.1319178	0.6534799	0.1793550	0.6060428	0.2278067	0.8725201	0.8393459
61	0.3581234	0.5304537	0.4583452	0.4583451	0.1287003	0.6566976	0.1809607	0.6044372	0.2287461	0.8718379	0.8405095
62	0.3466337	0.5207836	0.4480610	0.4480609	0.1254827	0.6599143	0.1825695	0.6028283	0.2296700	0.8711029	0.8417643
63	0.3350886	0.5110562	0.4377257	0.4377256	0.1222652	0.6631320	0.1841817	0.6012161	0.2305866	0.8703625	0.8430304
64	0.3234909	0.5012694	0.4273381	0.4273379	0.1190478	0.6663497	0.1857961	0.5996017	0.2315134	0.8697081	0.8441503
65	0.3118377	0.4914232	0.4168978	0.4168977	0.1158302	0.6695674	0.1874124	0.5979854	0.2321913	0.8678473	0.8473423
66	0.3001441	0.4815053	0.4064043	0.4064041	0.1126127	0.6727841	0.1890293	0.5963685	0.2330918	0.8671477	0.8485447
67	0.2883955	0.4715261	0.3958564	0.3958563	0.1093952	0.6760018	0.1906468	0.5947511	0.2339365	0.8662193	0.8501430
68	0.2765932	0.4614829	0.3852540	0.3852539	0.1061777	0.6792195	0.1922638	0.5931340	0.2347438	0.8651602	0.8519691
69	0.2647396	0.4513741	0.3745971	0.3745970	0.1029602	0.6824372	0.1938794	0.5915185	0.2355235	0.8640264	0.8539279
70	0.2528339	0.4411972	0.3638837	0.3638836	0.0997427	0.6856549	0.1954927	0.5899051	0.2362607	0.8627505	0.8561365
71	0.2408782	0.4309509	0.3531137	0.3531135	0.0965252	0.6888726	0.1971030	0.5882948	0.2369844	0.8614810	0.8583391
72	0.2288720	0.4206347	0.3422866	0.3422865	0.0933077	0.6920894	0.1987091	0.5866887	0.2376738	0.8601224	0.8607012

73	0.2168158	0.4102467	0.3314016	0.3314016	0.0907902	0.6953071	0.2003103	0.5850875	0.2383270	0.8586721	0.8632289
74	0.2047106	0.3997850	0.3204582	0.3204581	0.0868727	0.6985248	0.2019055	0.5834923	0.2389493	0.8571633	0.8658658
75	0.1925563	0.3892483	0.3094552	0.3094551	0.0836552	0.7017425	0.2034936	0.5819042	0.2395362	0.8555795	0.8686407
76	0.1803538	0.3786361	0.2983926	0.2983925	0.0804377	0.7049602	0.2050733	0.5803245	0.2400801	0.8538936	0.8716030
77	0.1681040	0.3679463	0.2872689	0.2872688	0.0772201	0.7081769	0.2066433	0.5787545	0.2405922	0.8521645	0.8746502
78	0.1558043	0.3571758	0.2760841	0.2760840	0.0740027	0.7113946	0.2082030	0.5771948	0.2410619	0.8503491	0.8778595
79	0.1434576	0.3463323	0.2648367	0.2648366	0.0707852	0.7146123	0.2097508	0.5756471	0.2414904	0.8484600	0.8812100
80	0.1310653	0.3354030	0.2535262	0.2535262	0.0675676	0.7178300	0.2112853	0.5741125	0.2418711	0.8464741	0.8847443
81	0.1186289	0.3243900	0.2421523	0.2421522	0.0643501	0.7210477	0.2128052	0.5725926	0.2422076	0.8444154	0.8884209
82	0.1061490	0.3132926	0.2307140	0.2307140	0.0611327	0.7242644	0.2143090	0.5710889	0.2424974	0.8422765	0.8922517
83	0.0936257	0.3021082	0.2192101	0.2192100	0.0579152	0.7274821	0.2157956	0.5696022	0.2427363	0.8400525	0.8962579
84	0.0810609	0.2908359	0.2076402	0.2076401	0.0546976	0.7306998	0.2172634	0.5681344	0.2429250	0.8377470	0.9004240
85	0.0684555	0.2794743	0.1960034	0.1960033	0.0514801	0.7339175	0.2187108	0.5666870	0.2430628	0.8353659	0.9047449
86	0.0558102	0.2680214	0.1842988	0.1842987	0.0482626	0.7371352	0.2201362	0.5652616	0.2431462	0.8329000	0.9092394
87	0.0431264	0.2564759	0.1725258	0.1725258	0.0450451	0.7403520	0.2215379	0.5638599	0.2431734	0.8303474	0.9139132
88	0.0304019	0.2448380	0.1606832	0.1606832	0.0418276	0.7435697	0.2229148	0.5624831	0.2431445	0.8277161	0.9187540

```
89 0.0176410 0.2331046 0.1487704 0.1487703 0.0386101 0.7467874 0.2242649
             0.5611330 0.2430580 0.8250054 0.9237653

90 0.0048451 0.2212741 0.1367862 0.1367862 0.0353926 0.7500051 0.2255866
             0.5598112 0.2429150 0.8222255 0.9289307

91-0.0079843 0.2093453 0.1247303 0.1247303 0.0321751 0.7532218 0.2268779
             0.5585199 0.2427126 0.8193703 0.9342635

92-0.0208471 0.1973162 0.1126012 0.1126012 0.0289576 0.7564395 0.2281377
             0.5572602 0.2424498 0.8164404 0.9397660

93-0.0337411 0.1851857 0.1003983 0.1003982 0.0257401 0.7596572 0.2293640
             0.5560338 0.2421274 0.8134441 0.9454245

94-0.0466690 0.1729540 0.0881205 0.0881204 0.0225226 0.7628749 0.2305551
             0.5548428 0.2417436 0.8103788 0.9512465

95-0.0596255 0.1606186 0.0757670 0.0757669 0.0193051 0.7660926 0.2317091
             0.5536888 0.2413010 0.8072599 0.9572054

96-0.0726097 0.1481775 0.0633368 0.0633368 0.0160876 0.7693103 0.2328244
             0.5525734 0.2407974 0.8040817 0.9633141

97-0.0856237 0.1356313 0.0508290 0.0508290 0.0128701 0.7725270 0.2338991
             0.5514987 0.2402332 0.8008499 0.9695645

98-0.0986636 0.1229768 0.0382423 0.0382423 0.0096526 0.7757447 0.2349319
             0.5504659 0.2396098 0.7975732 0.9759415

99-0.1117308 0.1102147 0.0255759 0.0255759 0.0064350 0.7789624 0.2359210
             0.5494769 0.2389274 0.7942556 0.9824401

100-0.1248229 0.0973431 0.0128291 0.0128291 0.0032176 0.7821801 0.2368645
             0.5485333 0.2381868 0.7909024 0.9890516

101-0.1379396 0.0843605 0.0000002 0.0000002 0.0000001 0.7853969 0.2377607
             0.5476371 0.2373897 0.7875214 0.9957625

0
NOSE SECTION DATA:

NOSE HALF ANGLE = 0.78327  STATION A =  -0.22266
OPAQUE SURFACE LENGTH = 0.11956
TRANSPARENT SURFACE LENGTH =1.45205
TOTAL LENS SURFACE LENGTH =1.57160
```

```
LENS INDEX OF REFRACTION DATA
 THE INDEX GRADIENT IS: N2(R) = SQRT((9.00)+( 5.351)*R**2)
 WITH THE CENTER OF SYMMETRY LOCATED AT   0.050
 (MINUS IMPLIES THE OSYM IS ON THE IMAGE SIDE).
 PERCENT CHANGE OF THE LENS INDEX GRADIENT:
   INSIDE SURFACE FROM CENTER TO EDGE :  49.88858
   INSIDE SURFACE TO OUTSIDE SURFACE AT THICKEST POINT :    0.36591
   OUTSIDE SURFACE FROM CENTER TO EDGE :  49.34212


1SKEW RAY TRACE PARAMETERS:

    ALFAP= 0.4000000  GRID= 0.3000000  SEE LENS PARAMETERS ABOVE.

 RAY      RAYY       RAYZ       XO         YO         XI         YI         ZI
             OPL        YIM        ZIM      NTNCTY        XDIAPT       YDIAPT


   1 0.0        0.3000000 0.1307886-0.1494352 0.2557881-0.1287202 0.2210370
       5.04583168 -2.1801453-0.1453156 0.5102614   -0.126E+01   -0.137E+01

   2 0.0        0.6000000 0.5384317-0.3217840 0.6207671-0.3018253 0.5424452
       4.45595169 -1.4455128-0.2271336 0.4481558   -0.775E+00   -0.111E+01

   3 0.0        0.9000000 0.9583030-0.4993026 0.9974844-0.4872602 0.8703845
       4.09892273 -1.1834154-0.2429521 0.3635889   -0.433E+00   -0.103E+01

   4 0.3000000 0.0        0.0109681 0.2269354 0.1305237 0.1305212 0.0
       4.85042477 -1.6185007 0.0       0.5535472    0.100E+06    0.100E+06

   5 0.3000000 0.3000000 0.1424869 0.1713301 0.2579772 0.1139907 0.2314239
       4.93159103 -1.9860687 0.3676595 0.5334762   -0.988E+01    0.368E+01

   6 0.3000000 0.6000000 0.4431463 0.0442133 0.5327001 0.0265410 0.5320314
       4.60996151 -1.7169704 0.0316697 0.4739231    0.442E+00   -0.183E+01

   7 0.3000000 0.9000000 0.8111566-0.1113788 0.8637780-0.1123655 0.8564321
       4.27614594 -1.4330120-0.1198373 0.3925338   -0.162E+00   -0.127E+01

   8 0.6000000 0.0        0.2600275 0.4473460 0.3610061 0.3610038 0.0
```

```
            4.66151619 -1.4761887 0.0        0.5169492    0.1C0E+C6    0.100E+06

         9 0.6000000 0.30000CC 0.3363692 0.4150693 0.4317581 0.3448501 0.2597798
            4.65313148 -1.5641460 0.1932485 0.5009179    0.1C6E+C2    -0.711E+01

        10 C.6000000 0.6000000 0.5420605 0.3281044 0.6192006 0.2887600 0.5477414
            4.53353596 -1.5893183 0.1321886 0.4537812    0.130E+01    -0.219E+01

        11 0.6000000 0.9000000 0.8309218 0.2059760 C.8806287 0.1906774 0.8597310
            4.31594181 -1.4822788 0.0079514 0.3868141    0.252E+00    -0.150E+01

        12 0.9000000 0.0       0.5180798 0.6639546 C.5948910 0.5948853 0.0
            4.56C61363 -1.3724556 0.0        0.4602101    0.100E+06    0.100E+06

        13 0.9000000 0.3000000 0.5713329 0.6414395 0.6435080 0.5810593 0.2765256
            4.53502178 -1.4060097 0.1153301 0.4473754    0.262E+01    -0.283E+01

        14 0.9000000 0.6000000 0.7219925 0.5777416 0.7806184 0.5374358 0.5661314
            4.452C9980 -1.4449883 0.1326690 0.4111363    0.121E+01    -0.205E+01

        15 0.9000000 0.9000000 0.9483795 0.4820271 0.9865439 0.4622759 0.8715199
            4.30145073 -1.4332008 0.0648745 0.3594230    0.465E+00    -0.159E+01

        16 1.1999998 0.0       0.7783279 0.8796349 0.8306387 0.8306248 0.0
            4.496C8326 -1.3109426 0.0        0.3974670    0.100E+06    0.100E+06

        17 1.1999998 0.3000000 0.8187981 0.8625243 0.8675712 0.8187382 0.2869341
            4.47258854 -1.3300571 0.0765226 0.3879091    0.136E+01    -0.211E+01

        18 1.1999998 0.6000000 0.9357986 0.8130573 0.9743750 0.7823852 C.5807928
            4.40475750 -1.3604498 0.1072606 0.3611534    0.908E+00    -0.185E+01

        19-C.3000000 0.0       0.4567428-0.6129578 0.5509578-0.5509512 C.0
            4.38281155 -0.9380237 0.0        0.4409877    0.100E+06    0.100E+06

        20-0.3C00000 0.3000000 0.6123005-0.6787266 0.6885747-0.6313385 0.2748162
            4.28067303 -0.9621467-0.2031004 0.4222168   -0.118E+01    -0.822E+00

        21-0.3000000 0.6000000 0.9397941-0.8171884 0.9814265-0.7927174 C.5786383
            4.05062485 -0.9309339-0.2432328 0.3676401   -0.671E+00    -0.890E+00
 1

 MIRRCR IMAGE SKEW RAYS FCLLOW
```

IMAGE RAY	RAY	RAYY	RAYZ	OPL	YIM	ZIM	NTNCTY
22	1	0.0	-0.3000000	5.04583168	-2.1801453	0.1453156	0.5102614
23	2	0.0	-0.6000000	4.45595169	-1.4455128	0.2271336	0.4481558
24	3	0.0	-0.9000000	4.09892273	-1.1834154	0.2429521	0.3635889
25	5	0.3000000	-0.3000000	4.93159103	-1.9860687	-0.3676595	0.5334762
26	6	0.3000000	-0.6000000	4.60996151	-1.7169704	-0.0316697	0.4739231
27	7	0.3000000	-0.9000000	4.27614594	-1.4330120	0.1198373	0.3925338
28	9	0.6000000	-0.3000000	4.65313148	-1.5641460	-0.1932485	0.5009179
29	10	0.6000000	-0.6000000	4.53353596	-1.5893183	-0.1321886	0.4537812
30	11	0.6000000	-0.9000000	4.31594181	-1.4822788	-0.0079514	0.3868141
31	13	0.9000000	-0.3000000	4.53502178	-1.4060097	-0.1153301	0.4473754
32	14	0.9000000	-0.6000000	4.45209980	-1.4449883	-0.1326690	0.4111363
33	15	0.9000000	-0.9000000	4.30145073	-1.4332008	-0.0648745	0.3594230
34	17	1.1999998	-0.3000000	4.47258854	-1.3300571	-0.0765226	0.3879091
35	18	1.1999998	-0.6000000	4.40475750	-1.3604498	-0.1072606	0.3611534
36	20	-0.3000000	-0.3000000	4.28067303	-0.9621467	0.2031004	0.4222168
37	21	-0.3000000	-0.6000000	4.05062485	-0.9309339	0.2432328	0.3676401

END OF SKEW RAY TRACE.

TOTAL NUMBER OF RAYS TRACED = 37
TOTAL NUMBER OF MIRROR IMAGE RAYS = 16
TOTAL NUMBER OF RAYS STRIKING IMAGE PLANE = 37

1

IMAGE PLANE SPOT DIAGRAM ANALYSIS:

THICKNESS =0.0500000   U =0.0   ALFAP =0.4000000   R =1.0000000

CENTROID: ZCENTR = 0.0, YCENTR = -1.4490051

STANDARD DEVIATIONS: SIGMAY = 0.0911858 SIGMAZ = 0.0264883

RMS SPOT SIZE: RMSRAD = 0.3430366

SPOT DIAGRAM ENERGY DENSITY VS. RADIUS FROM CENTROID:

GG	RADIUS	FRACTION
1	0.0050000	0.0
2	0.0100000	0.0
3	0.0150000	0.0
4	0.0200000	0.0
5	0.0250000	0.0
6	0.0300000	0.0270270
7	0.0350000	0.0810810
8	0.0400000	0.0810810
9	0.0450000	0.0810810
10	0.0500000	0.0810810
11	0.0550000	0.0810810
12	0.0600000	0.0810810
13	0.0649999	0.0810810
14	0.0699999	0.1351351
15	0.0749999	0.1351351
16	0.0799999	0.1621621
17	0.0849999	0.1621621
18	0.0899999	0.1621621
19	0.0949999	0.1621621
20	0.0999999	0.1621621
21	0.1049999	0.1621621
22	0.1099999	0.1621621
23	0.1149999	0.1621621
24	0.1199999	0.1621621
25	0.1249999	0.2702702
26	0.1299999	0.2702702
27	0.1349999	0.3243243
28	0.1399999	0.4054054
29	0.1449999	0.4594594
30	0.1499999	0.4594594

31	0.1549999	0.4594594
32	0.1599998	0.4594594
33	0.1649998	0.4594594
34	0.1699998	0.4864864
35	0.1749998	0.4864864
36	0.1799998	0.4864864
37	0.1849998	0.4864864
38	0.1899998	0.4864864
39	0.1949998	0.5405405
40	0.1999998	0.5405405
41	0.2049998	0.5405405
42	0.2099998	0.5405405
43	0.2149998	0.5405405
44	0.2199998	0.5405405
45	0.2249998	0.5945945
46	0.2299998	0.6486486
47	0.2349998	0.6486486
48	0.2399998	0.6486486
49	0.2449998	0.6486486
50	0.2499998	0.6486486
51	0.2549998	0.6486486
52	0.2599998	0.6486486
53	0.2649997	0.6486486
54	0.2699997	0.7027027
55	0.2749997	0.7027027
56	0.2799997	0.7027027
57	0.2849997	0.7027027
58	0.2899997	0.7027027
59	0.2949997	0.7027027
60	0.2999997	0.7027027
61	0.3049997	0.7027027
62	0.3099997	0.7027027
63	0.3149997	0.7027027
64	0.3199997	0.7027027
65	0.3249997	0.7027027
66	0.3299997	0.7027027
67	0.3349997	0.7027027
68	0.3399997	0.7027027
69	0.3449997	0.7027027
70	0.3499997	0.7027027
71	0.3549997	0.7027027
72	0.3599997	0.7567567
73	0.3649997	0.7567567
74	0.3699996	0.7567567
75	0.3749996	0.7567567
76	0.3799996	0.7567567
77	0.3849996	0.7567567
78	0.3899996	0.7567567

```
 79  0.3949996  0.7567567
 80  0.3999996  0.7567567
 81  0.4049996  0.7567567
 82  0.4099996  0.7567567
 83  0.4149996  0.7567567
 84  0.4199996  0.7567567
 85  0.4249996  0.7567567
 86  0.4299996  0.7567567
 87  0.4349996  0.7567567
 88  0.4399996  0.7567567
 89  0.4449996  0.7567567
 90  0.4499996  0.7567567
 91  0.4549996  0.7567567
 92  0.4599996  0.7567567
 93  0.4649996  0.7567567
 94  0.4699996  0.7567567
 95  0.4749995  0.7567567
 96  0.4799995  0.7567567
 97  0.4849995  0.7567567
 98  0.4899995  0.7567567
 99  0.4949995  0.7567567
100  0.4999995  0.7567567
SPOT DIAGRAM CALCULATIONS COMPLETE.


END OF PROGRAM


 TO OBTAIN PLOTS FROM THE PLOTTER OR THE PRINTER,
 ISSUE THE FOLLOWING COMMAND:
         FOR PRINTER PLOTS          ENTER "CHARTS PRINTER"
         FOR PLOTTER GRAPHS         ENTER "CHARTS PLOTTER"
 END OF PROGRAM
```

APPENDIX D

HIN LENS PERFORMANCE PLOTS

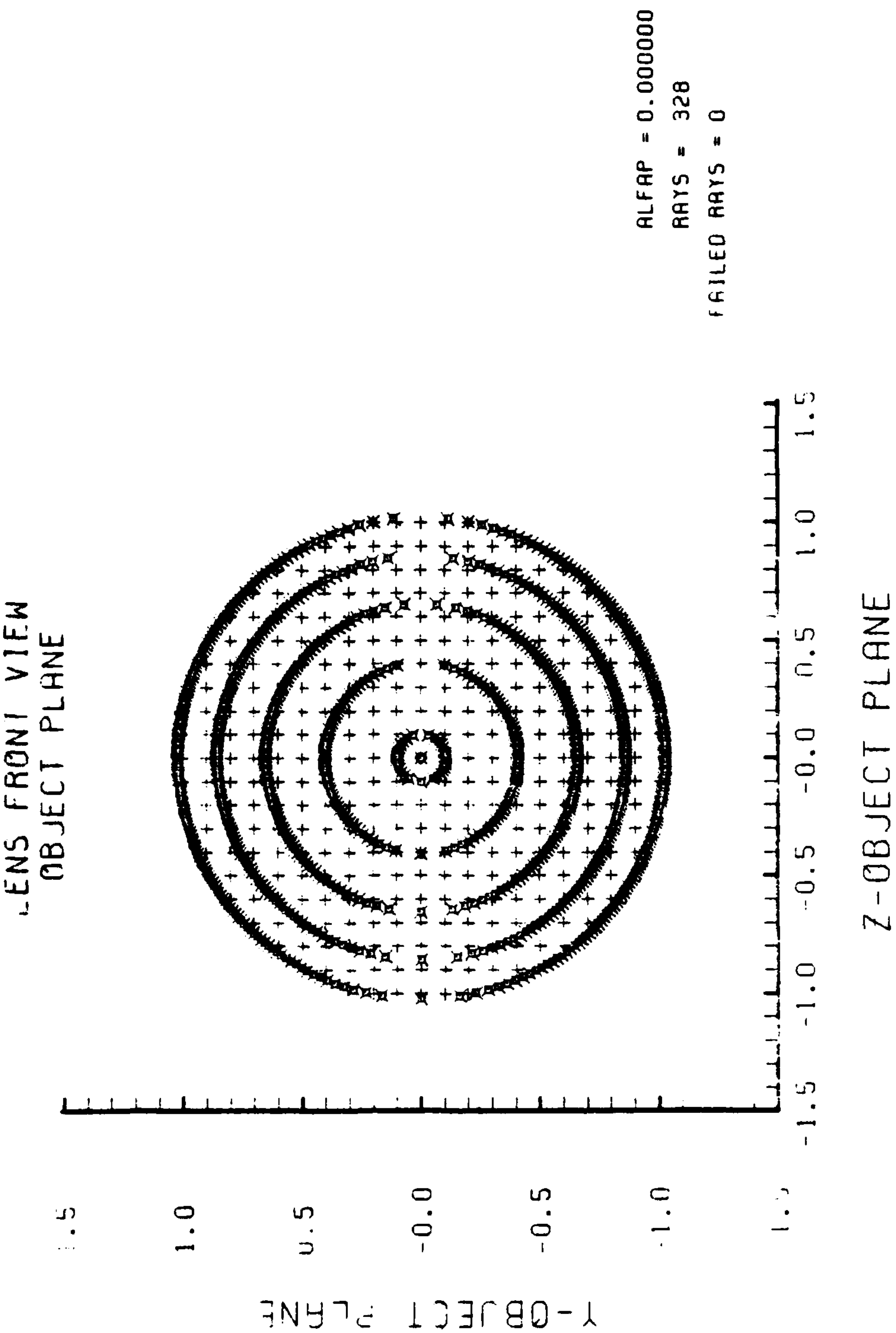

Figure D-1. Object Plane at $\alpha_p = 0.0$ Radians for Hin Lens Design Shown in Figure 11

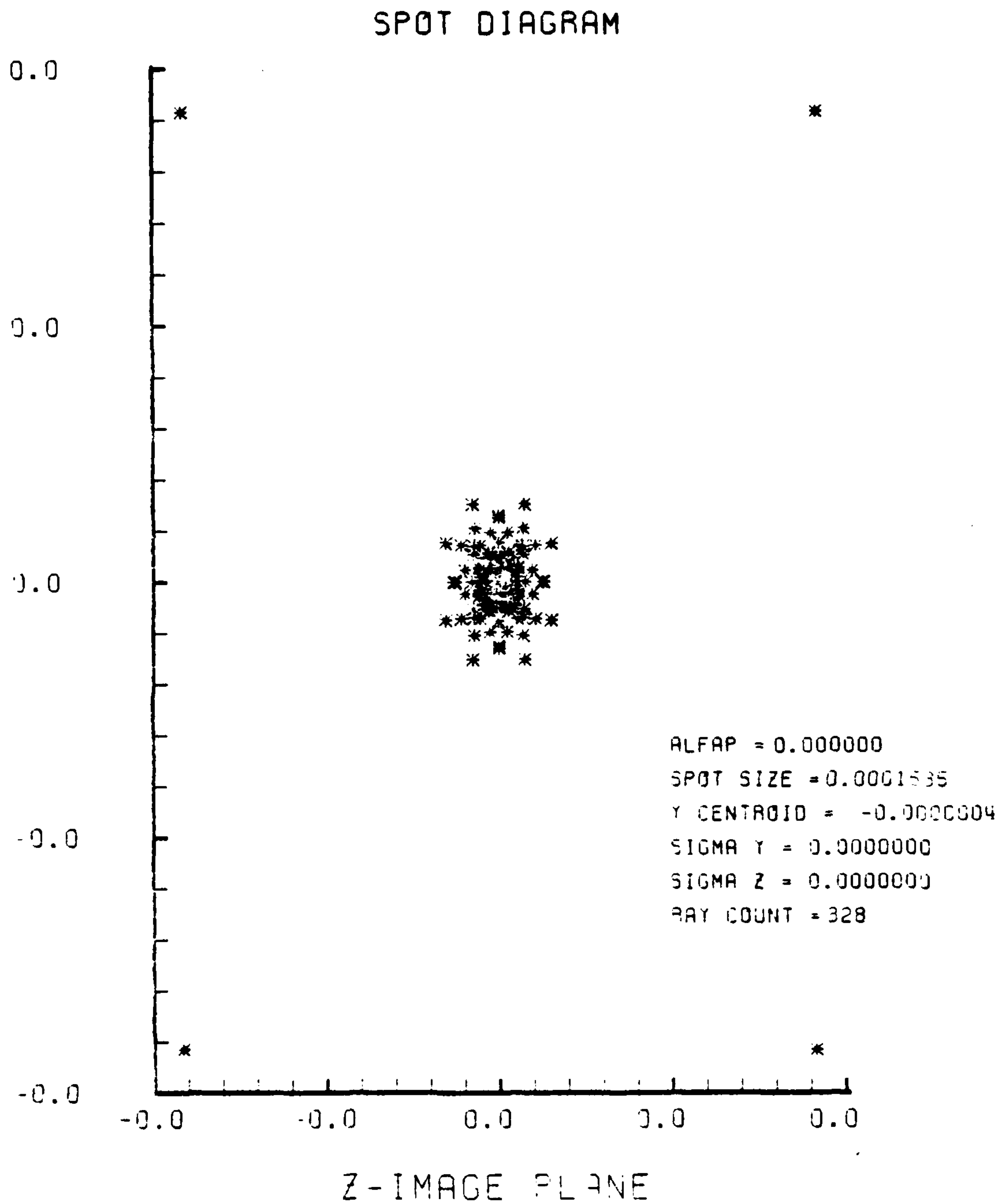

Figure D-2. Spot Diagram Corresponding to Object Plane of Figure D-1

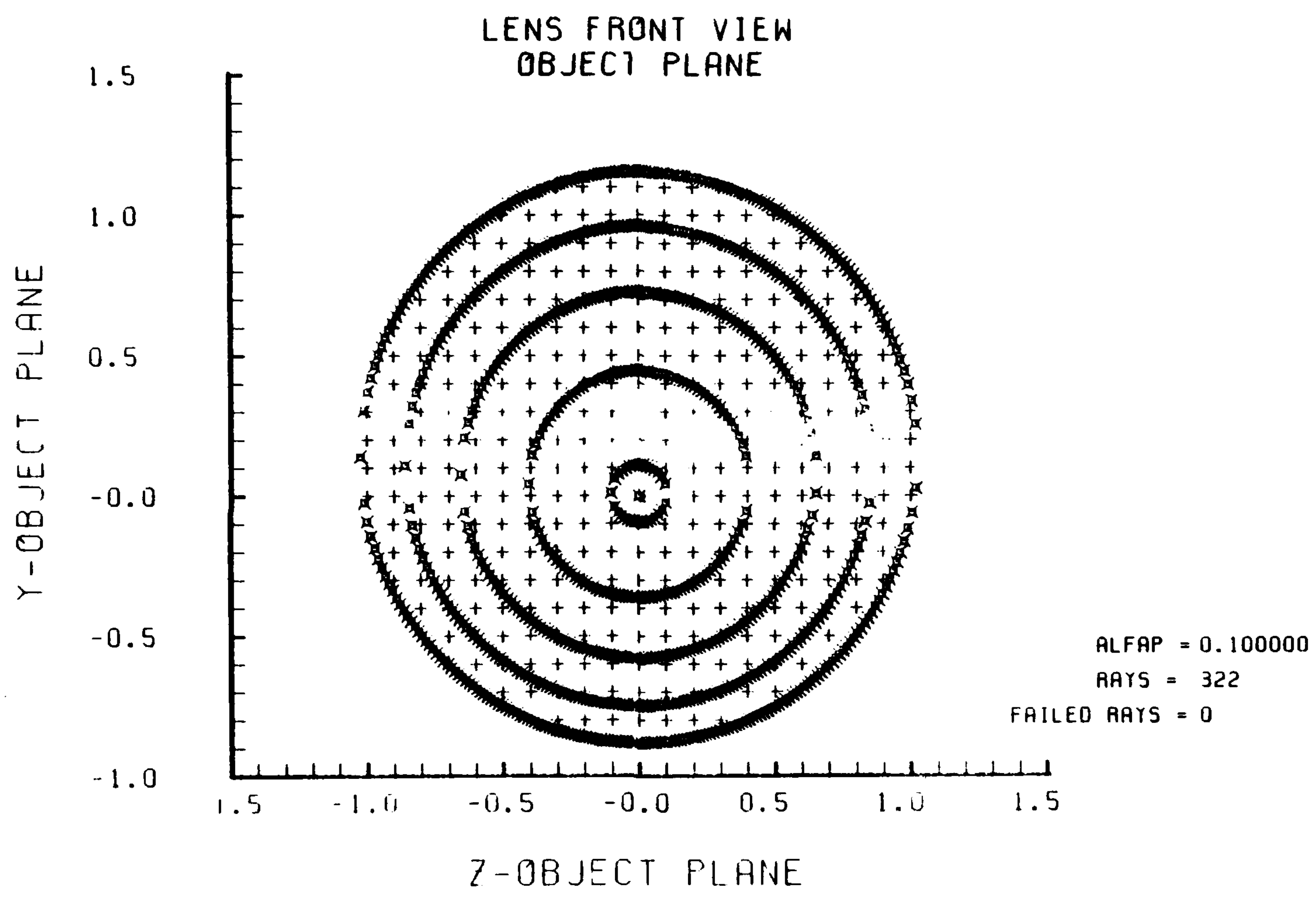

Figure D-3. Object Plane at $\alpha_p = 0.1$ Radians for HIN Lens Shown in Figure 11

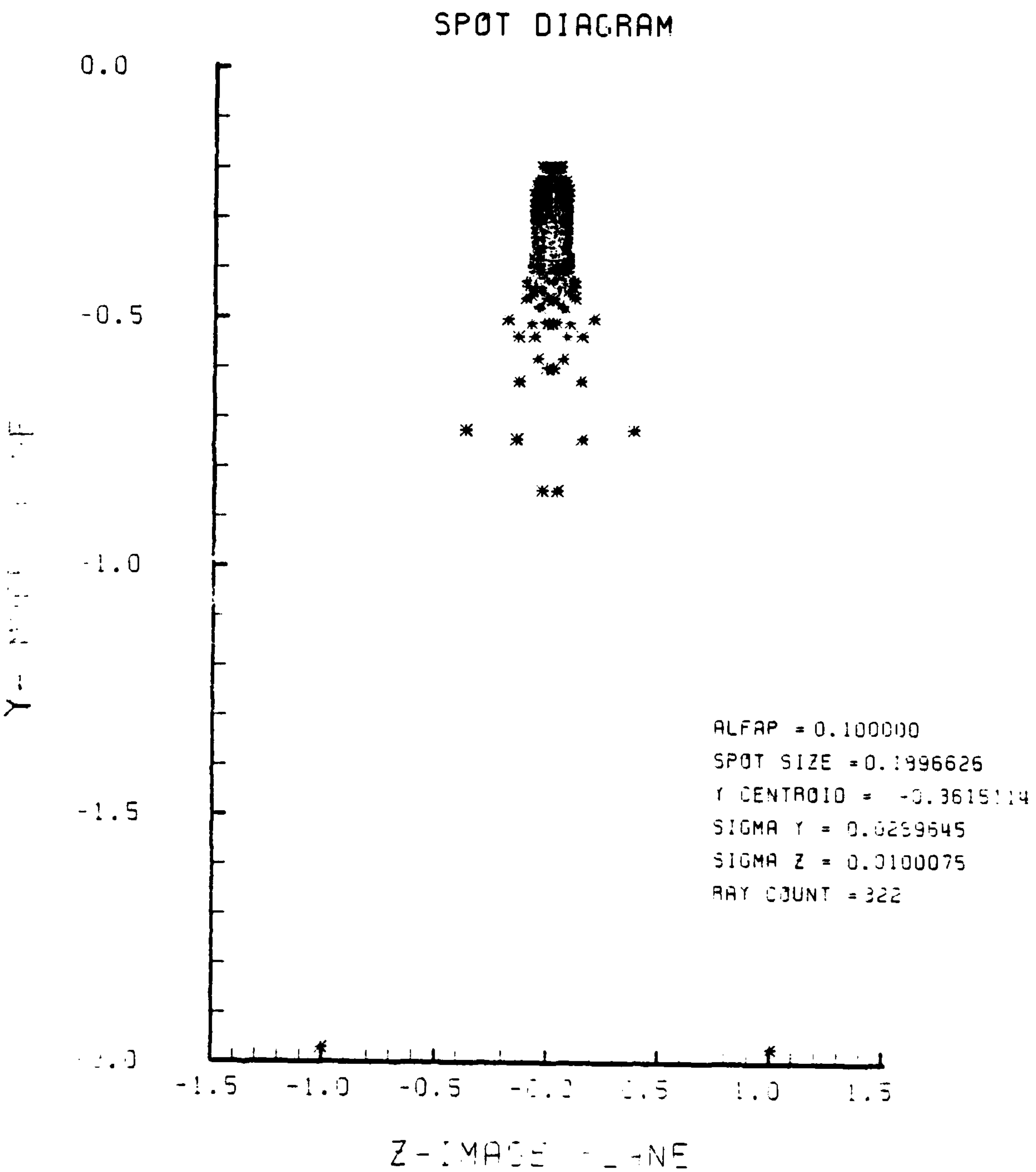

Figure D-4. Spot Diagram Corresponding to Figure D-3

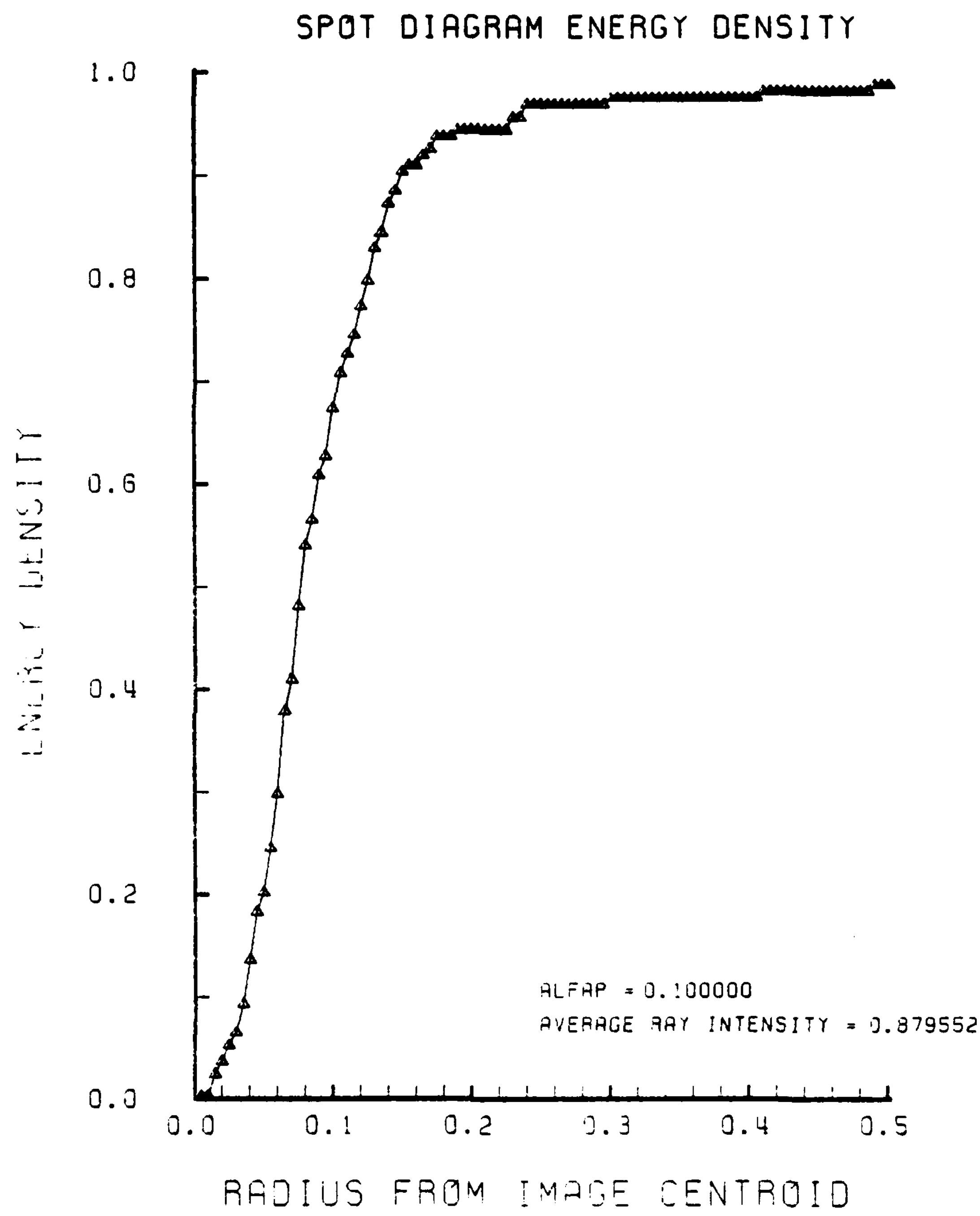

Figure D-5. Encircled Energy Plot for the Spot Diagram of Figure D-4

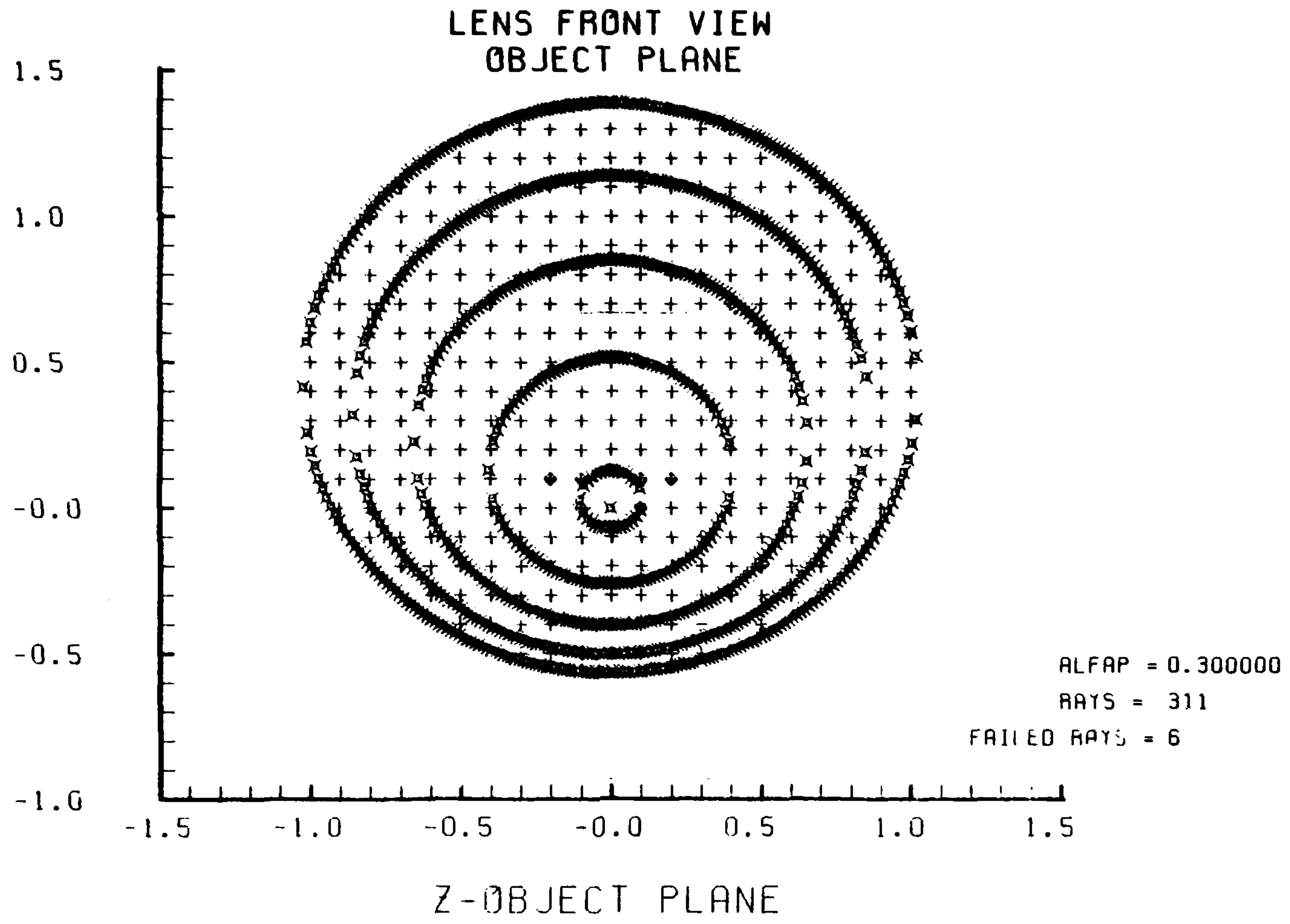

Figure D-6. HIN Object Plane at $\alpha_p = 0.2$ Radians, $N_2 = 1.5$

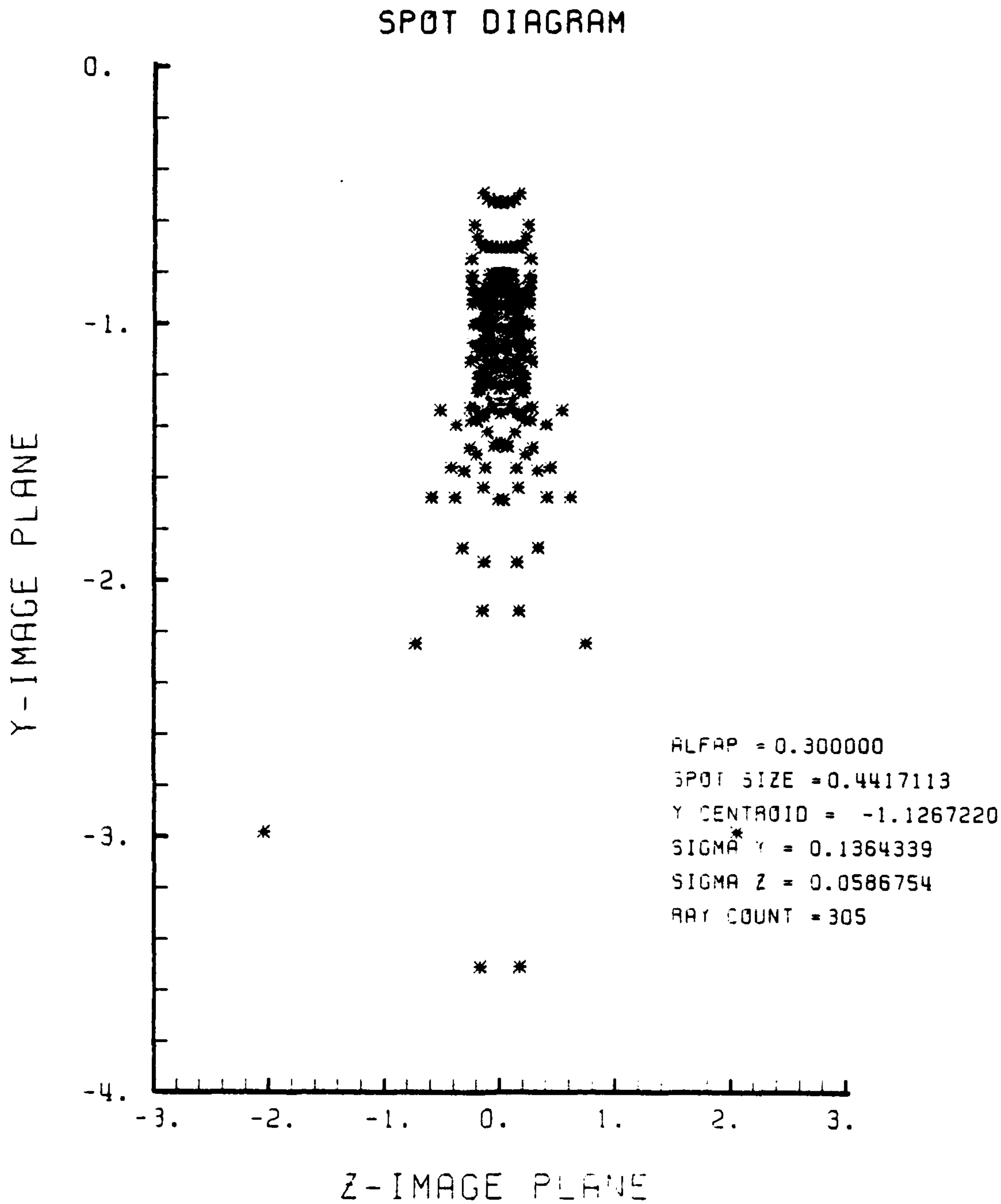

Figure D-7. Spot Diagram of HIN Lens at $\alpha_p = 0.2$ Radians, $N_2 = 1.5$

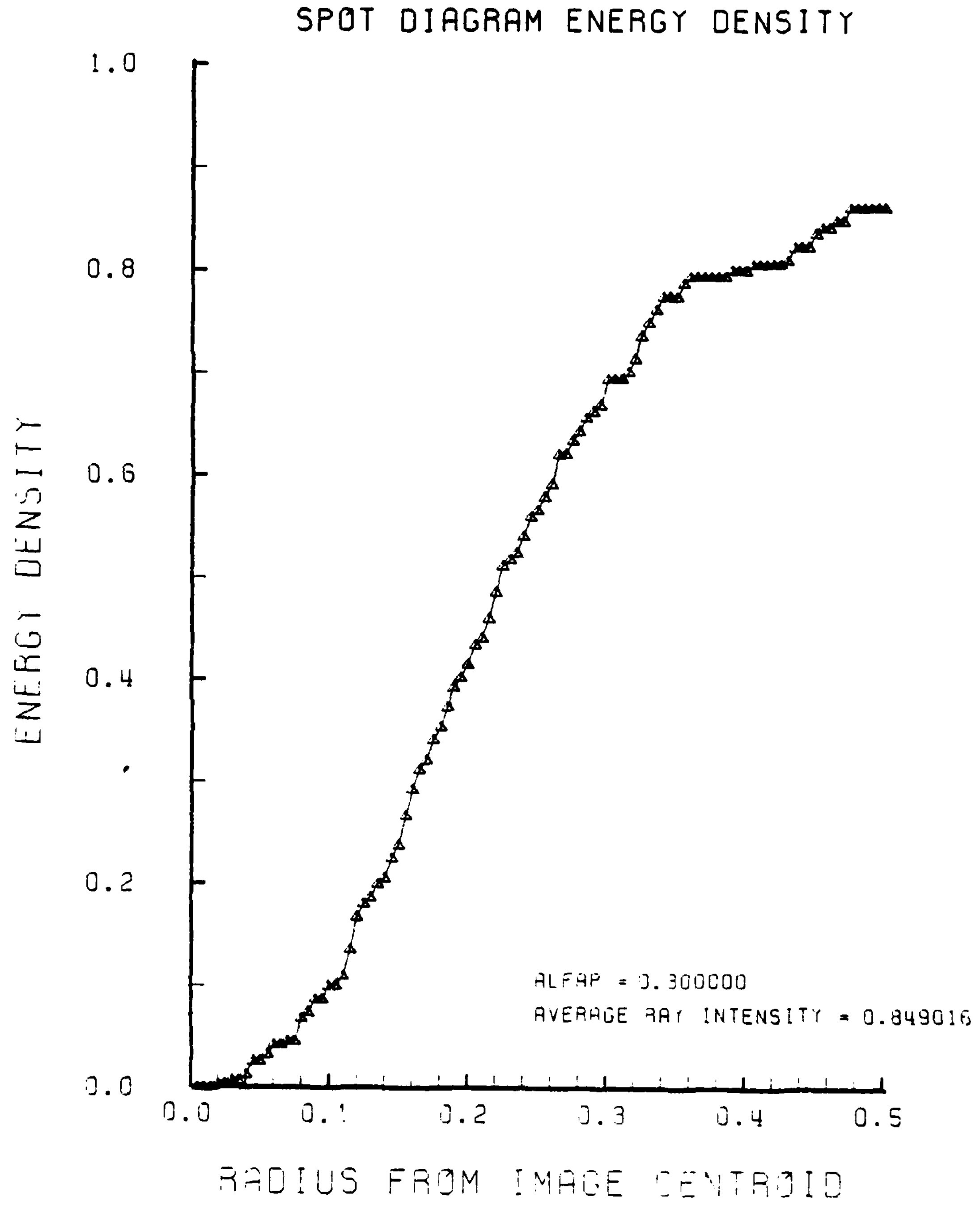

Figure D-8. Encircled Energy Plot of HIN Lens at α_p = 0.2 Radians, N_2 = 1.5

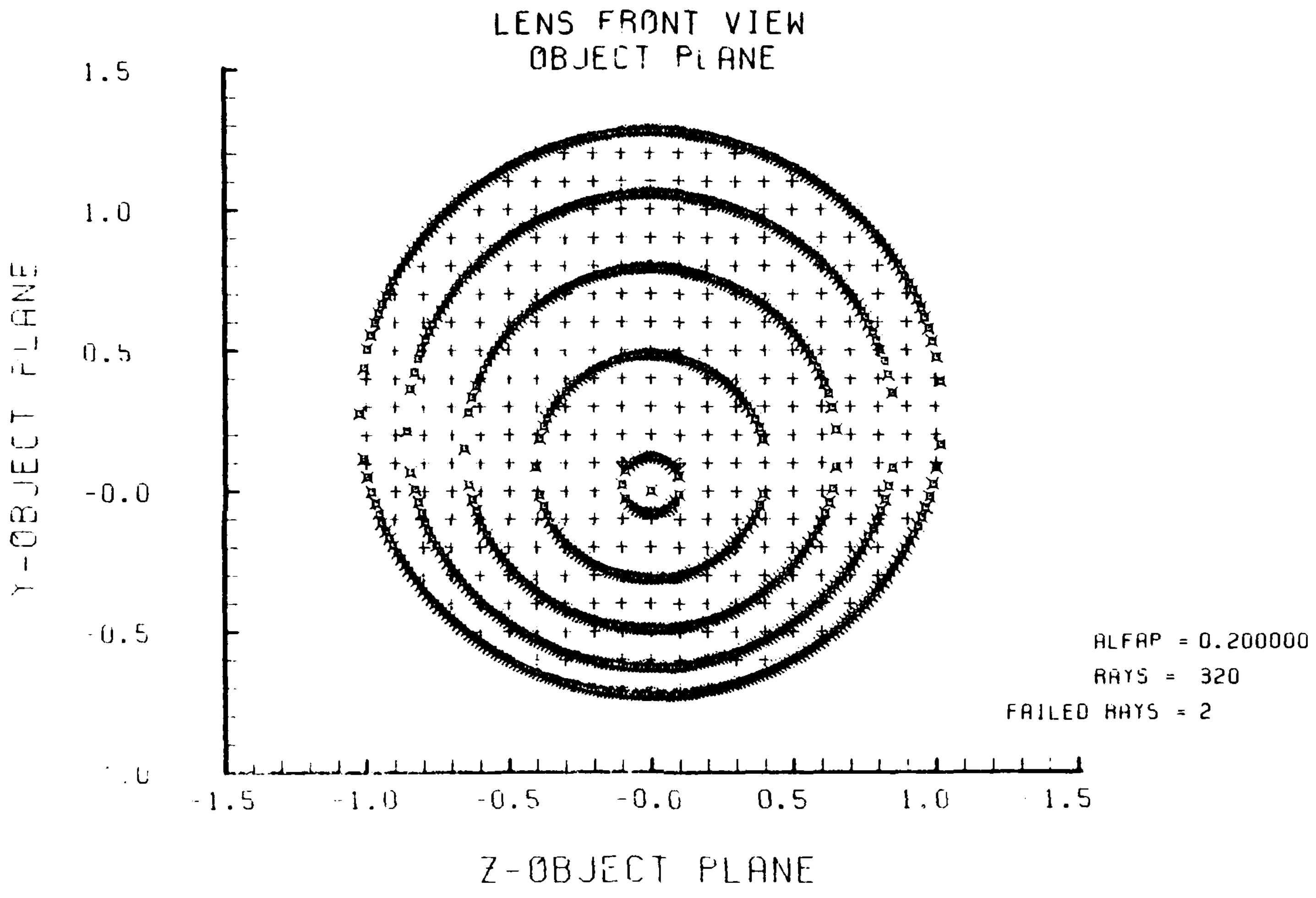

Figure D-9. HIN Object Plane at α_p = 0.3 Radians, N_2 = 1.5

AD-A125 167 AERODYNAMICALLY EFFICIENT GRADIENT REFRACTIVE INDEX MISSILE SEEKER LENS(U) NAVAL POSTGRADUATE SCHOOL MONTEREY CA H M CARR OCT 82 NPS67-82-012 3/6

UNCLASSIFIED F/G 16/4 NL

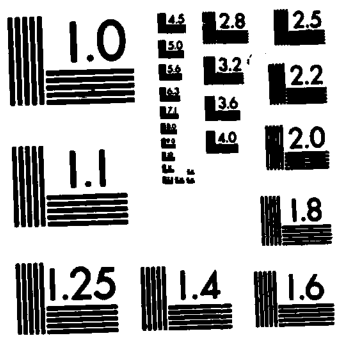

MICROCOPY RESOLUTION TEST CHART
NATIONAL BUREAU OF STANDARDS-1963-A

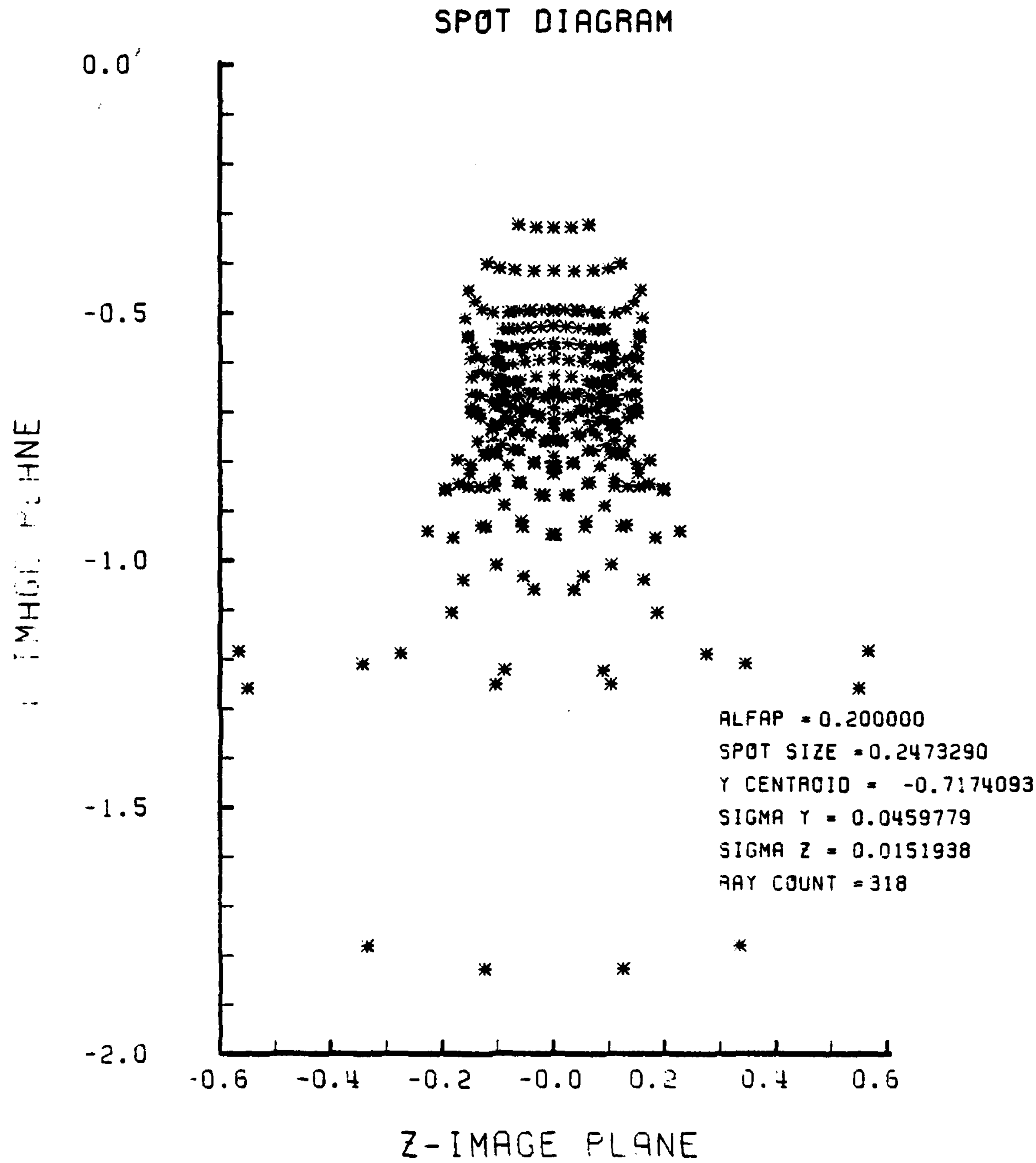

Figure D-10. Spot Diagram of HIN Lens at $\alpha_p = 0.3$ Radians, $N_2 = 1.5$

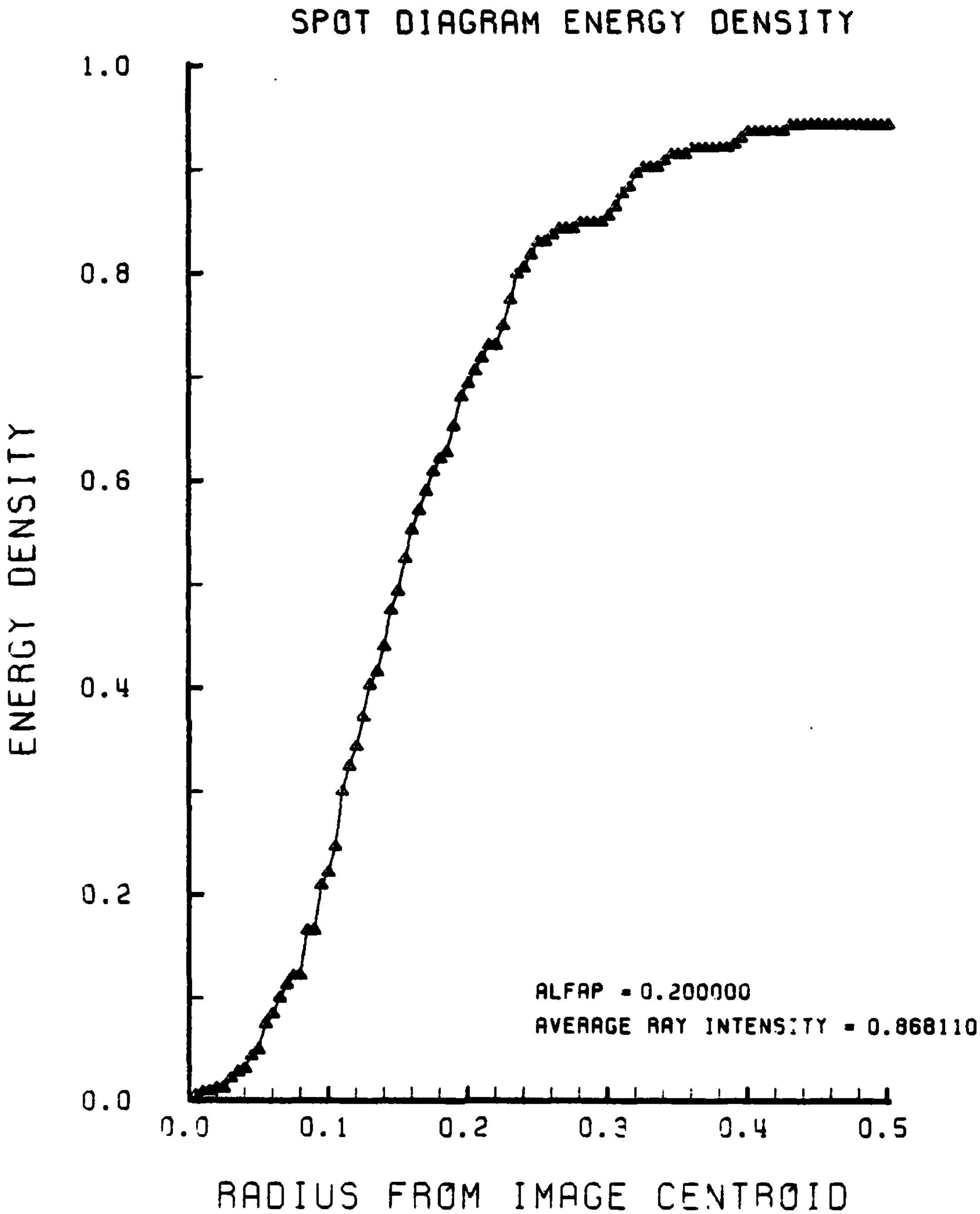

Figure D-11. HIN Lens Encircled Energy at α_p = 0.3 Radians, N_2 = 1.5

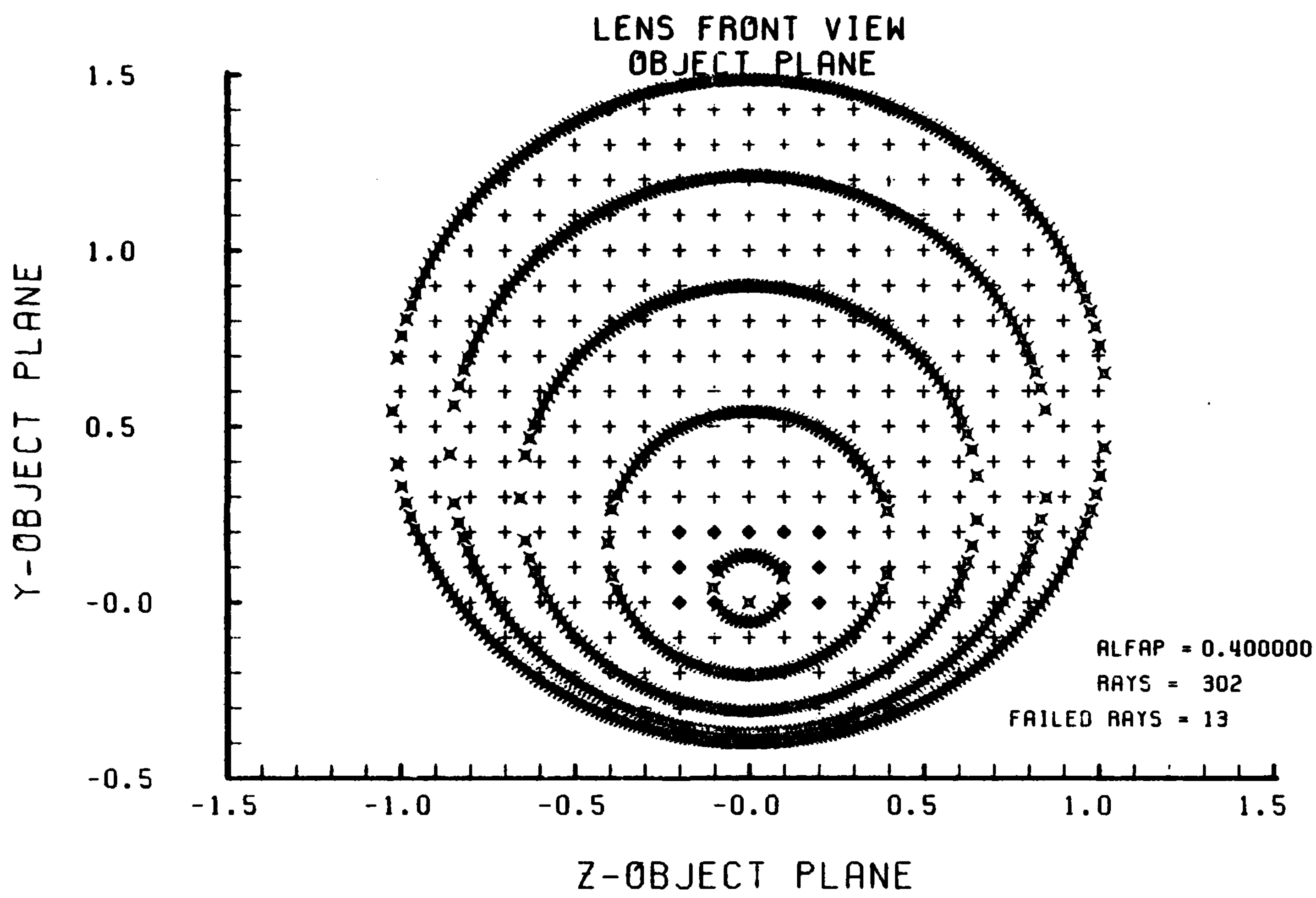

Figure D-12. HIN Object Plane at α_p = 0.4 Radians, N_2 = 1.5

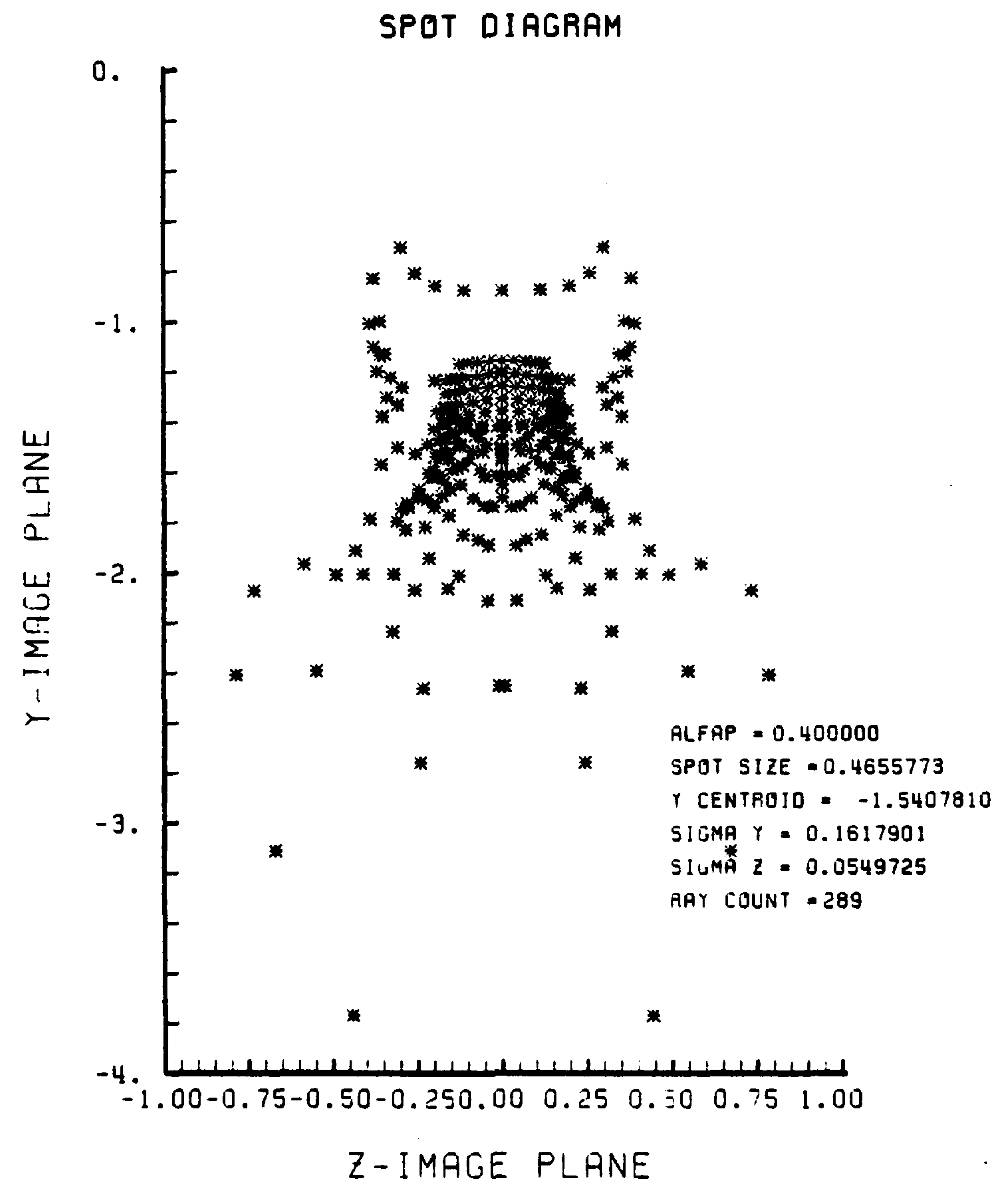

Figure D-13. Spot Diagram of HIN lens at $\alpha_p = 0.4$ Radians, $N_2 = 1.5$

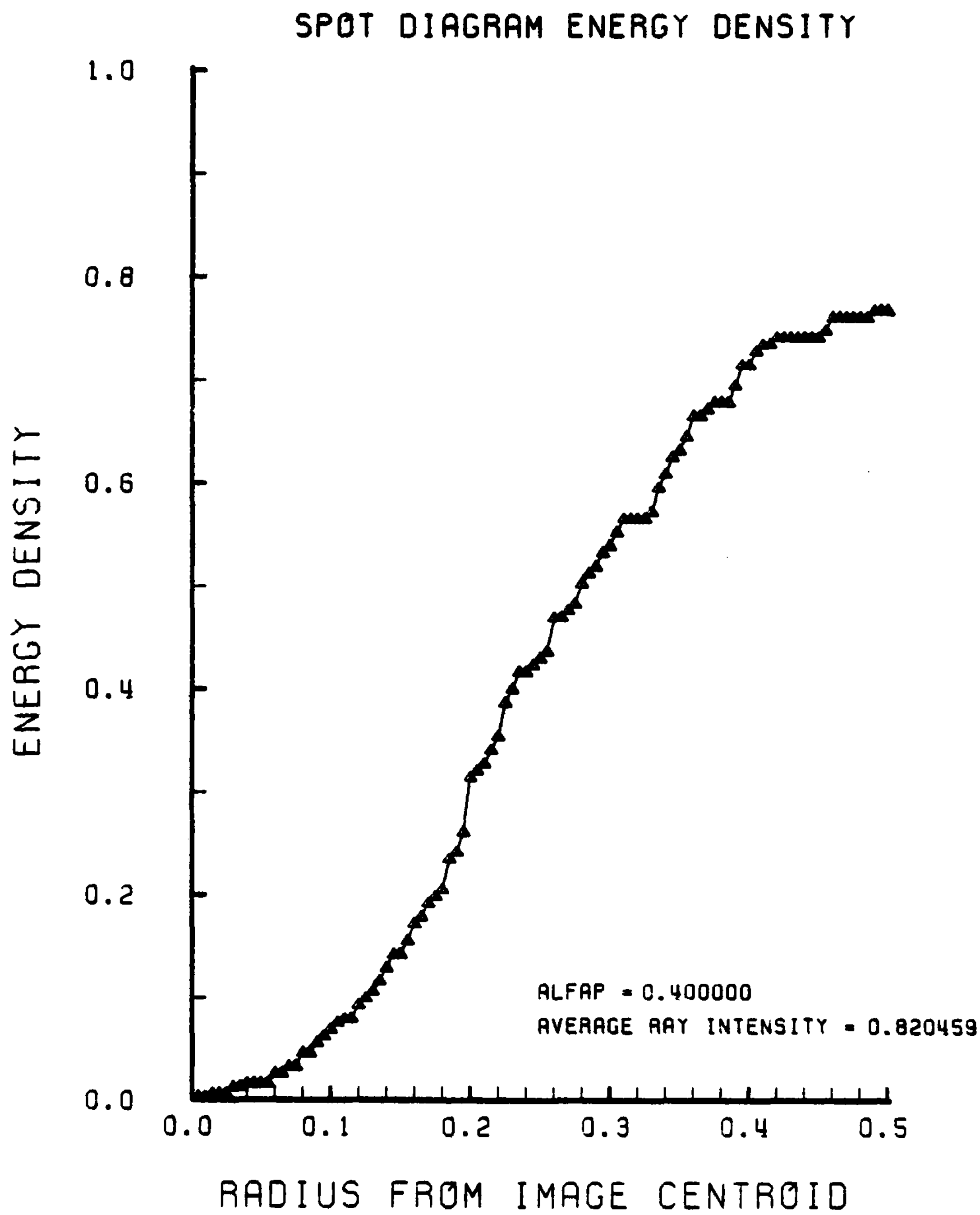

Figure D-14. Encircled Energy Plot at $\alpha_p = 0.4$ Radians, $N_2 = 1.5$

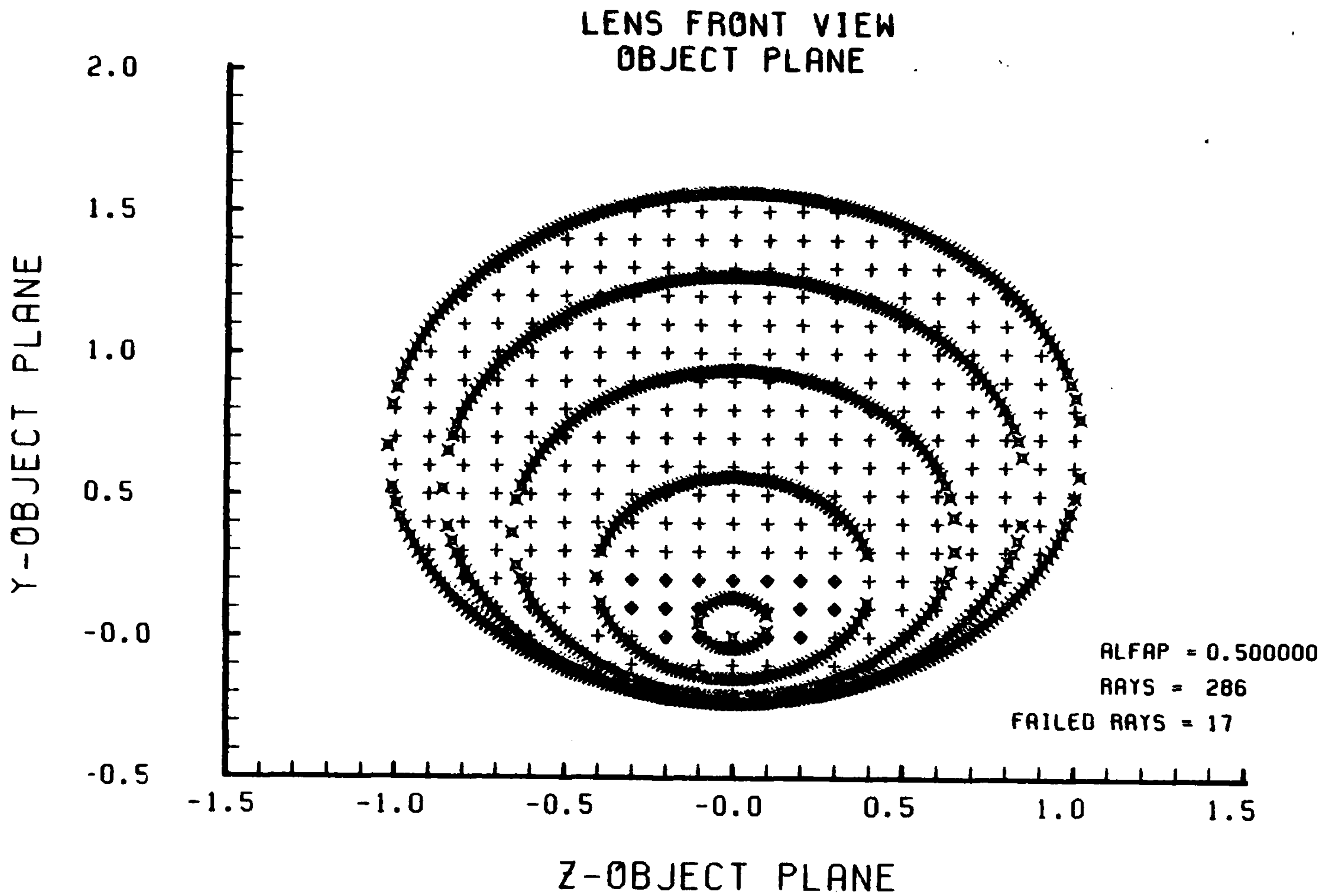

Figure D-15. HIN Lens Object Plane at $\alpha_p = 0.5$ Radians, $N_2 = 1.5$

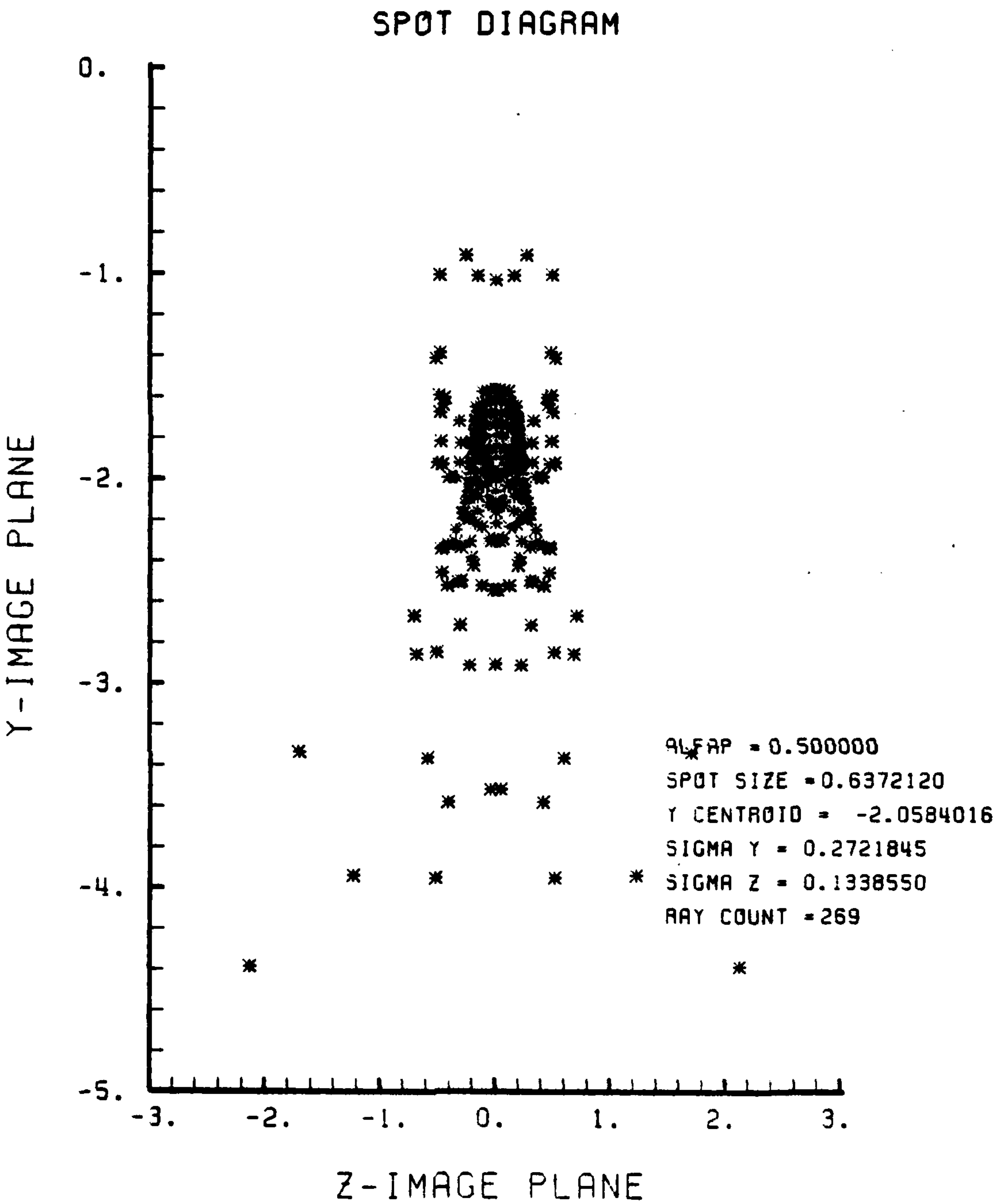

Figure D-16. **Spot Diagram of HIN Lens at α_p = 0.5 Radians, N_2 = 1.5**

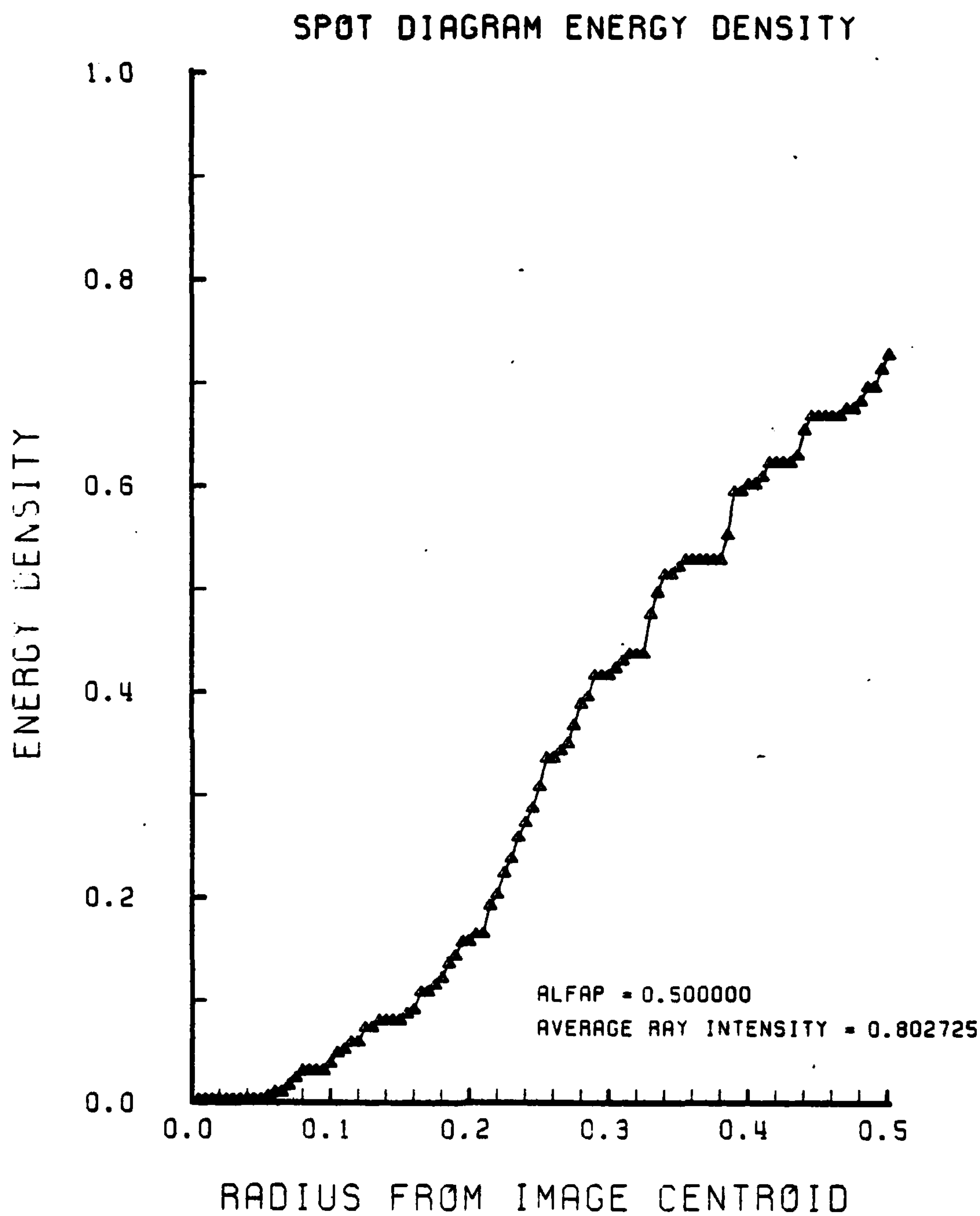

Figure D-17. **Encircled Energy Plot at α_p = 0.5 Radians, N_2 = 1.5**

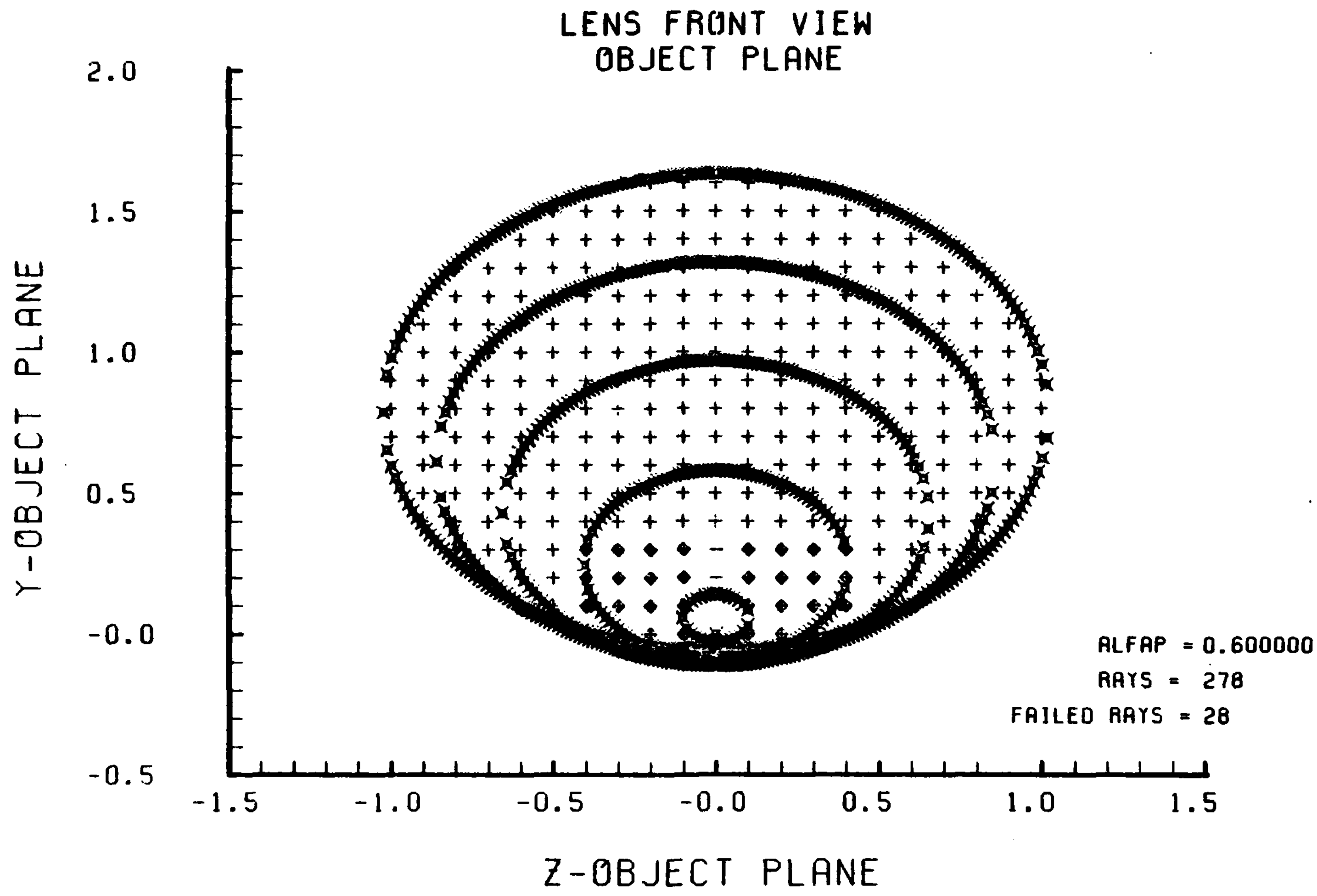

Figure D-18. HIN Object Plane at α_p = 0.6 Radians, N_2 = 1.5. Overlapping Portions of Inner Ellipses are hidden lines.

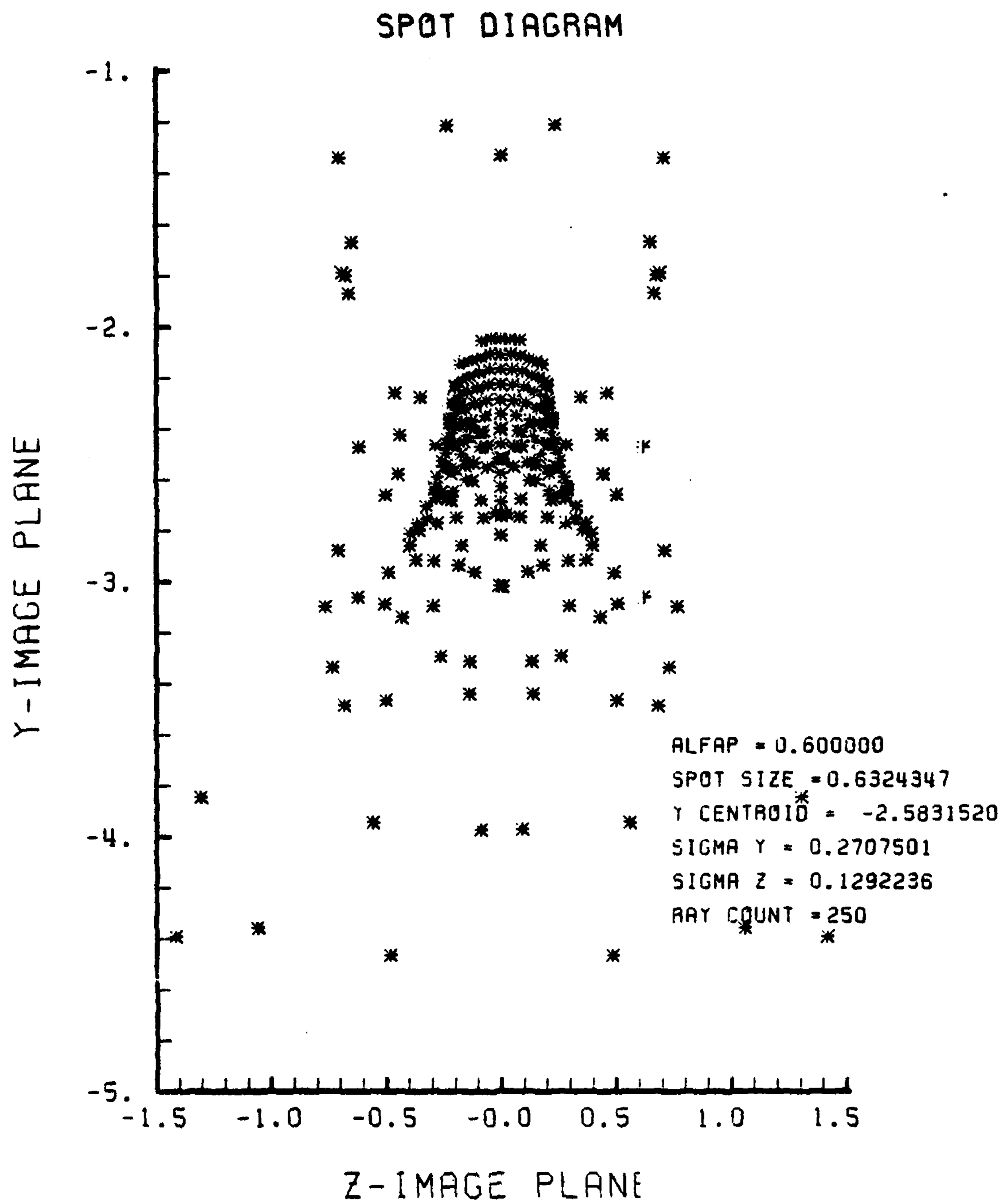

Figure D-19. Spot Diagram of HIN Lens at α_p = 0.6 Radians, N_2 = 1.5

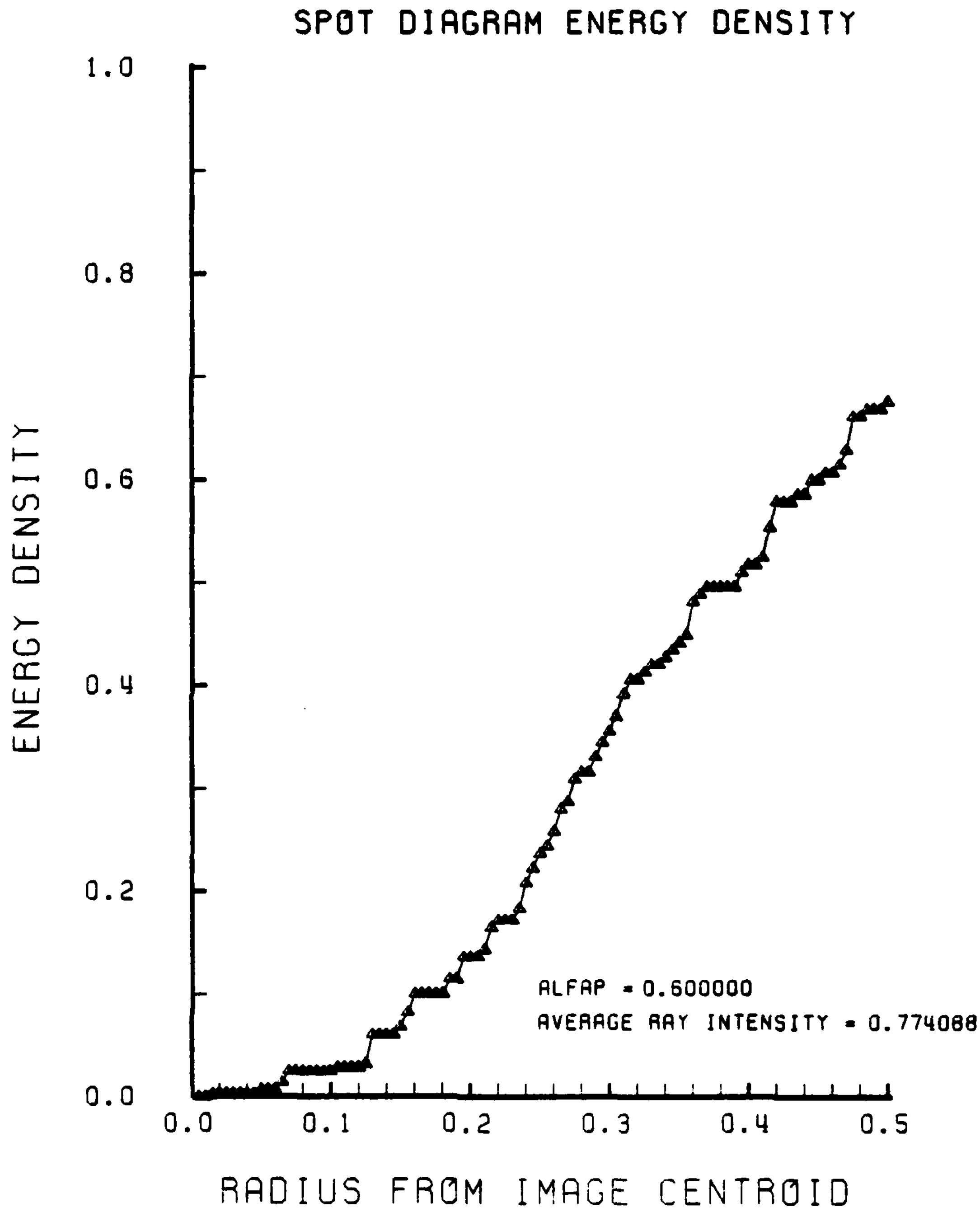

Figure D-20. Encircled Energy Plot at $\alpha_p = 0.6$ Radians, $N_2 = 1.5$

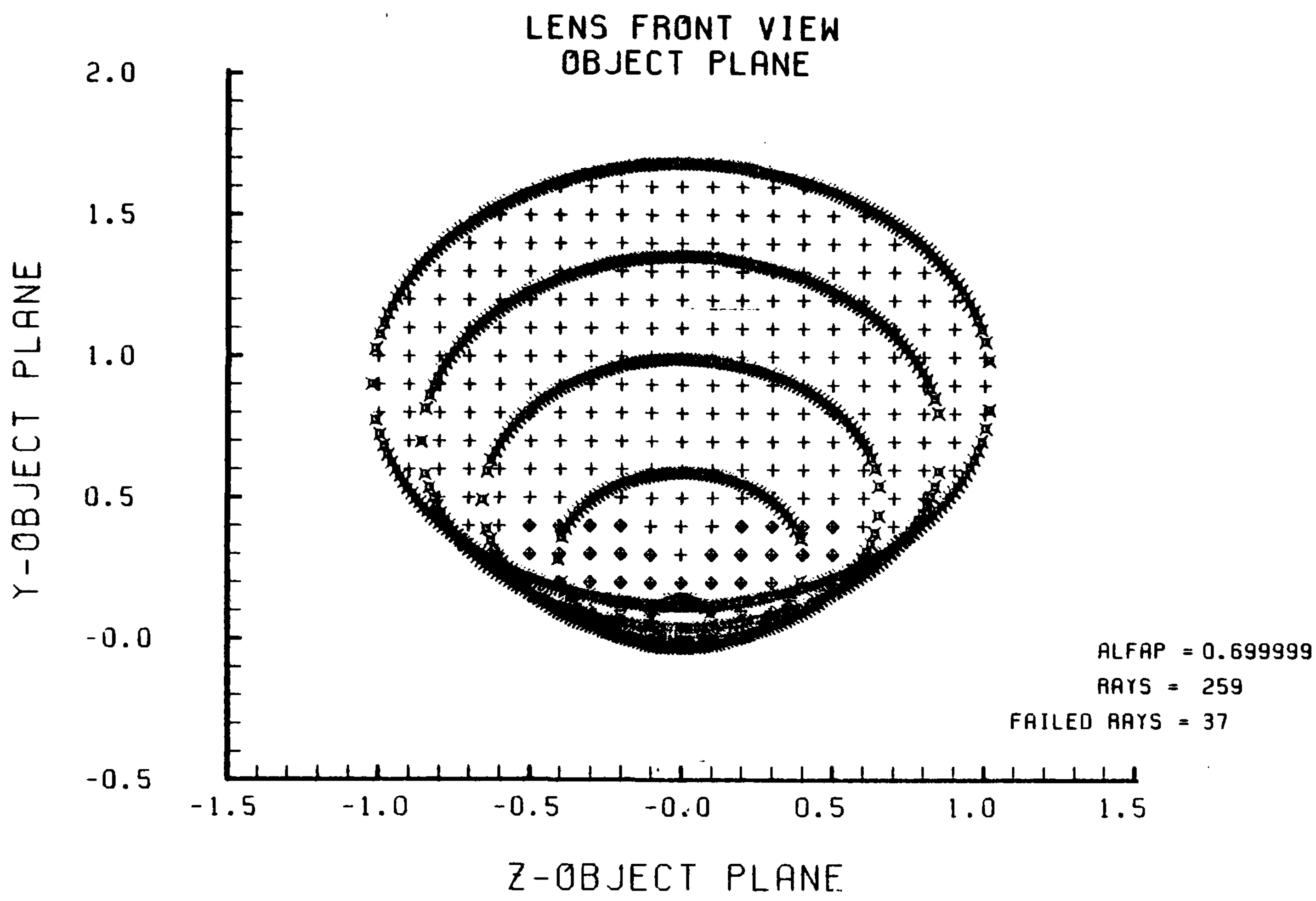

Figure D-21. HIN Object Plane at $\alpha_p = 0.7$ Radians, $N_2 = 1.5$. Overlapping Portions of Inner Ellipses are Hidden Lines.

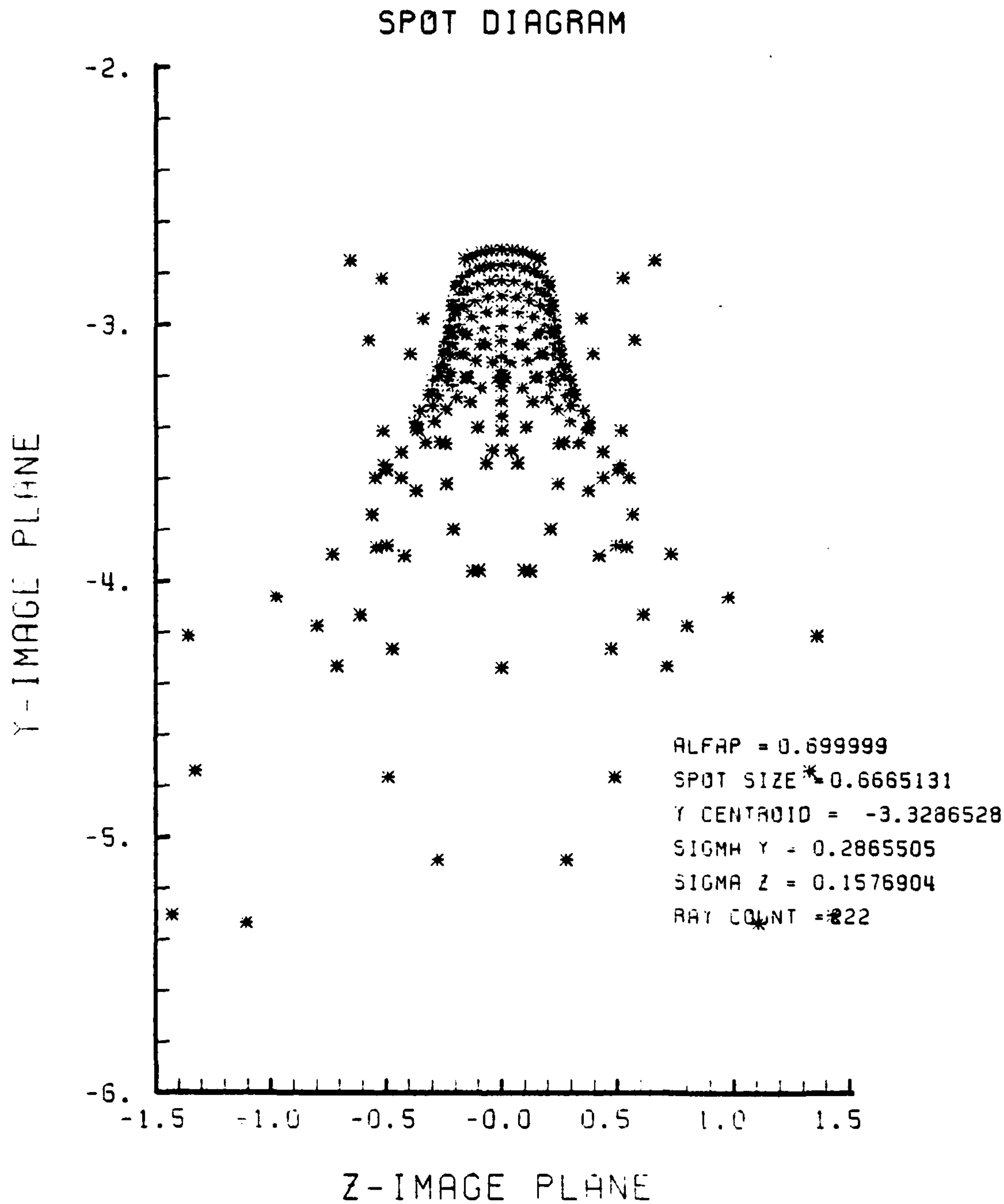

Figure D-22. Spot Diagram of HIN Lens at α_p = 0.7 Radians, N_2 = 1.5

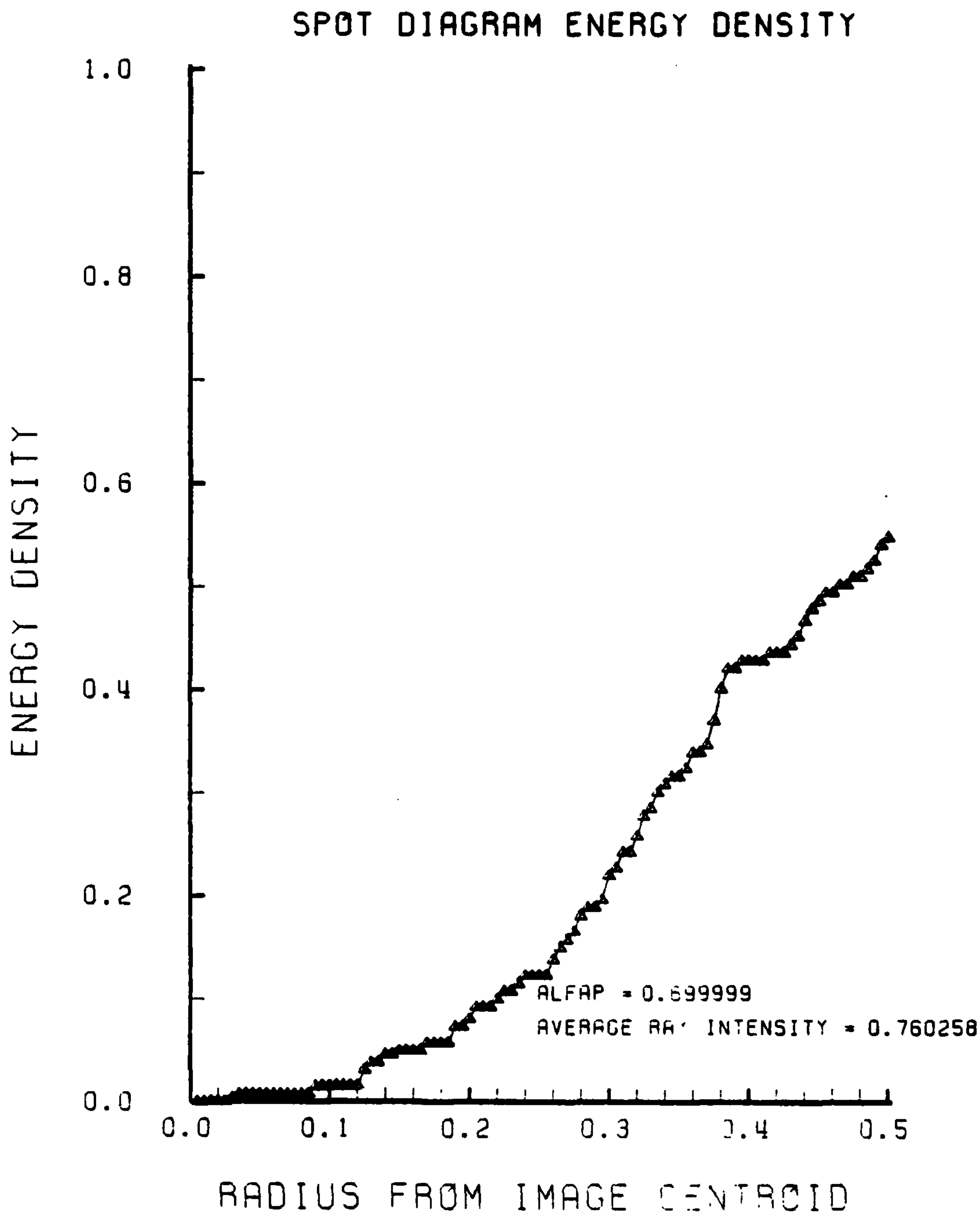

Figure D-23. Encircled Energy Plot at $\alpha_p = 0.7$ Radians, $N_2 = 1.5$

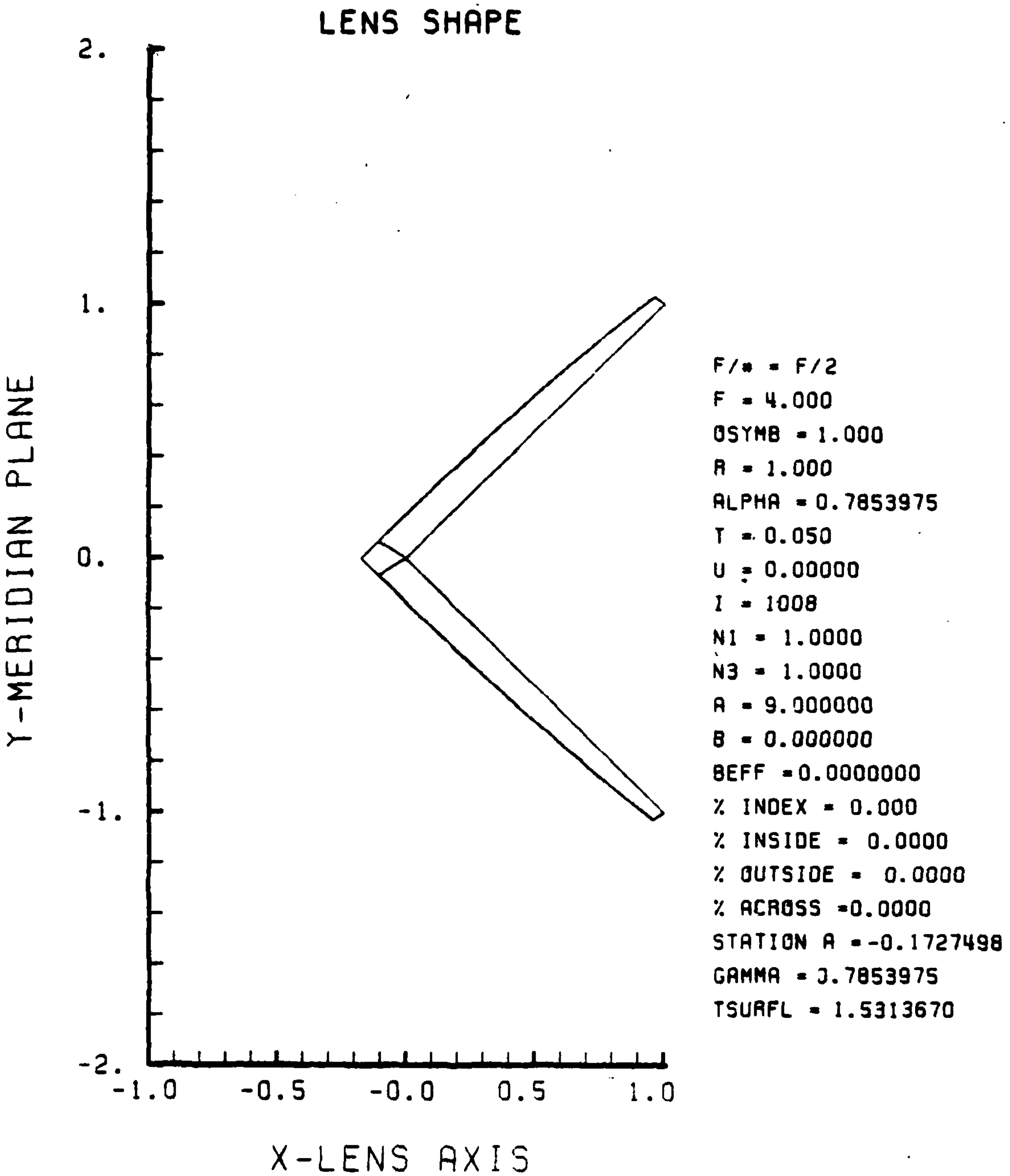

Figure D-24. HIN Lens Design for N_2 = 3.0

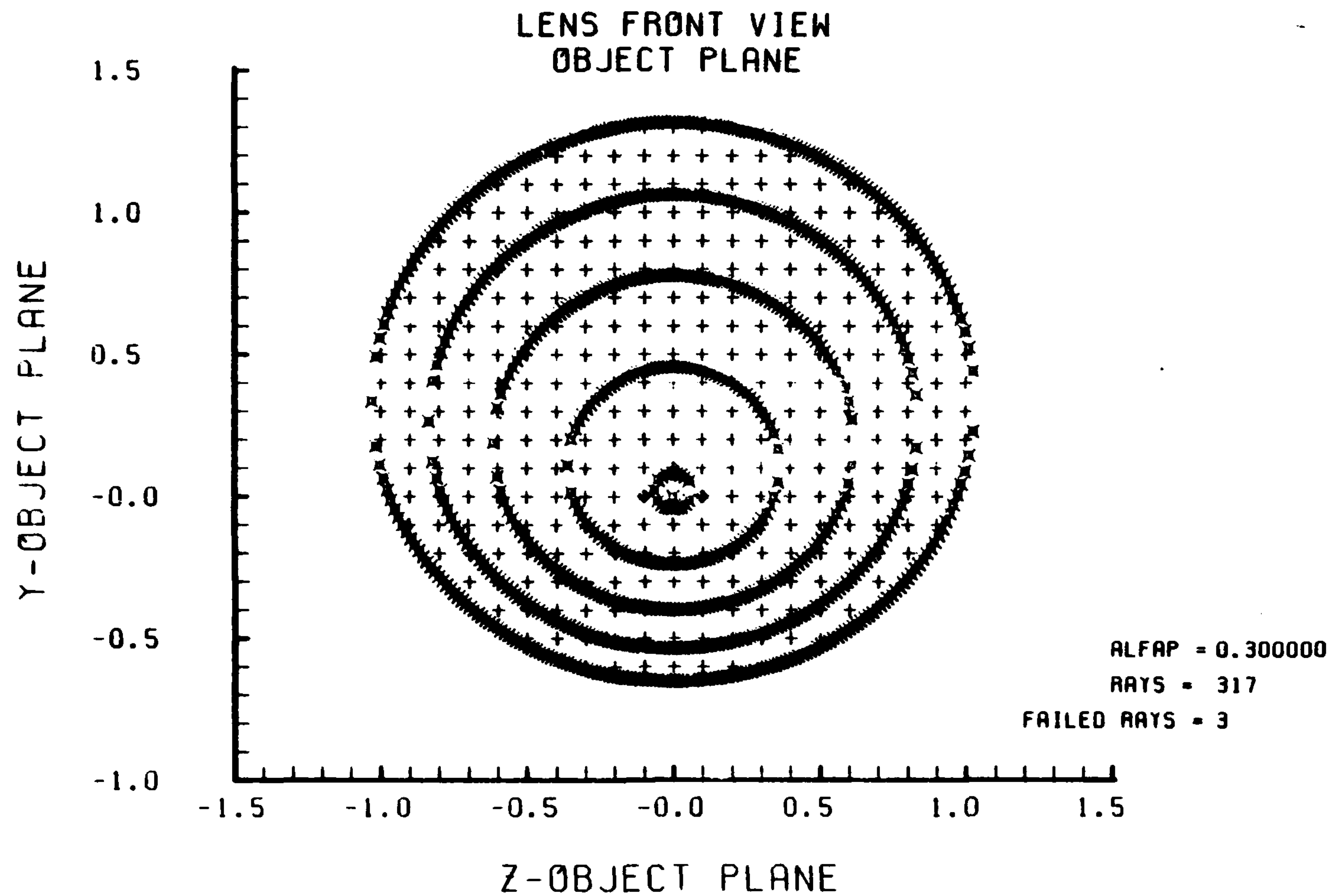

Figure D-25. Object Plane of HIN Lens in Figure D-24 at α_p = 0.3 Radians

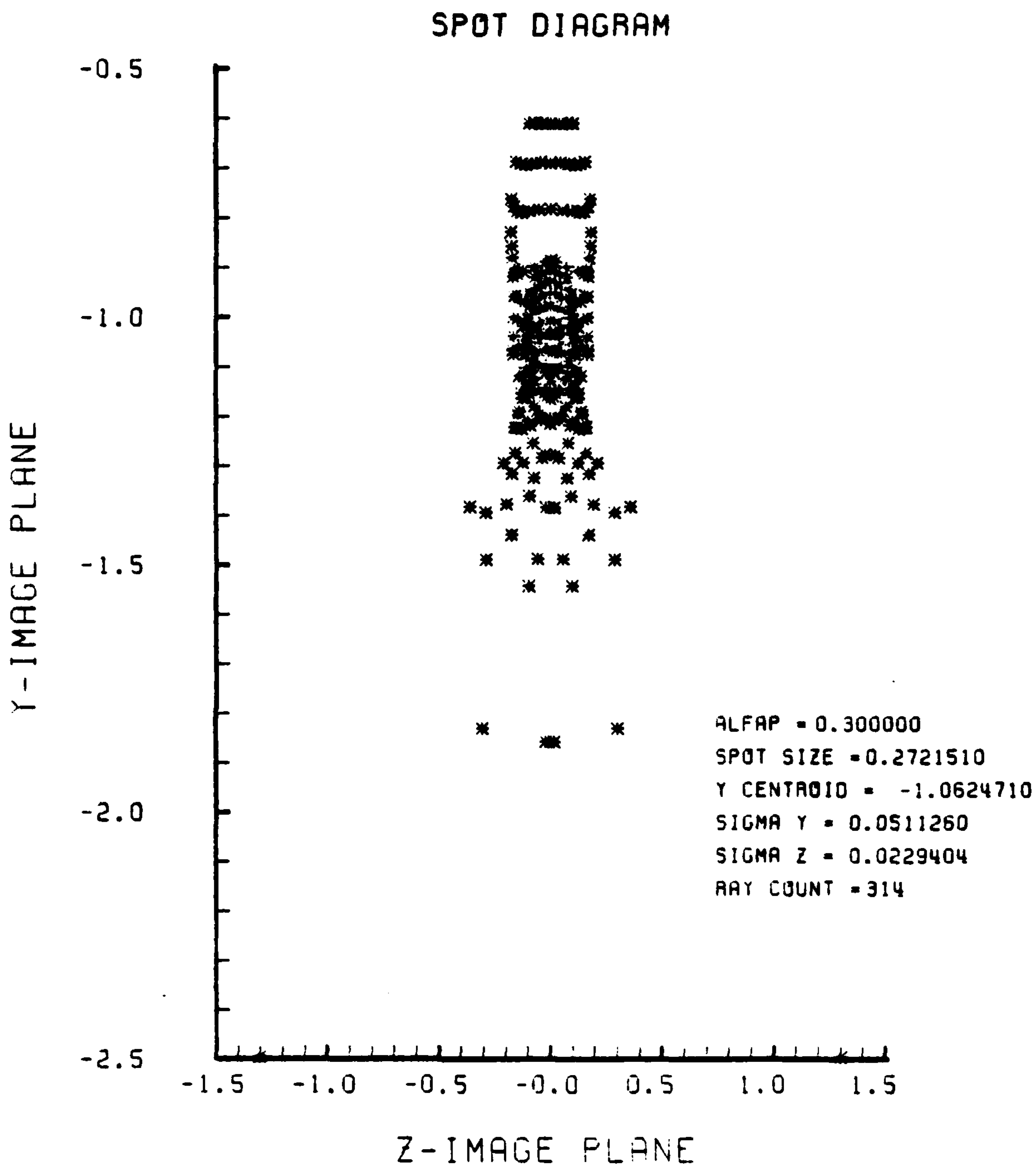

Figure D-26. Spot Diagram Corresponding to Figure D-25

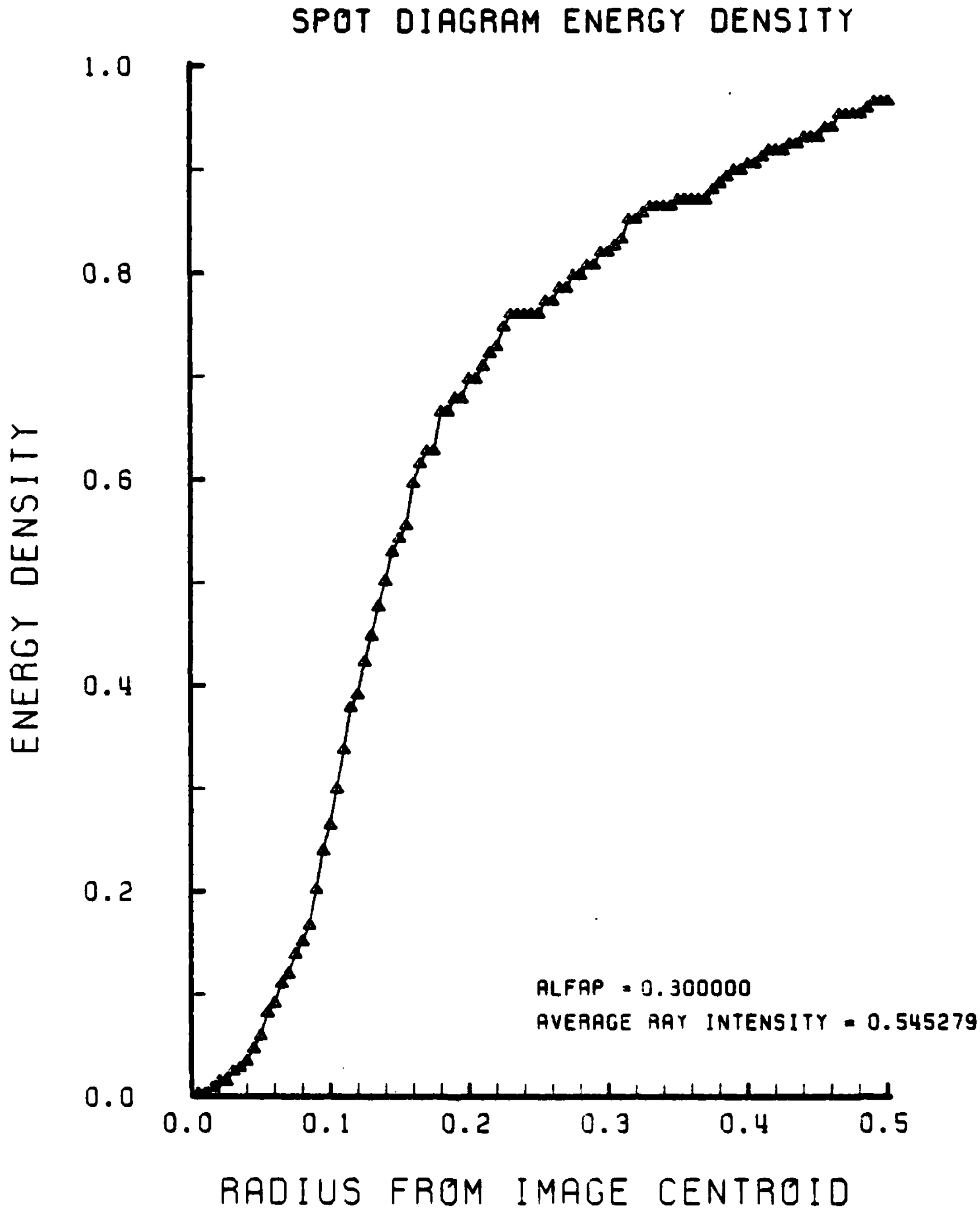

Figure D-27. Encircled Energy Plot for Spot Diagram of Figure D-26

APPENDIX E

GRIN LENS PERFORMANCE PLOTS IN THE LOW RANGE OF INDICES OF REFRACTION (a = 2.25)

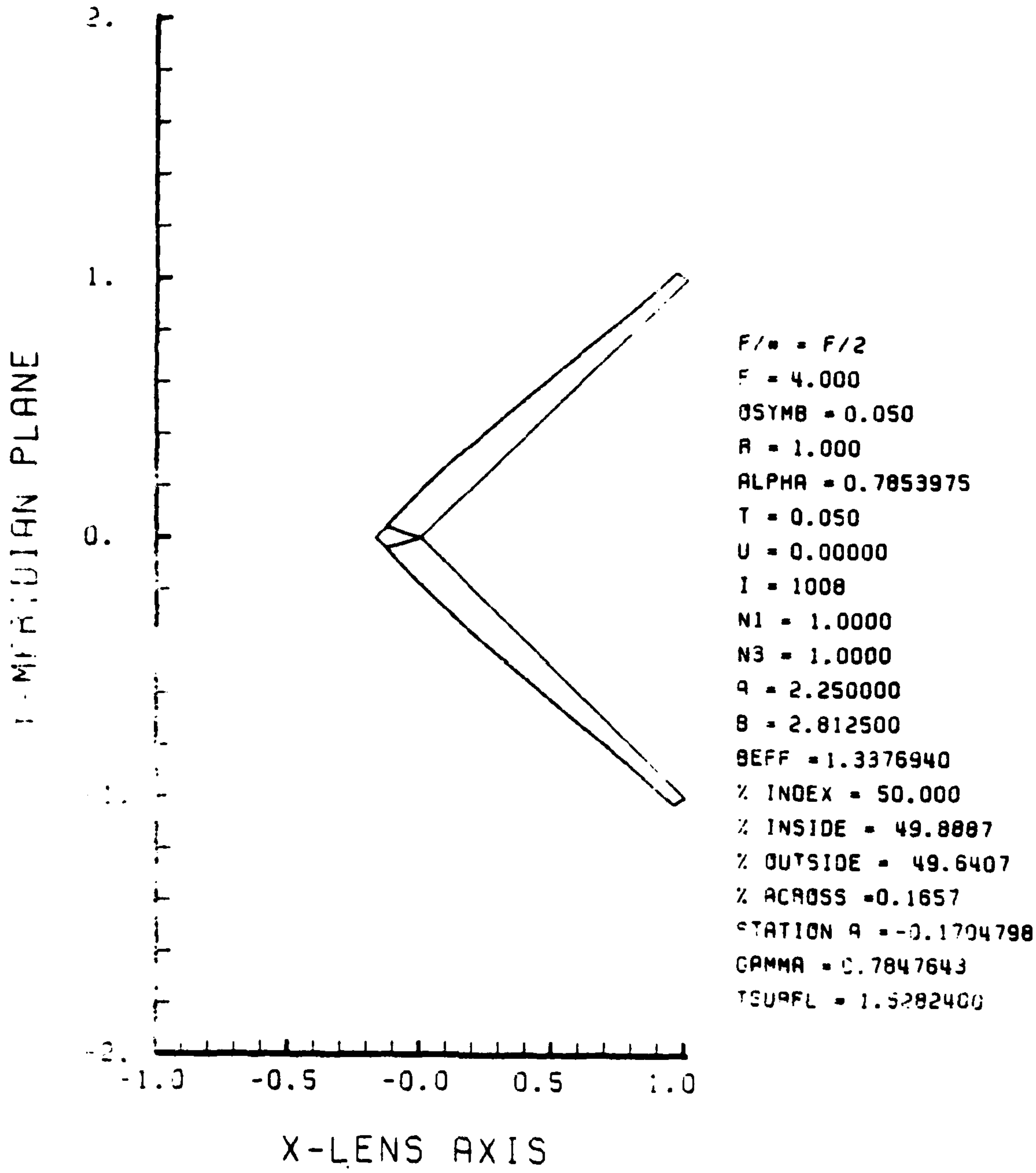

Figure E-1. GRIN Lens Shape at +50%, OB = 0.05, a = 2.25

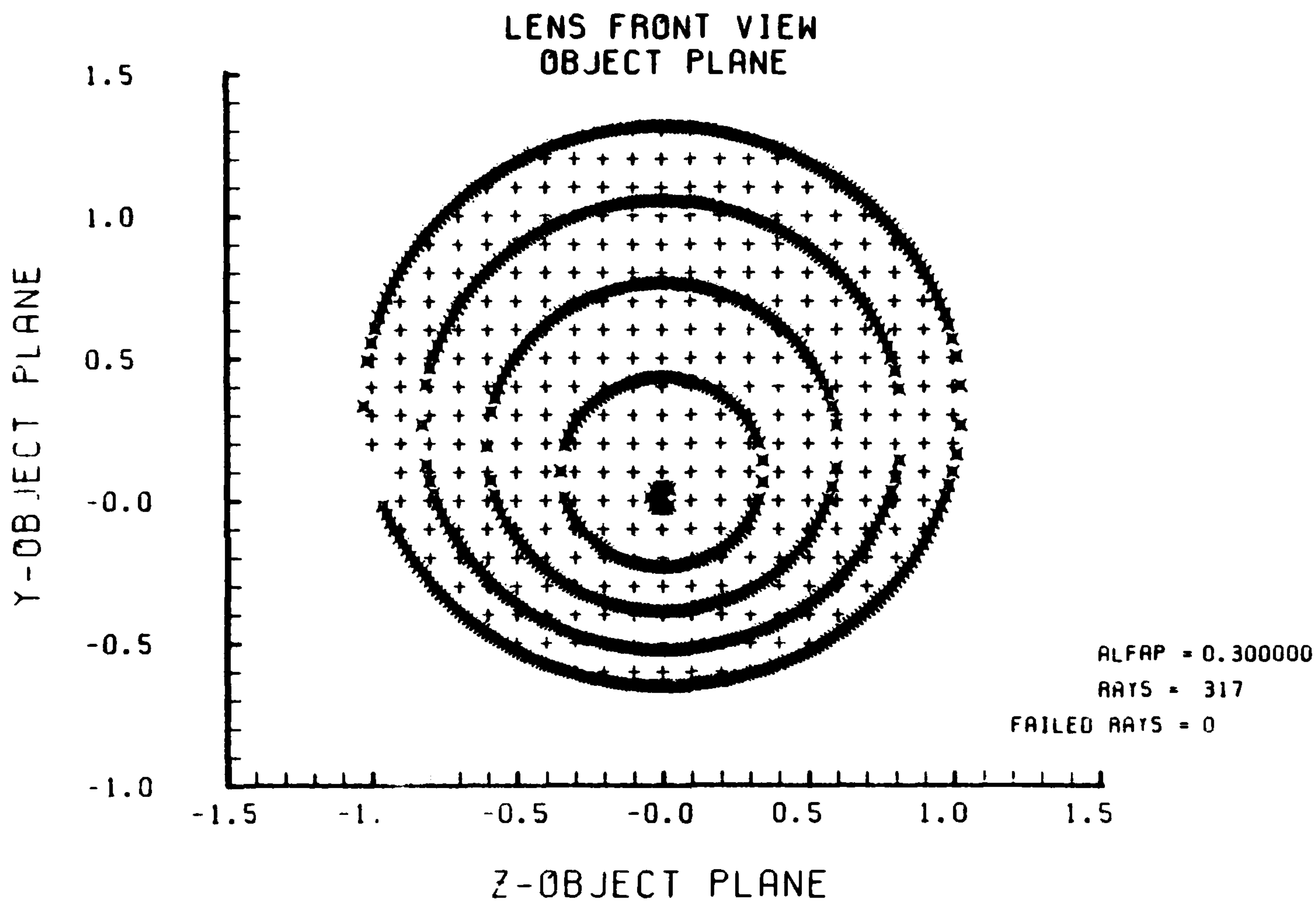

Figure E-2. Grid Plane at $\alpha_p = 0.3$ for Lens of Figure E-1

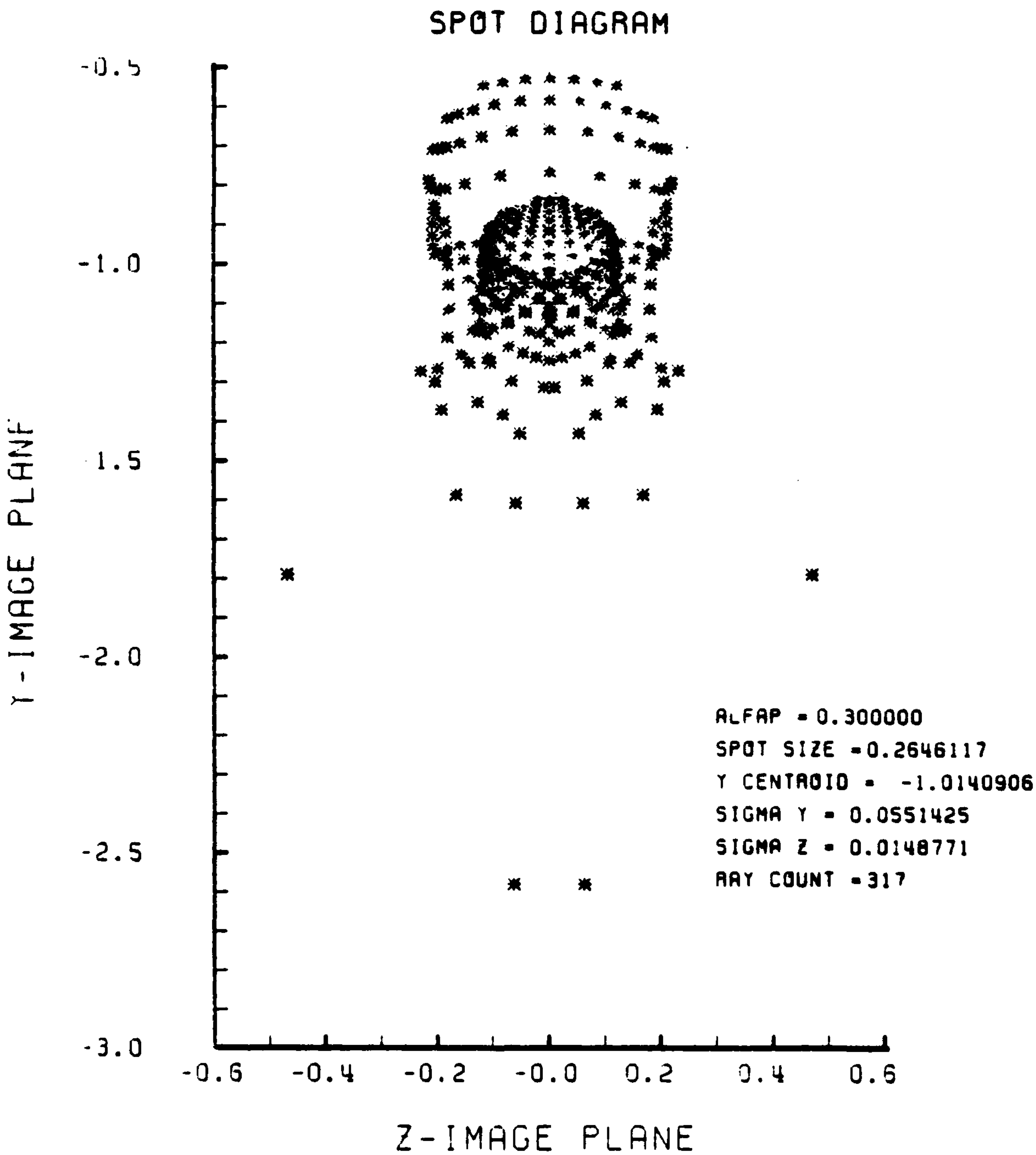

Figure E-3. Spot Diagram for Grid of Figure E-2

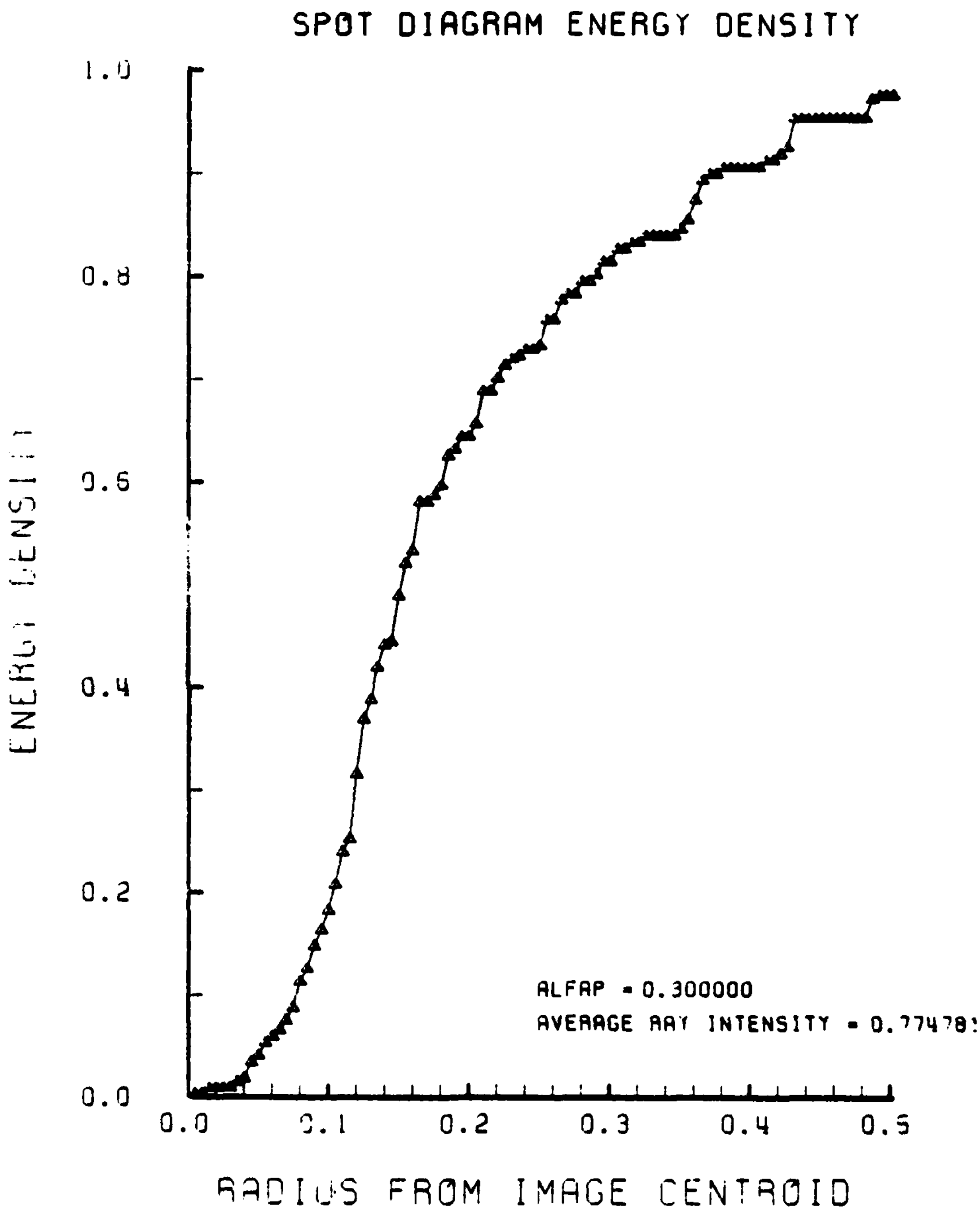

Figure E-4. Encircled Energy of Figure E-3

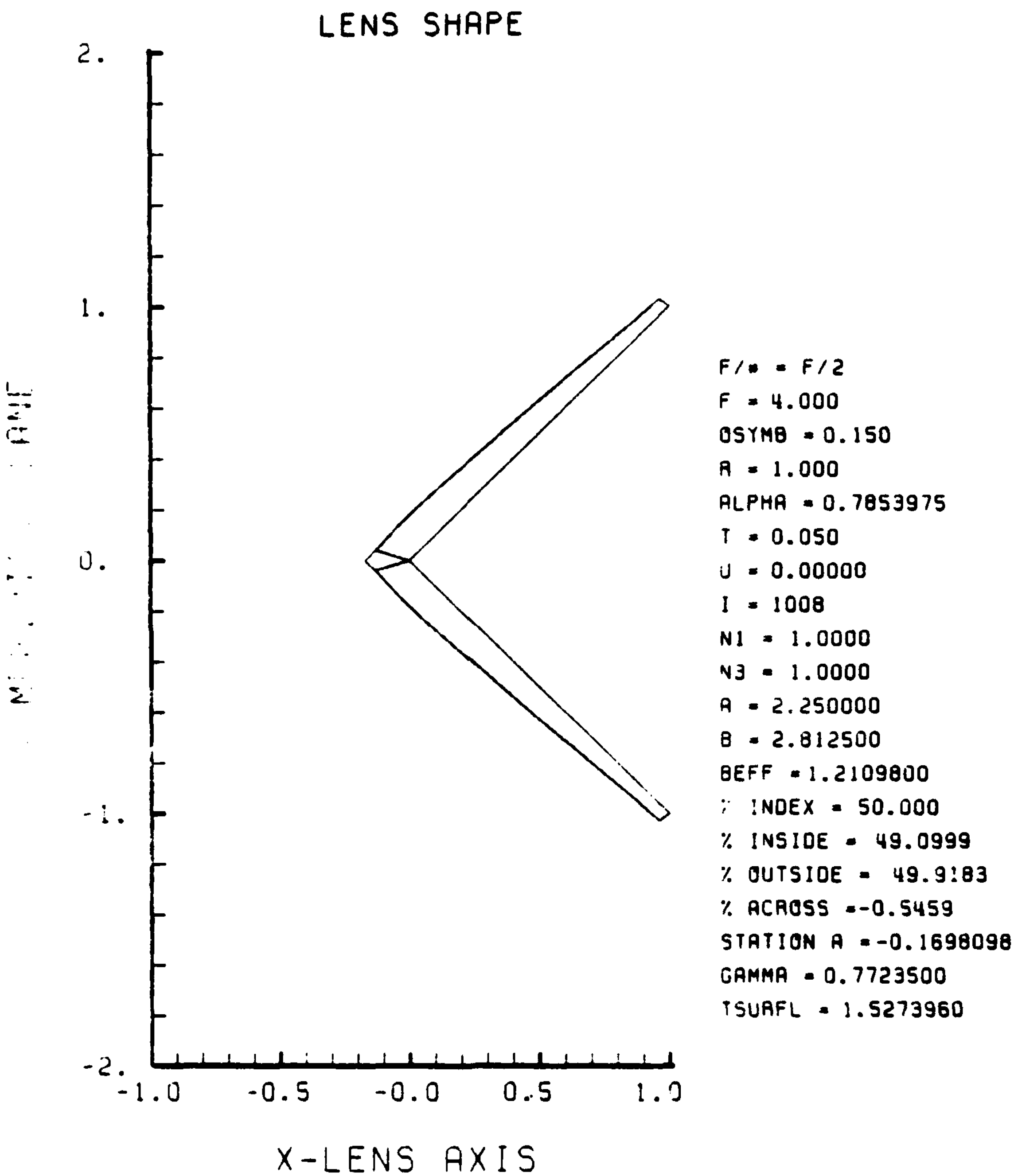

Figure E-5. GRIN Lens Shape at +50%, OB = 0.15, a = 2.25

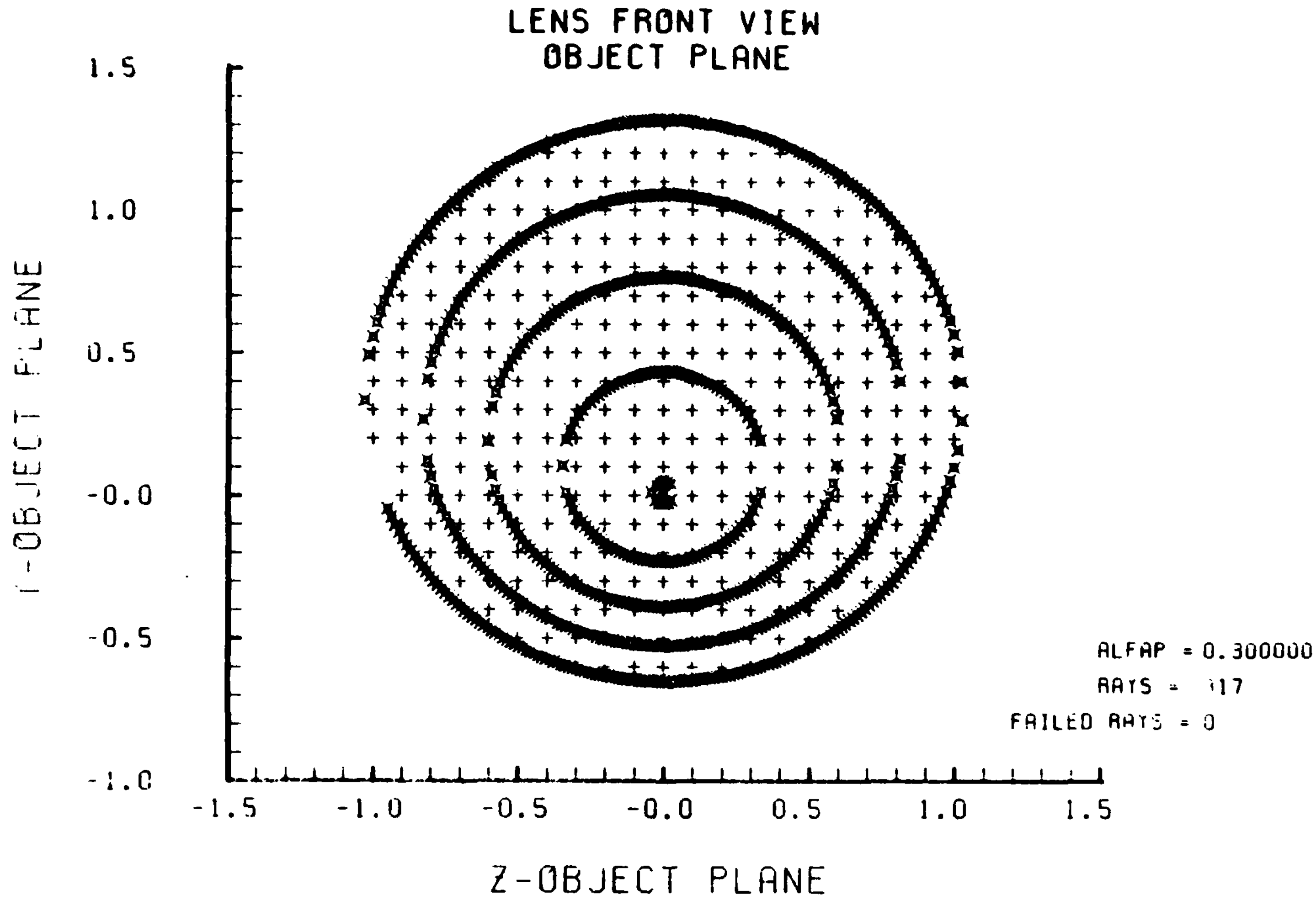

Figure E-6. Grid Plane at $\alpha_p = 0.3$ for Lens of Figure E-5

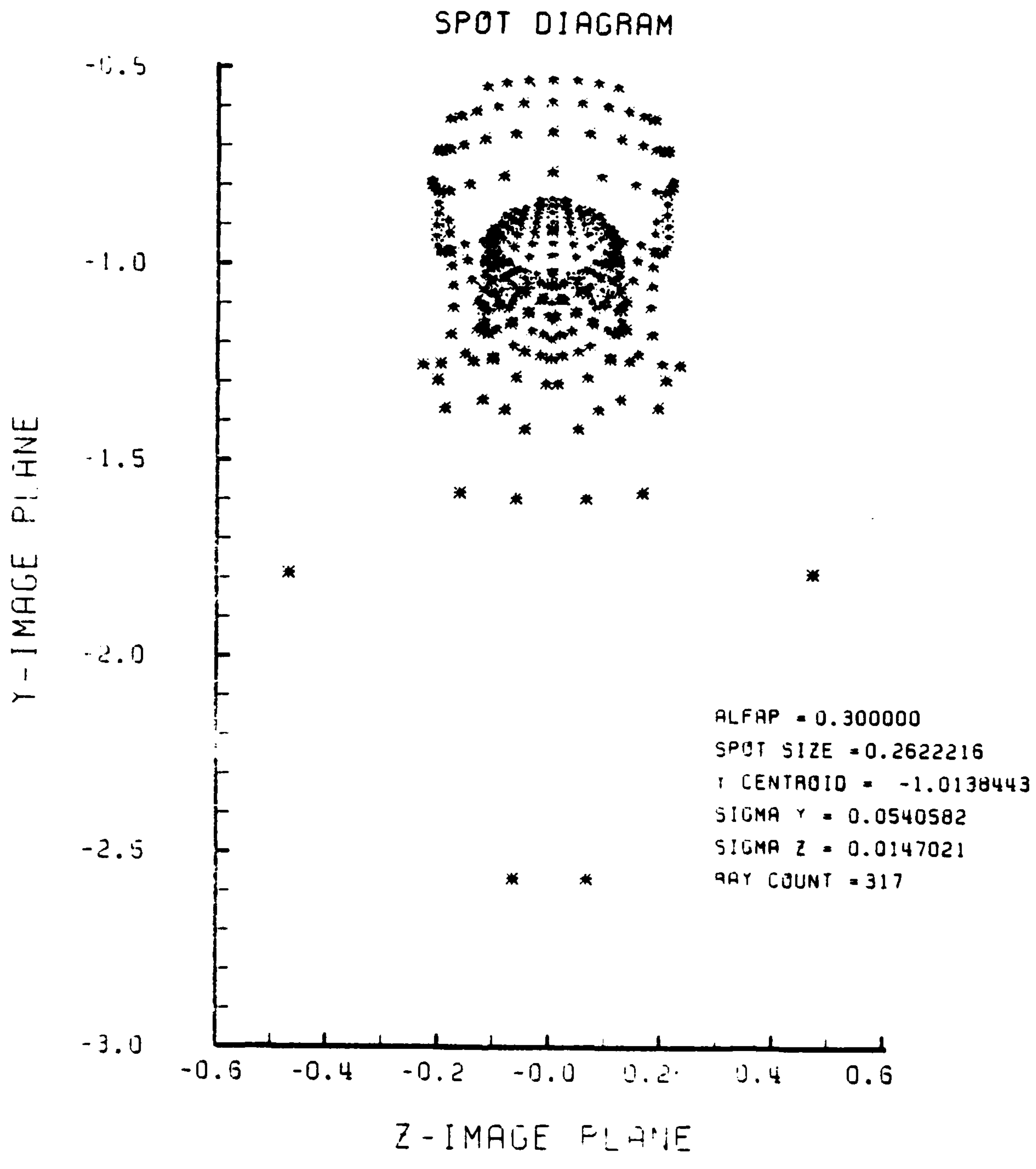

Figure E-7. Spot Diagram for Grid of Figure E-6

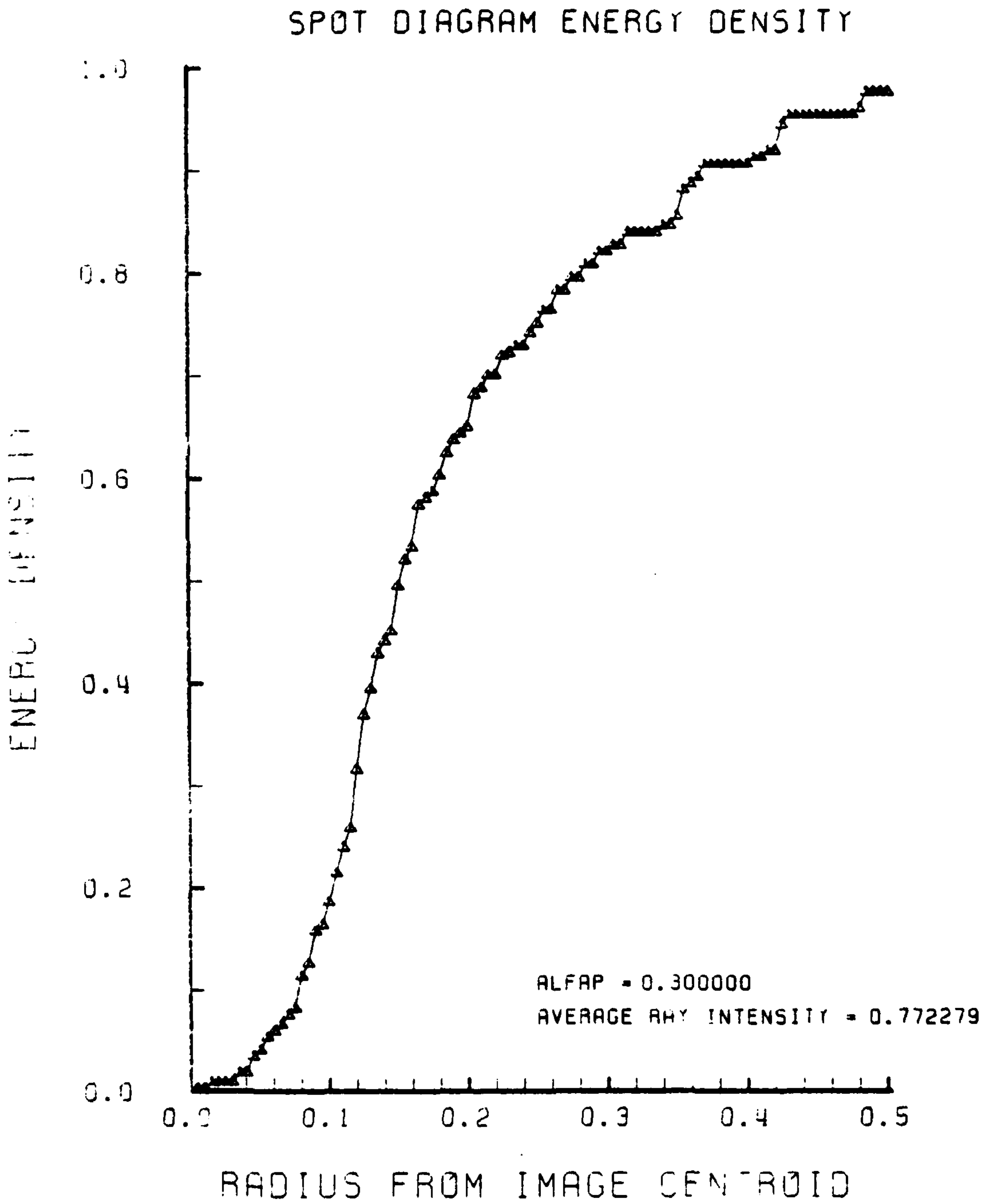

Figure E-8. Encircled Energy of Figure E-7

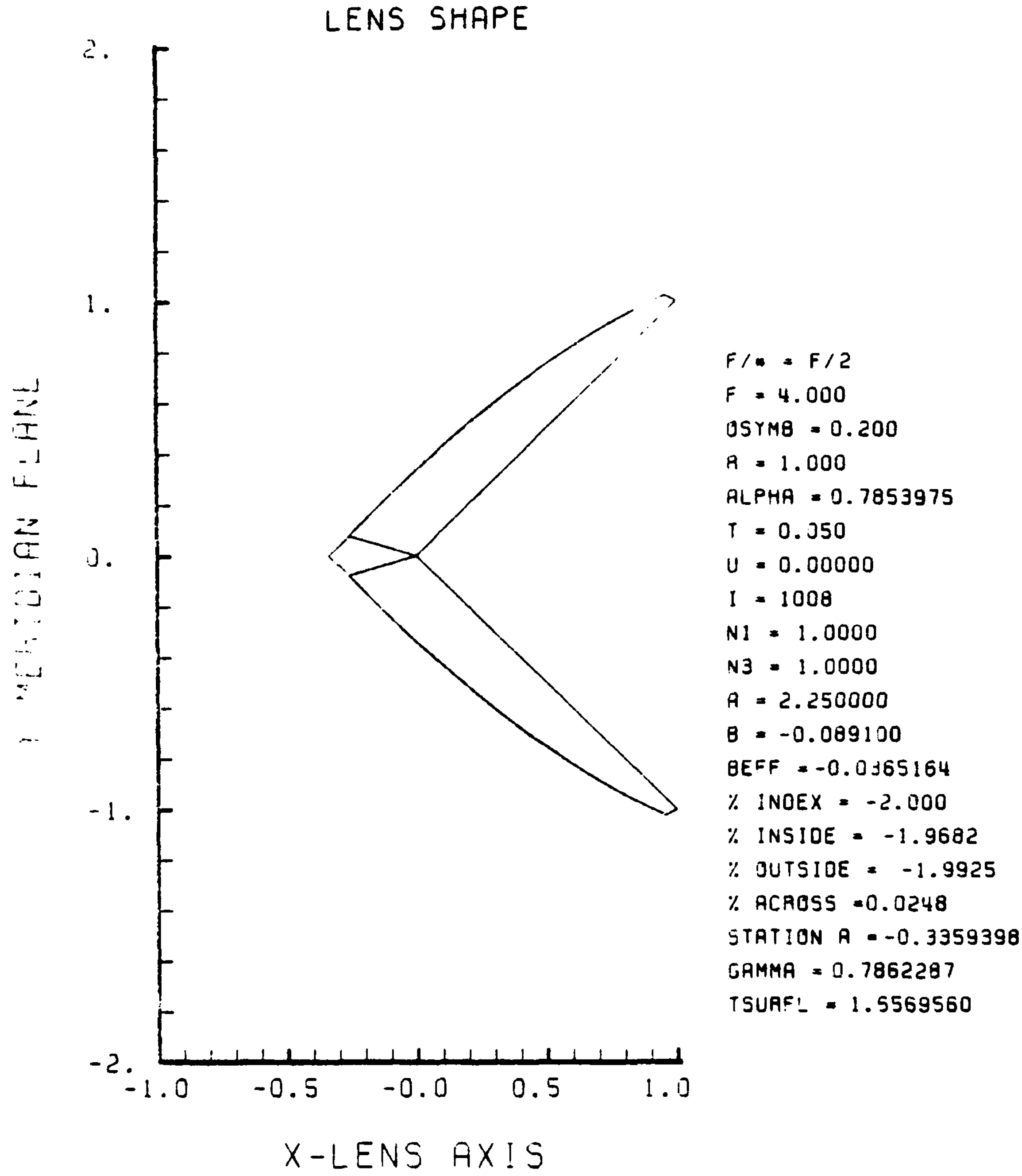

Figure E-9. GRIN Lens Shape at -2%, OB = 0.20, a = 2.25

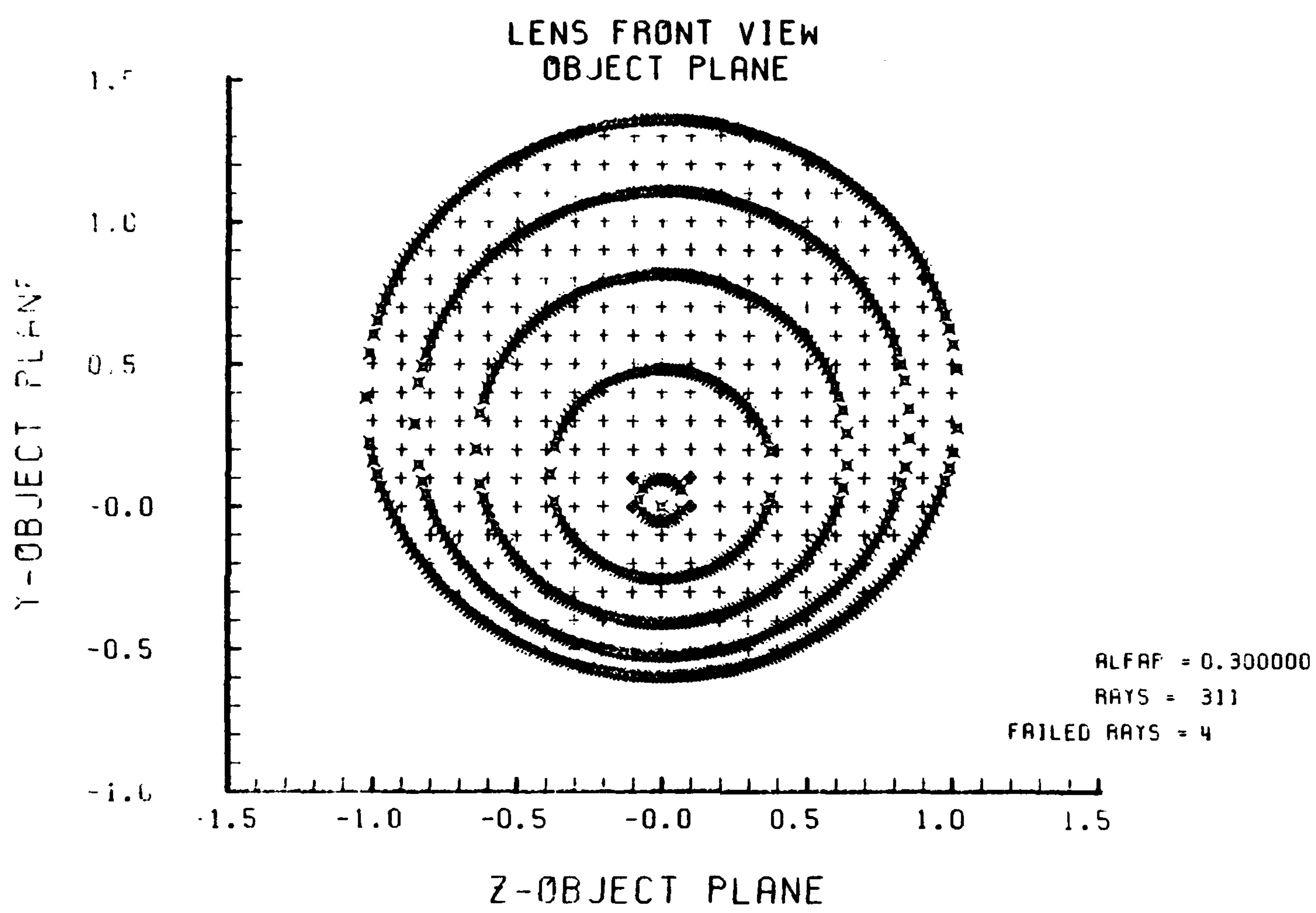

Figure E-10. Grid Plane at $\alpha_p = 0.3$ for Lens of Figure E-9

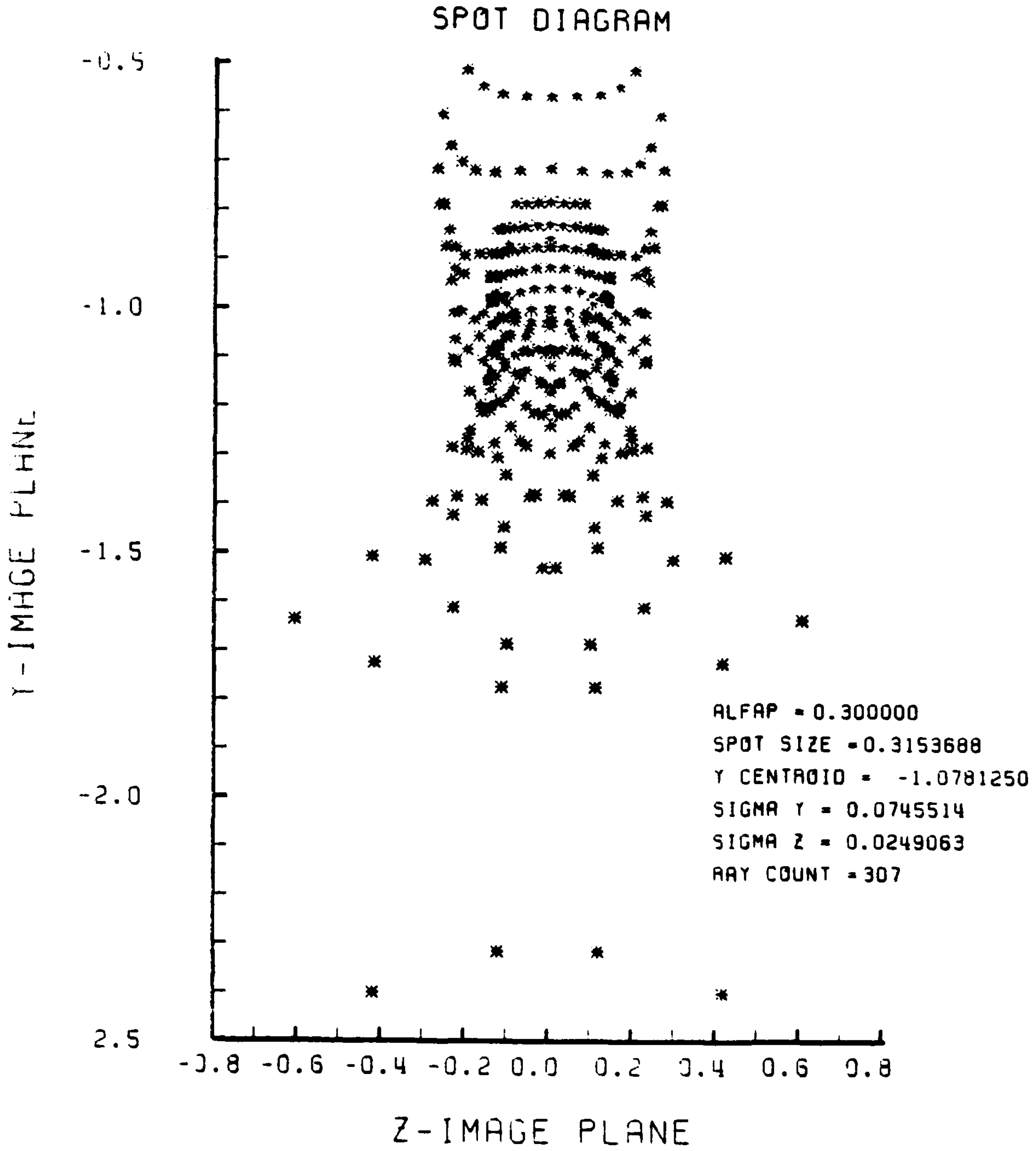

Figure E-11. Spot Diagram for Grid of Figure E-10

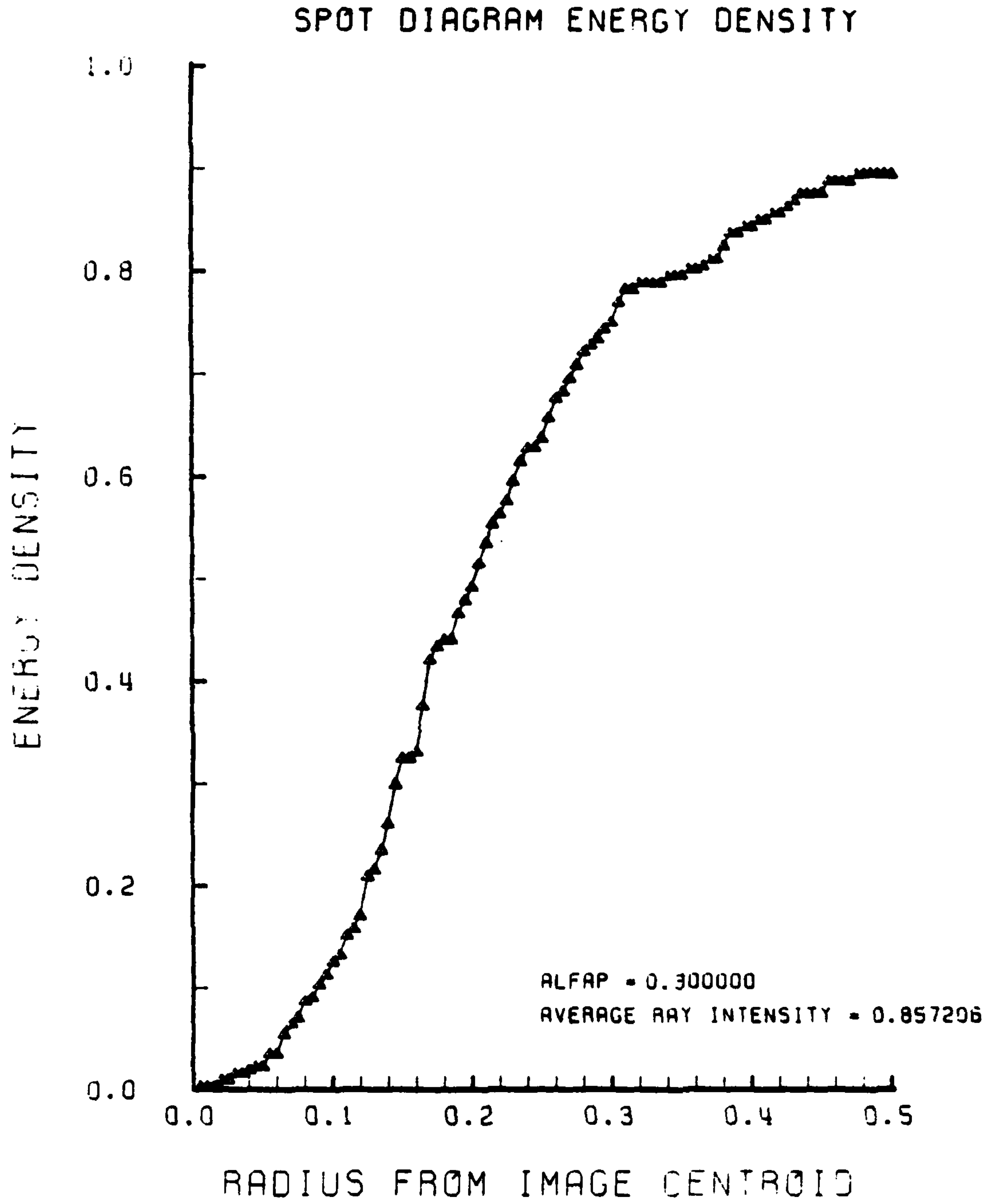

Figure E-12. Encircled Energy of Figure E-11

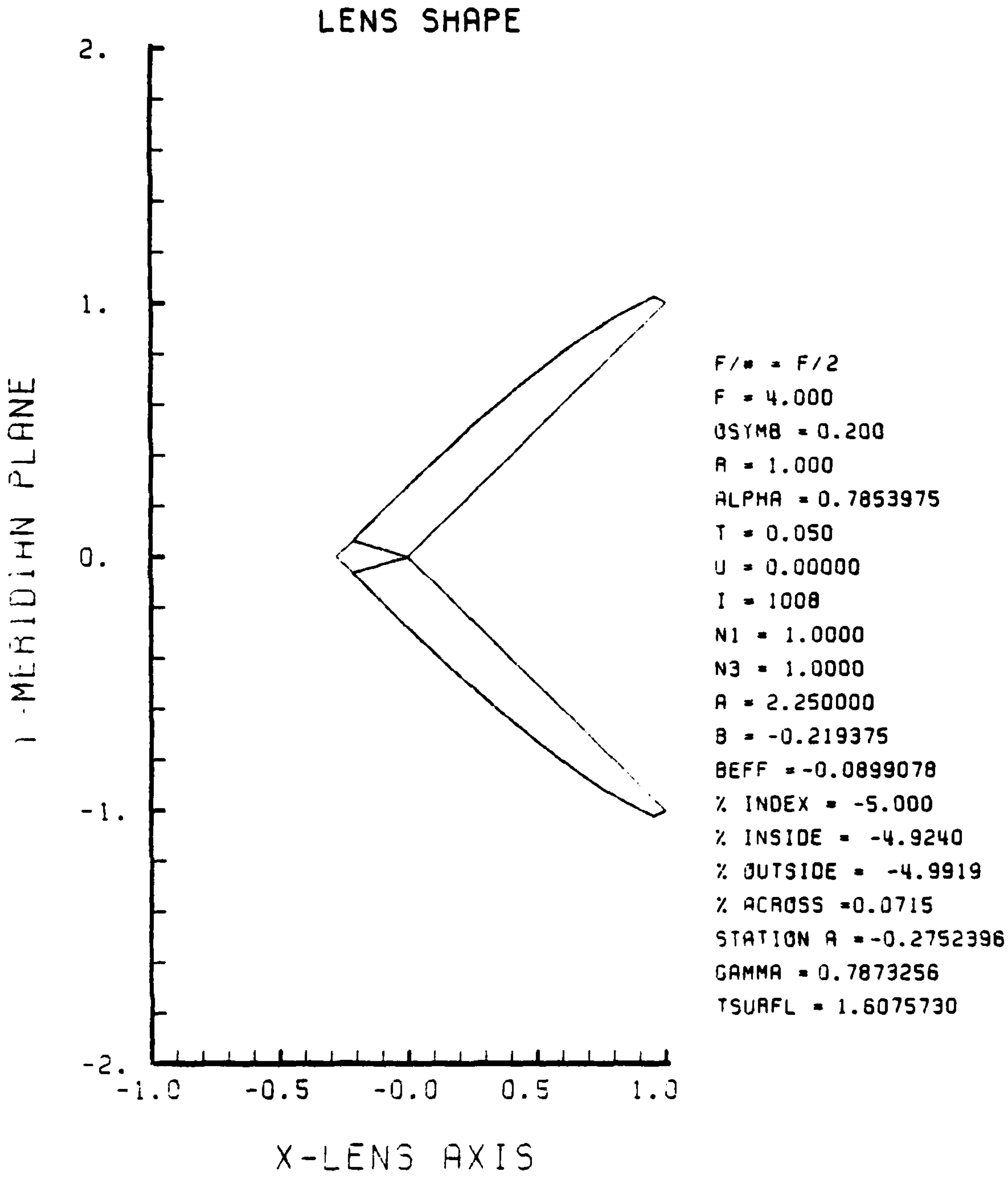

Figure E-13. GRIN Lens Shape at -5%, OB = 0.20, a = 2.25

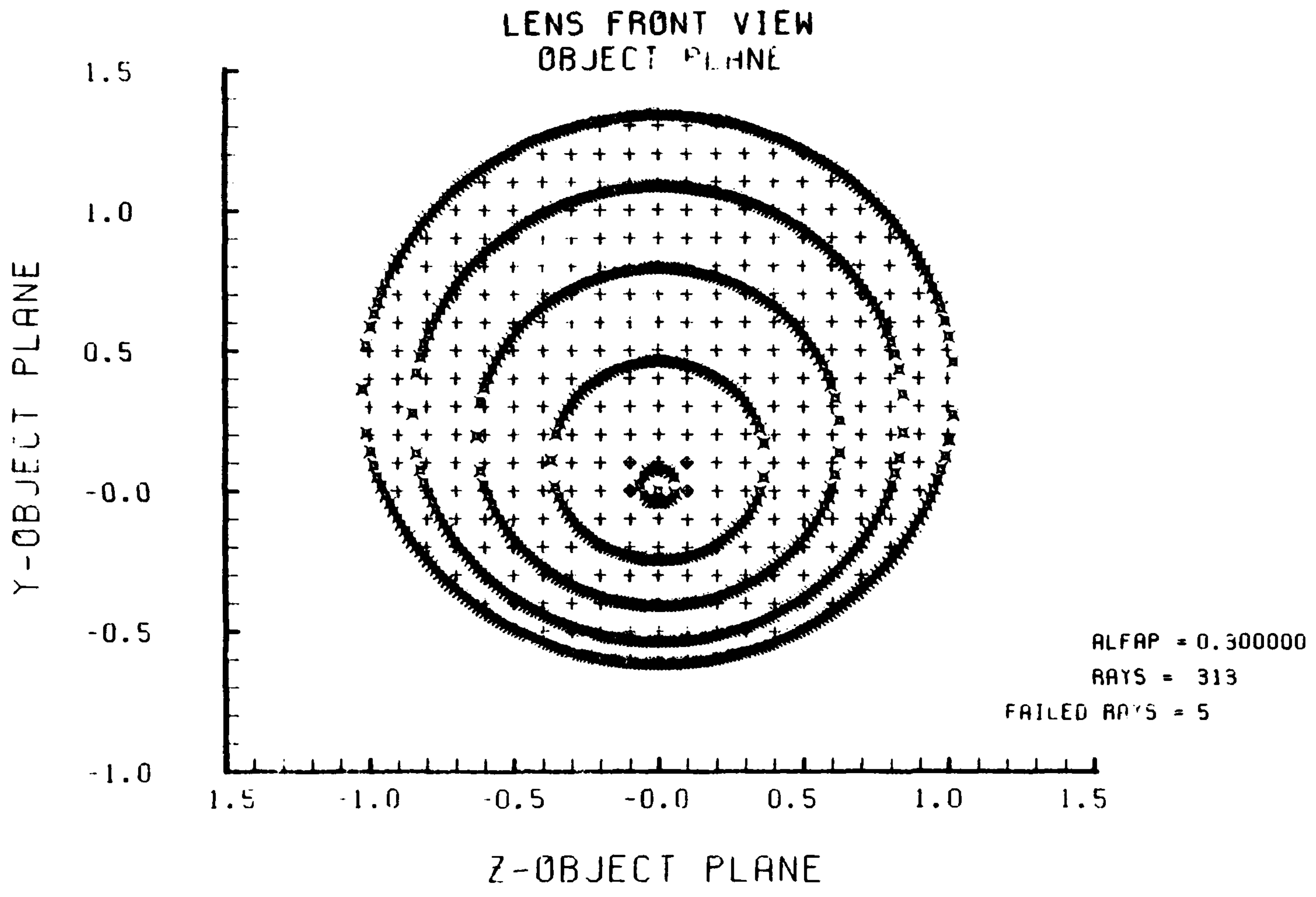

Figure E-14. Grid Plane at $\alpha_p = 0.3$ for Lens of Figure E-13

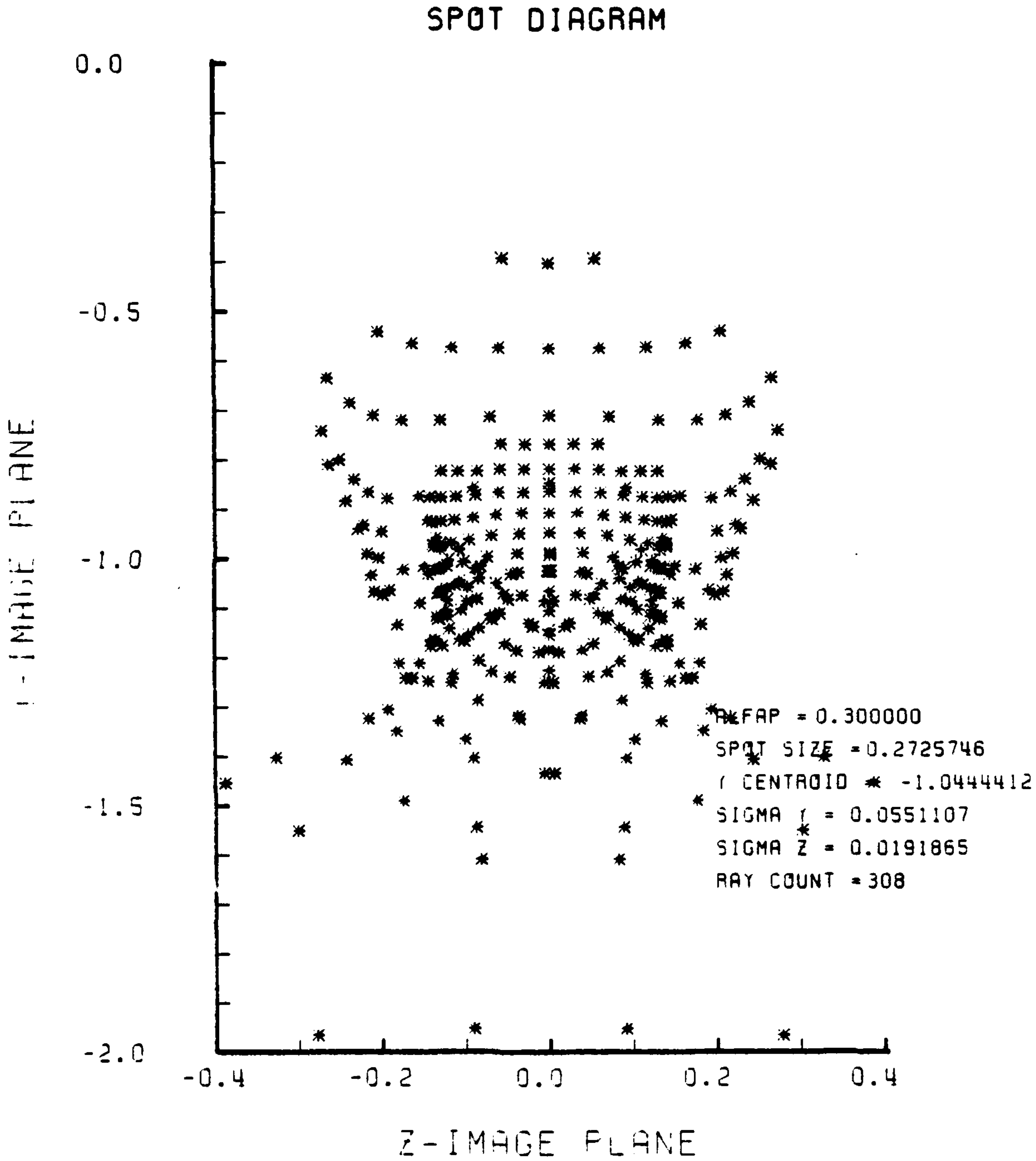

Figure E-15. Spot Diagram for Grid of Figure E-14

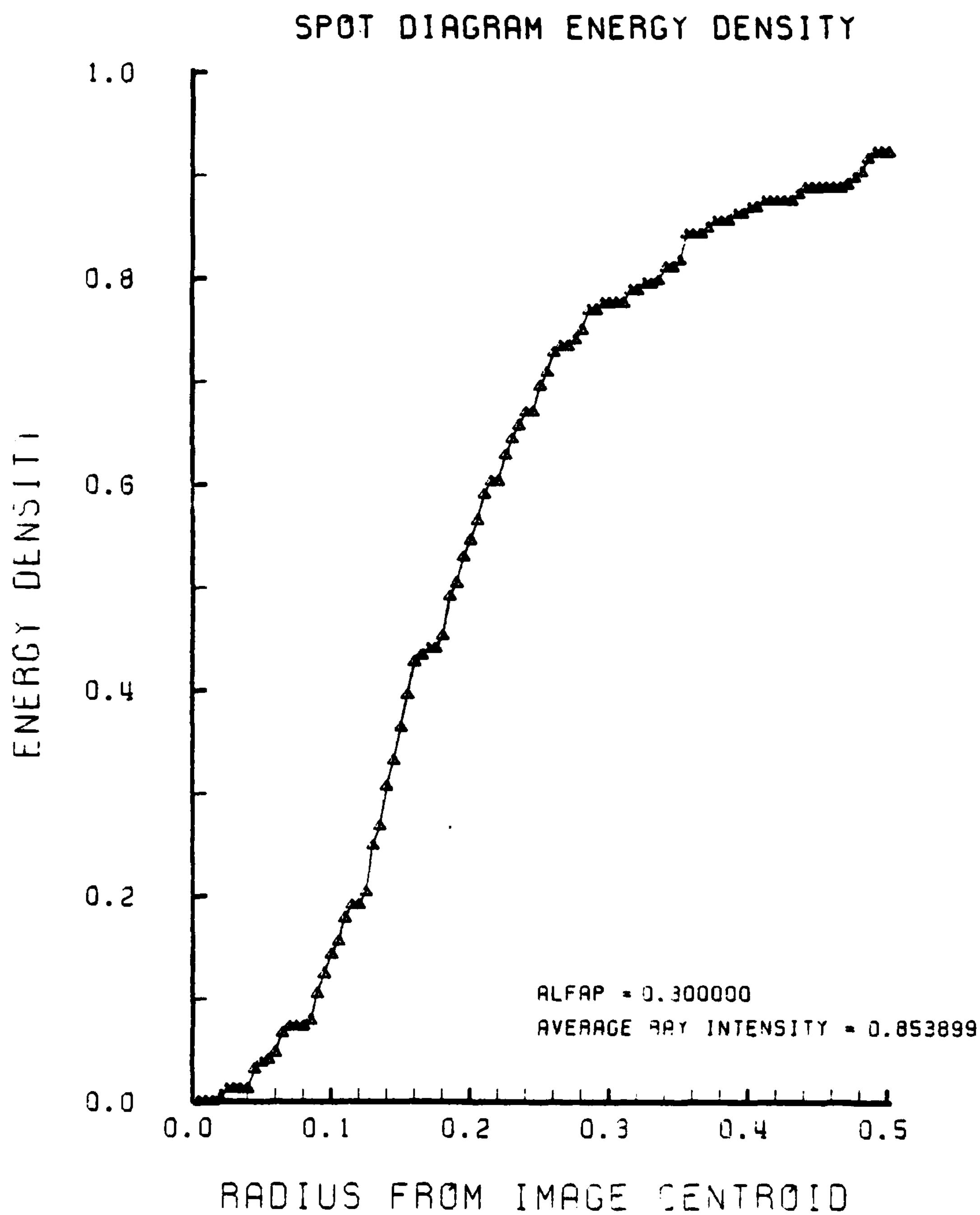

Figure E-16. Encircled Energy of Figure E-15

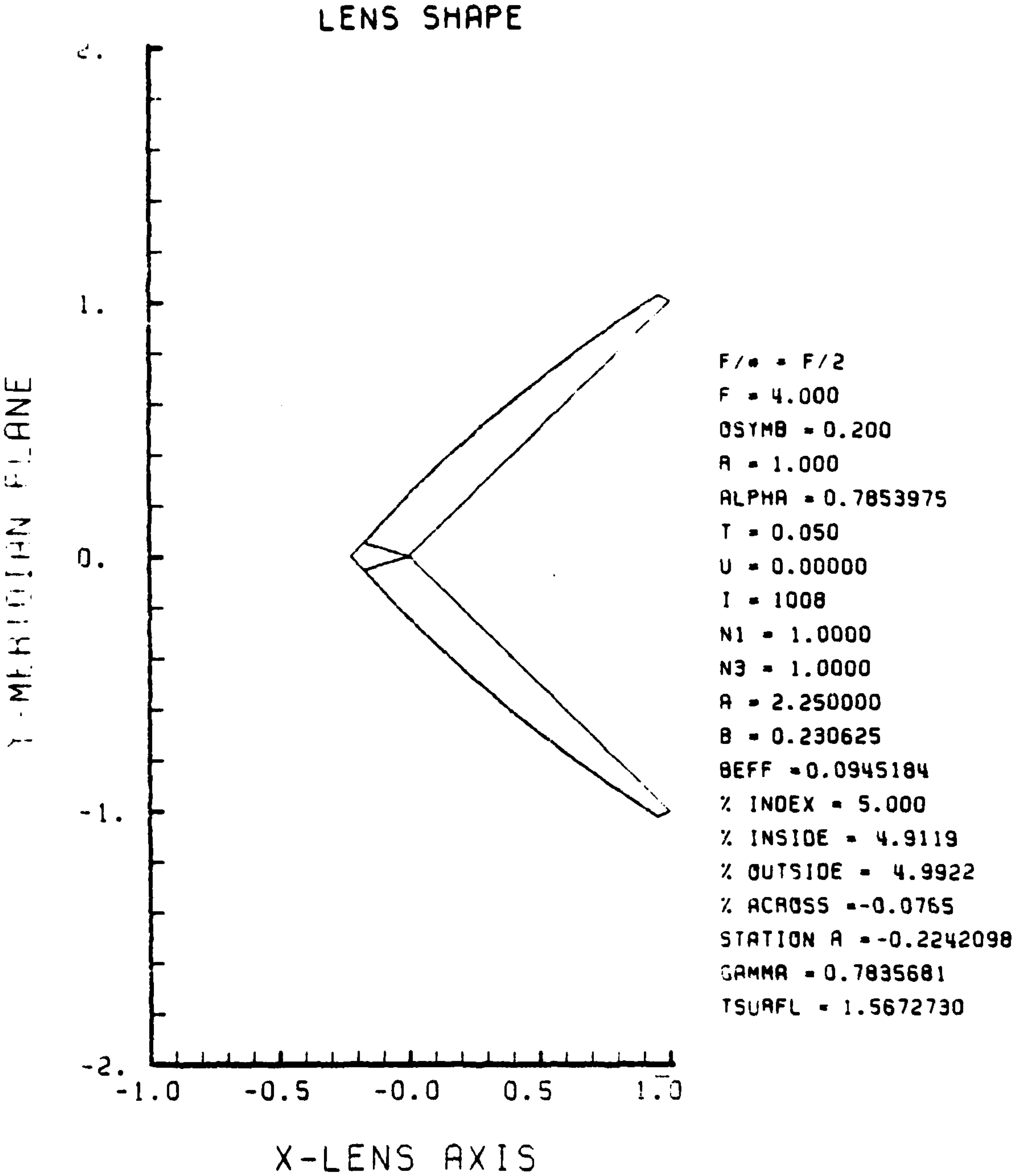

Figure E-17. GRIN Lens Shape at +5%, OB = 0.20, a = 2.25

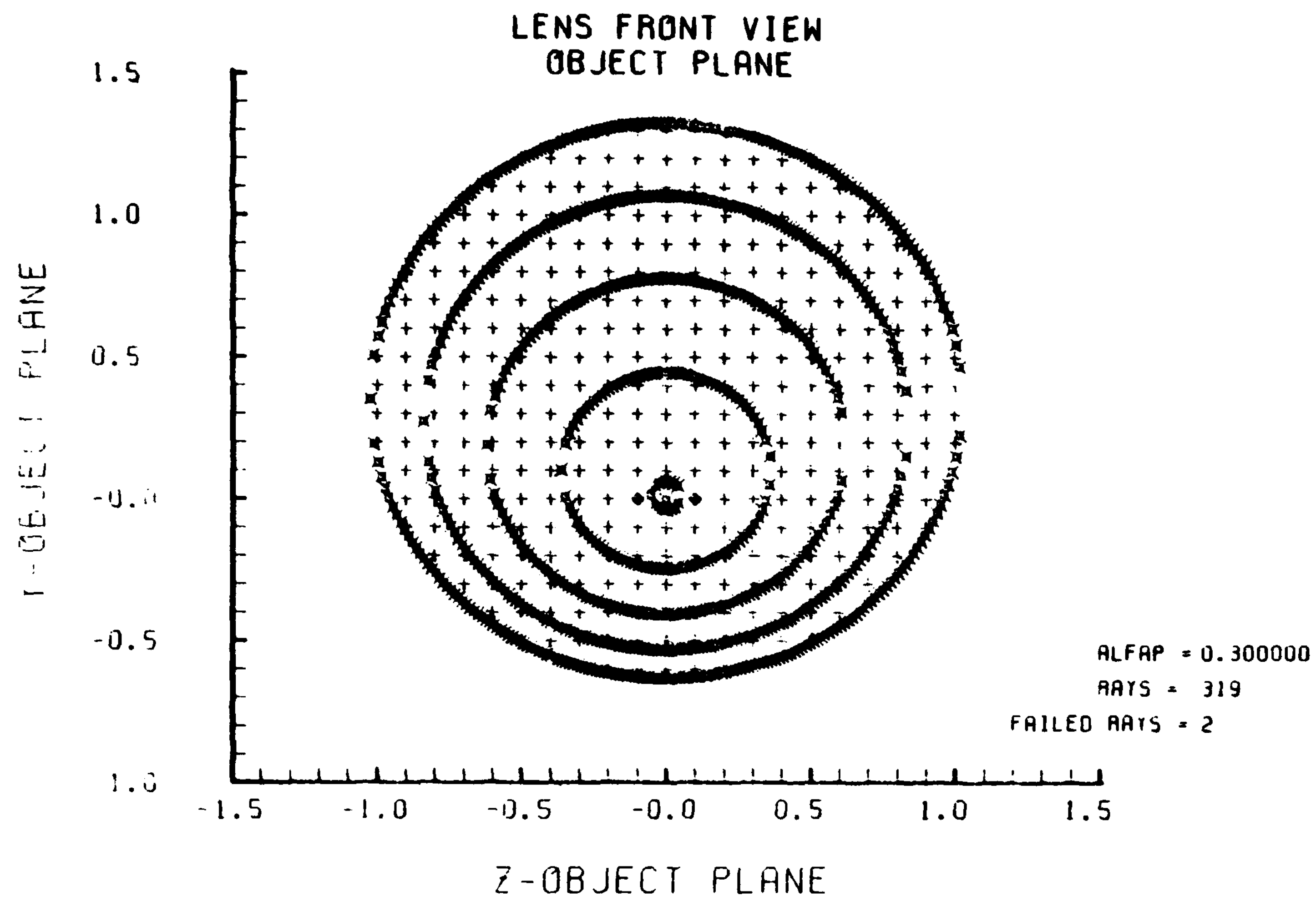

Figure E-18. Grid Plane at $\alpha_p = 0.3$ for Lens of Figure E-17

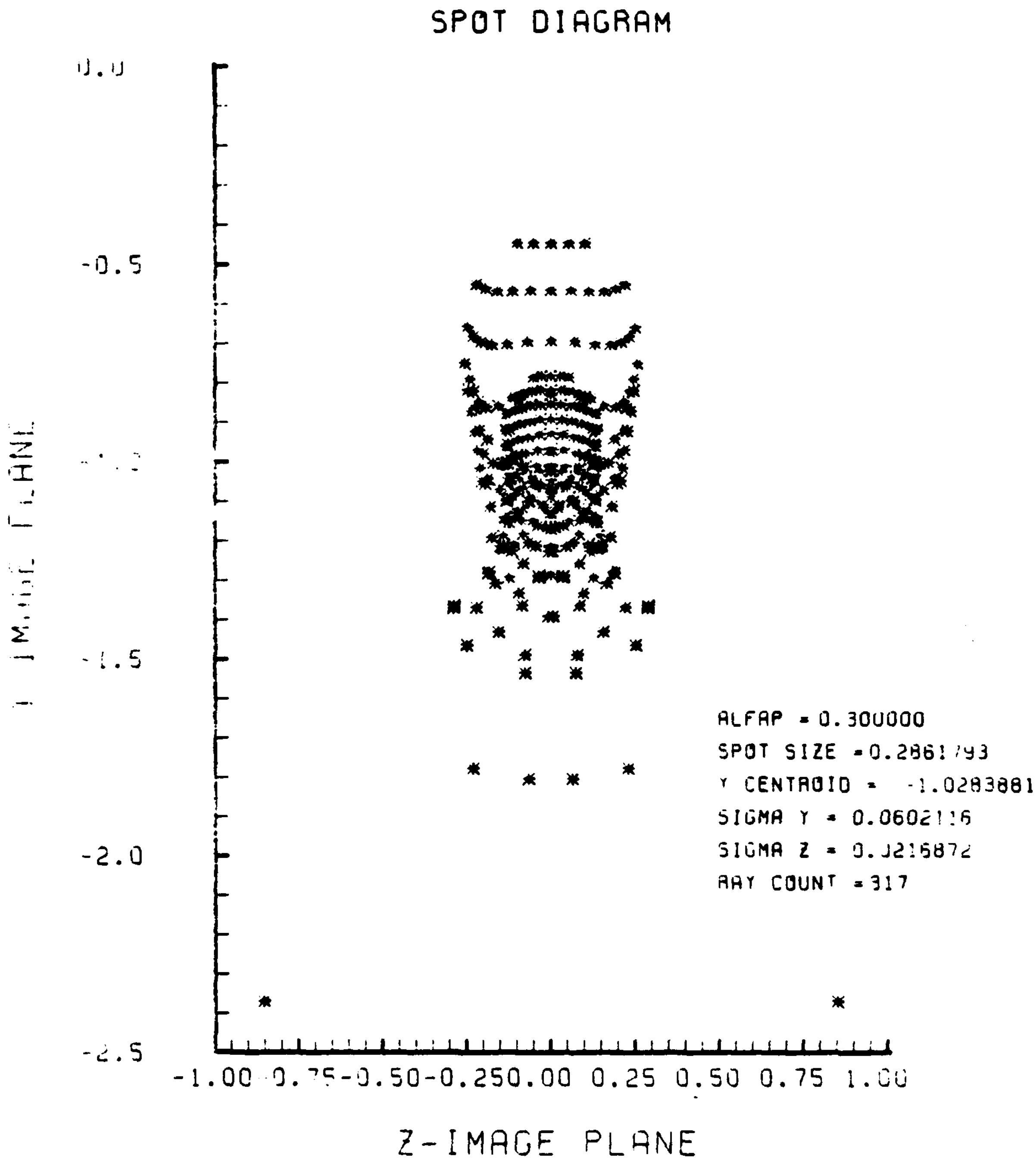

Figure E-19. Spot Diagram for Grid of Figure E-18

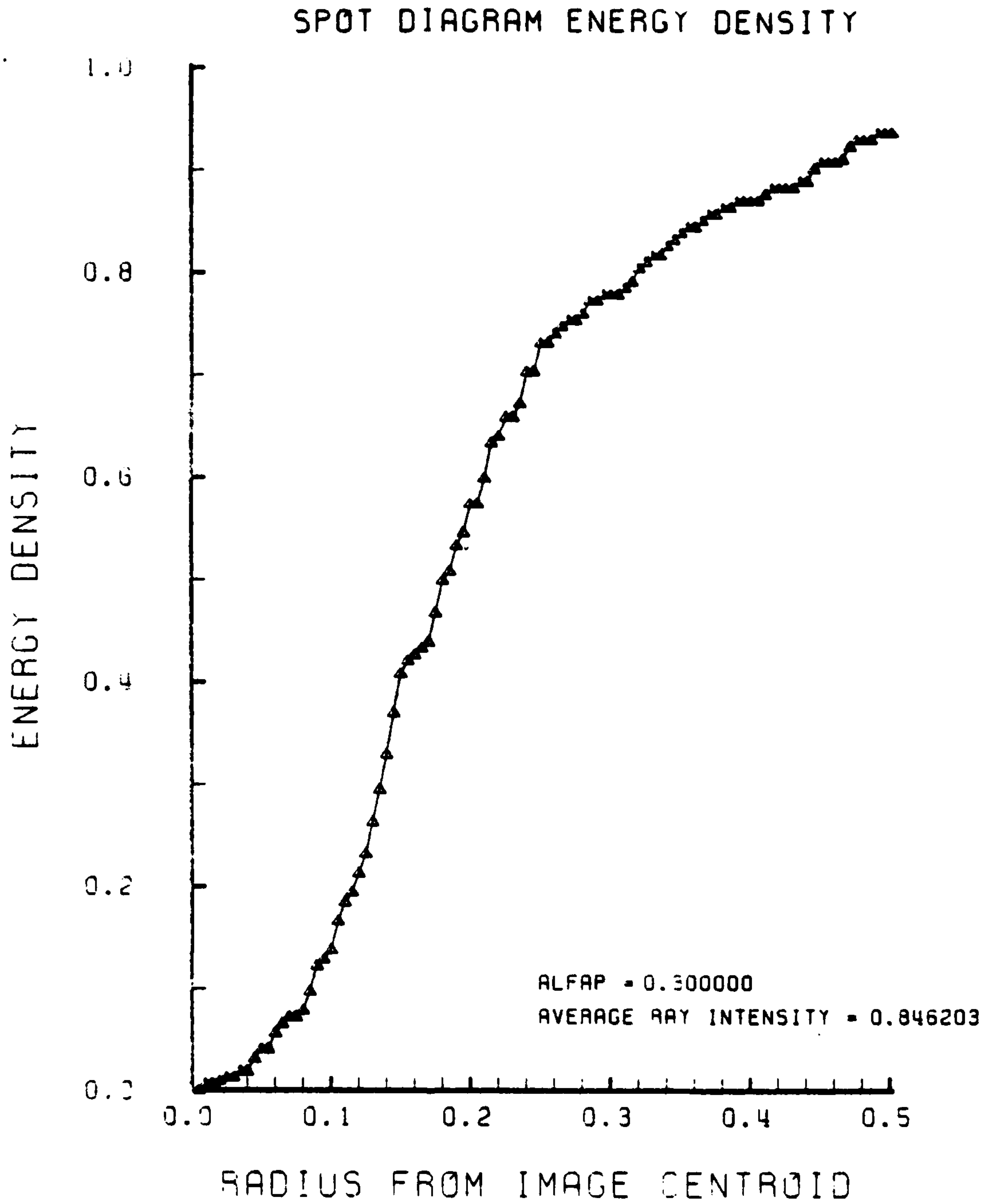

Figure E-20. Encircled Energy of Figure E-19

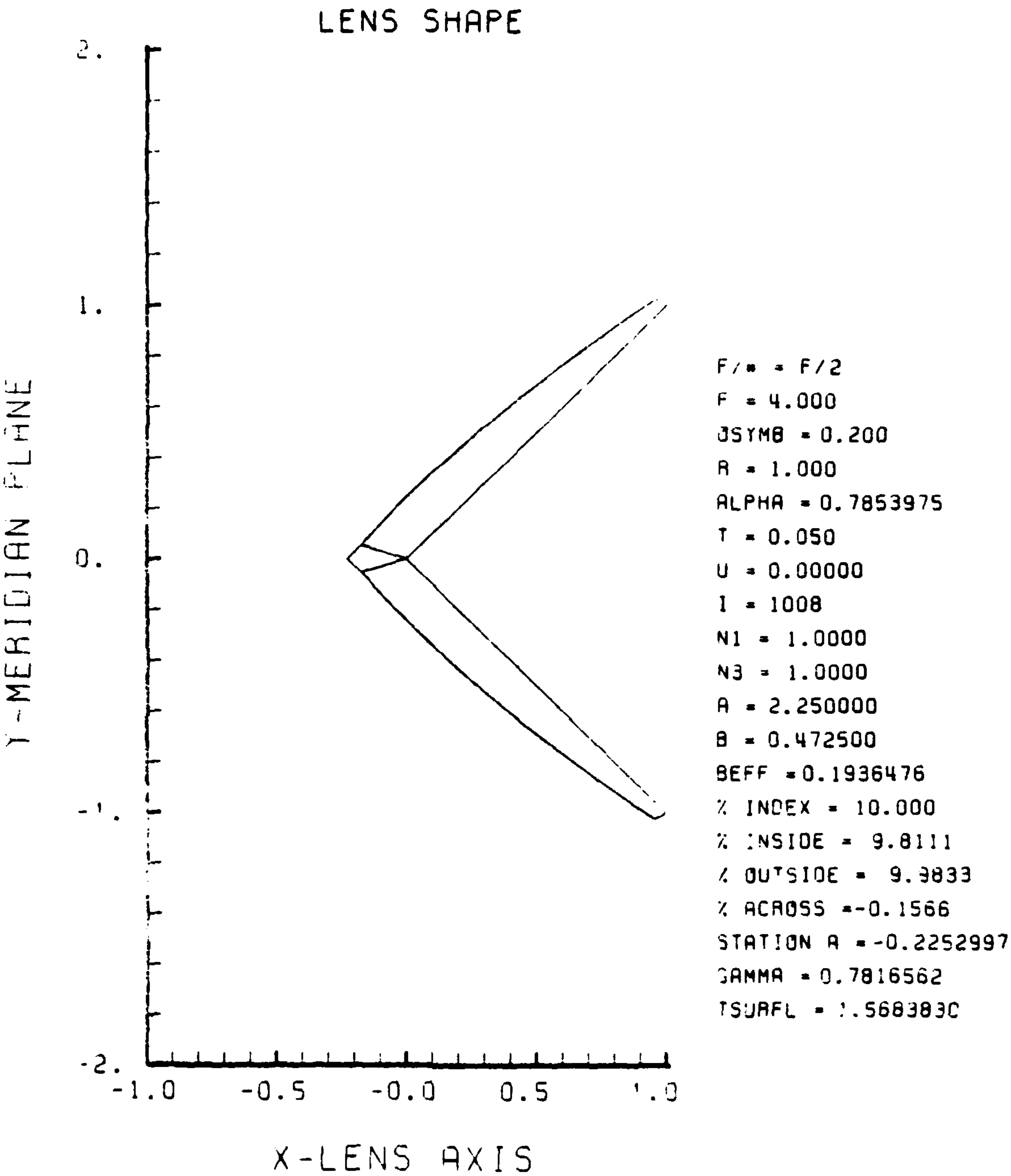

Figure E-21. GRIN Lens Shape at +10%, σB = 0.20, a = 2.25

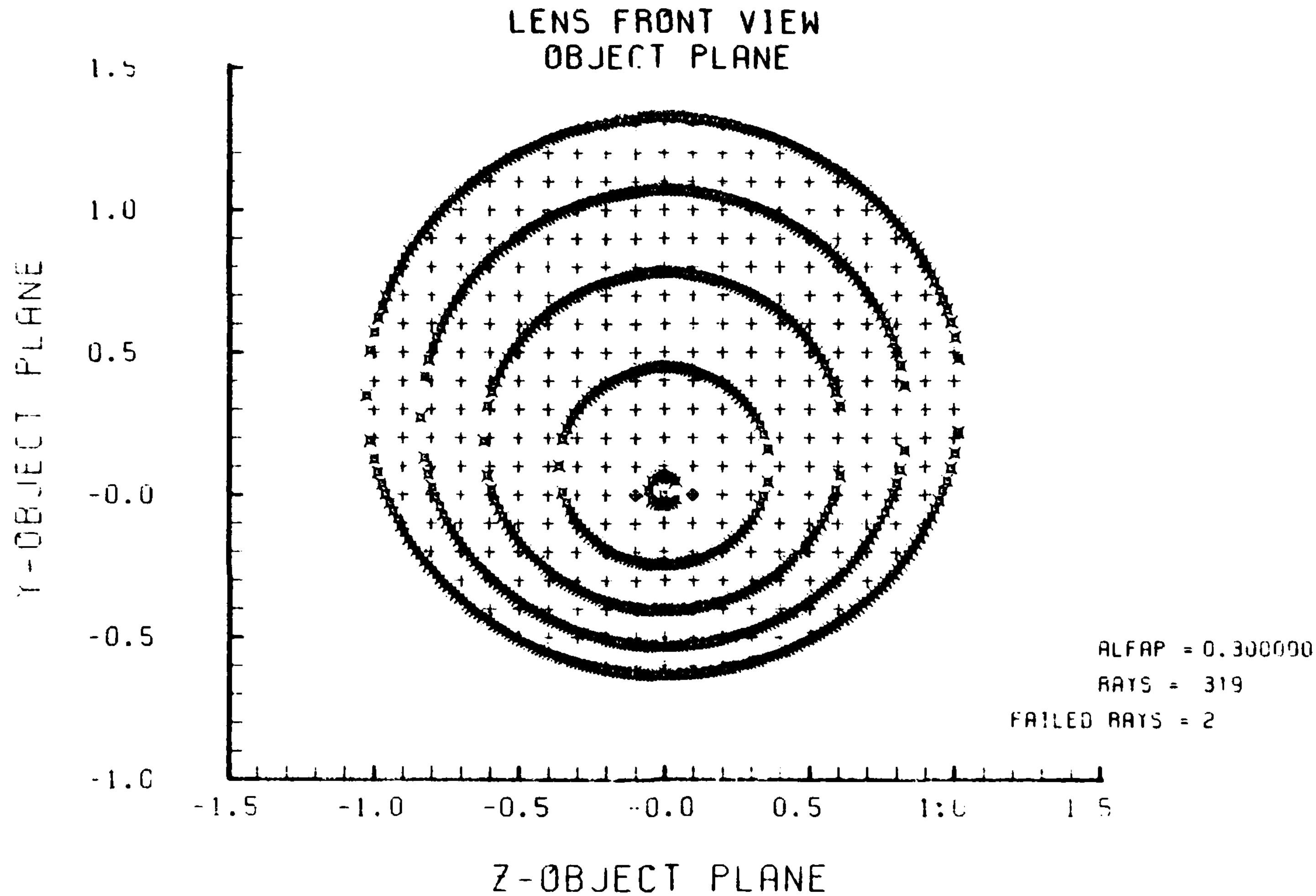

Figure E-22. Grid Plane at $\alpha_p = 0.3$ for Lens of Figure E-21

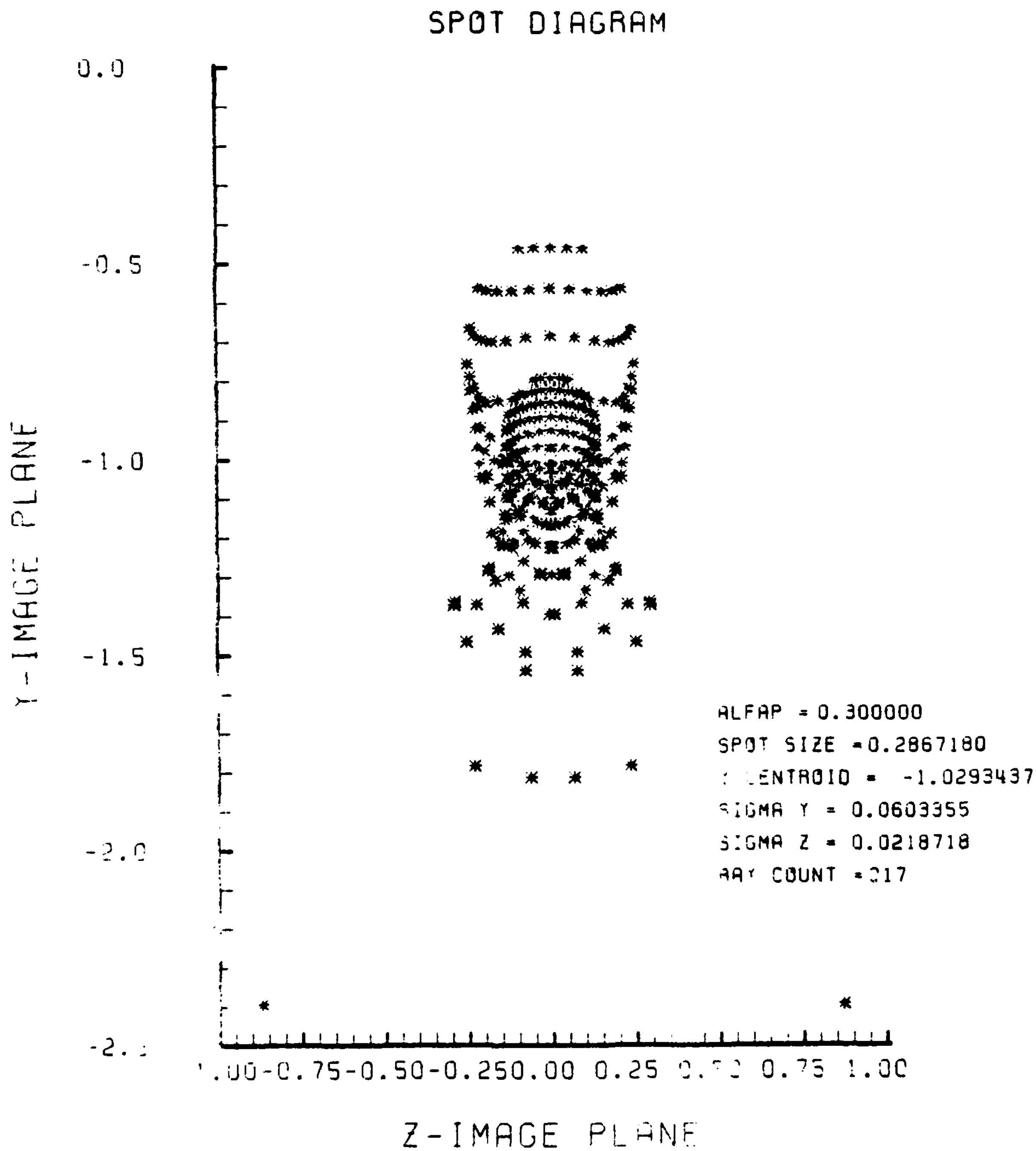

Figure E-23. Spot Diagram for Grid of Figure E-22

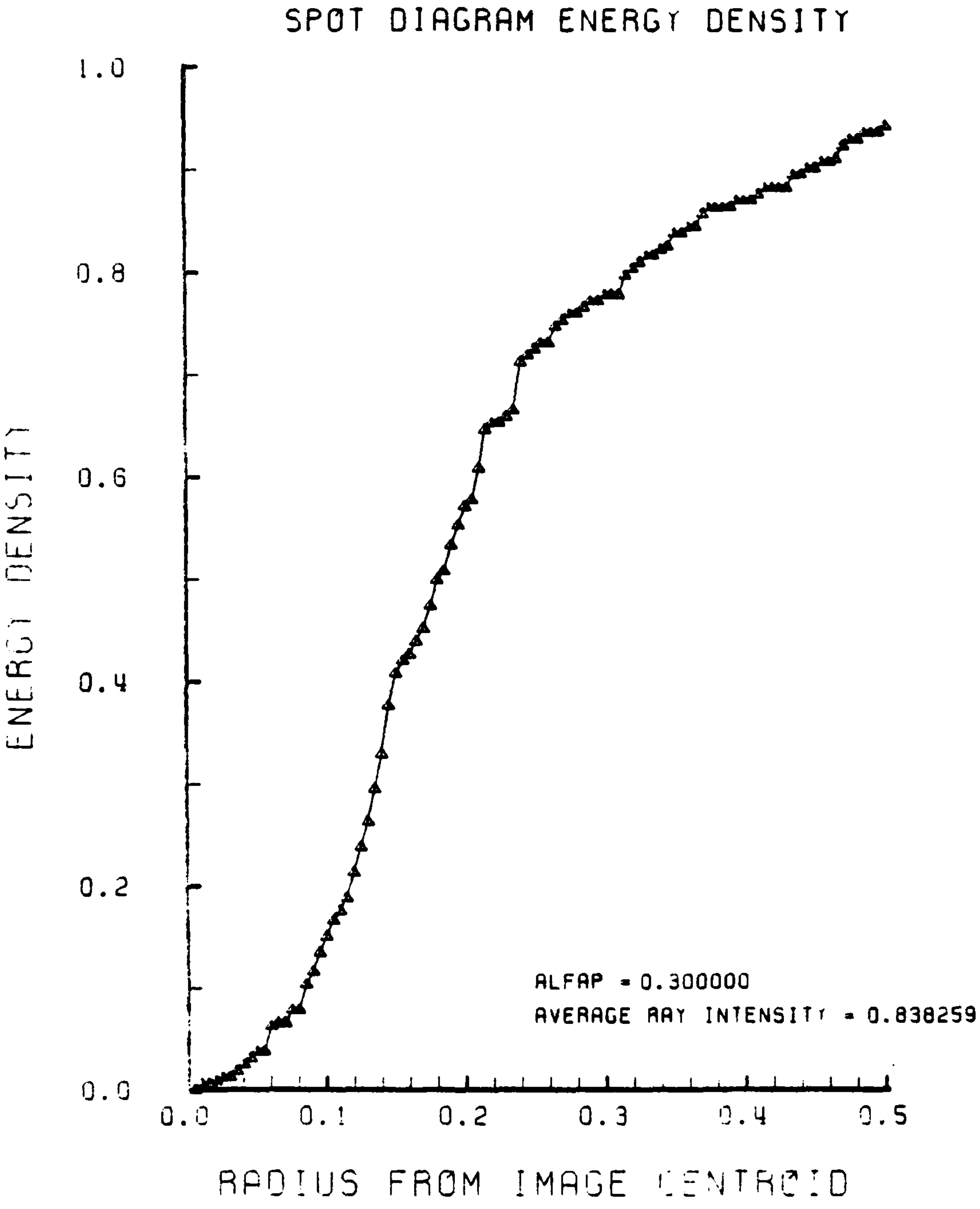

Figure E-24. Encircled Energy of Figure E-23

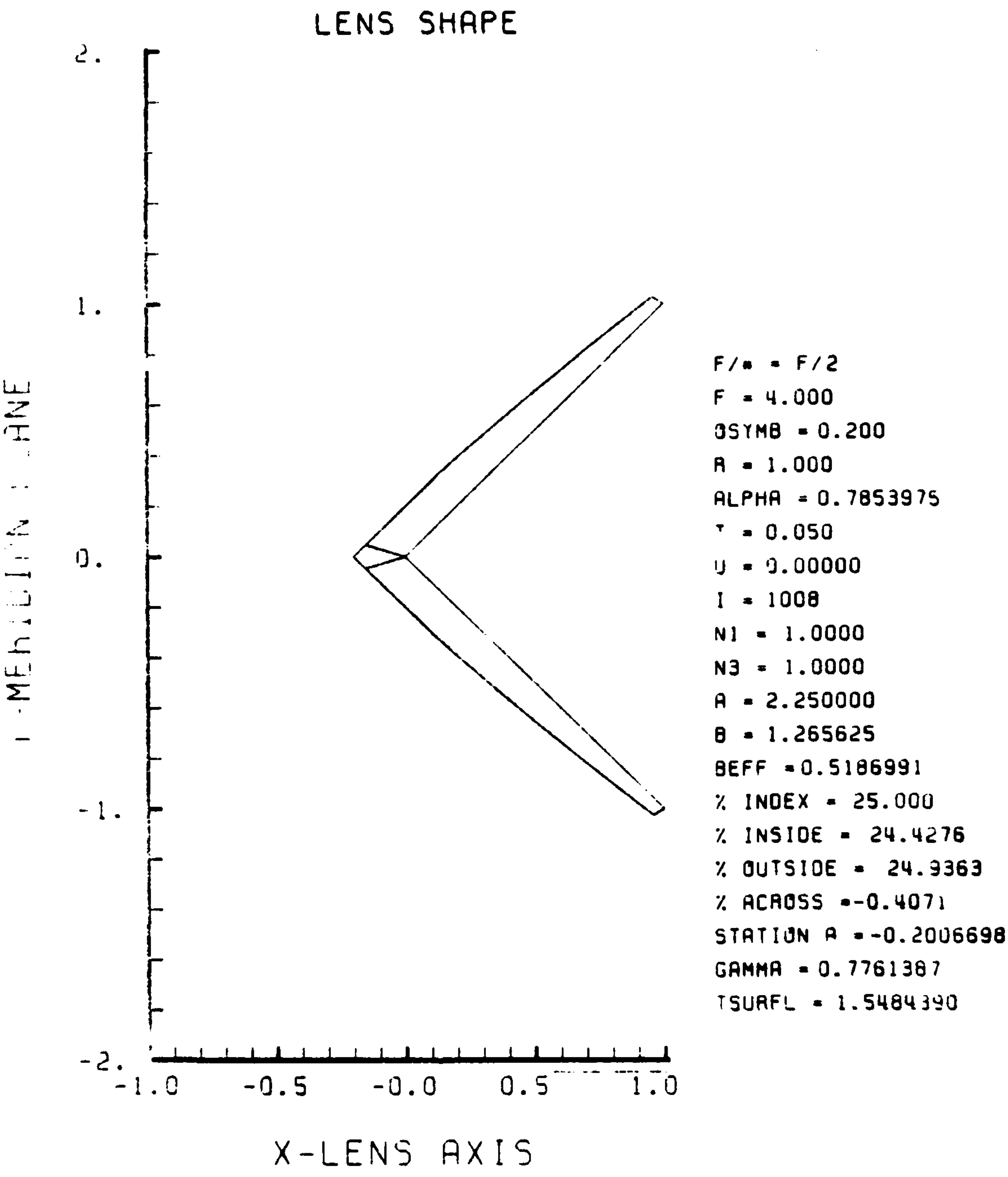

Figure E-25. GRIN Lens Shape at +25%, OB = 0.20, a = 2.25

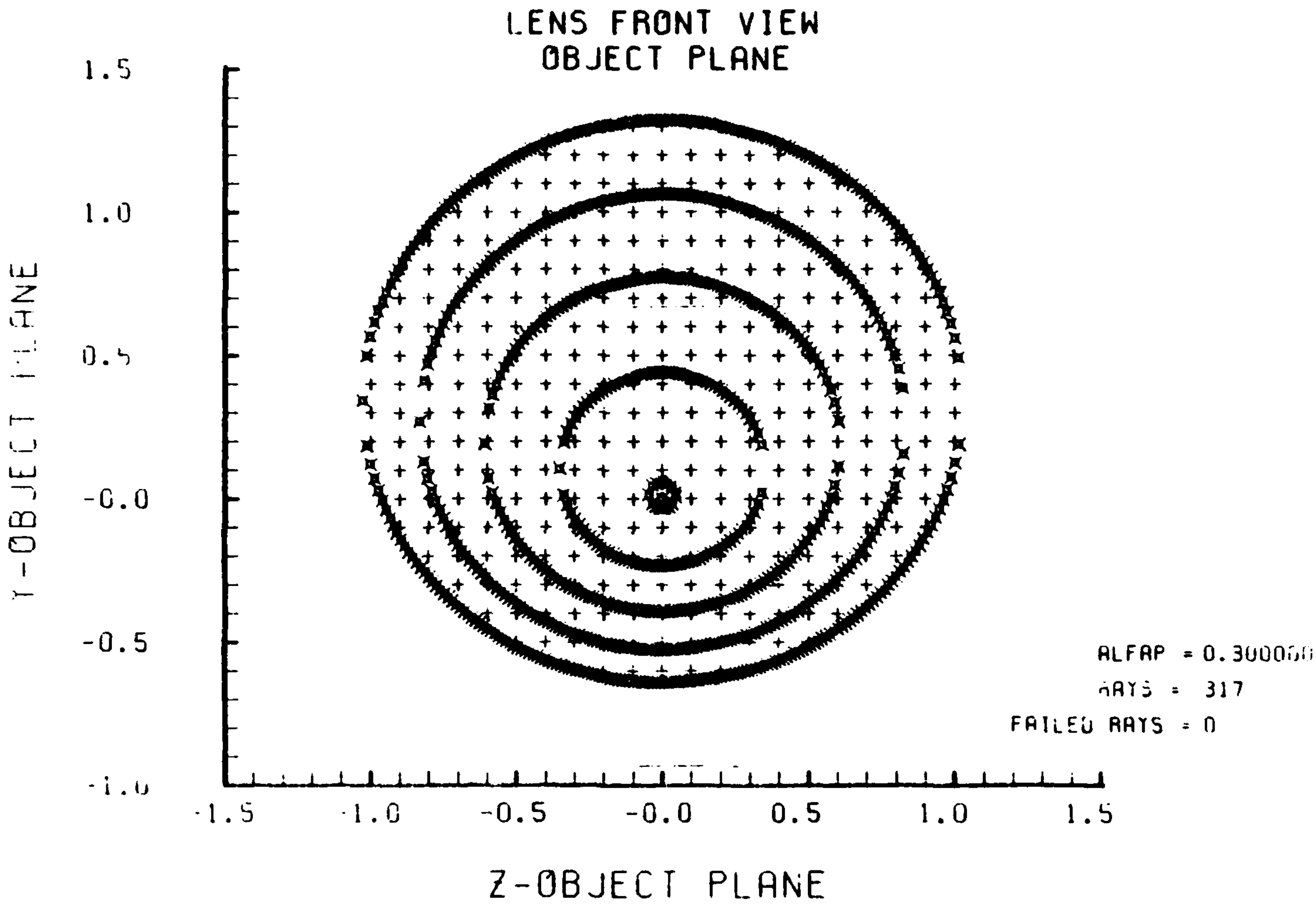

Figure E-26. Grid Plane at $\alpha_p = 0.3$ for Lens of Figure E-25

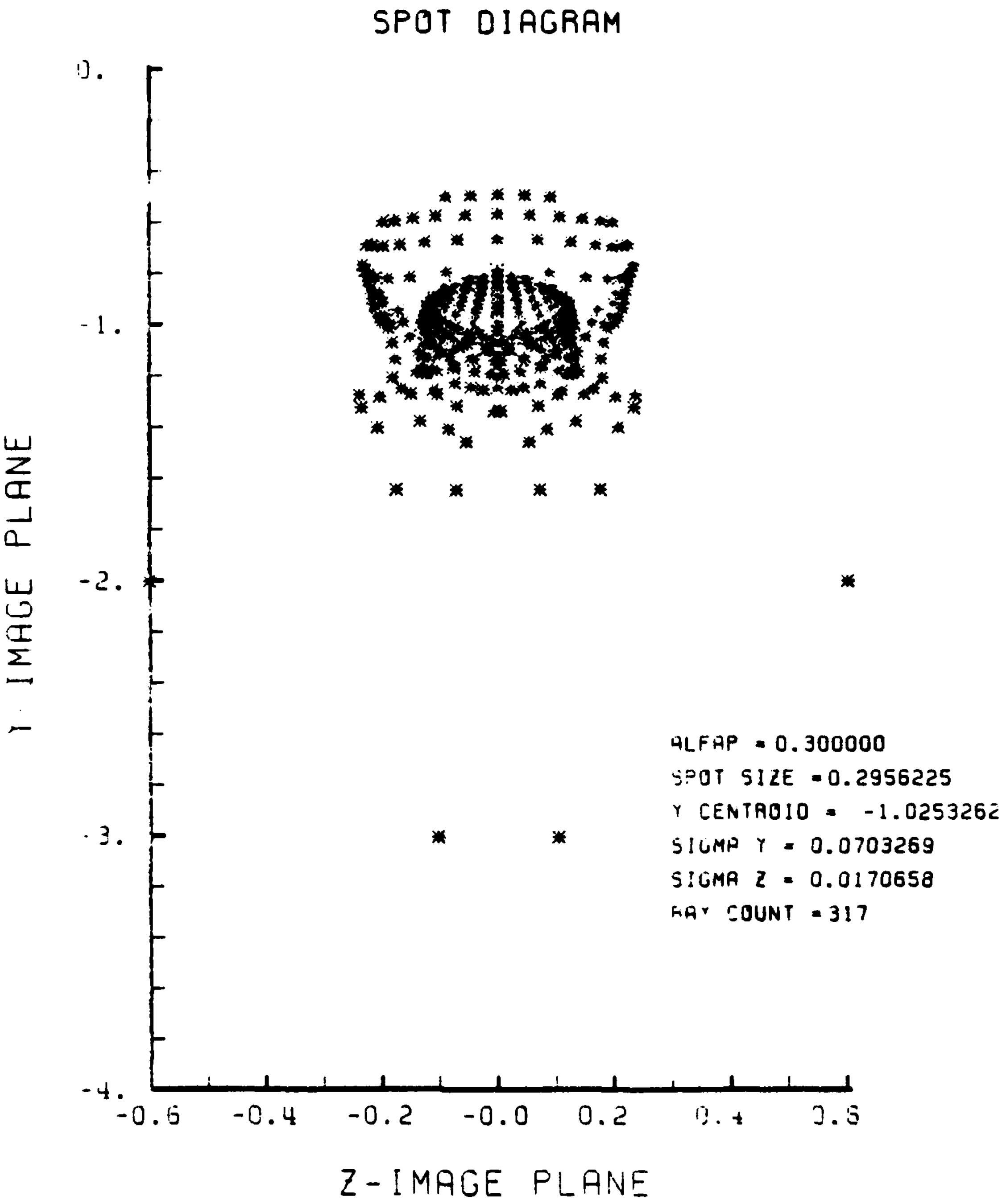

Figure E-27. Spot Diagram for Grid of Figure E-26

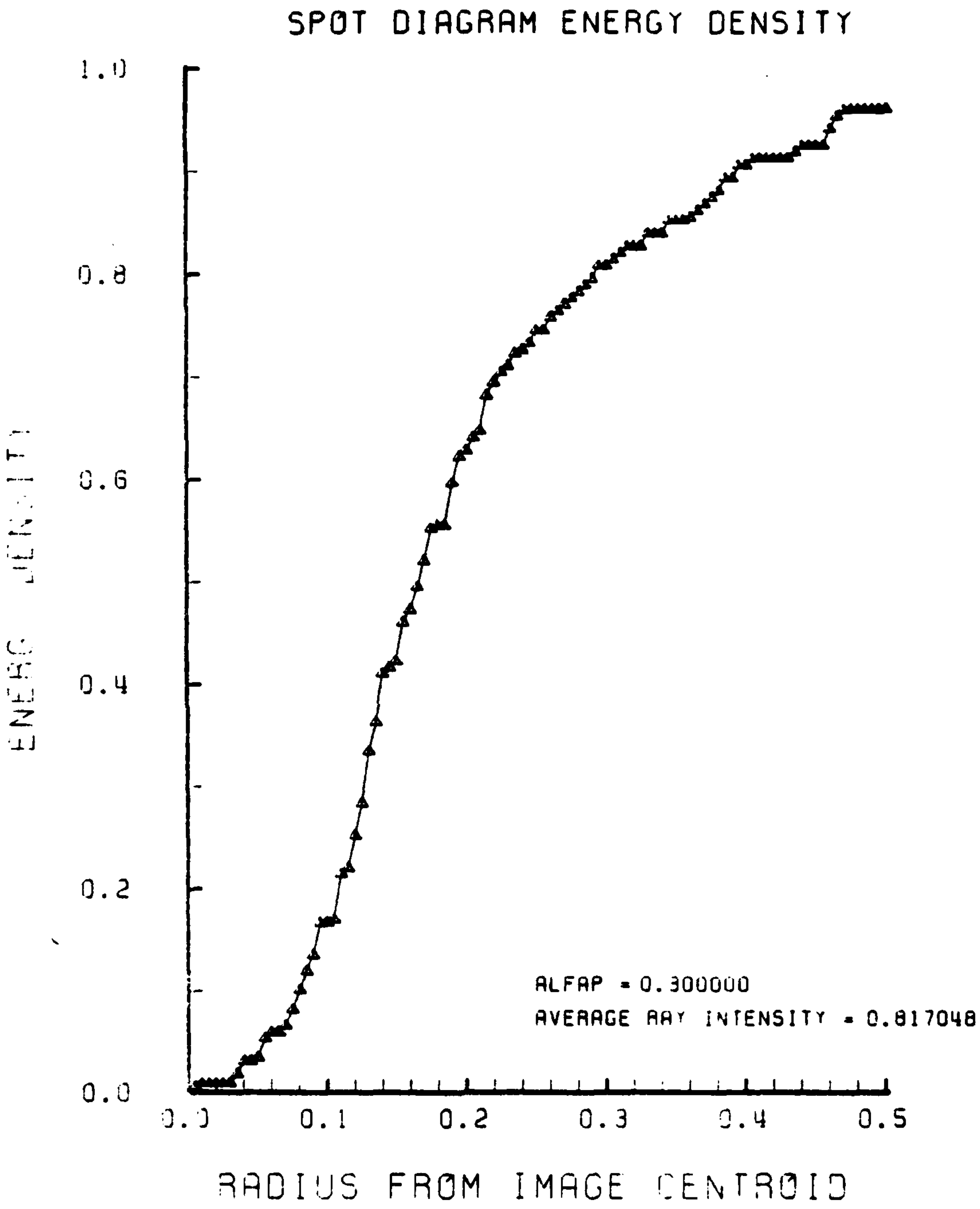

Figure E-28. Encircled Energy of Figure E-27

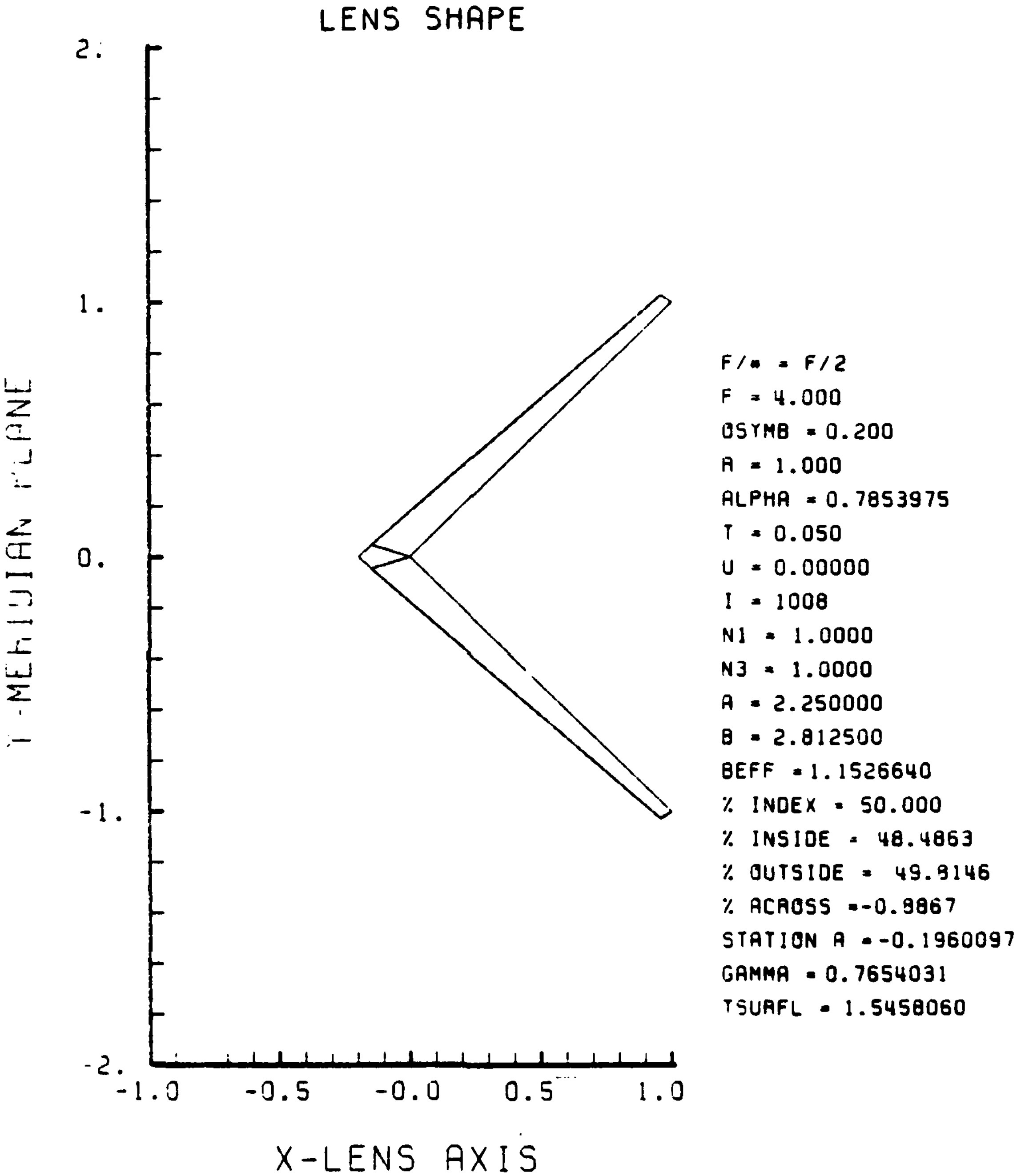

Figure E-29. GRIN Lens Shape at +50%, OB = 0.20, a = 2.25

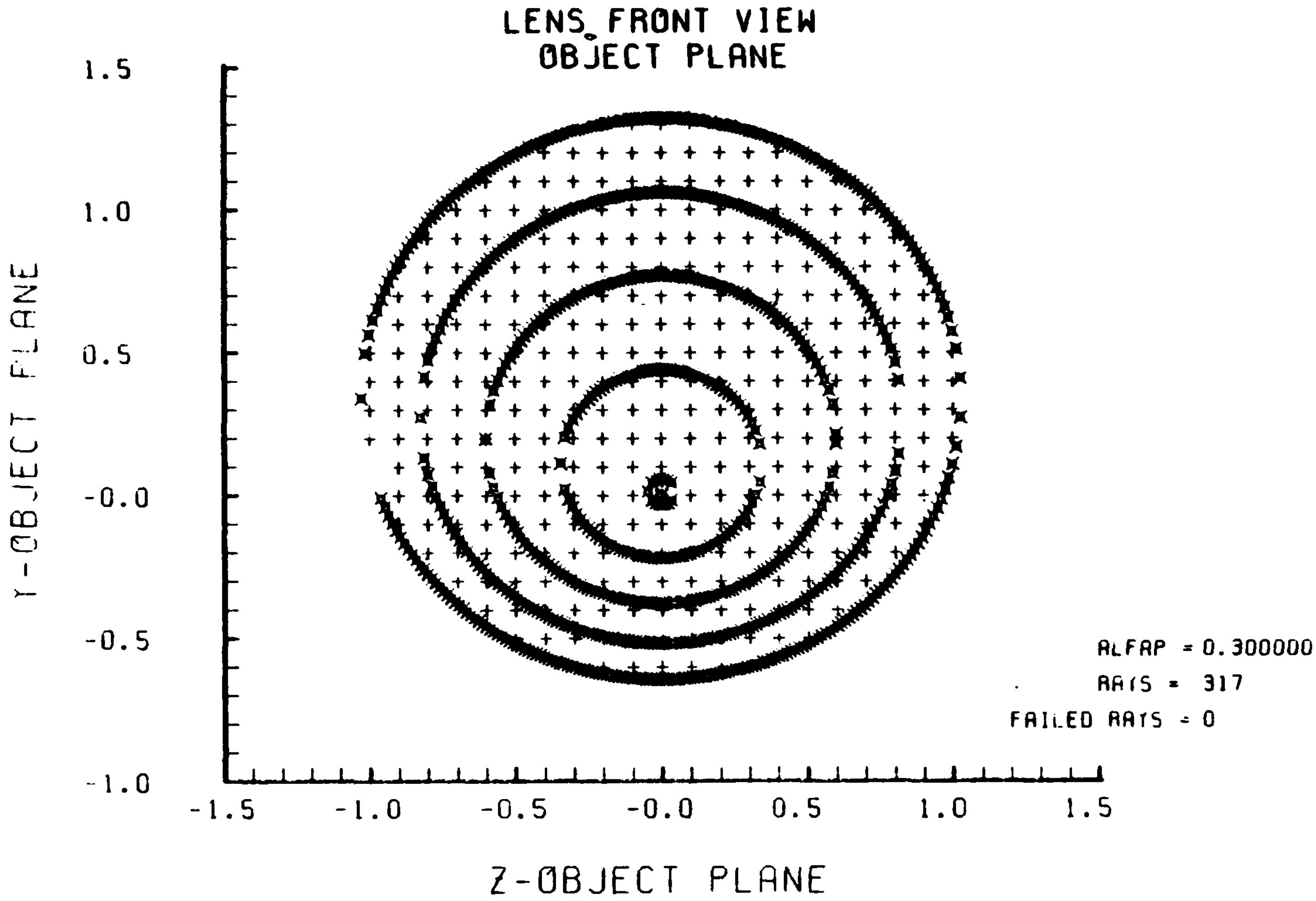

Figure E-30. Grid Plane at α_p = 0.3 for Lens of Figure E-29

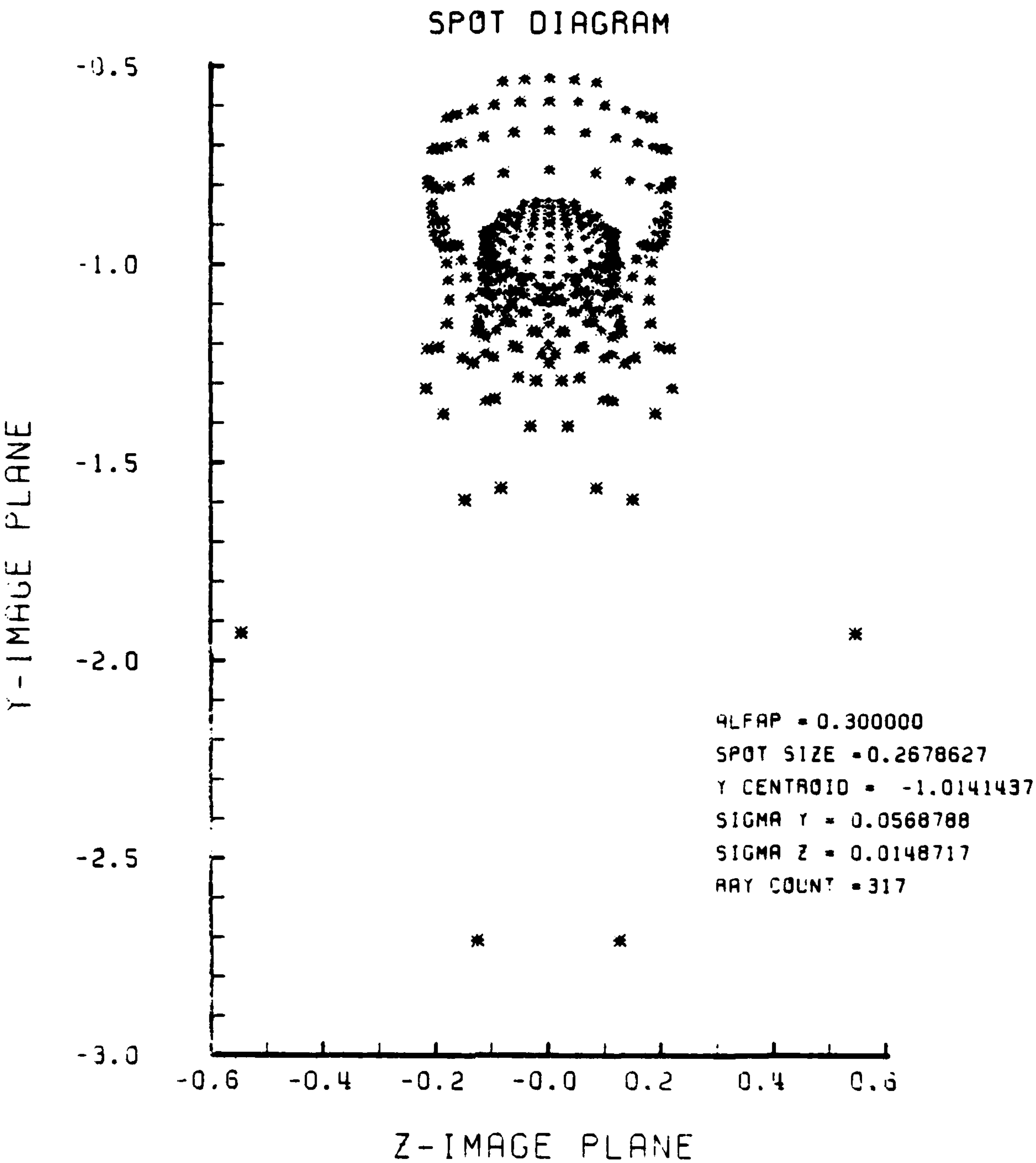

Figure E-31. Spot Diagram for Grid of Figure E-30

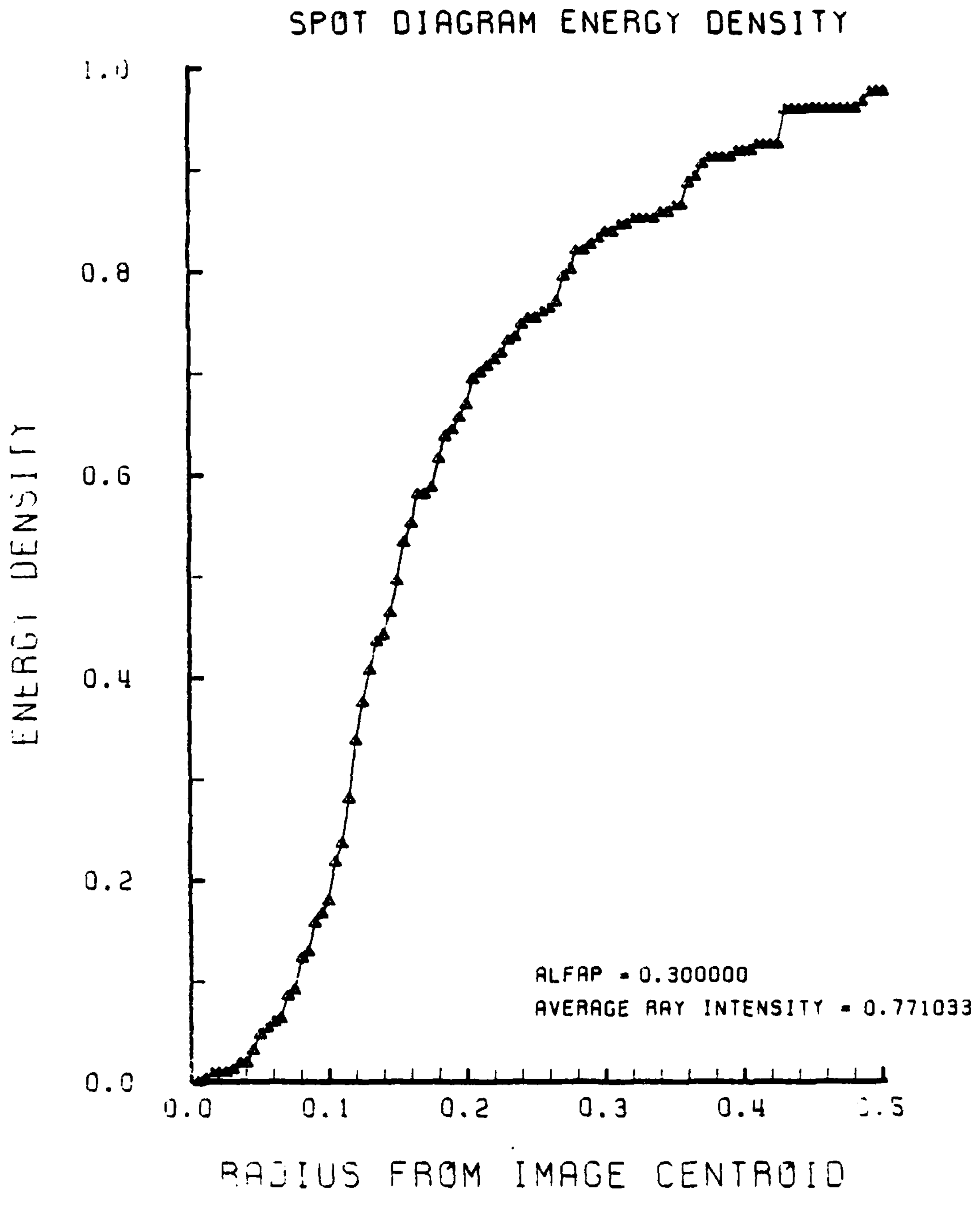

Figure E-32. Encircled Energy of Figure E-31

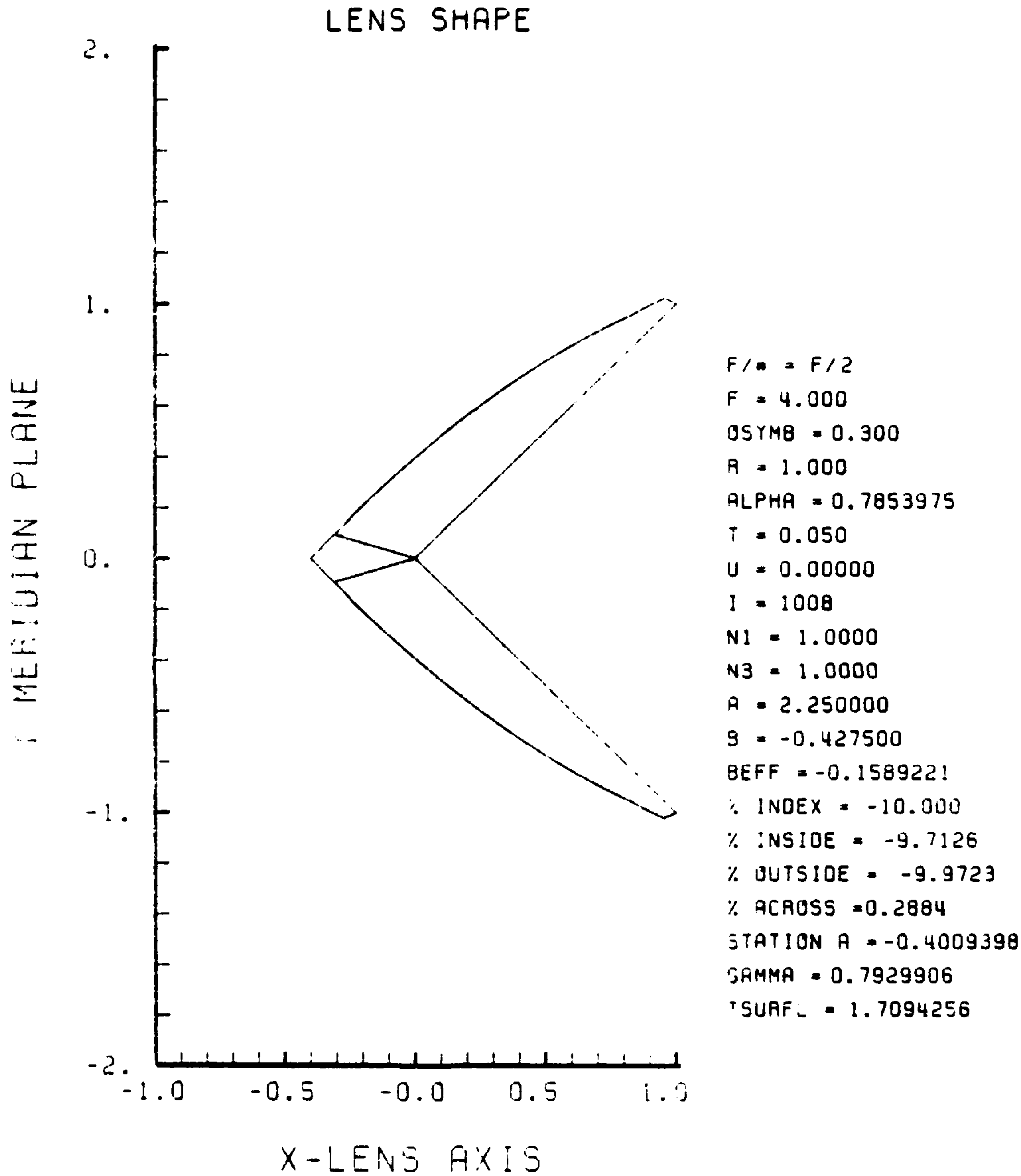

Figure E-33. GRIN Lens Shape at -10%, OB = 0.30, a = 2.25

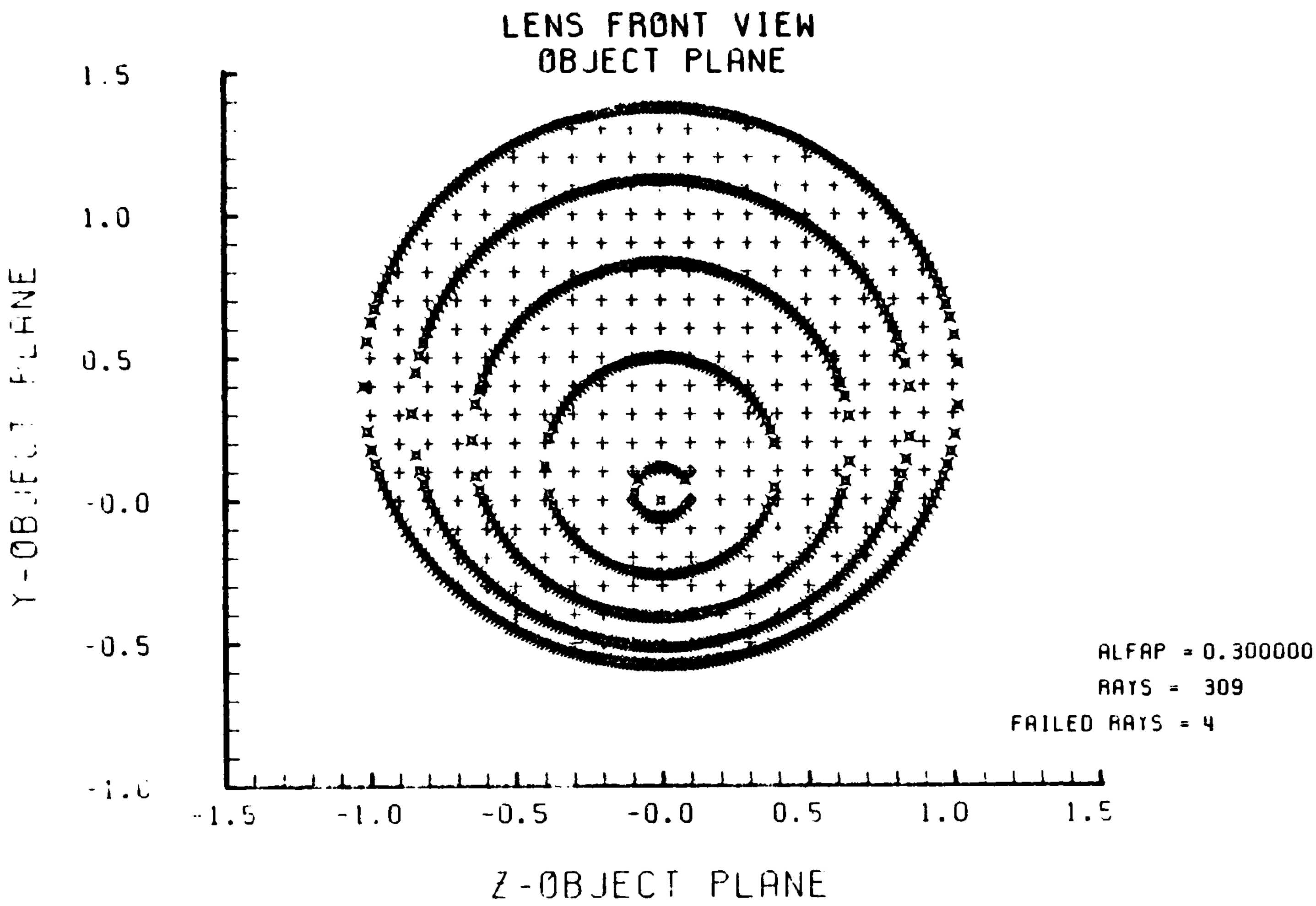

Figure E-34. Grid Plane at α_p = 0.3 for Lens of Figure E-33

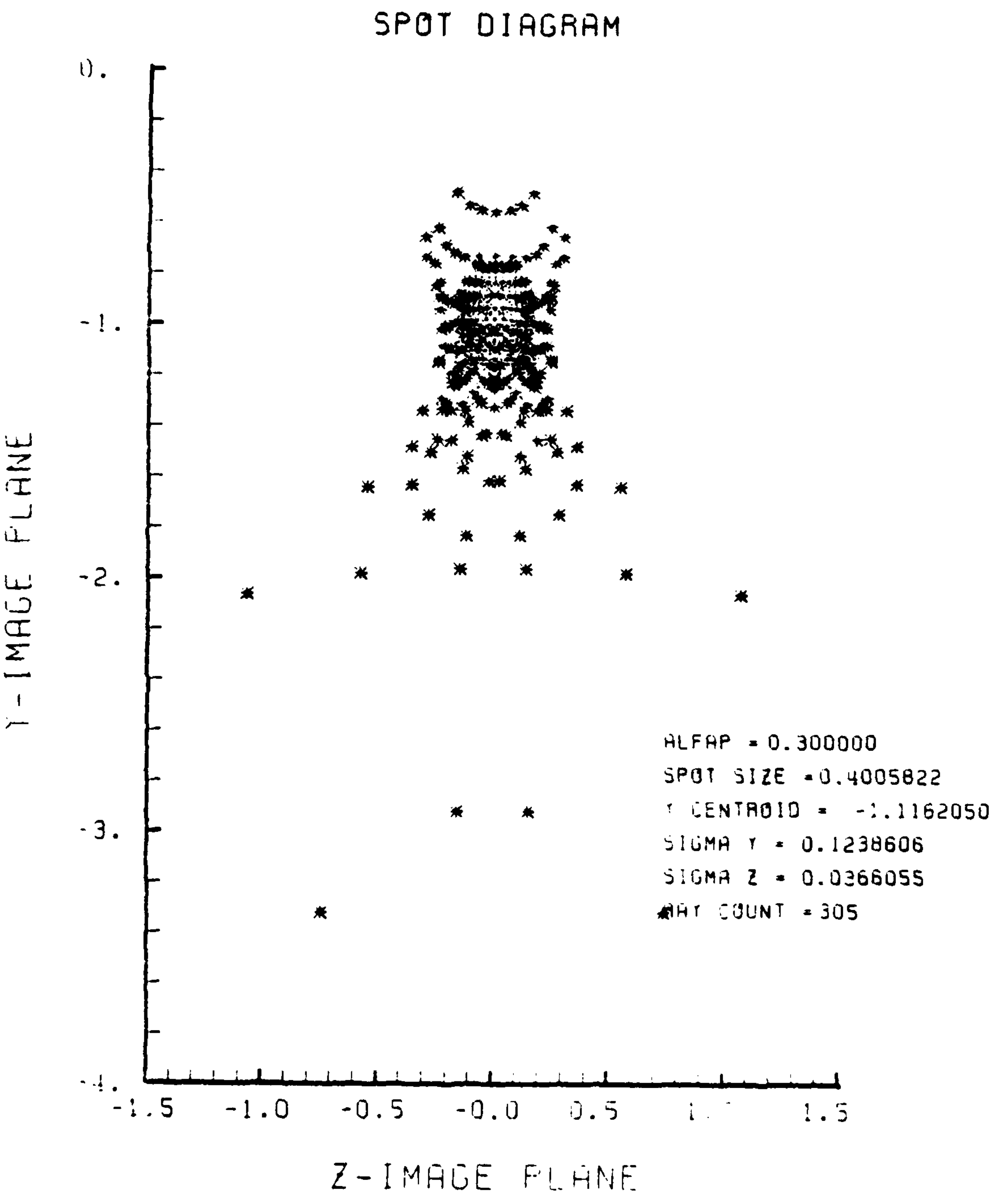

Figure E-35. Spot Diagram for Grid of Figure E-34

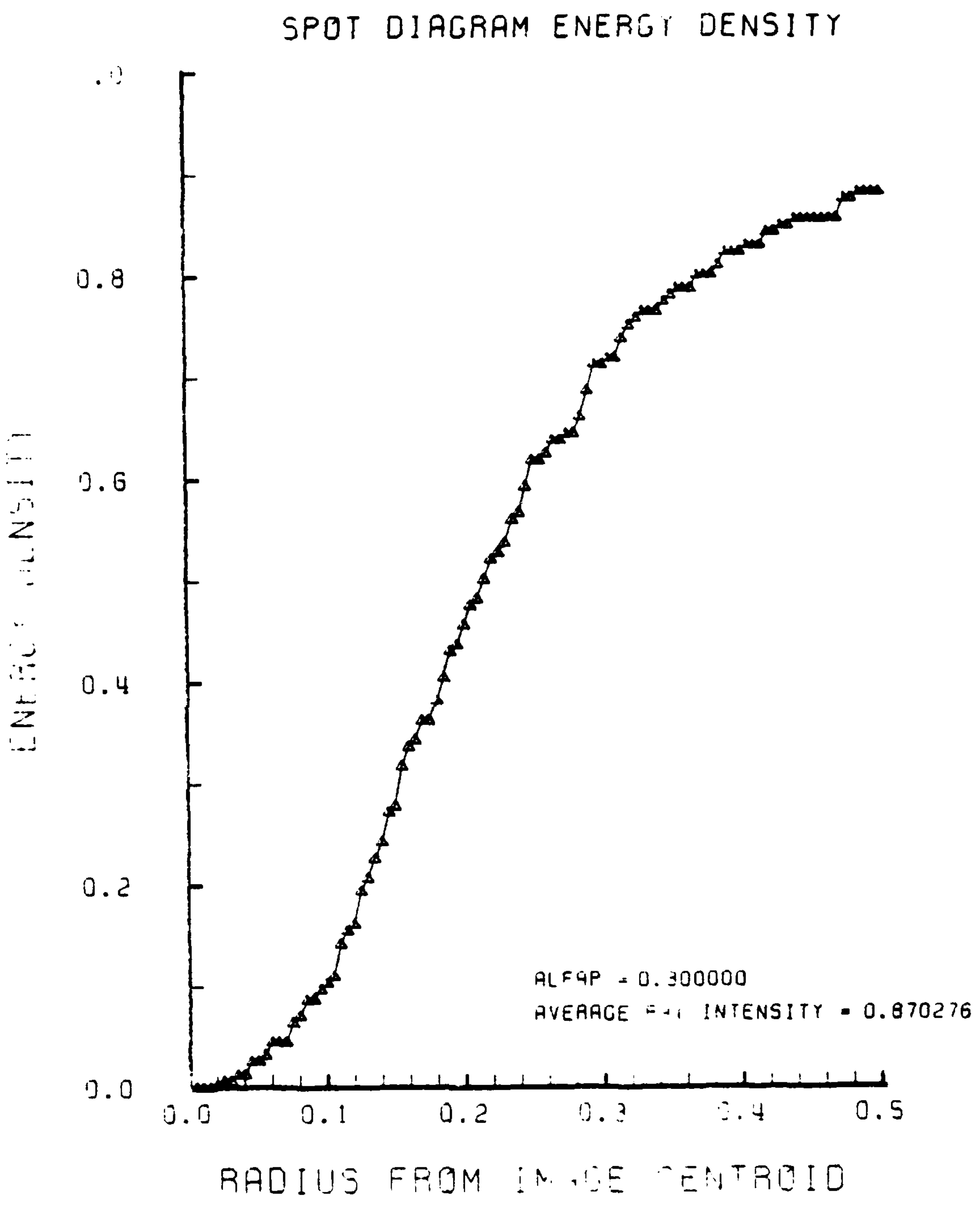

Figure E-36. Encircled Energy of Figure E-35

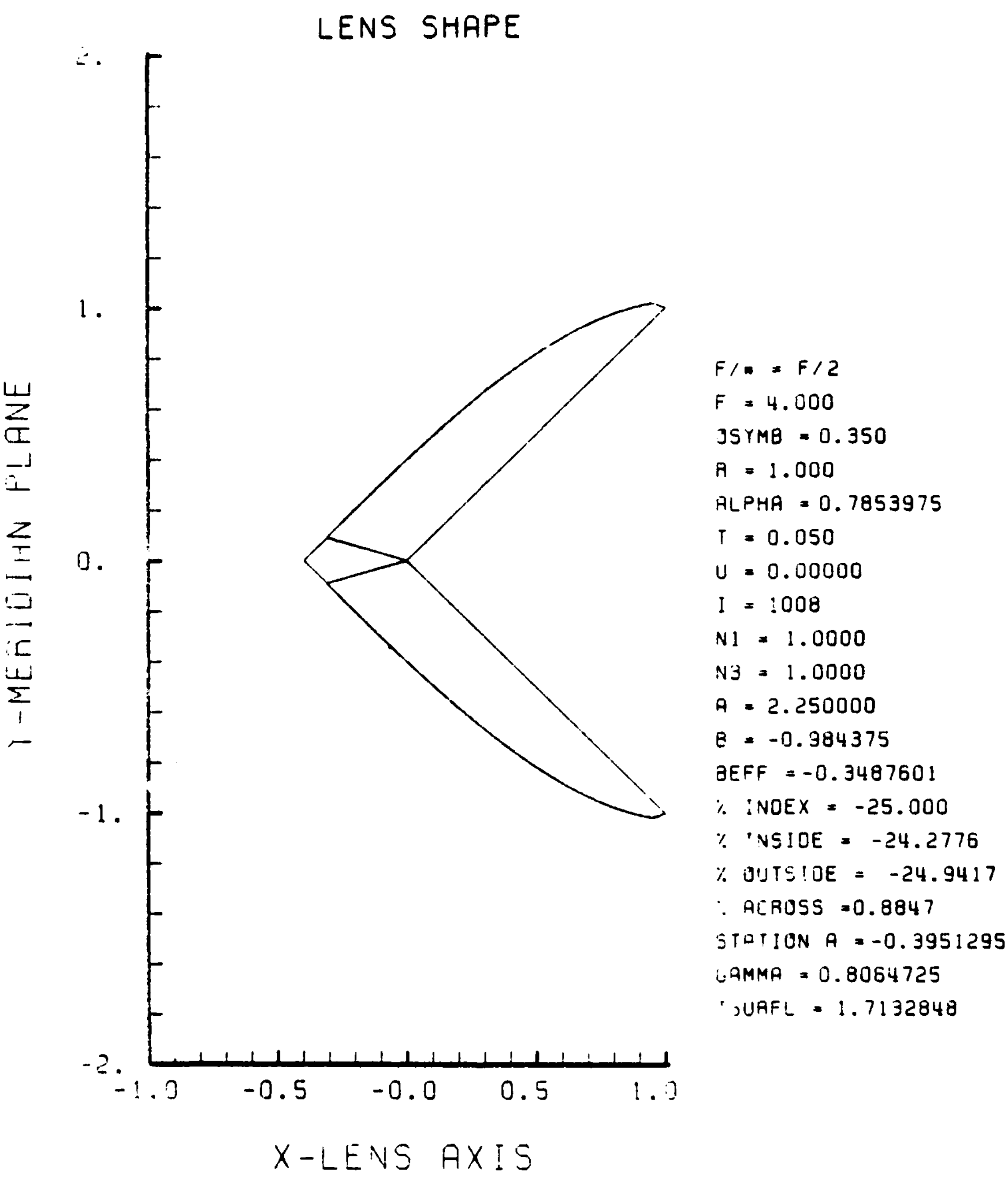

Figure E-37. GRIN Lens Shape at -25%, OB = 0.35, a = 2.25

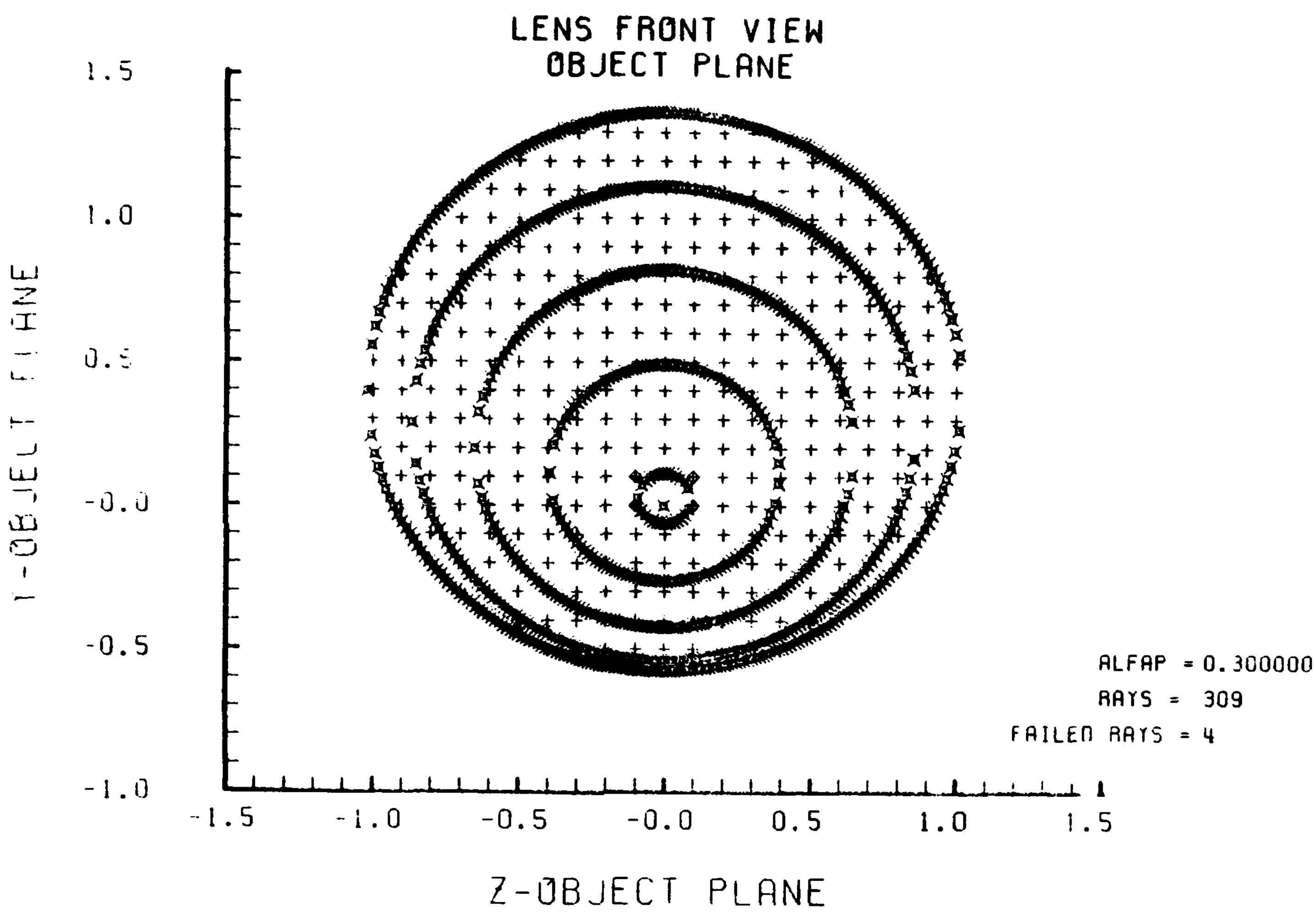

Figure E-38. Grid Plane at α_p = 0.3 for Lens of Figure E-37

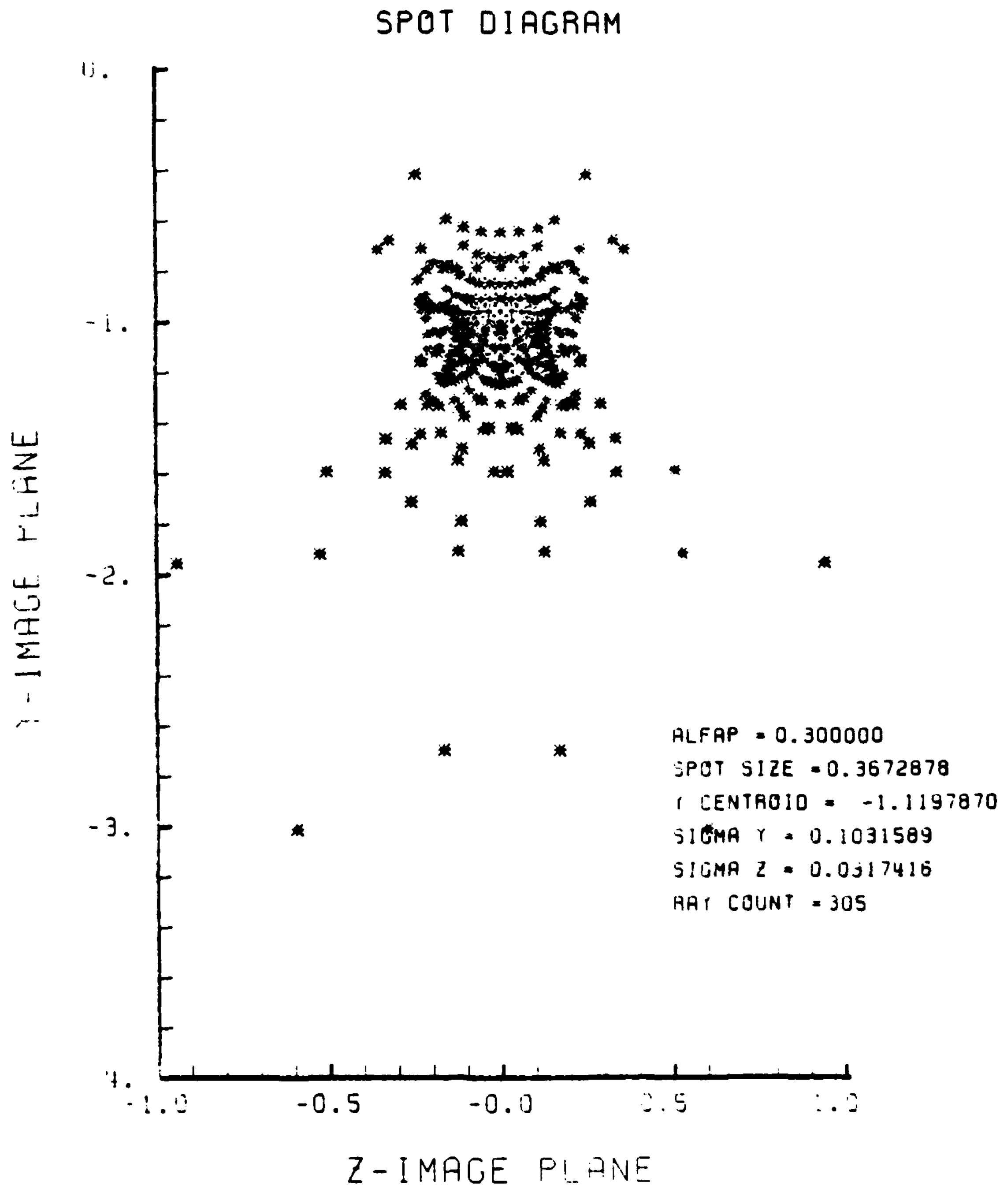

Figure E-39. Spot Diagram for Grid of Figure E-38

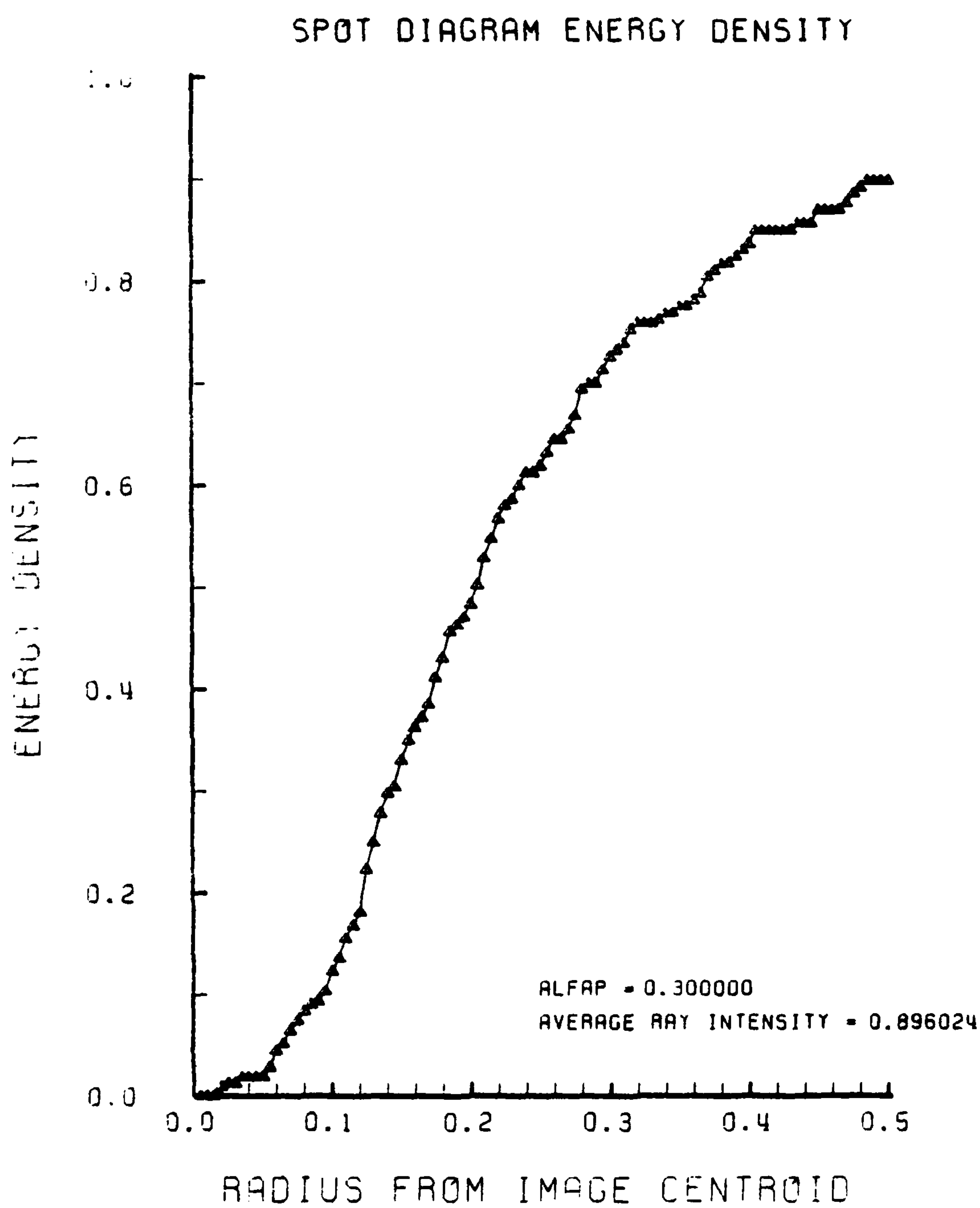

Figure E-40. Encircled Energy of Figure E-39

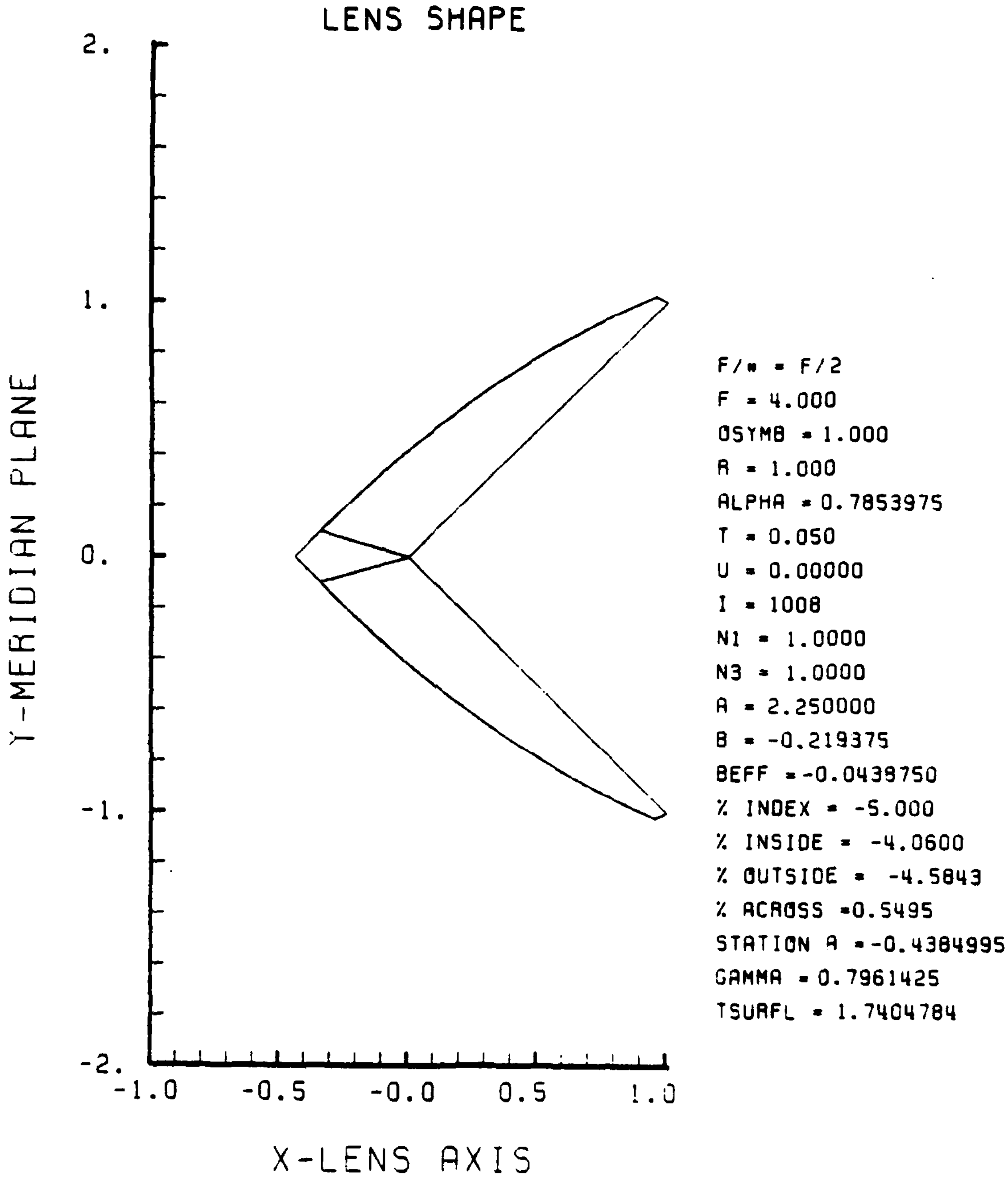

Figure E-41. GRIN Lens Shape at -5%, OB = 1.00, a = 2.25

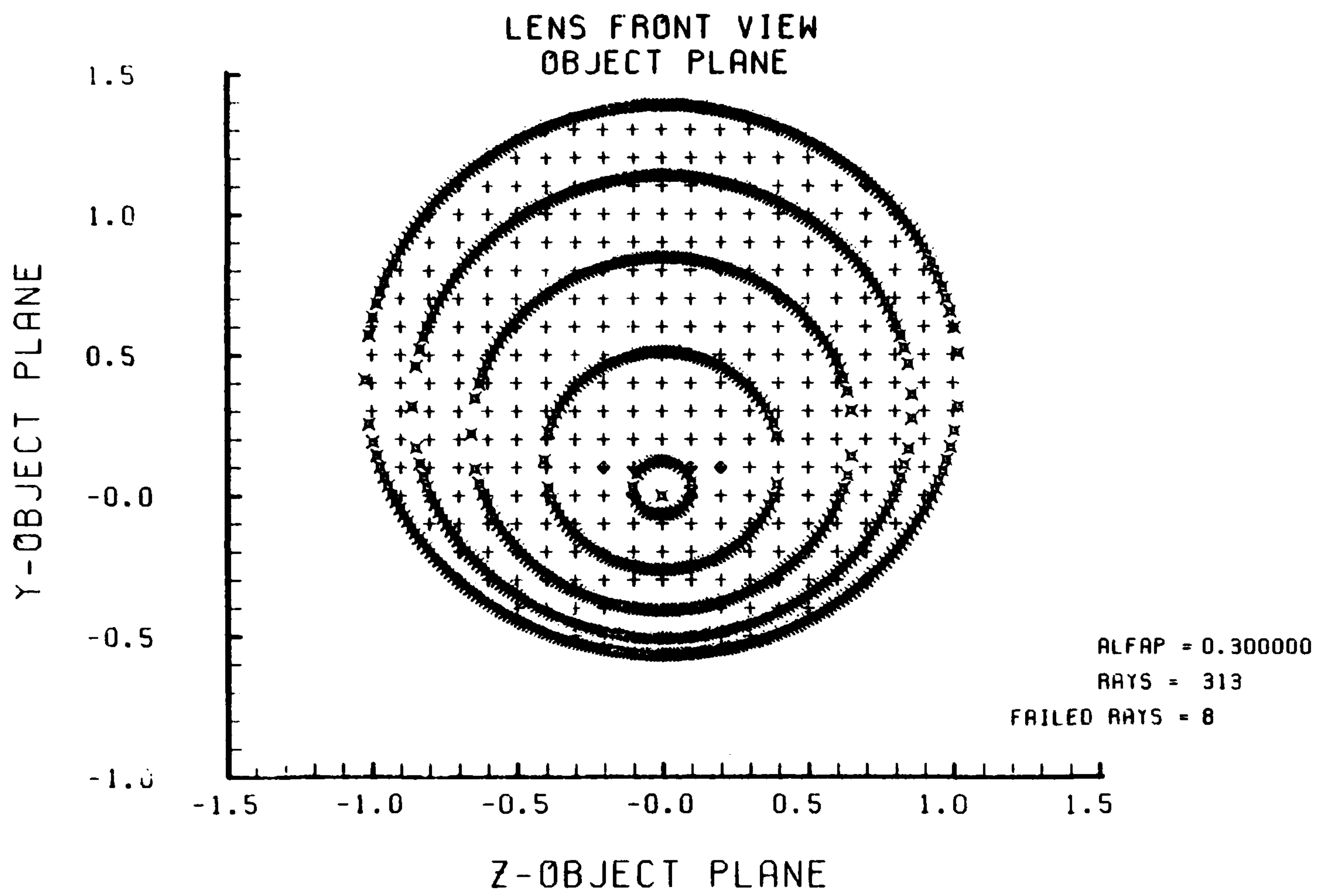

Figure E-42. Grid Plane at $\alpha_p = 0.3$ for Lens of Figure E-41

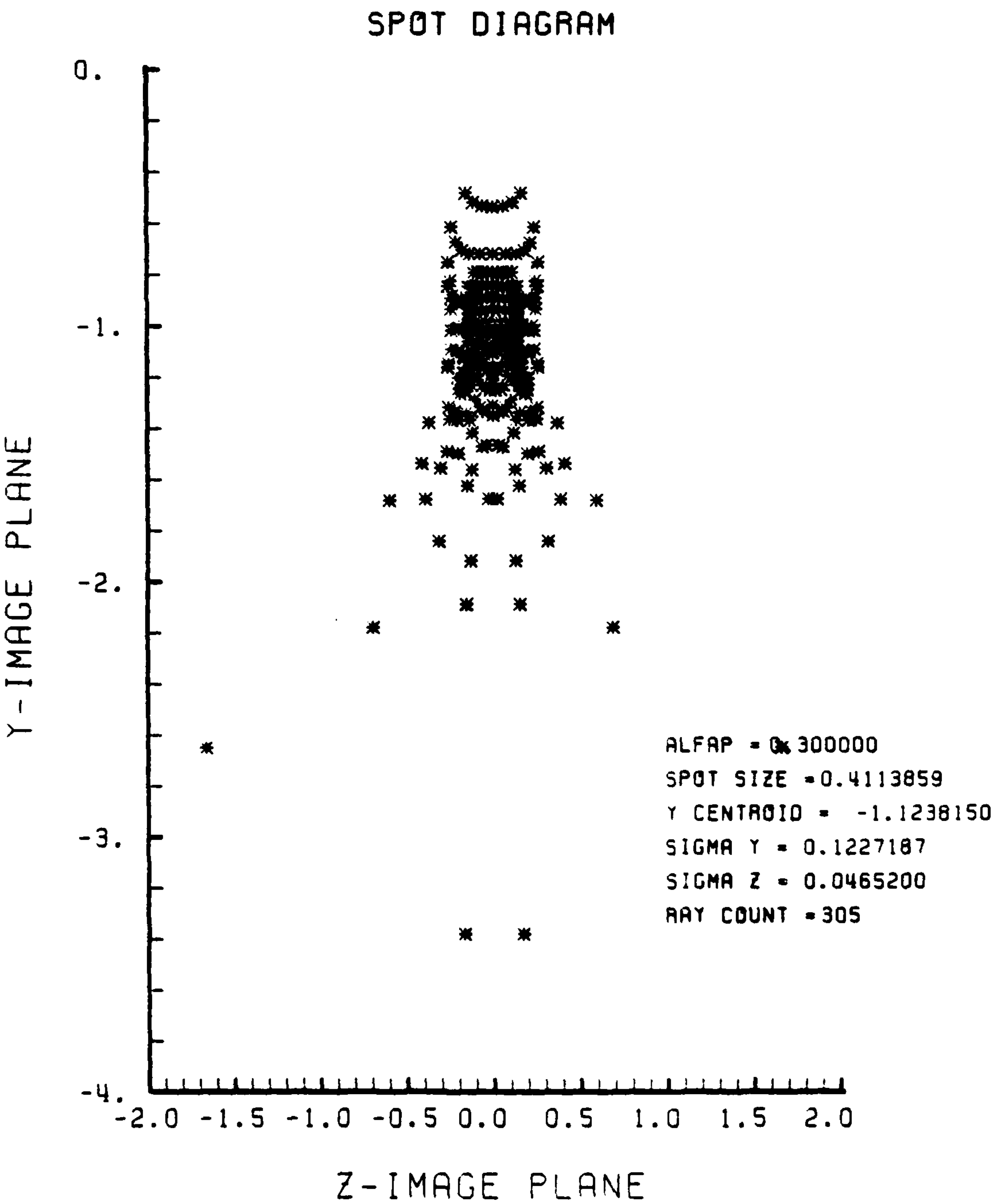

Figure E-43. Spot Diagram for Grid of Figure E-42

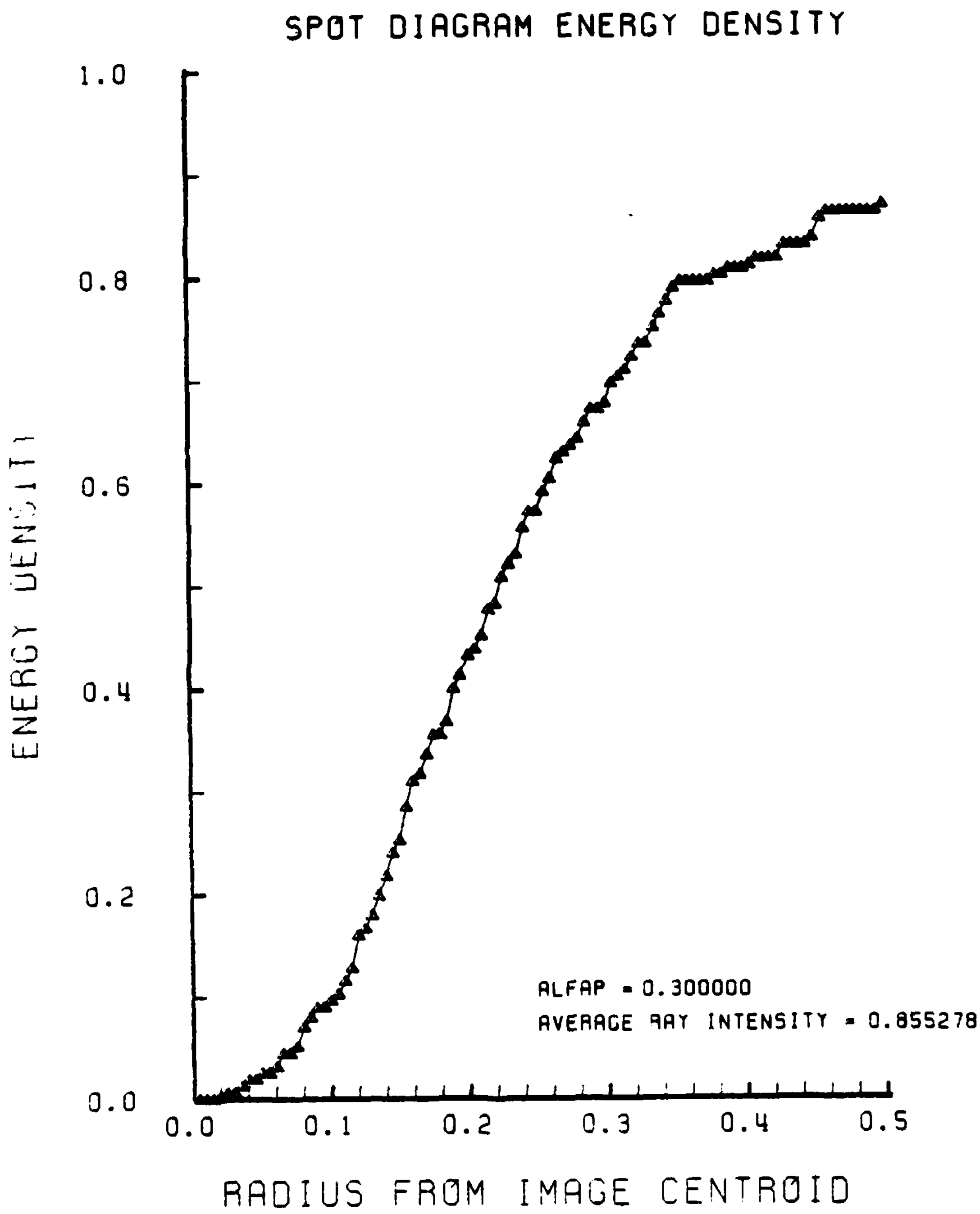

Figure E-44. Encircled Energy of Figure E-43

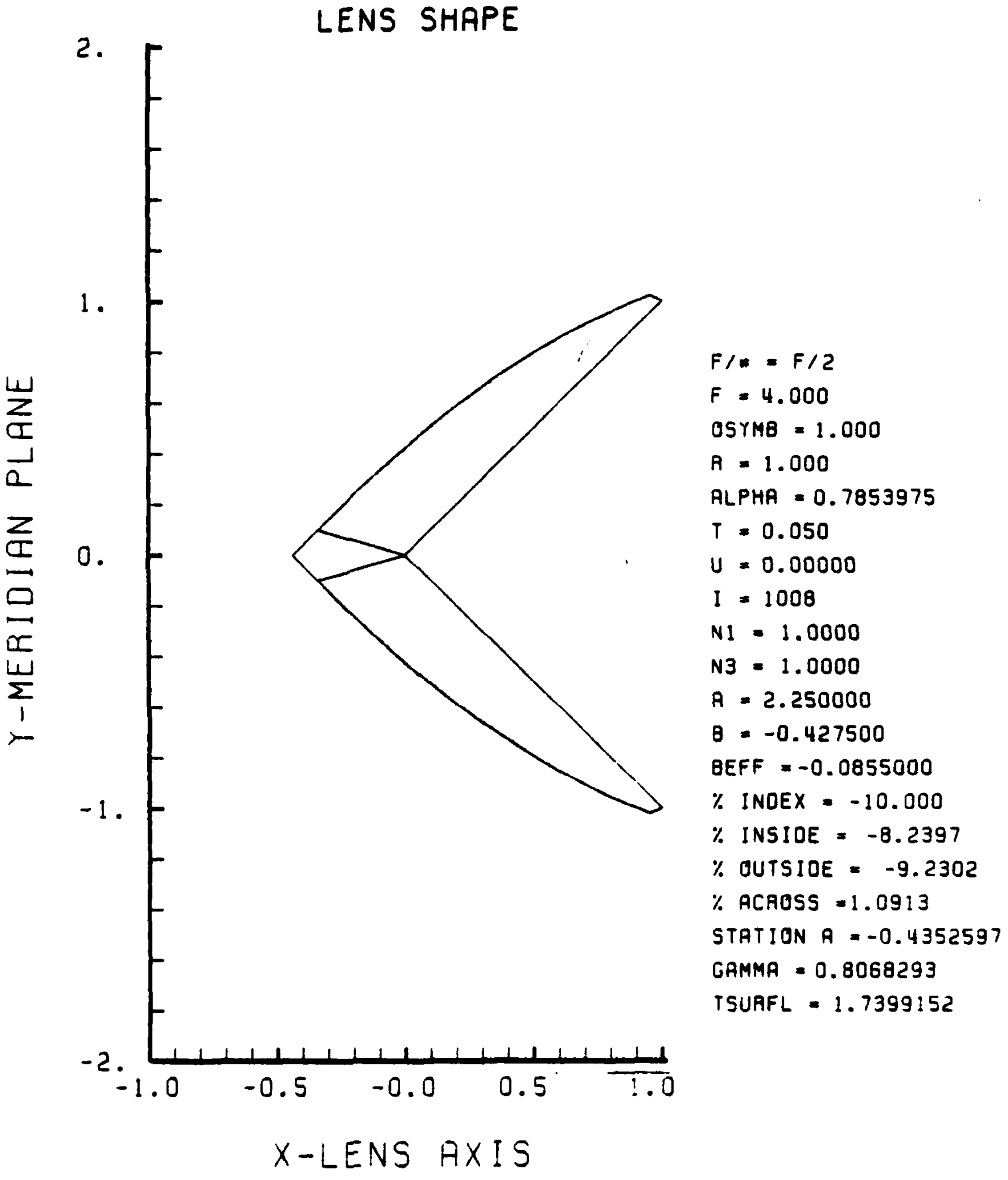

Figure E-45. GRIN Lens Shape at -10%, OB = 1.00
a = 2.25

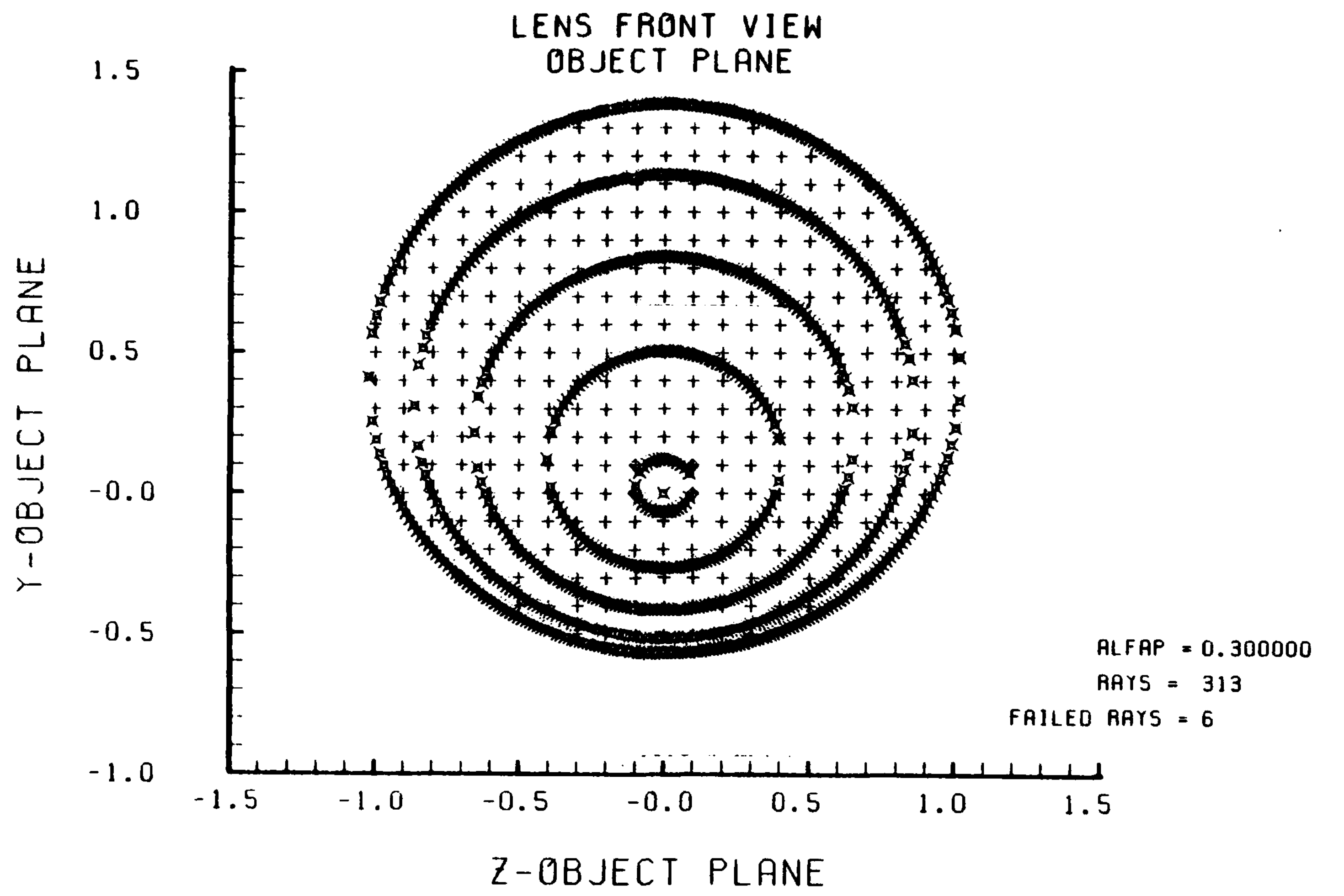

Figure E-46. Grid Plane at α_p = 0.3 for Lens of Figure E-45

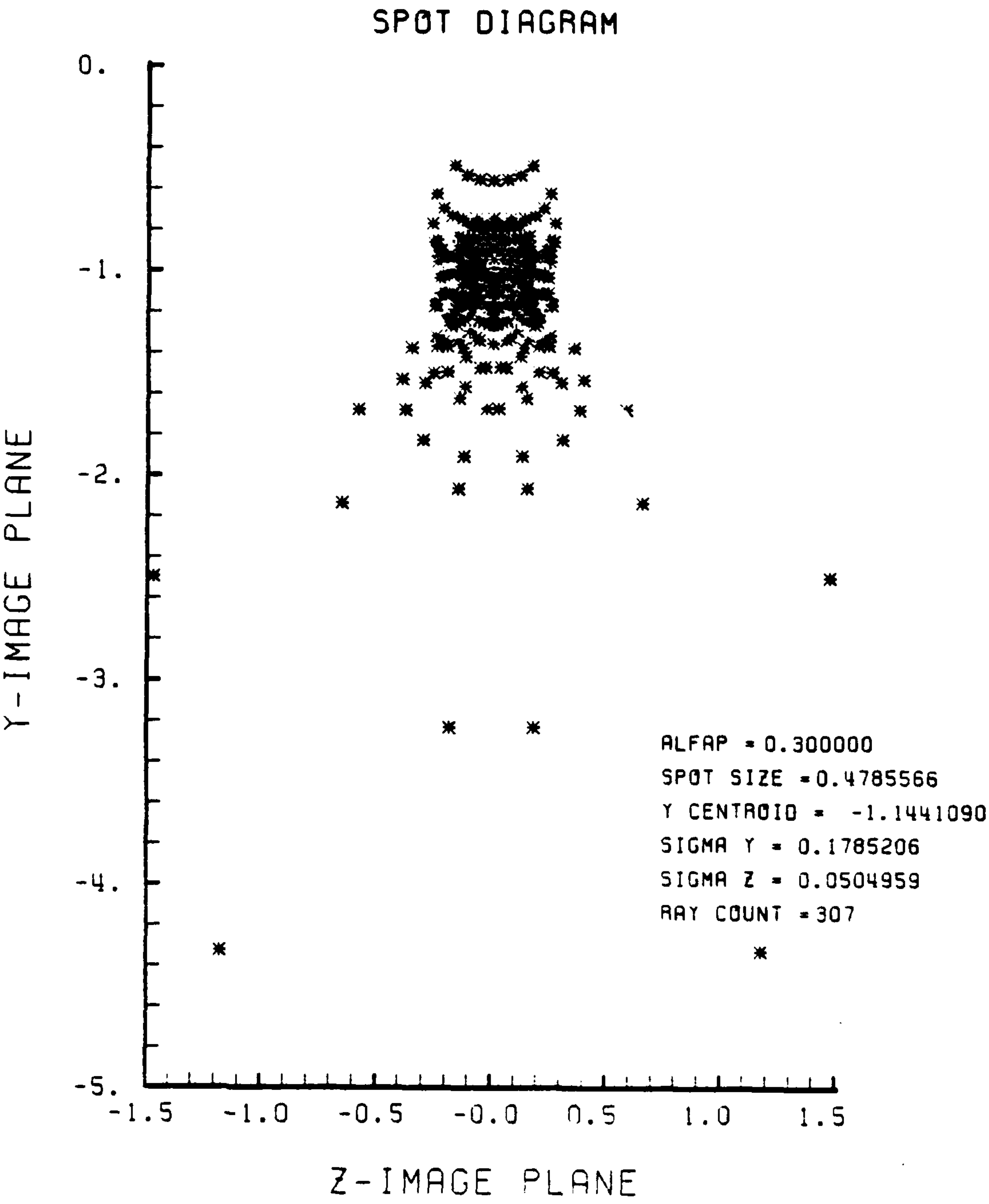

Figure E-47. Spot Diagram for Grid of Figure E-46

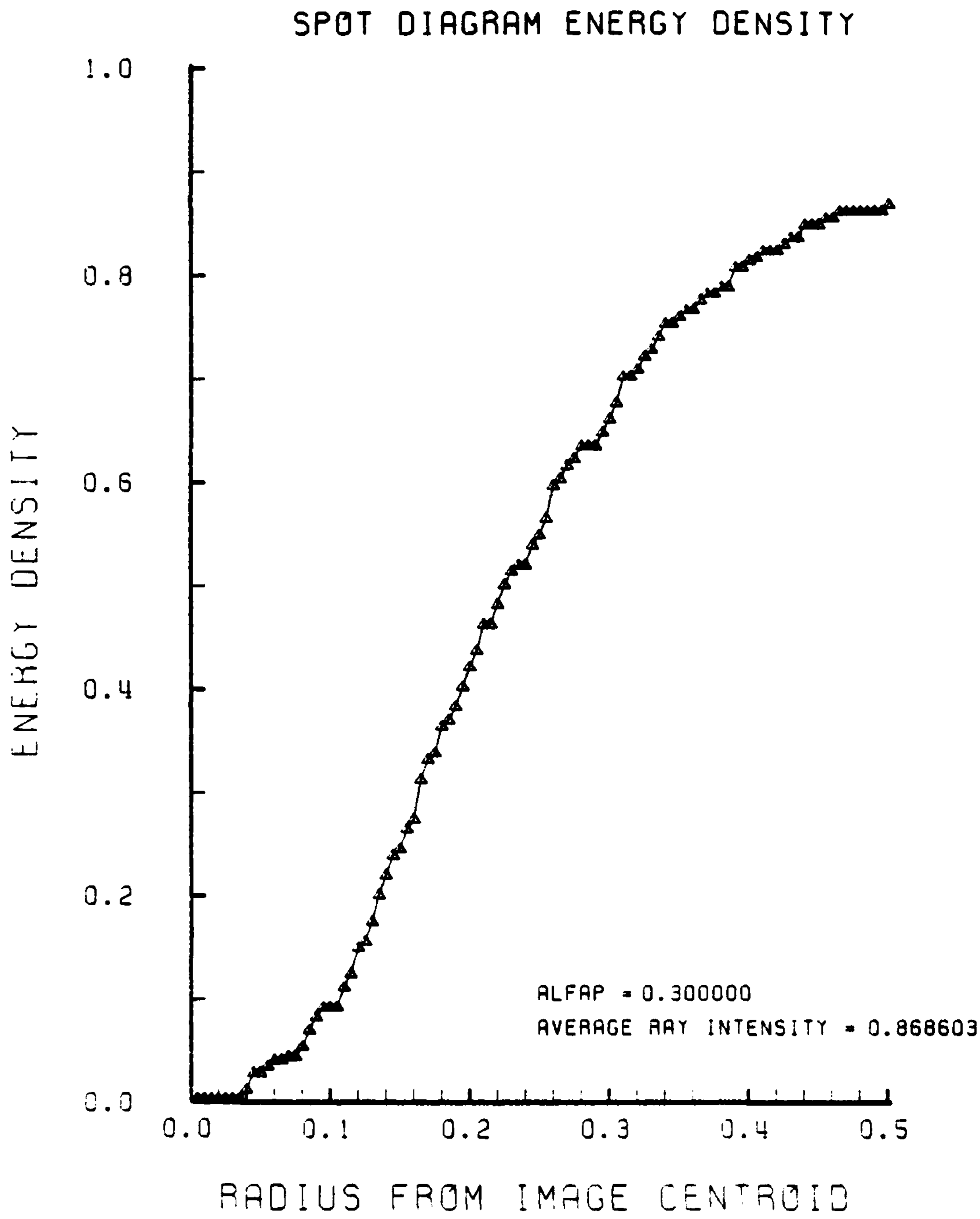

Figure E-48. Encircled Energy of Figure E-47

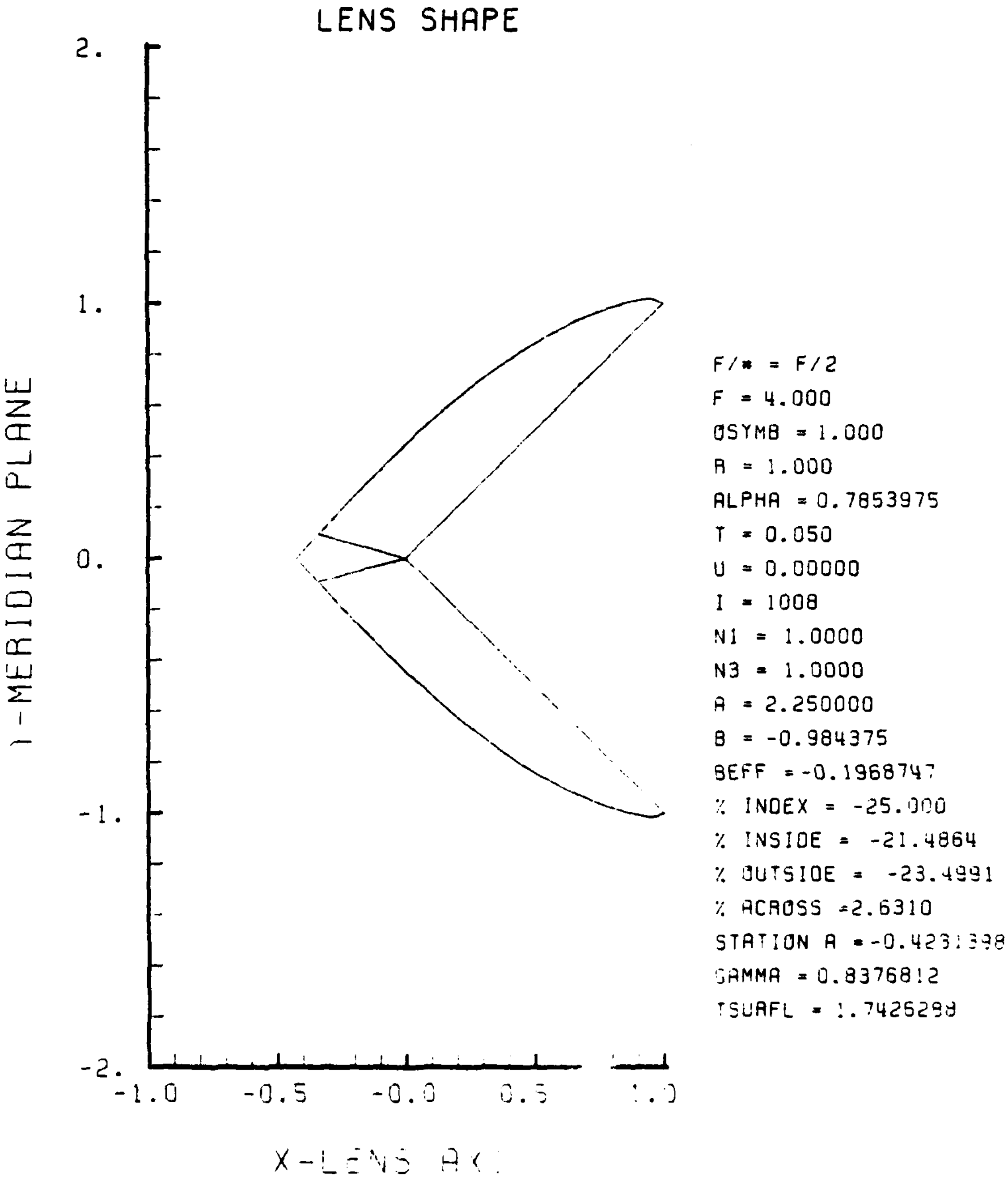

Figure E-49. GRIN Lens Shape at -25%, OB = 1.00, a = 2.25

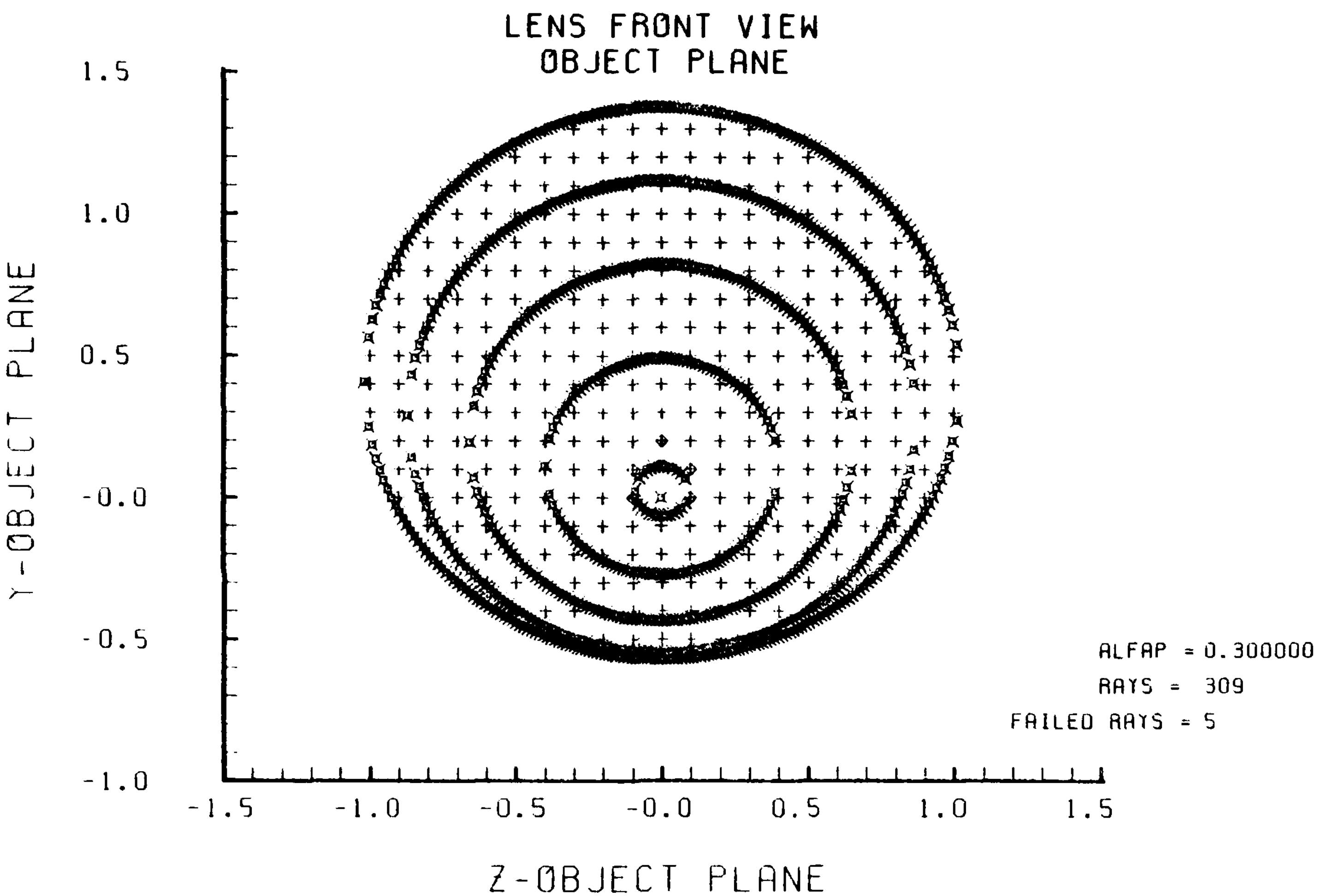

Figure E-50. Grid Plane at α_p = 0.3 for Lens of Figure E-49

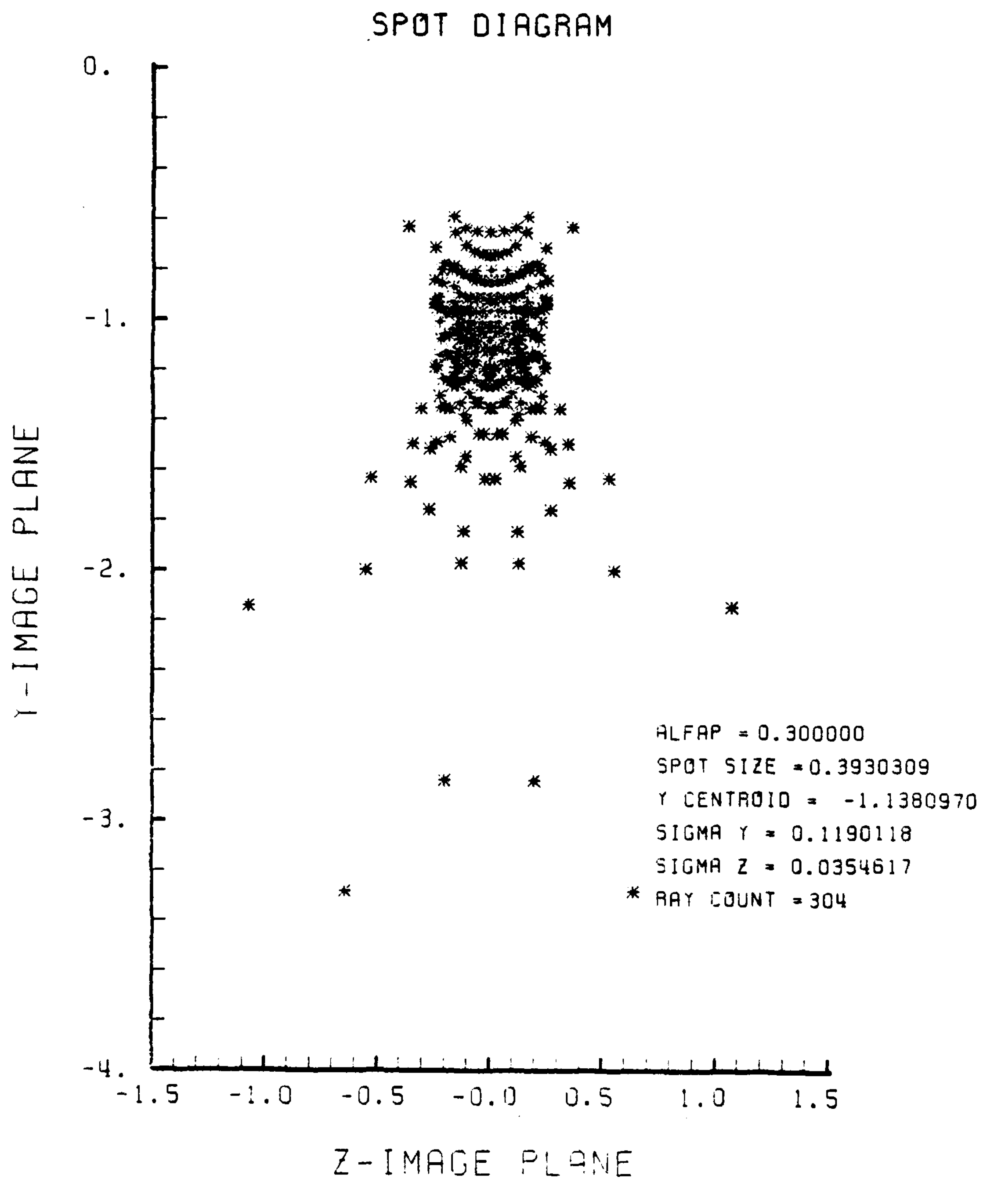

Figure E-51. Spot Diagram for Grid of Figure E-50

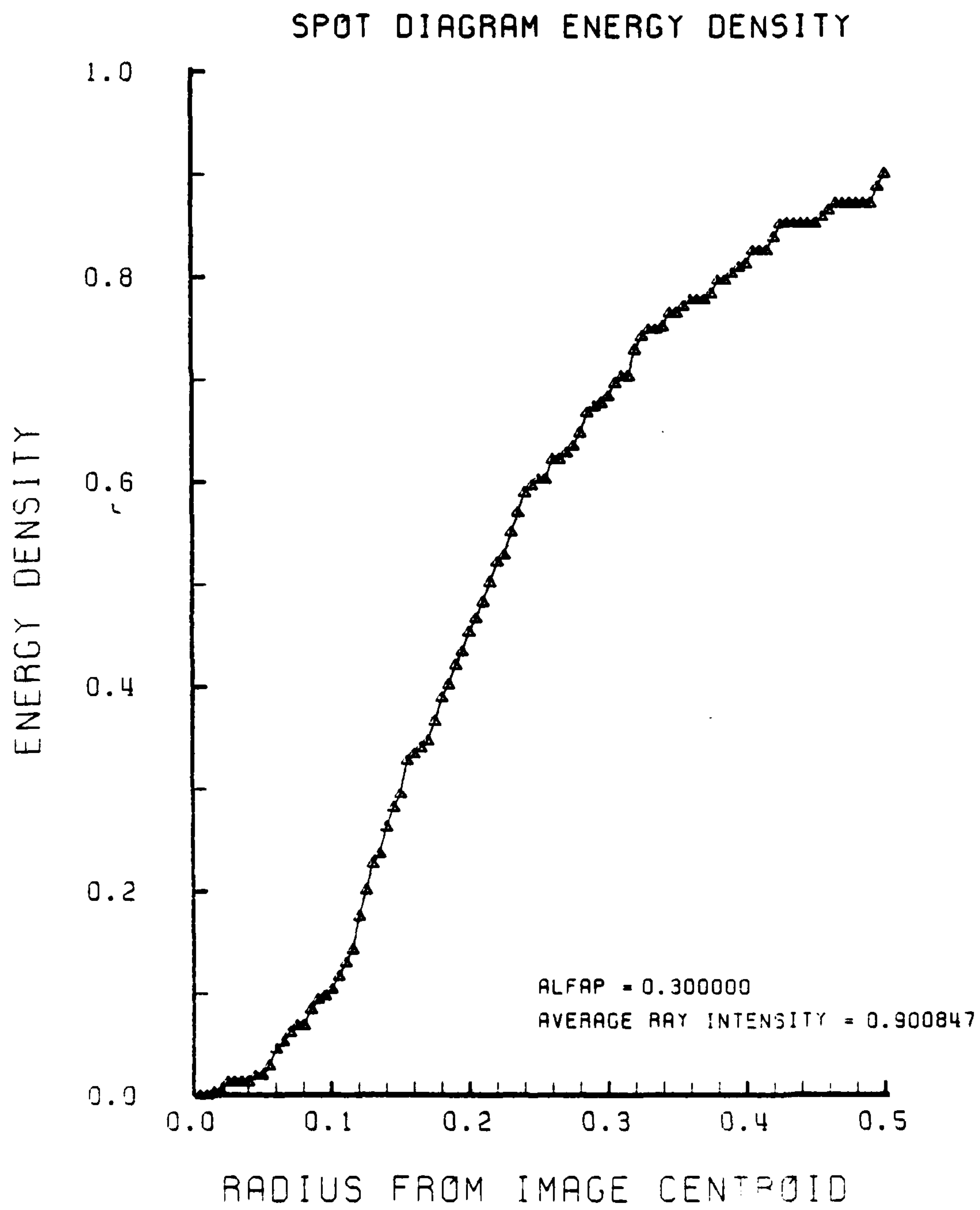

Figure E-52. Encircled Energy of Figure E-51

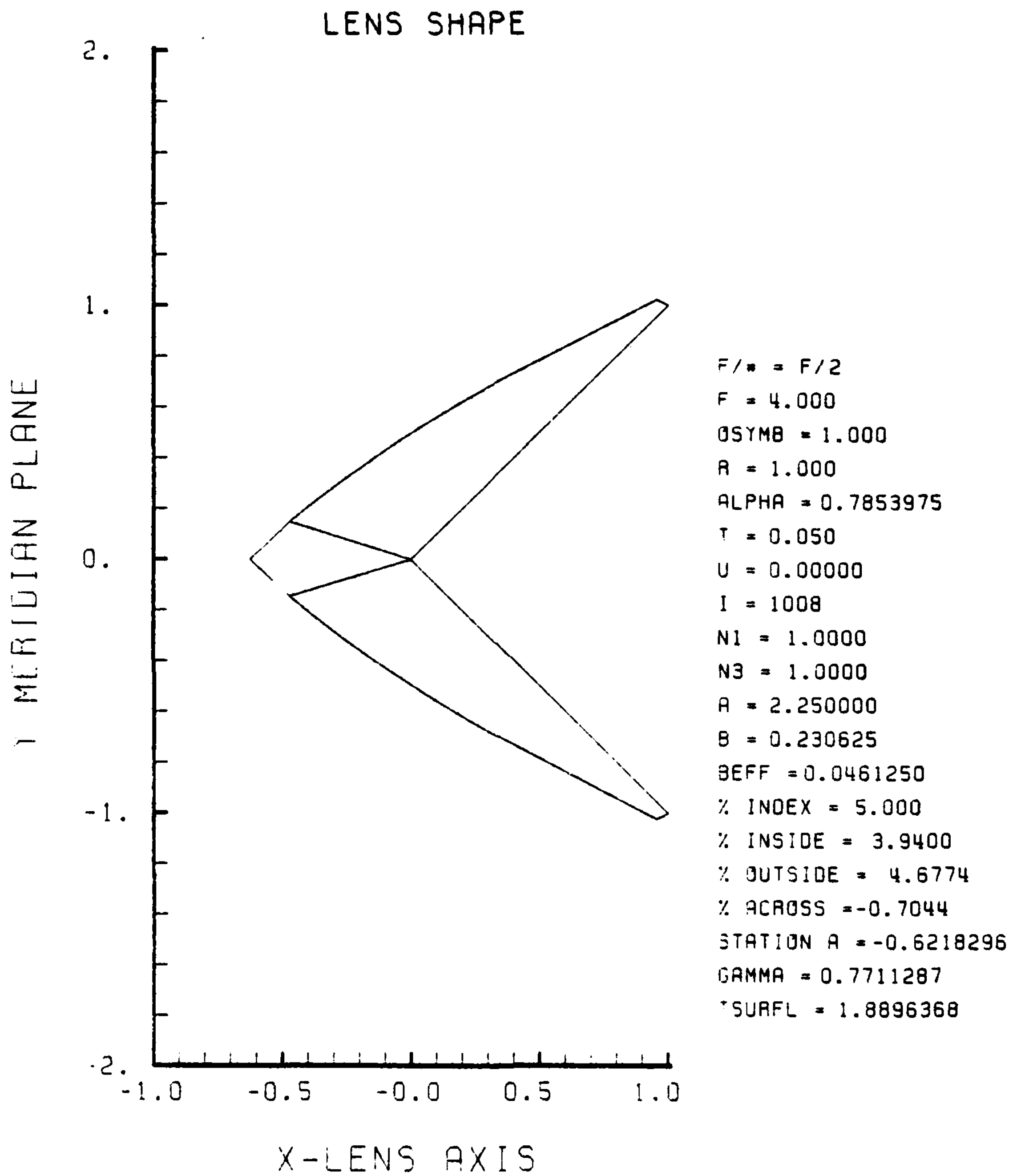

Figure E-53. GRIN Lens Shape at +5%, OB = 1.00, a = 2.25

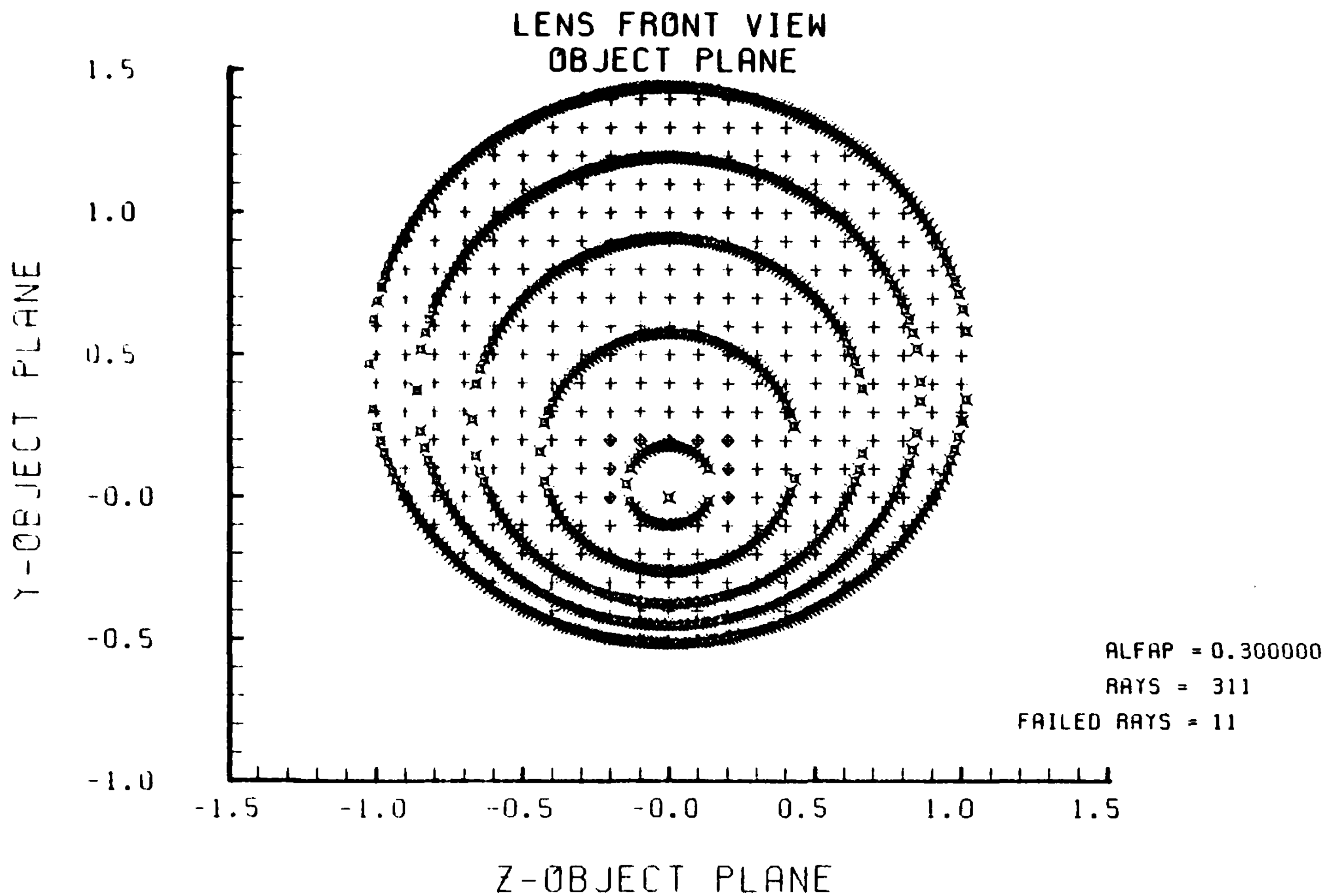

Figure E-54. Grid Plane at α_p = 0.3 for Lens of Figure E-53

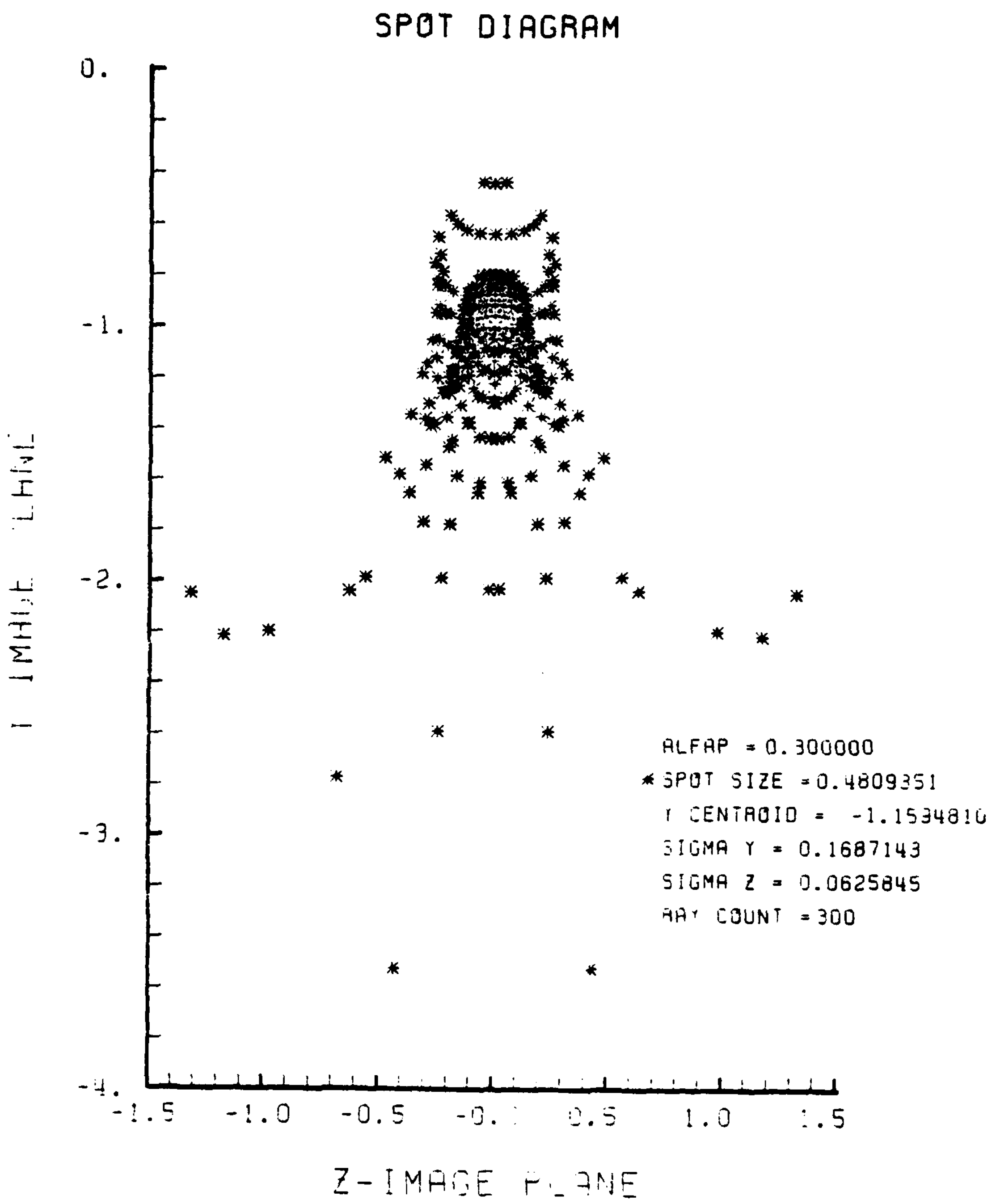

Figure E-55. Spot Diagram for Grid of Figure E-54

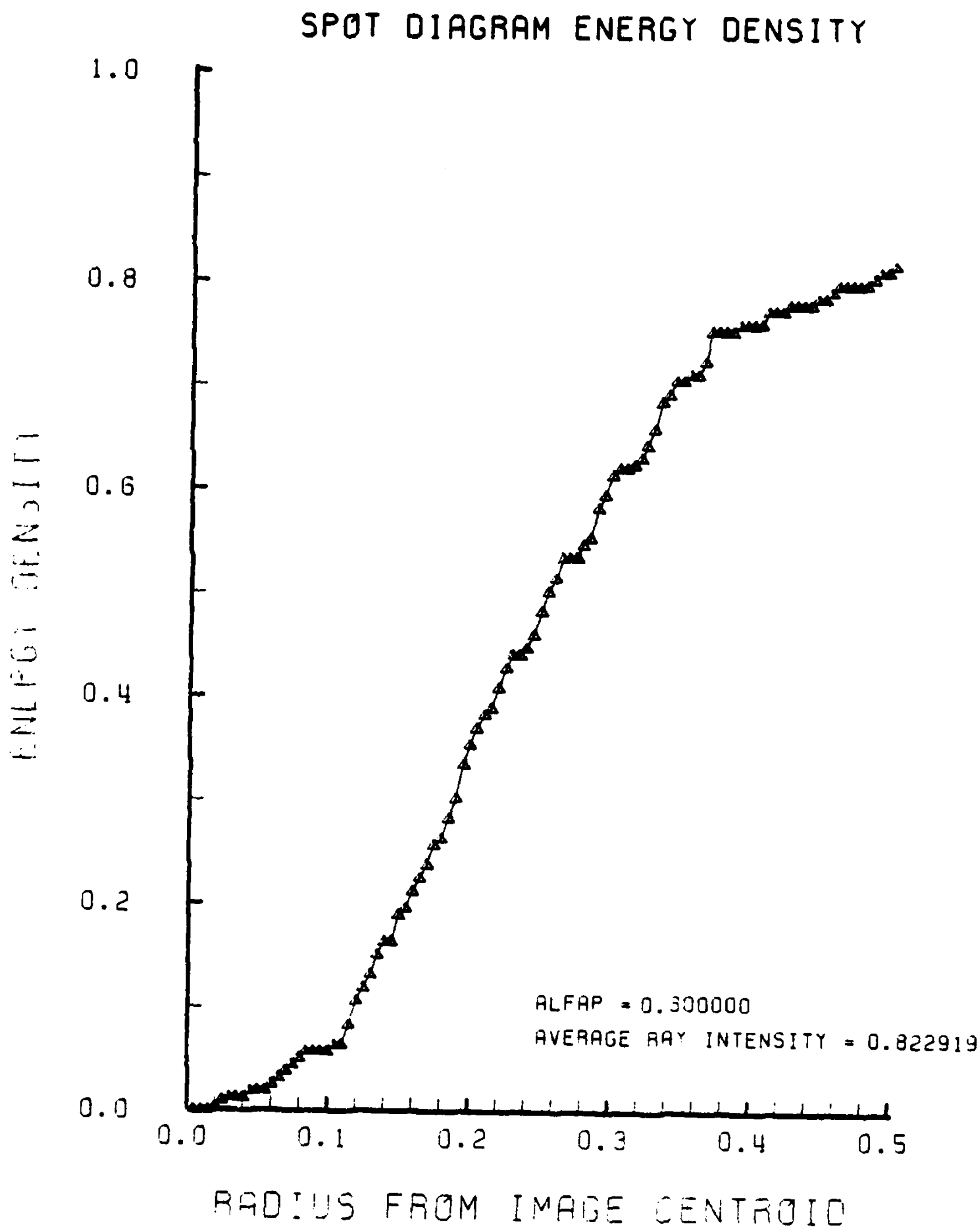

Figure E-56. Encircled Energy of Figure E-55

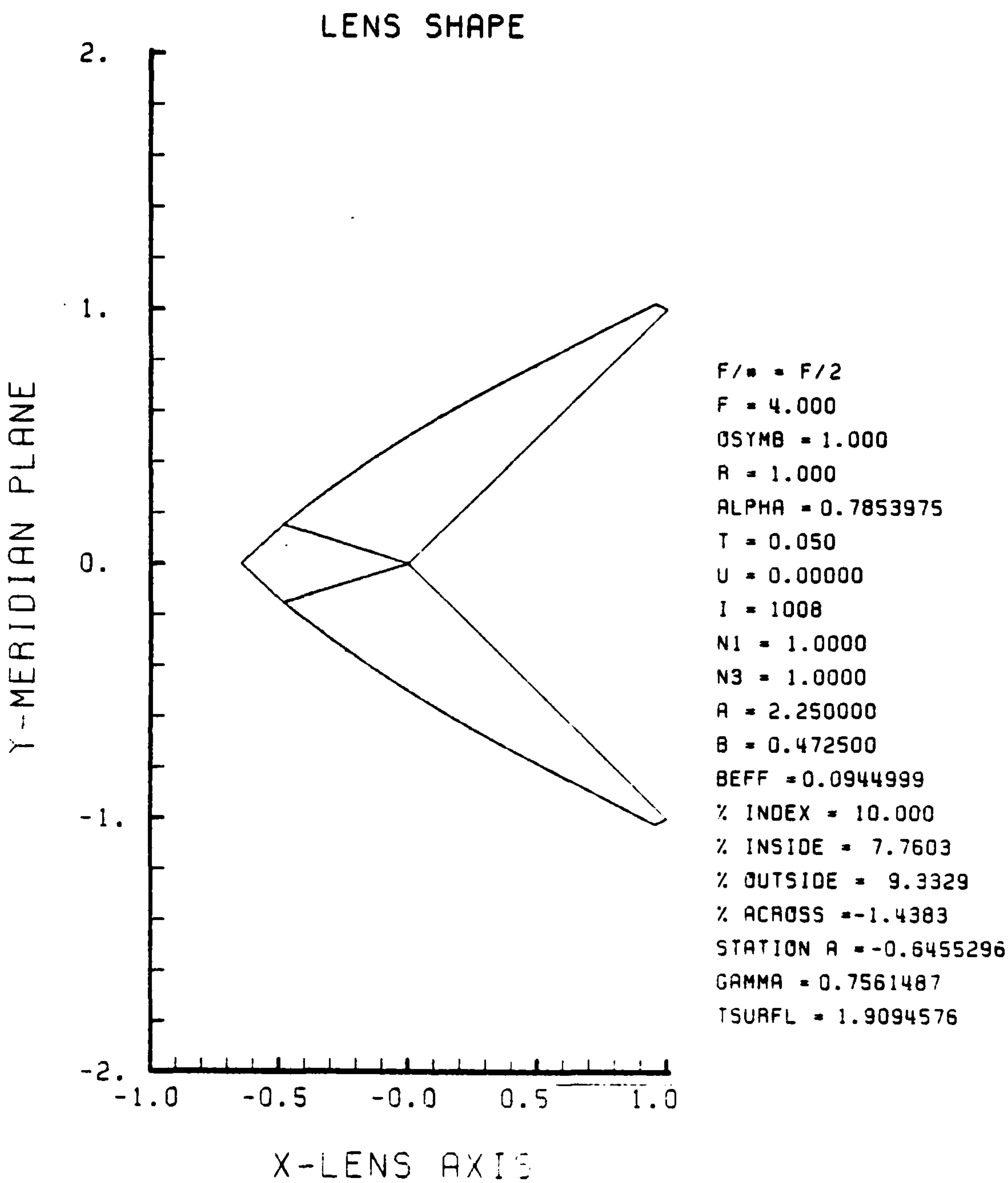

Figure E-57. GRIN Lens Shape at +10%, OB = 1.00, a = 2.25

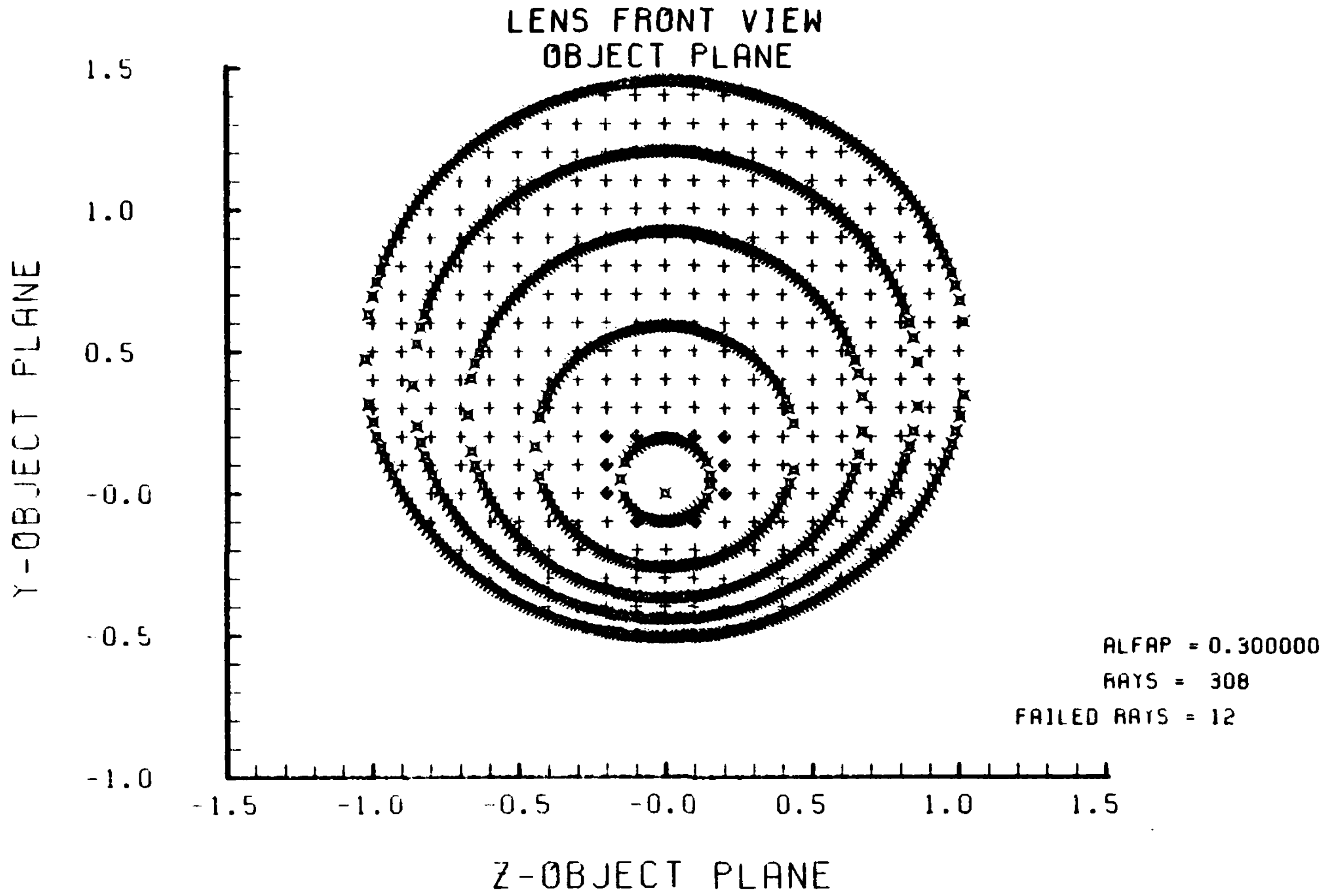

Figure E-58. Grid Plane at $\alpha_p = 0.3$ for Lens of Figure E-57

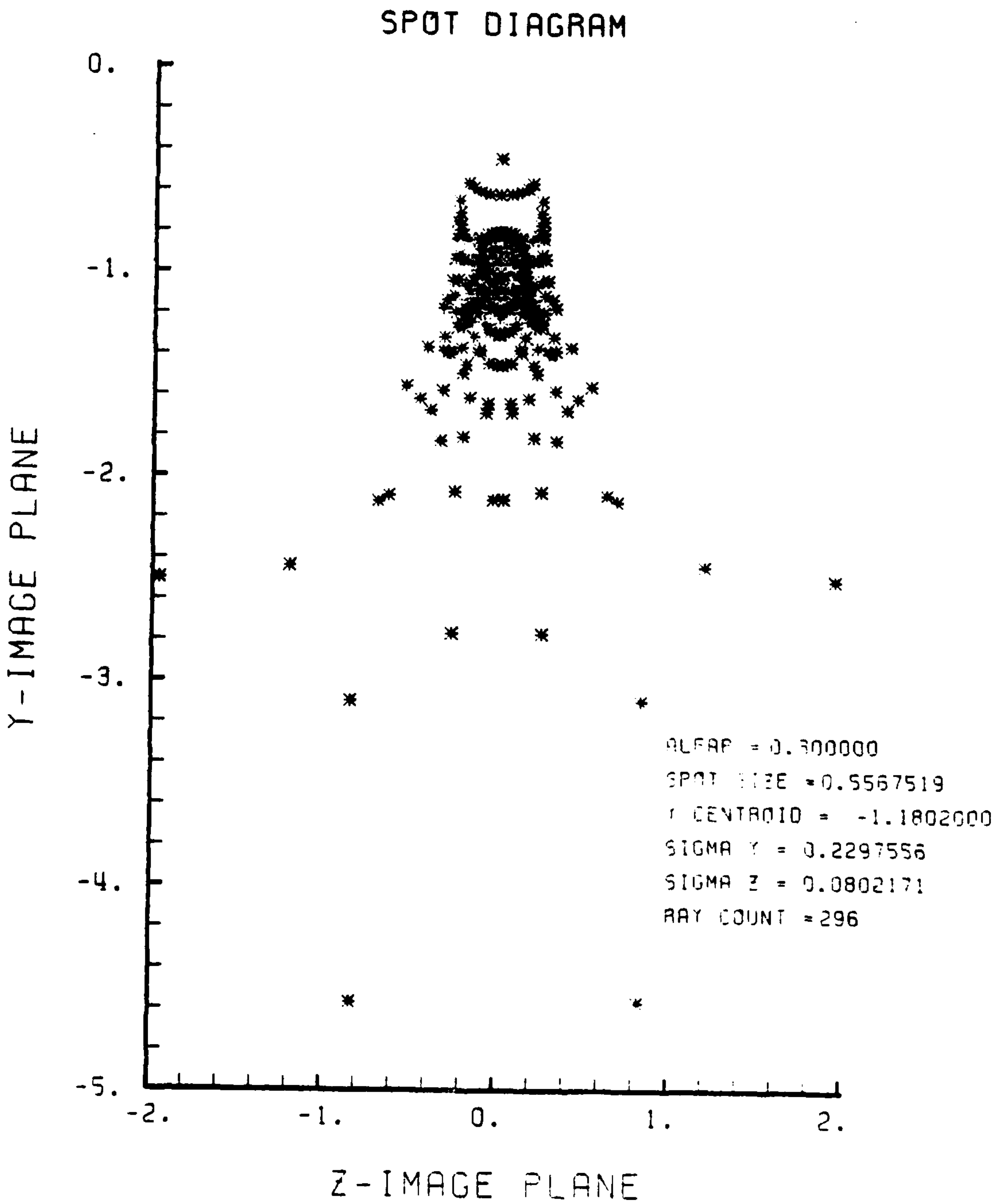

Figure E-59. Spot Diagram for Grid of Figure E-58

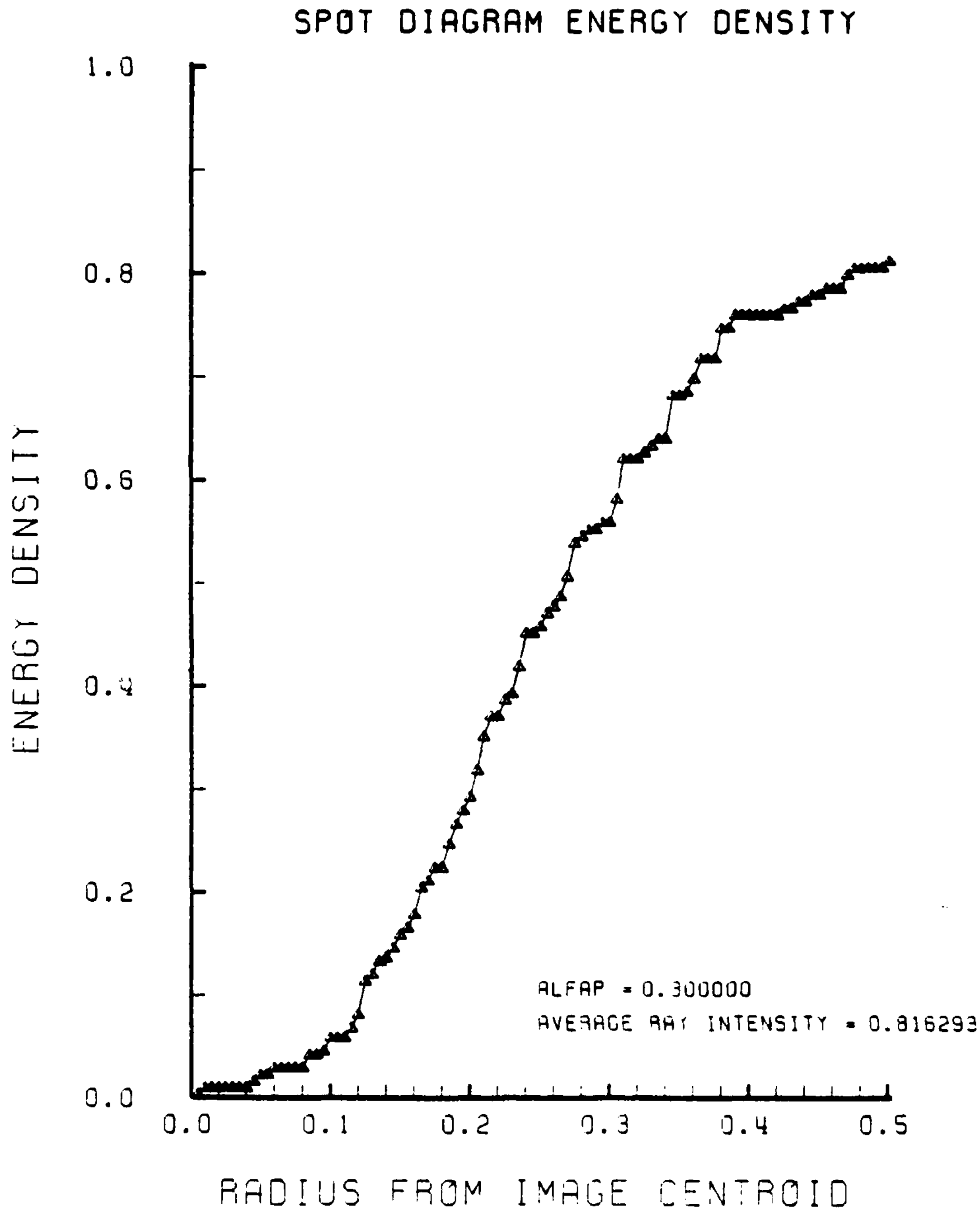

Figure E-60. Encircled Energy of Figure E-59

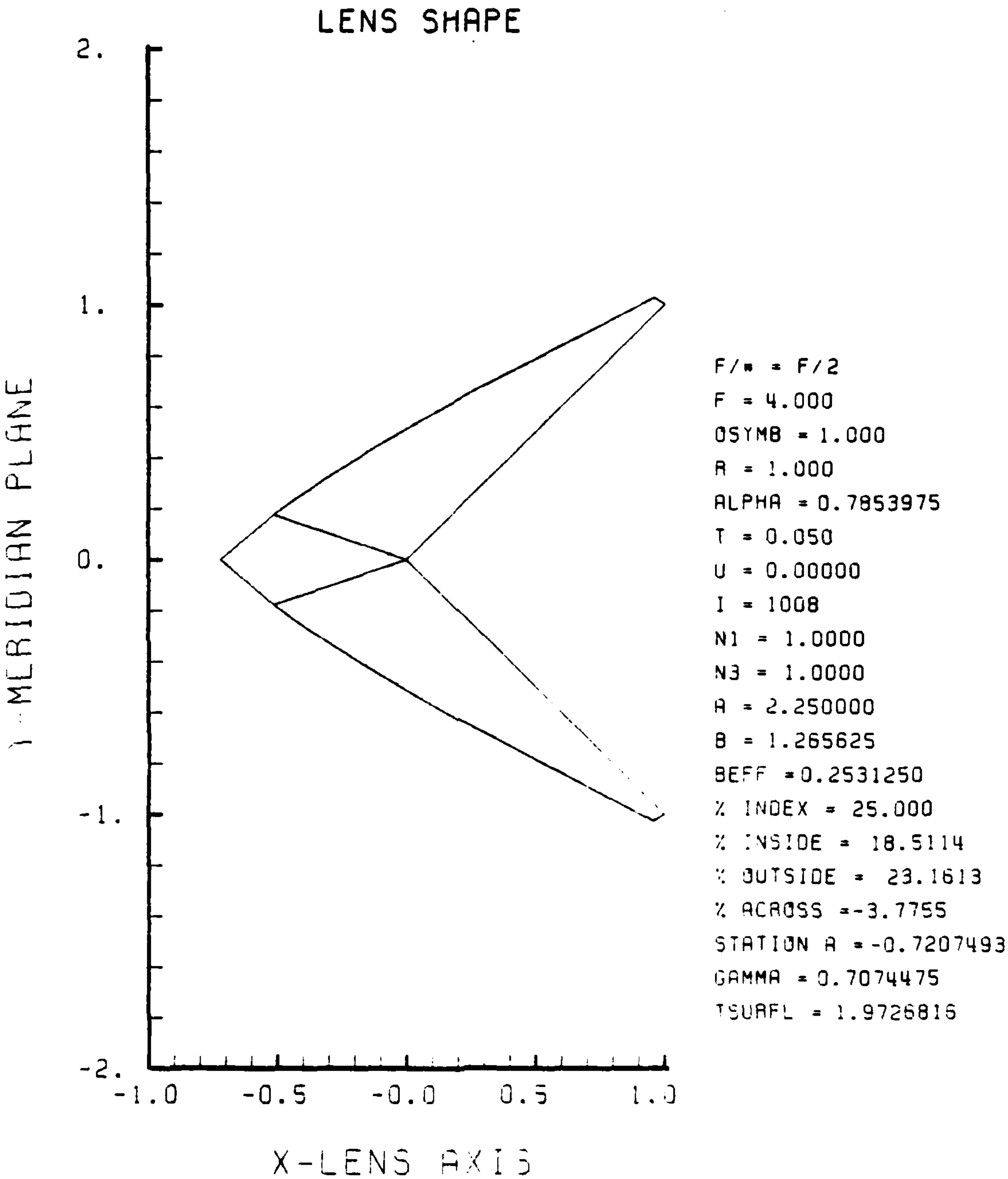

Figure E-61. GRIN Lens Shape at +25%, OB = 1.00, a = 2.25

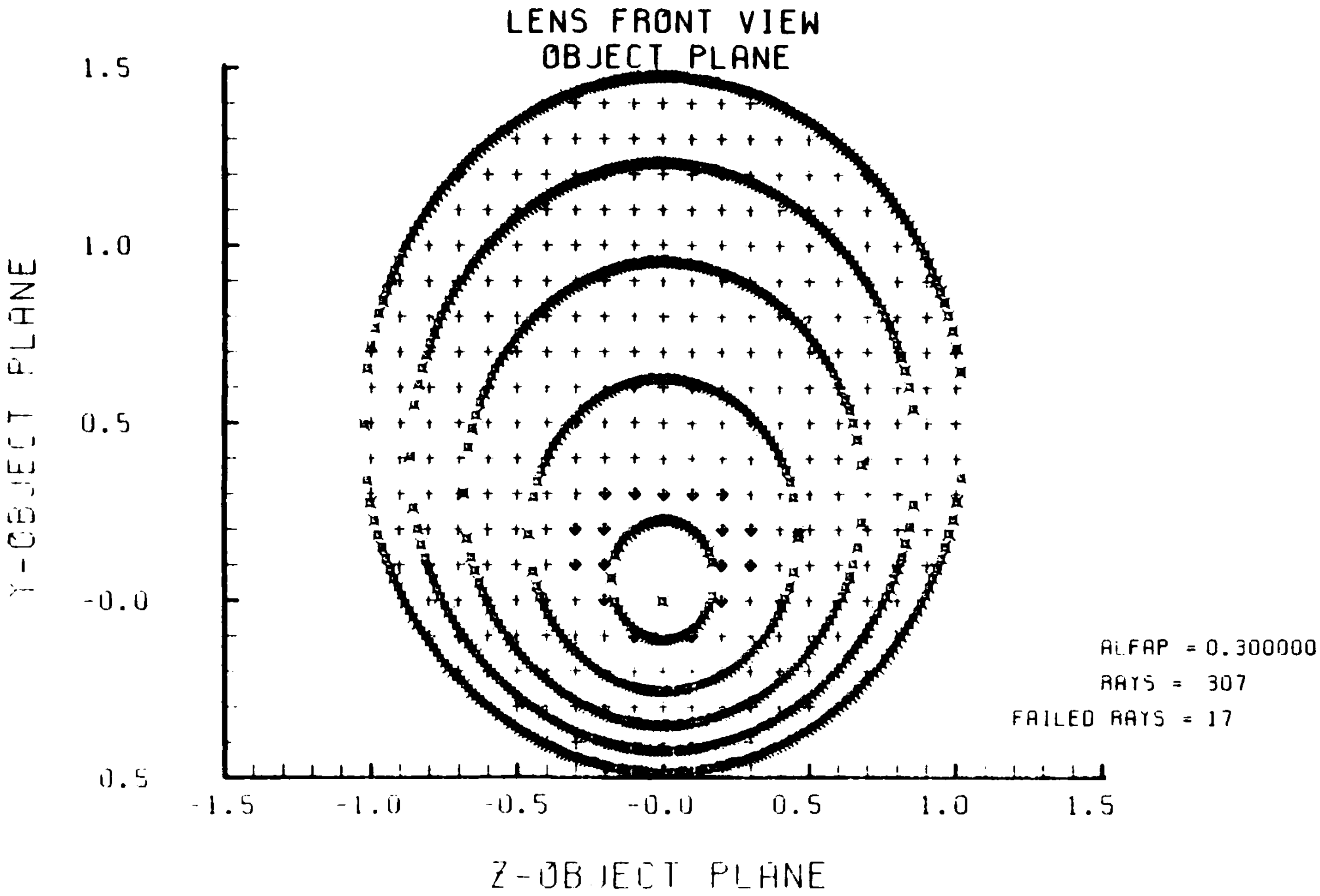

Figure E-62. Grid Plane at α_p = 0.3 for Lens of Figure E-61

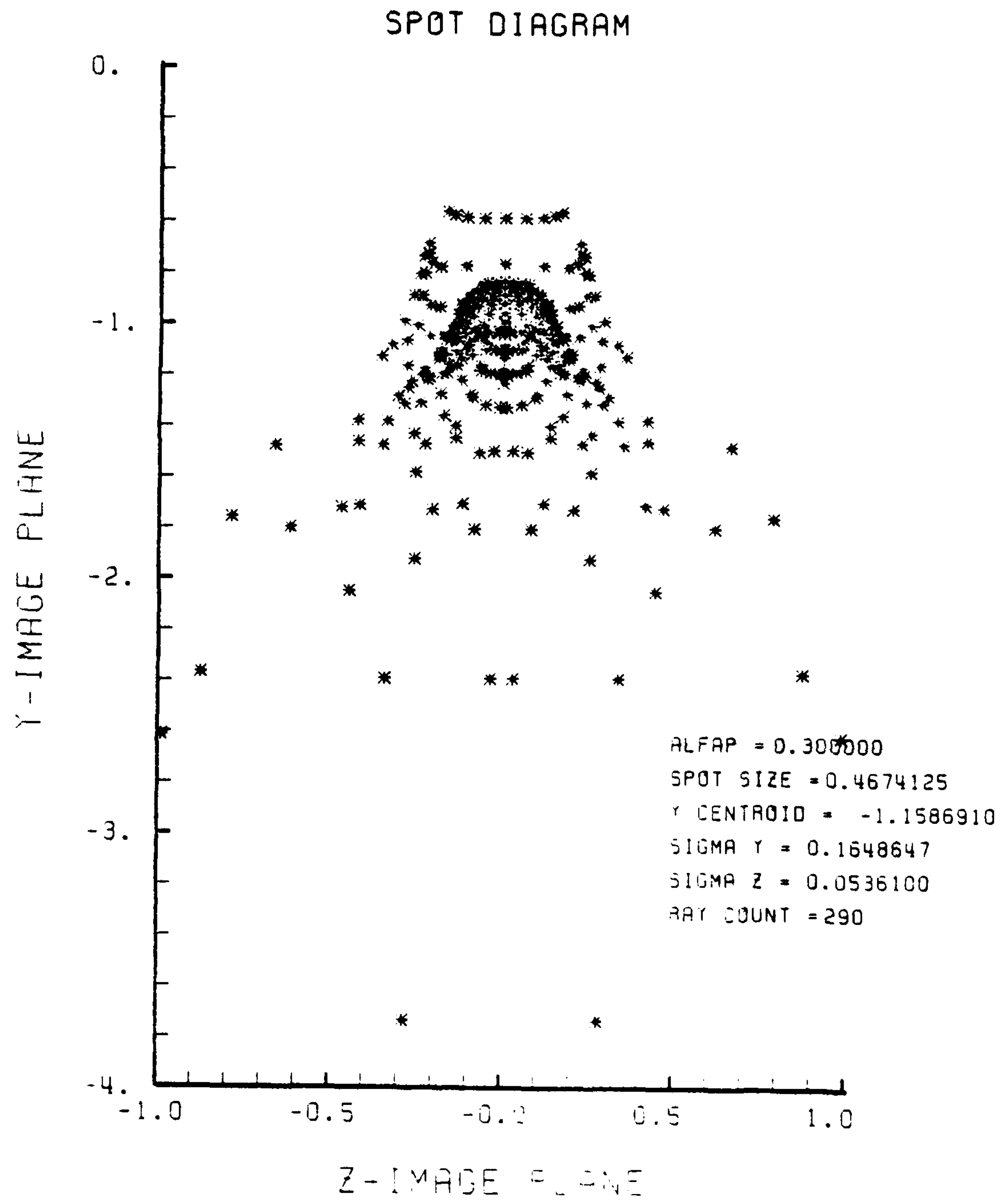

Figure E-63. Spot Diagram for Grid of Figure E-62

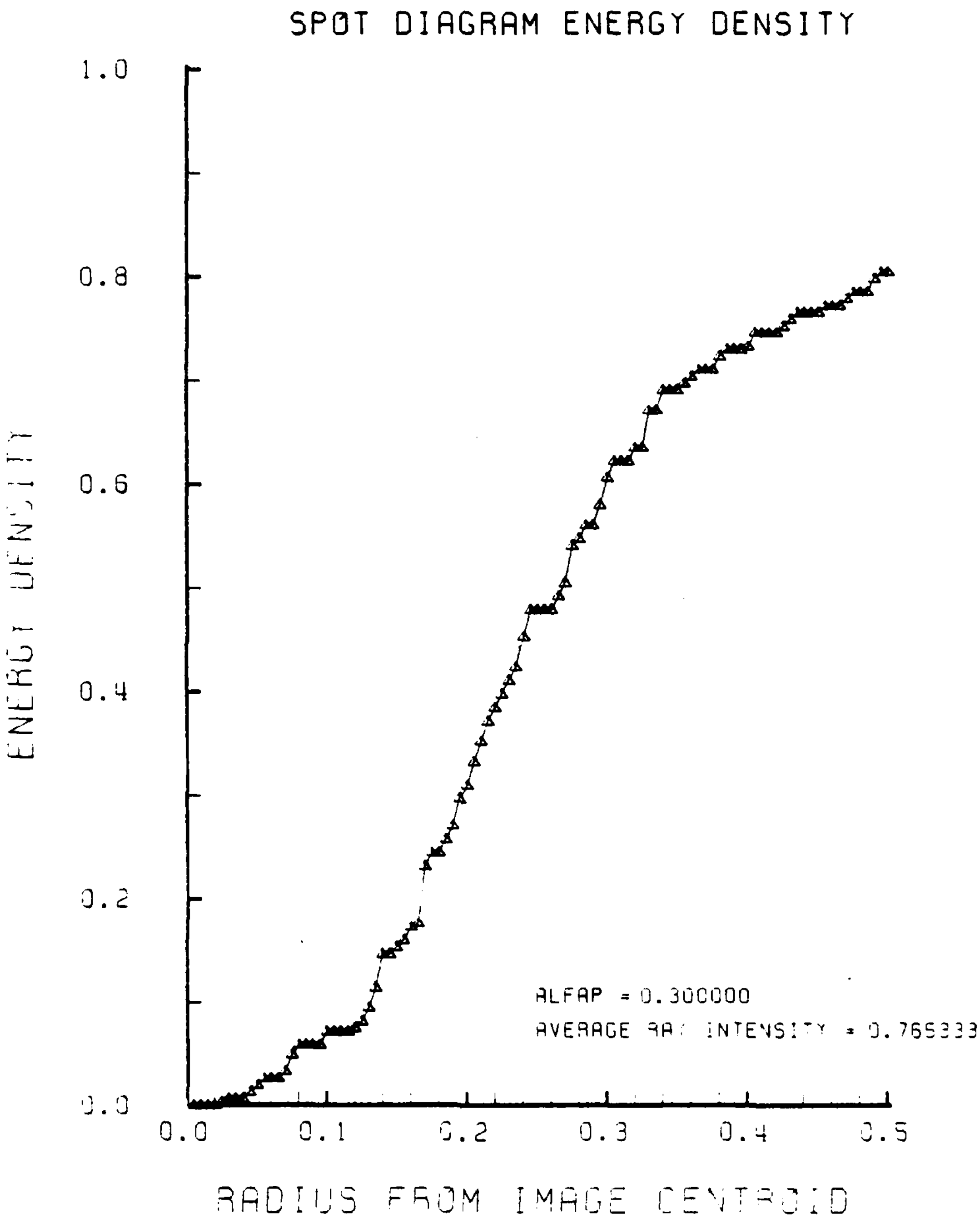

Figure E-64. Encircled Energy of Figure E-63

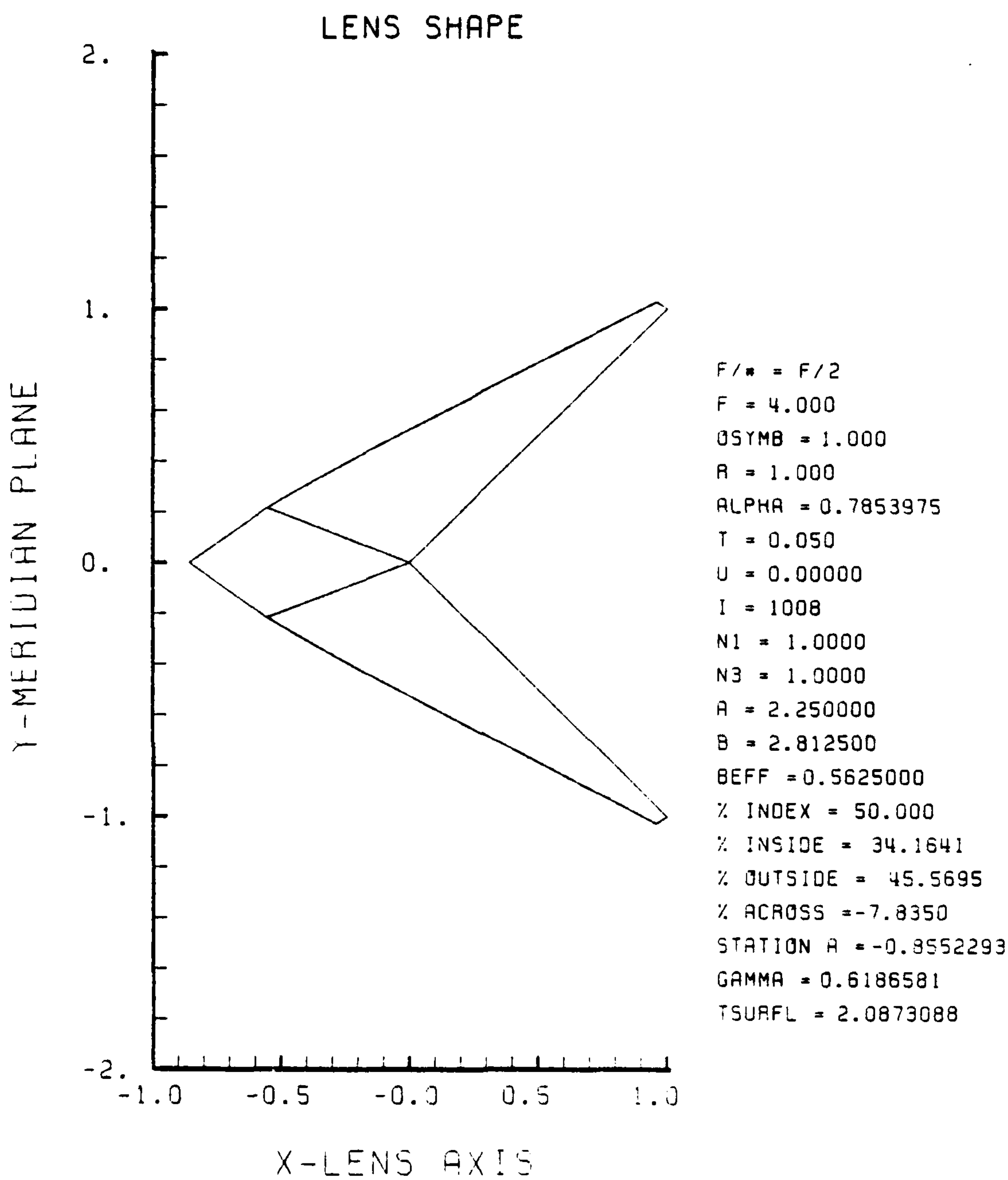

Figure E-65. GRIN Lens Shape at +50%, OB = 1.00, a = 2.25

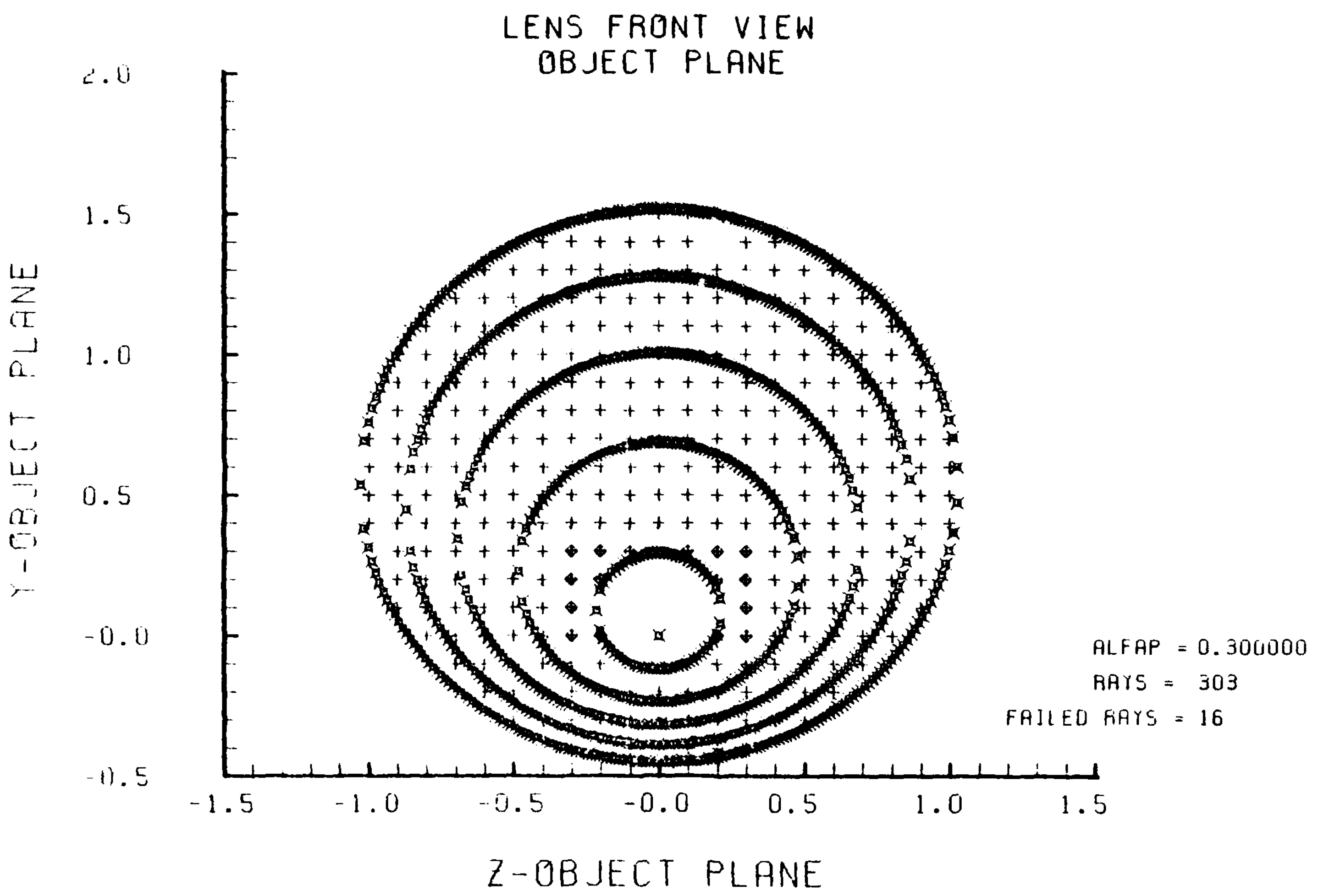

Figure E-66. Grid Plane at $\alpha_p = 0.3$ for Lens of Figure E-65

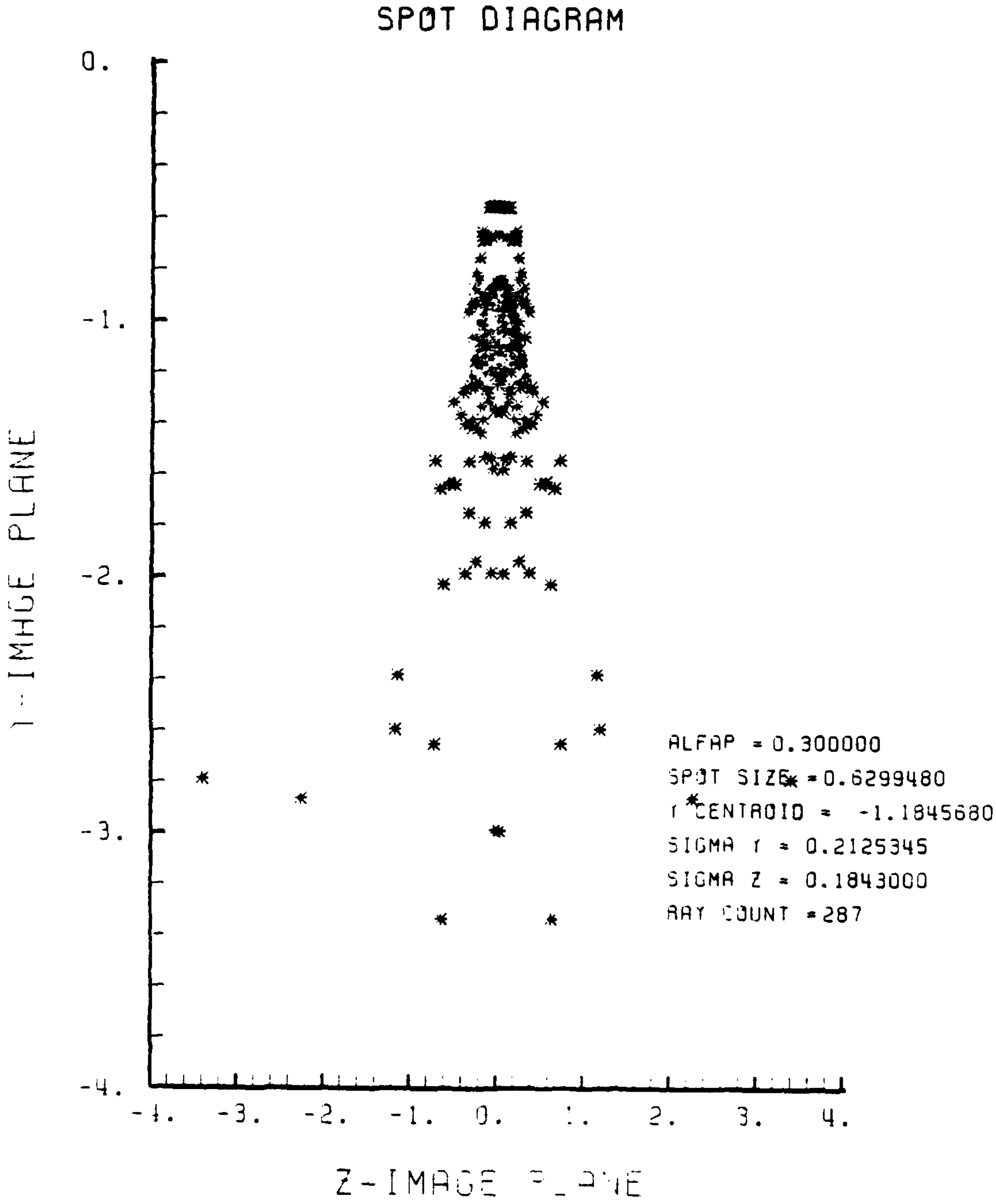

Figure E-67. Spot Diagram for Grid of Figure E-66

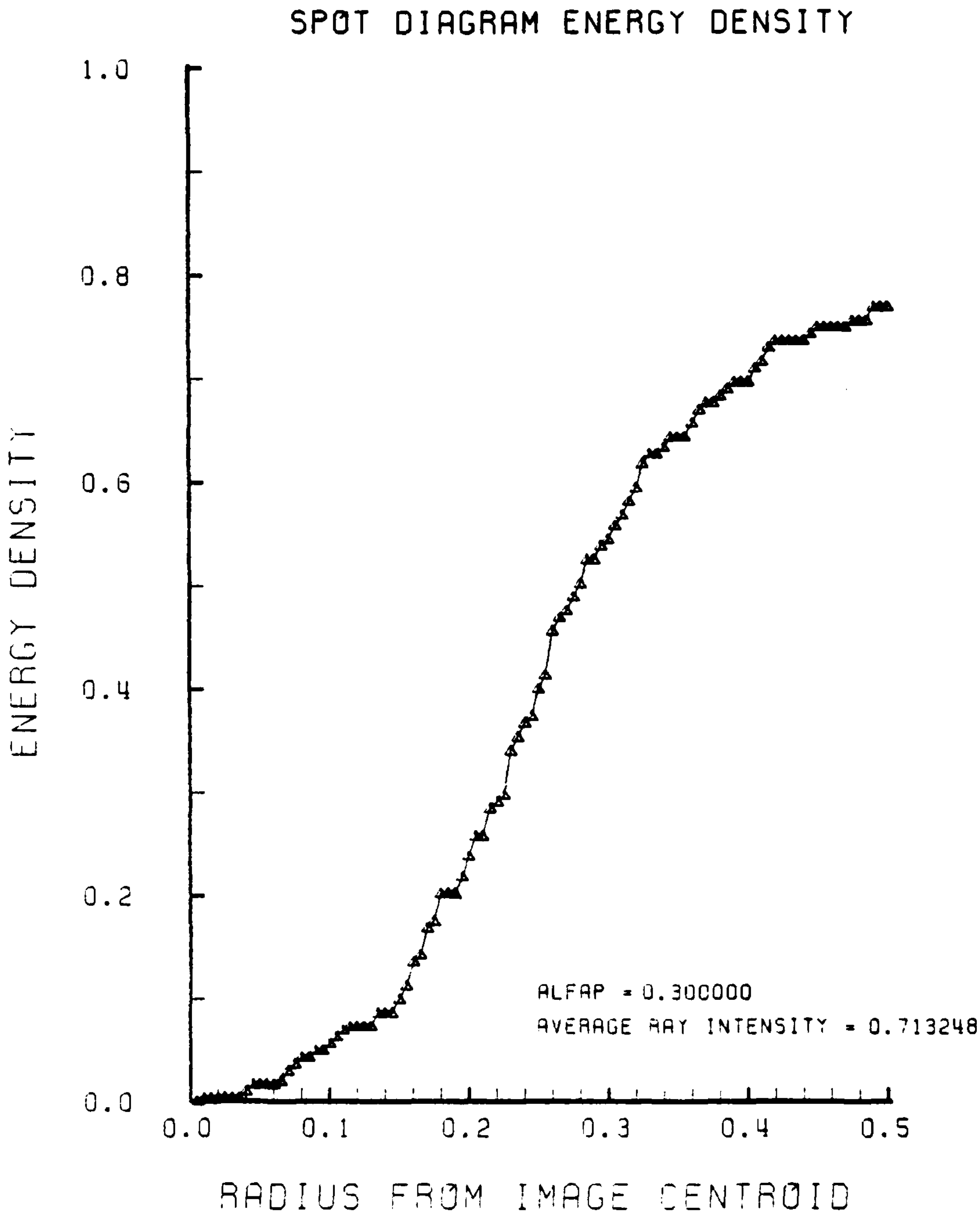

Figure E-68. Encircled Energy of Figure E-67

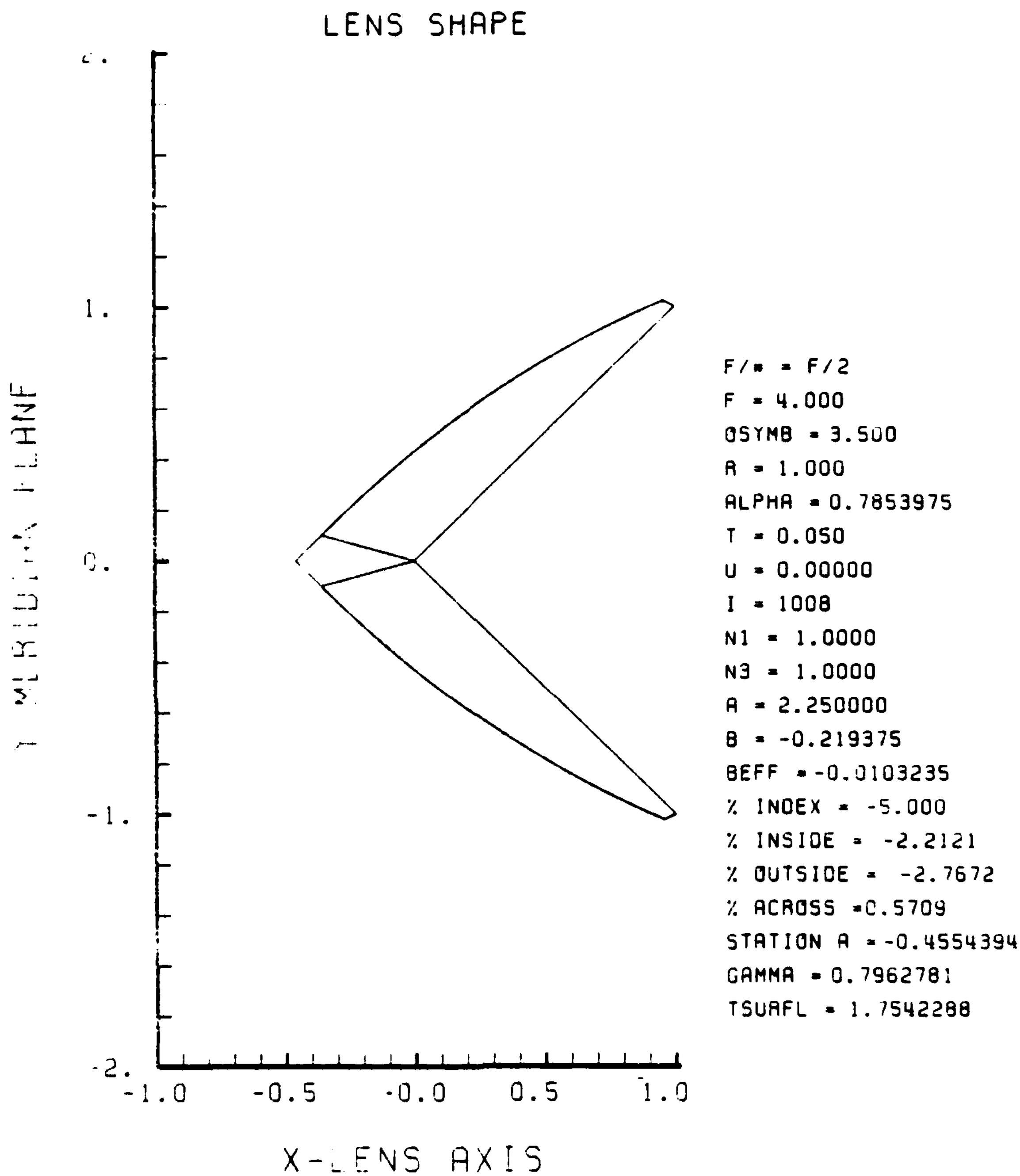

Figure E-69. GRIN Lens Shape at -5%, OB = 3.50, a = 2.25

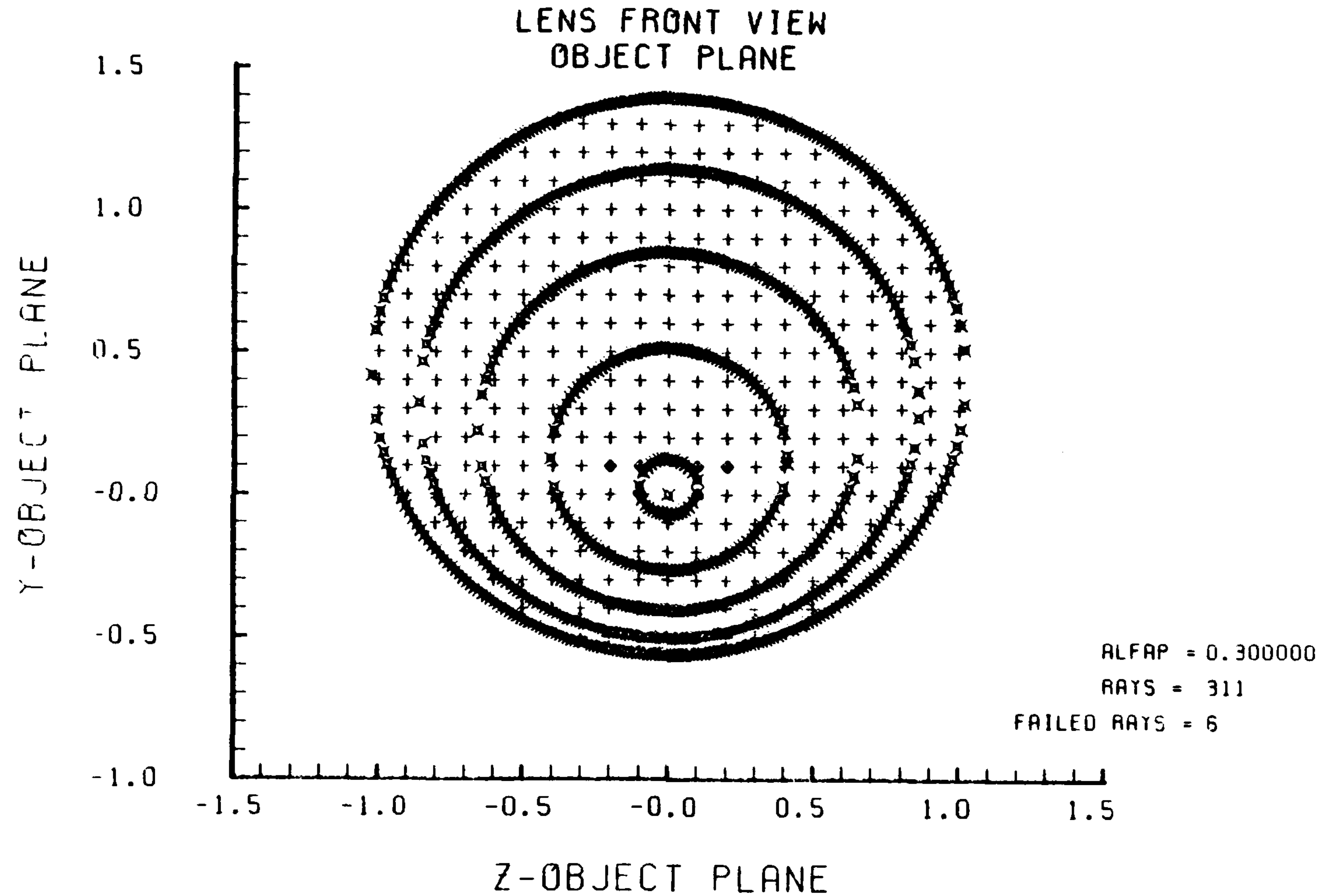

Figure E-70. Grid Plane at $\alpha_p = 0.3$ for Lens of Figure E-69

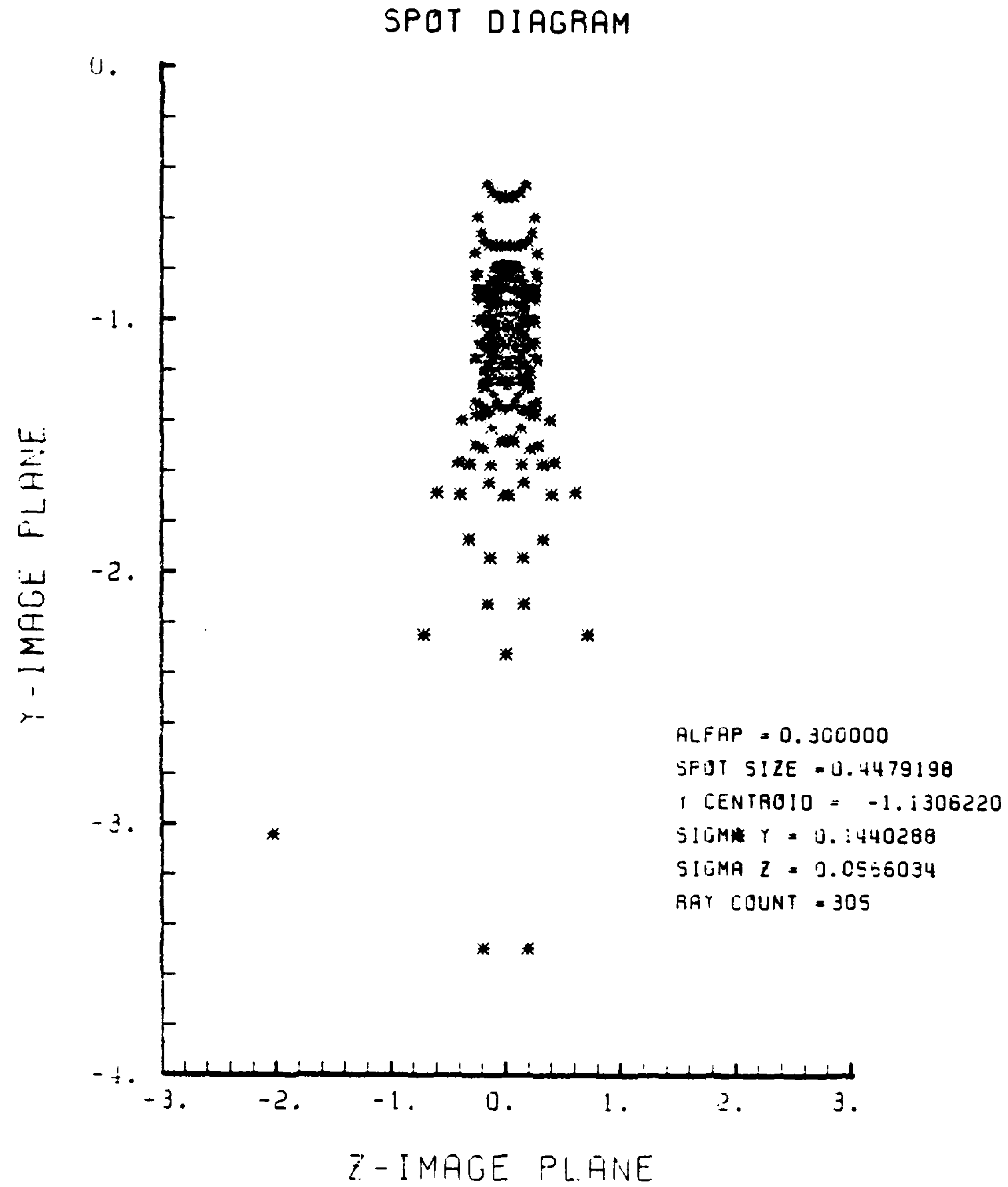

Figure E-71. Spot Diagram for Grid of Figure E-70

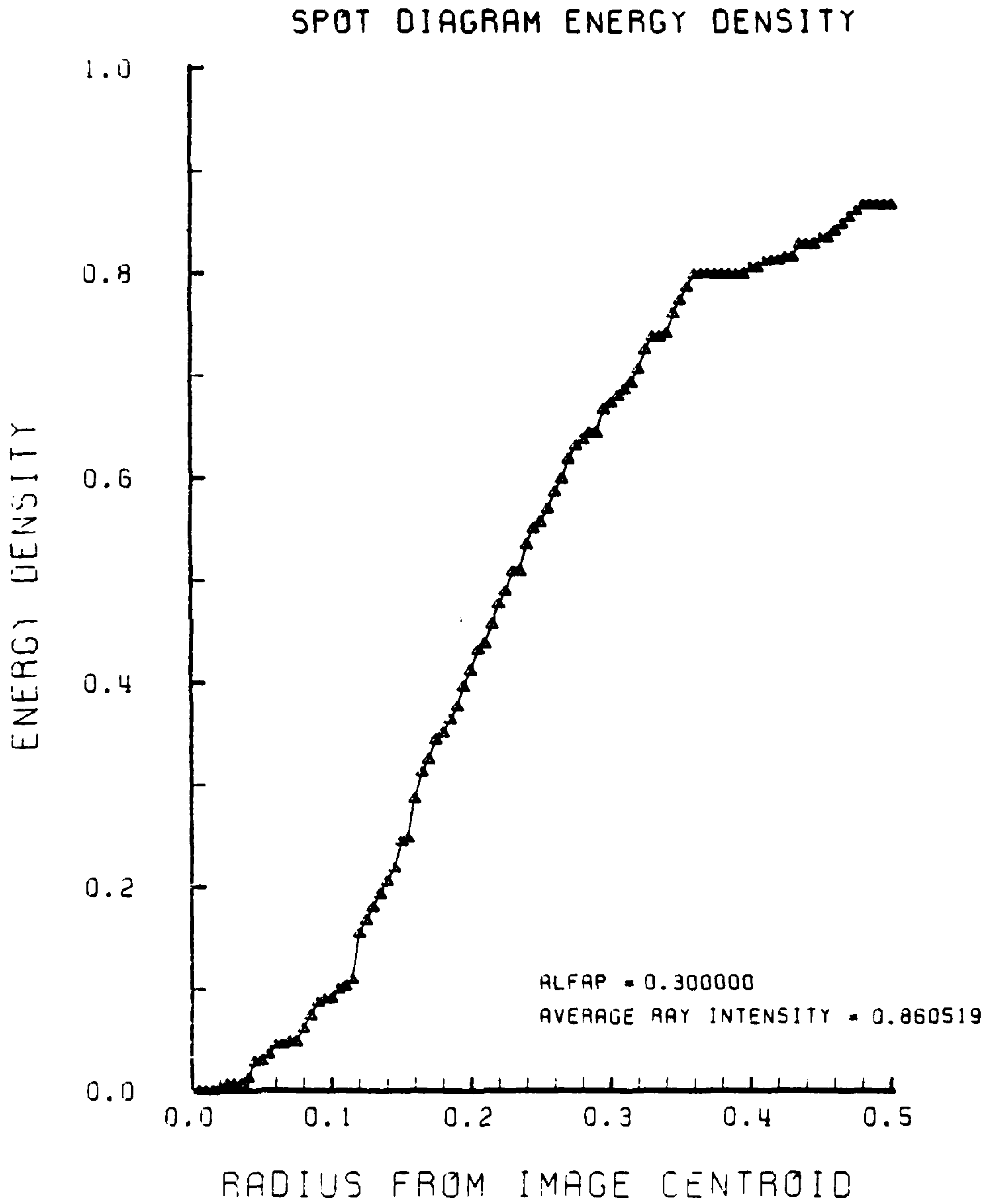

Figure E-72. Encircled Energy of Figure E-71

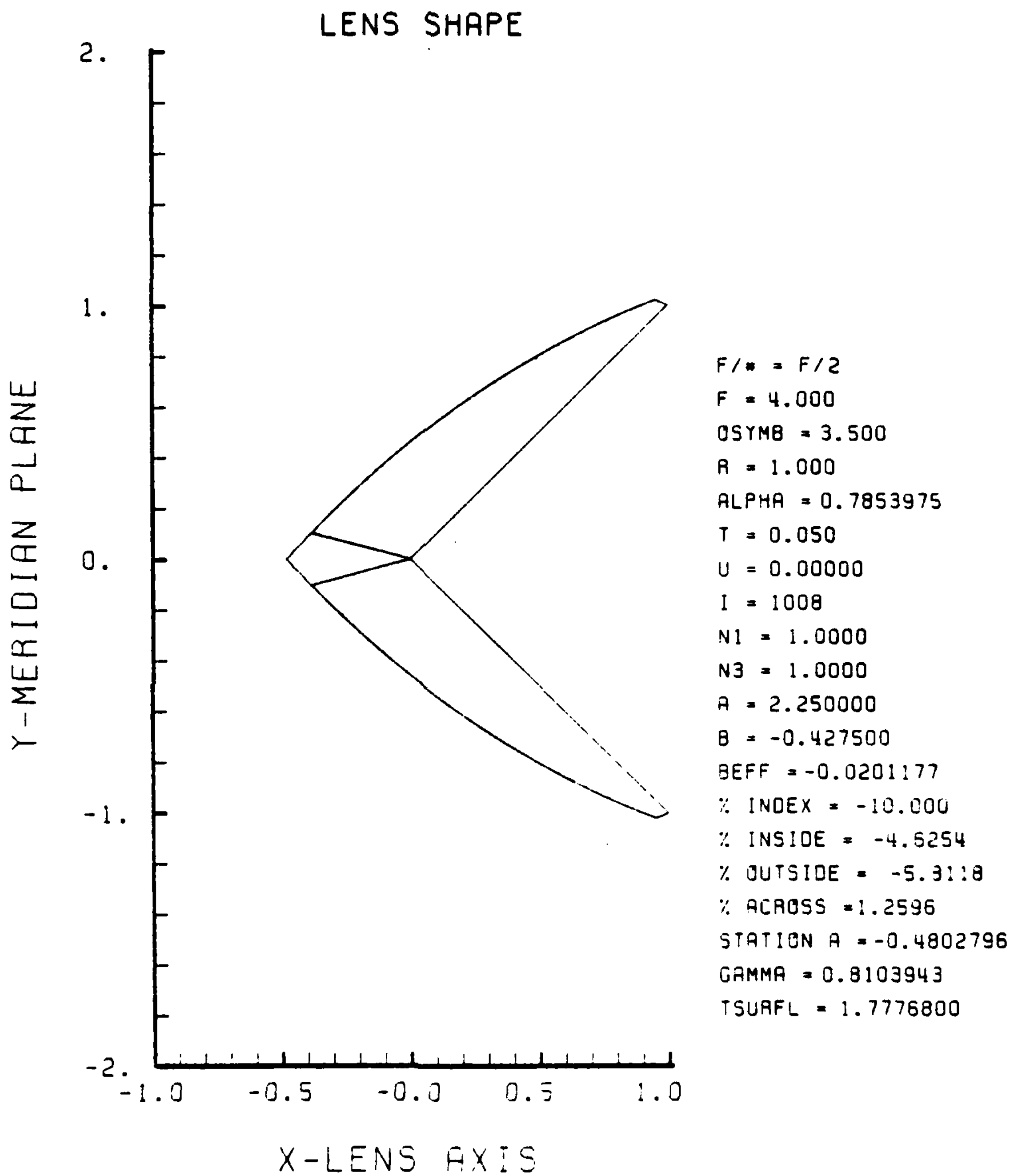

Figure E-73. GRIN Lens Shape at -10%, OB = 3.50,
a = 2.25

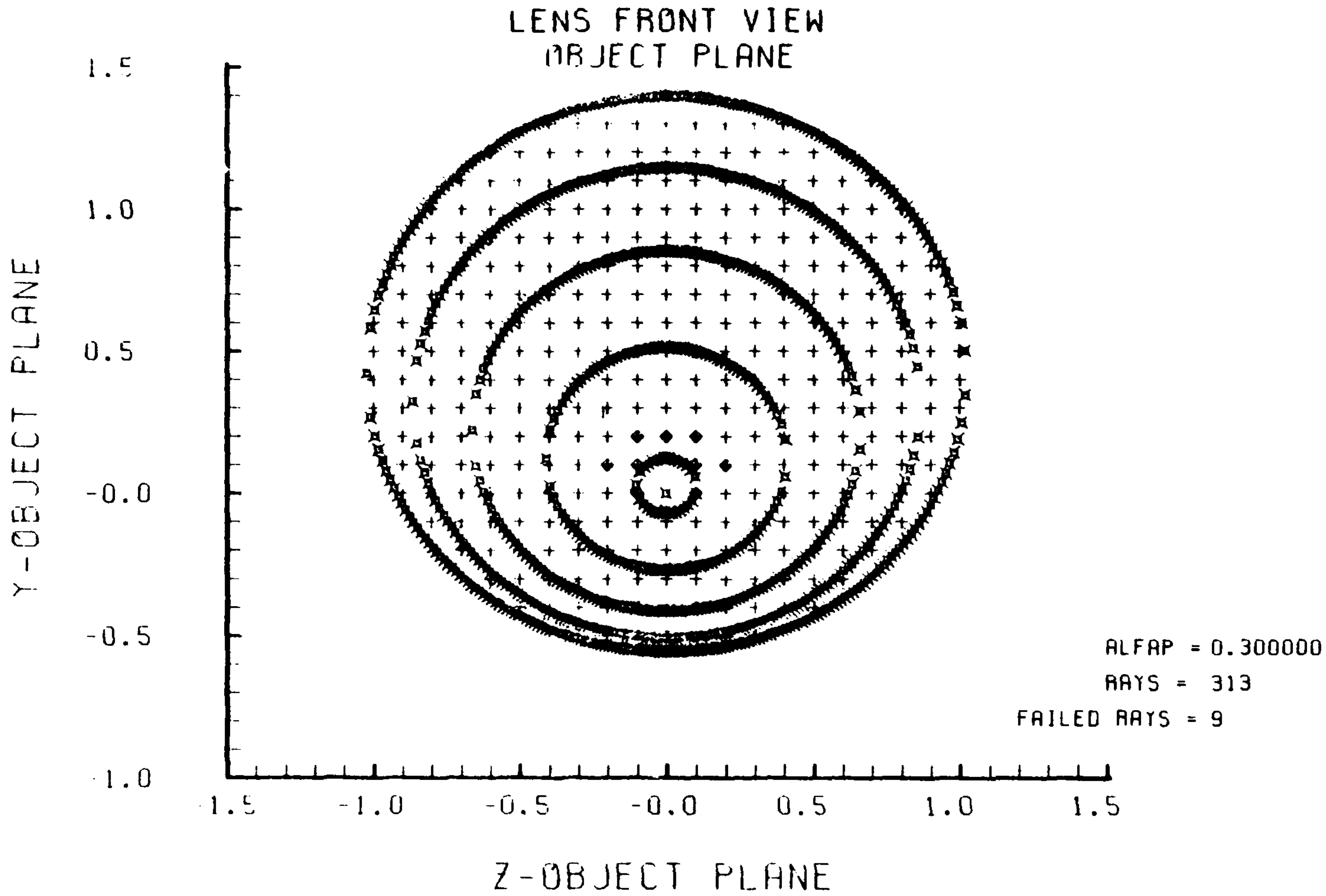

Figure E-74. Grid Plane at α_p = 0.3 for Lens of Figure E-73

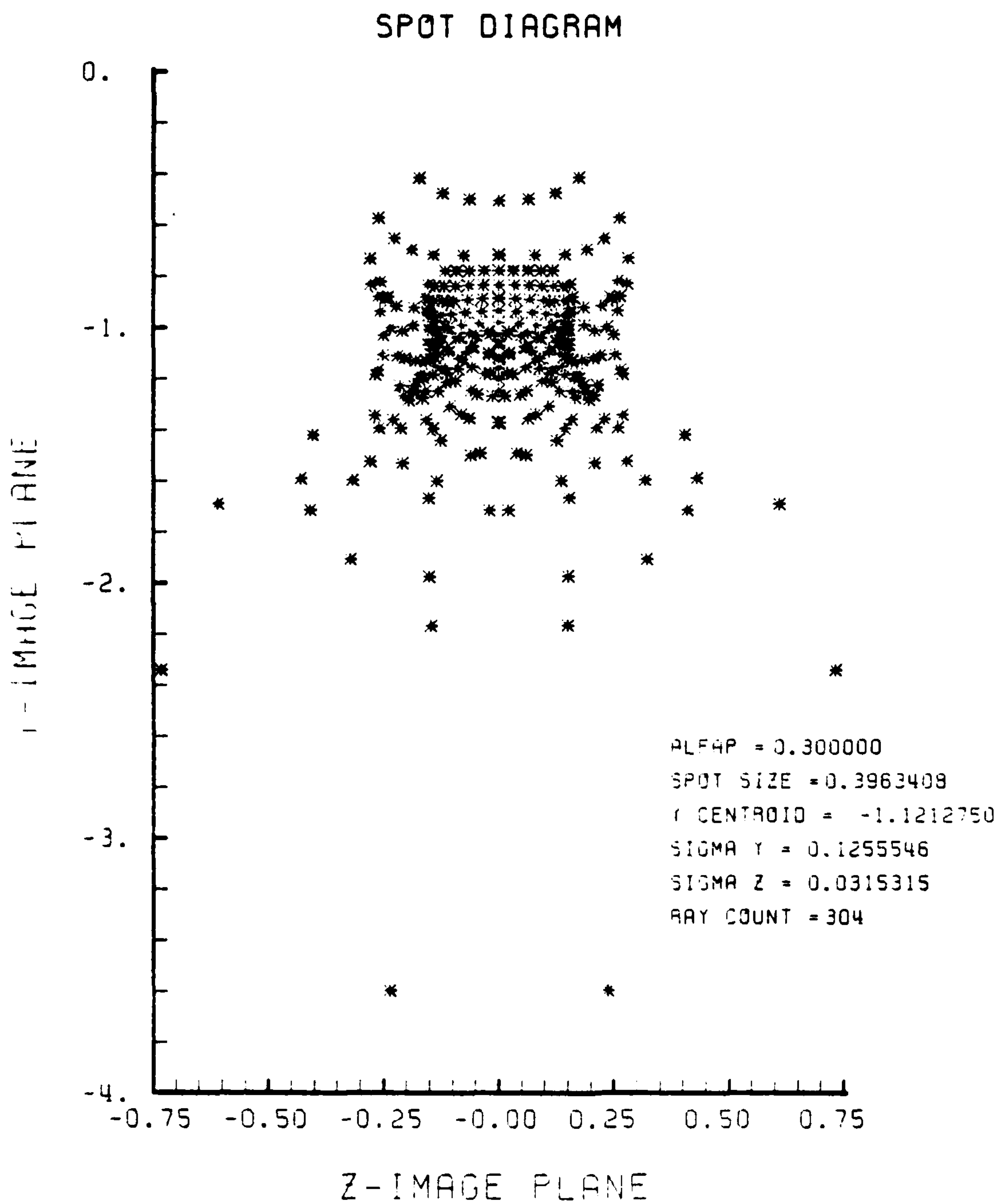

Figure E-75. Spot Diagram for Grid of Figure E-74

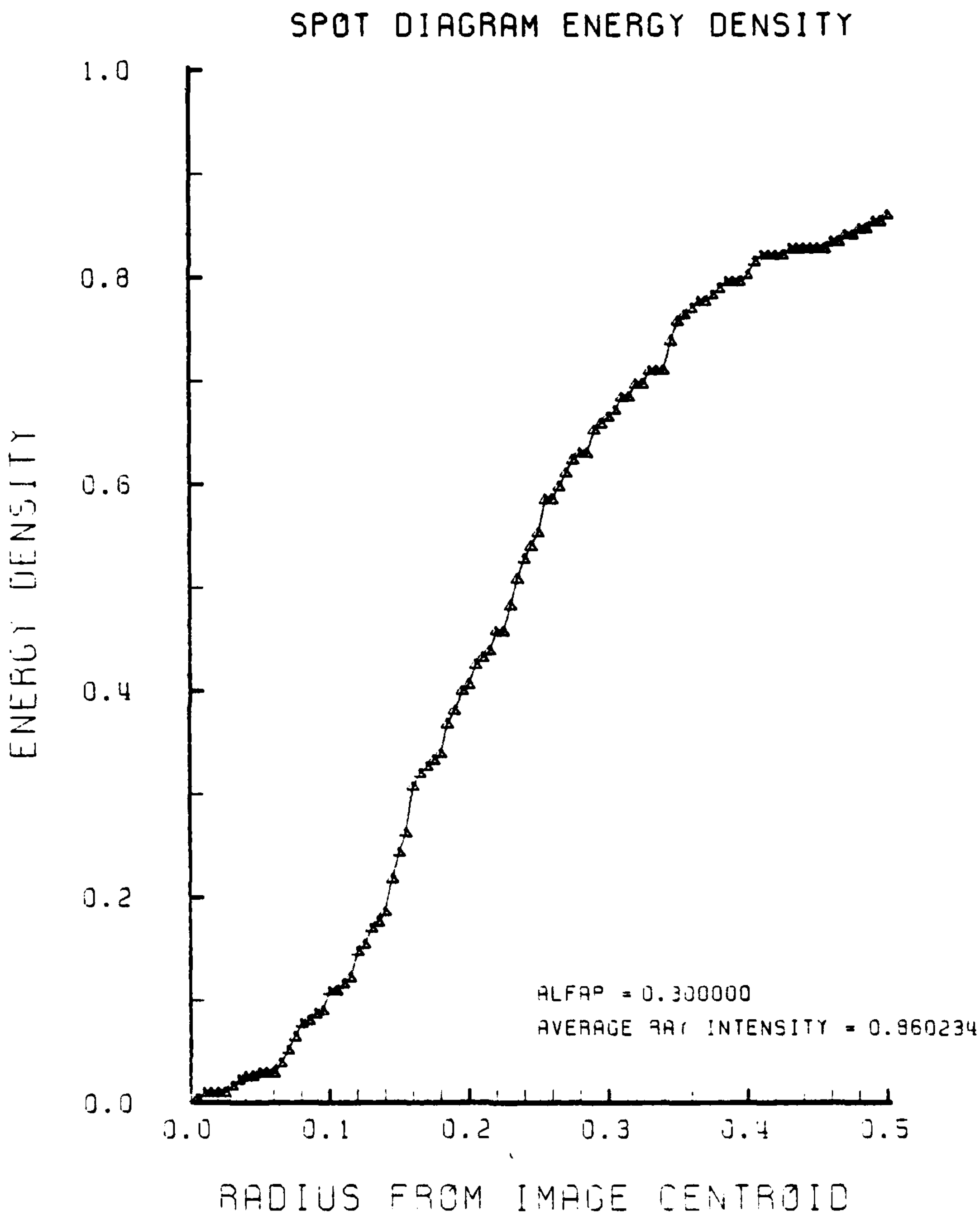

Figure E-76. Encircled Energy of Figure E-75

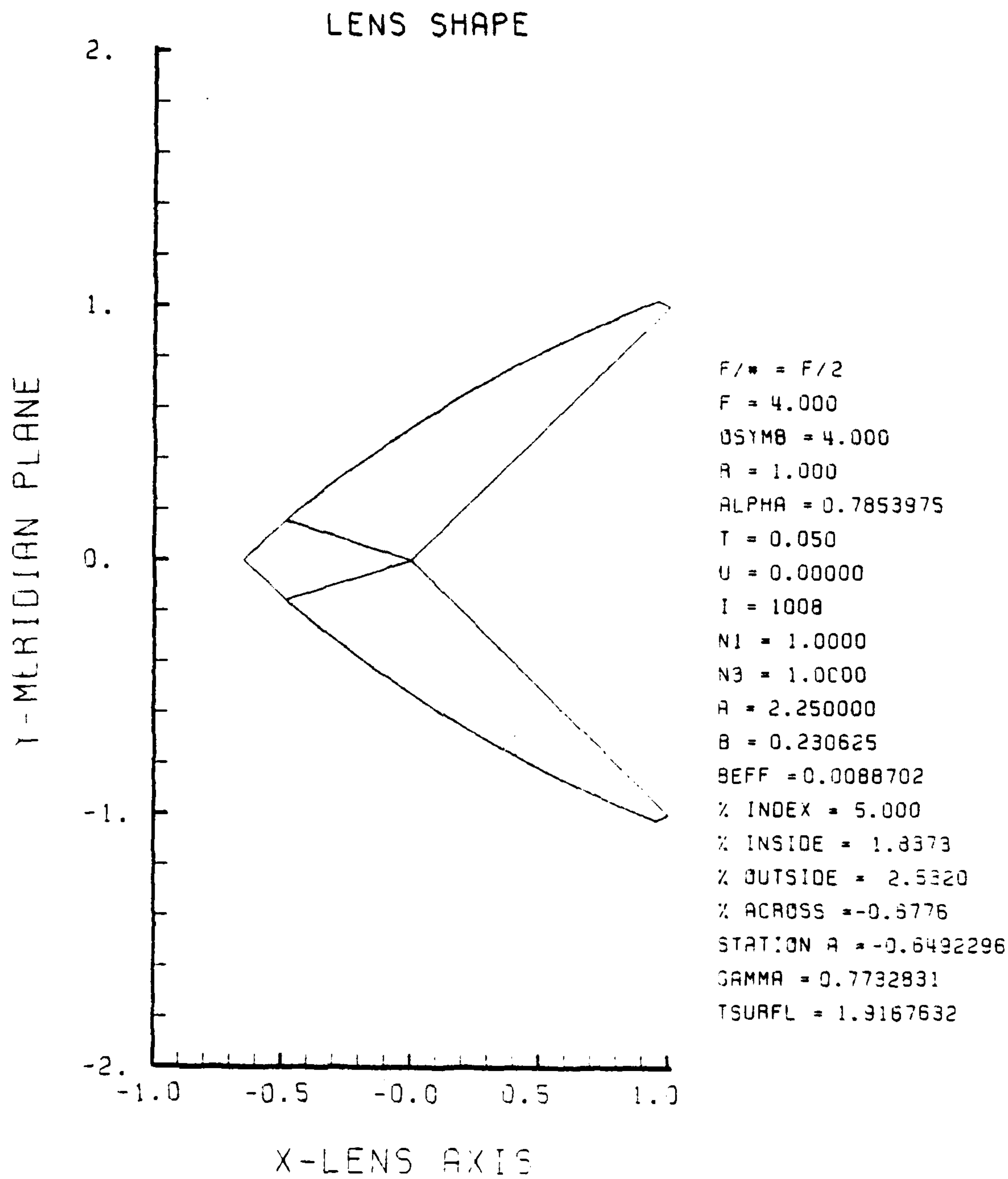

Figure E-77. GRIN Lens Shape at +5%, OB = 4.00, a = 2.25

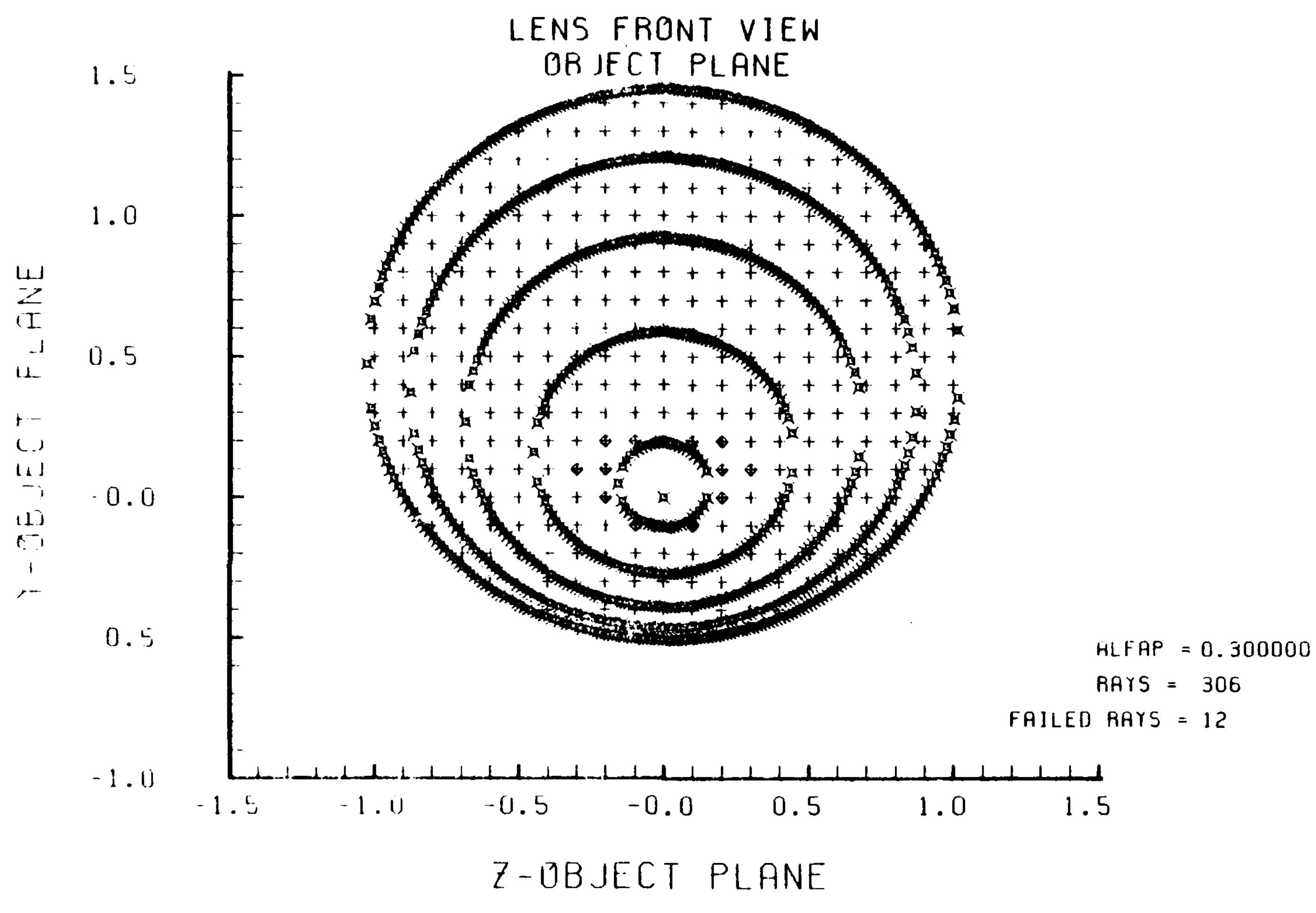

Figure E-78. Grid Plane at α_p = 0.3 for Lens of Figure E-77

AD-A125 167 AERODYNAMICALLY EFFICIENT GRADIENT REFRACTIVE INDEX MISSILE SEEKER LENS(U) NAVAL POSTGRADUATE SCHOOL MONTEREY CA H M CARR OCT 82 NPS67-82-012 4/6

UNCLASSIFIED F/G 16/4 NL

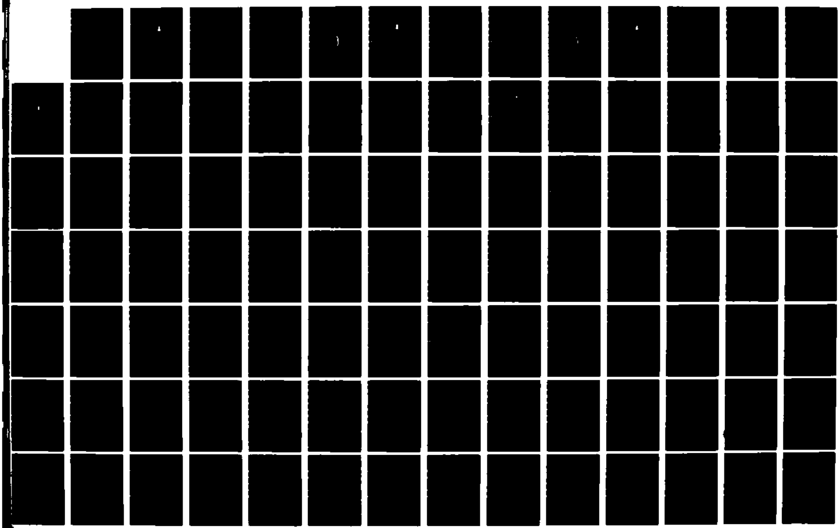

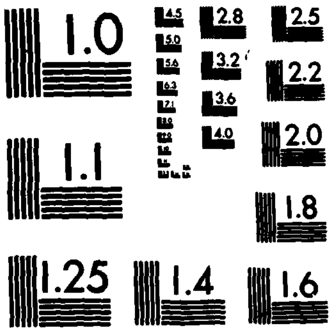
1.0
2.8
2.5
3.2
2.2
3.6
2.0
4.0
1.1
1.8
1.25
1.4
1.6

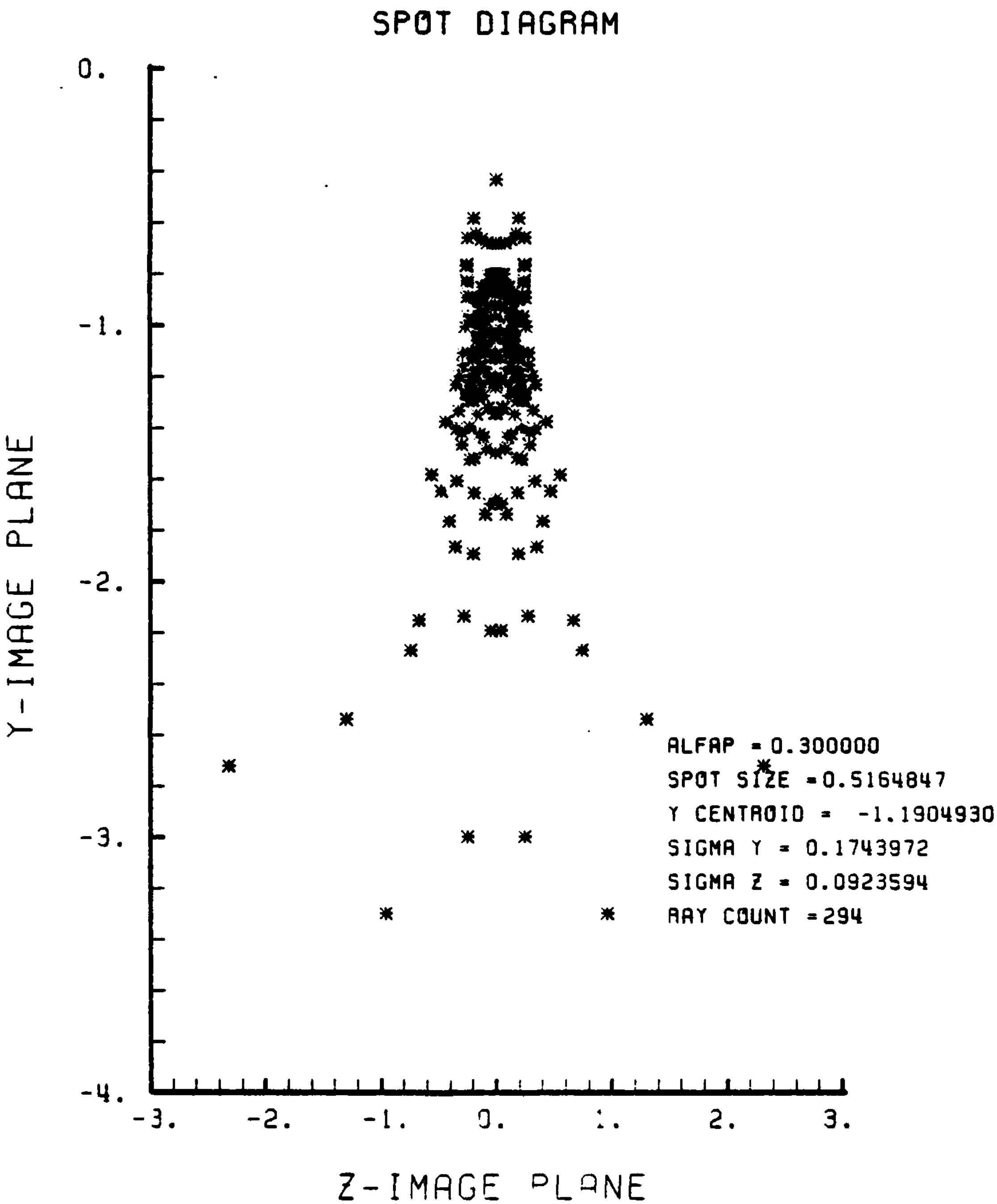

Figure E-79. Spot Diagram for Grid of Figure E-78

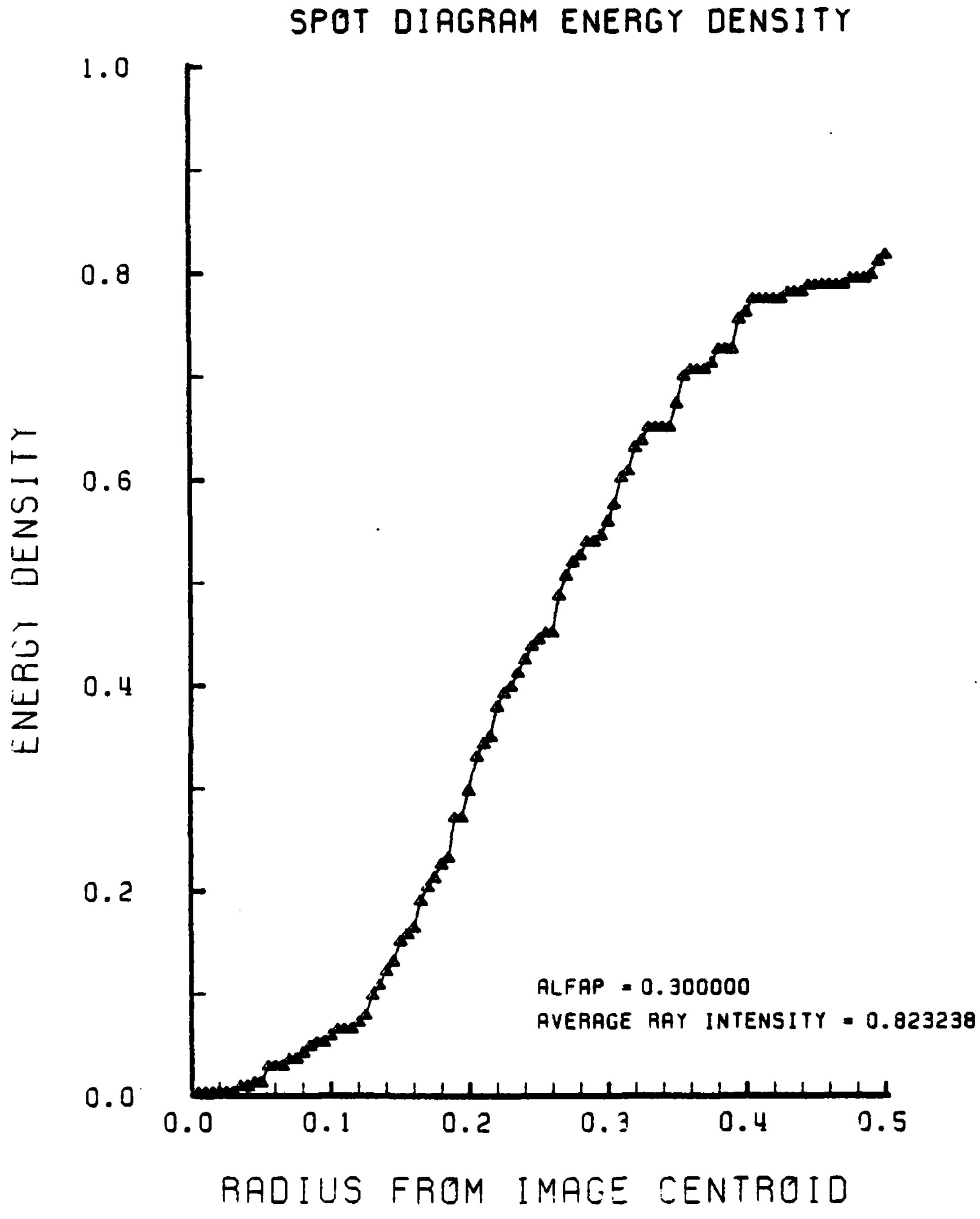

Figure E-80. Encircled Energy of Figure E-79

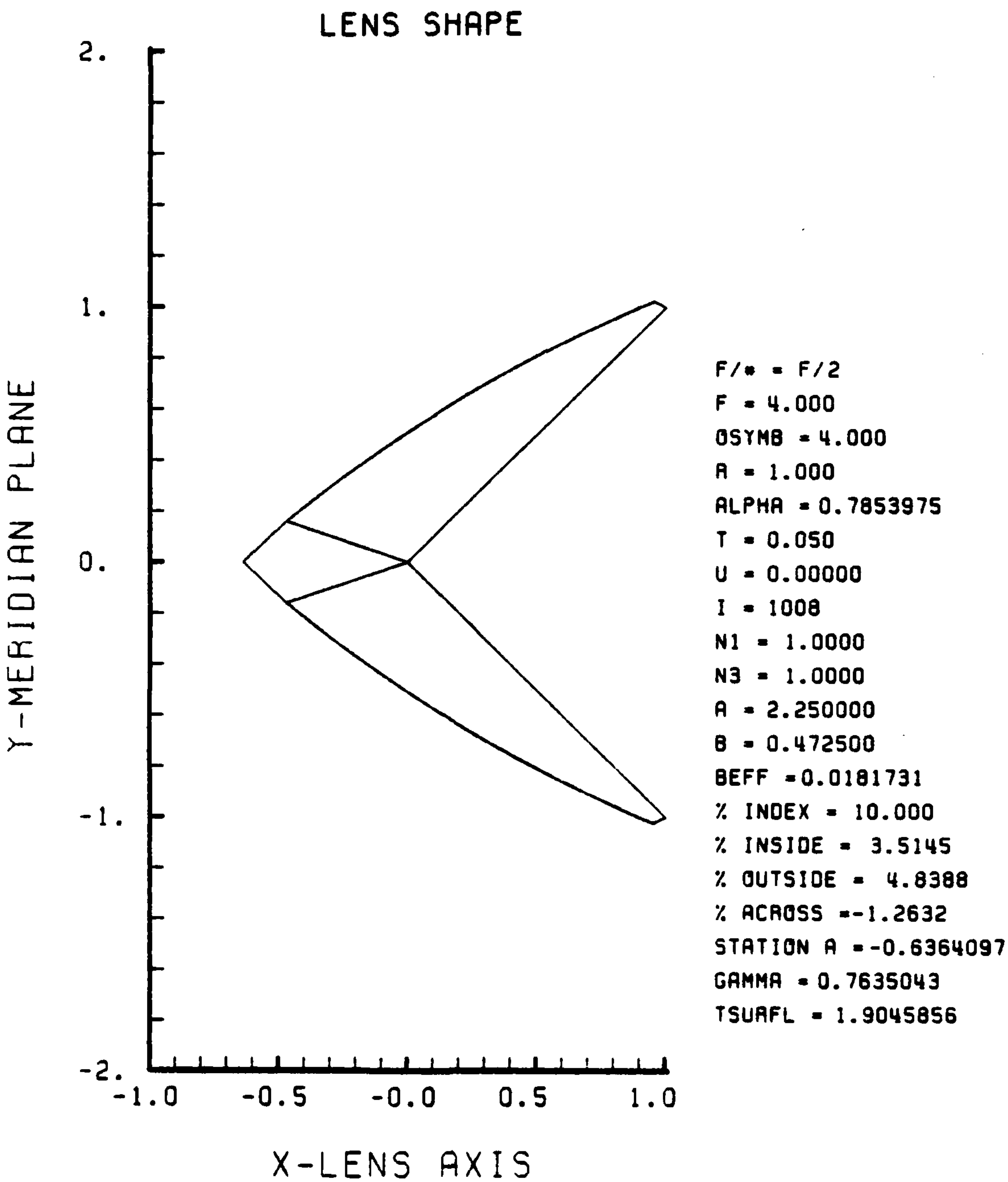

Figure E-81. GRIN Lens Shape at +10%, OB = 4.00, a = 2.25

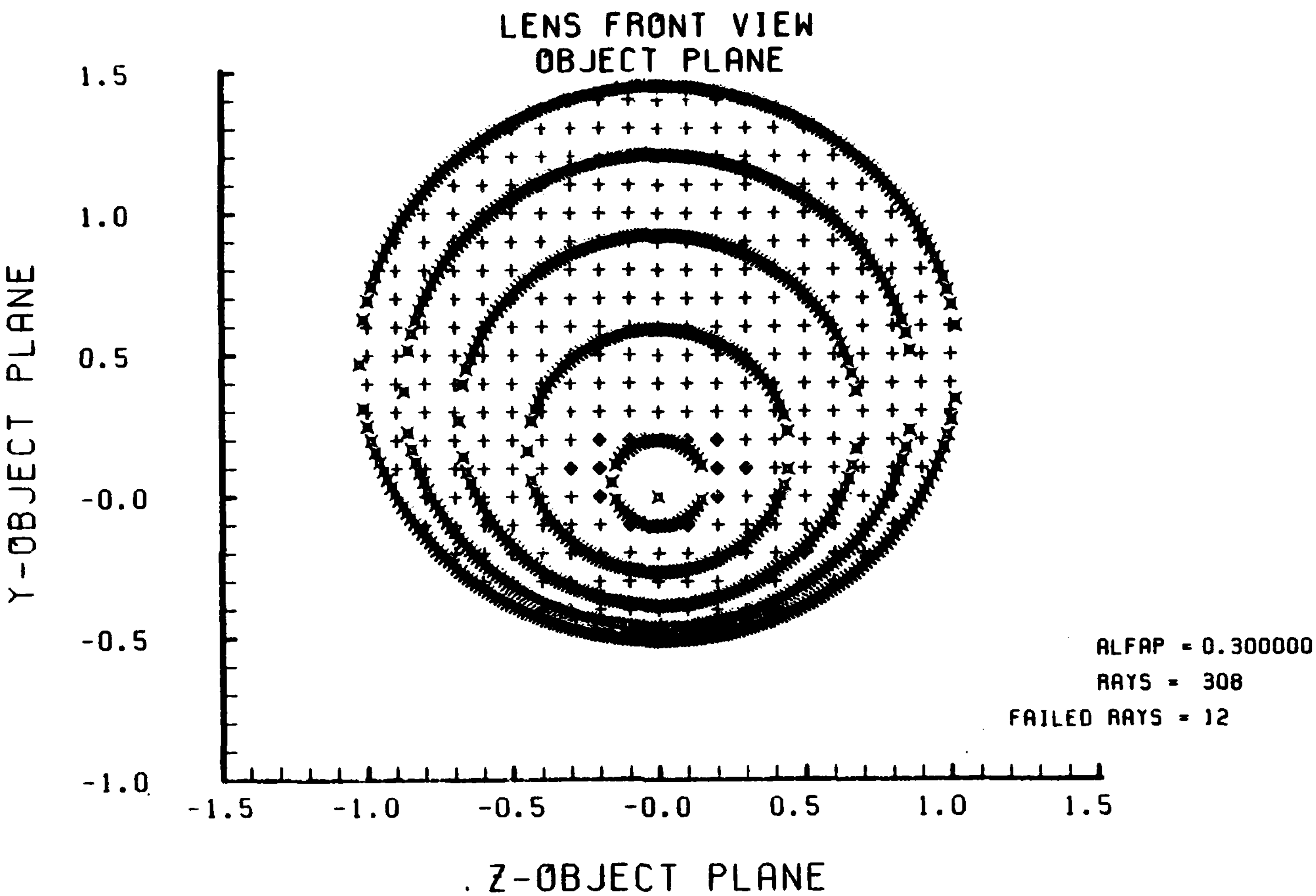

Figure E-82. Grid Plane at $\alpha_p = 0.3$ for Lens of Figure E-81

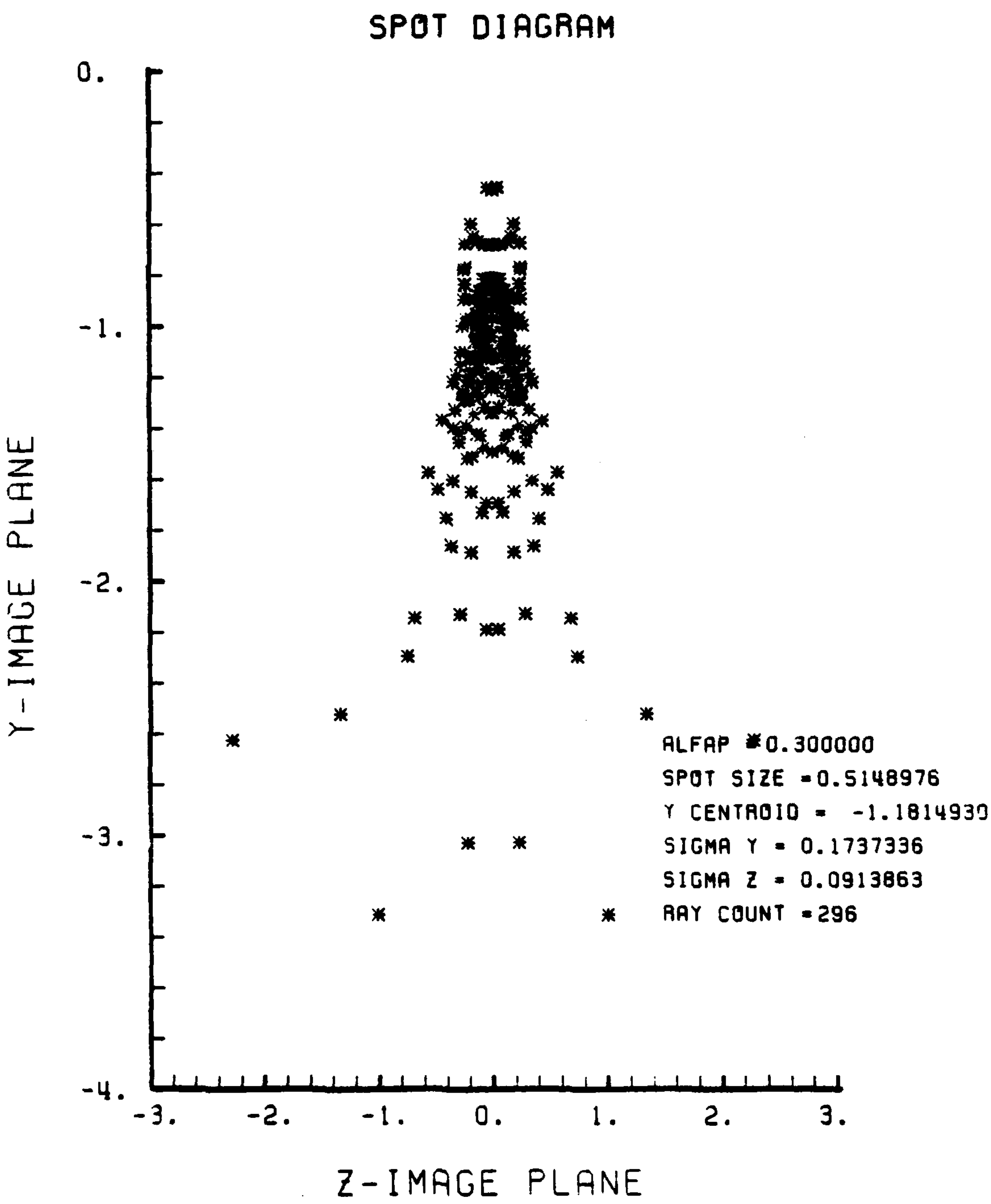

Figure E-83. Spot Diagram for Grid of Figure E-82

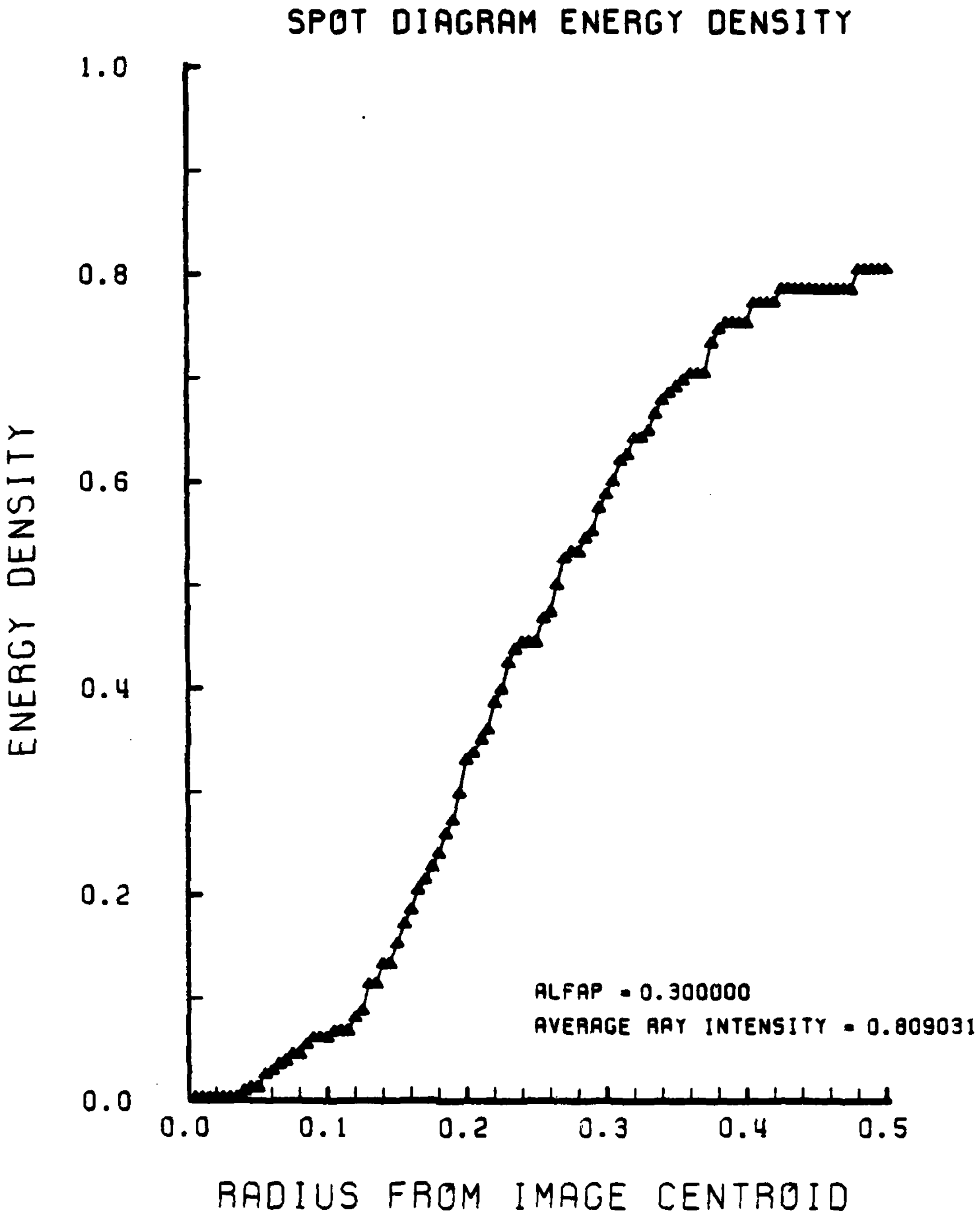

Figure E-84. Encircled Energy of Figure E-83

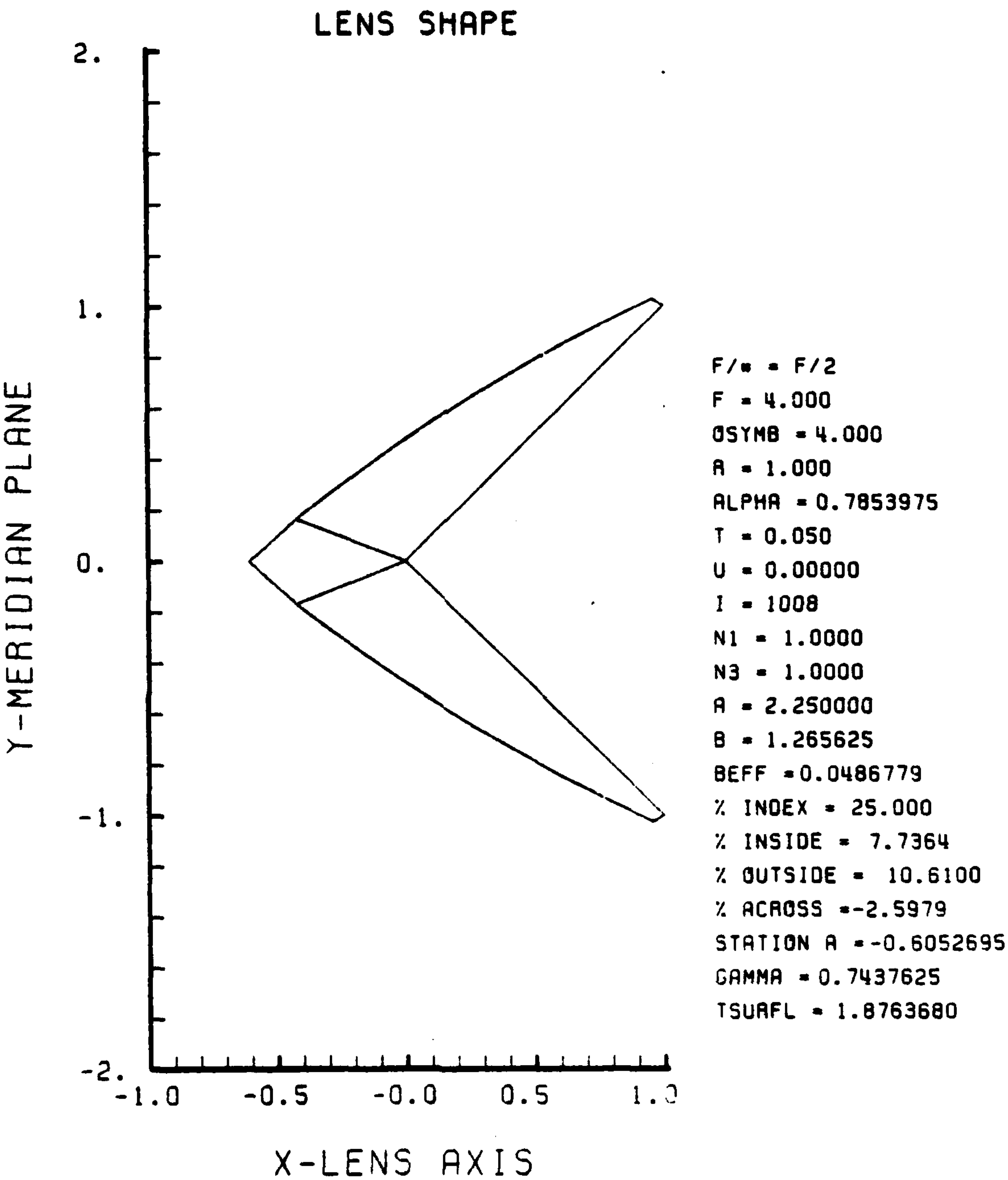

Figure E-85. GRIN Lens Shape at +25%, OB = 4.00, a = 2.25

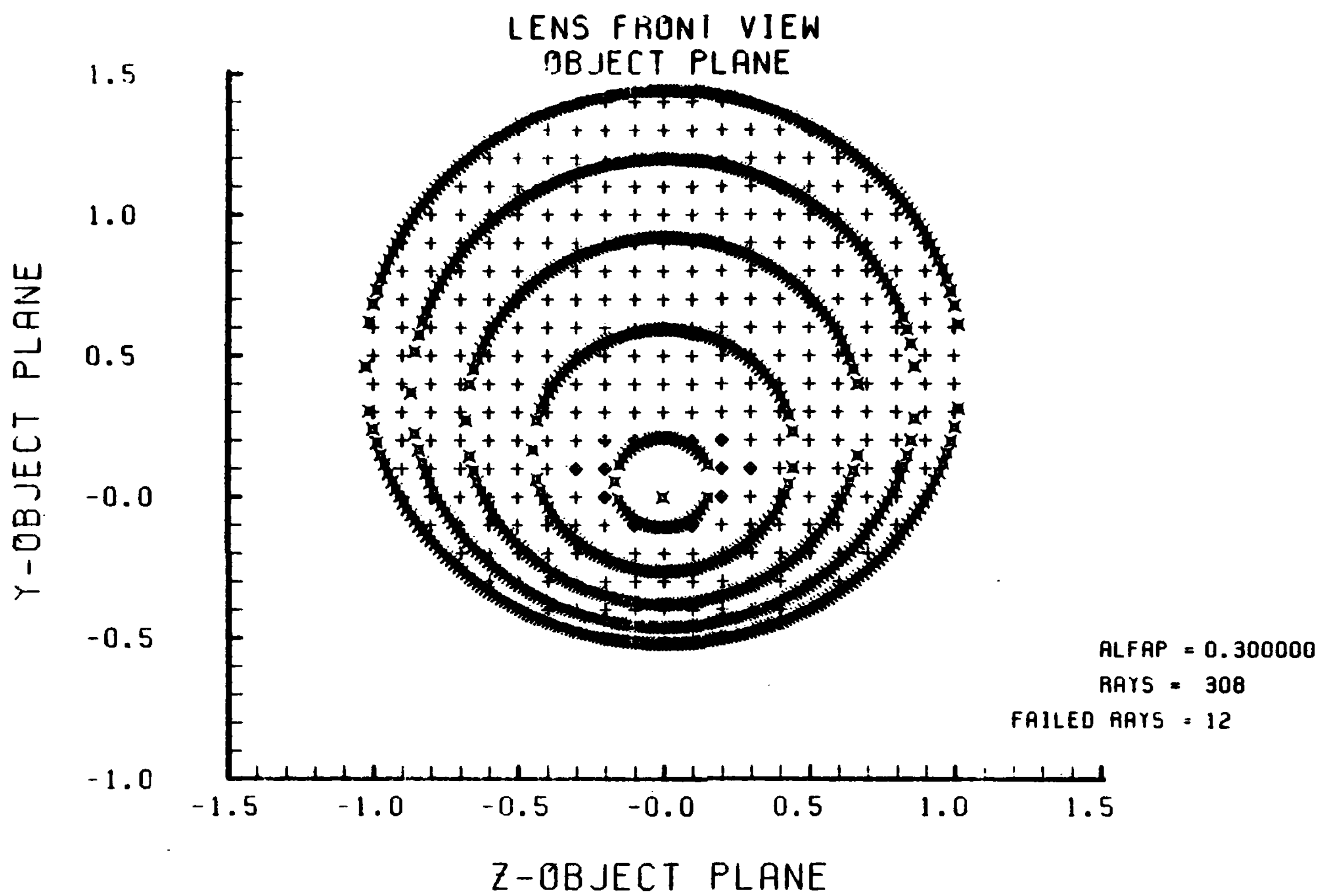

Figure E-36. Grid Plane at α_p = 0.3 for Lens of Figure E-85

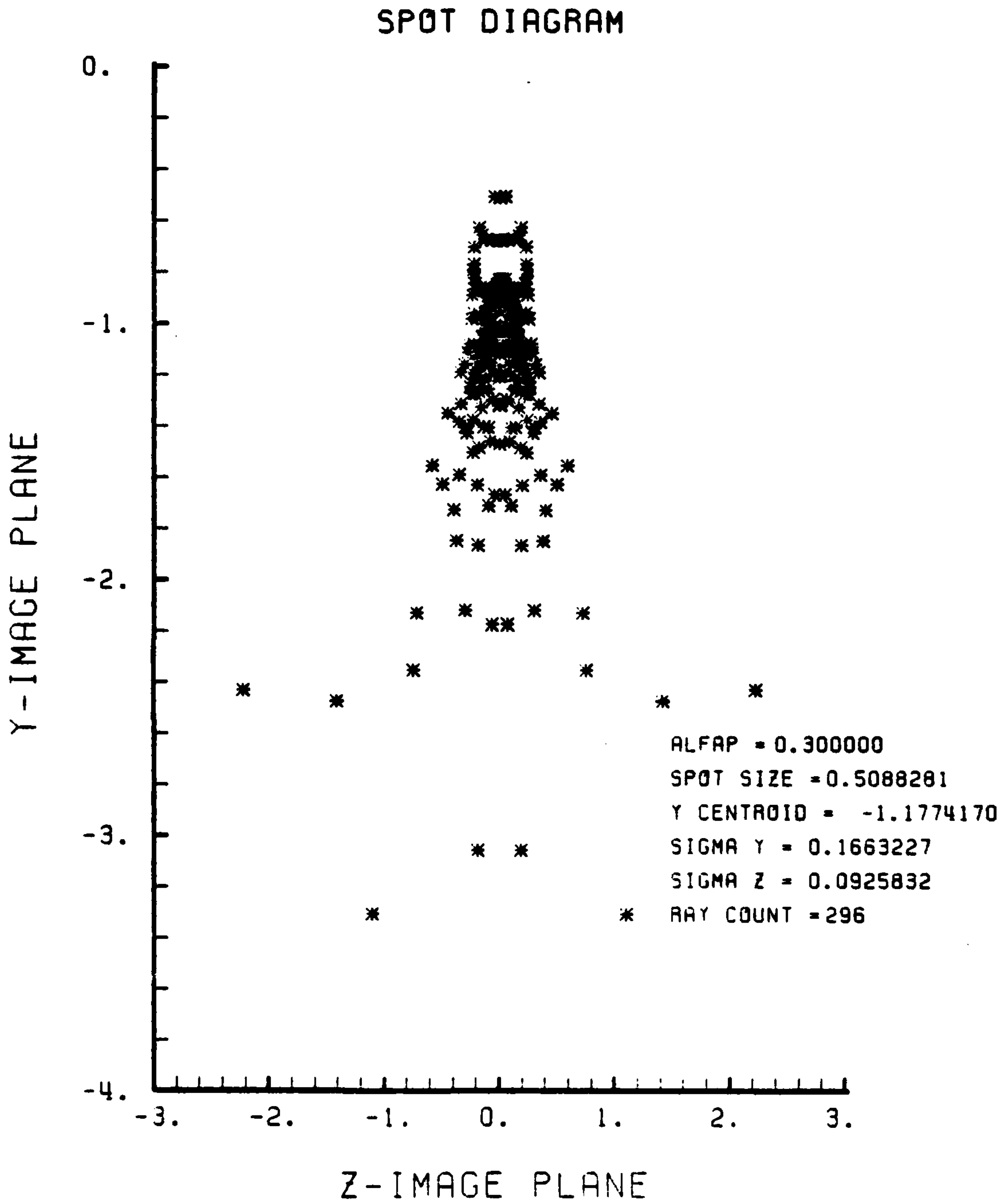

Figure E-87. Spot Diagram for Grid of Figure E-86

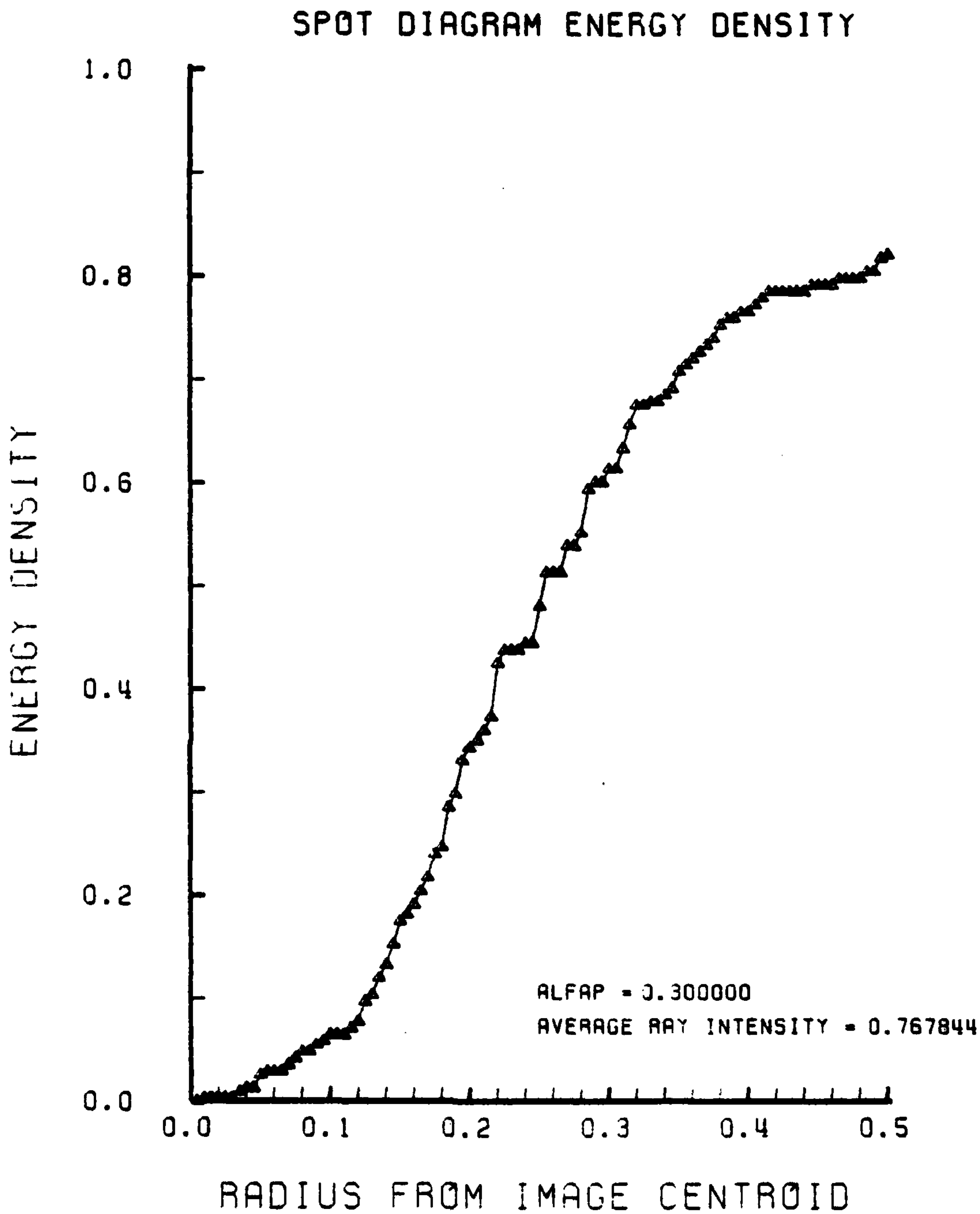

Figure E-88. Encircled Energy of Figure E-87

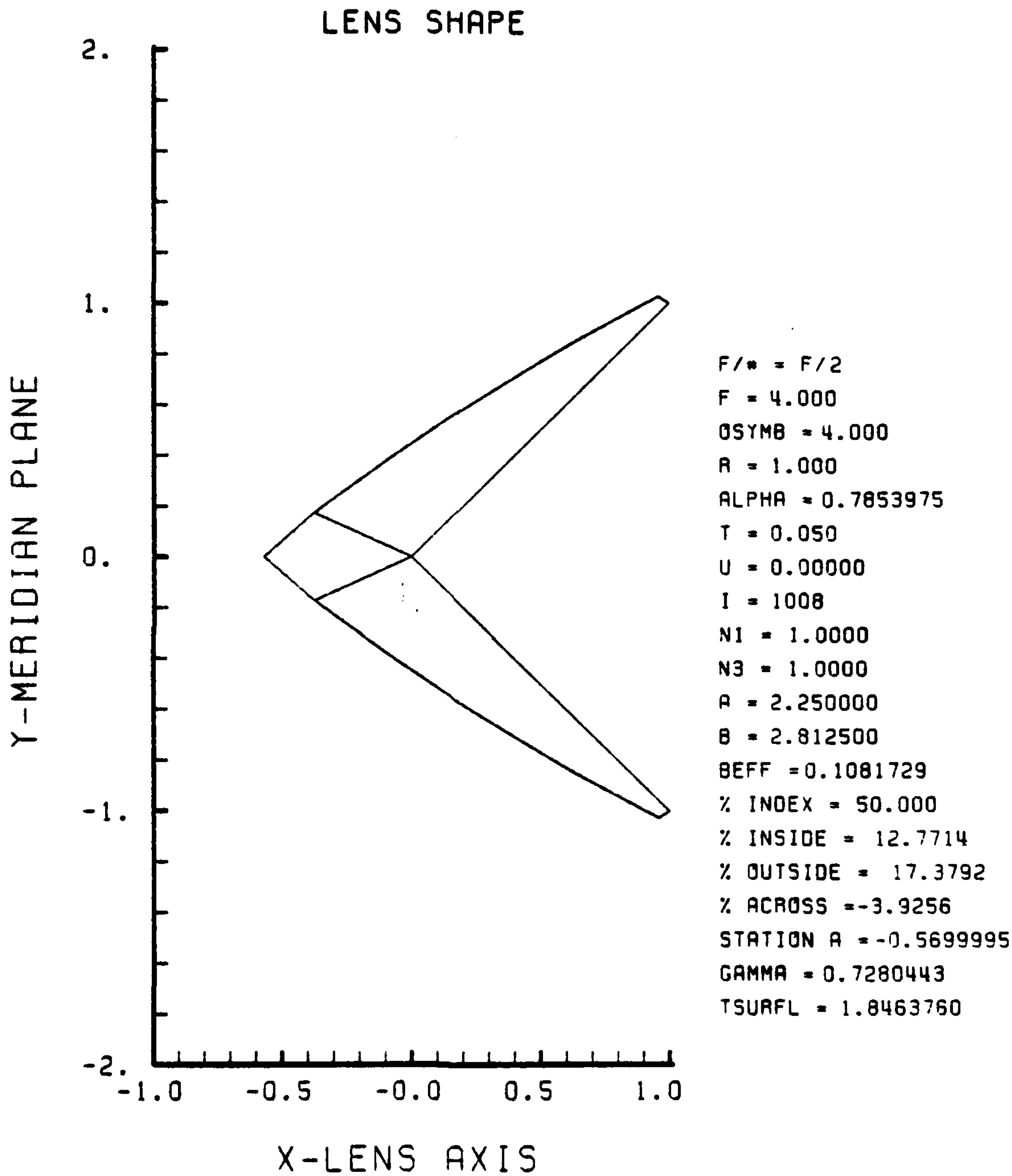

Figure E-89. GRIN Lens Shape at +50%, OB = 4.00, a = 2.25

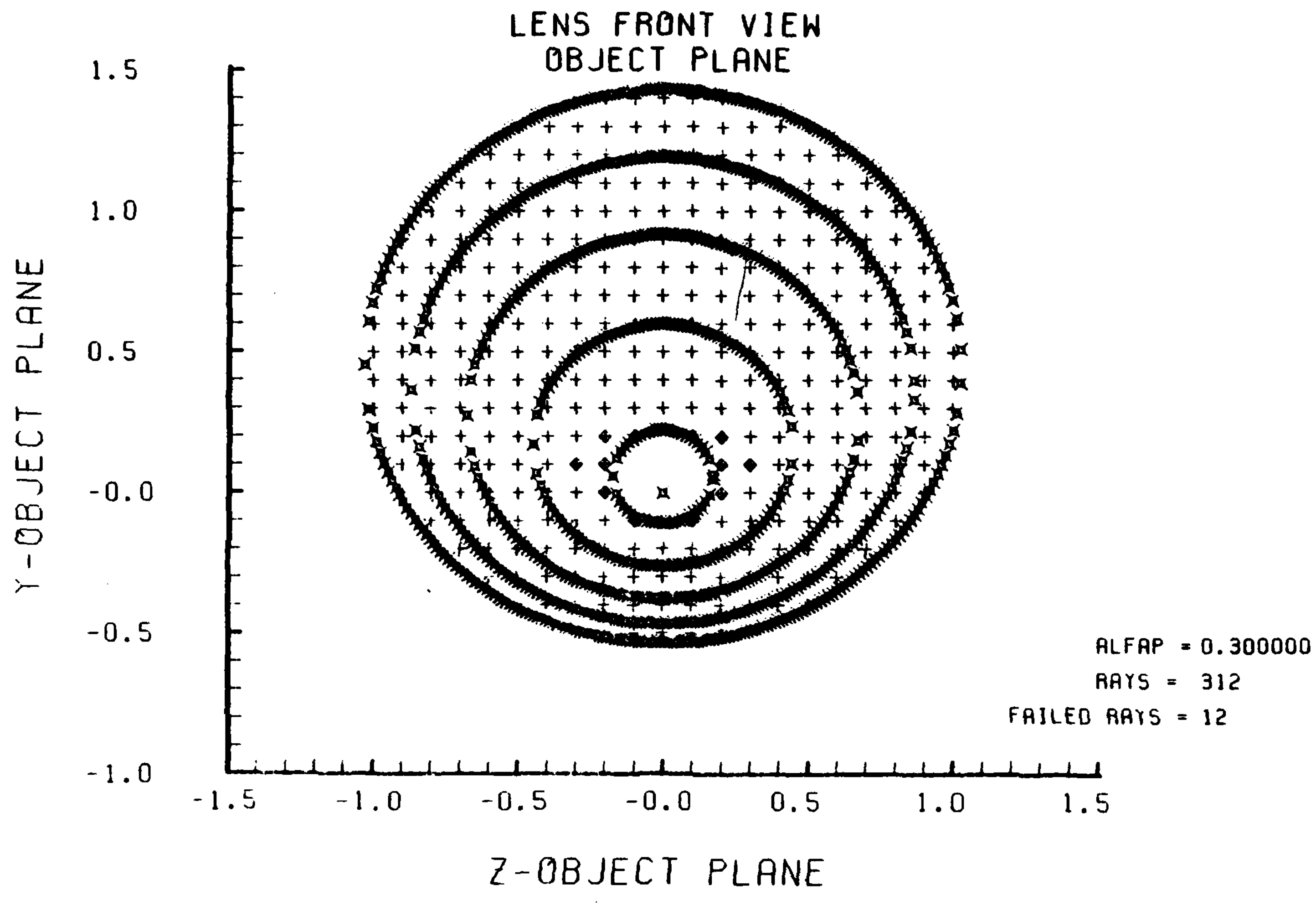

Figure E-90. Grid Plane at $\alpha_p = 0.3$ for Lens of Figure E-89

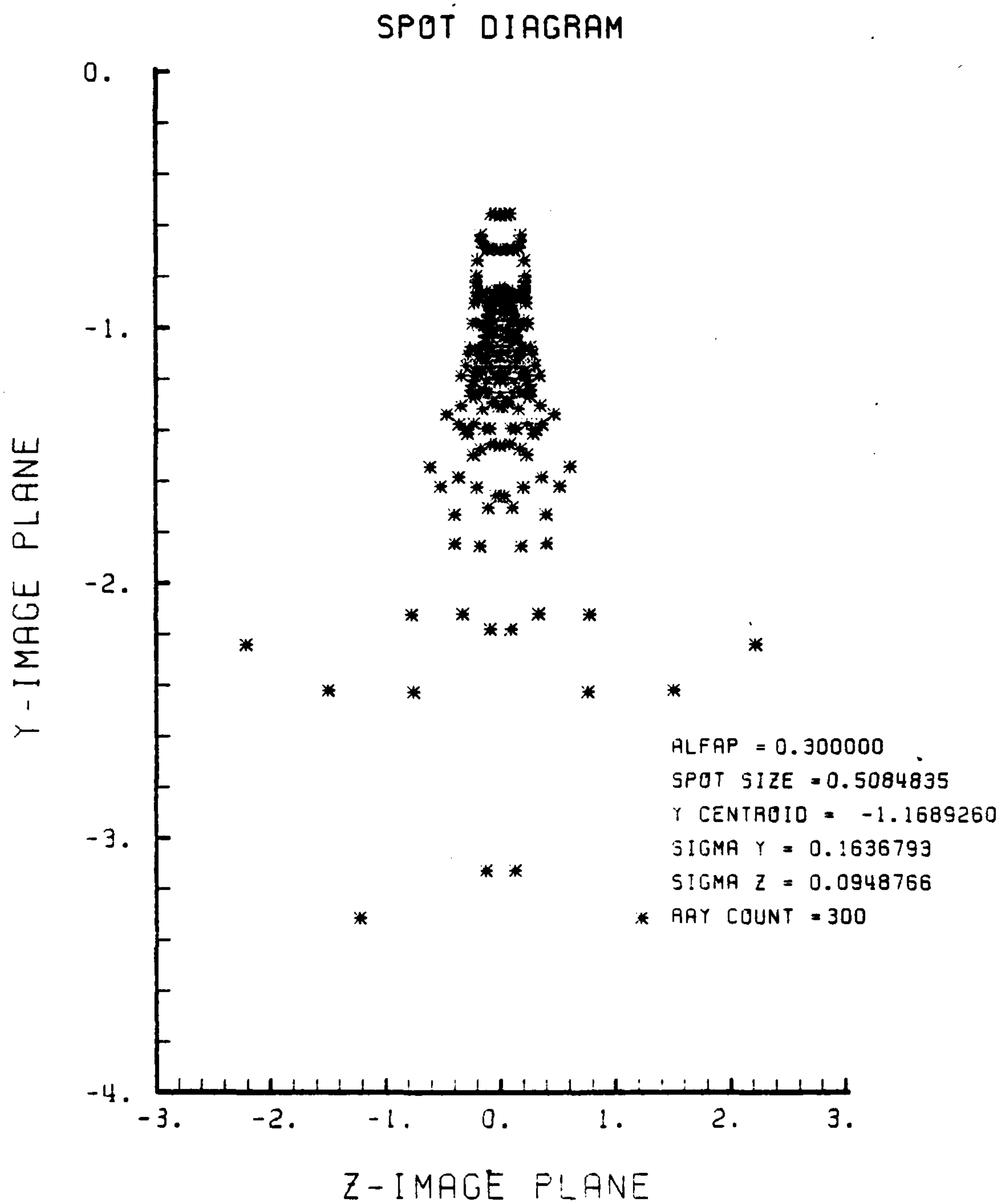

Figure E-91. Spot Diagram for Grid of Figure E-90

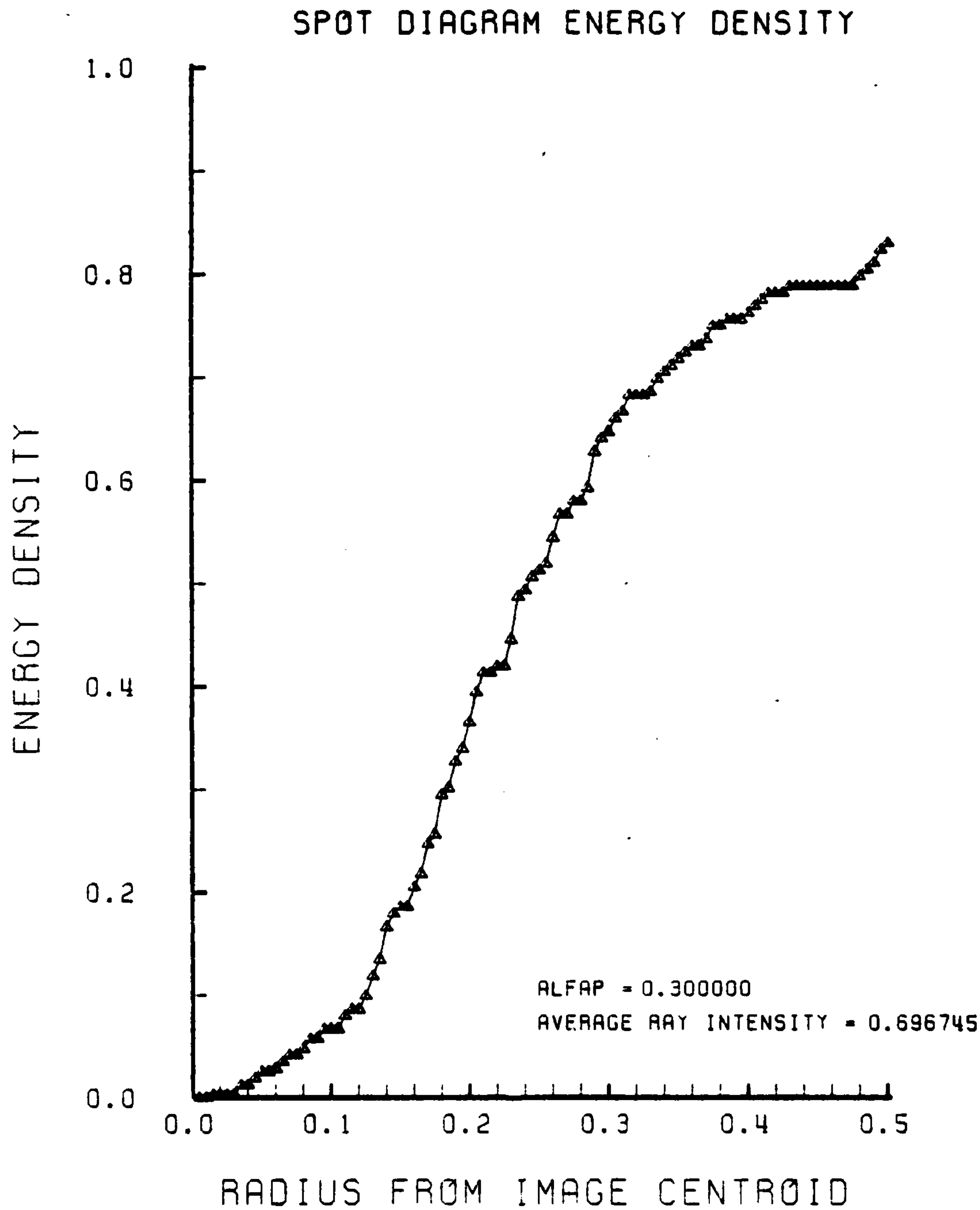

Figure E-92. Encircled Energy of Figure E-91

APPENDIX F

GRIN LENS PERFORMANCE PLOTS IN THE HIGH RANGE OF INDICES OF REFRACTION (a = 9.00)

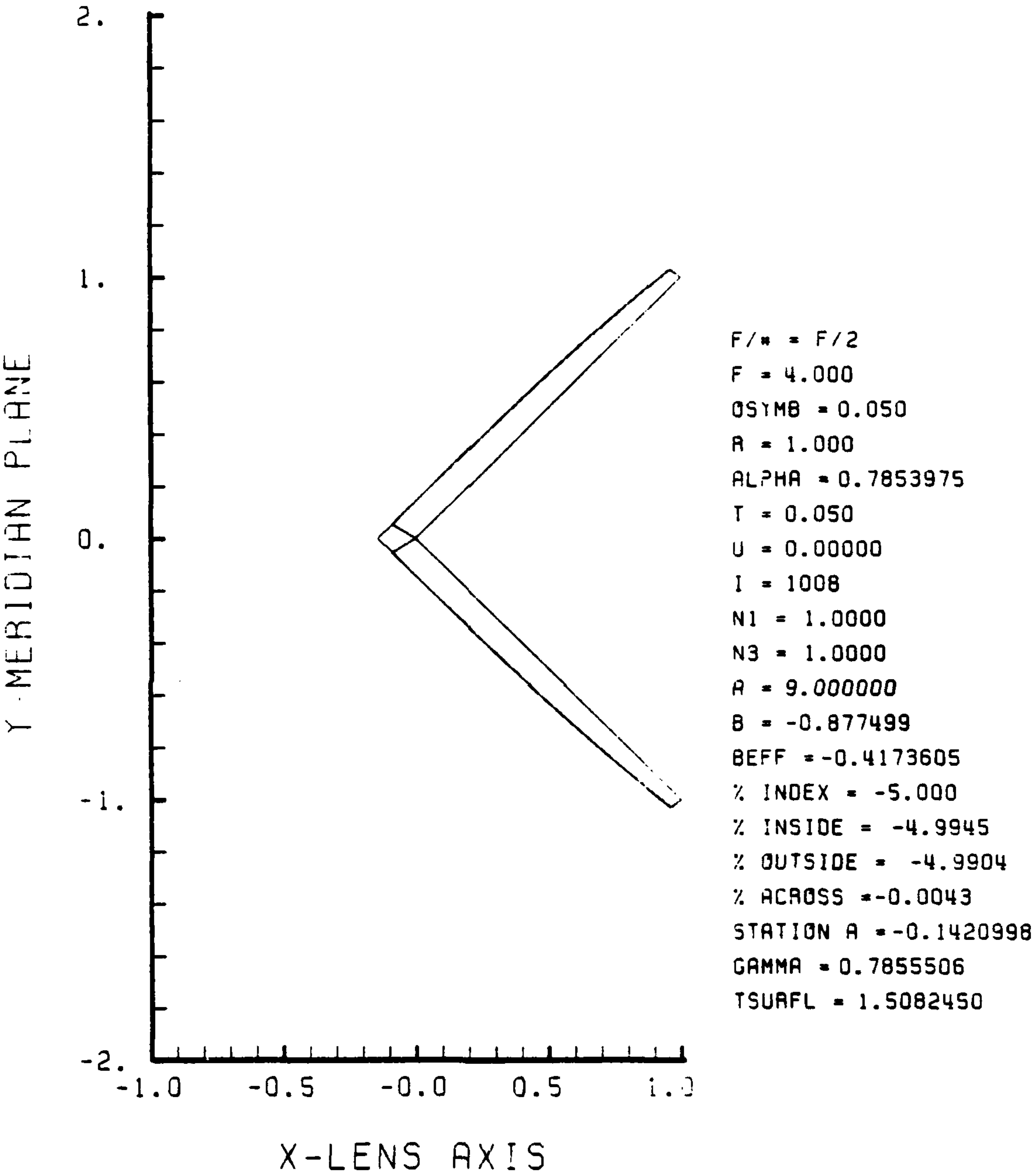

Figure F-1. GRIN Lens Shape at -5%, OB = 0.05, a = 9.00

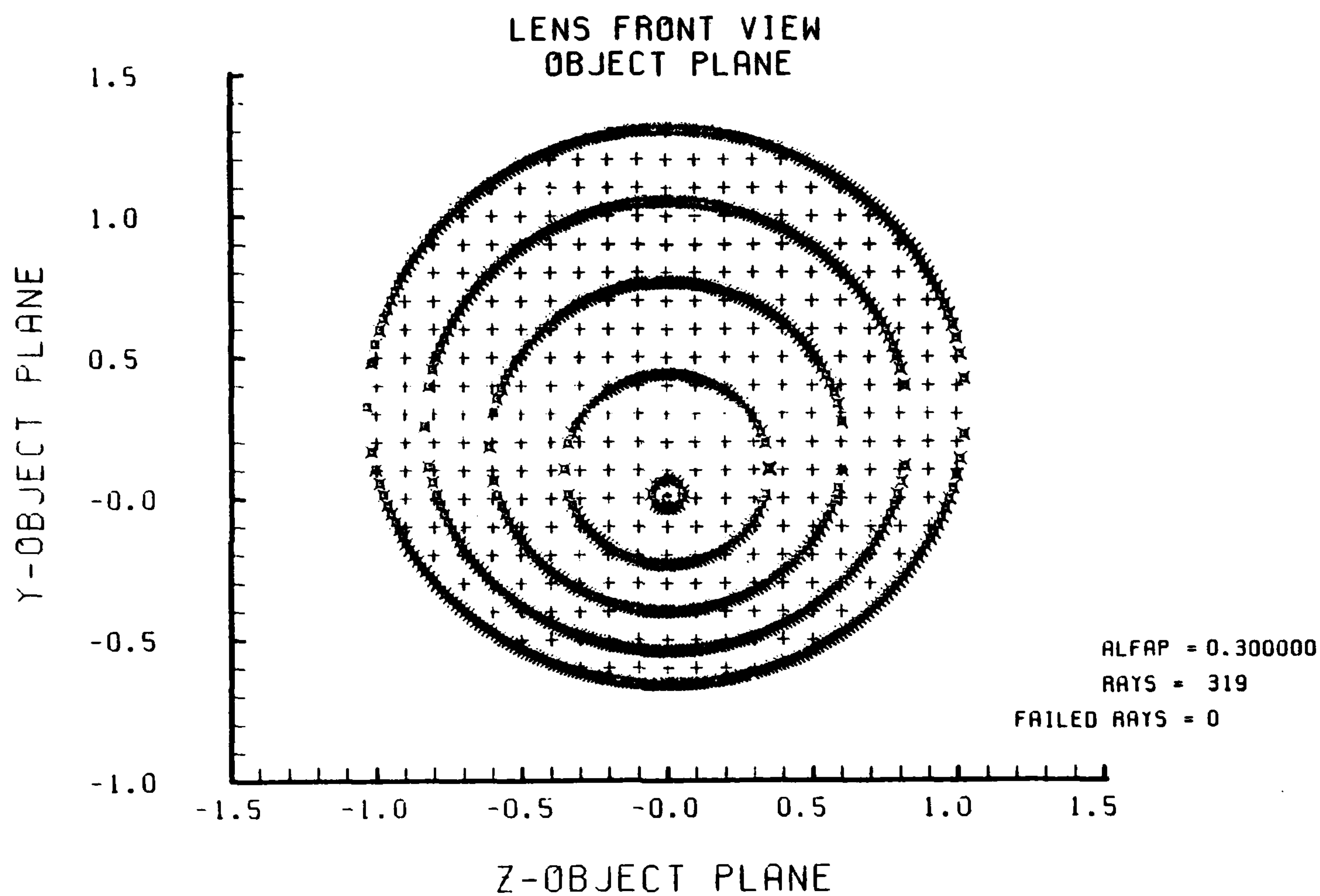

Figure F-2. Grid Plane at $\alpha_p = 0.3$ for Lens of Figure F-1

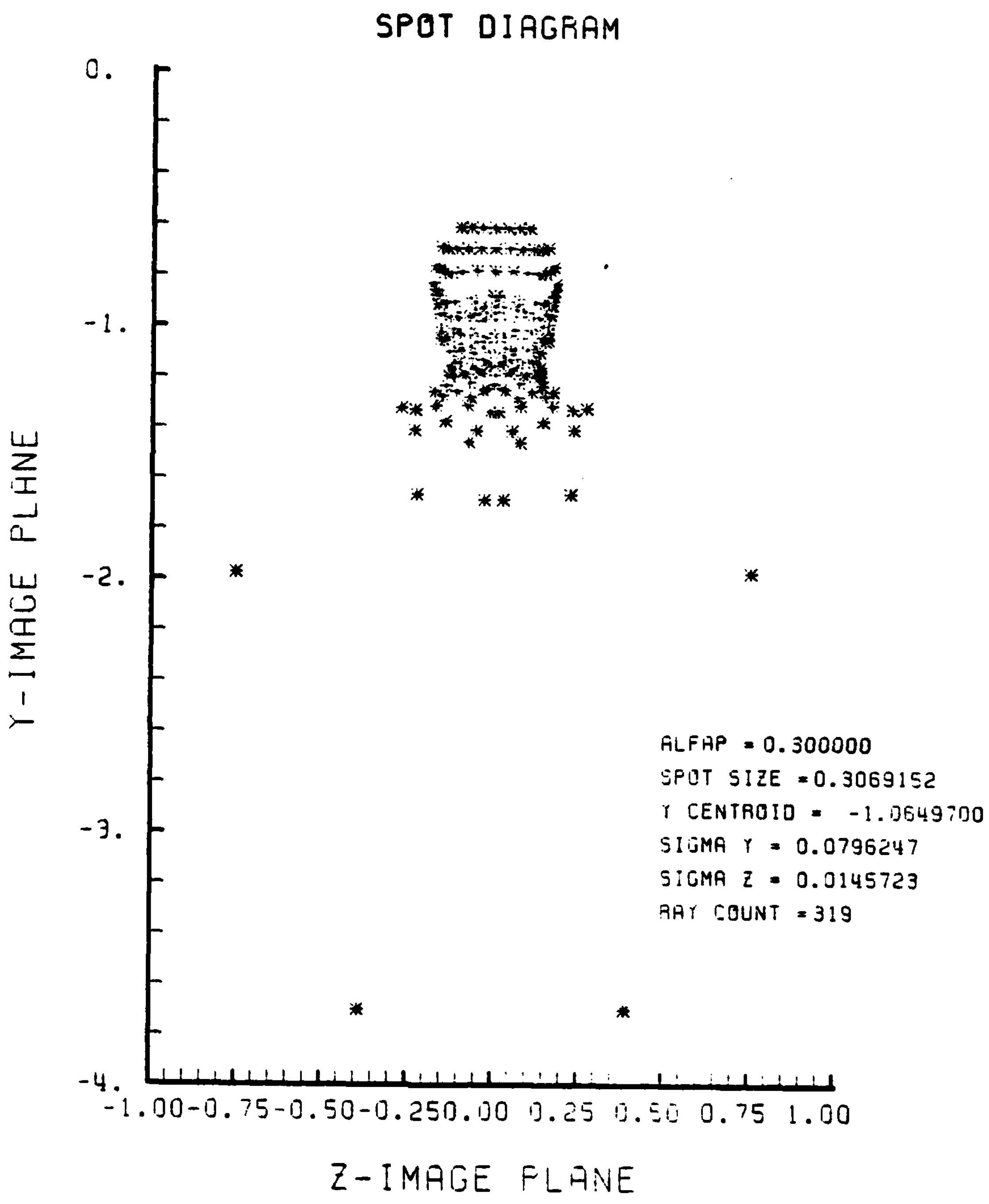

Figure F-3. Spot Diagram for Grid of Figure F-2

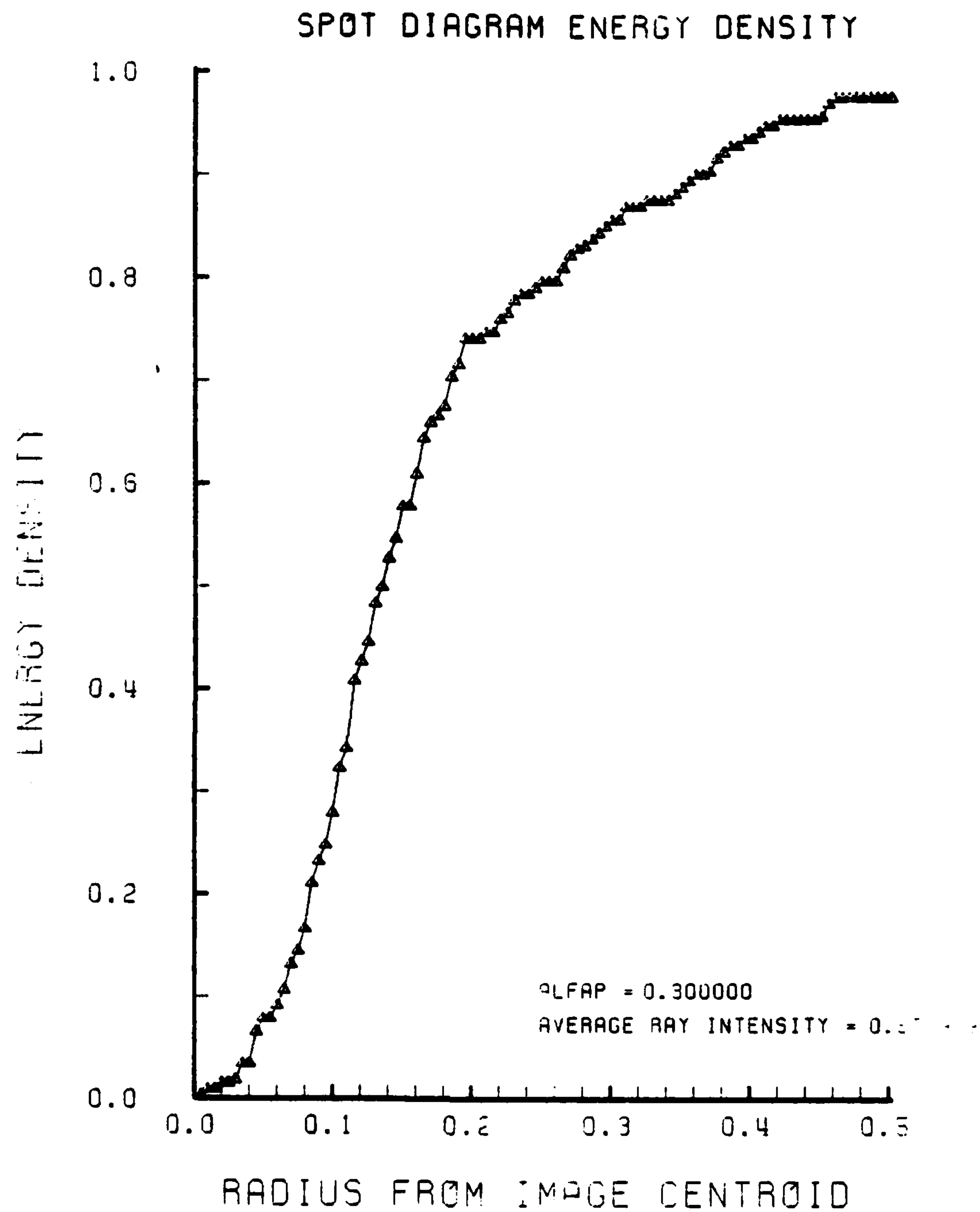

Figure F-4. Encircled Energy of Figure F-3

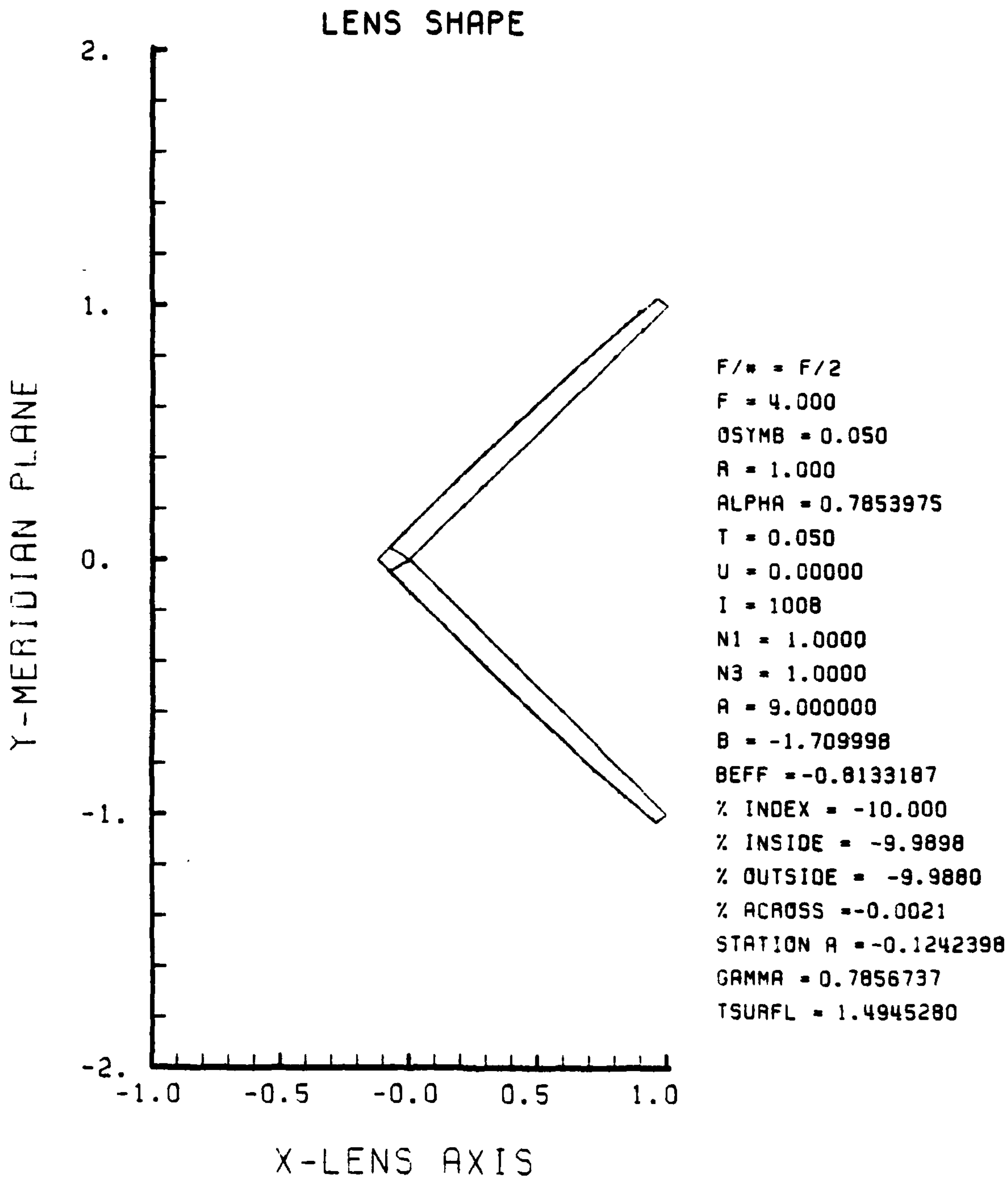

Figure F-5. GRIN Lens Shape at -10%, OB = 0.05, a = 9.00

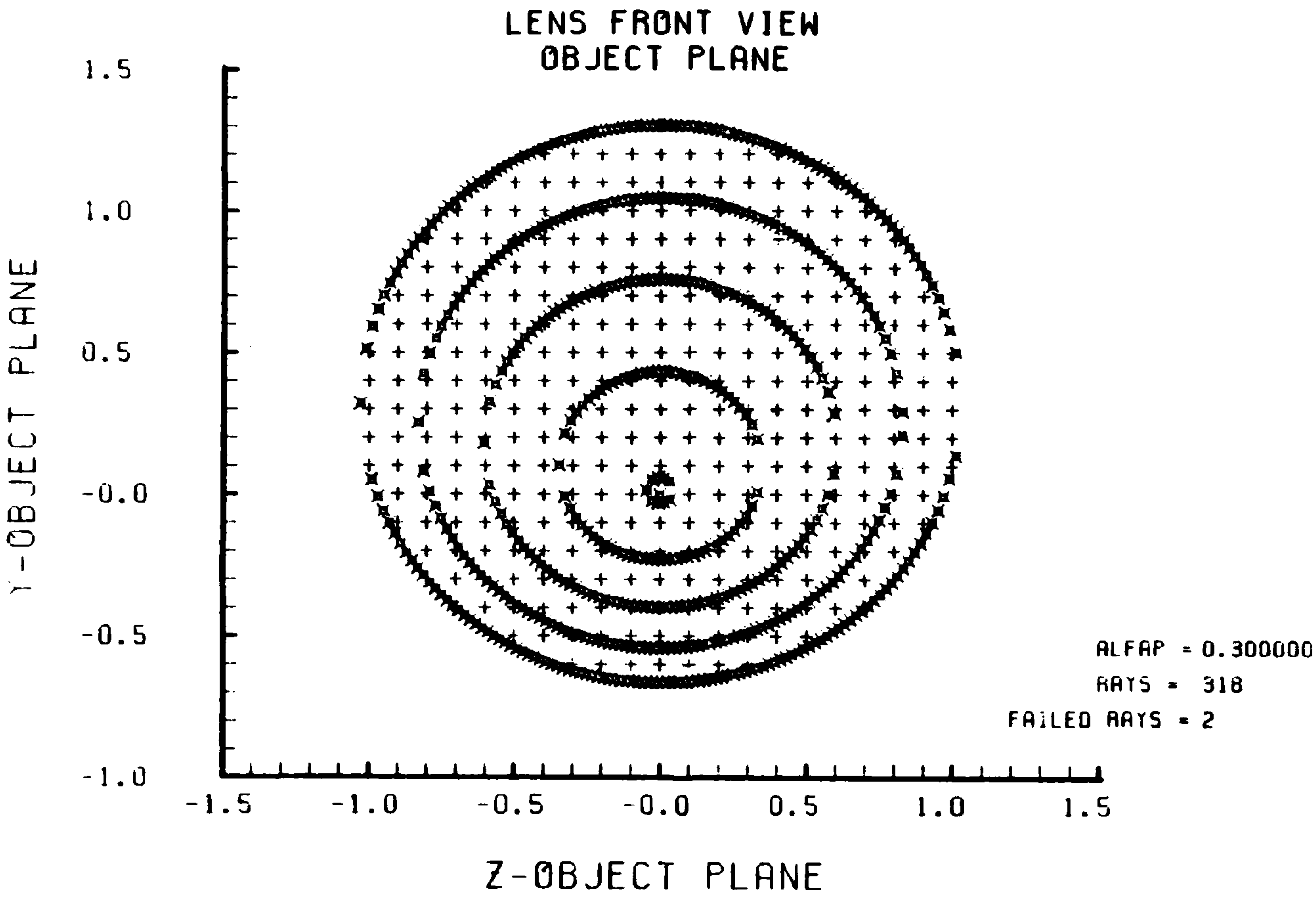

Figure F-6. Grid Plane at $\alpha_p = 0.3$ for Lens of Figure F-5

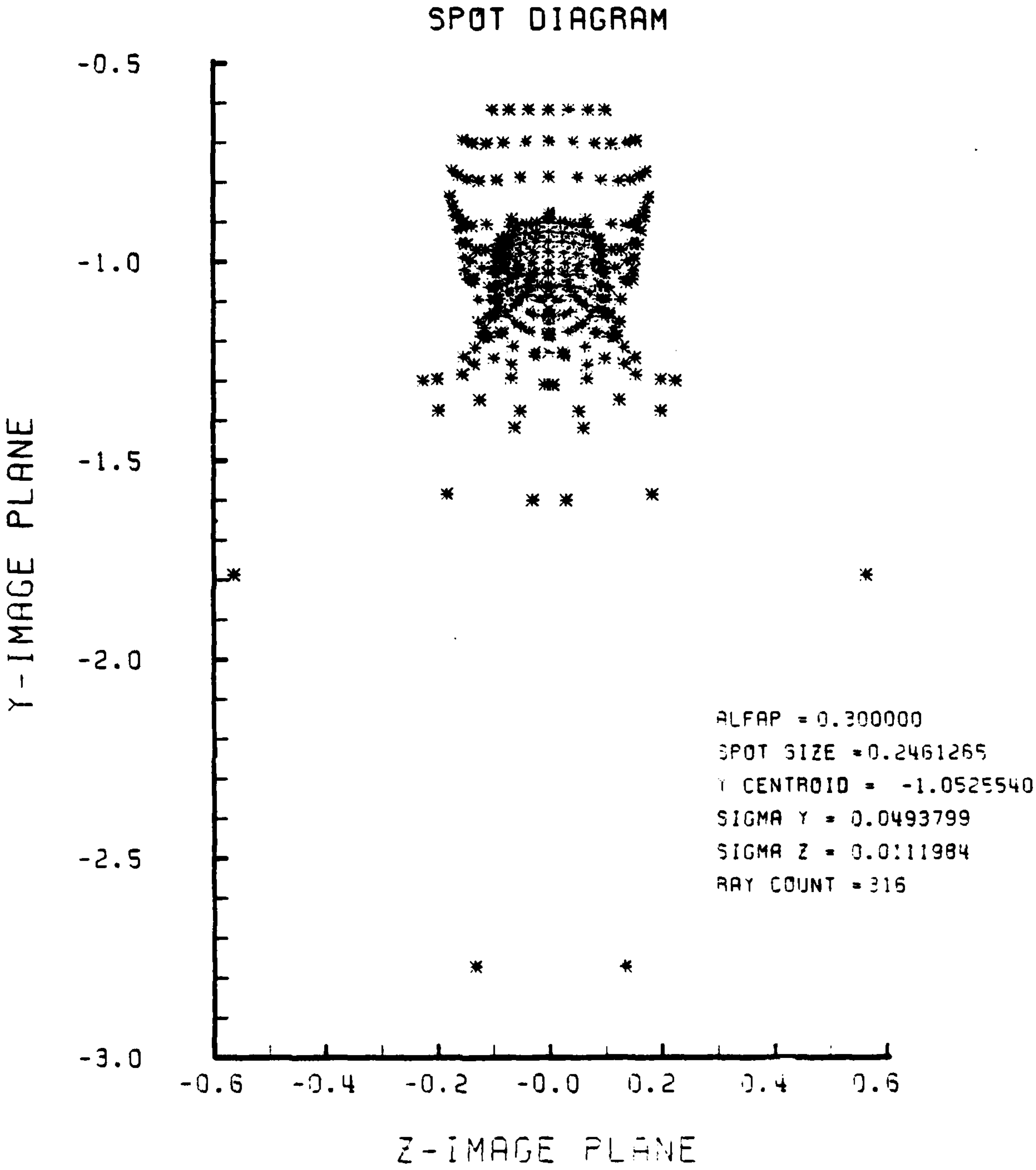

Figure F-7. Spot Diagram for Grid of Figure F-6

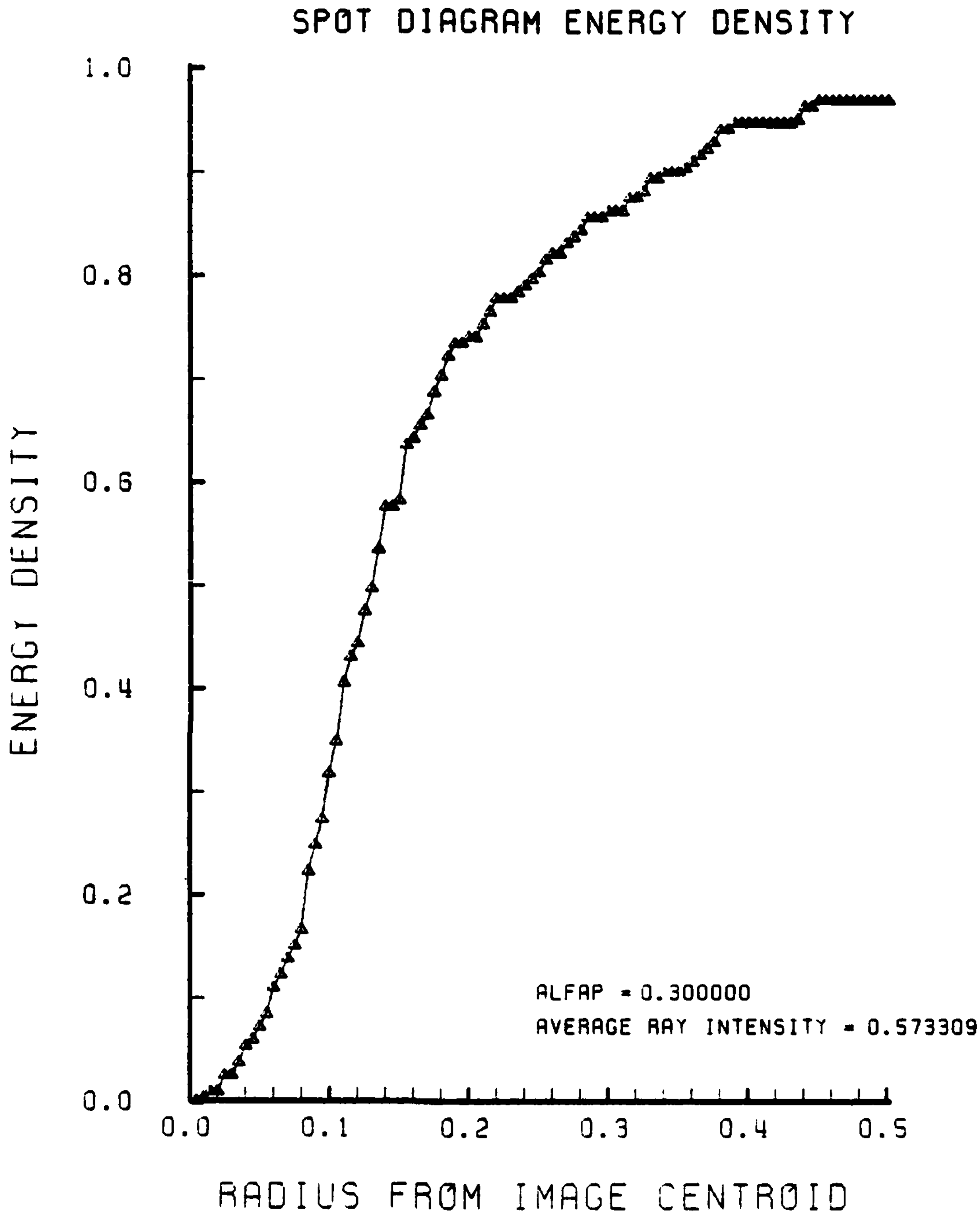

Figure F-8. Encircled Energy of Figure F-7

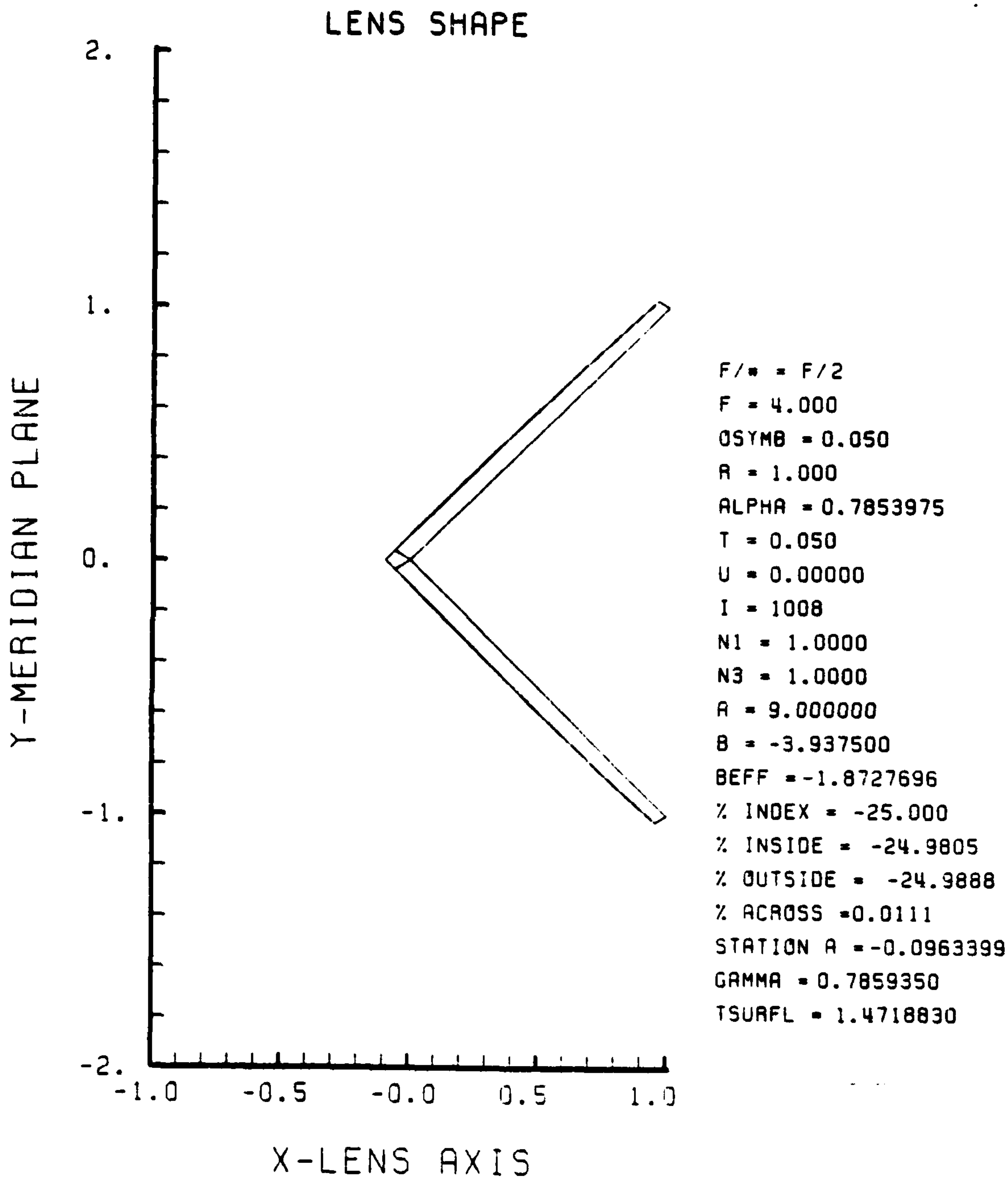

Figure F-9. GRIN Lens Shape at -25%, OB = 0.05, a = 9.00

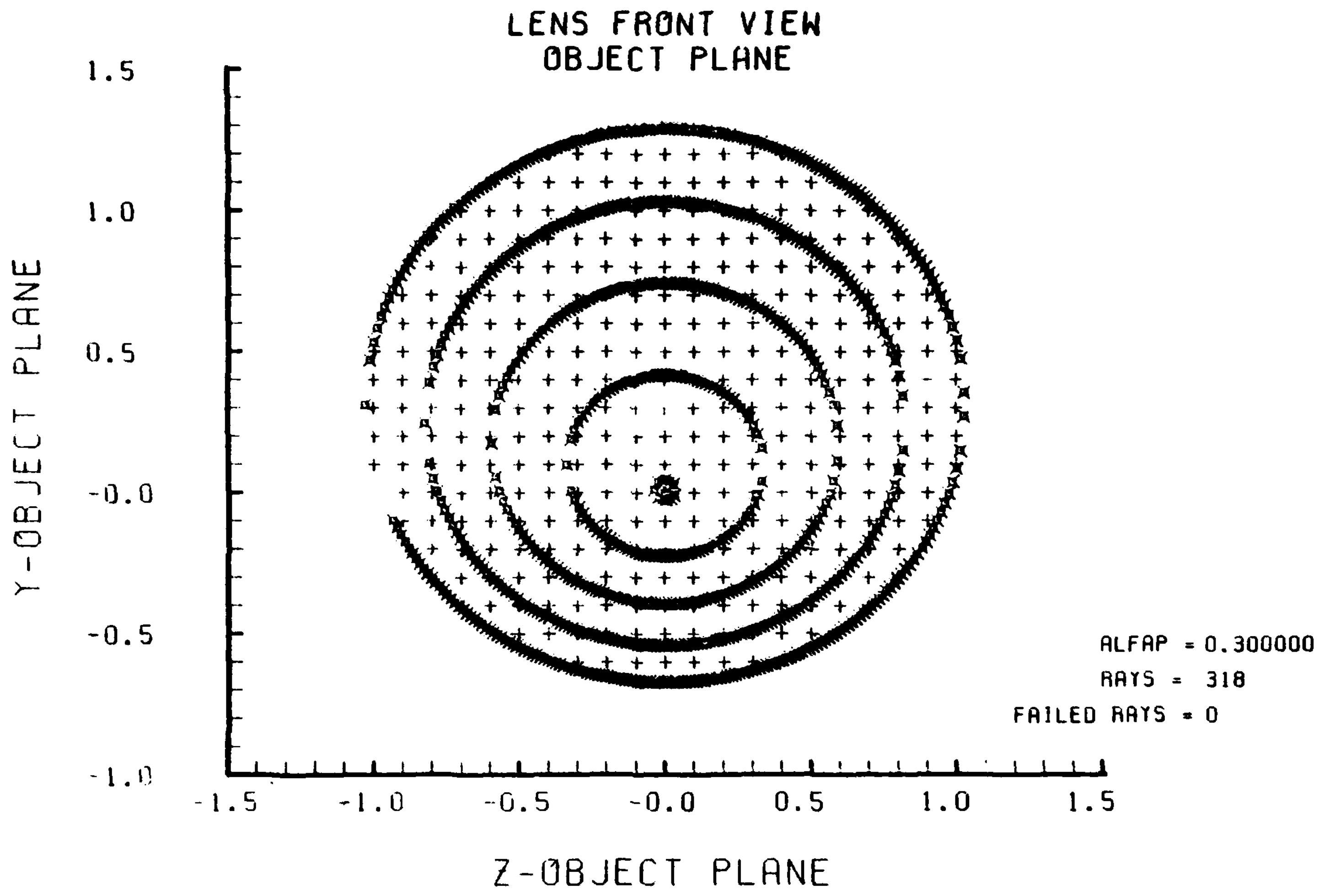

Figure F-10. Grid Plane at $\alpha_p = 0.3$ for Lens of Figure F-9

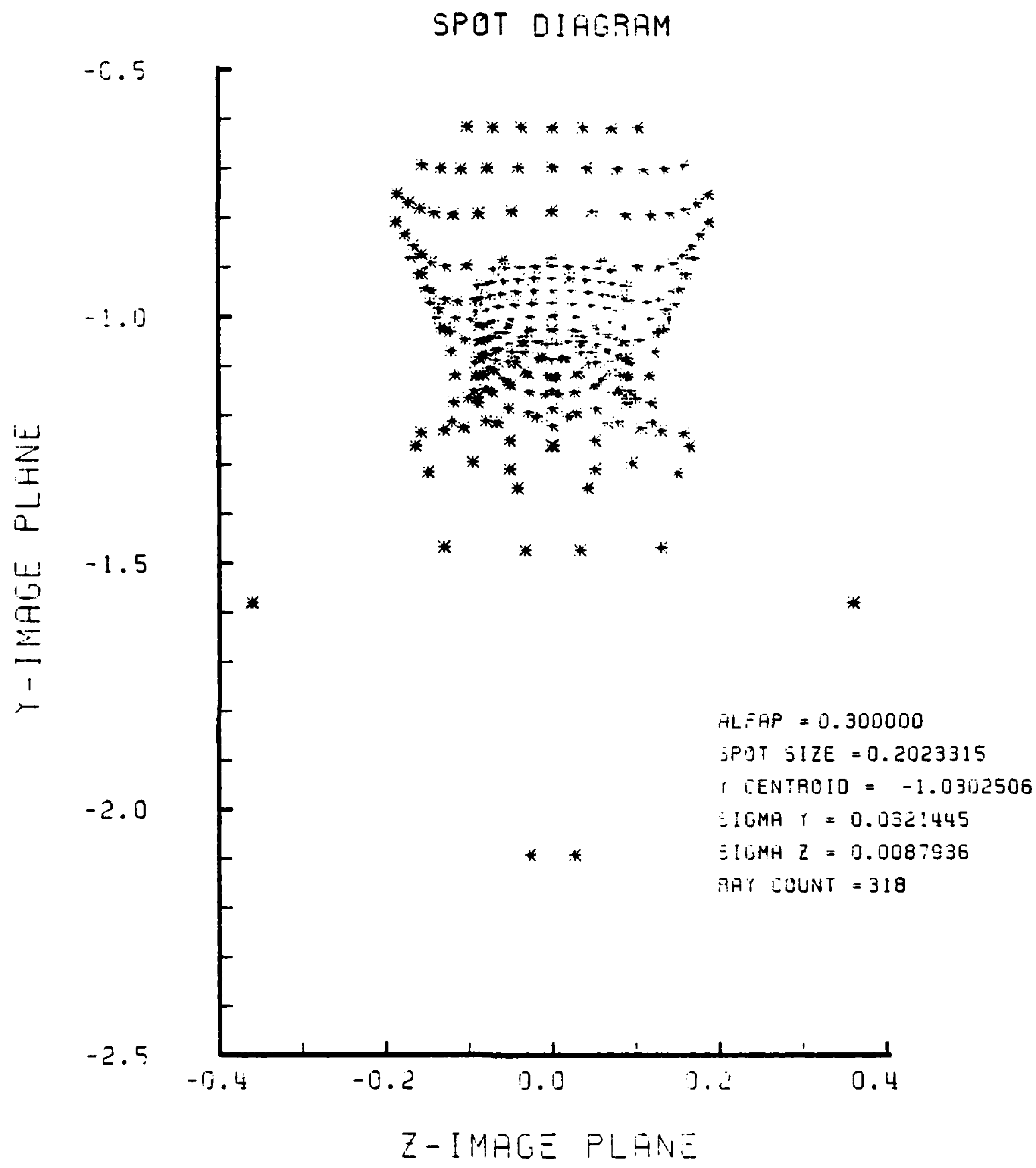

Figure F-11. Spot Diagram for Grid of Figure F-10

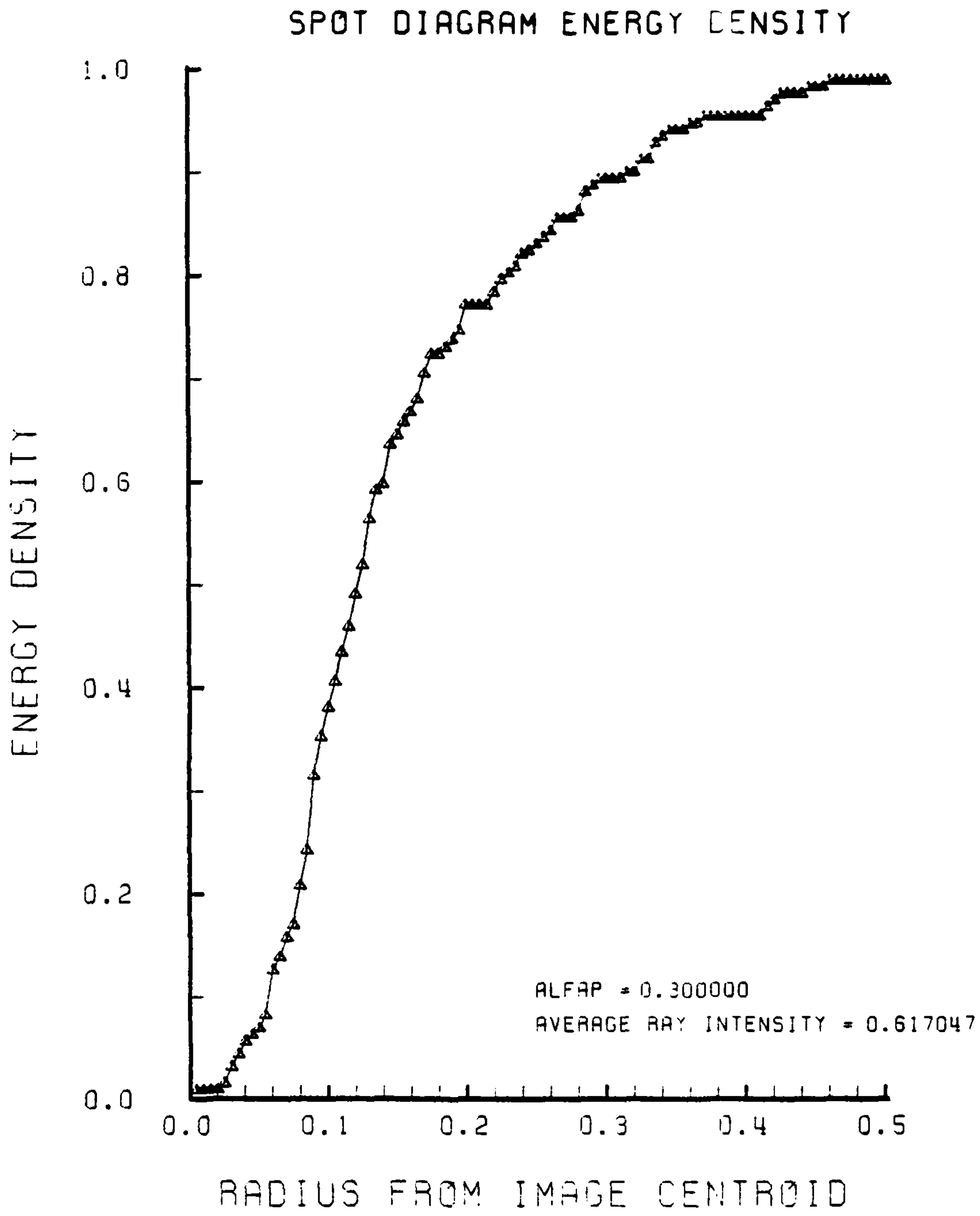

Figure F-12. Encircled Energy of Figure F-11

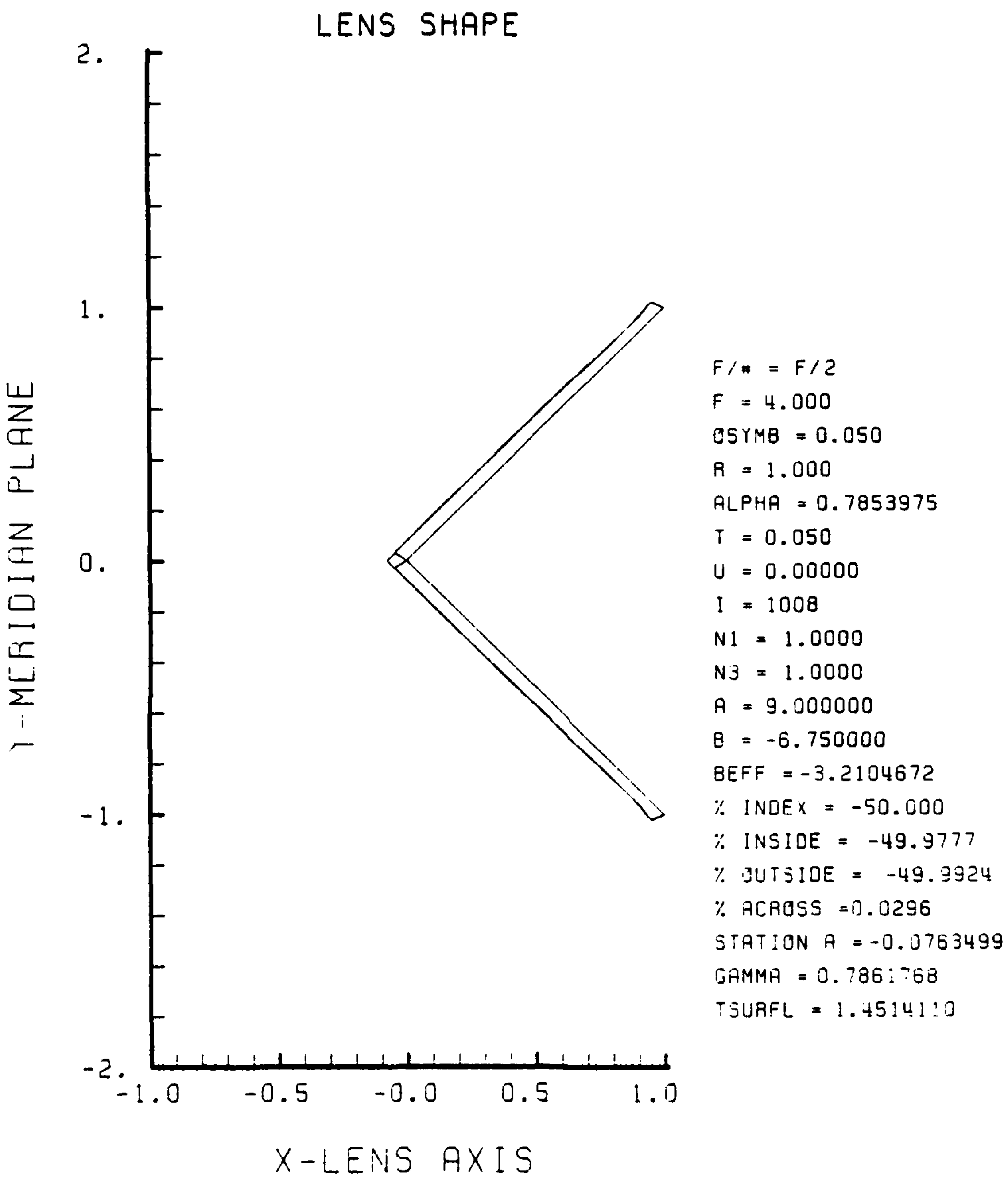

Figure F-13. GRIN Lens Shape at -50%, OB = 0.05, a = 9.00

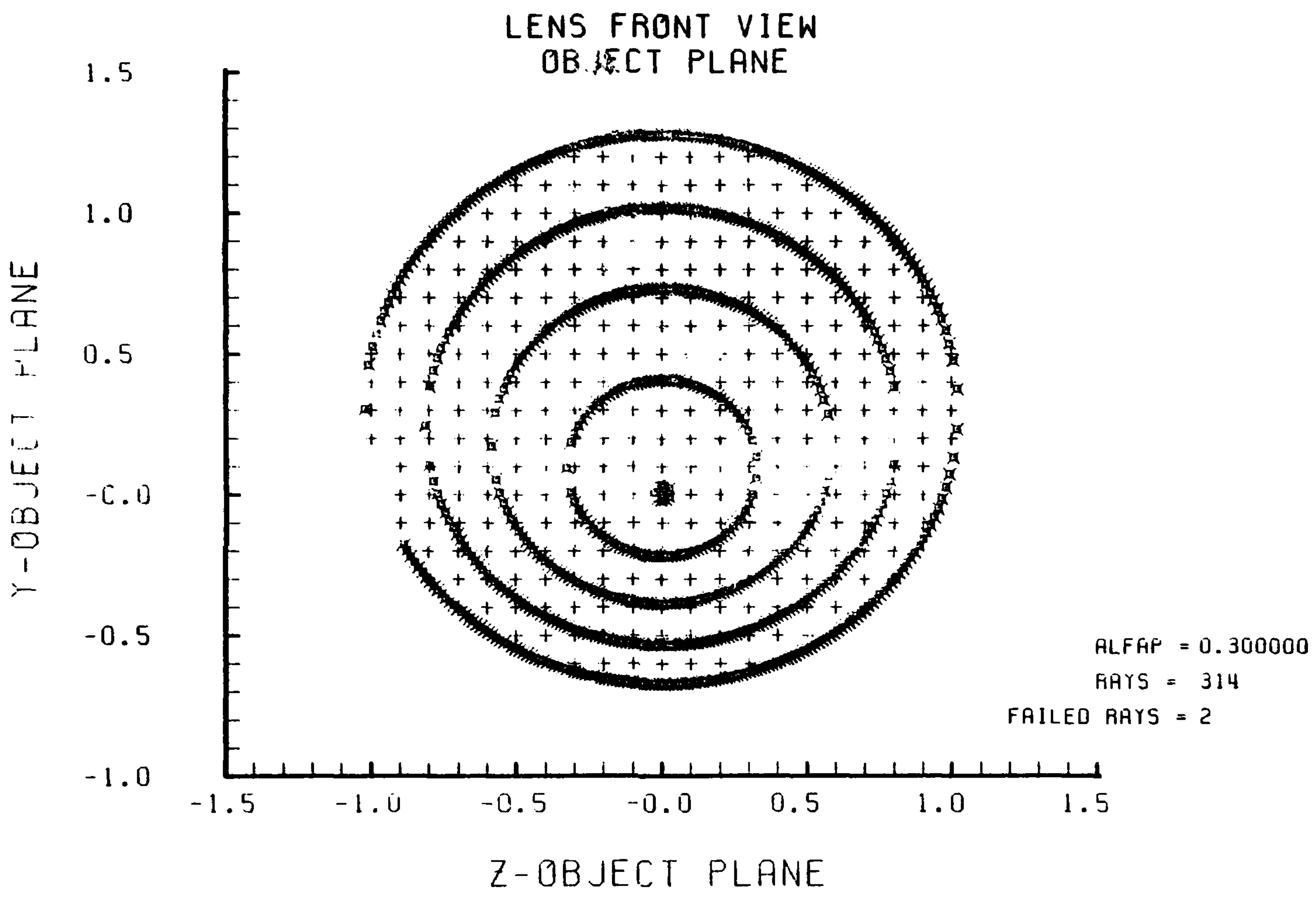

Figure F-14. Grid Plane at α_p = 0.3 for Lens of Figure F-13

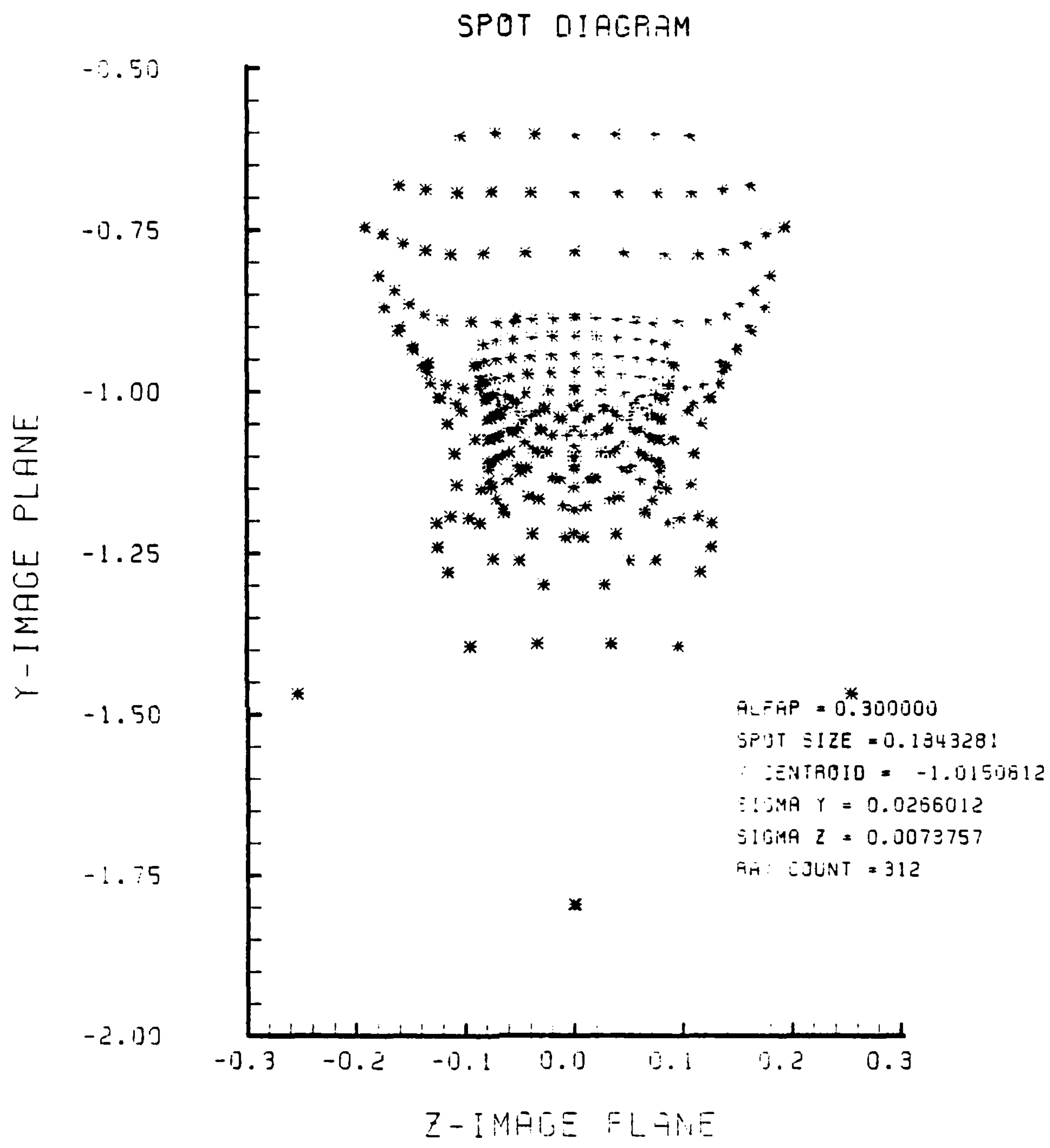

Figure F-15. Spot Diagram for Grid of Figure F-14

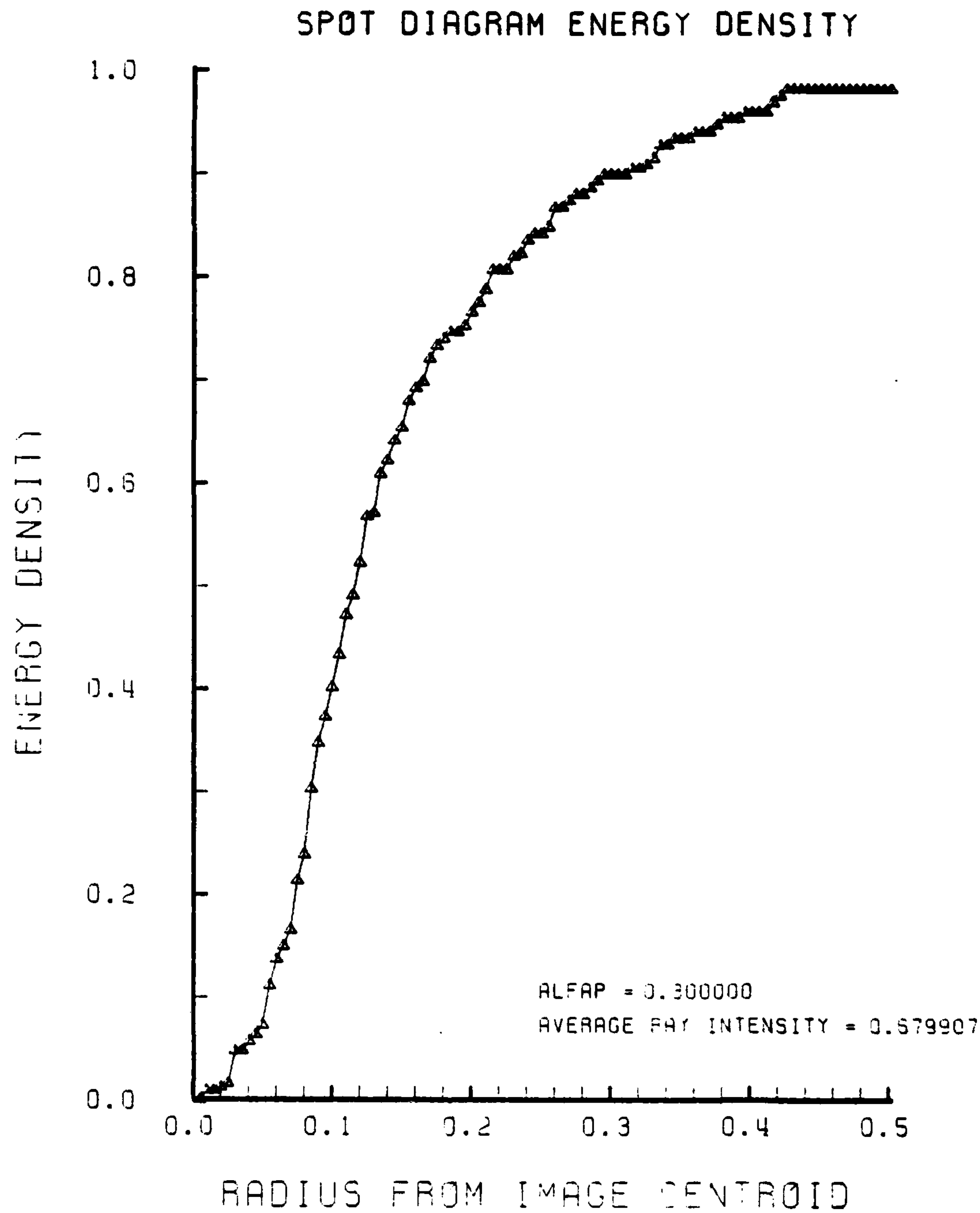

Figure F-16. Encircled Energy of Figure F-15

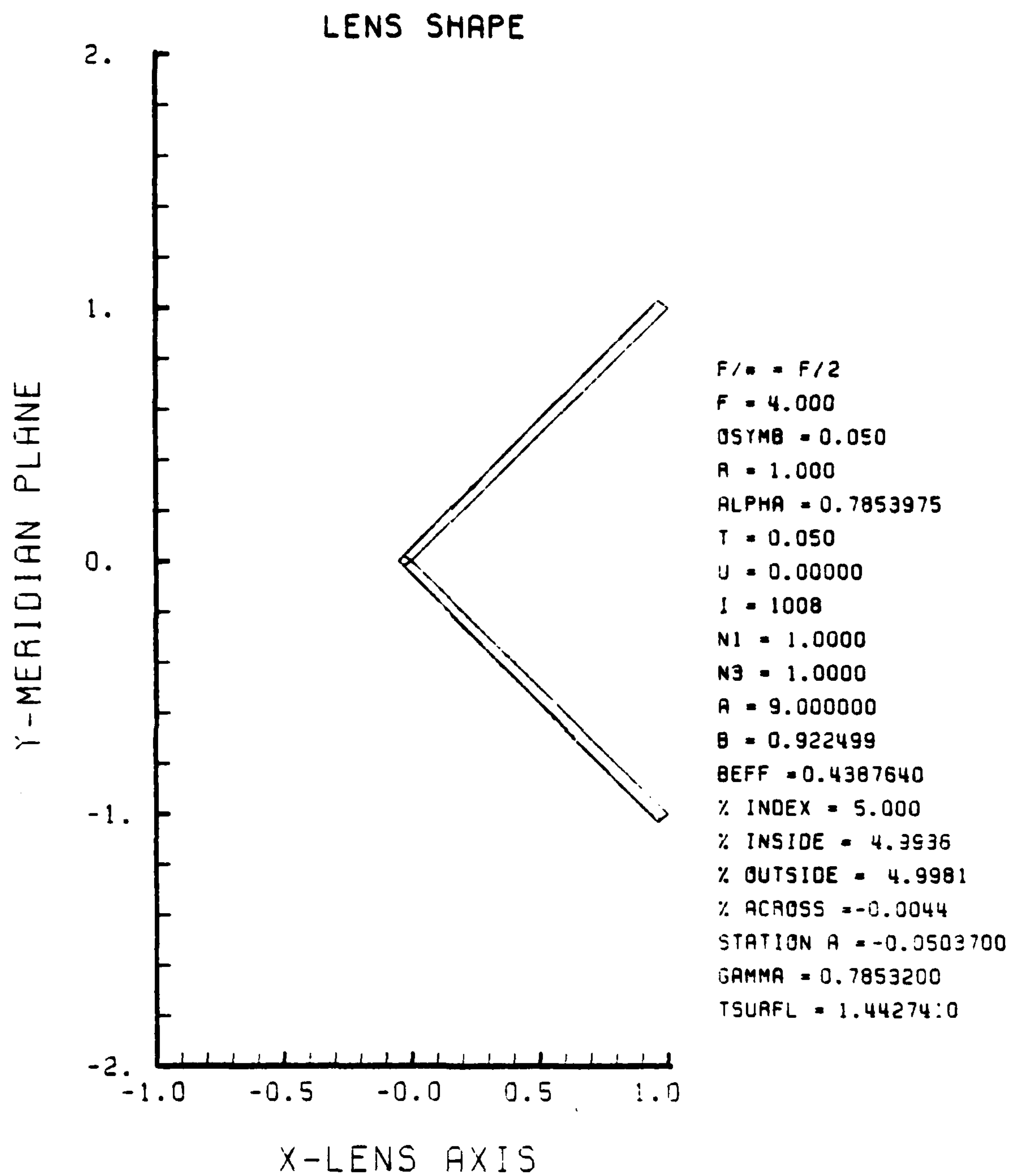

Figure F-17. GRIN Lens Shape at +5%, OB = 0.05, a = 9.00

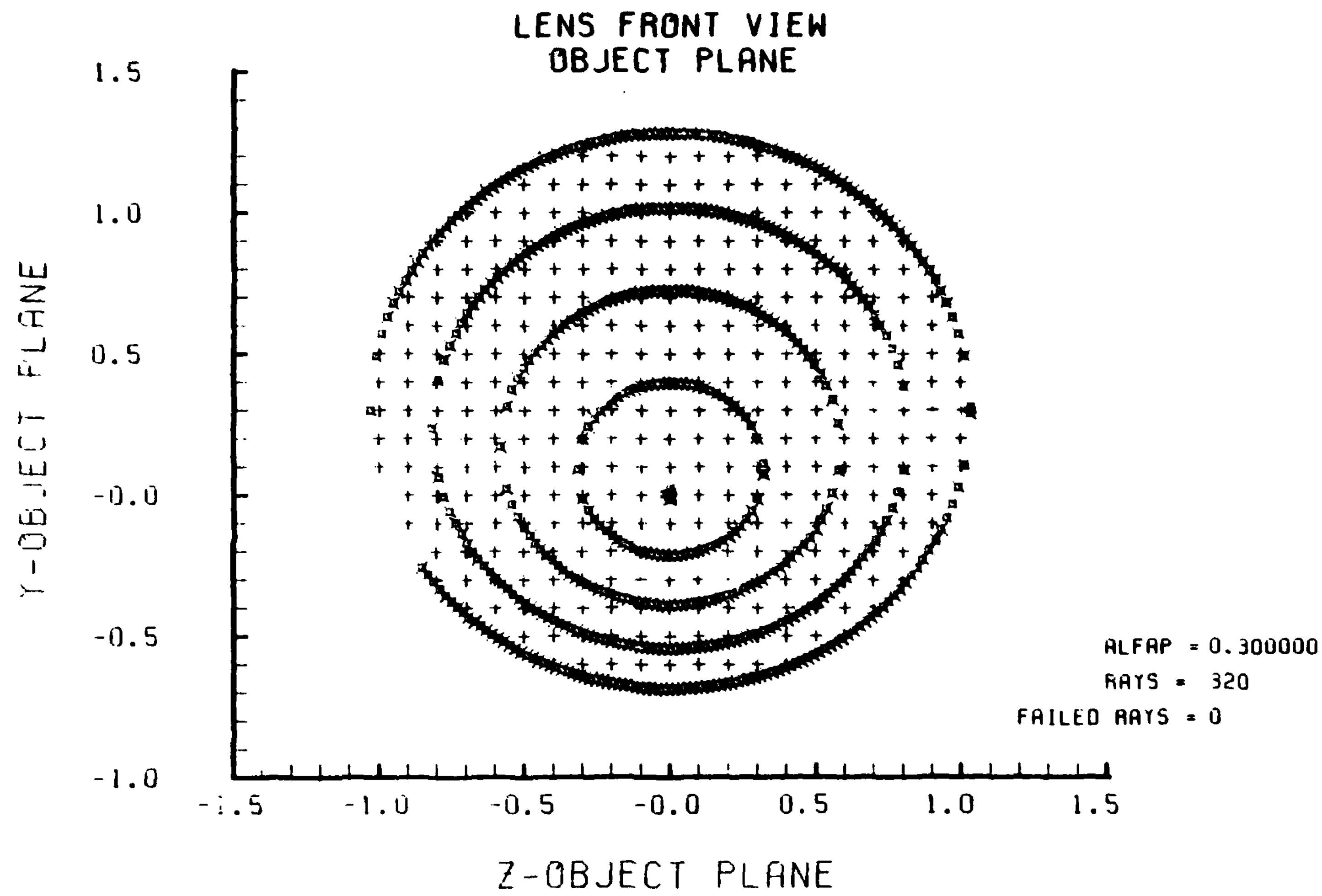

Figure F-18. Grid Plane at $\alpha_p = 0.3$ for Lens of Figure F-17

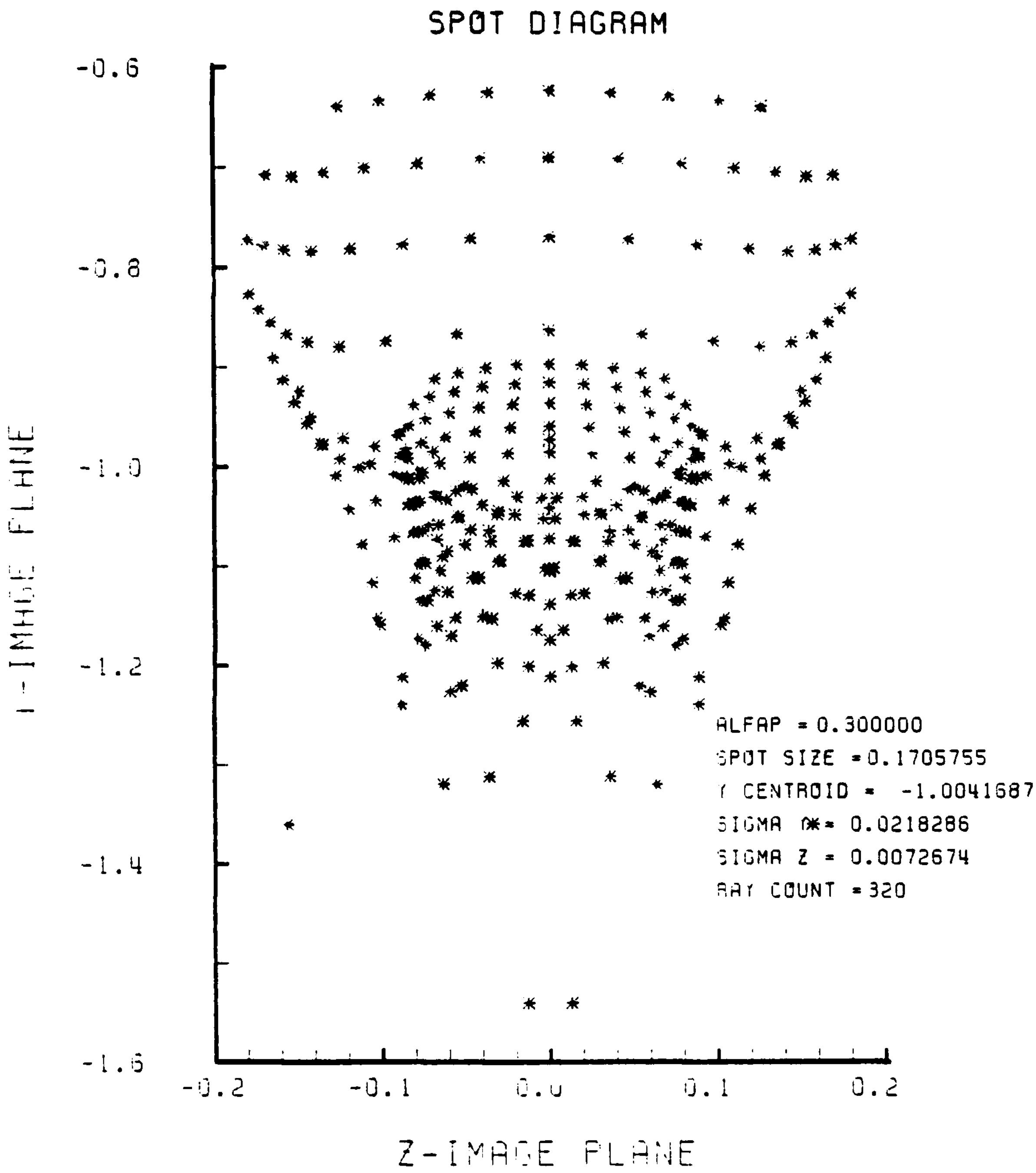

Figure F-19. Spot Diagram for Grid of Figure F-18

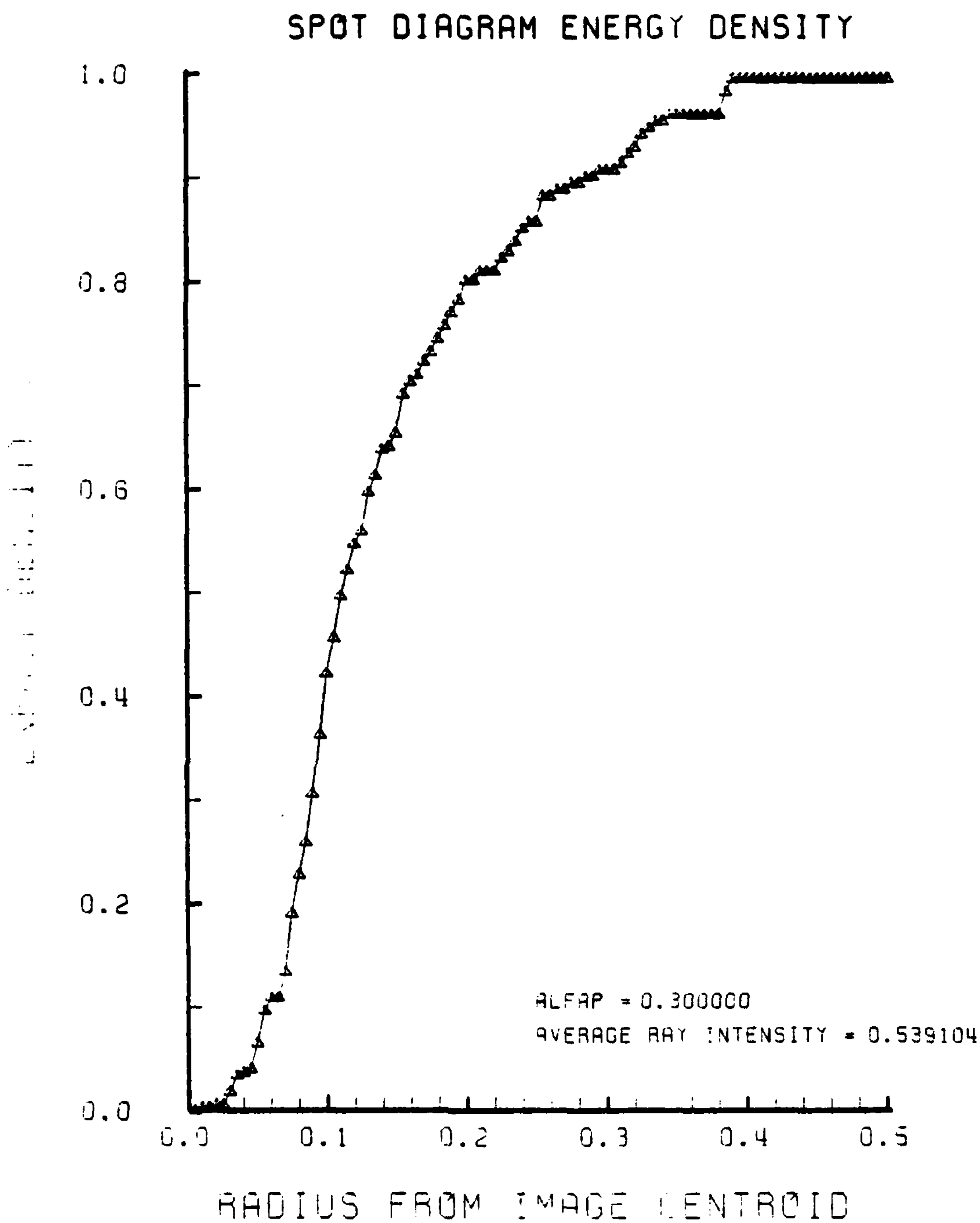

Figure F-20. Encircled Energy of Figure F-19

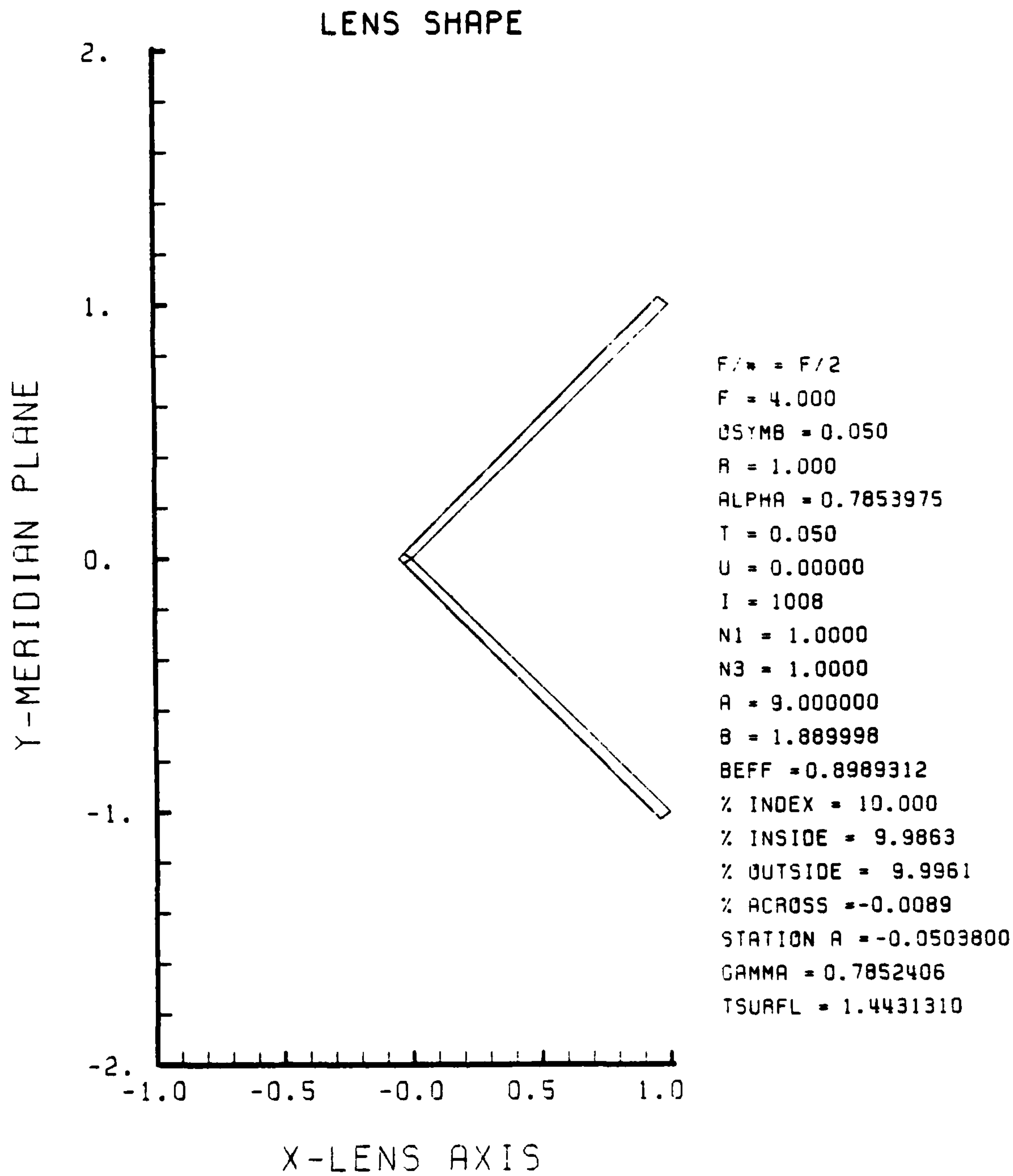

Figure F-21. GRIN Lens Shape for +10%, OB = 0.05, a = 9.00

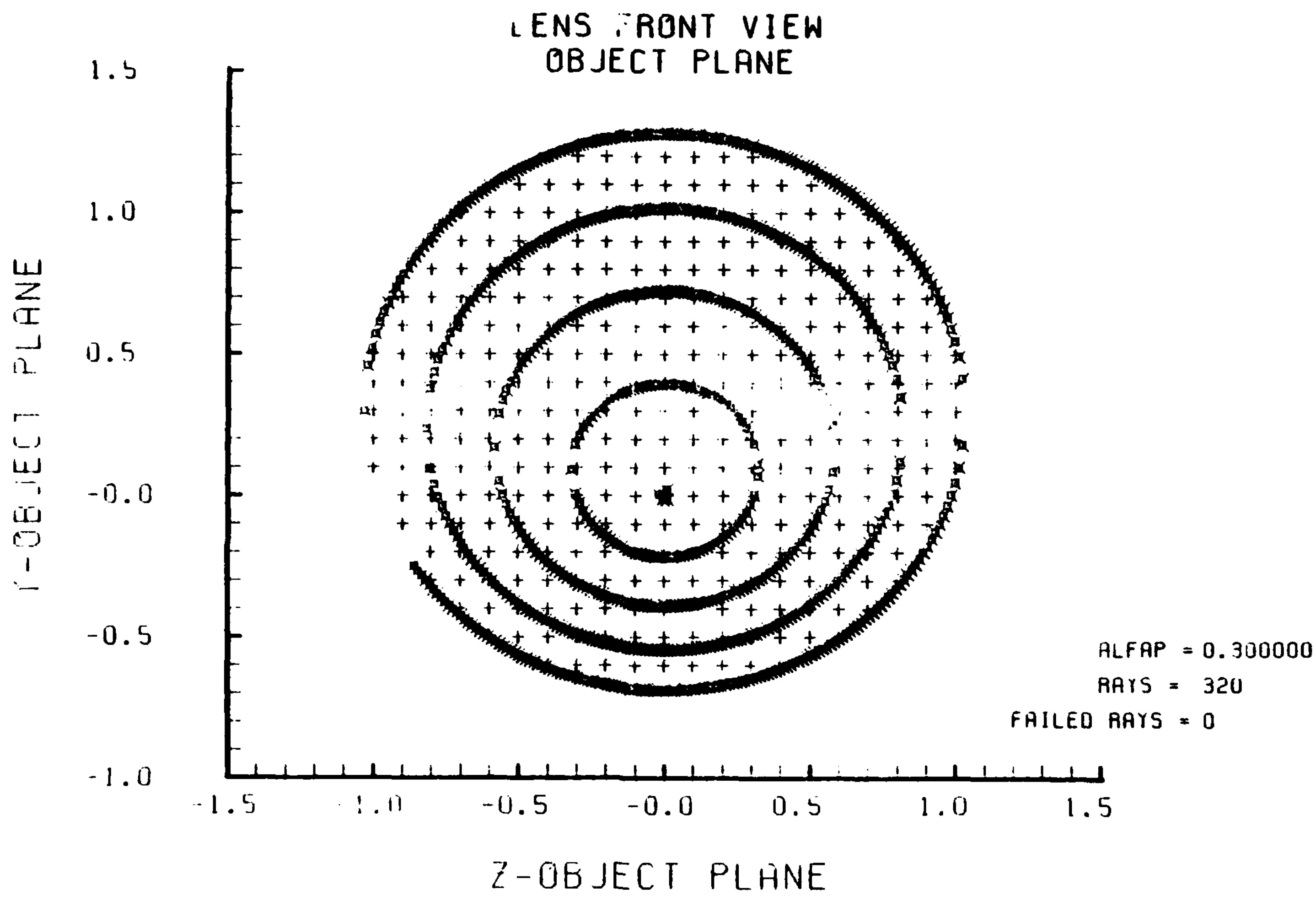

Figure F-22. Grid Plane at α_p = 0.3 Radians for Lens of Figure F-21

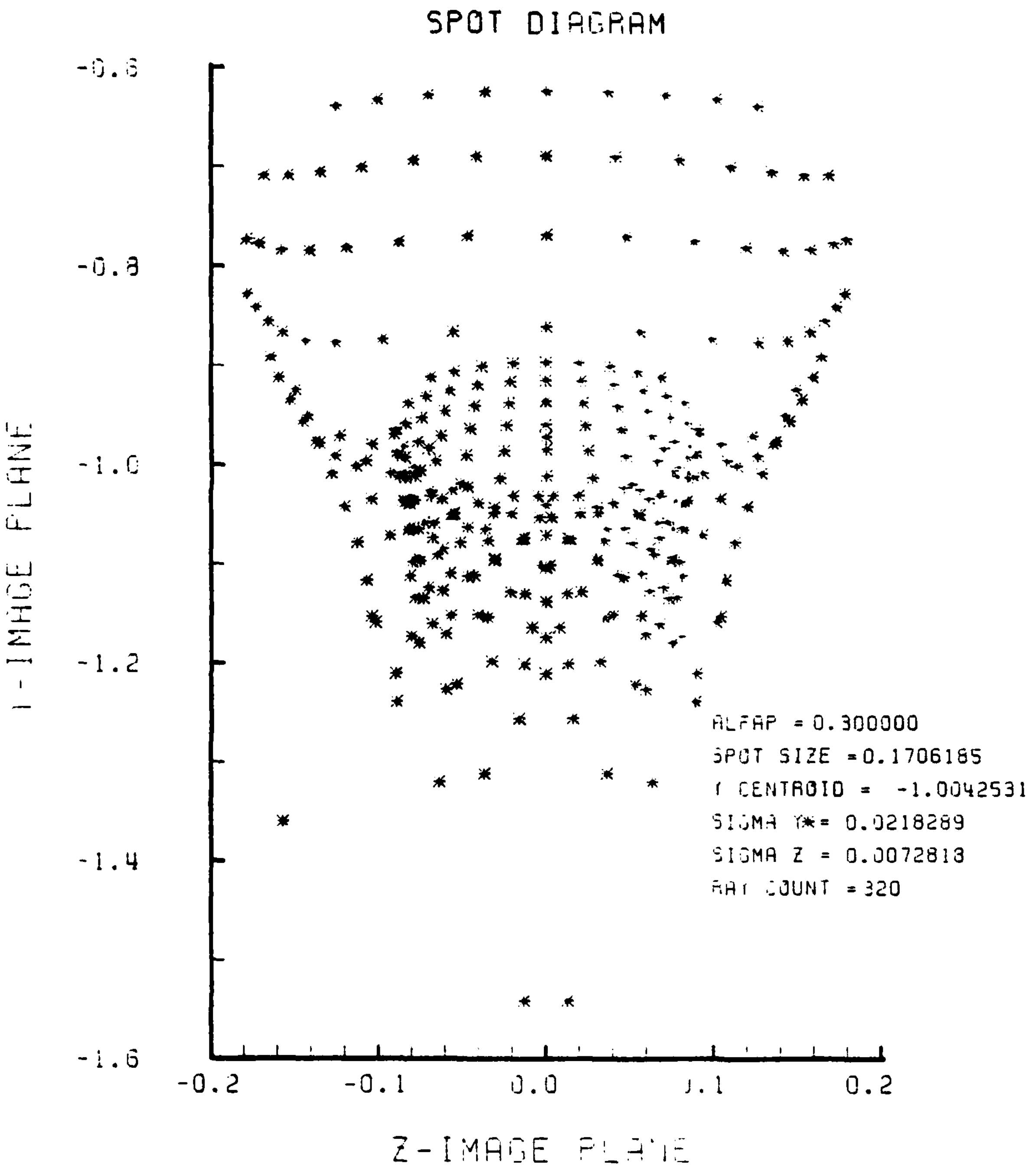

Figure F-23. Spot Diagram for Grid of Figure F-22

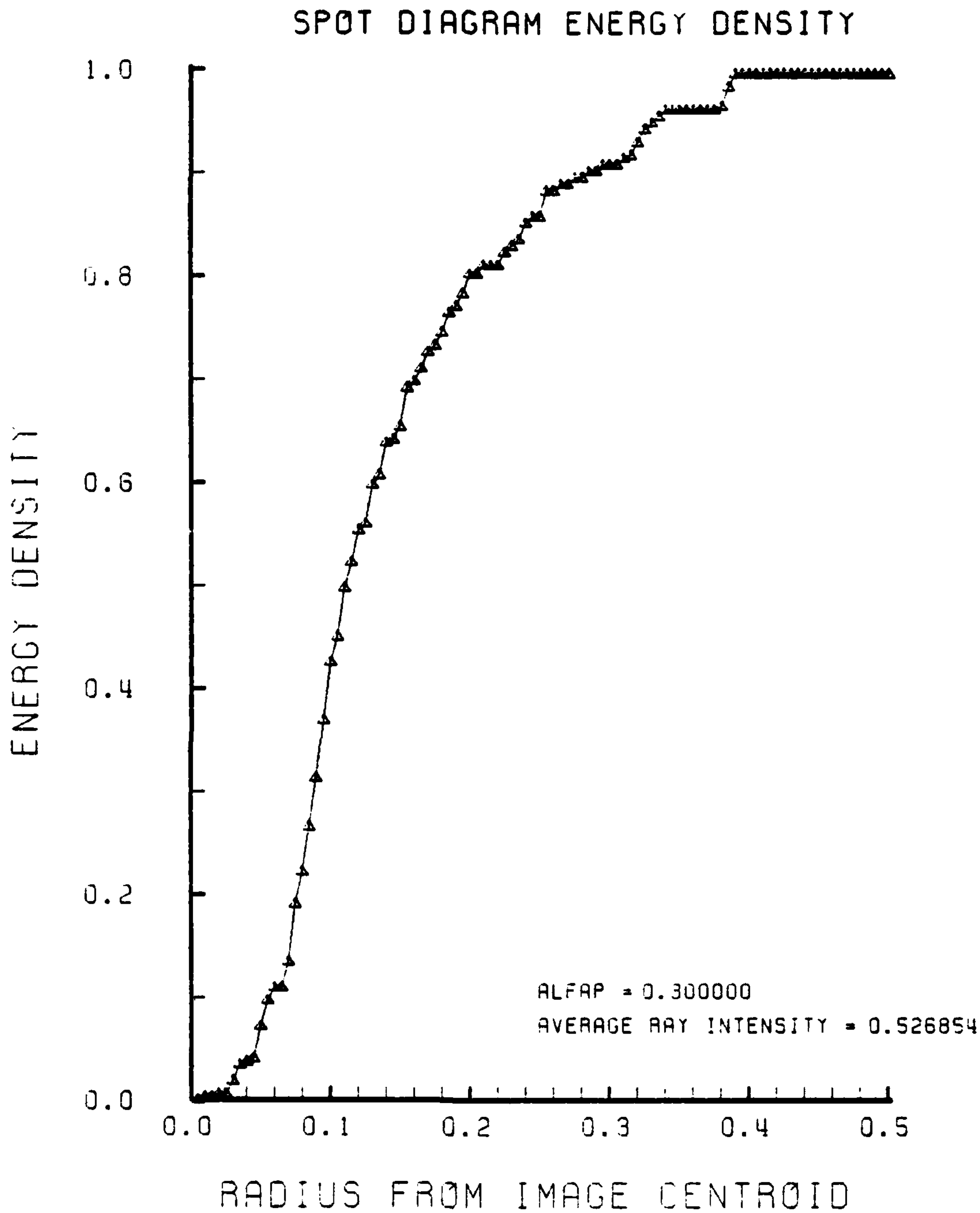

Figure F-24. Encircled Energy of Figure F-23

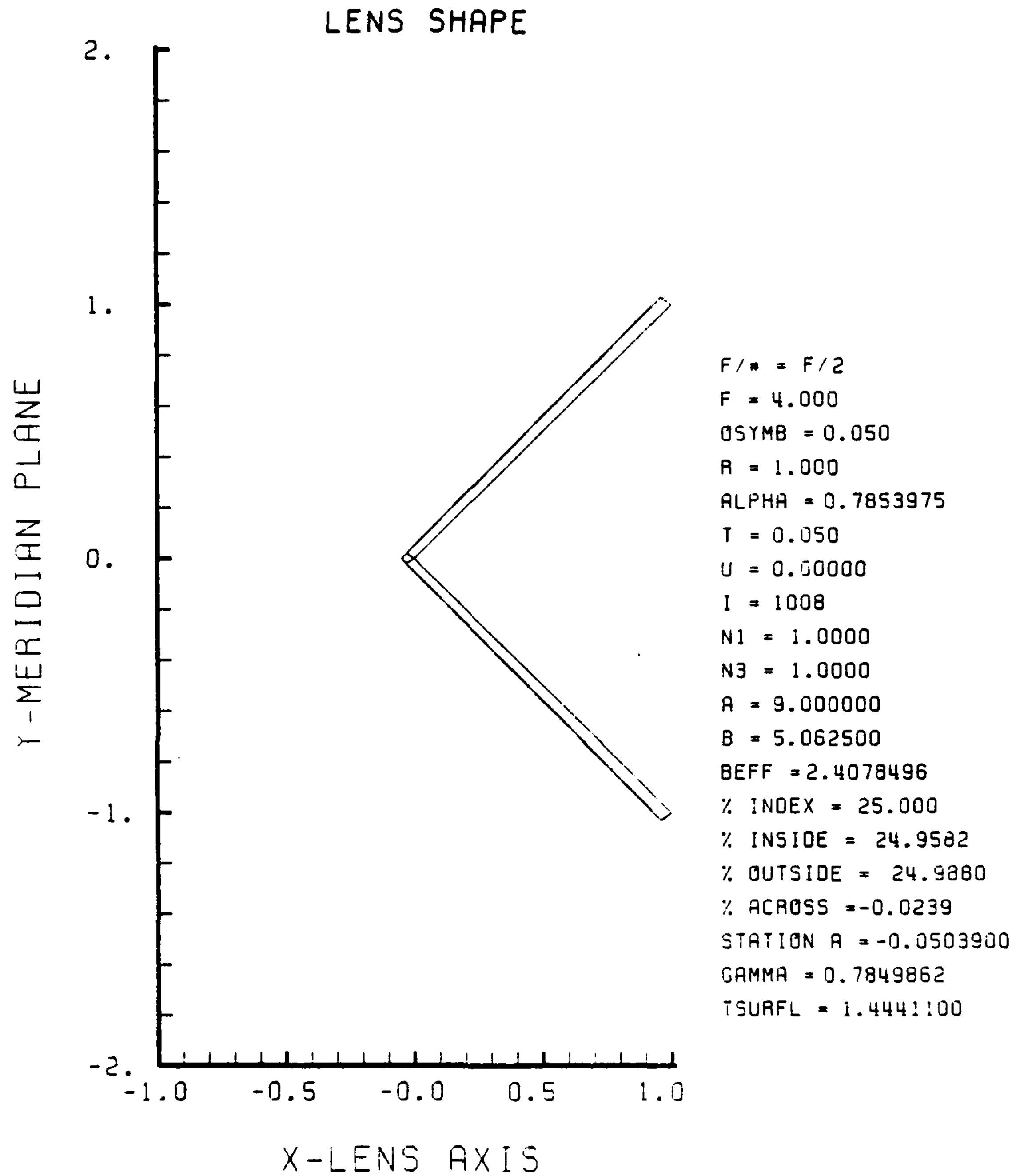

Figure F-25. GRIN Lens Shape for +25%, OB = 0.05, a = 9.00

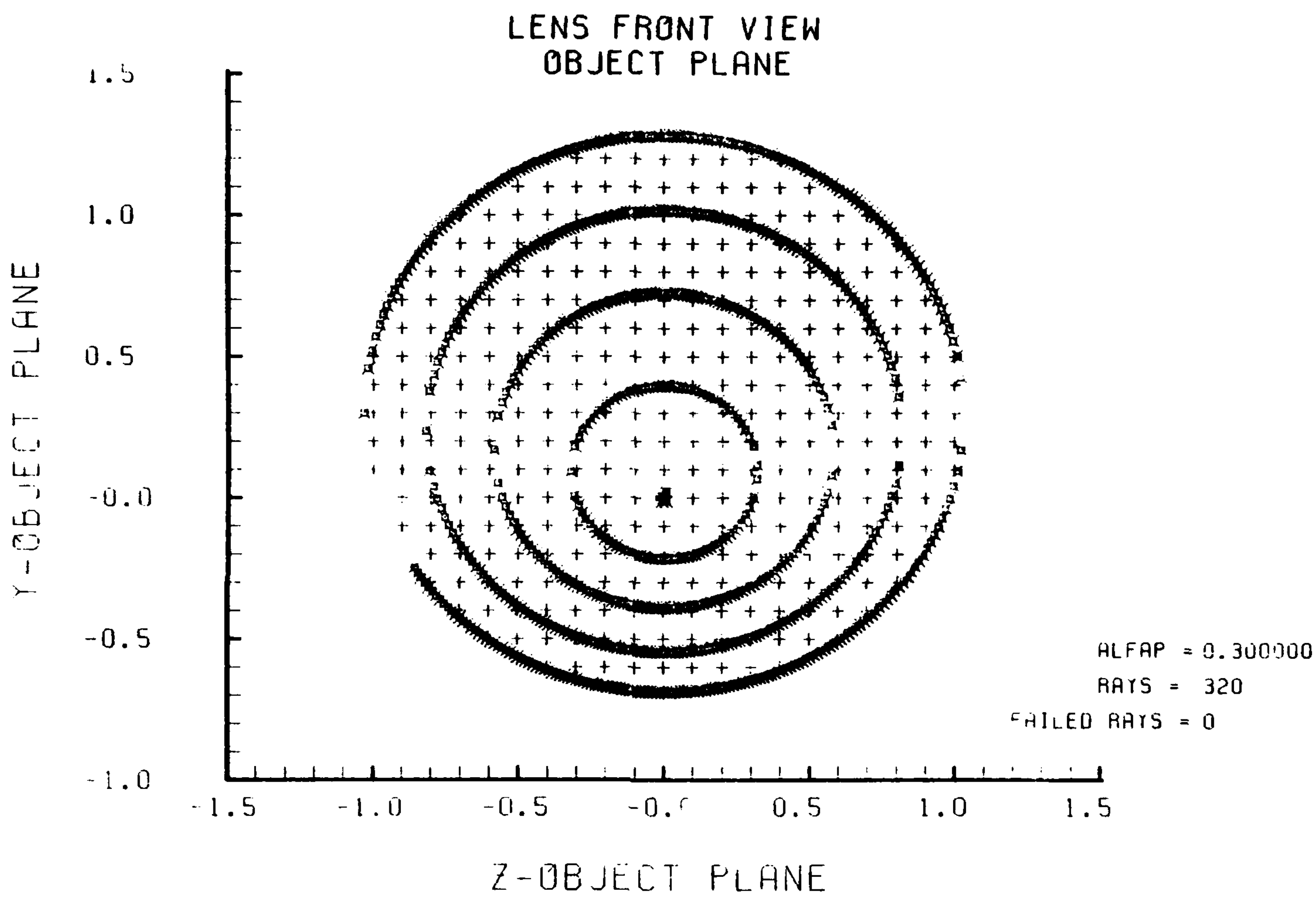

Figure F-26. Grid Plane at α_p = 0.3 for Lens of Figure F-25

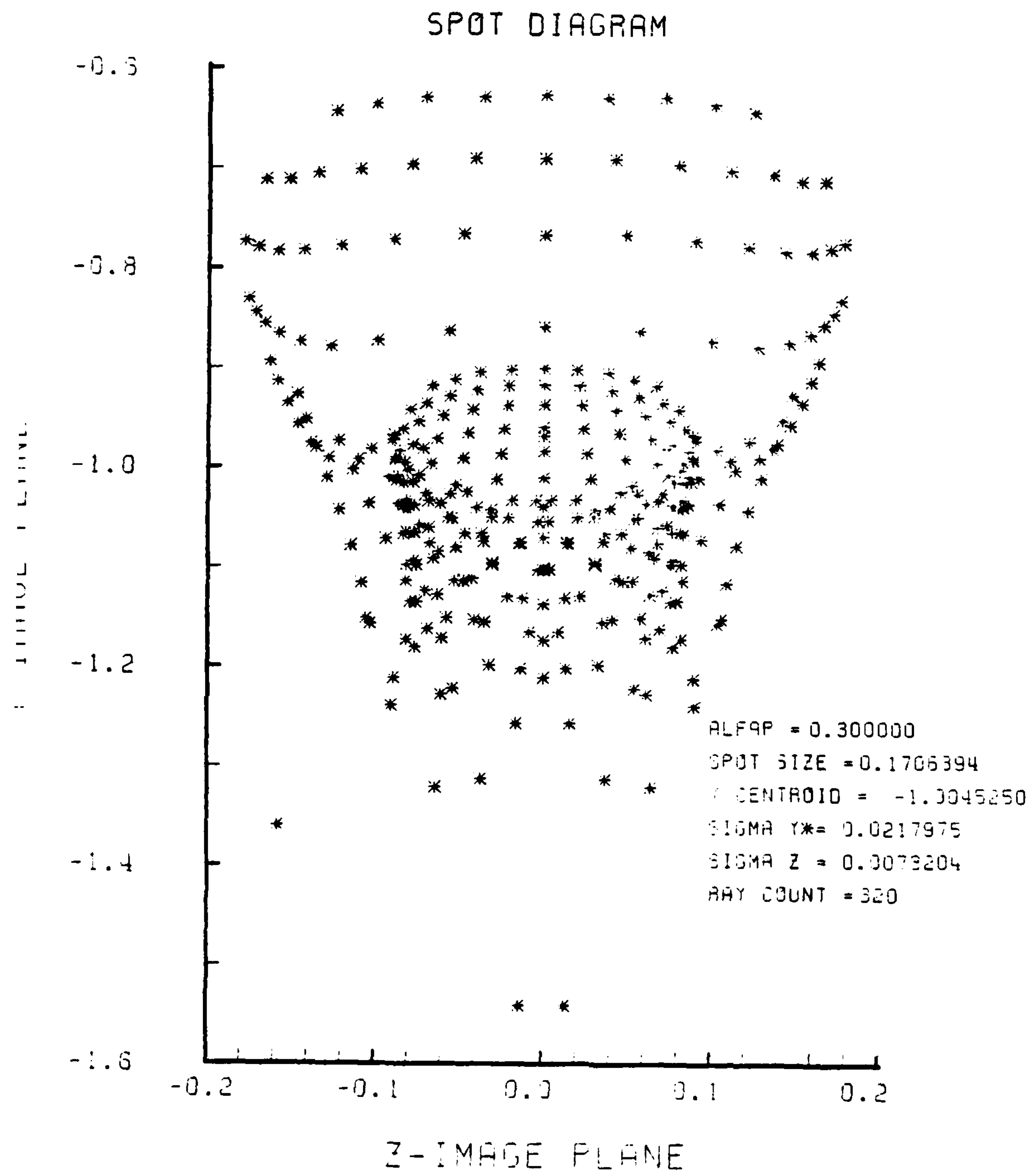

Figure F-27. Spot Diagram for Grid of Figure F-26

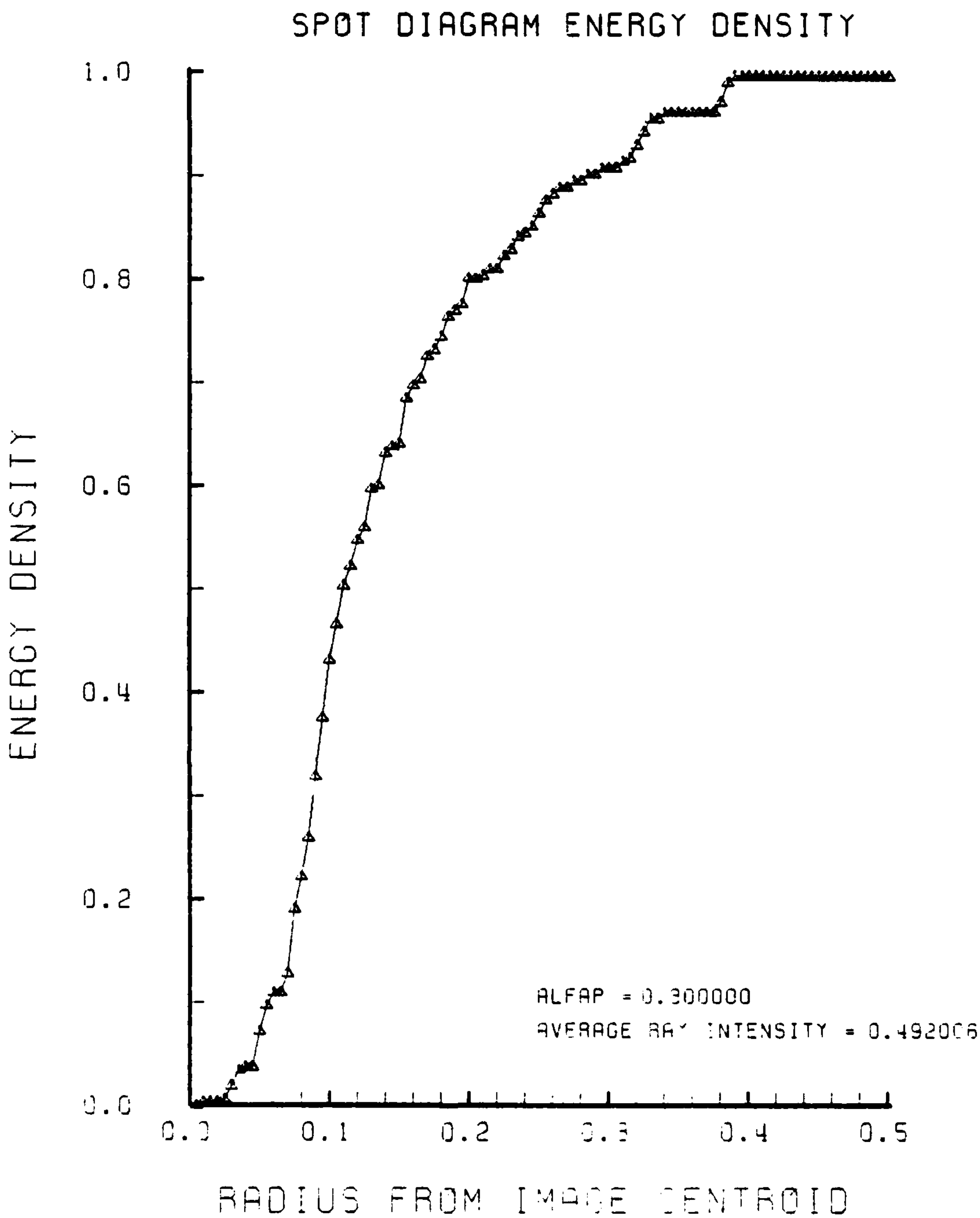

Figure F-28. Encircled Energy of Figure F-27

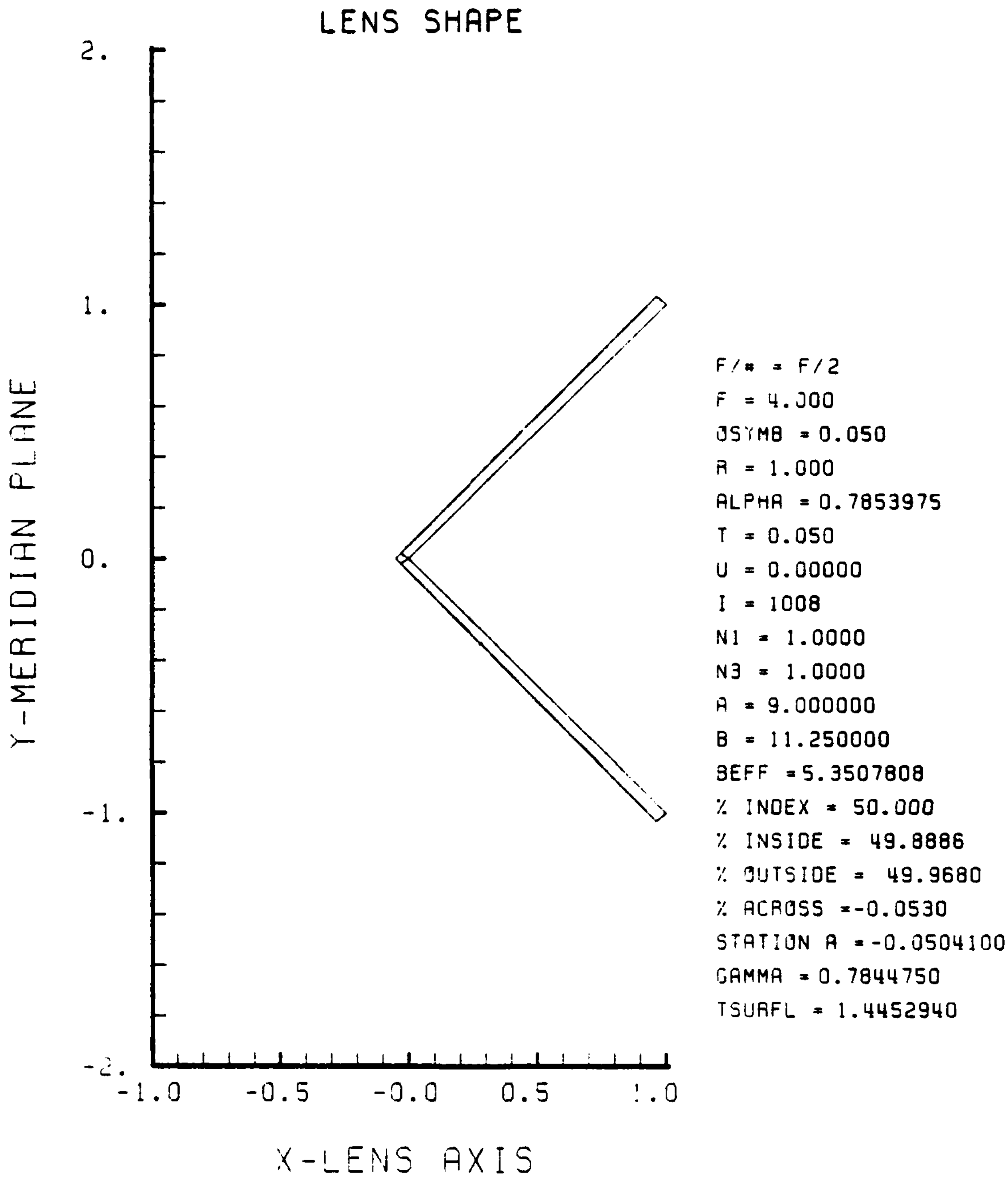

Figure F-29. GRIN Lens Shape at +50%, OB = 0.05, a = 9.00

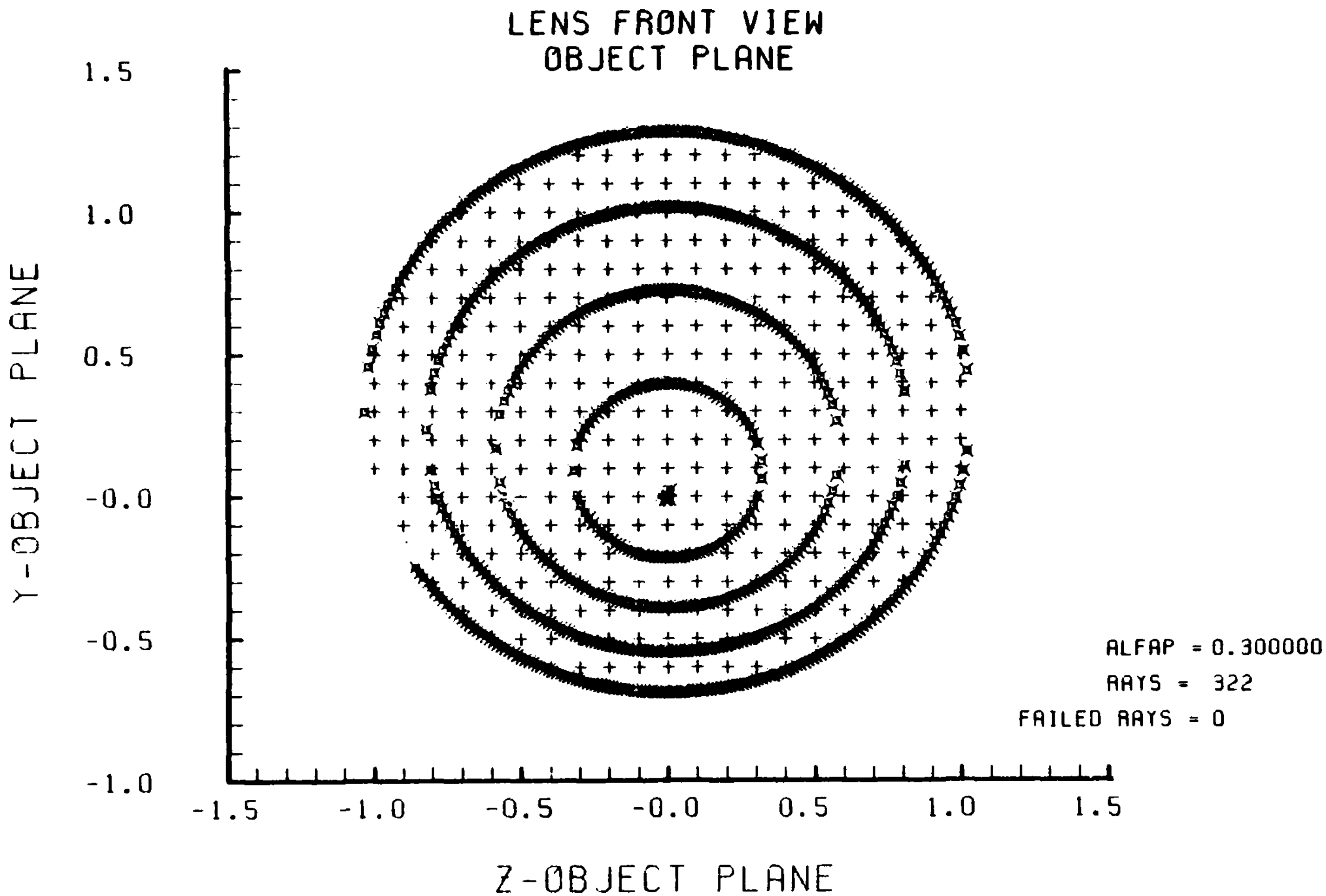

Figure F-30. Grid Plane at $\alpha_p = 0.3$ for Lens of Figure F-29

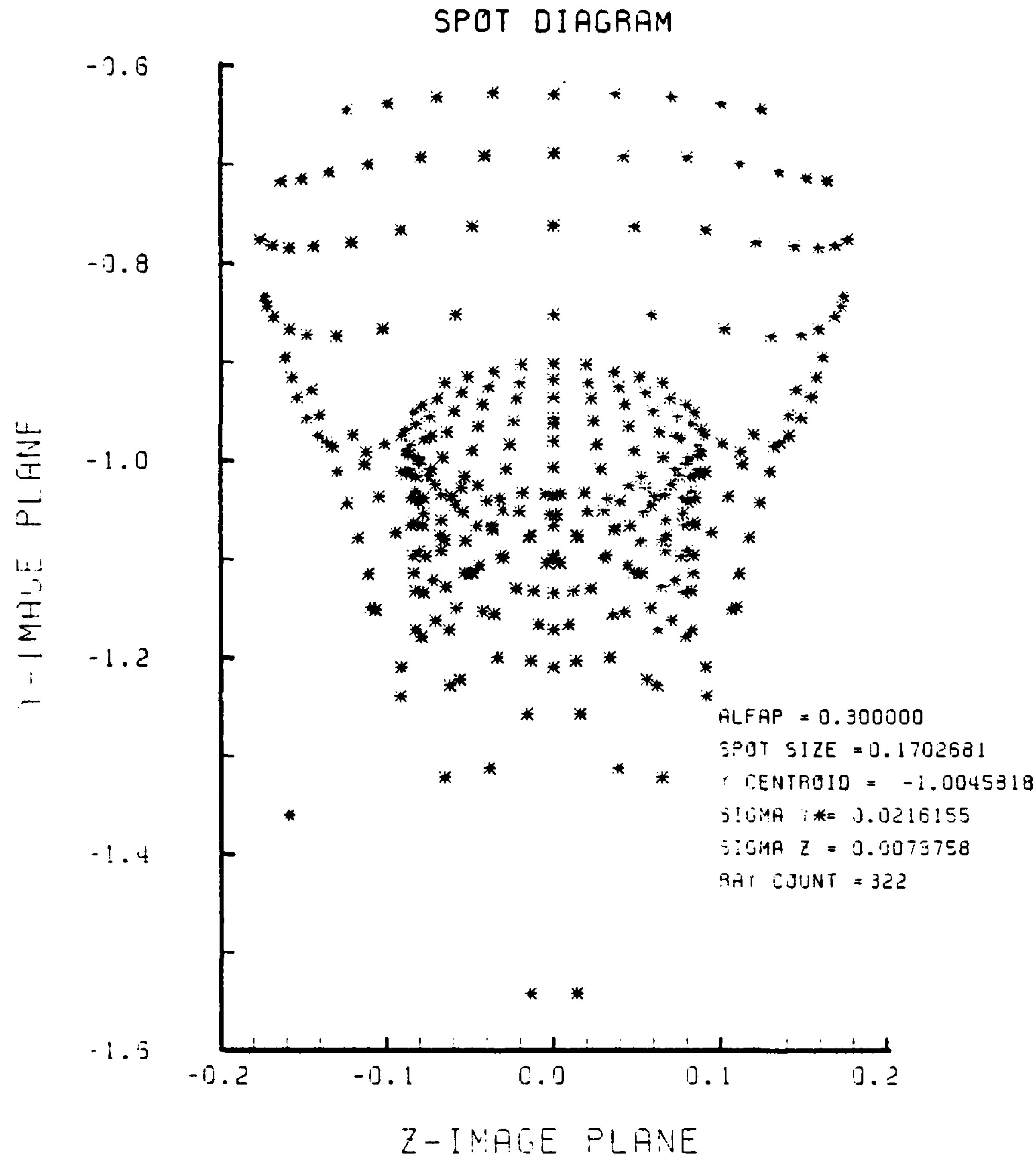

Figure F-31. Spot Diagram for Grid of Figure F-30

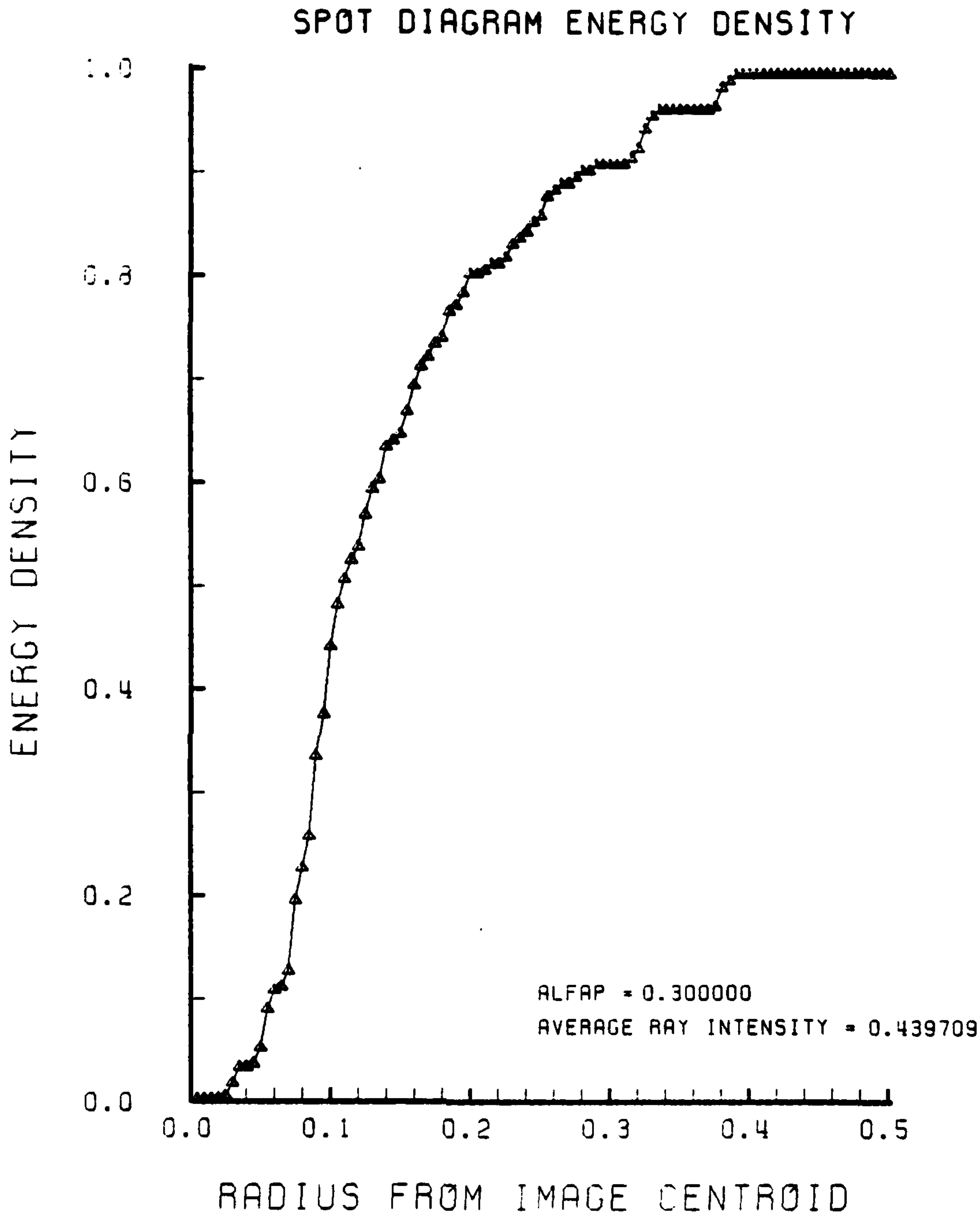

Figure F-32. Encircled Energy of Figure F-31

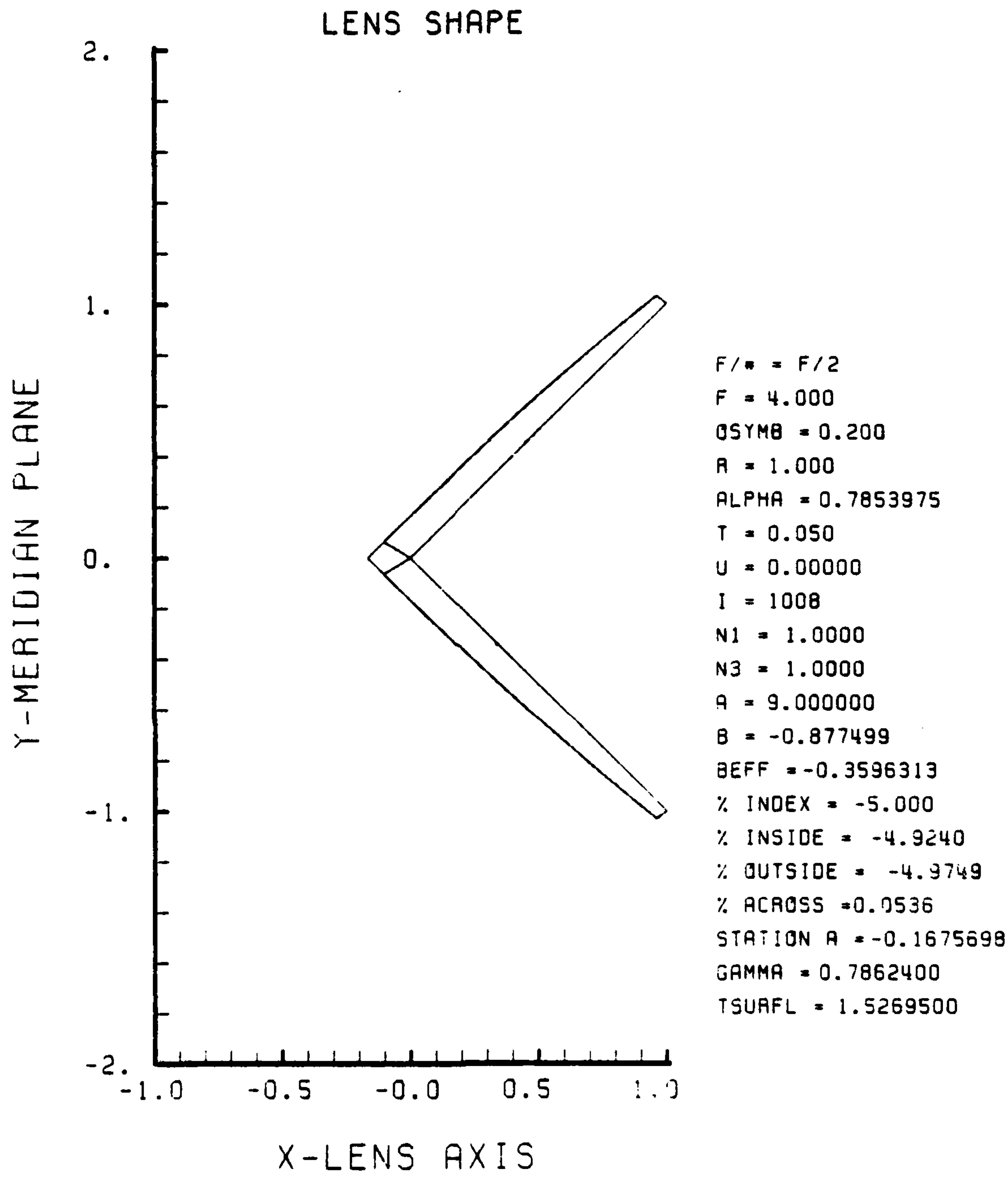

Figure F-33. GRIN Lens Shape at -5%, OB = 0.20, a = 9.00

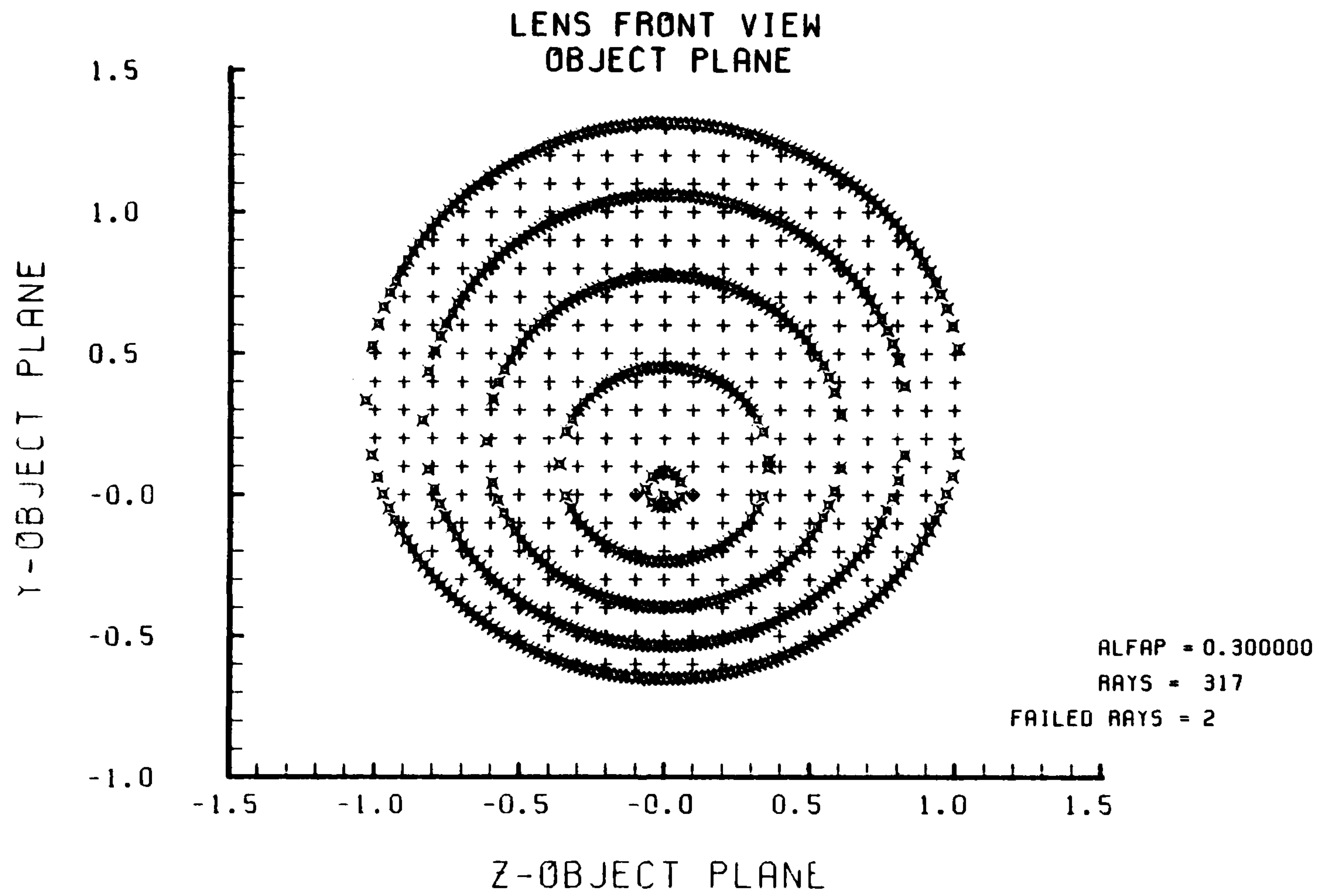

Figure F-34. Grid Plane at $\alpha_p = 0.3$ for Lens of Figure F-33

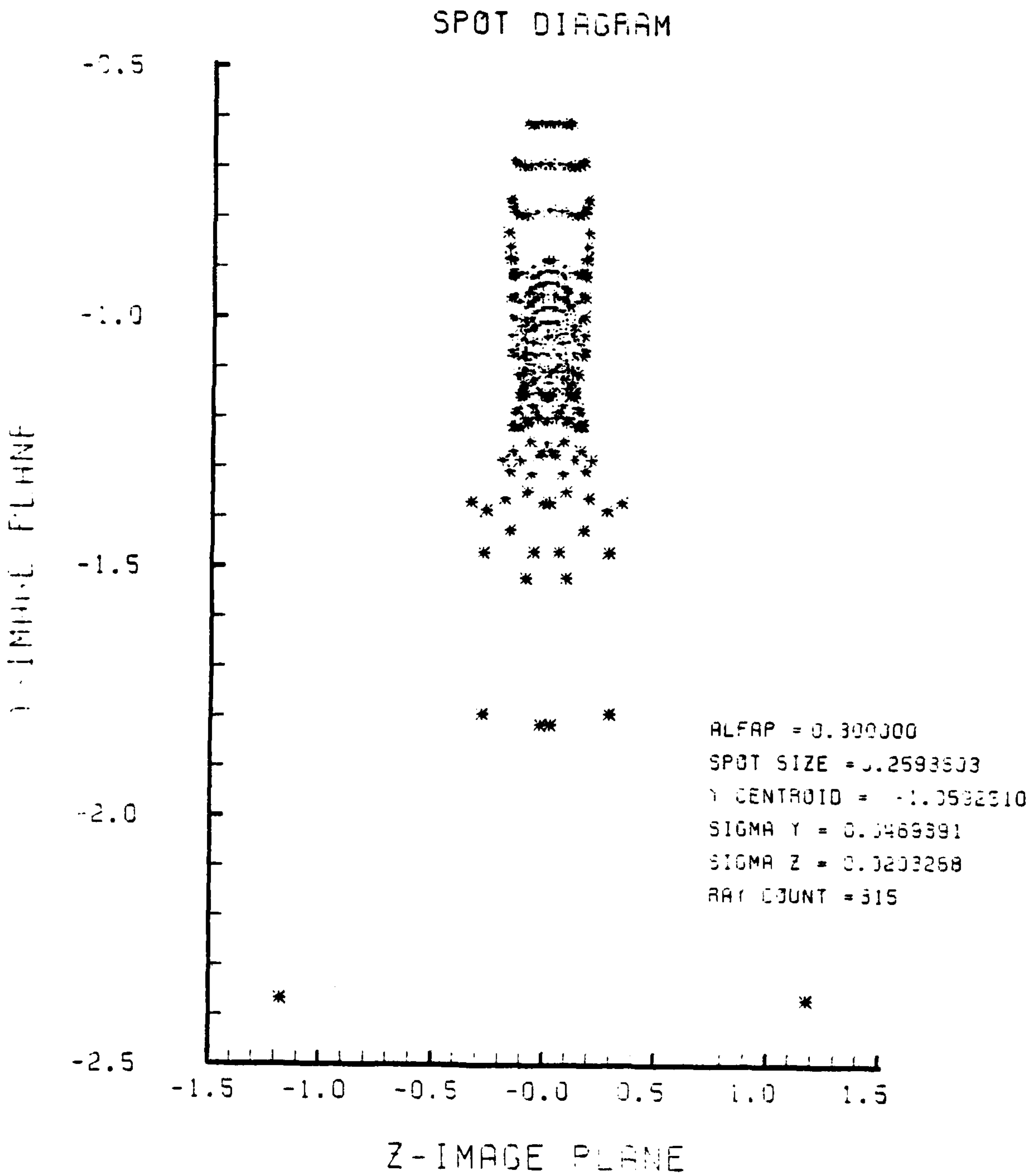

Figure F-35. Spot Diagram for Grid of Figure F-34

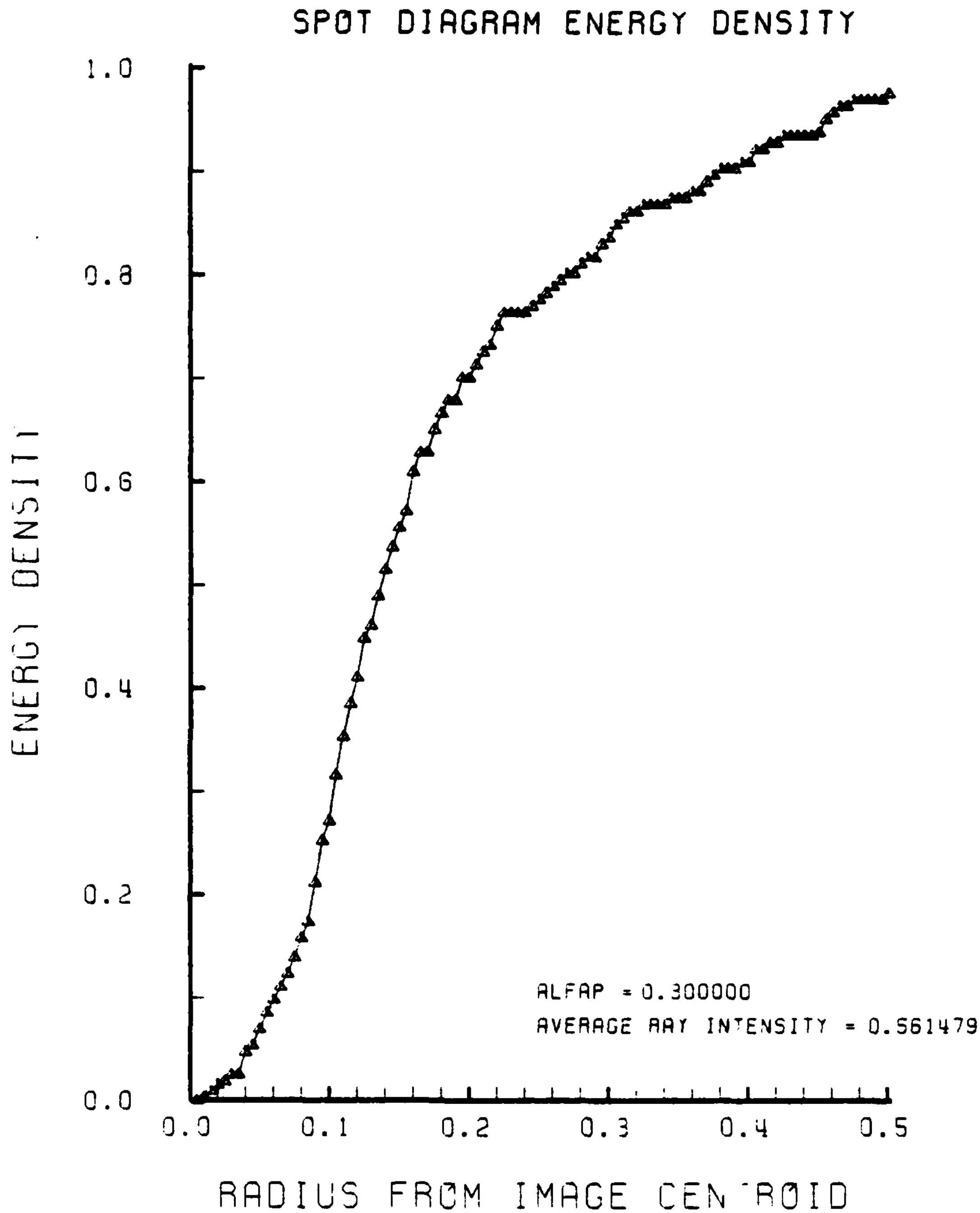

Figure F-36. Encircled Energy of Figure F-35

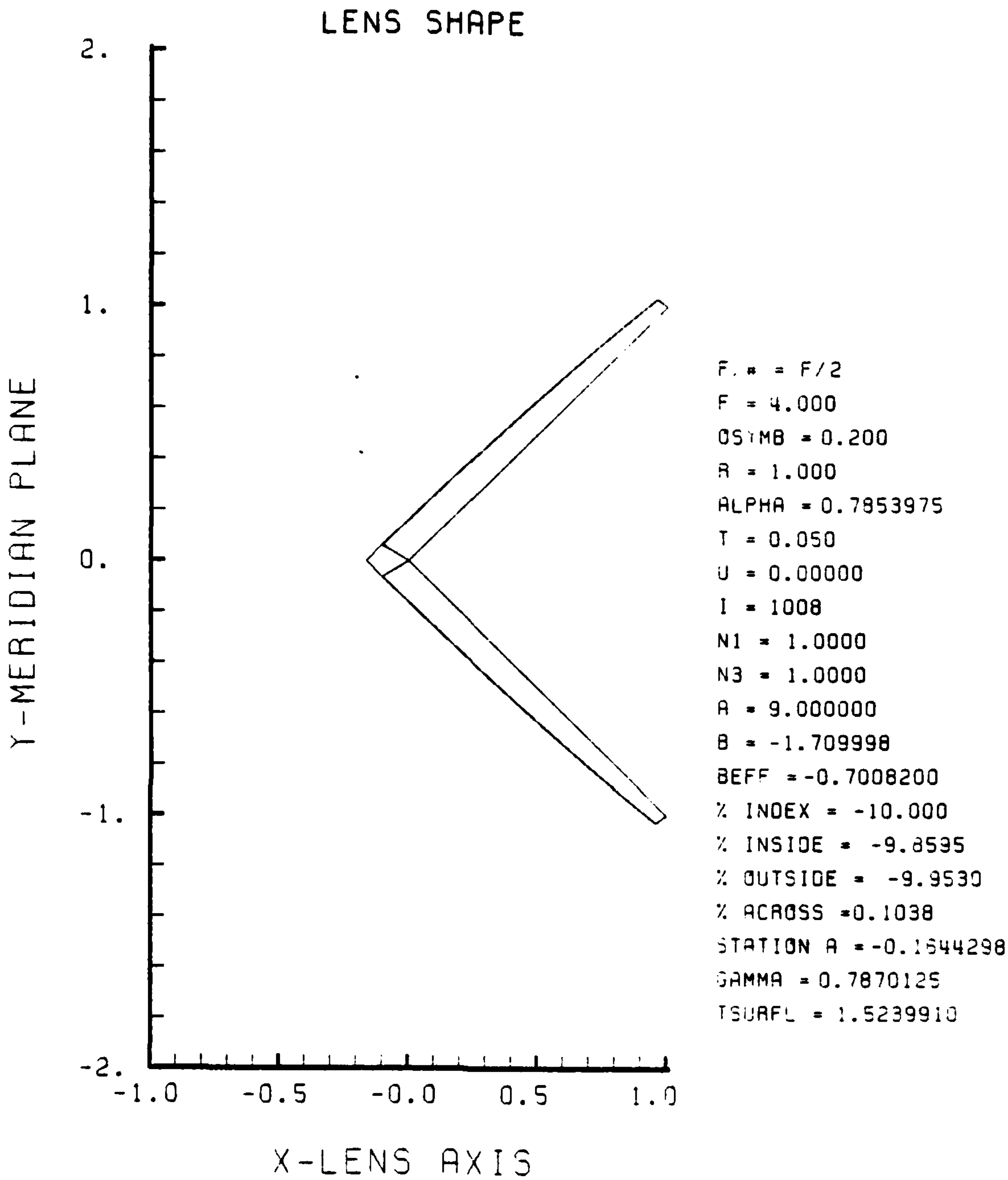

Figure F-37. GRIN Lens Shape at -10%, OB = 0.20, a = 9.00

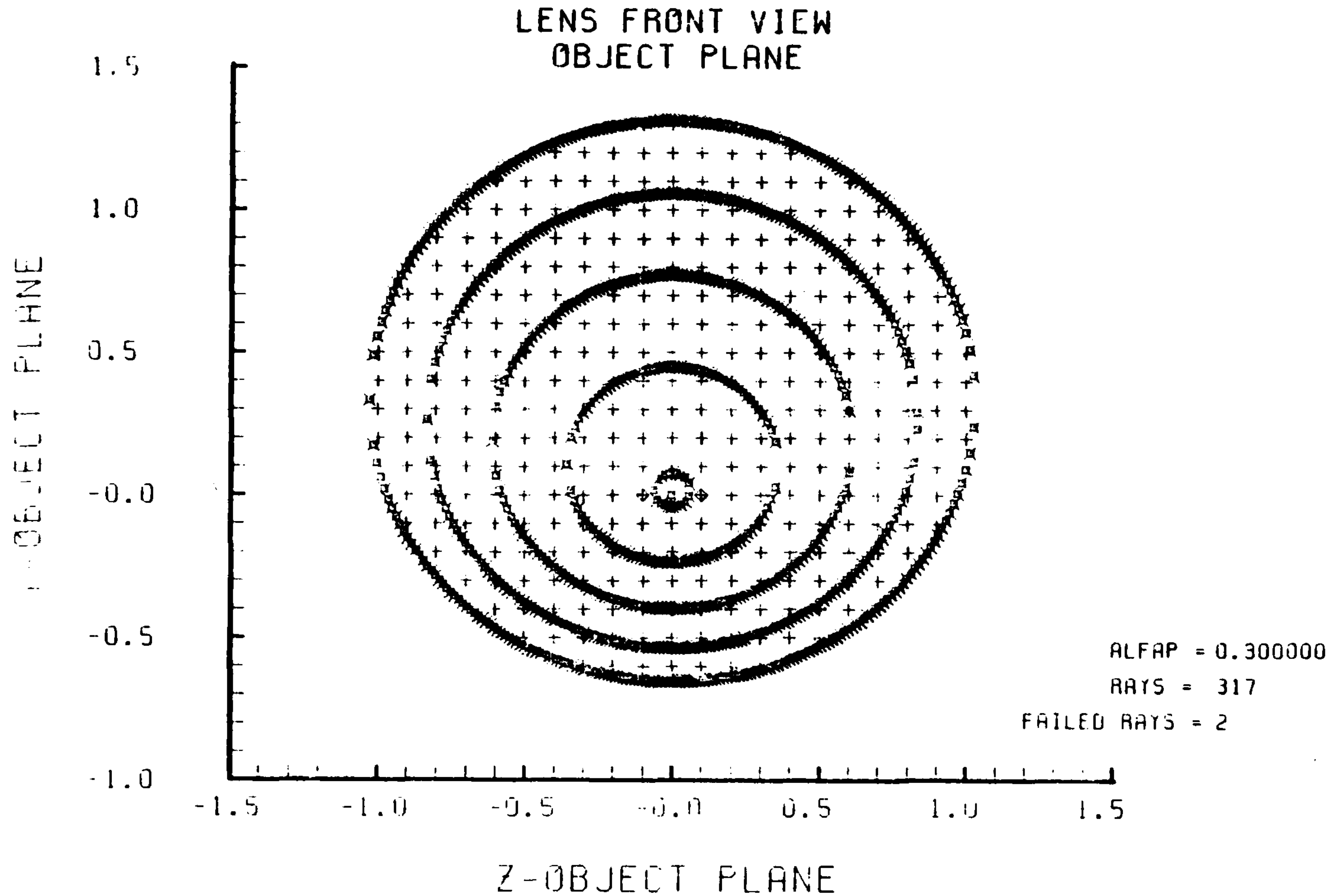

Figure F-38. Grid Plane at α_p = 0.3 for Lens of Figure F-37

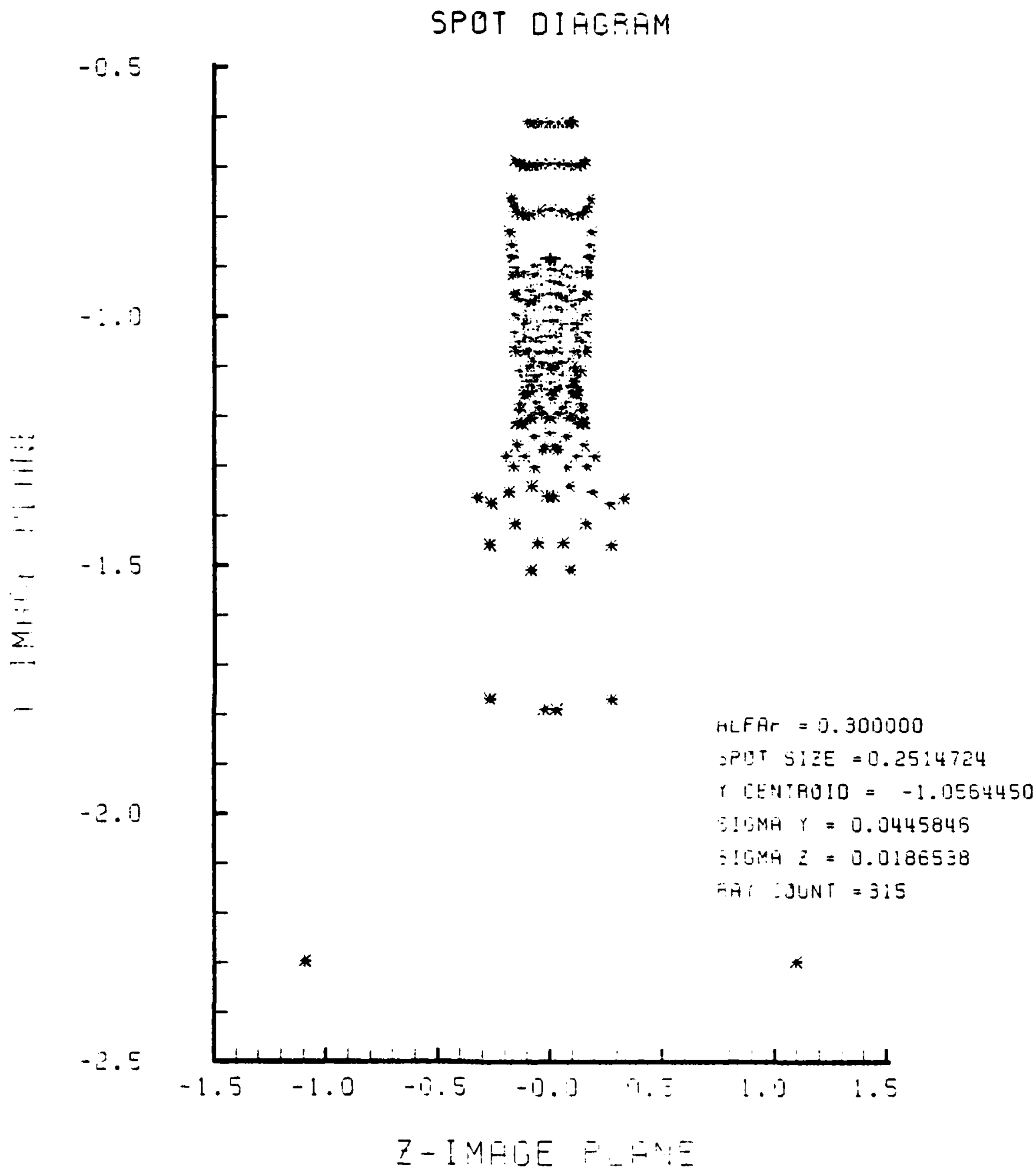

Figure F-39. Spot Diagram for Grid of Figure F-38

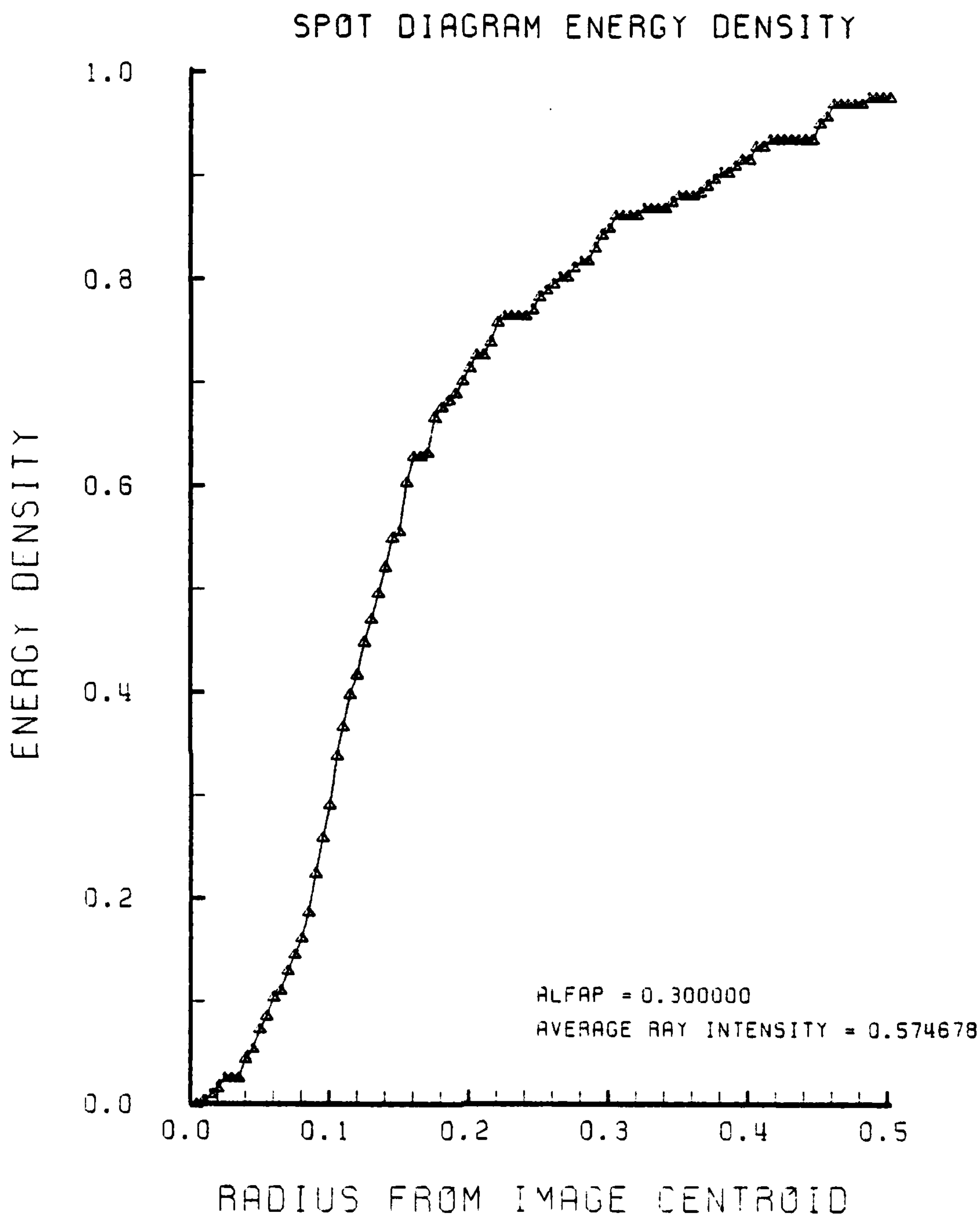

Figure F-40. Encircled Energy of Figure F-39

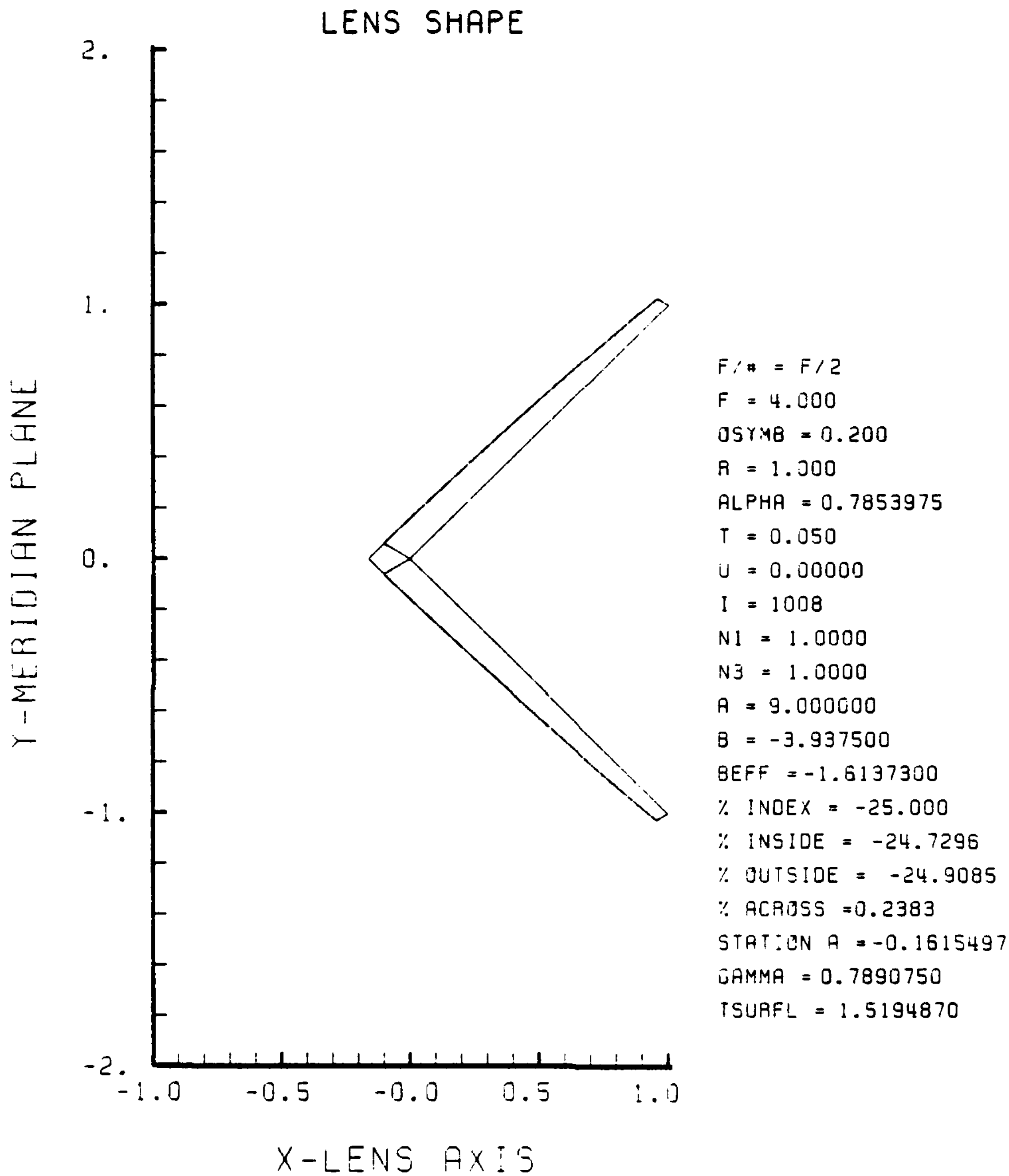

Figure F-41. GRIN Lens Shape at -25%, OB = 0.20, a = 9.00

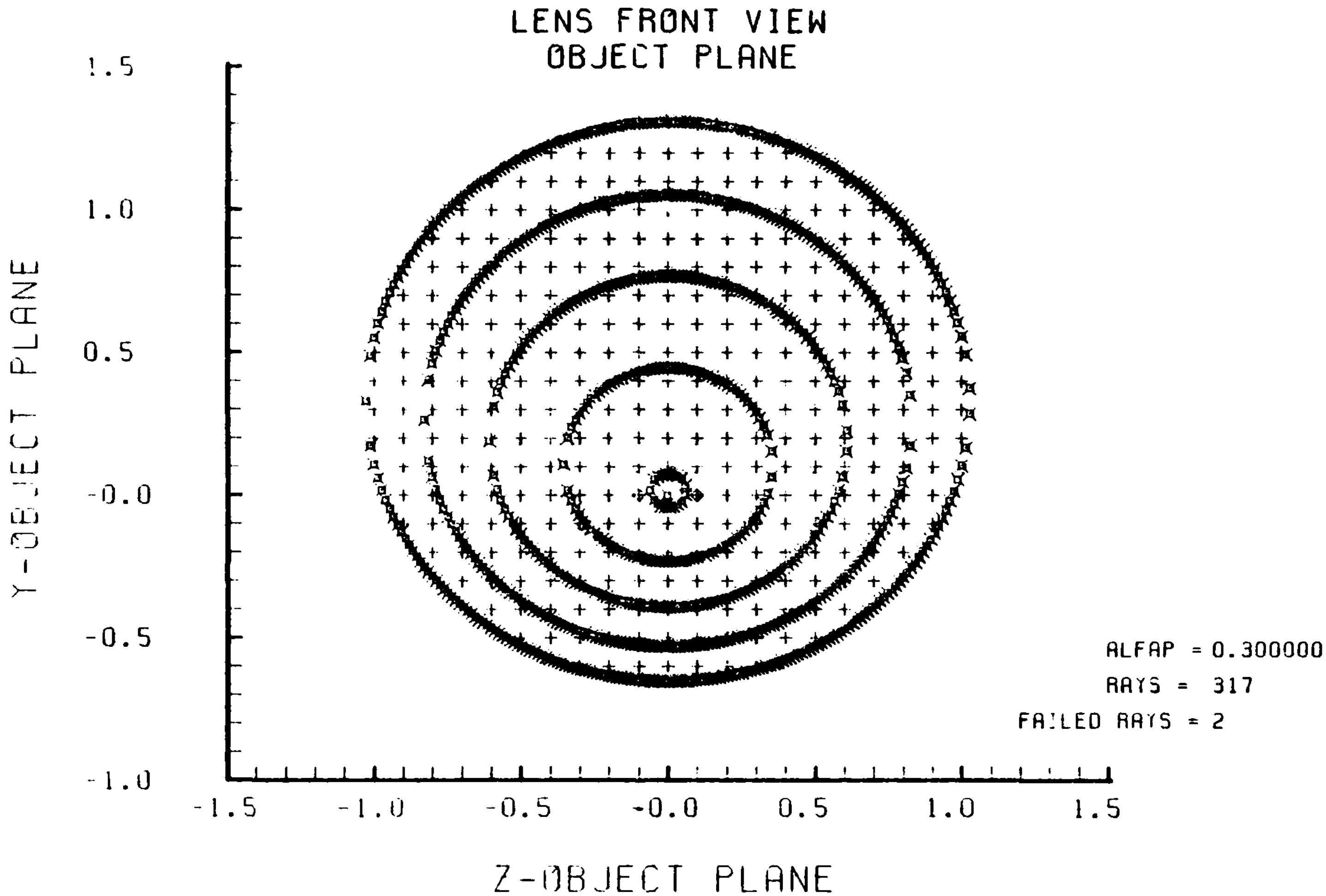

Figure F-42. Grid Plane at $\alpha_p = 0.3$ for Lens of Figure F-41

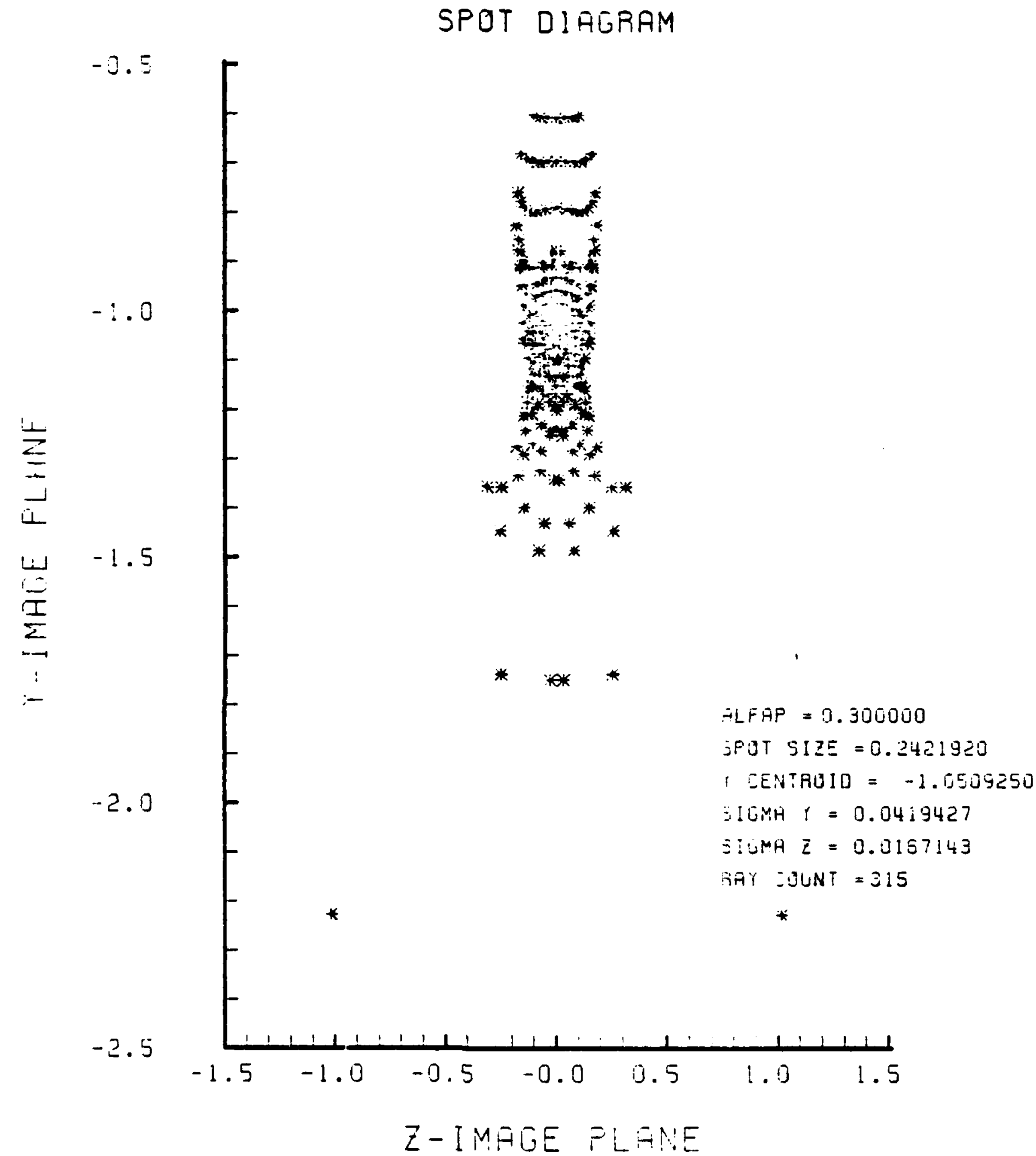

Figure F-43. Spot Diagram for Grid of Figure F-42

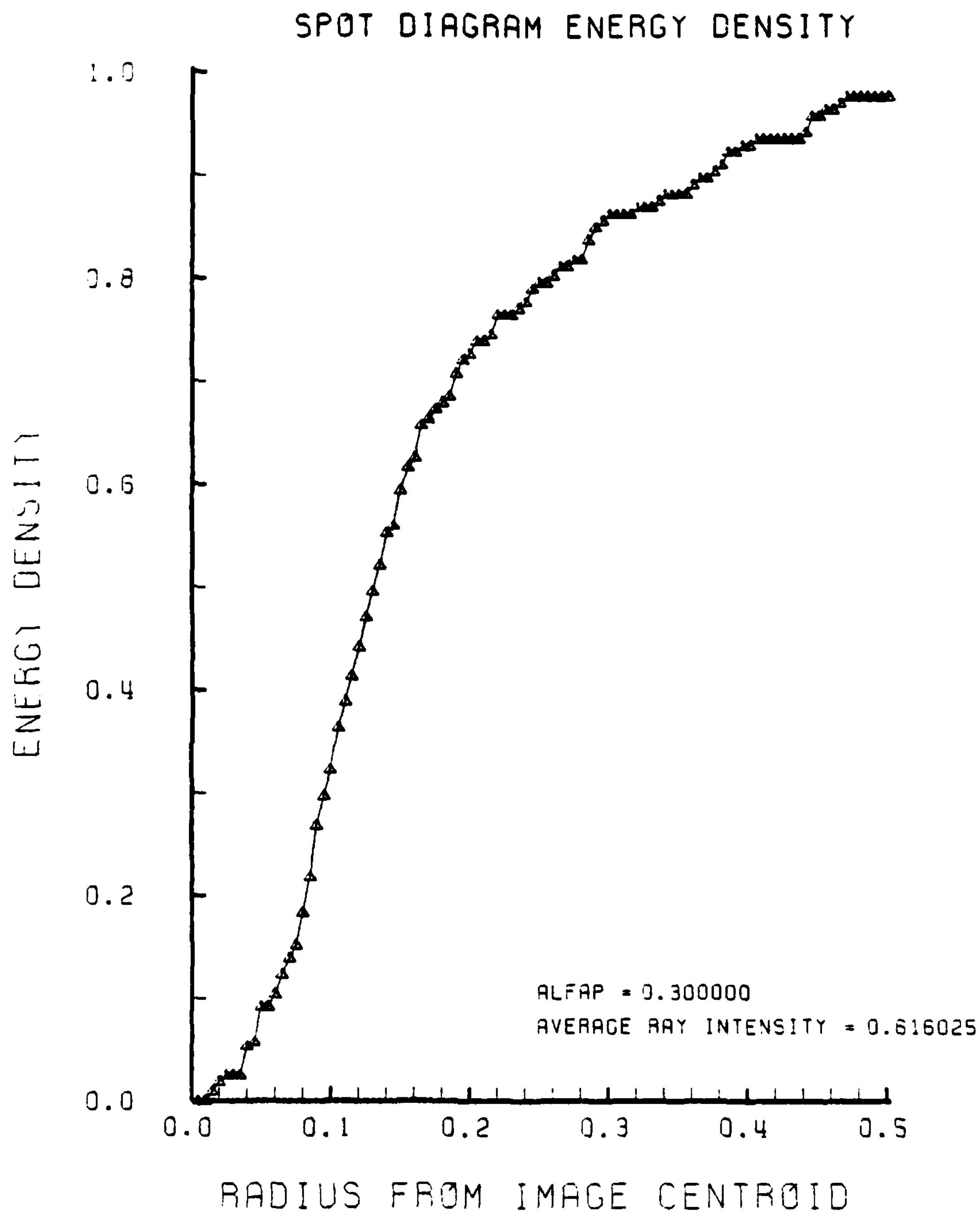

Figure F-44. Encircled Energy of Figure F-43

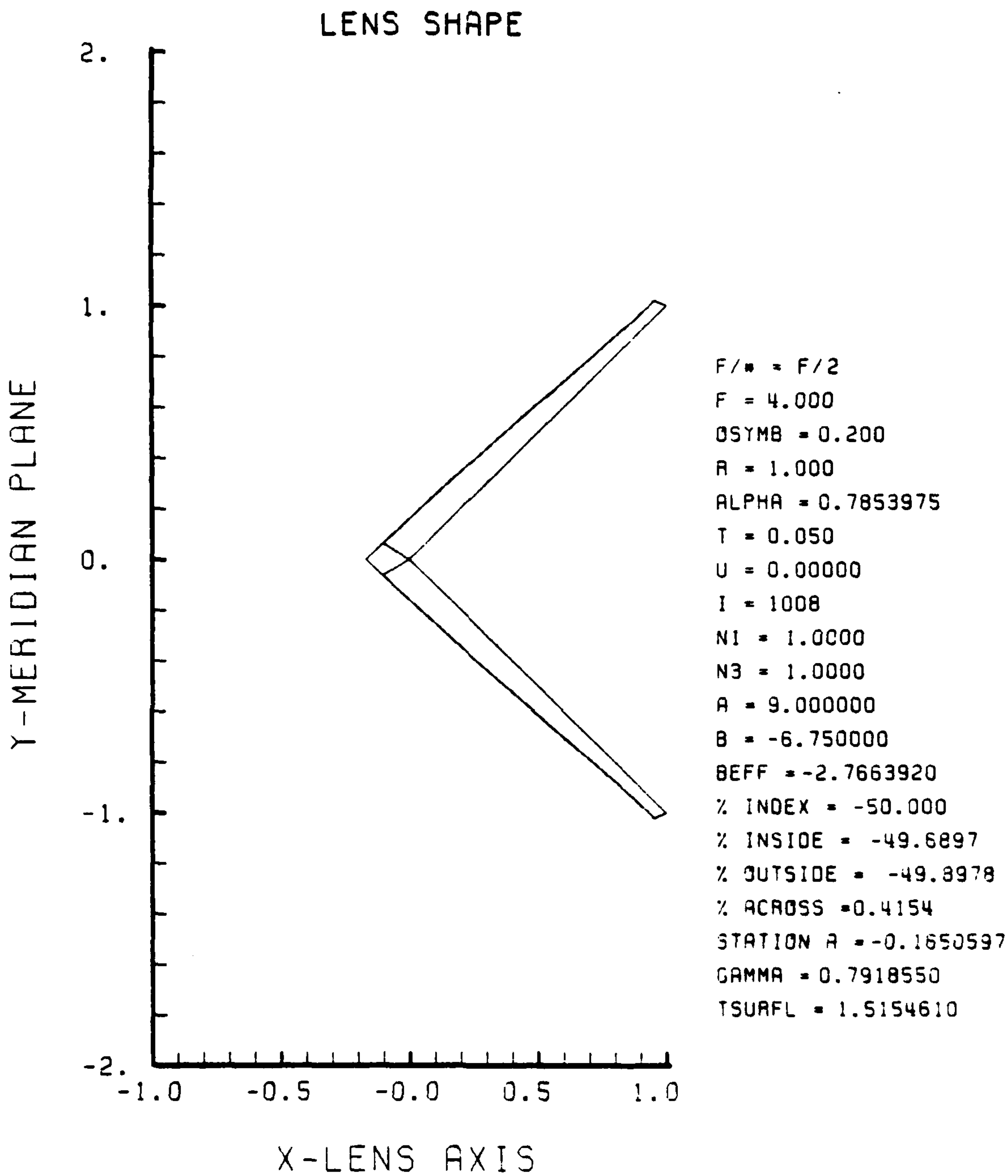

Figure F-45. GRIN Lens Shape for -50%, OB = 0.20, a = 9.00

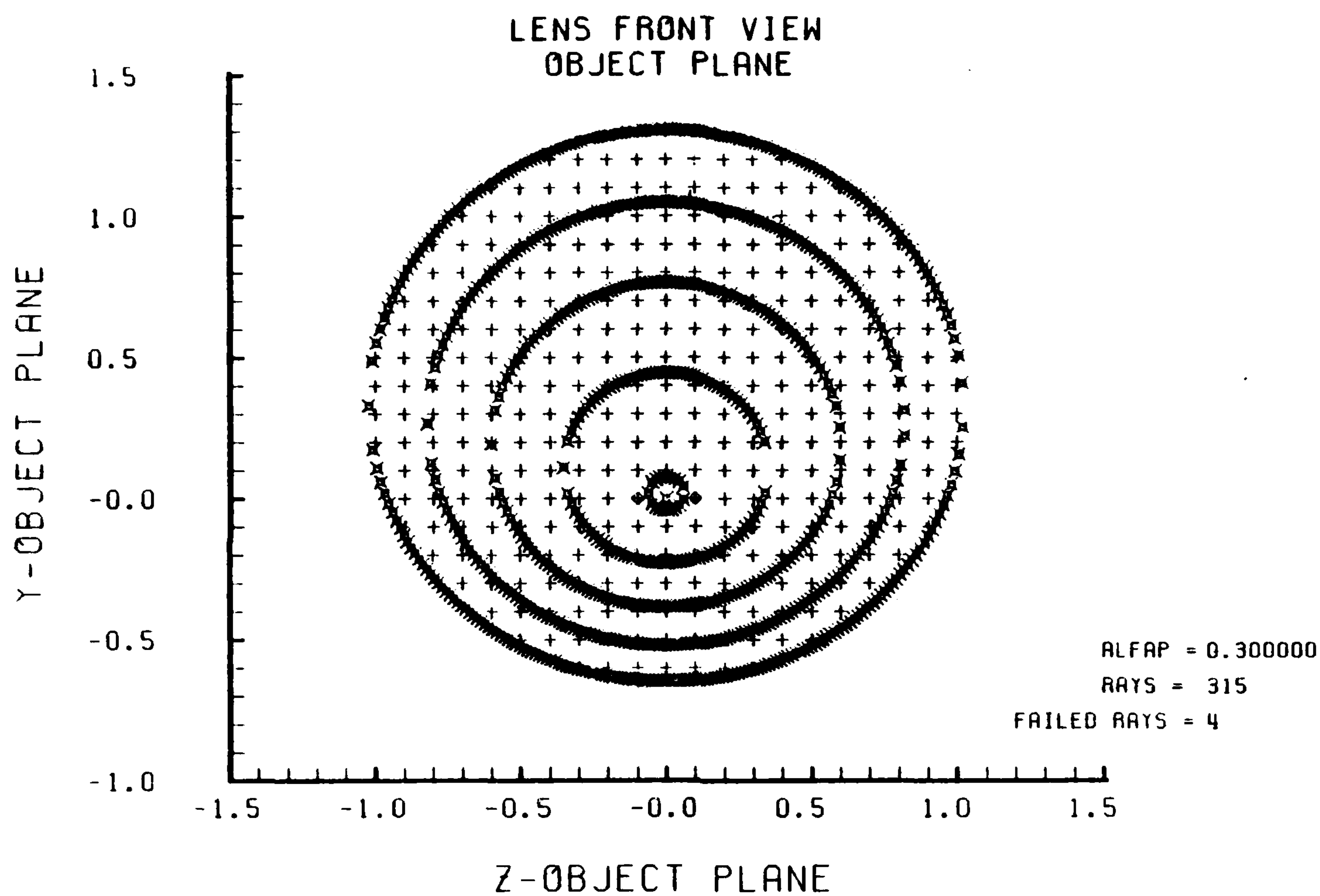

Figure F-46. Grid Plane at α_p = 0.3 for Lens of Figure F-45

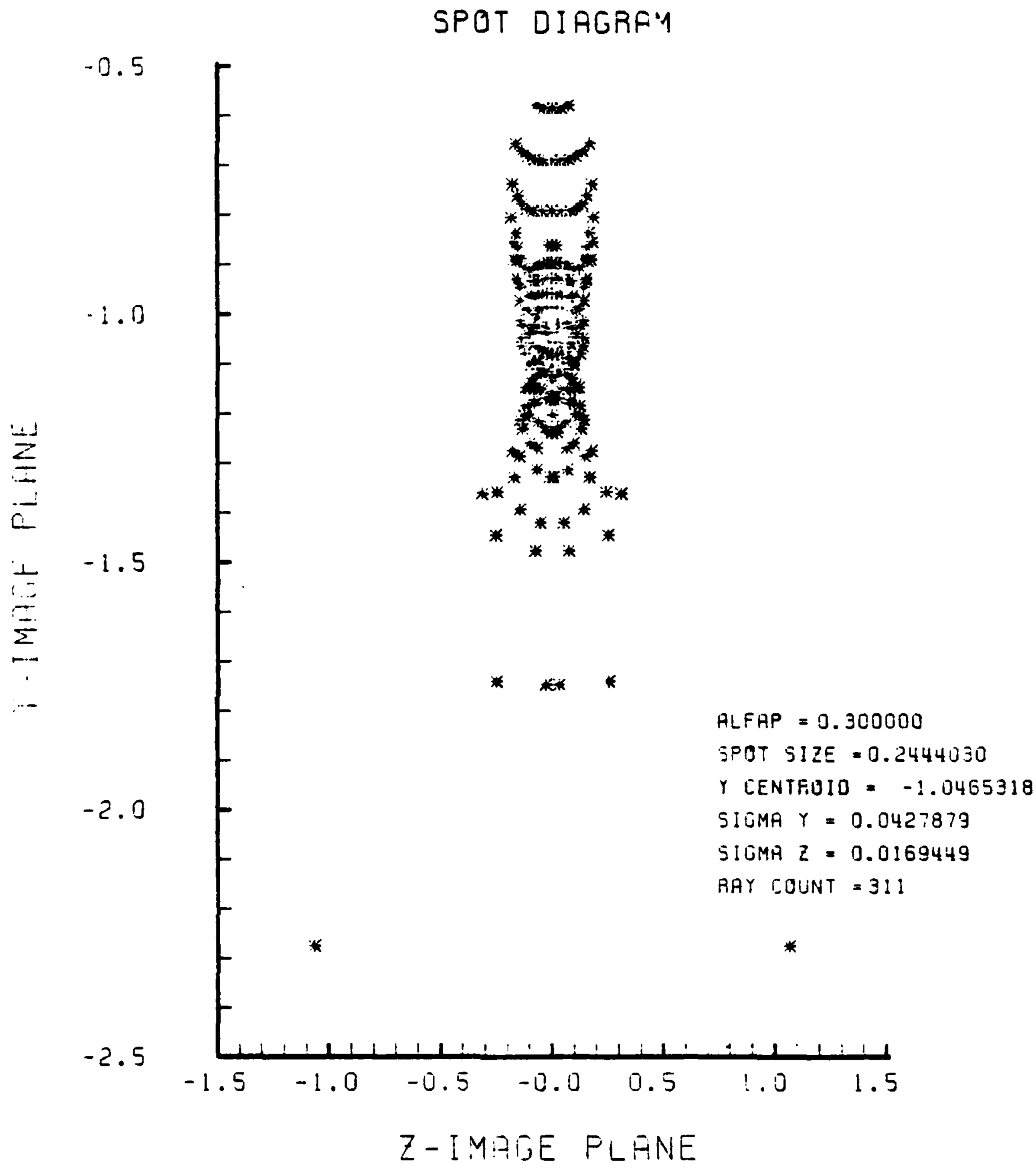

Figure F-47. Spot Diagram for Grid of Figure F-46

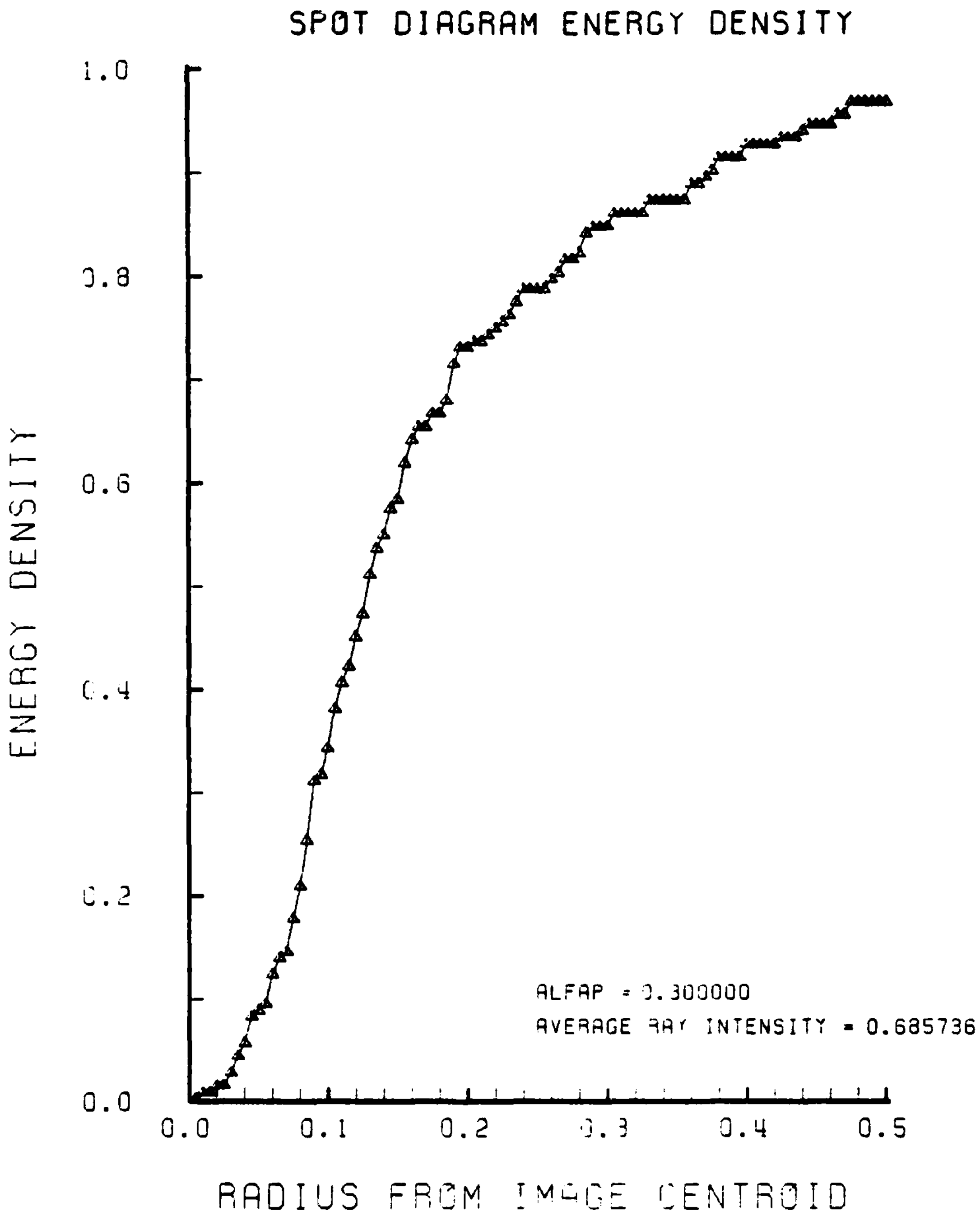

Figure F-48. Encircled Energy of Figure F-47

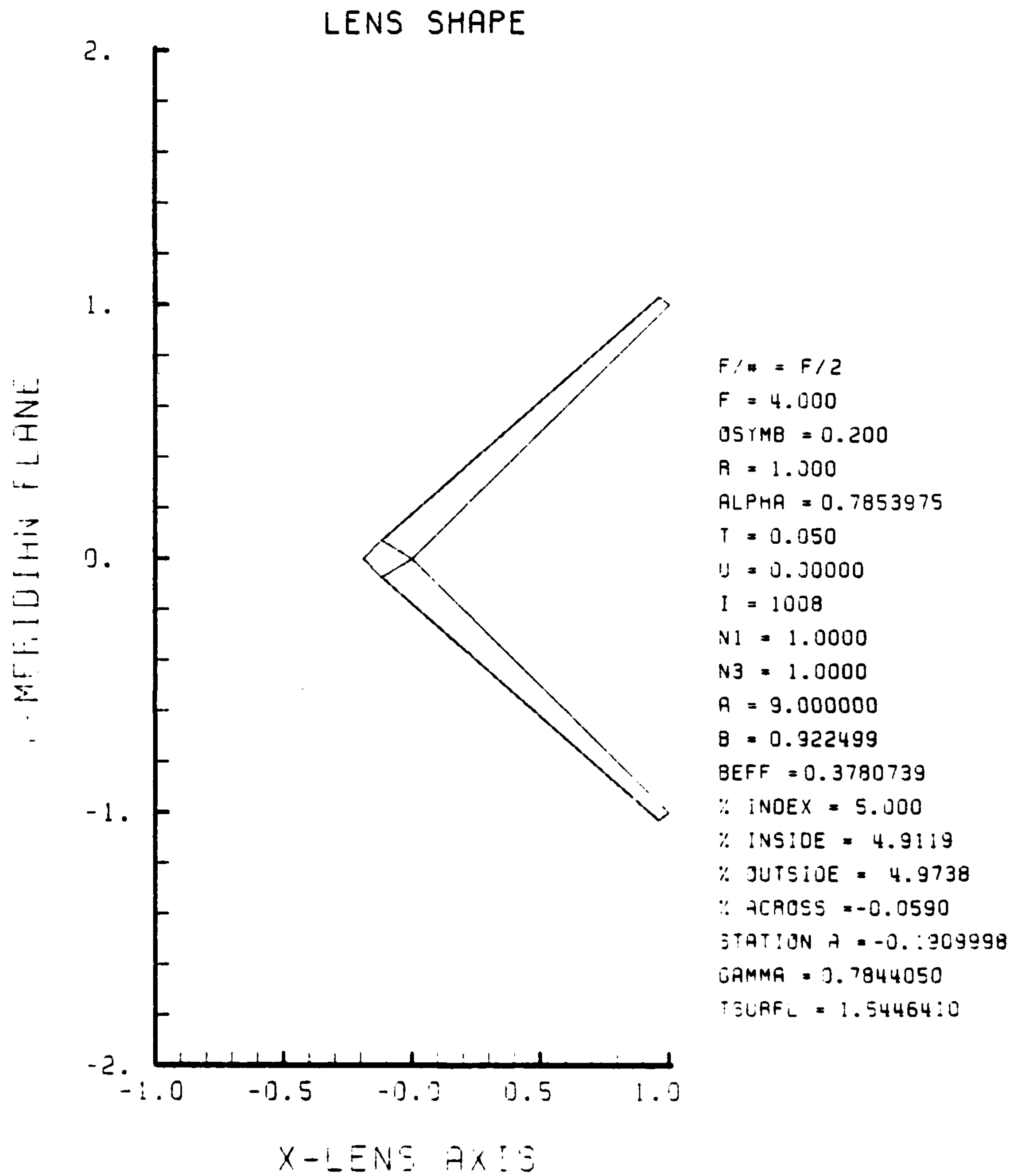

Figure F-49. GRIN Lens Shape for +5%, OB = 0.20, a = 9.00

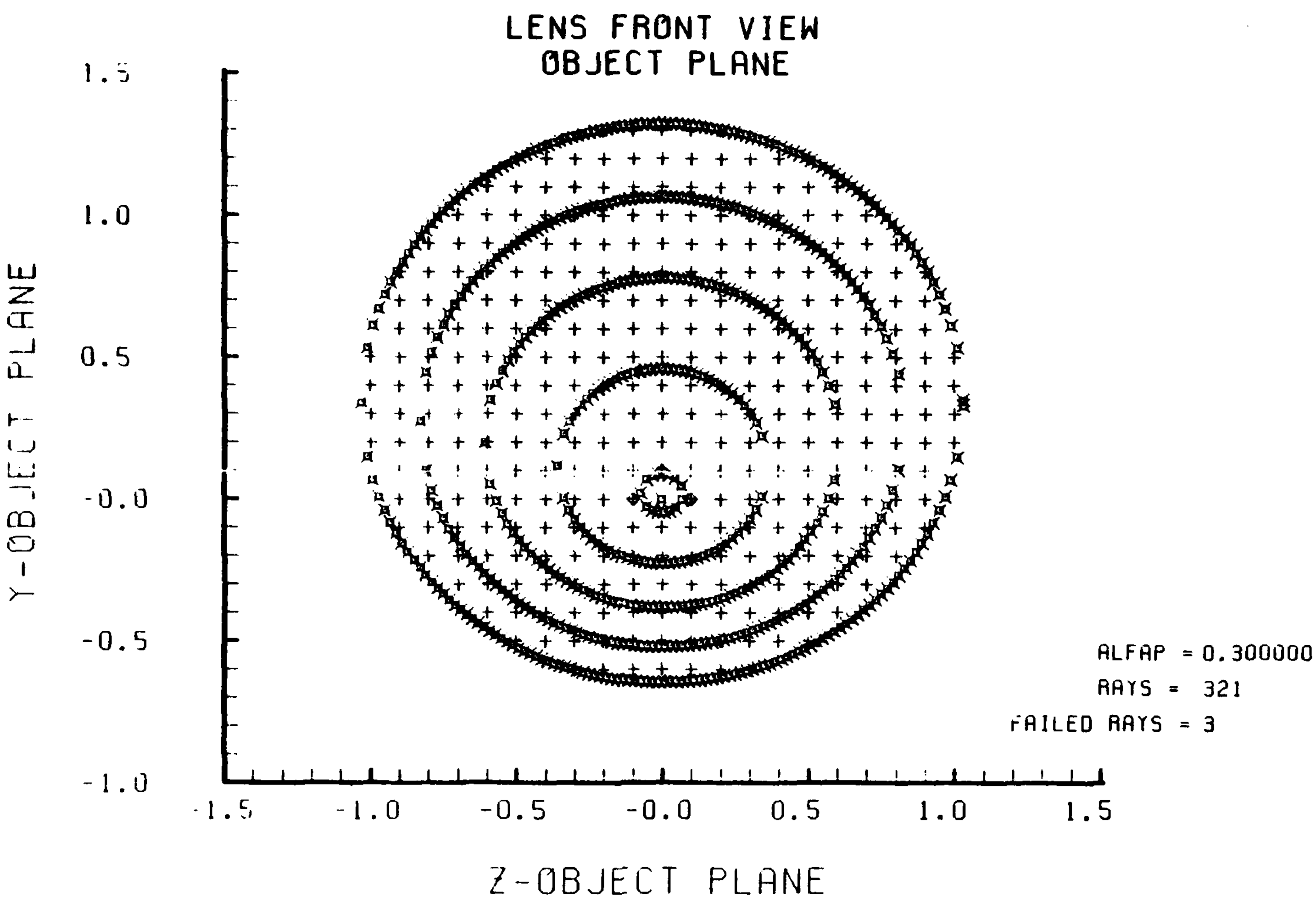

Figure F-50. Grid Plane at $\alpha_p = 0.3$ for Lens of Figure F-49

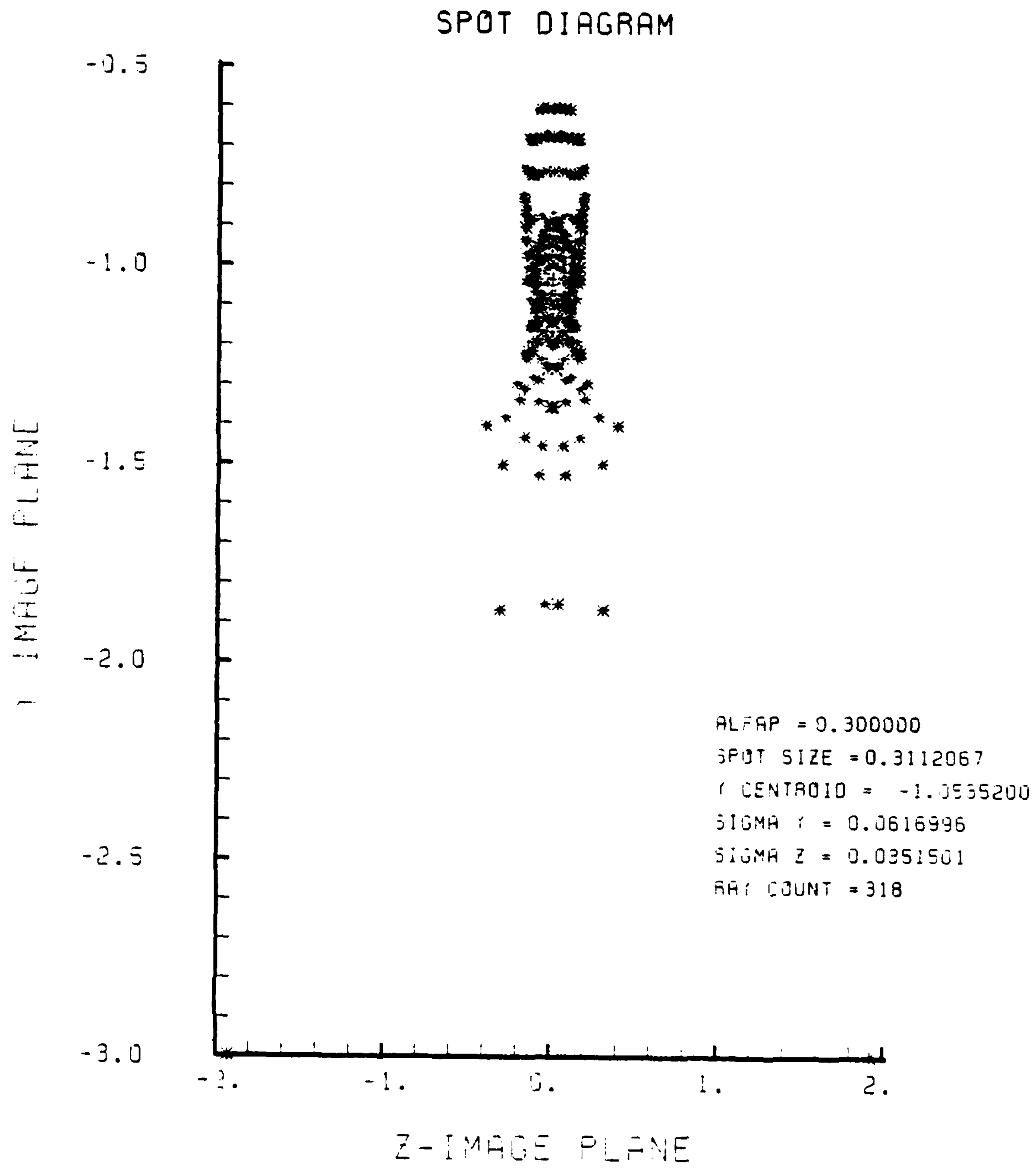

Figure F-51. Spot Diagram for Grid of Figure F-50

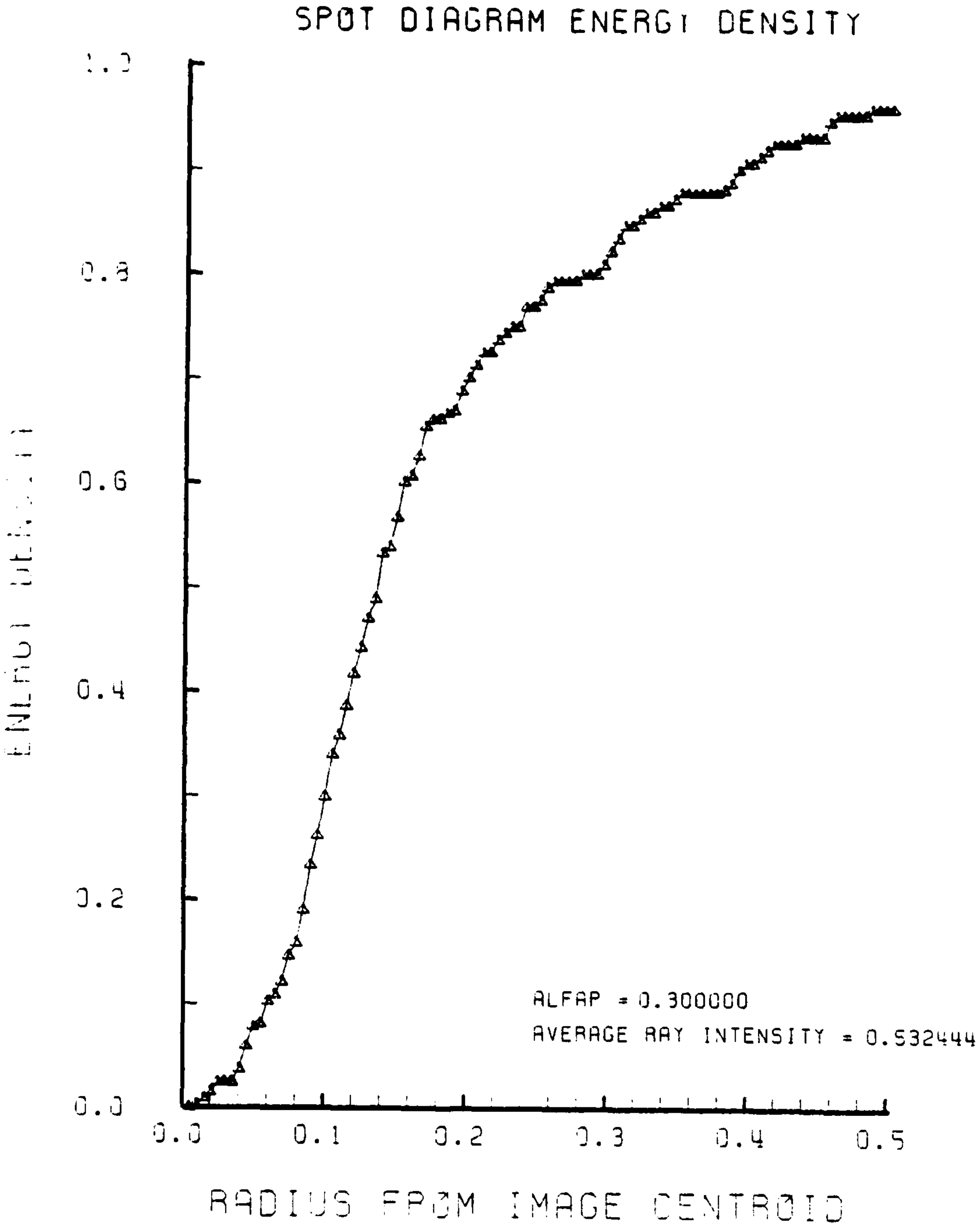

Figure F-52. Encircled Energy of Figure F-51

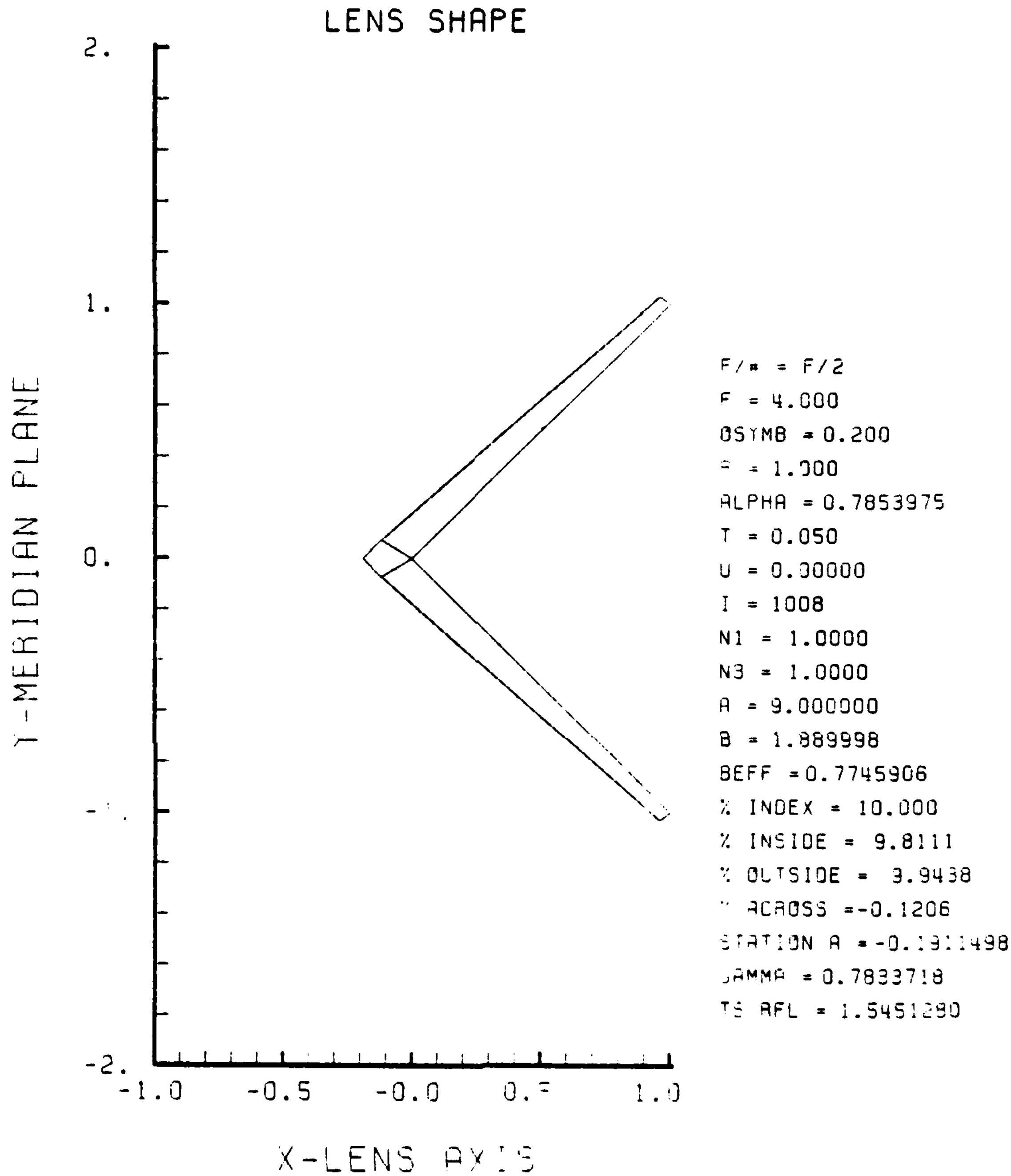

Figure F-53. GRIN Lens Shape at +10%, OB = 0.20, a = 9.00

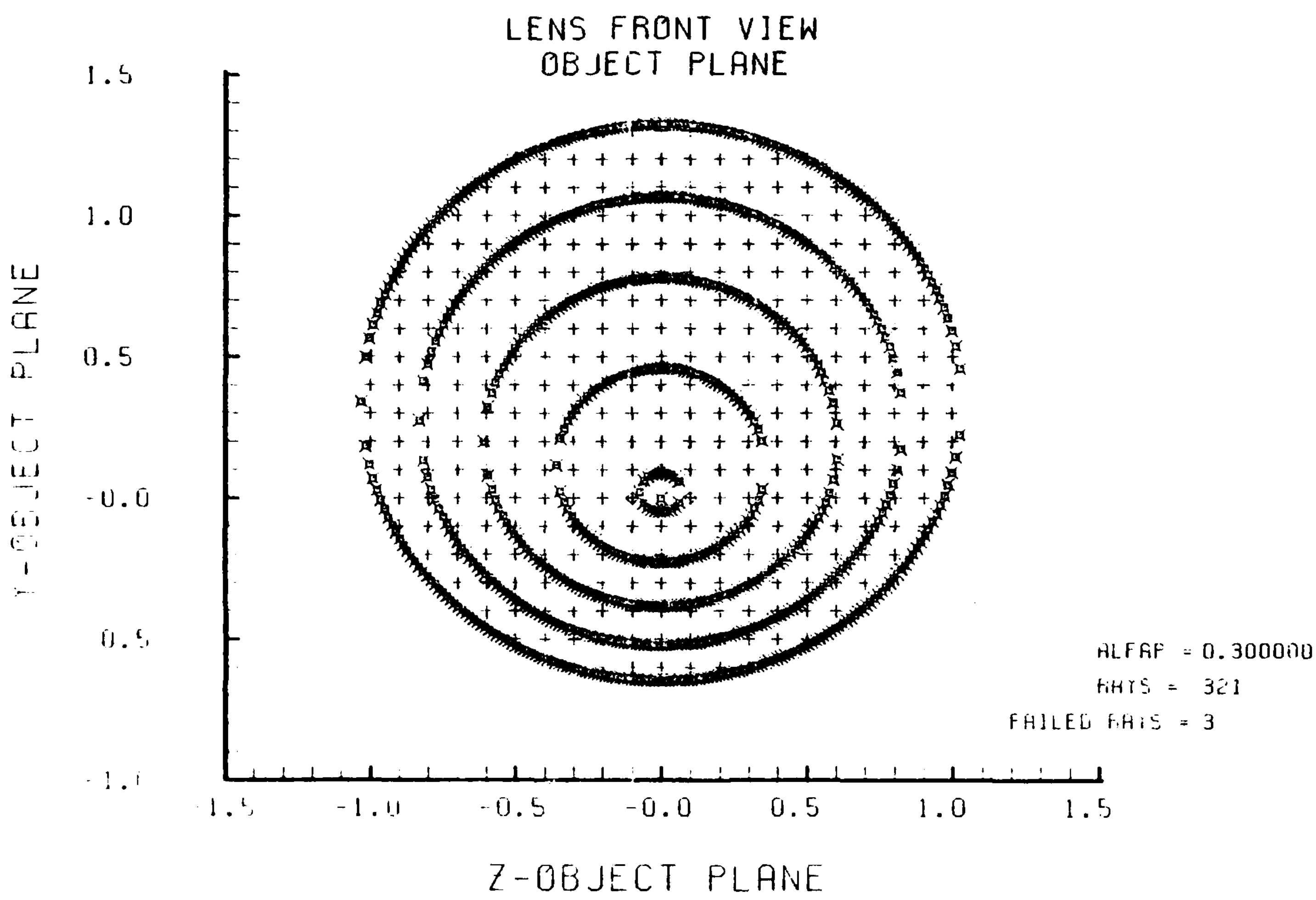

Figure F-54. Grid Plane at $\alpha_p = 0.3$ for Lens of Figure F-53

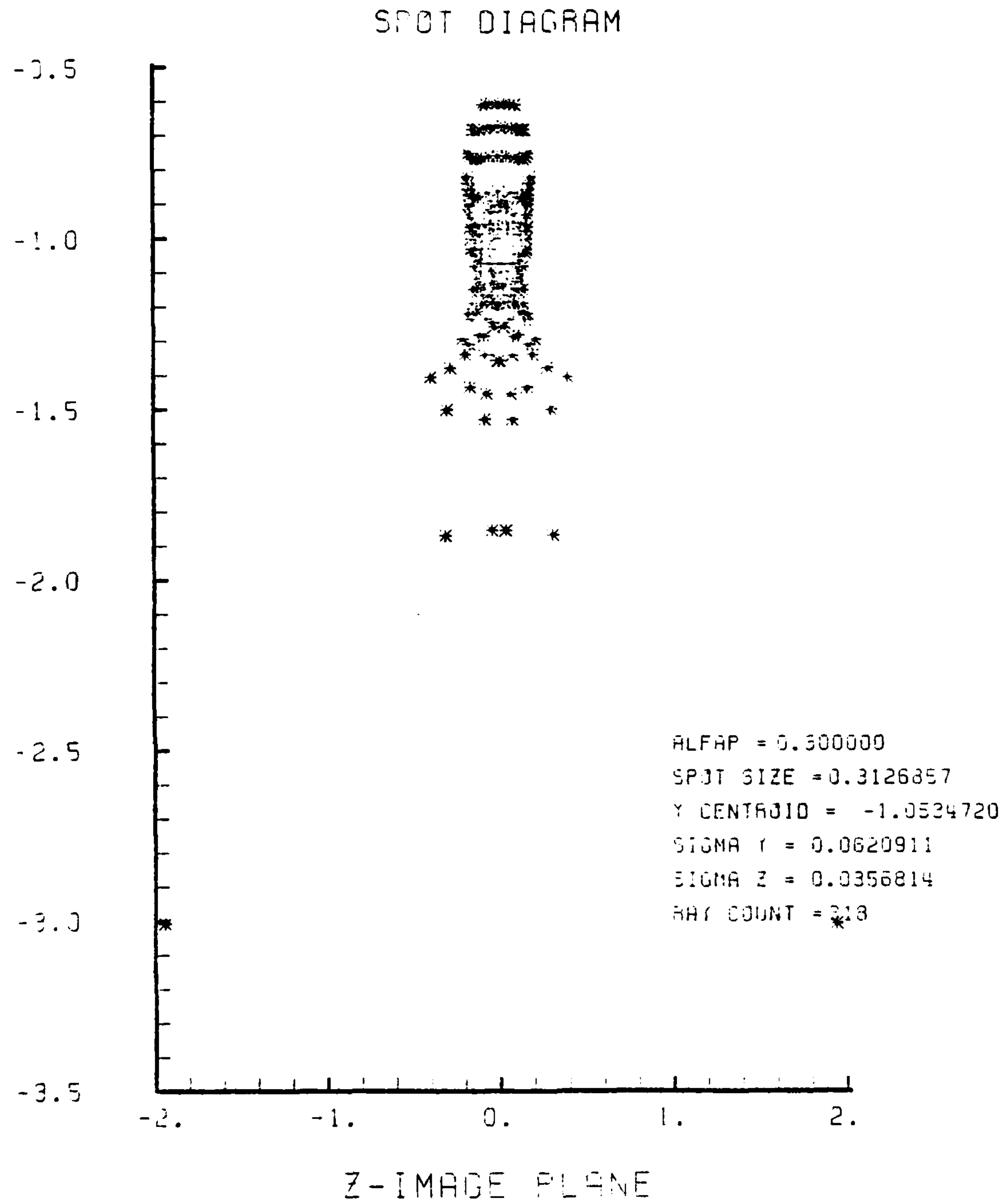

Figure F-55. Spot Diagram for Grid of Figure F-54

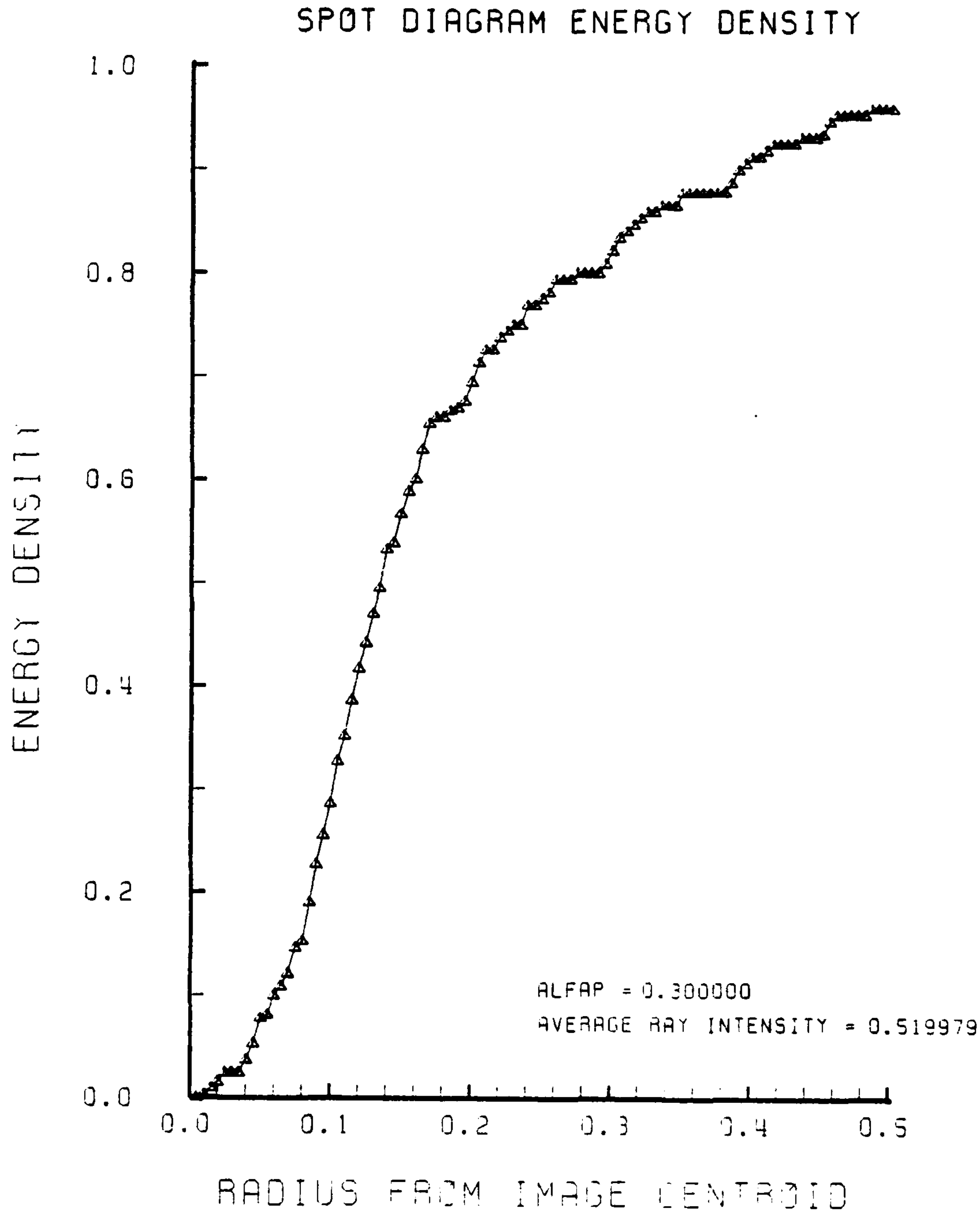

Figure F-56. Encircled Energy of Figure F-55

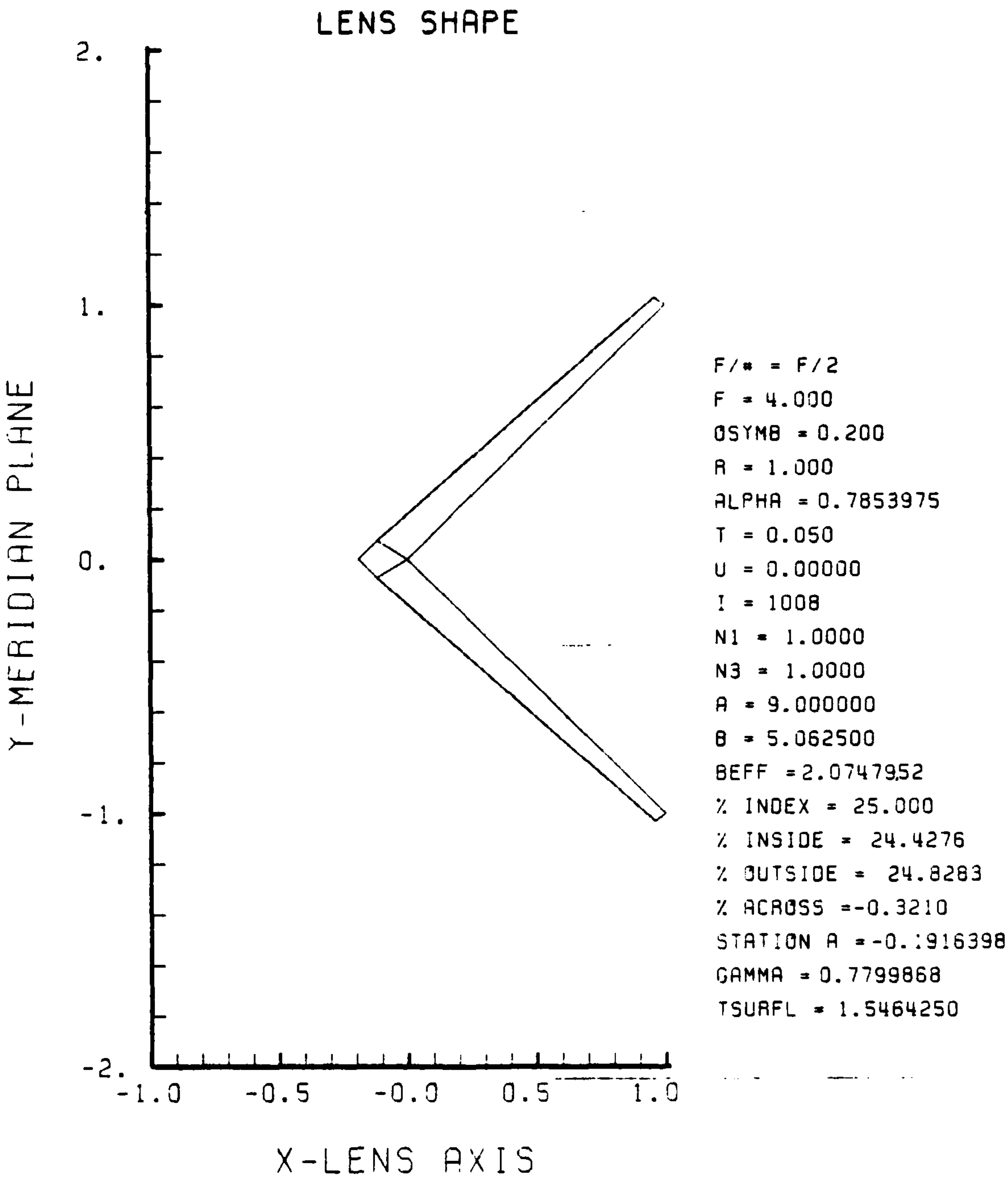

Figure F-57. GRIN Lens Shape at +25%, OB = 0.20, a = 9.00

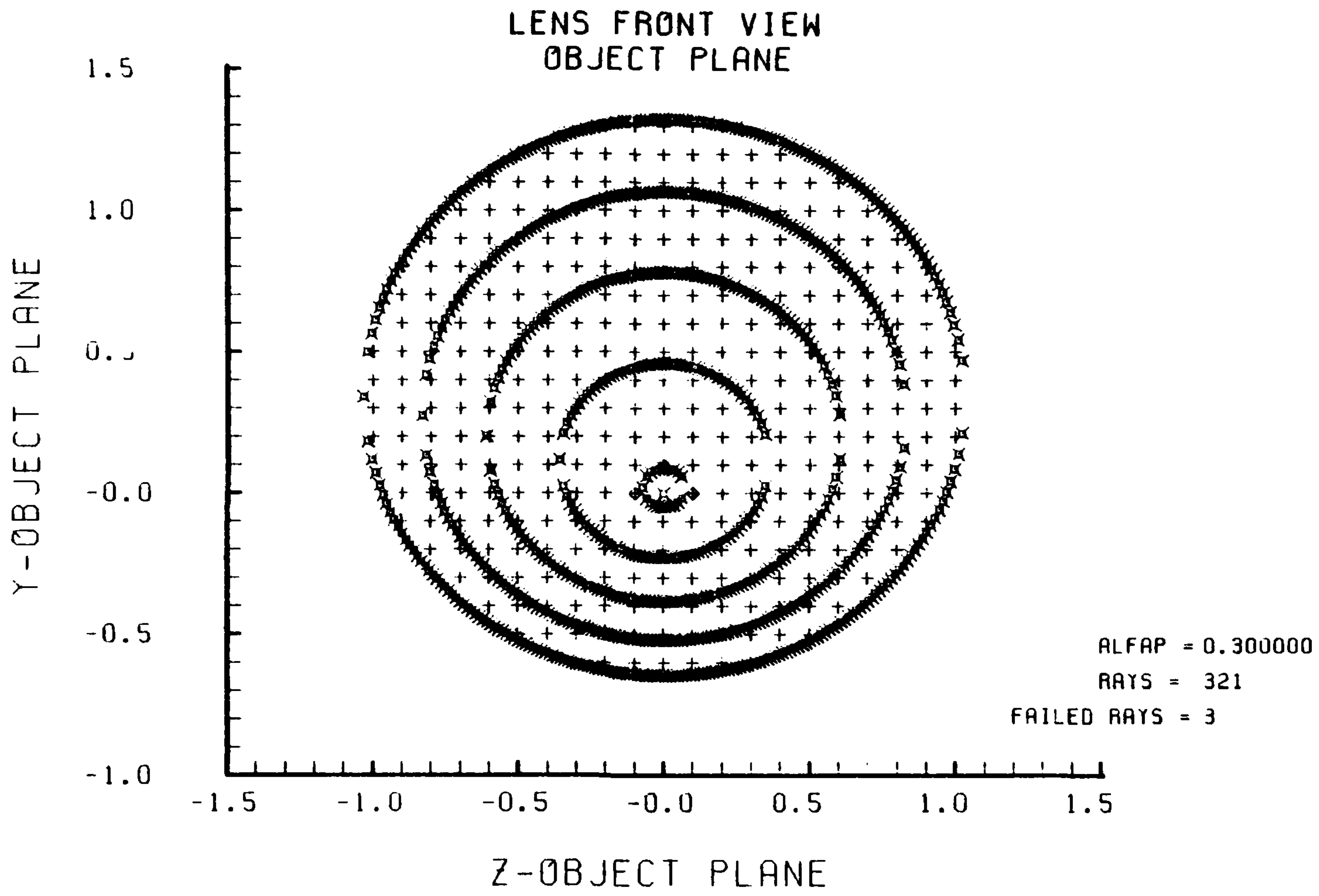

Figure F-58. Grid Plane at $\alpha_p = 0.3$ for Lens of Figure F-57

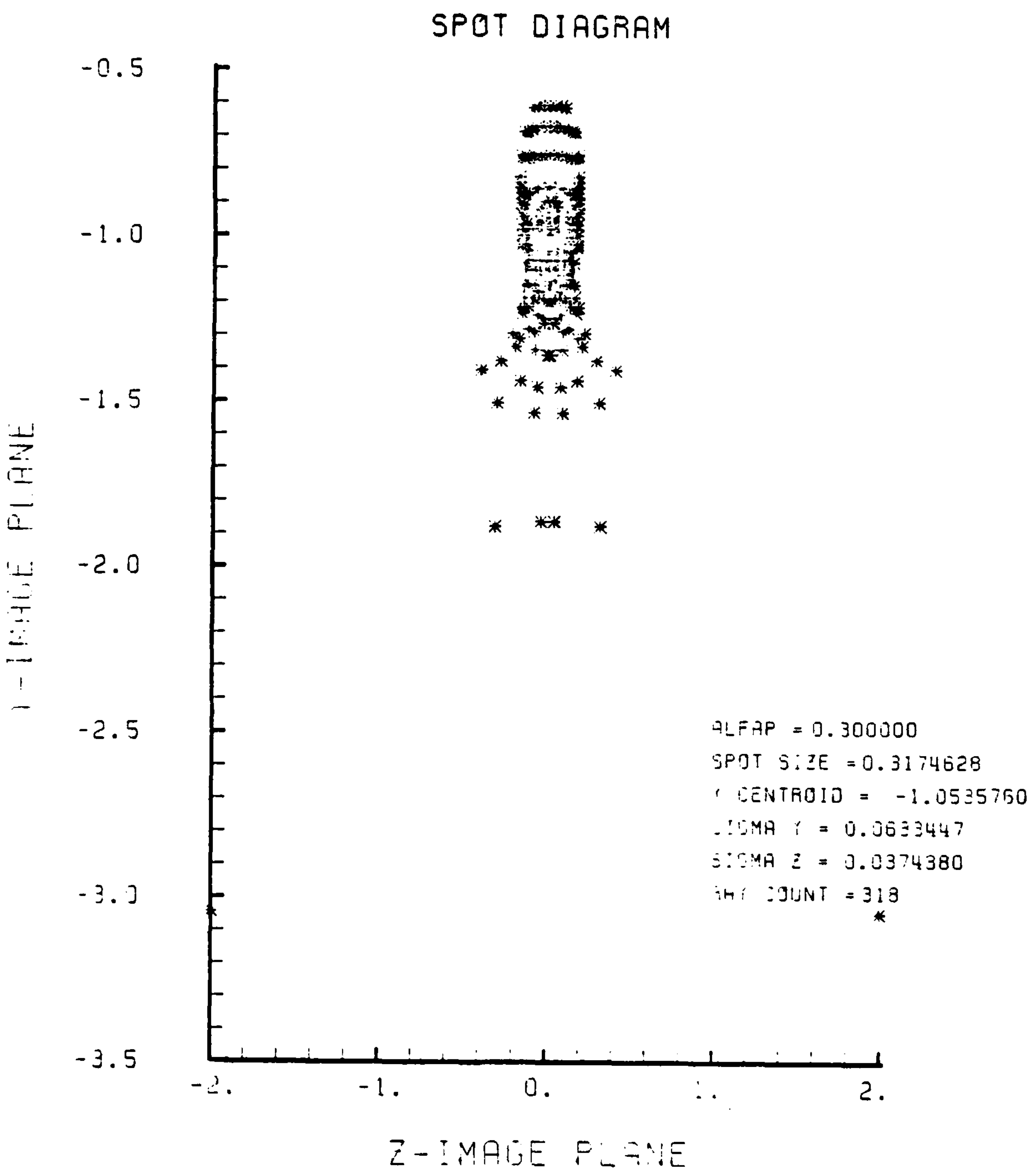

Figure F-59. Spot Diagram for Grid of Figure F-58

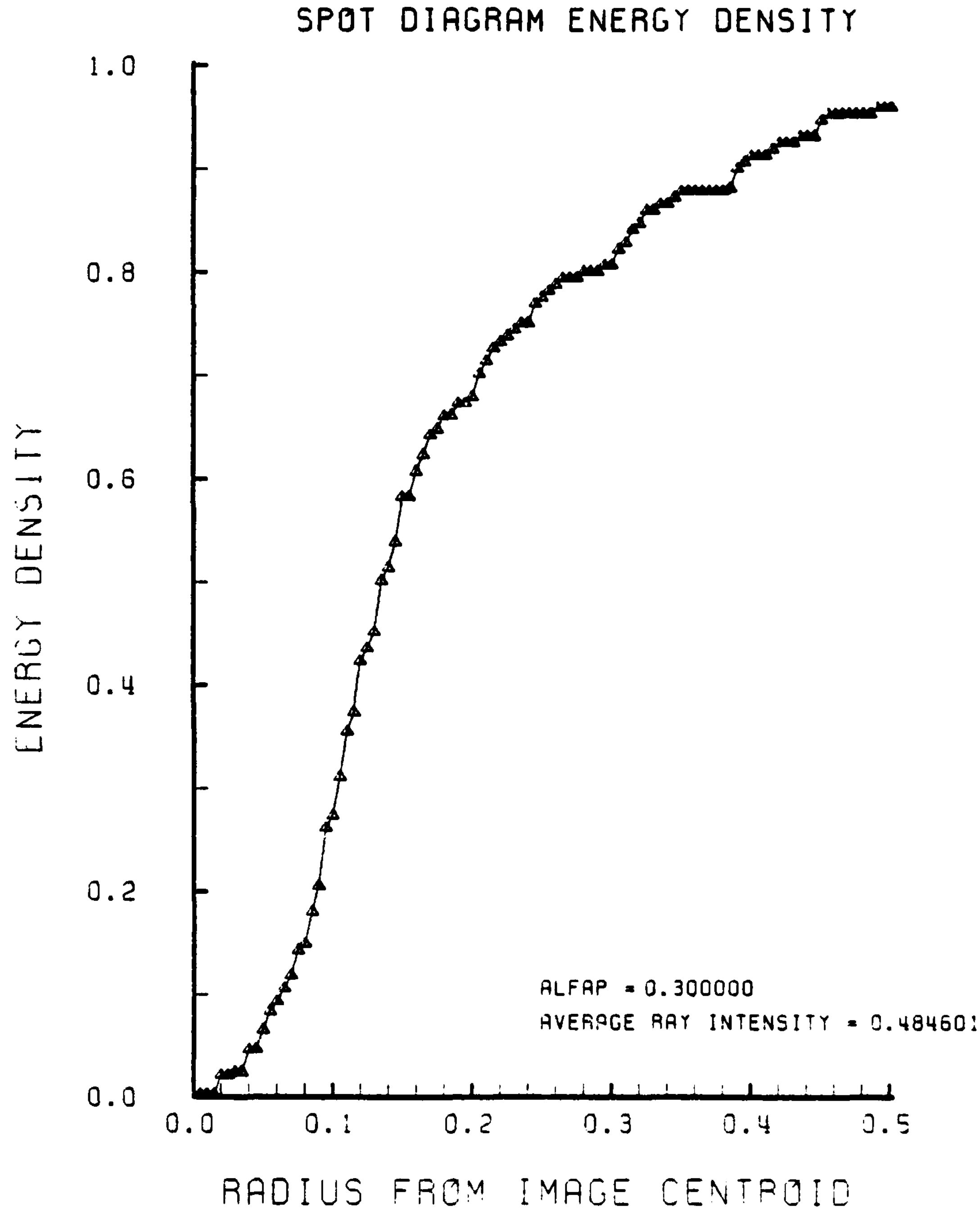

Figure F-60. Encircled Energy of Figure F-59

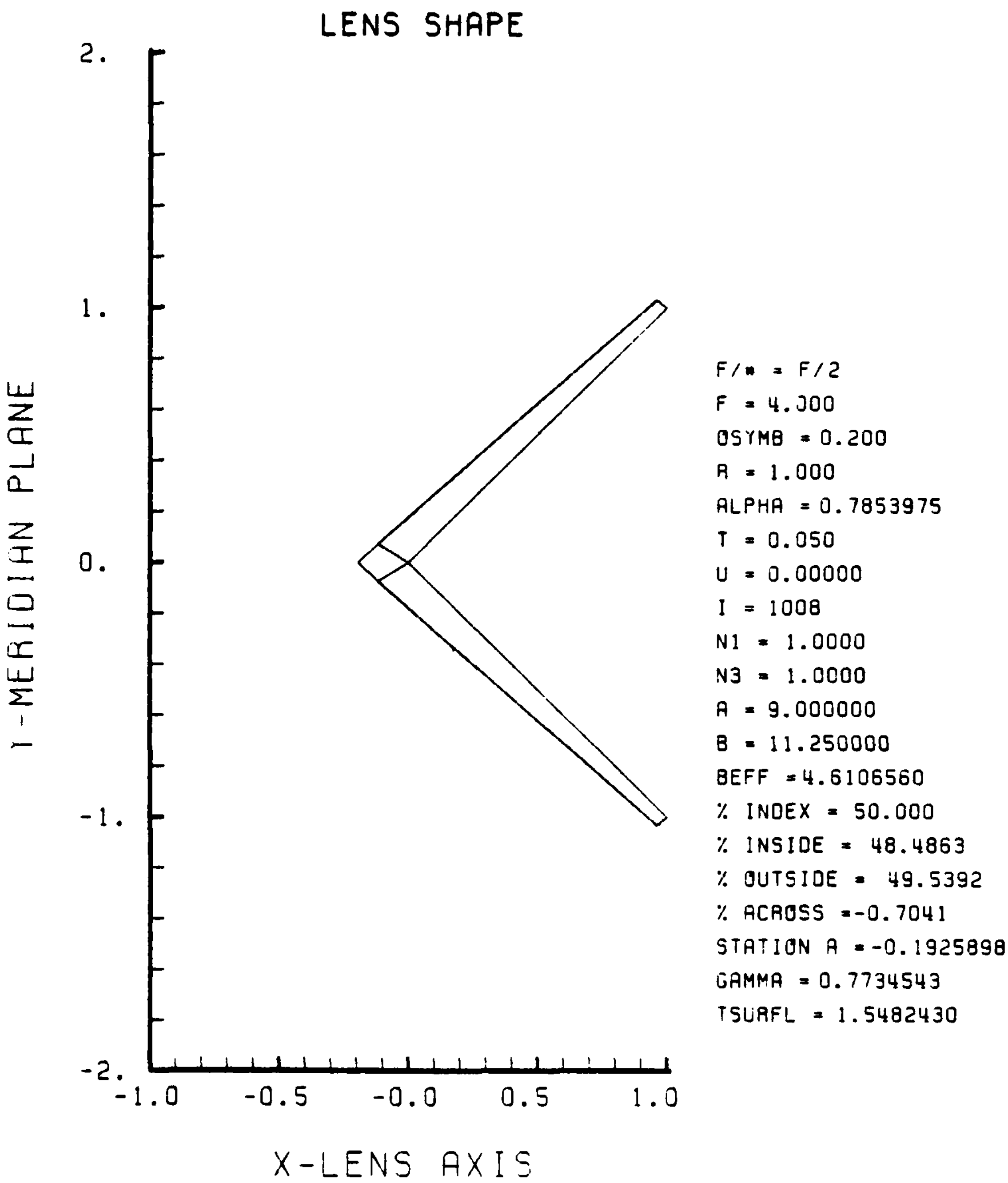

Figure F-61. GRIN Lens Shape at +50%, OB = 0.20, a = 9.00

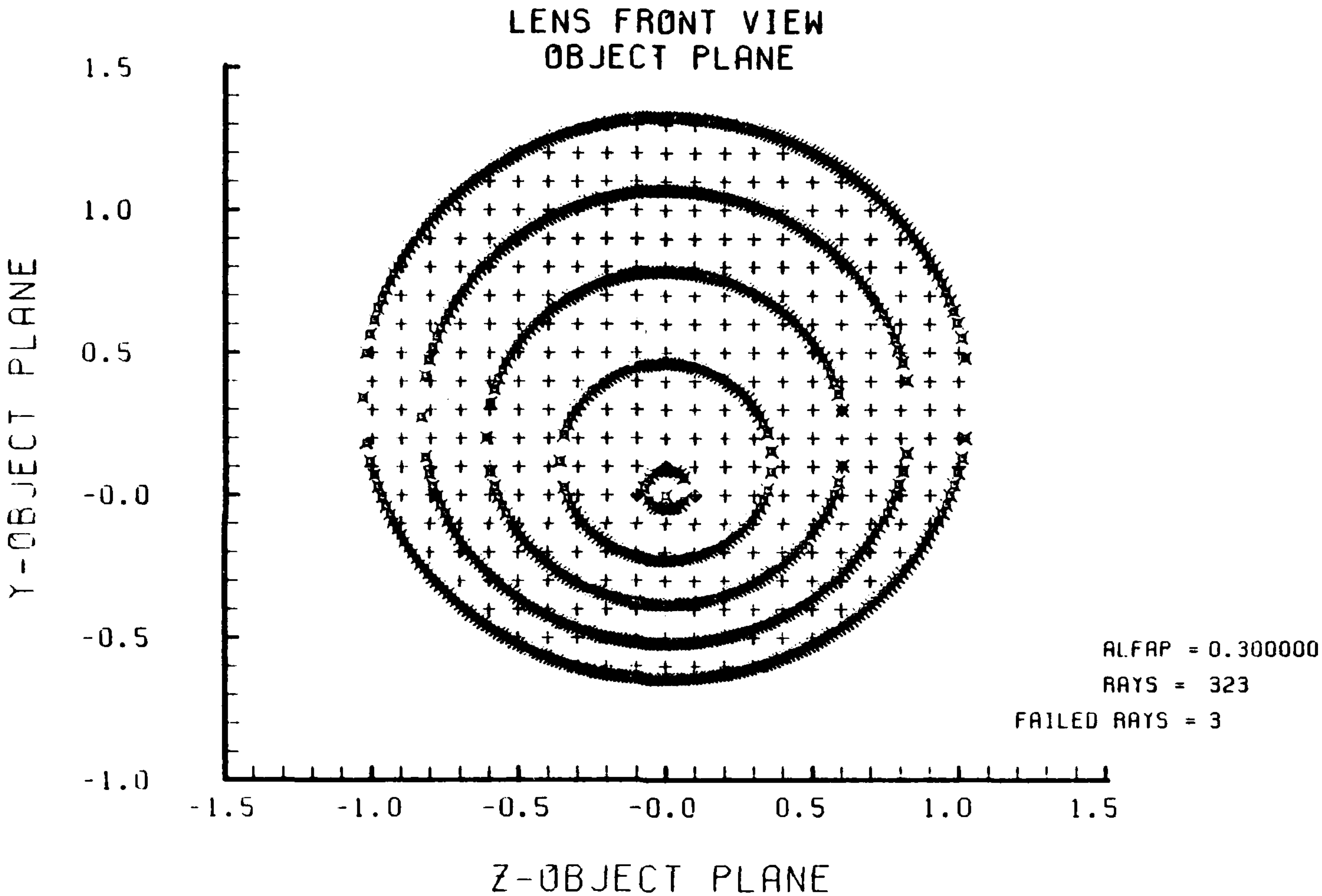

Figure F-62. Grid Plane at $\alpha_p = 0.3$ for Lens of Figure F-61

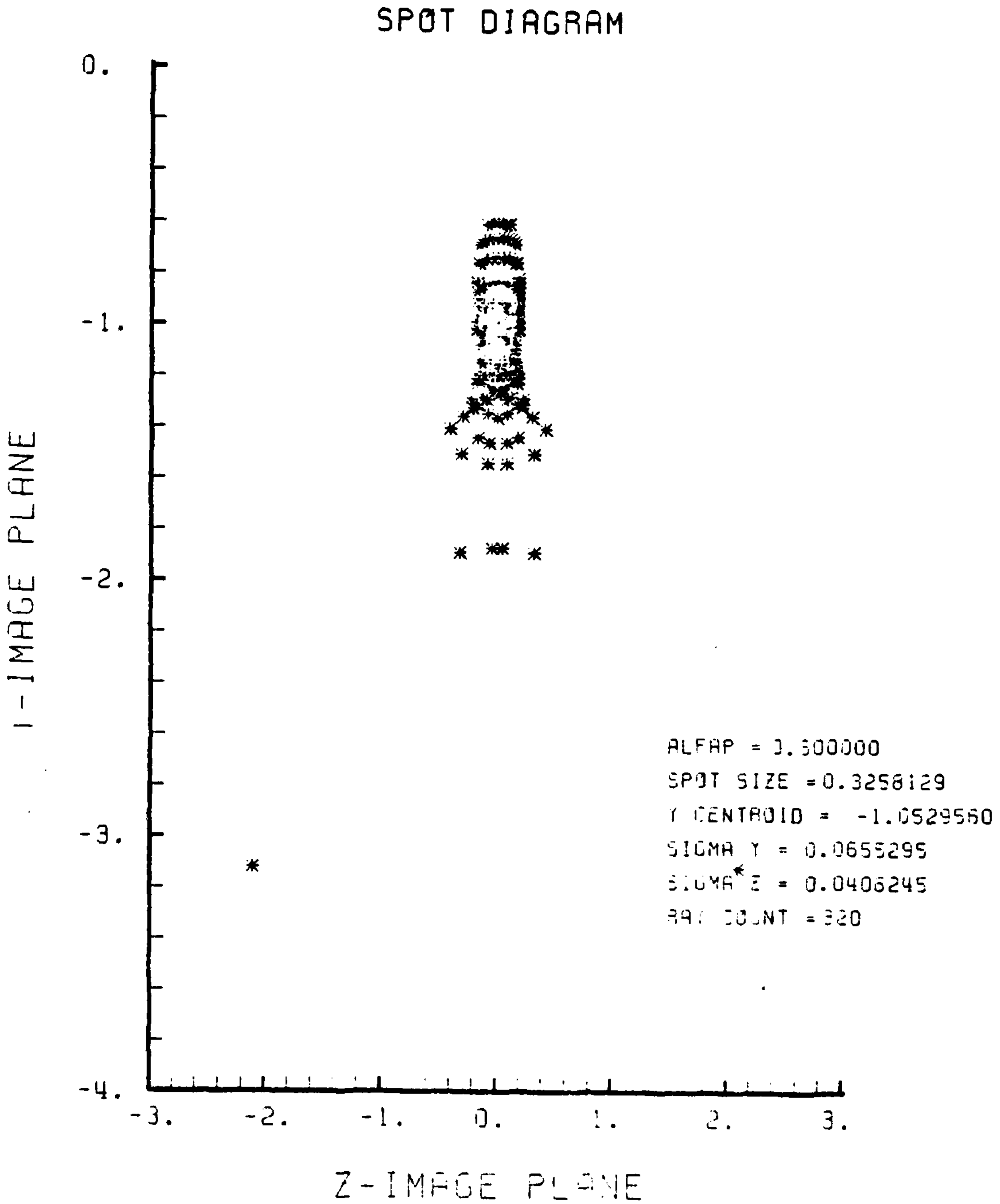

Figure F-63. Spot Diagram for Grid of Figure F-62

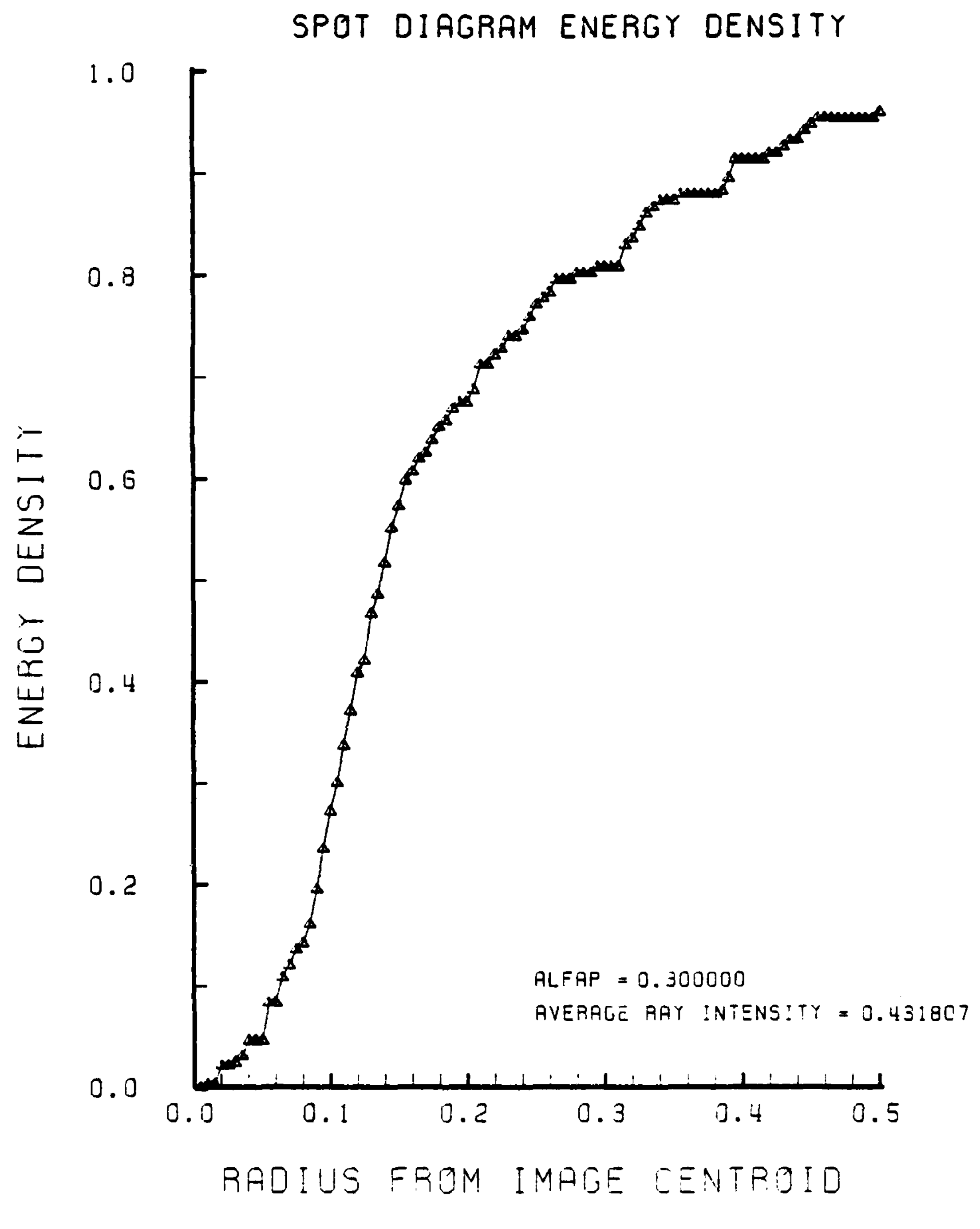

Figure F-64. Encircled Energy of Figure F-63

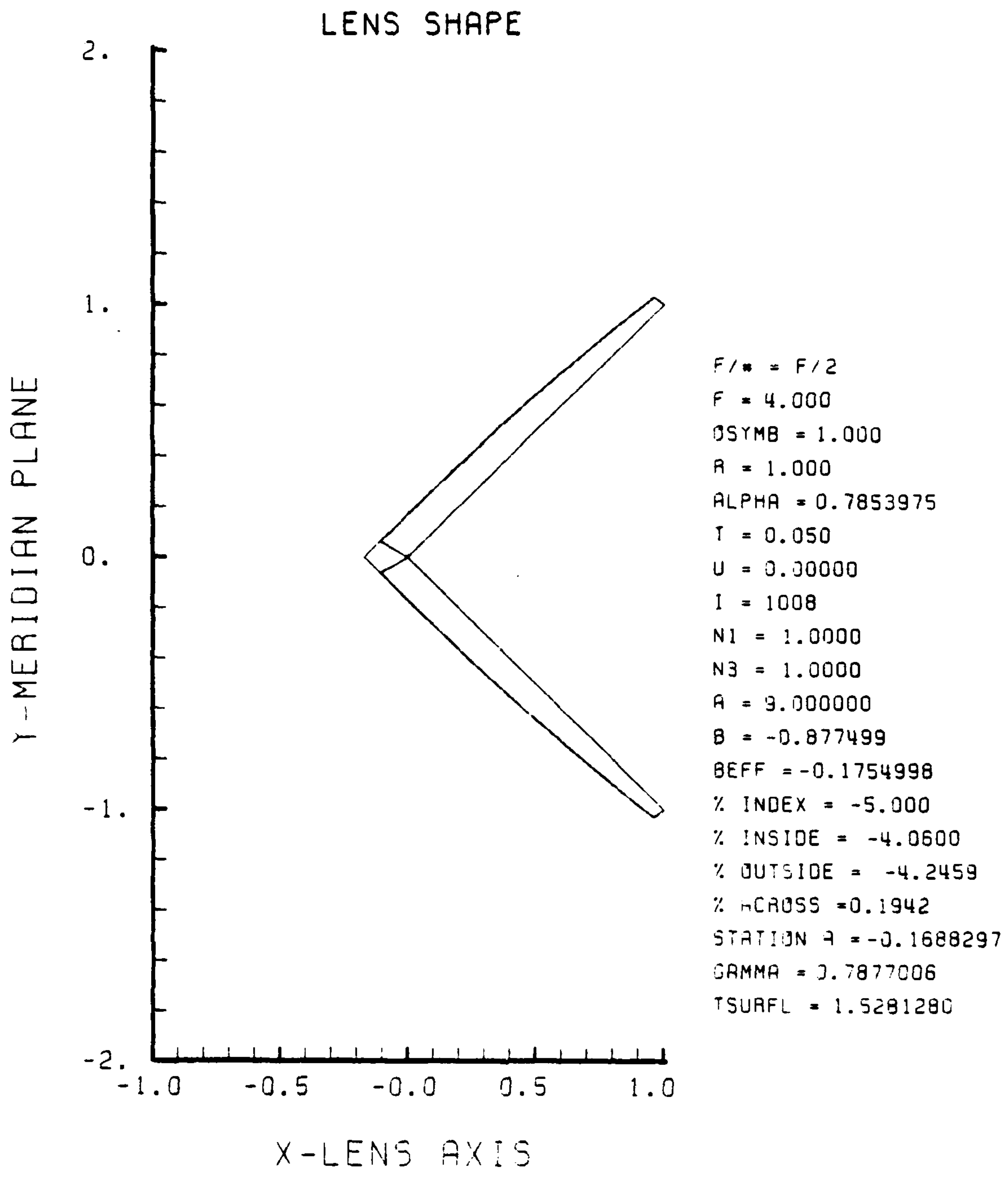

Figure F-65. GRIN Lens Shape at -5%, OB = 1.00, a = 9.00

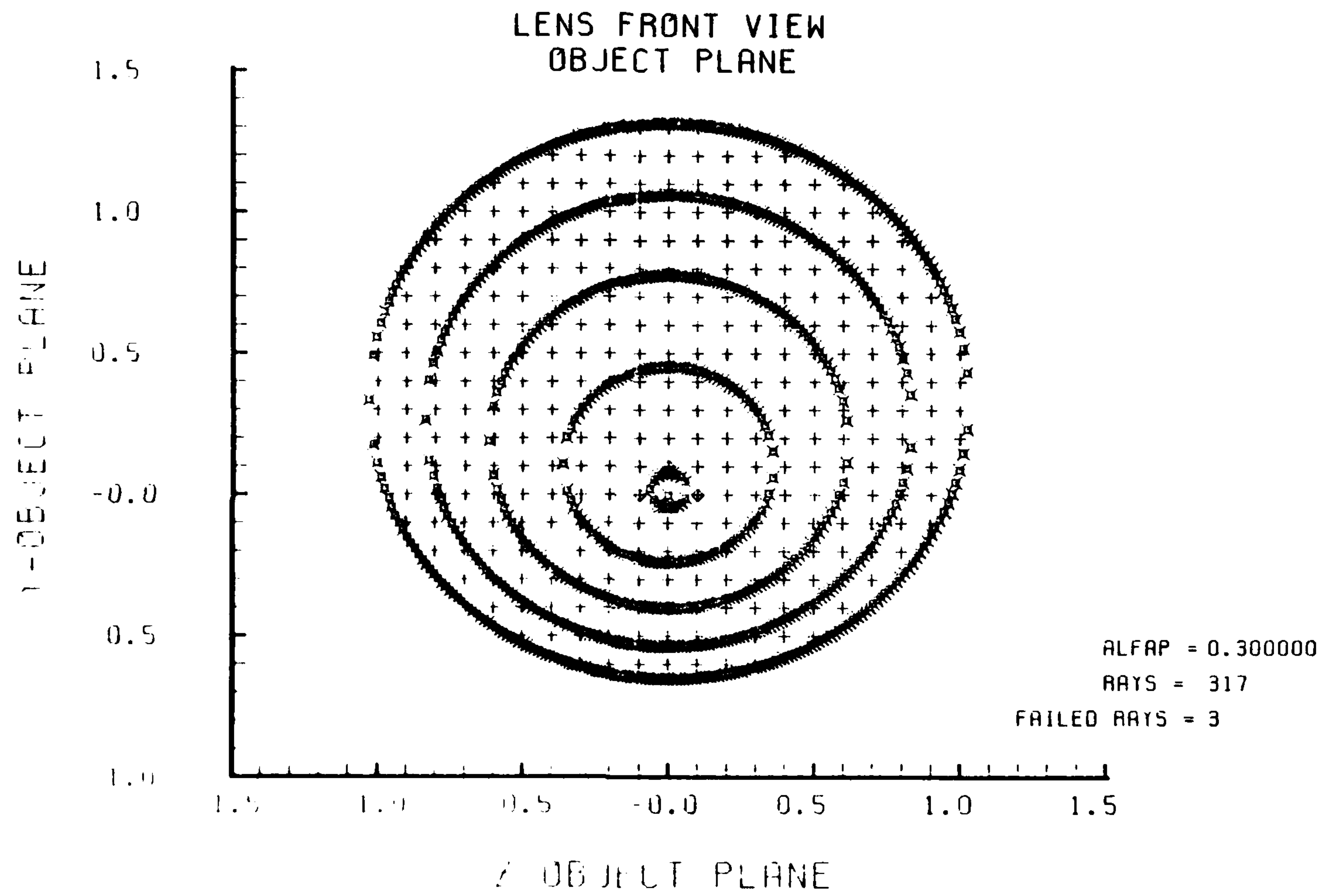

Figure F-66. Grid Plane at $\alpha_p = 0.3$ for Lens of Figure F-65

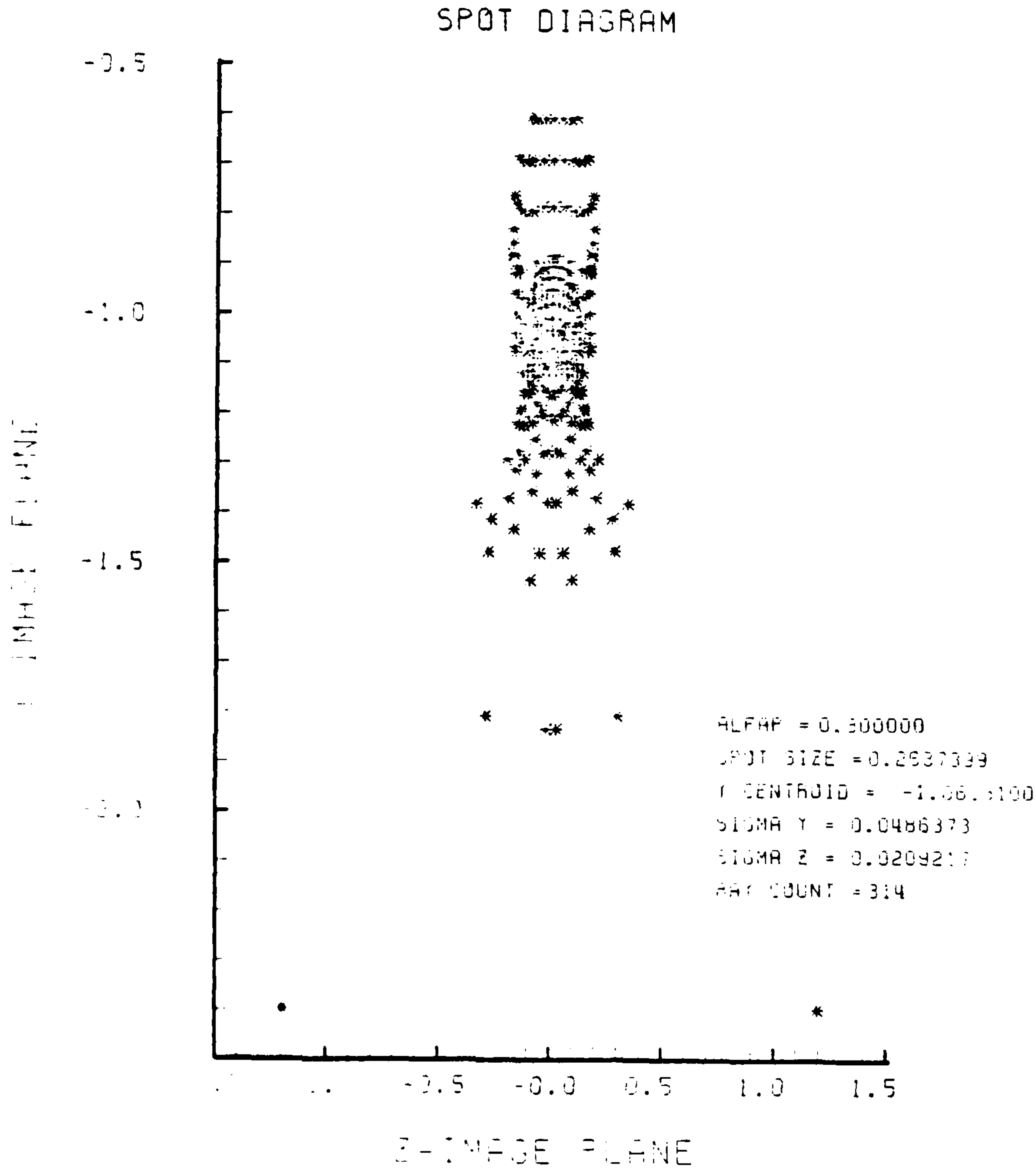

Figure F-67. Spot Diagram for Grid of Figure F-66

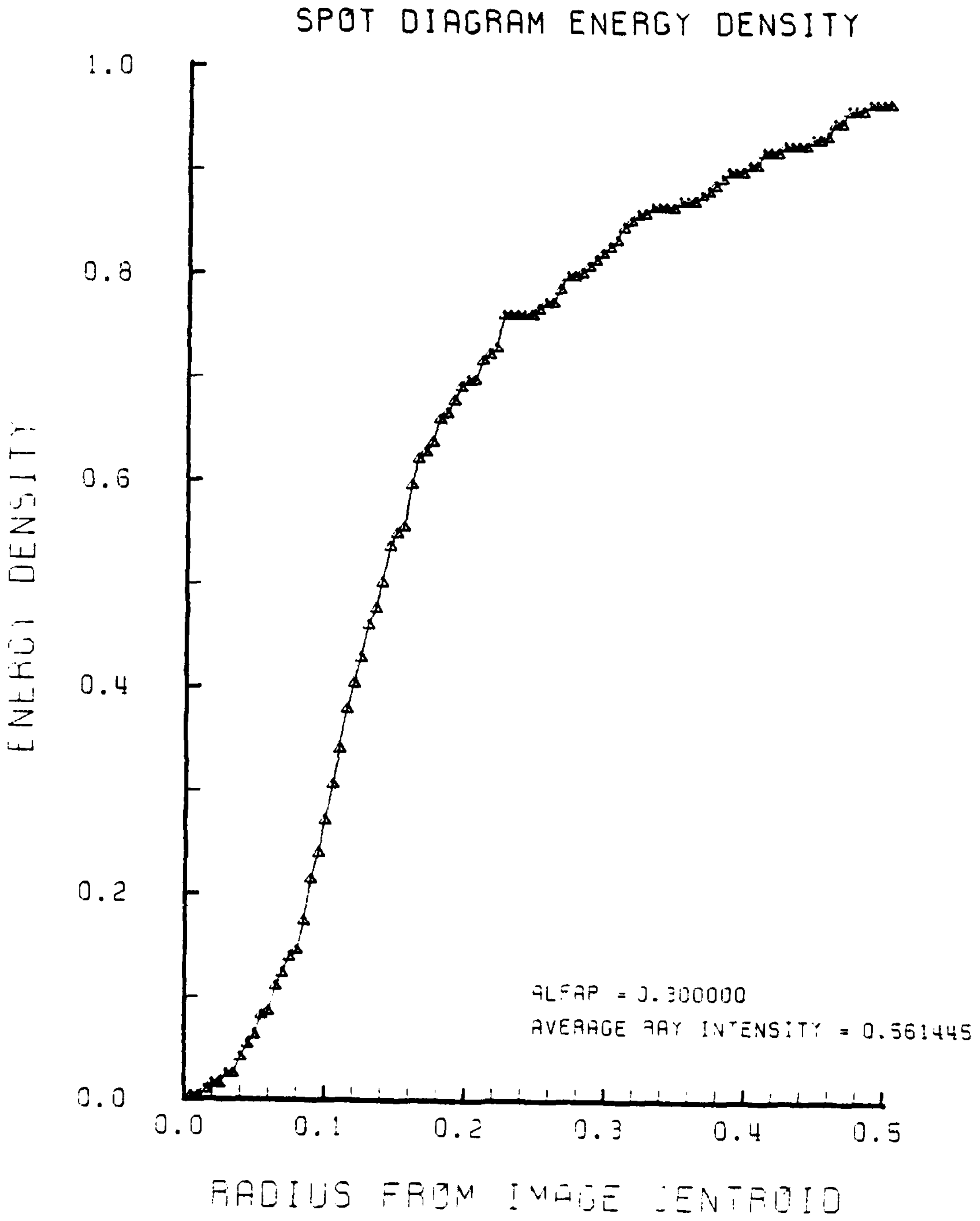

Figure F-68. Encircled Energy of Figure F-67

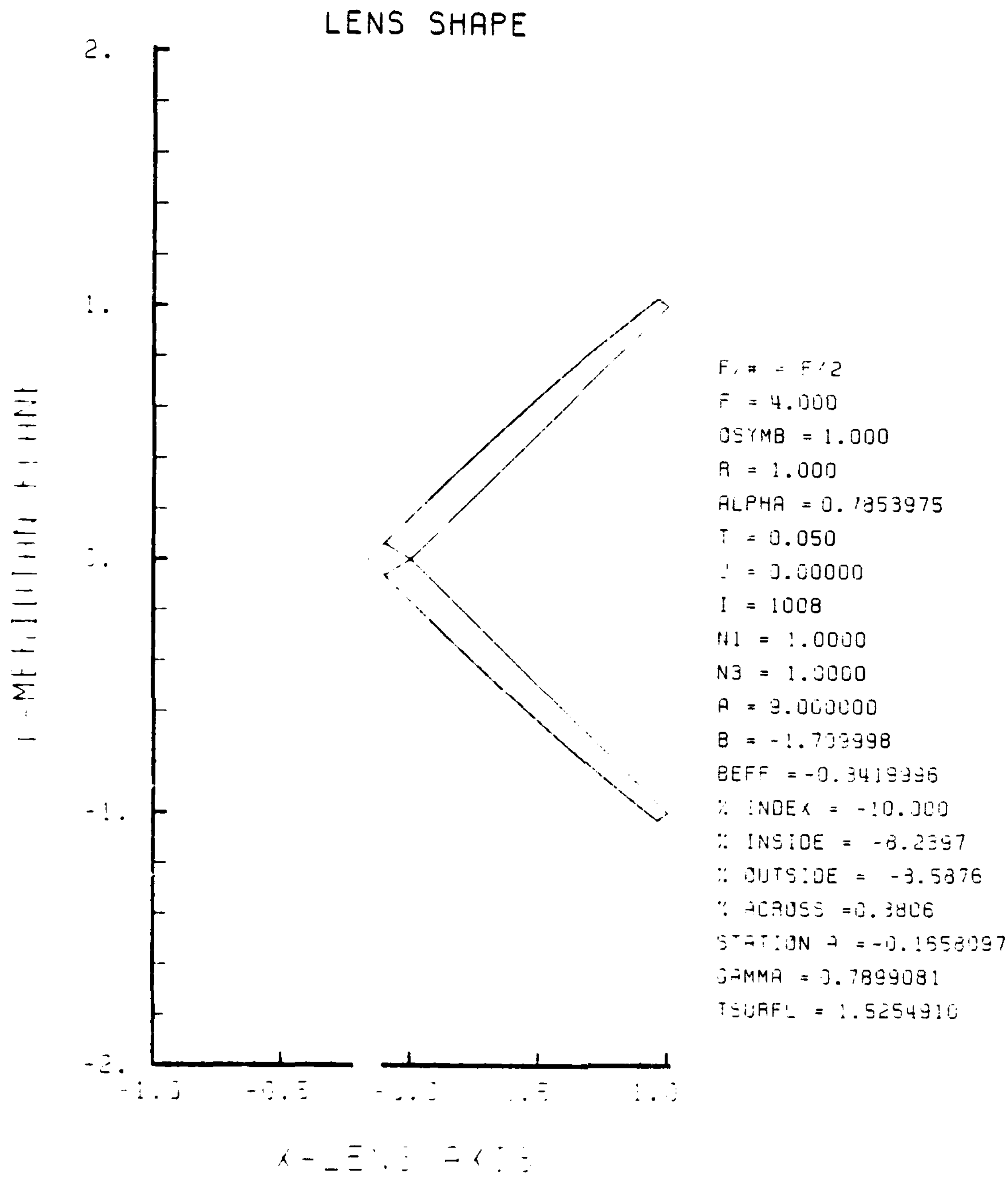

Figure F-69. GRIN Lens Shape at -10%, OB = 1.00, a = 9.00

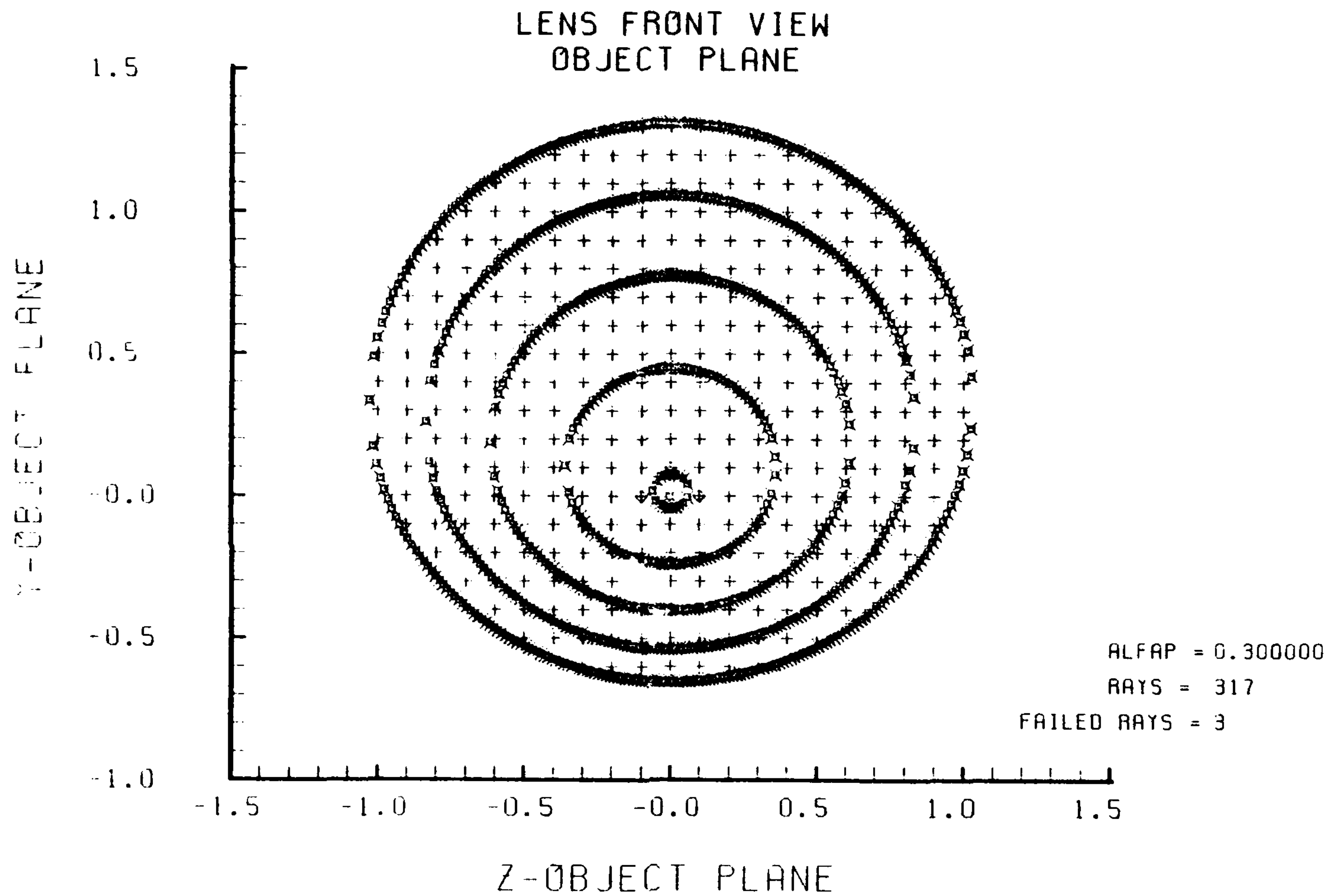

Figure F-70. Grid Plane at $\alpha_p = 0.3$ for Lens of Figure F-69

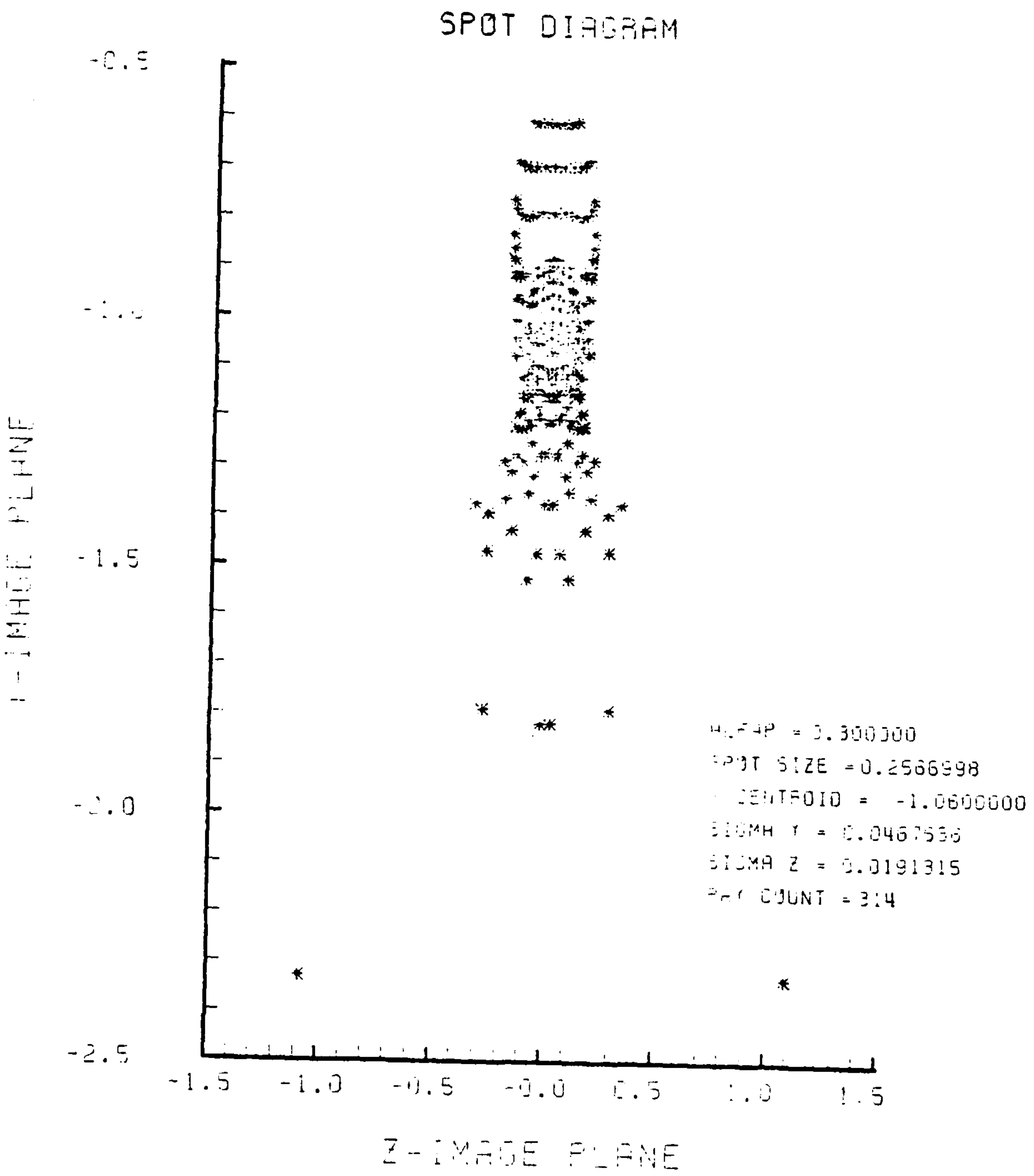

Figure F-71. Spot Diagram for Grid of Figure F-70

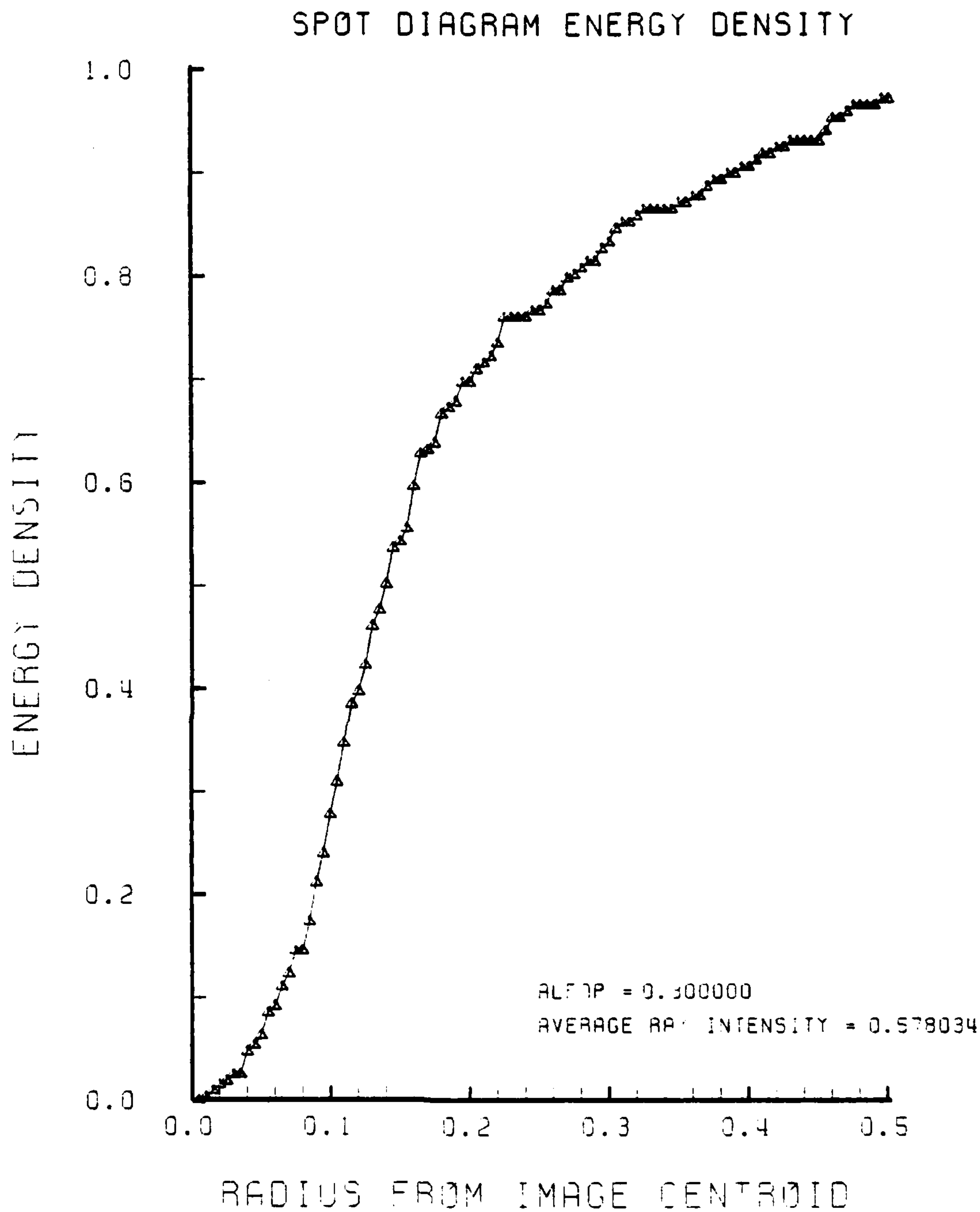

Figure F-72. Encircled Energy of Figure F-71

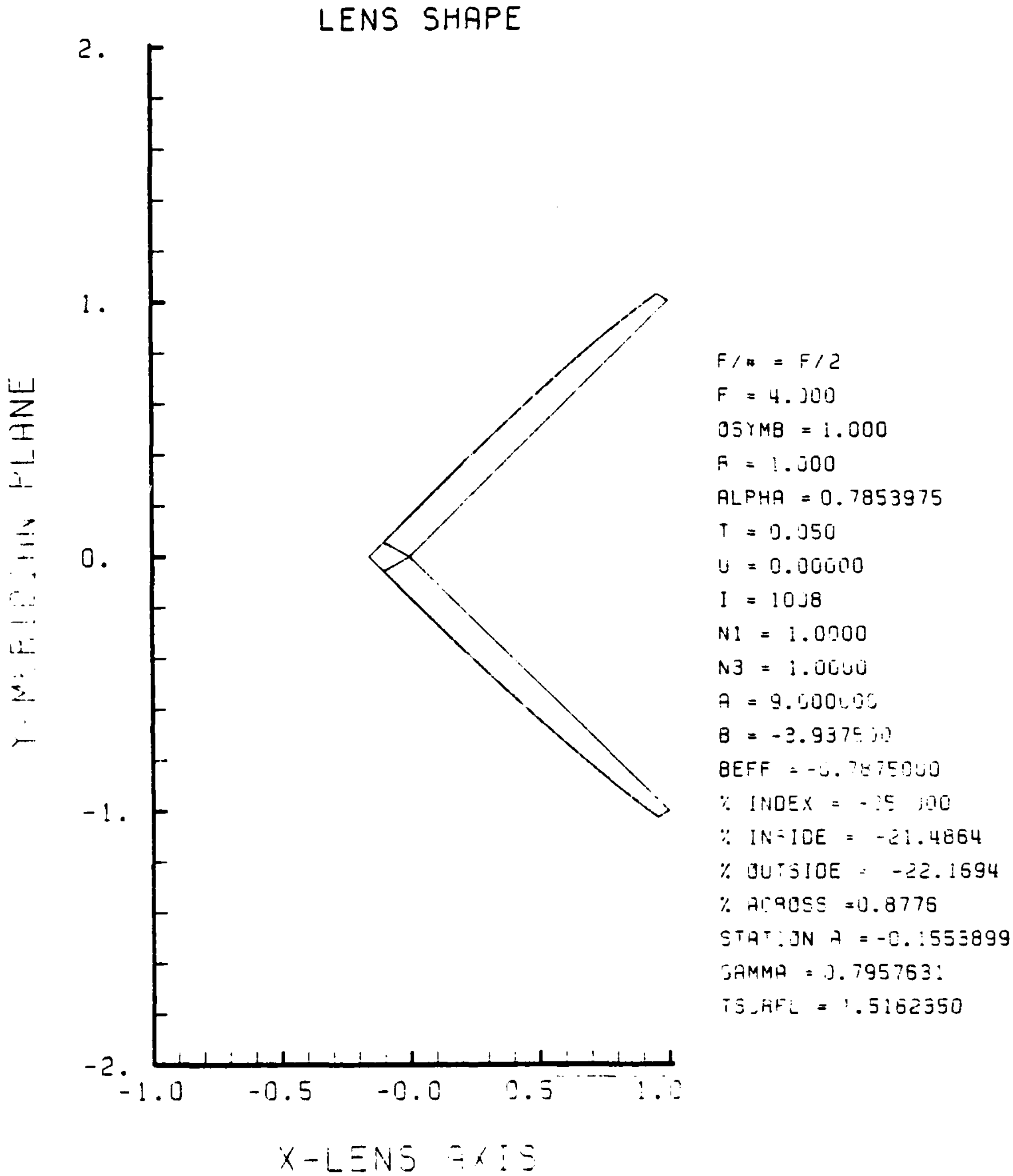

Figure F-73. GRIN Lens Shape at -25%, OB = 1.00, a = 9.00

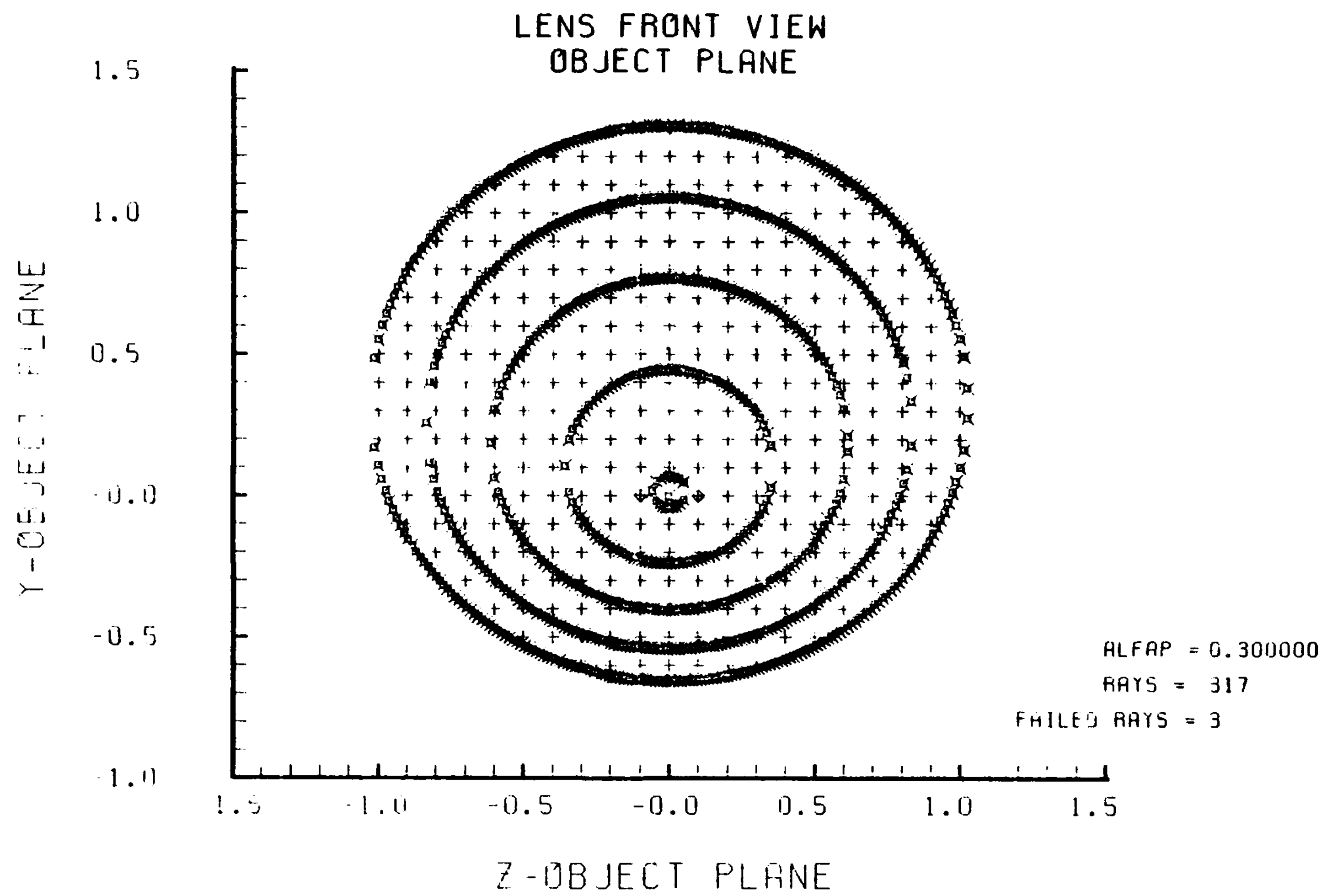

Figure F-74. Grid Plane at α_p = 0.3 for Lens of Figure F-73

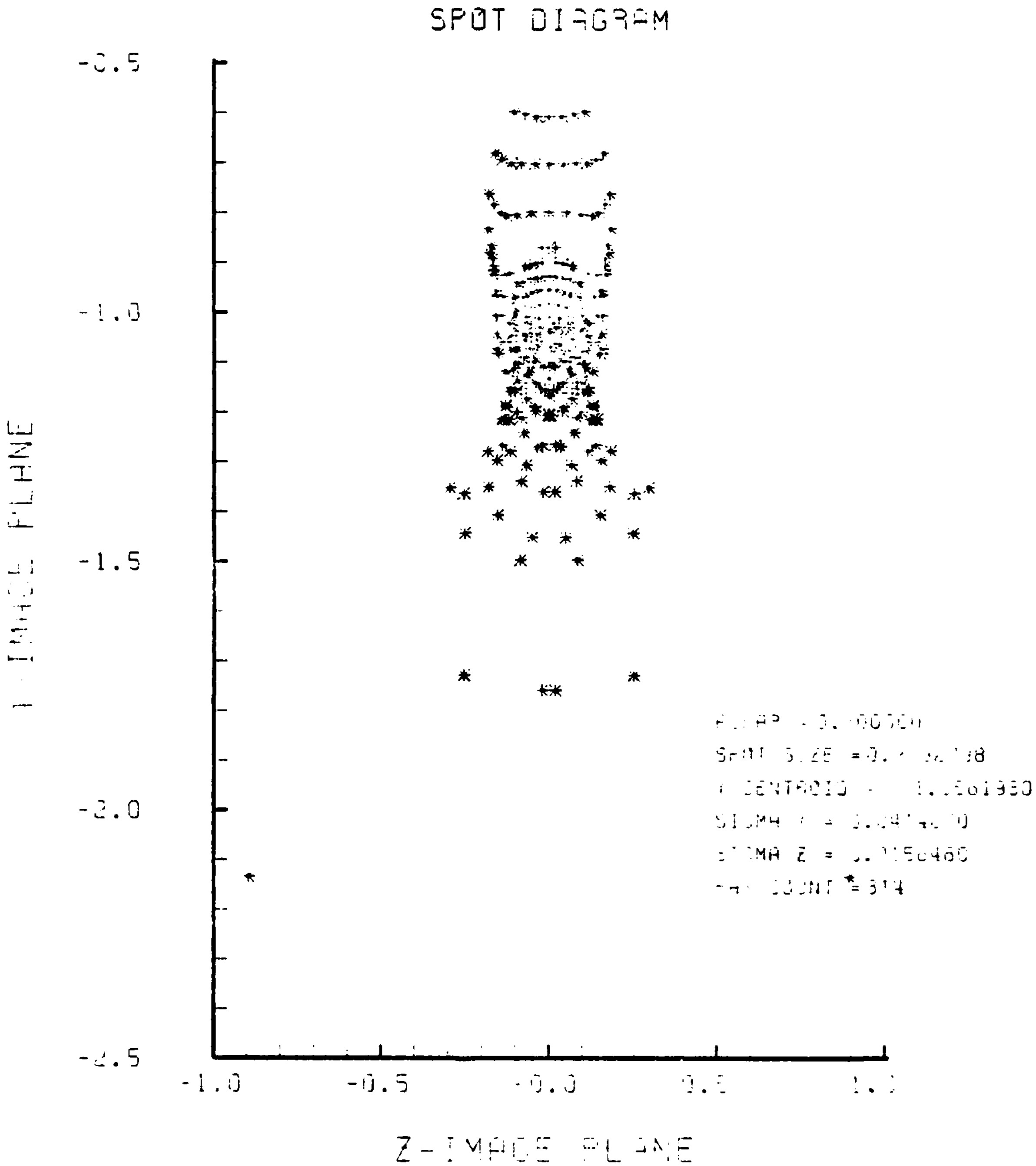

Figure F-75. Spot Diagram for Grid of Figure F-74

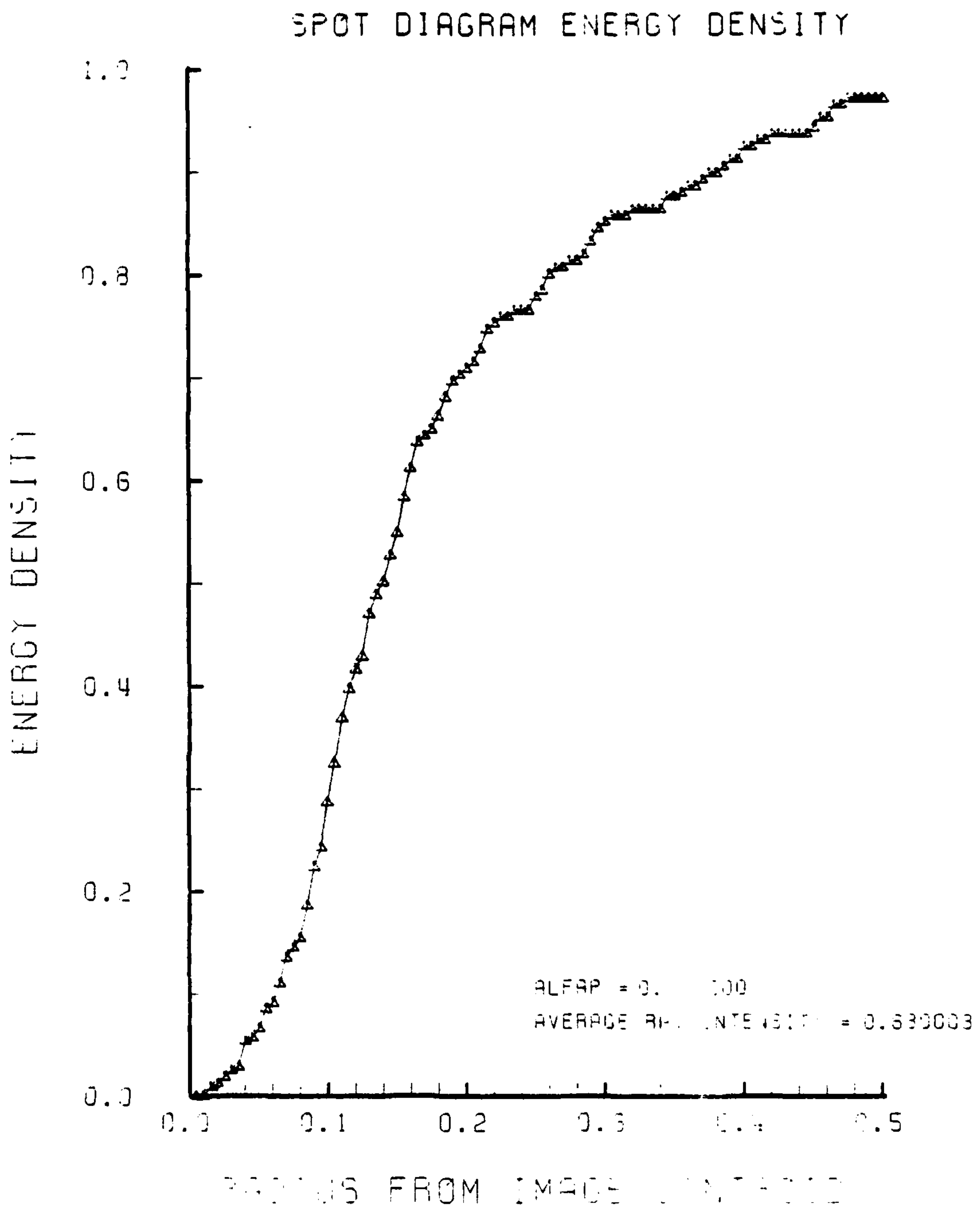

Figure F-76. Encircled Energy of Figure F-75

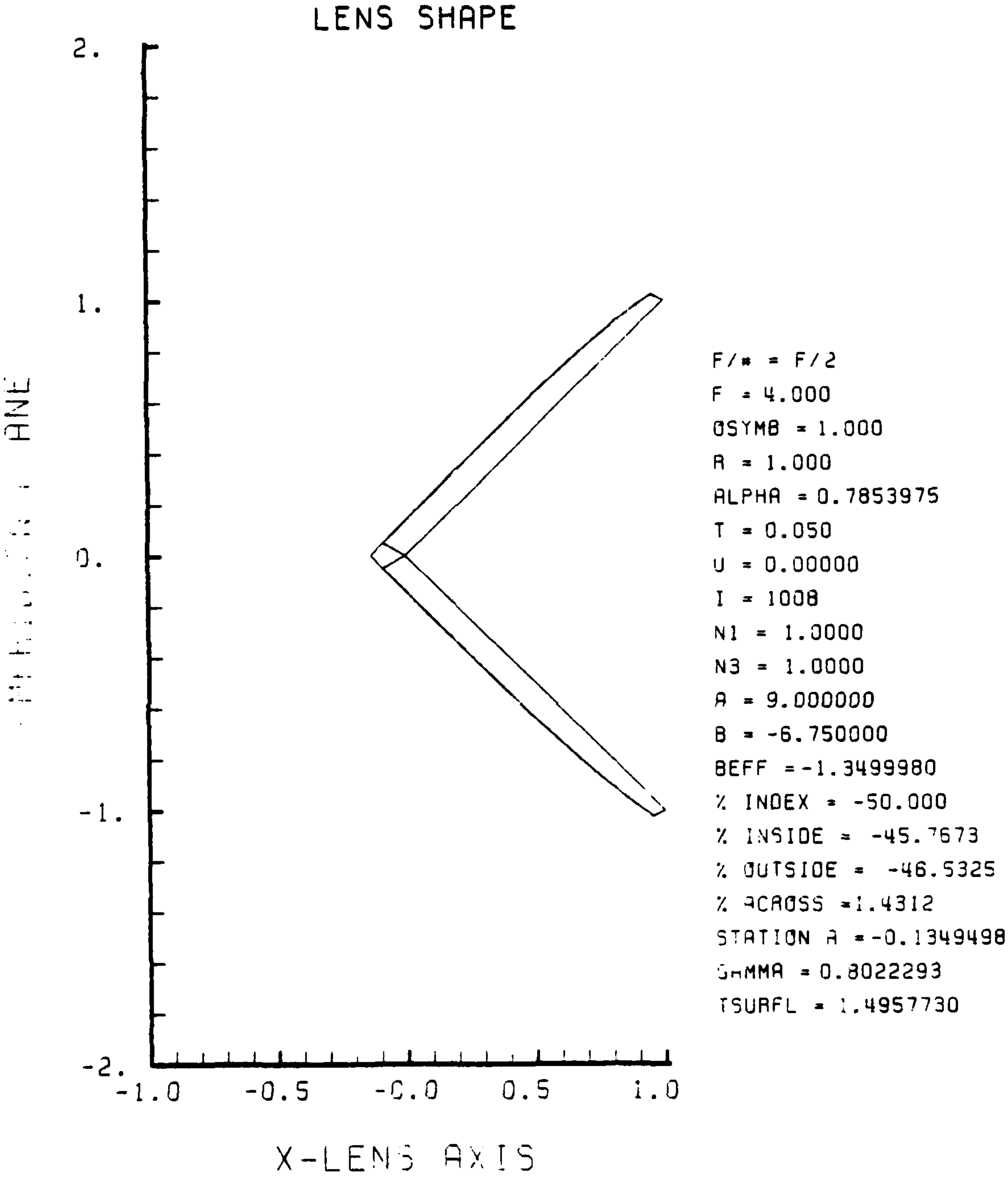

Figure F-77. GRIN Lens Shape at -50%, OB = 1.00, a = 9.00

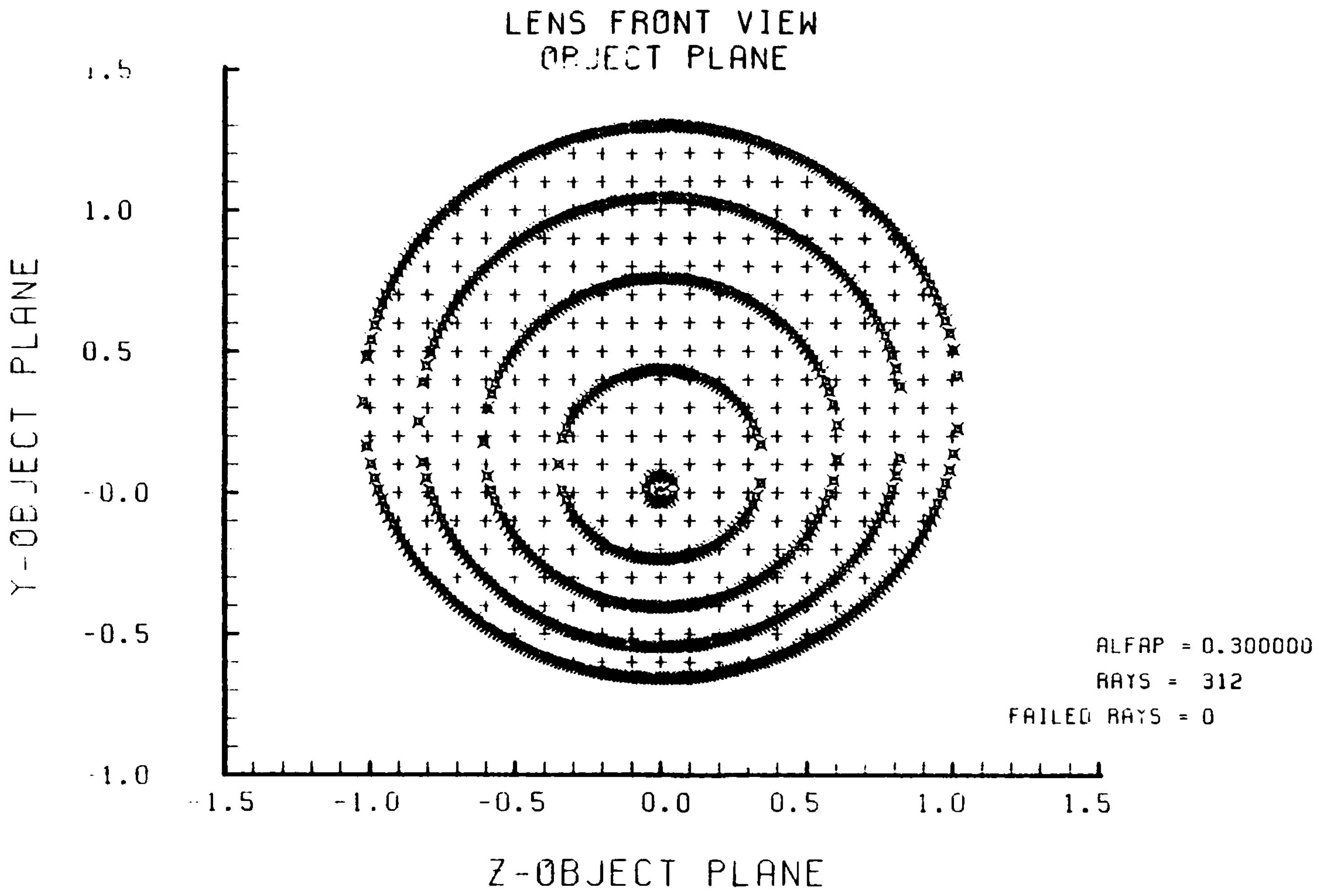

Figure F-78. Grid Plane at α_p = 0.3 for Lens of Figure F-77

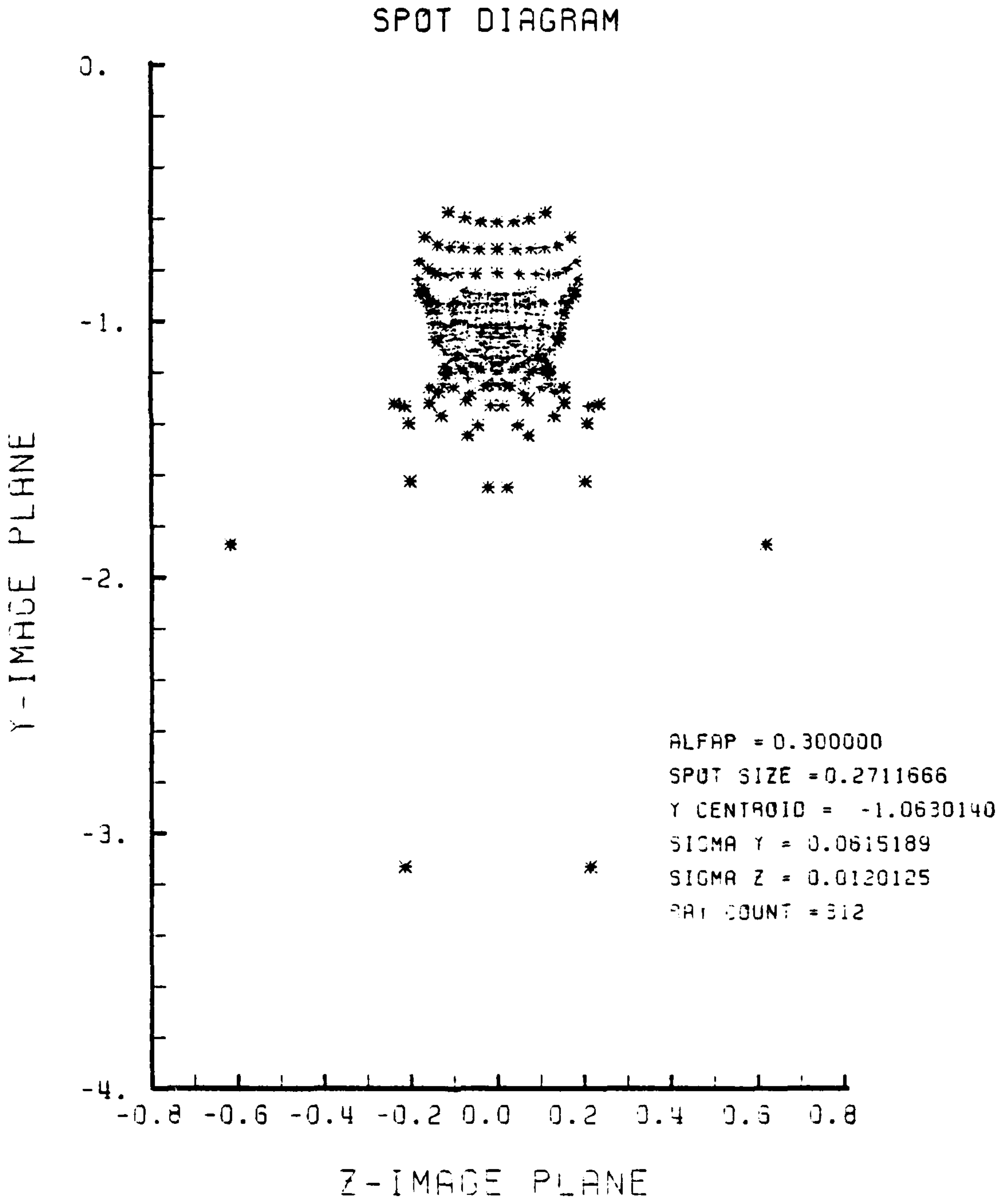

Figure F-79. Spot Diagram for Grid of Figure F-78

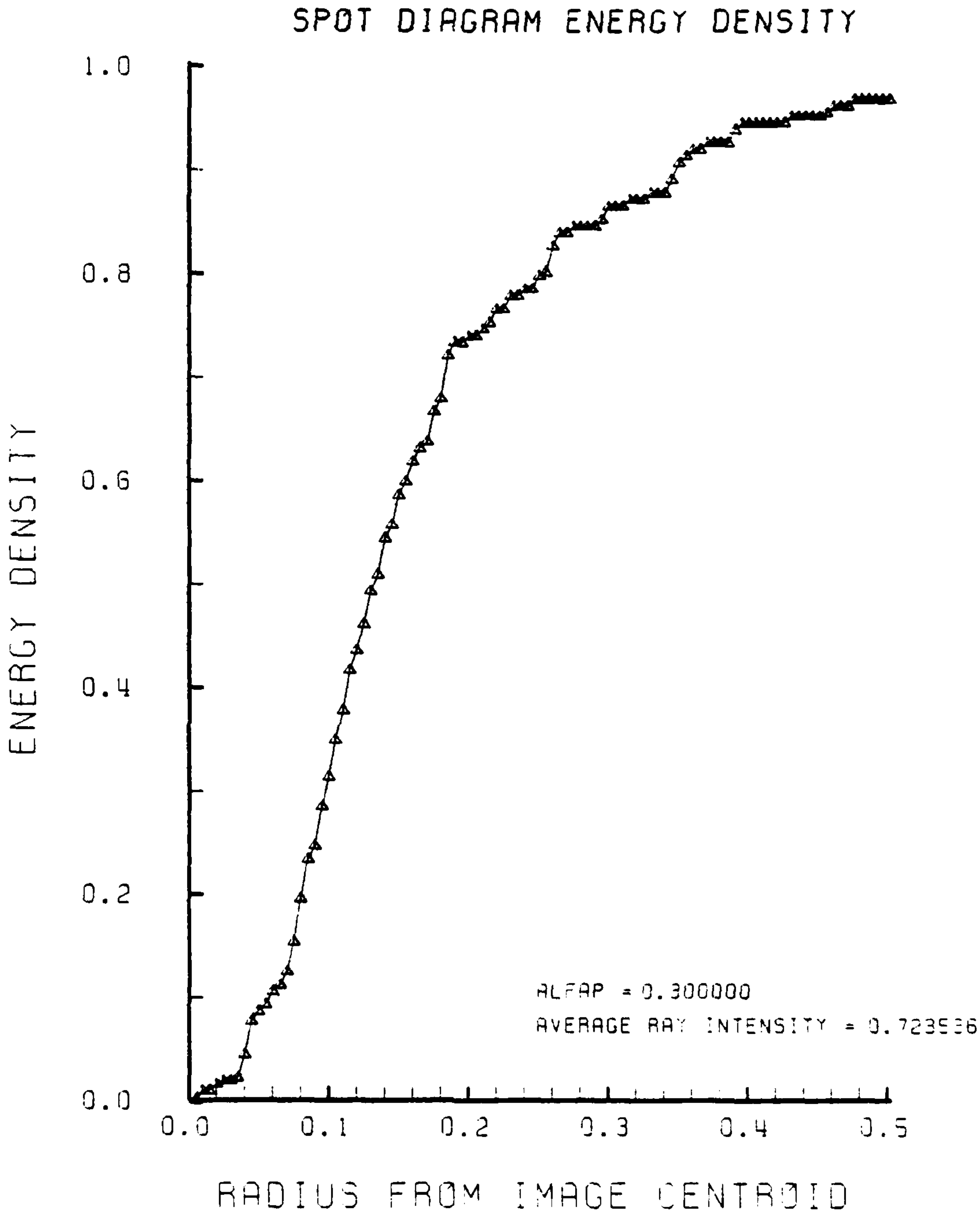

Figure F-80. Encircled Energy of Figure F-79

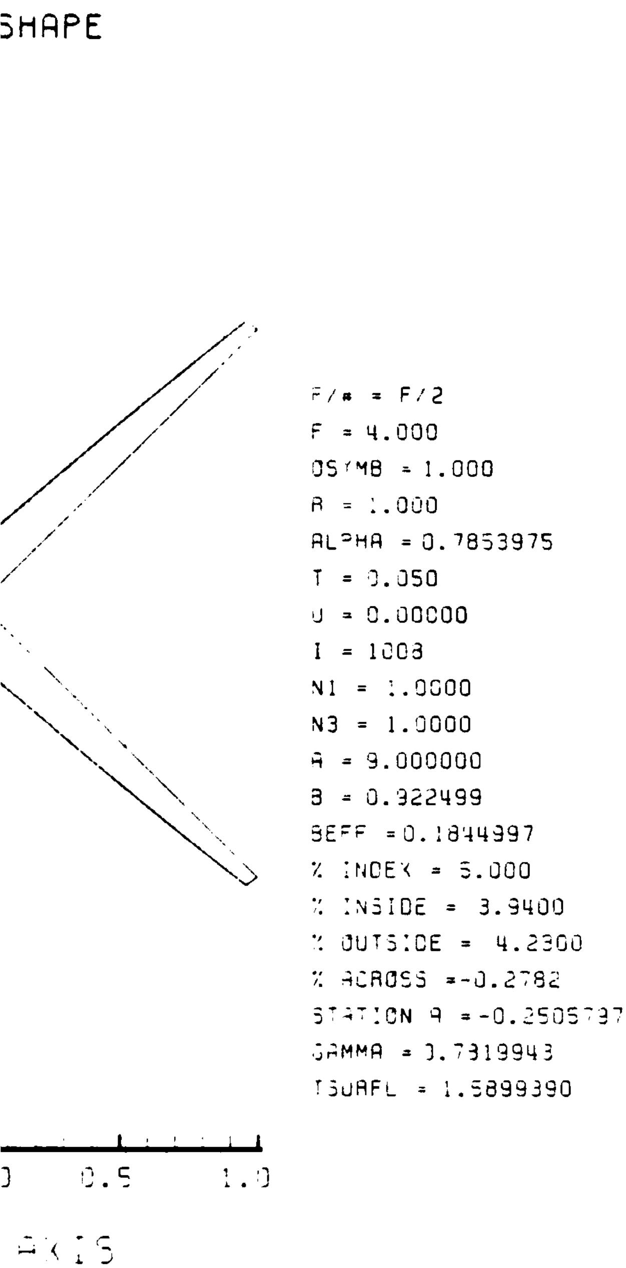

ns Shape at +5%, OB = 1.00,
0

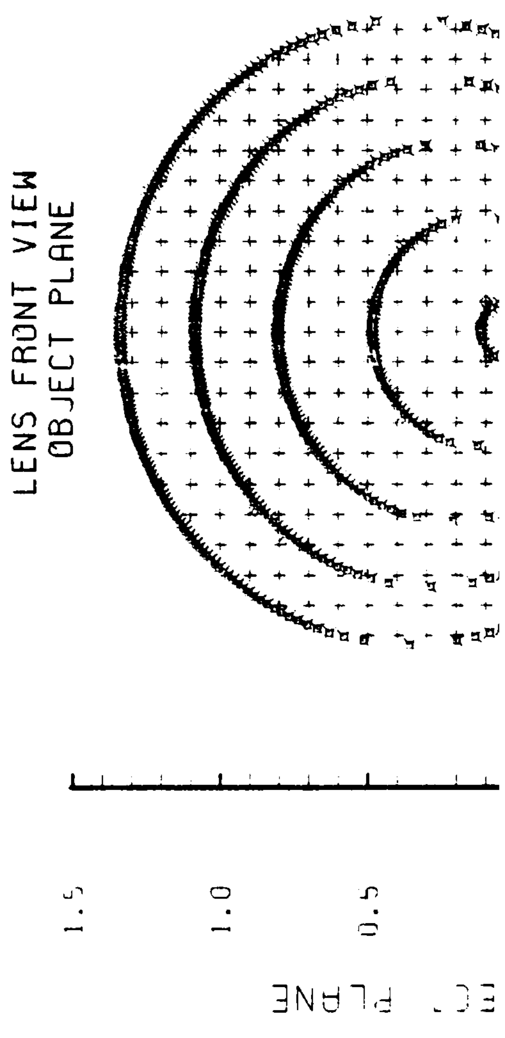

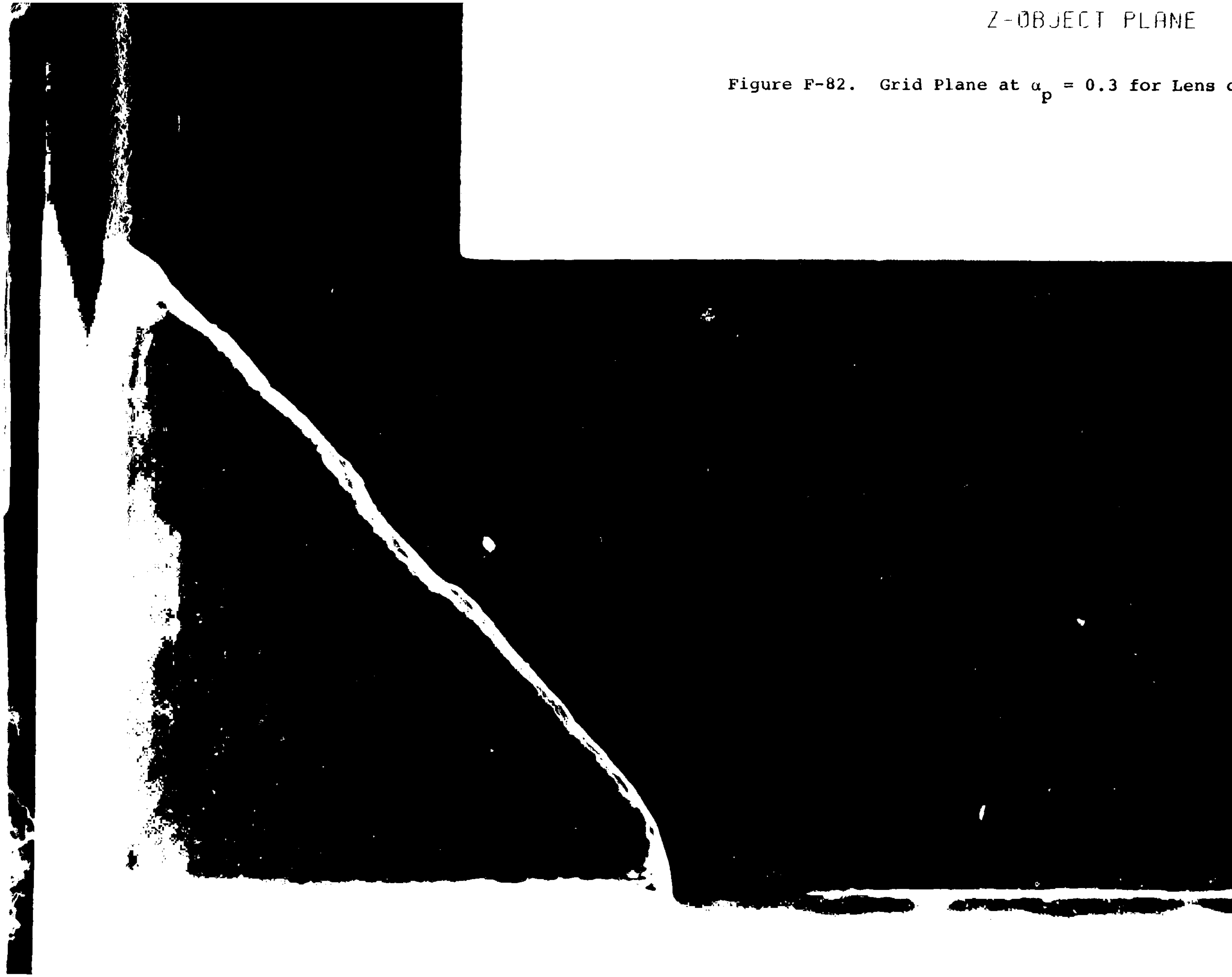

Figure F-82. Grid Plane at $\alpha_p = 0.3$ for Lens o

AD-A125 167 AERODYNAMICALLY EFFICIENT GRADIENT REFRACTIVE INDEX MISSILE SEEKER LENS(U) NAVAL POSTGRADUATE SCHOOL MONTEREY CA H M CARR OCT 82 NPS67-82-012 5/6

UNCLASSIFIED F/G 16/4 NL

1.0 1.1 1.25 1.4 1.6 1.8 2.0 2.2 2.5 2.8 3.2 3.6 4.0

MICROCOPY RESOLUTION TEST CHART
NATIONAL BUREAU OF STANDARDS-1963-A

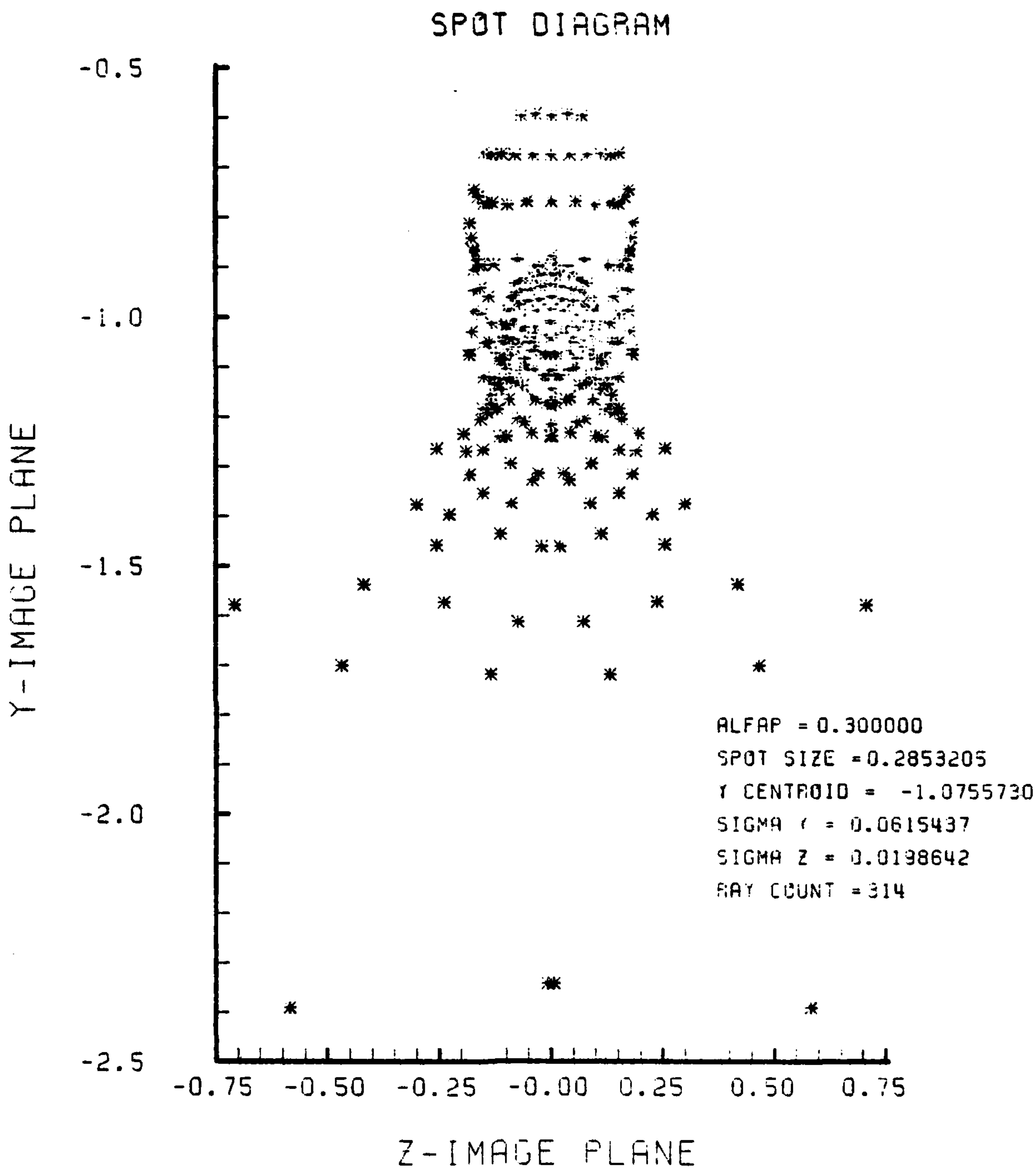

Figure F-83. Spot Diagram for Grid of Figure F-82

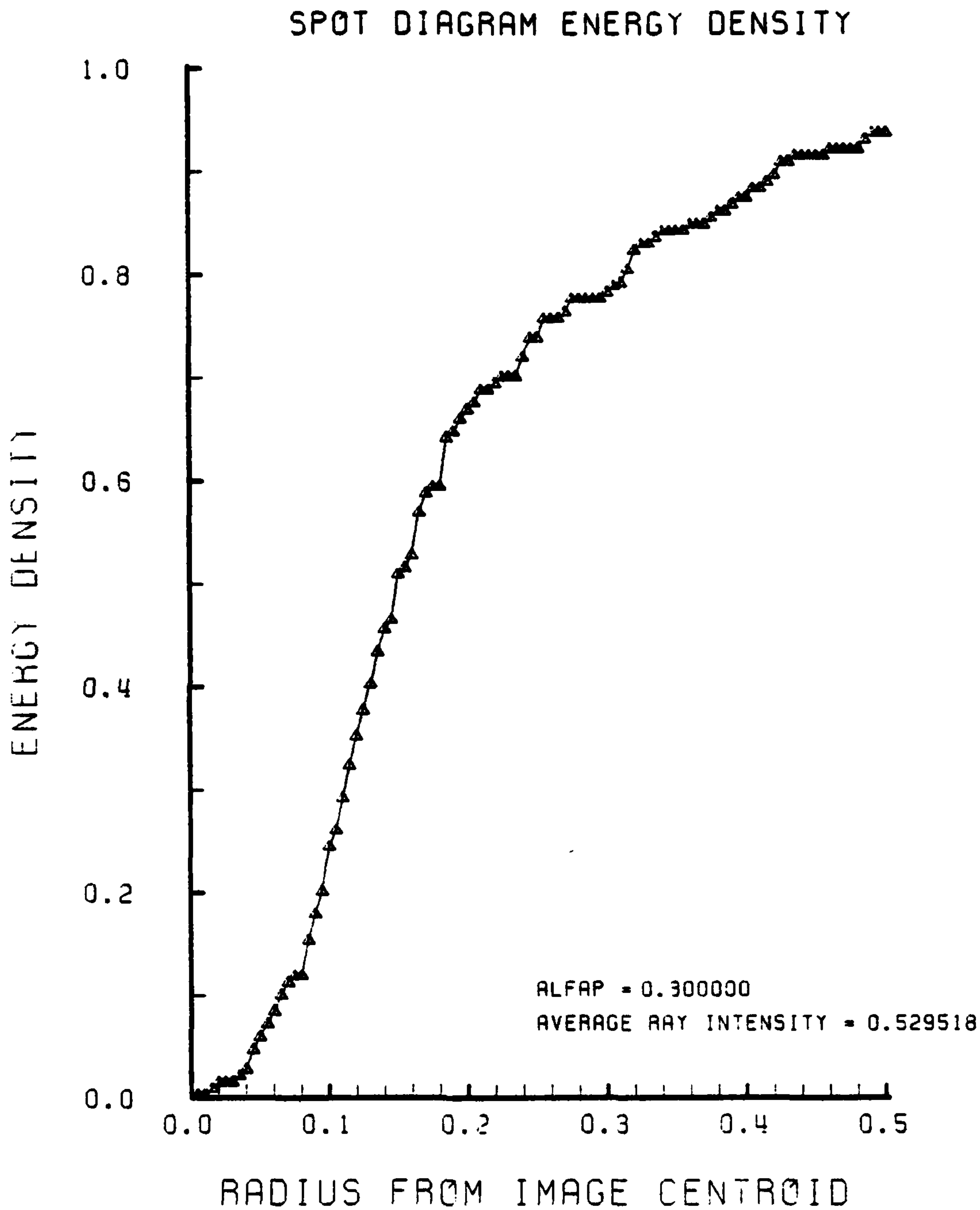

Figure F-84. Encircled Energy of Figure F-83

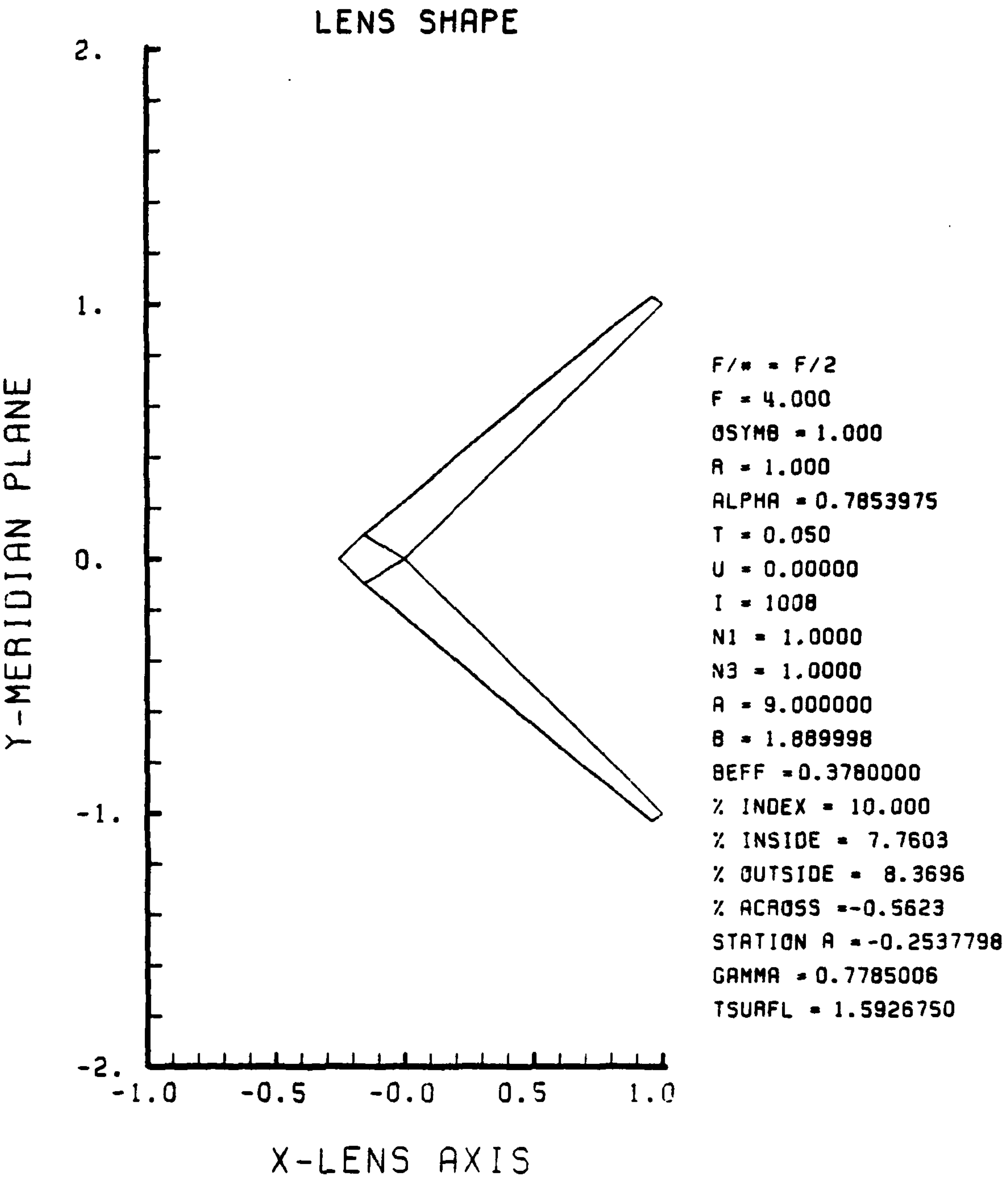

Figure F-85. GRIN Lens Shape at +10%, OB = 1.00, a = 9.00

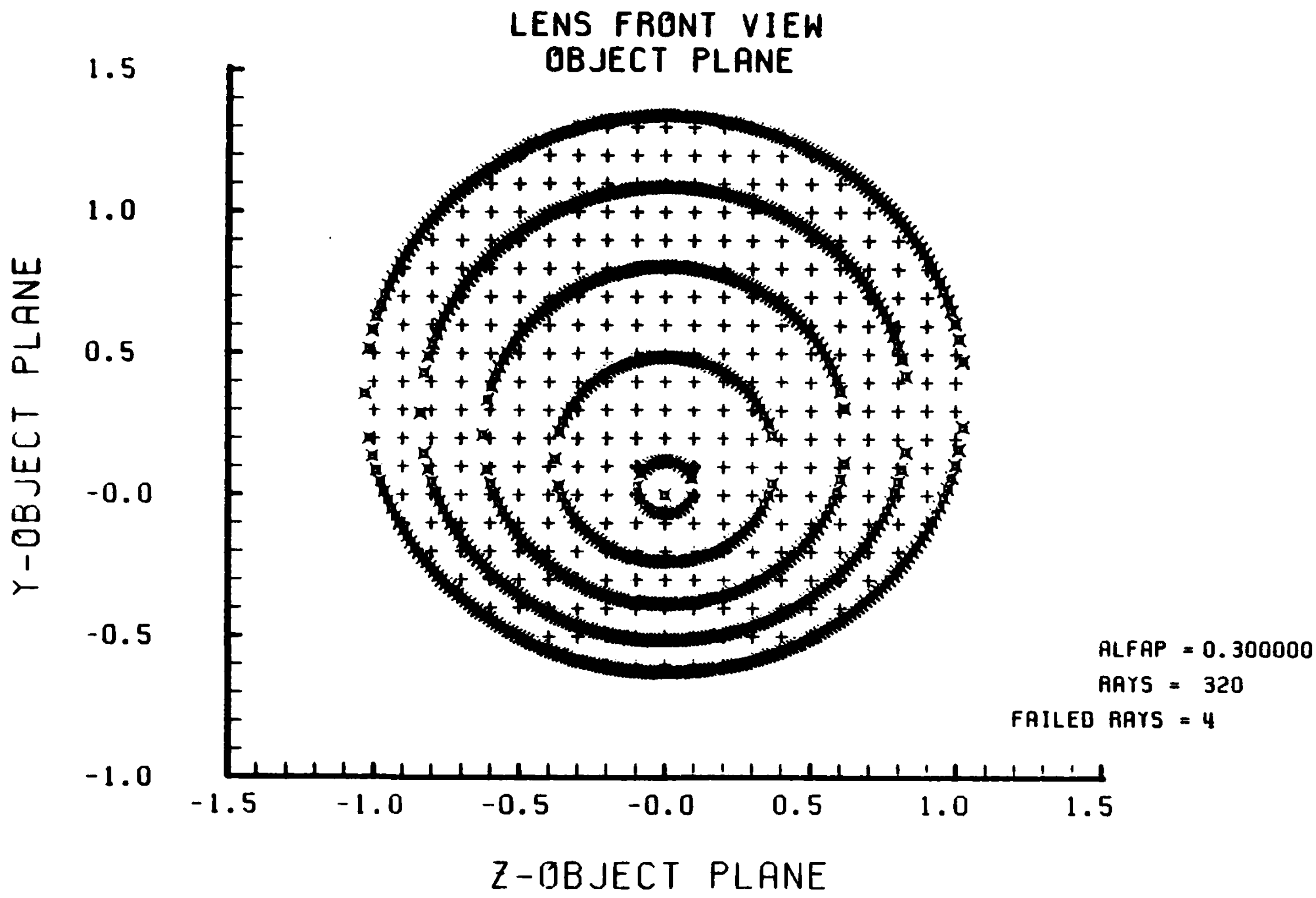

Figure F-86. Grid Plane at $\alpha_p = 0.3$ for Lens of Figure F-85

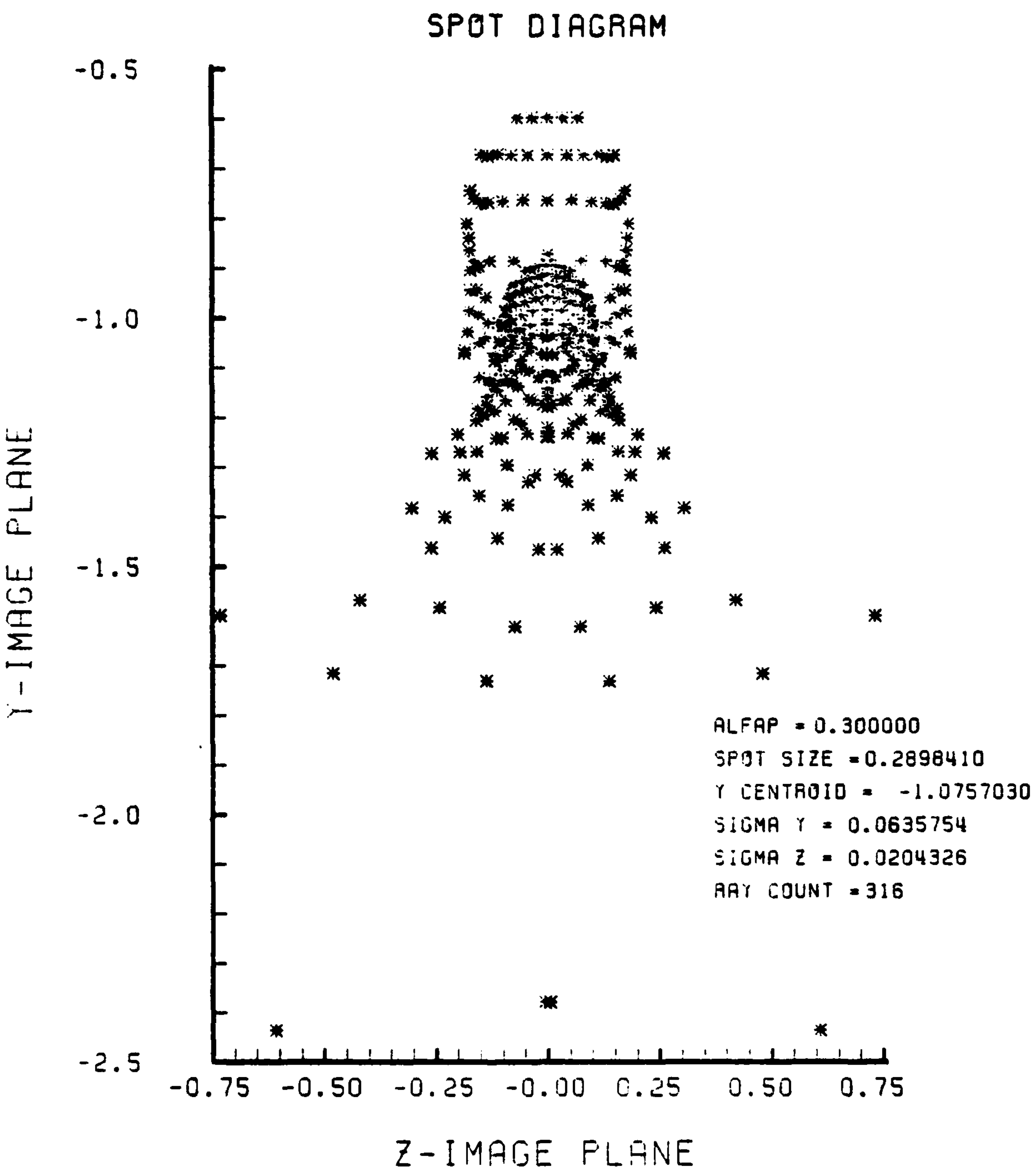

Figure F-87. Spot Diagram for Grid of Figure F-86

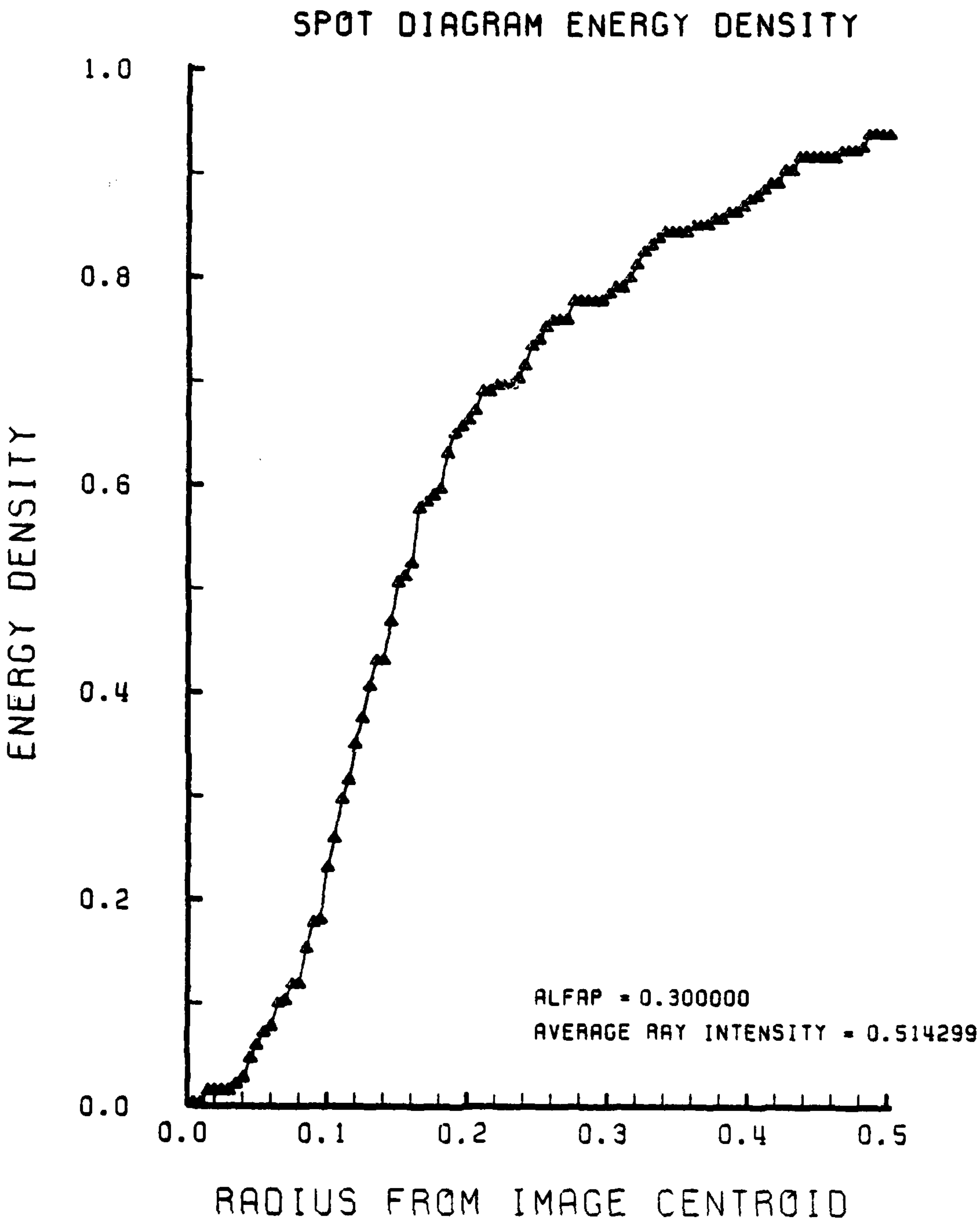

Figure F-88. Encircled Energy of Figure F-87

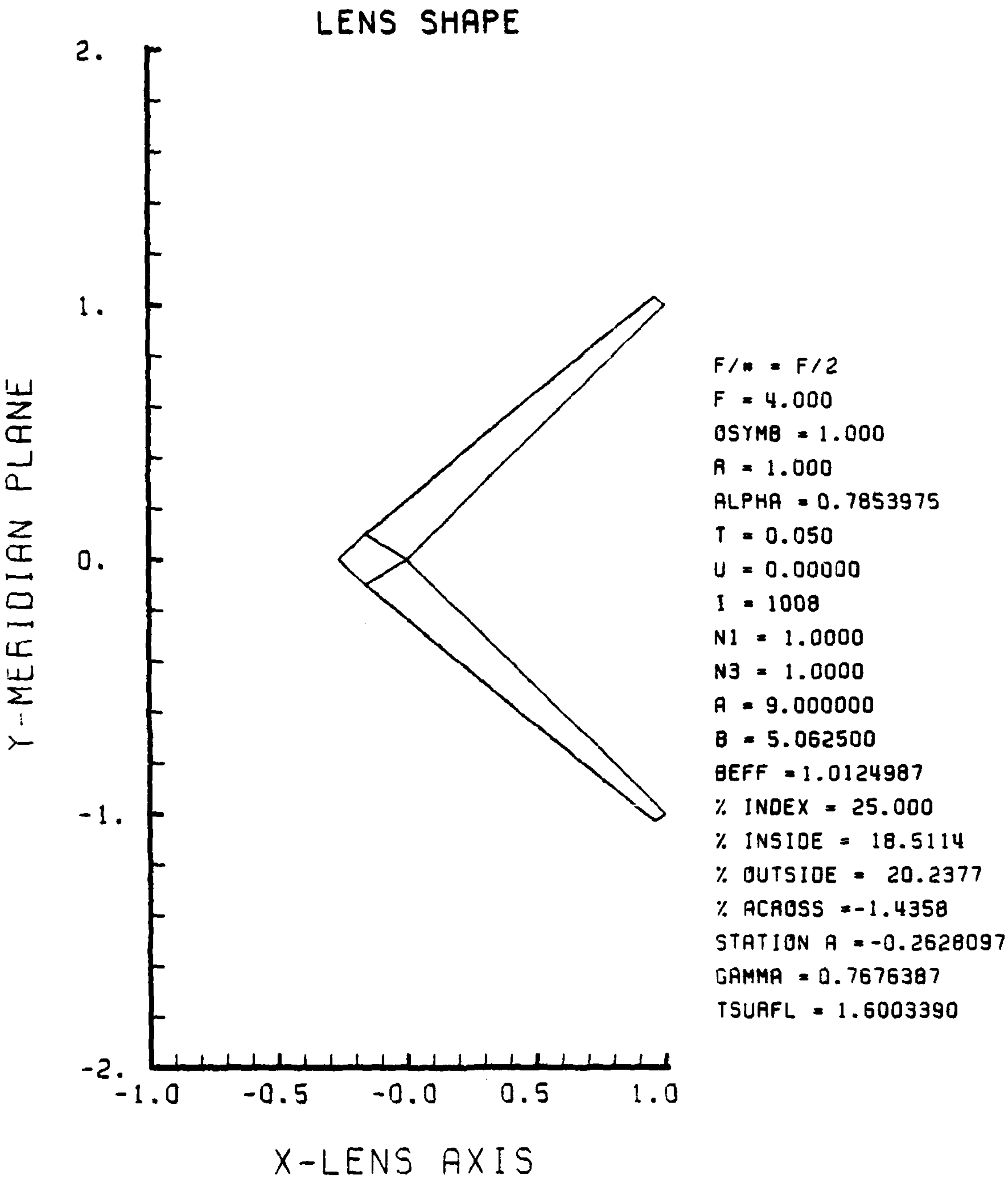

Figure F-89. GRIN Lens Shape at +25%, OB = 1.00, a = 9.00

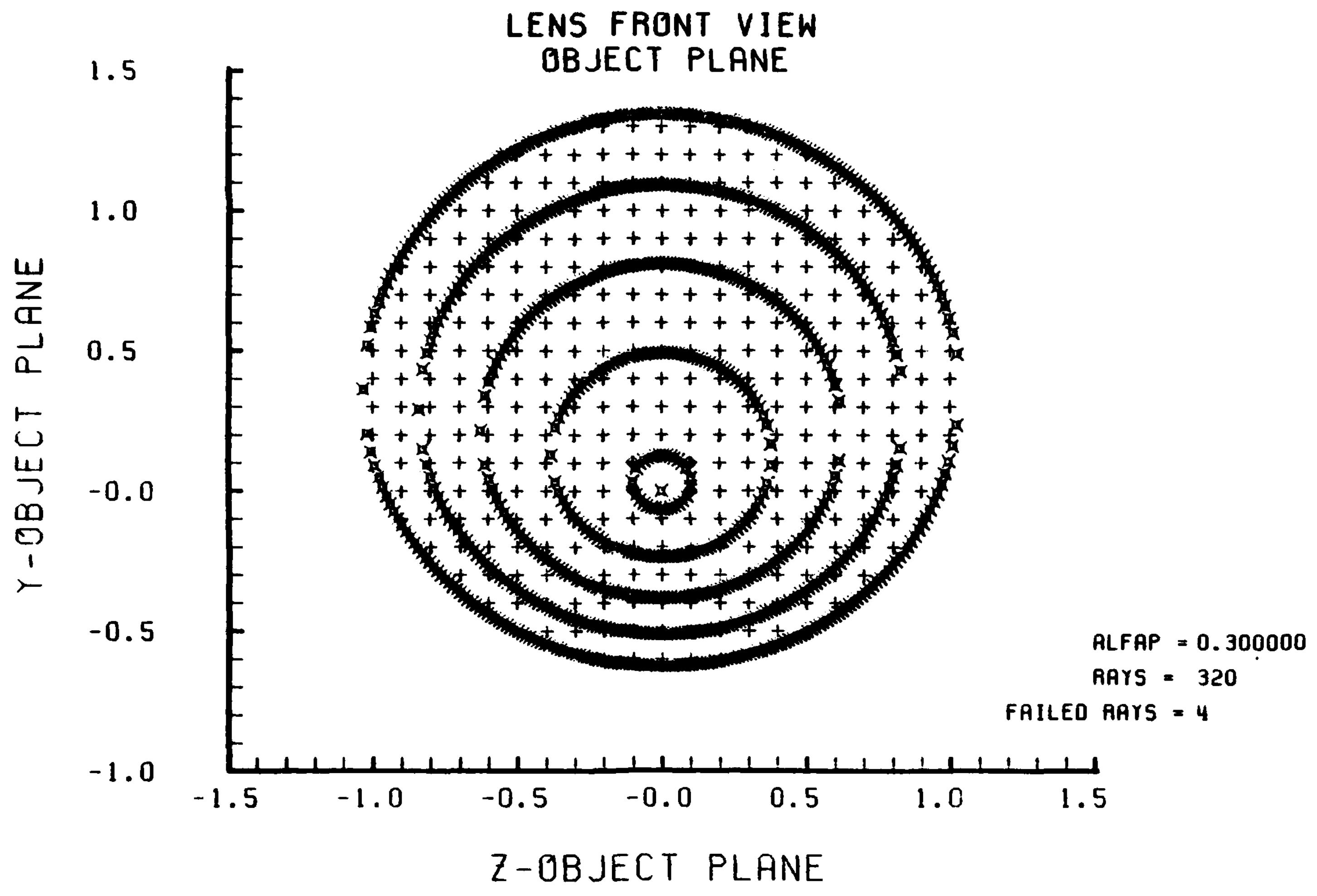

Figure F-90. Grid Plane at $\alpha_p = 0.3$ for Lens of Figure F-89

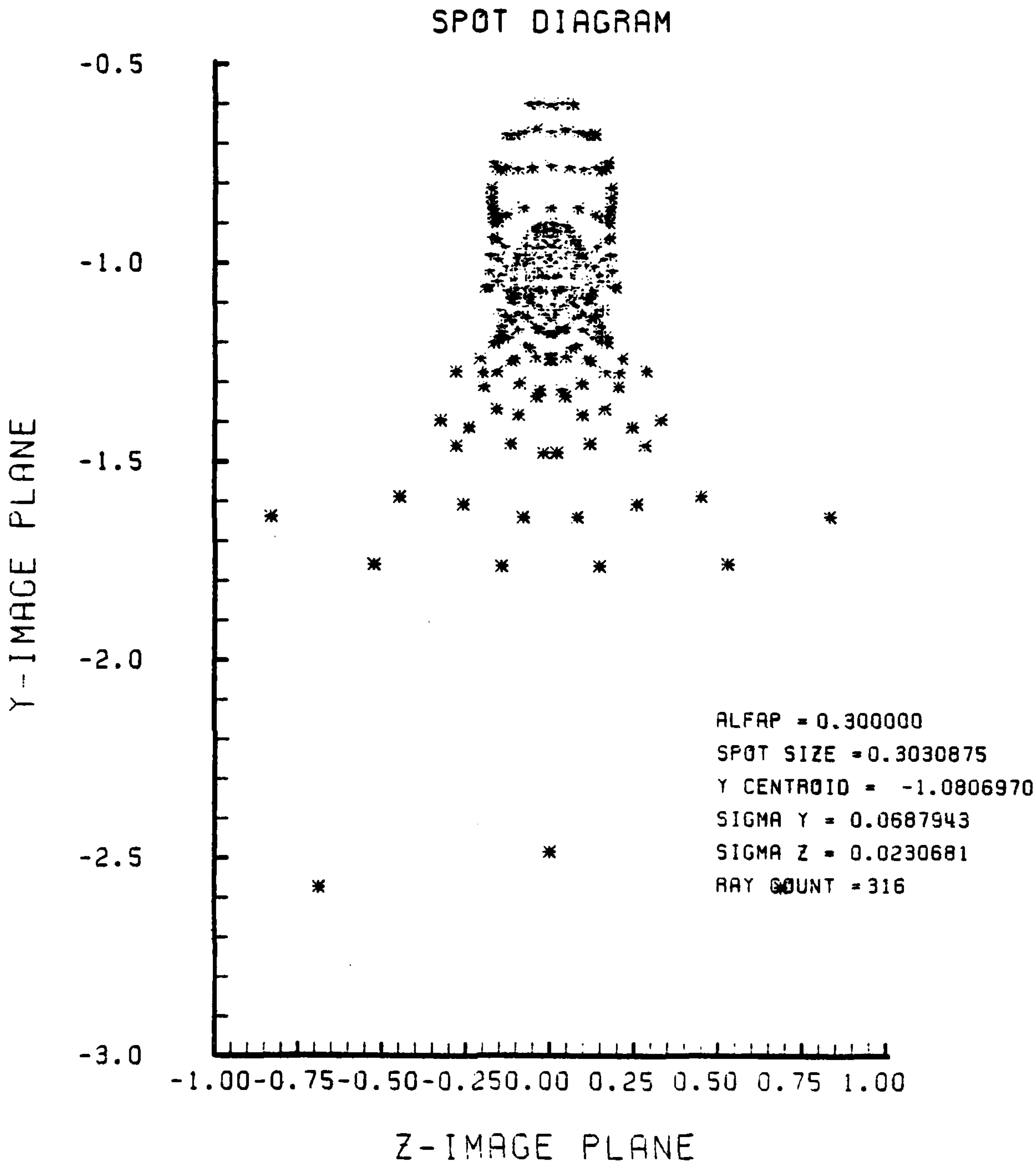

Figure F-91. Spot Diagram for Grid of Figure F-90

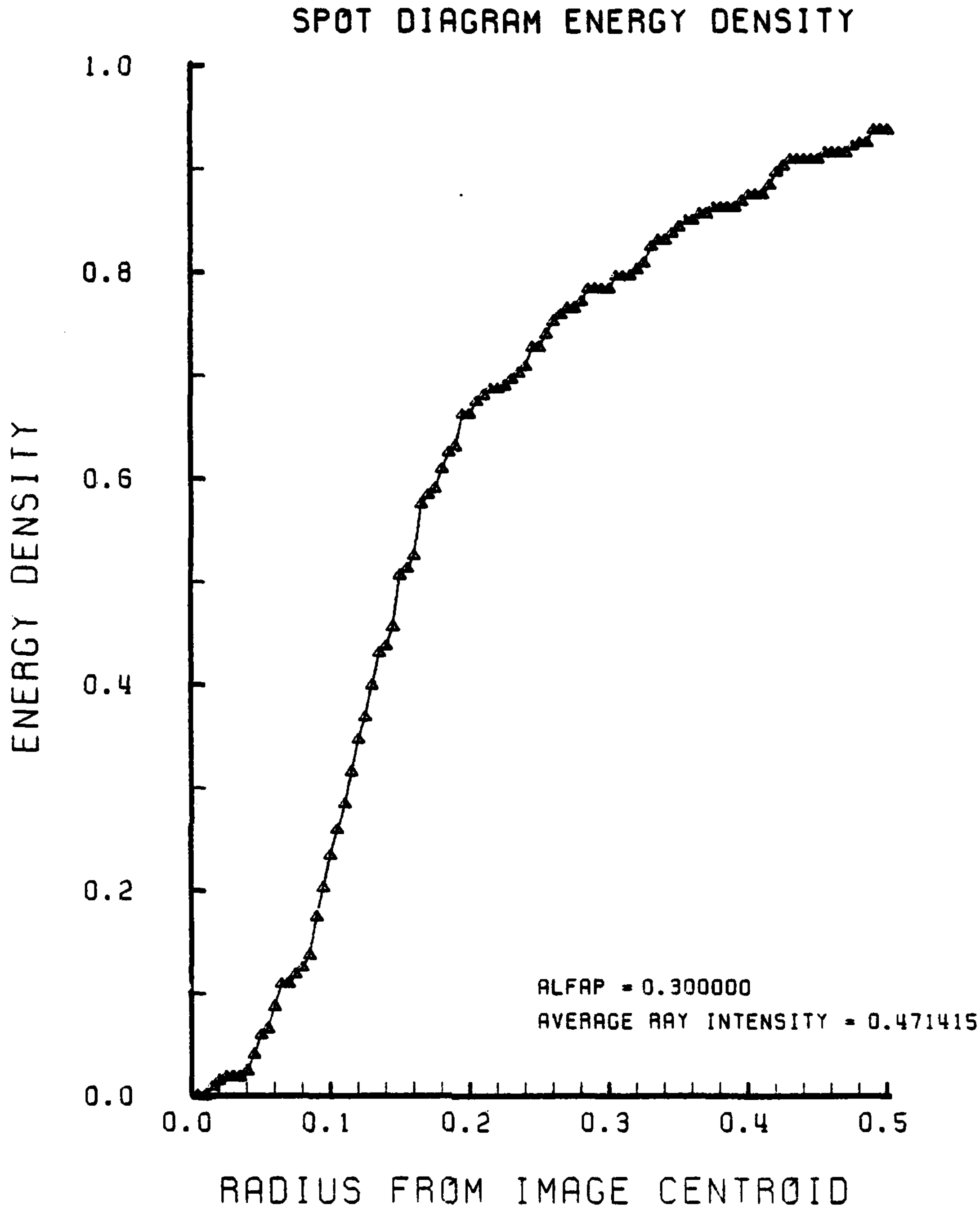

Figure F-92. Encircled Energy of Figure F-91

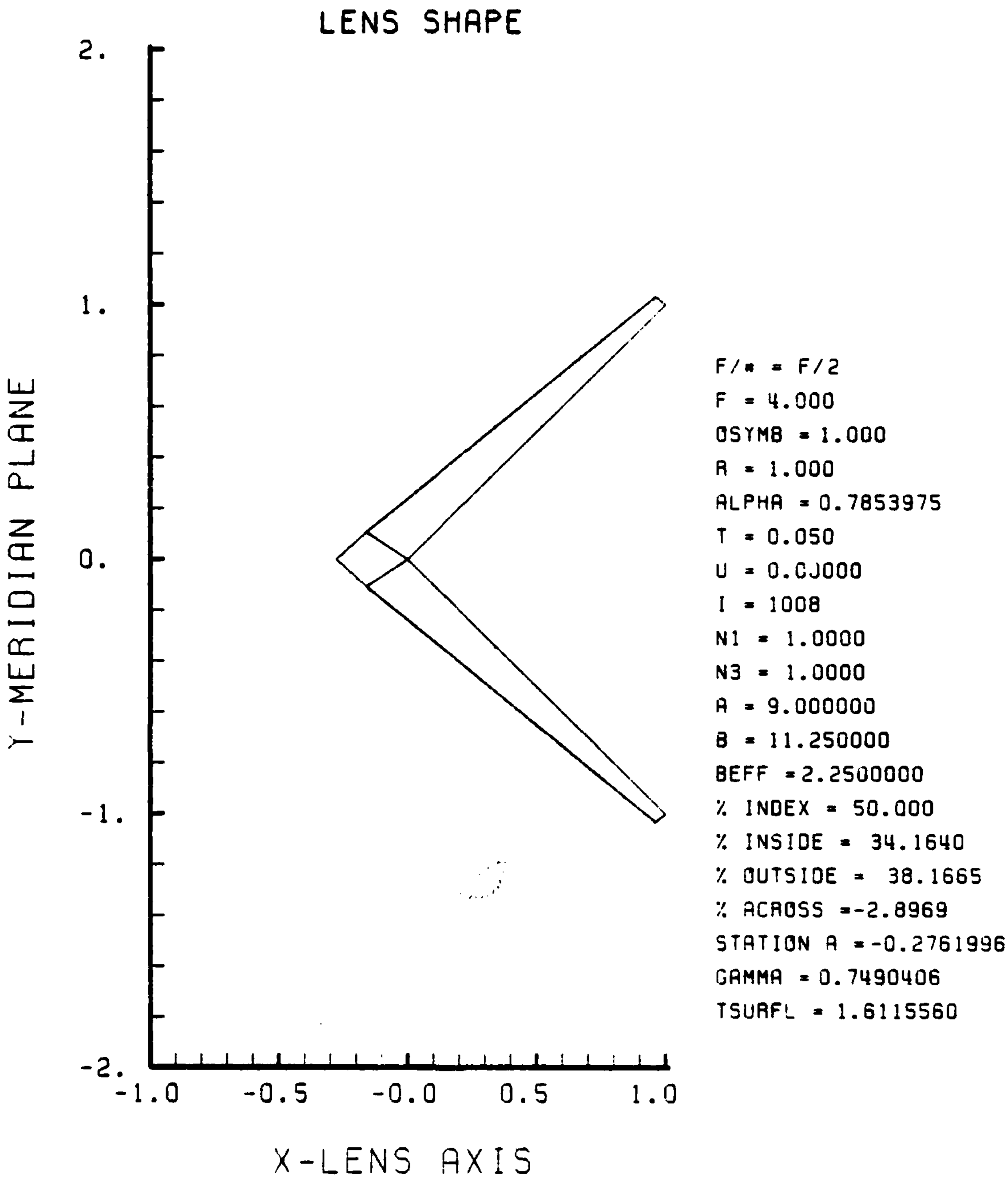

Figure F-93. GRIN Lens Shape at +50%, OB = 1.00, a = 9.00

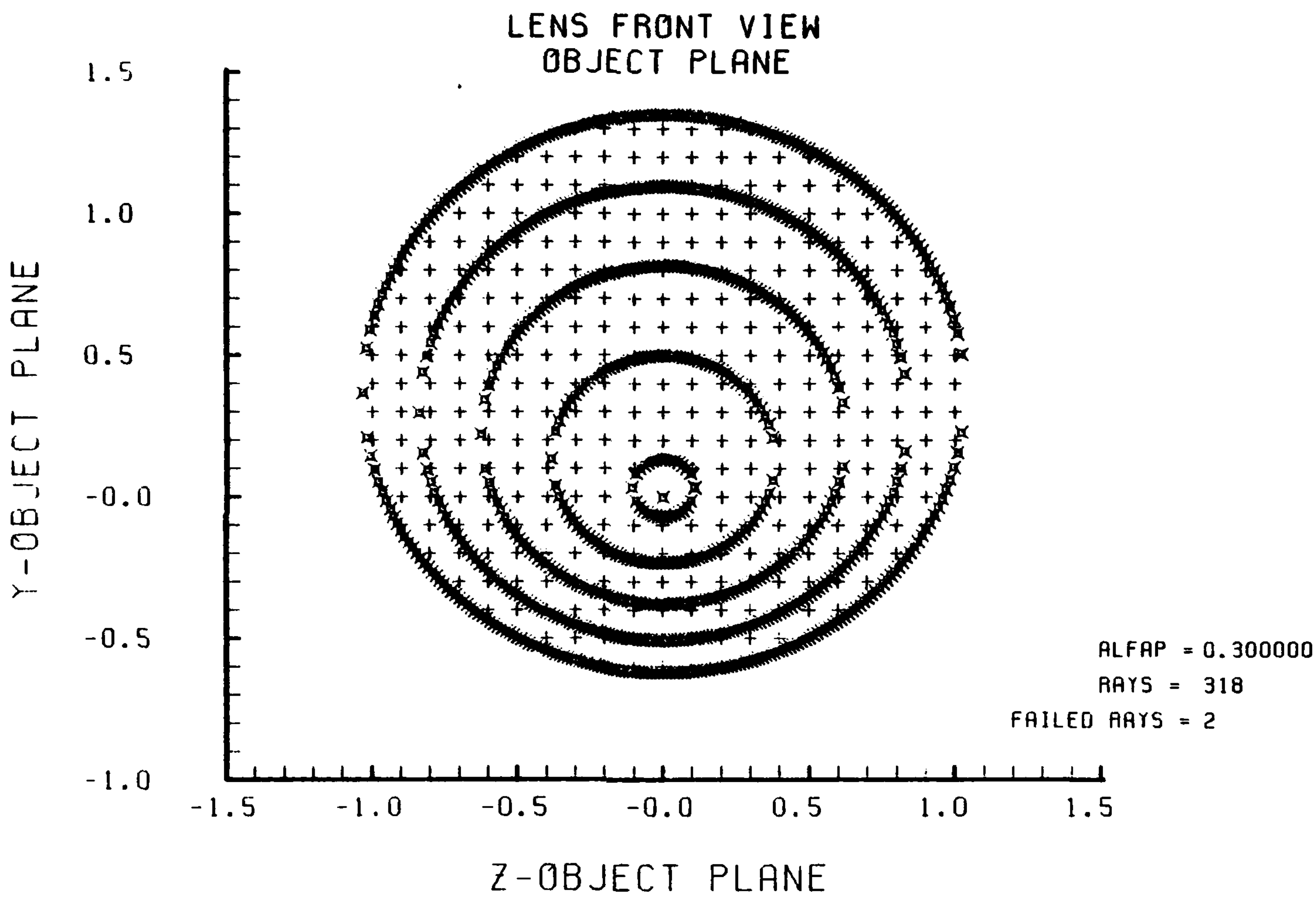

Figure F-94. Grid Plane at $\alpha_p = 0.3$ for Lens of Figure F-93

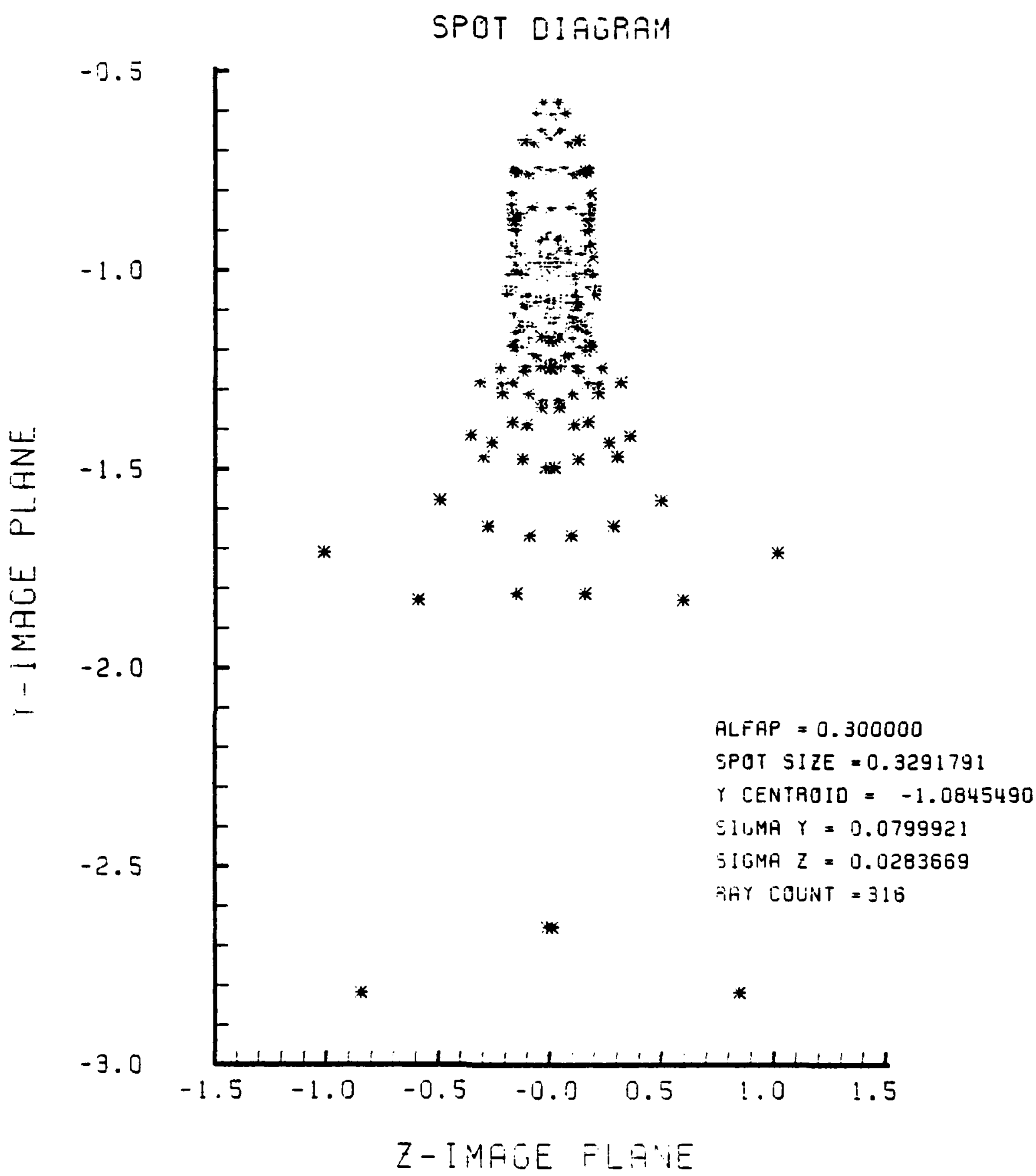

Figure F-95. Spot Diagram for Grid of Figure F-94

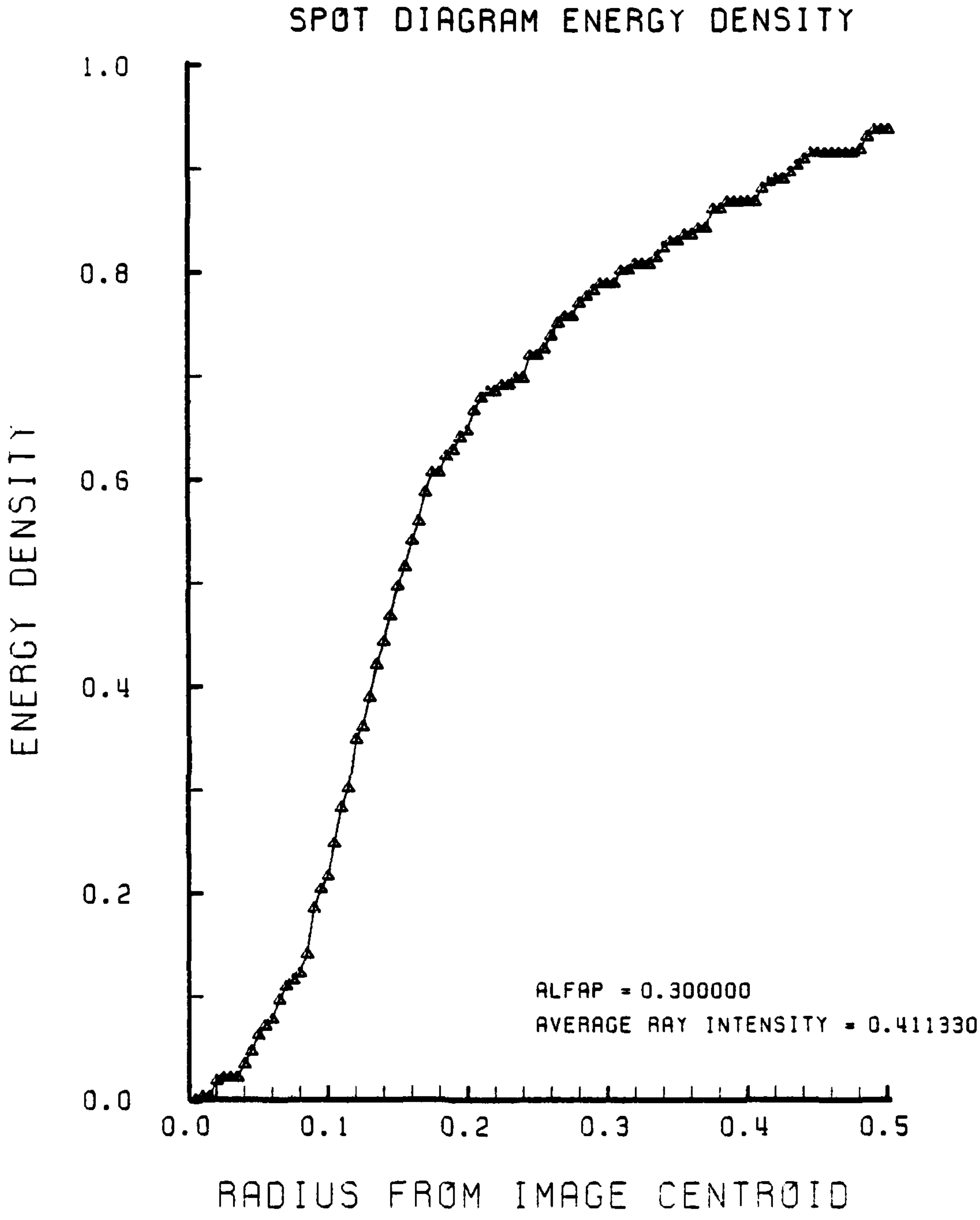

Figure F-96. Encircled Energy of Figure F-95

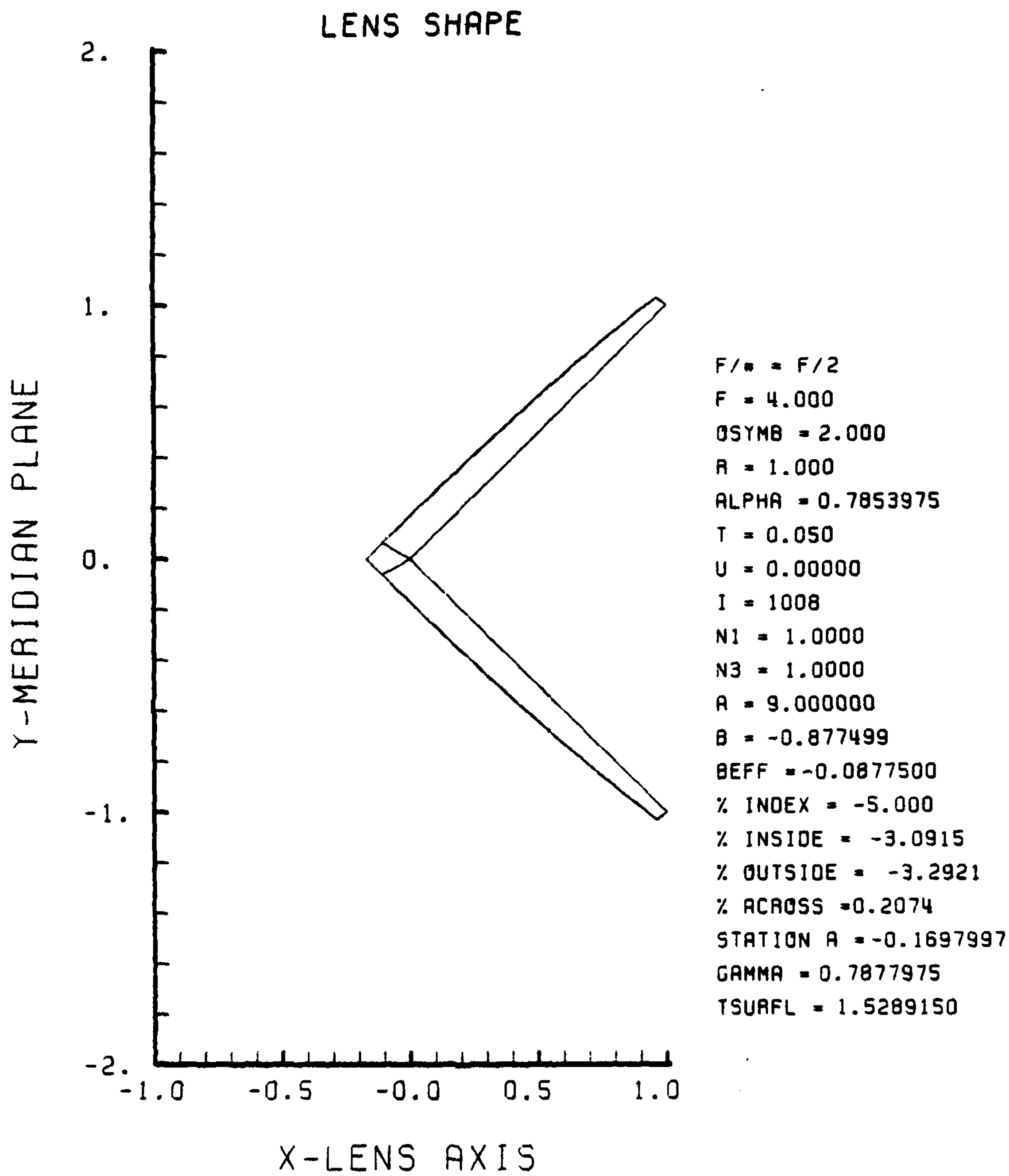

Figure F-97. GRIN Lens Shape at -5%, OB = 2.00, a = 9.00

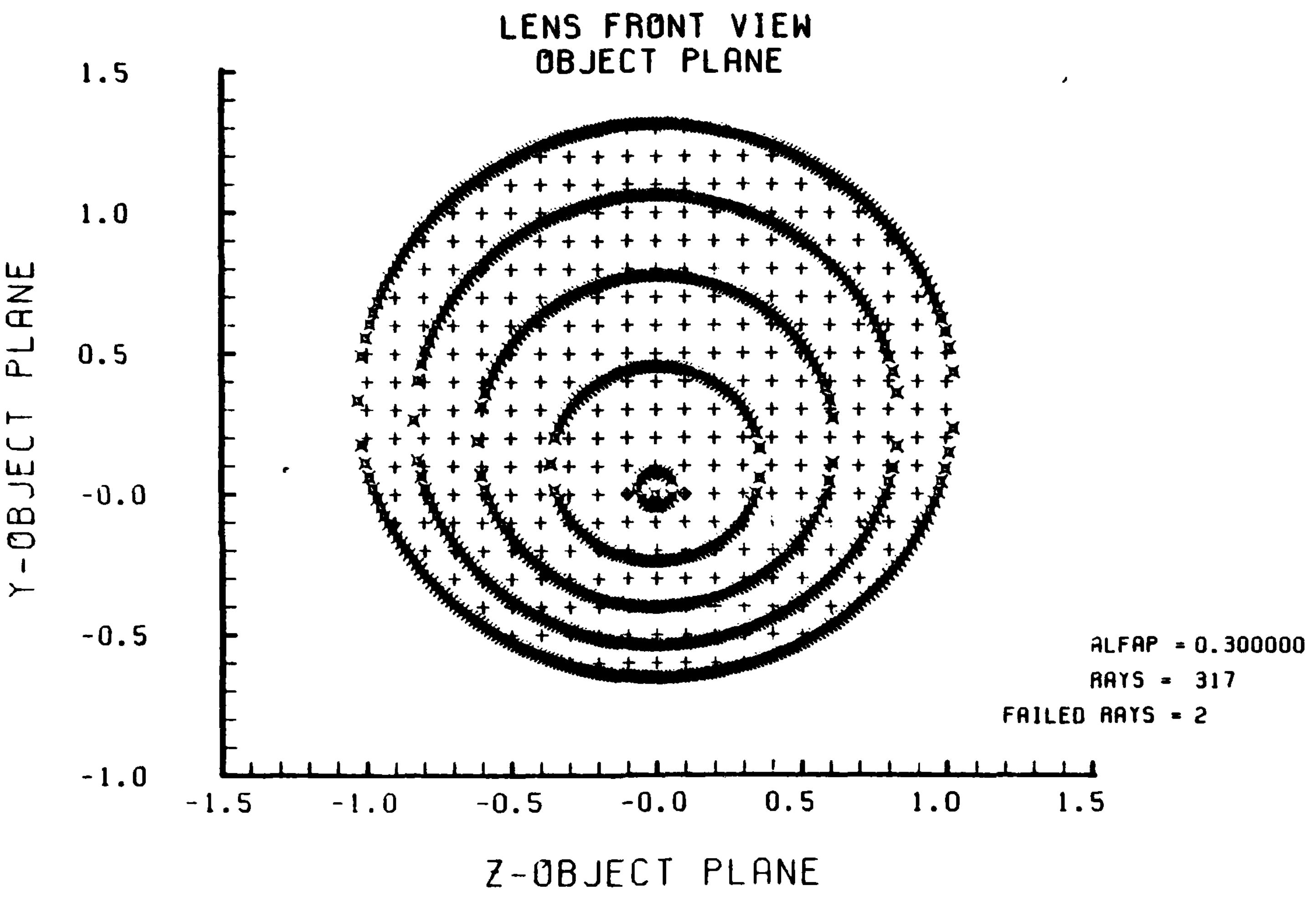

Figure F-98. Grid Plane at $\alpha_p = 0.3$ for Lens of Figure F-97

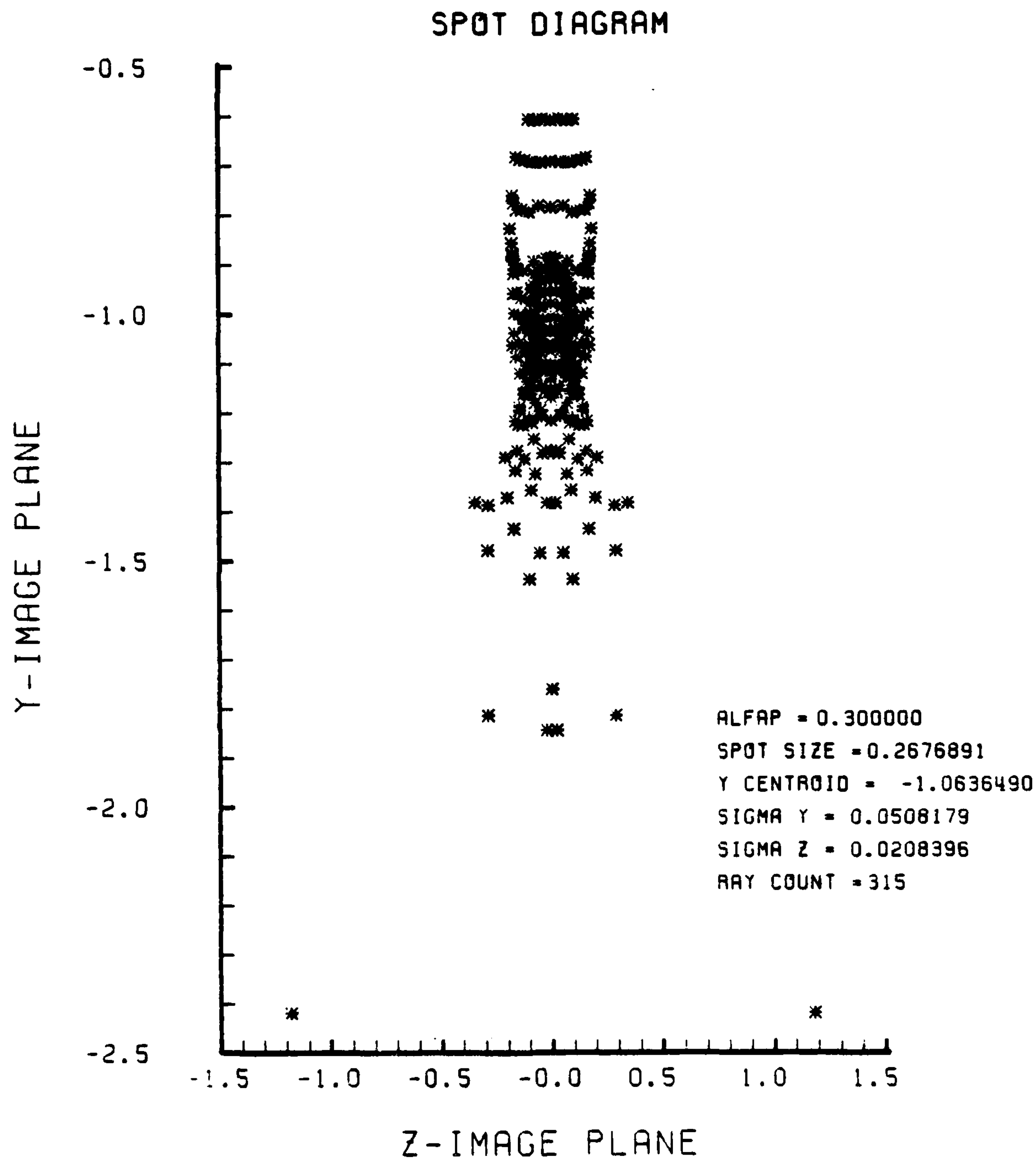

Figure F-99. Spot Diagram for Grid of Figure F-98

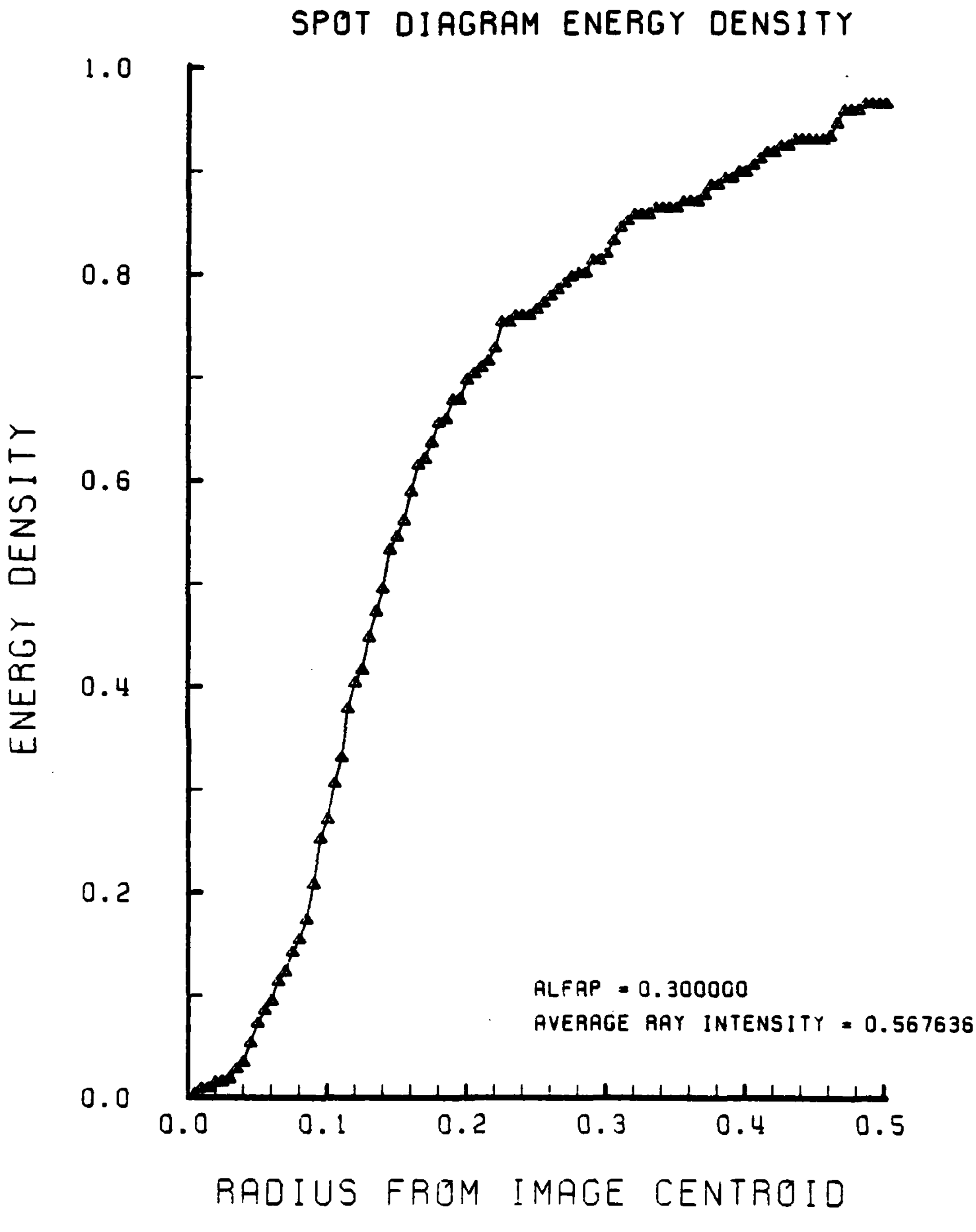

Figure F-100. Encircled Energy of Figure F-99

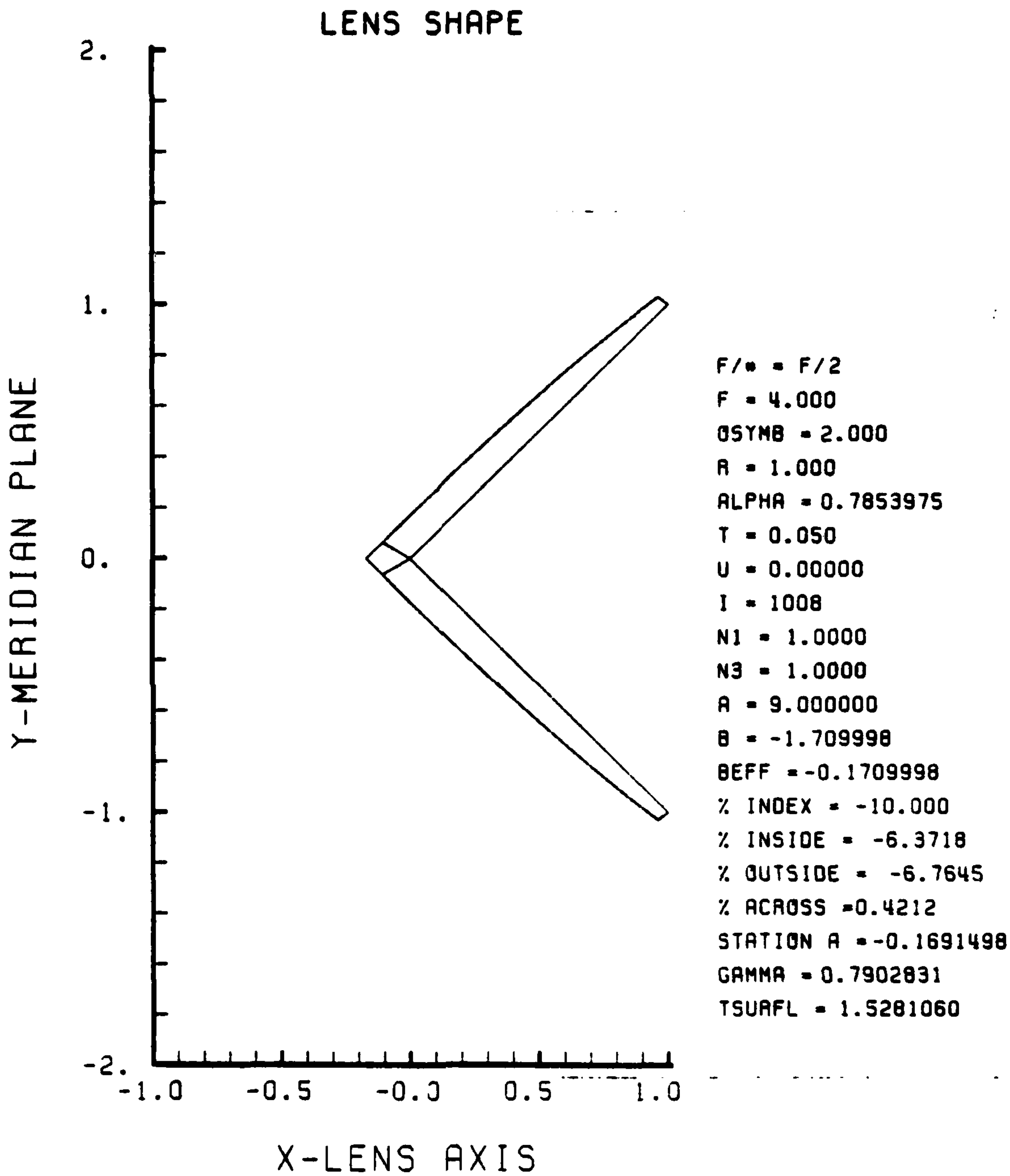

Figure F-101. GRIN Lens Shape at -10%, OB = 2.00, a = 9.00

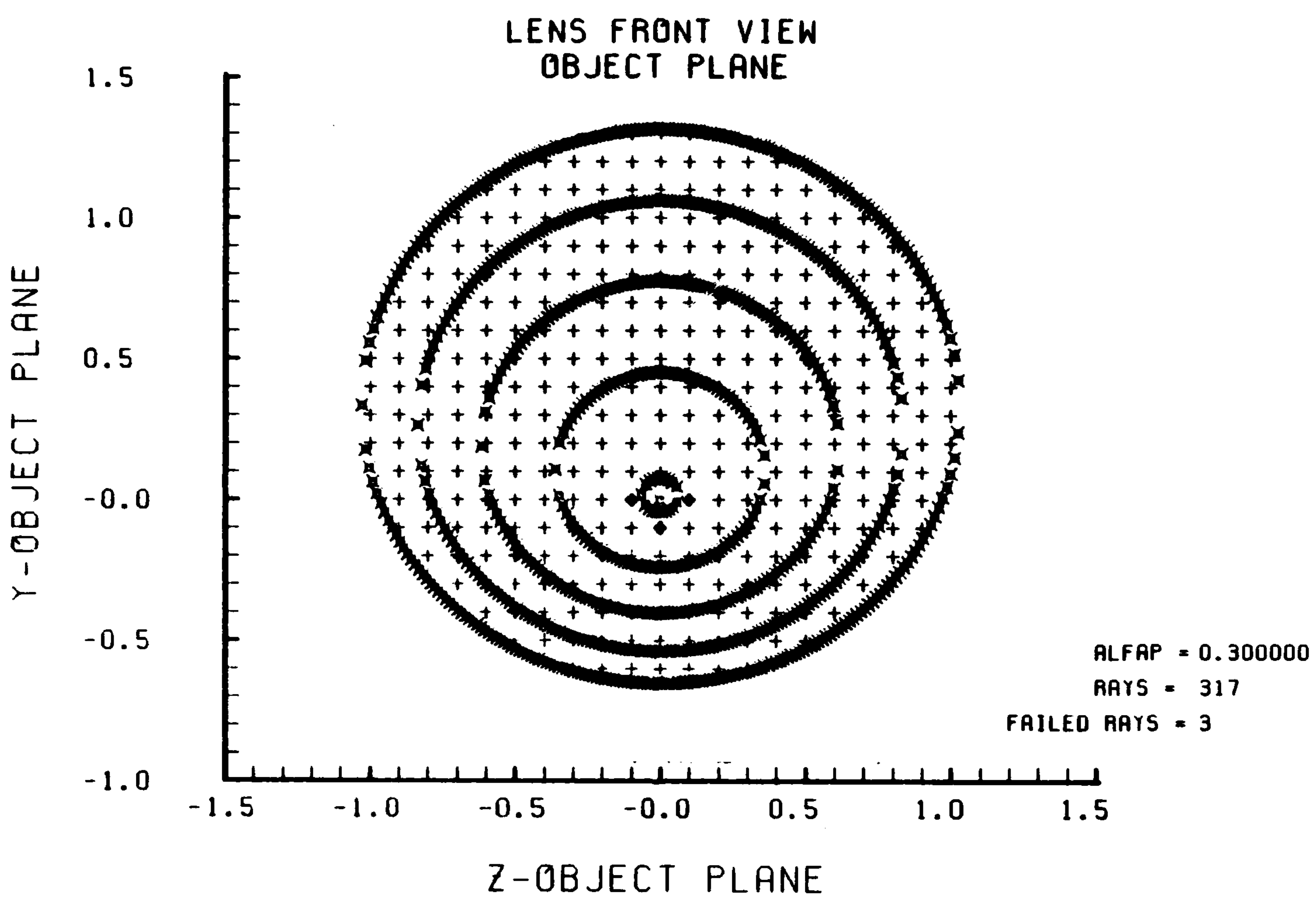

Figure F-102. Grid Plane at $\alpha_p = 0.3$ for Lens of Figure F-101

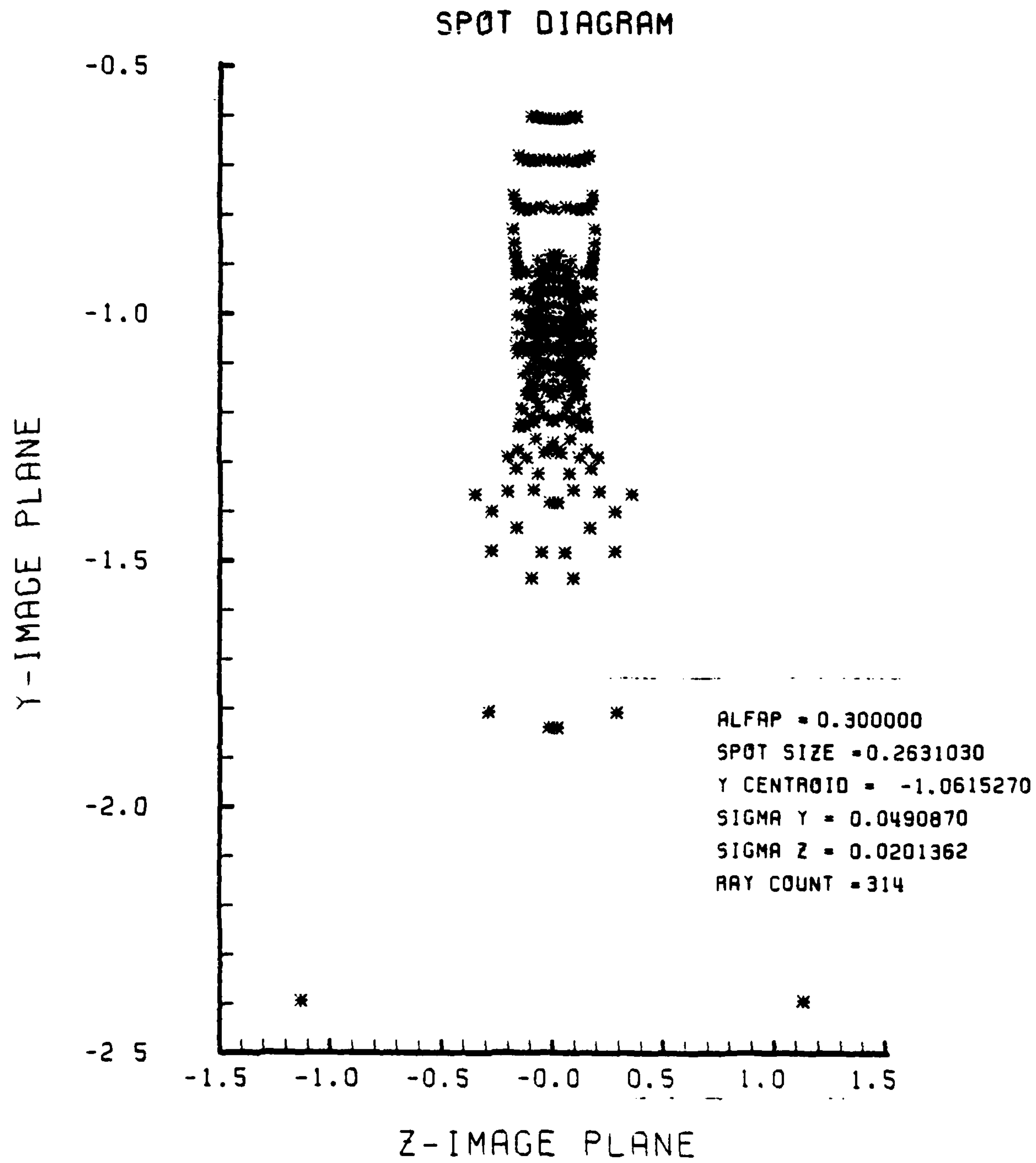

Figure F-103. Spot Diagram for Grid of Figure F-102

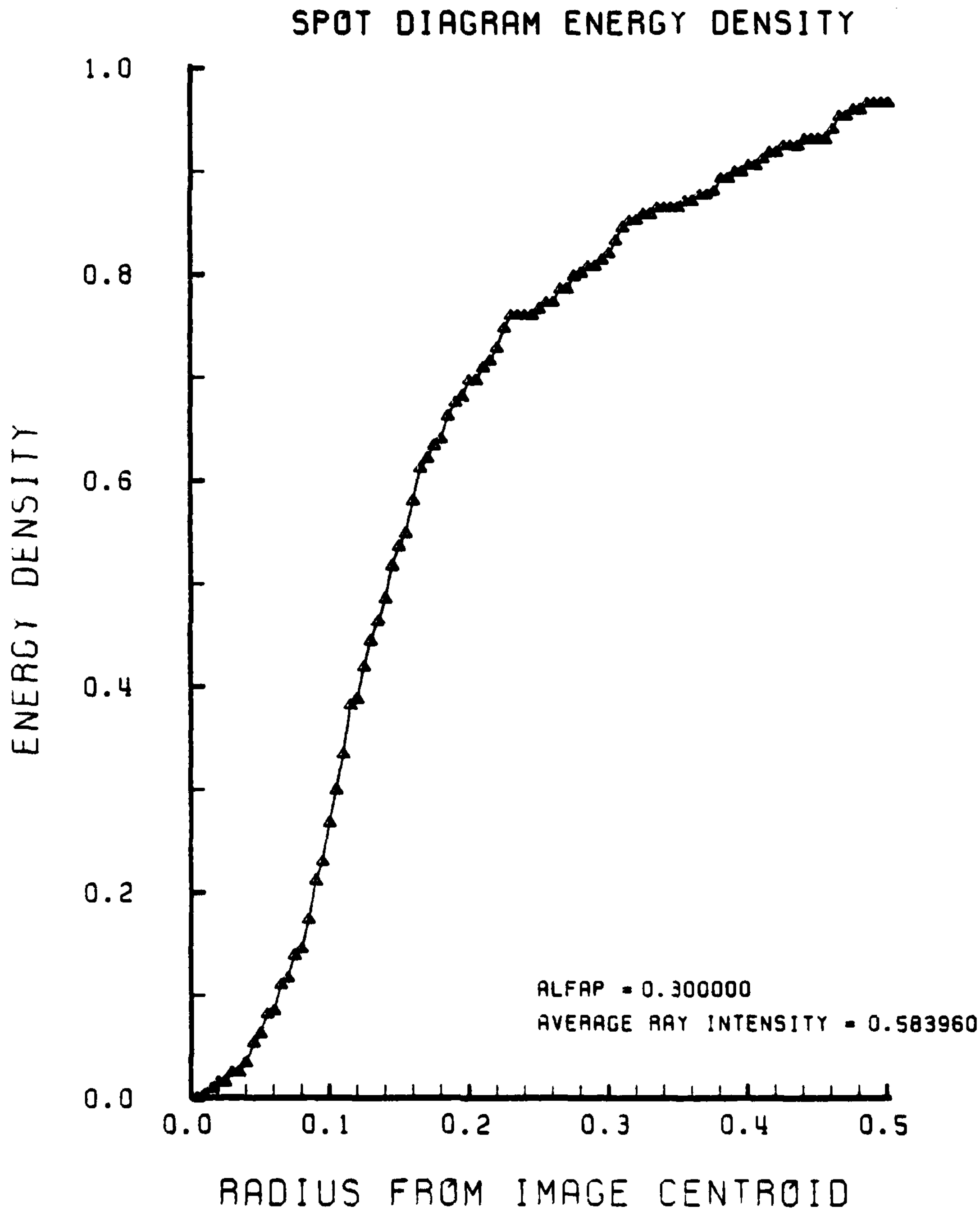

Figure F-104. Encircled Energy of Figure F-103

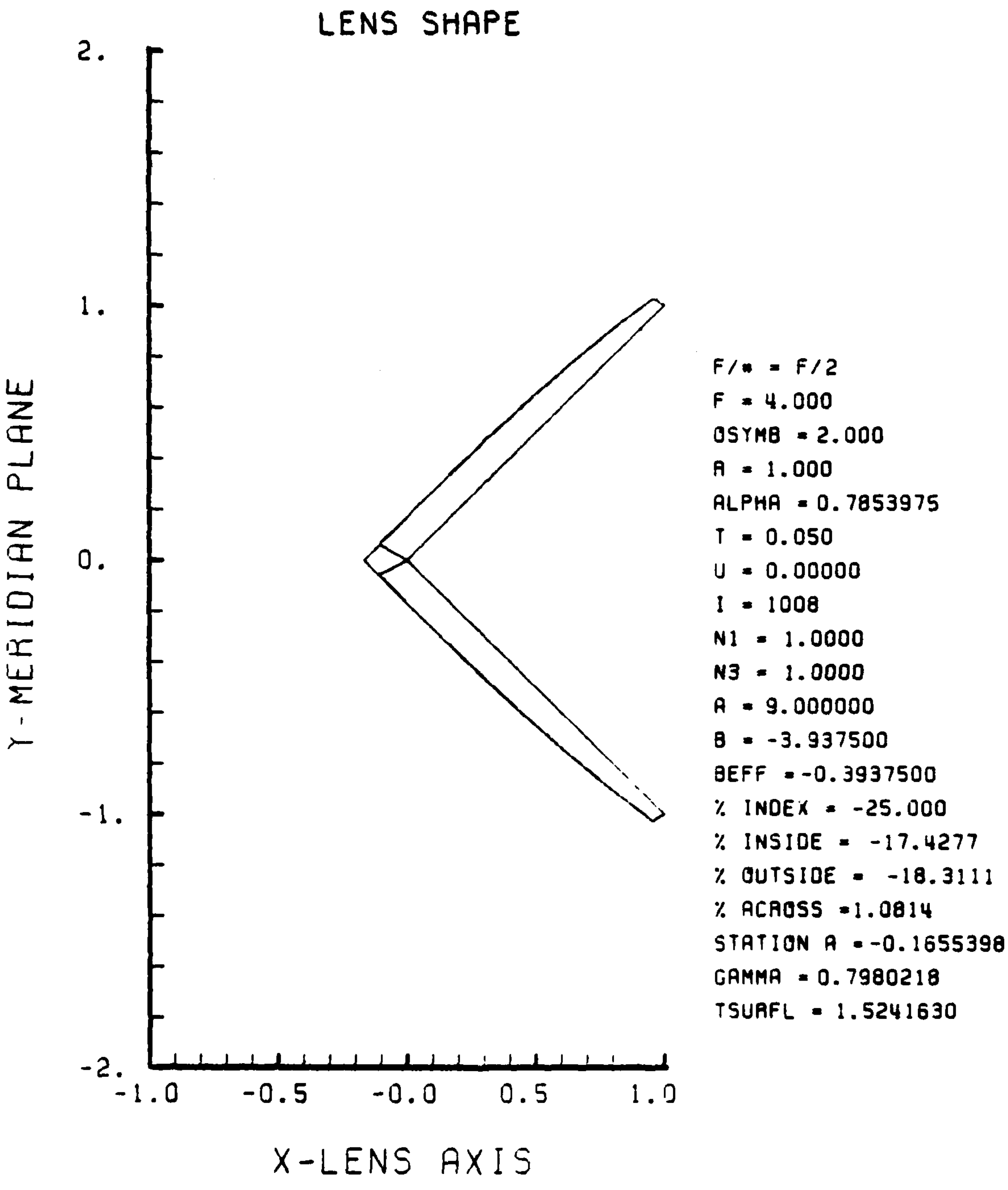

Figure F-105. GRIN Lens Shape at -25%, OB = 2.00, a = 9.00

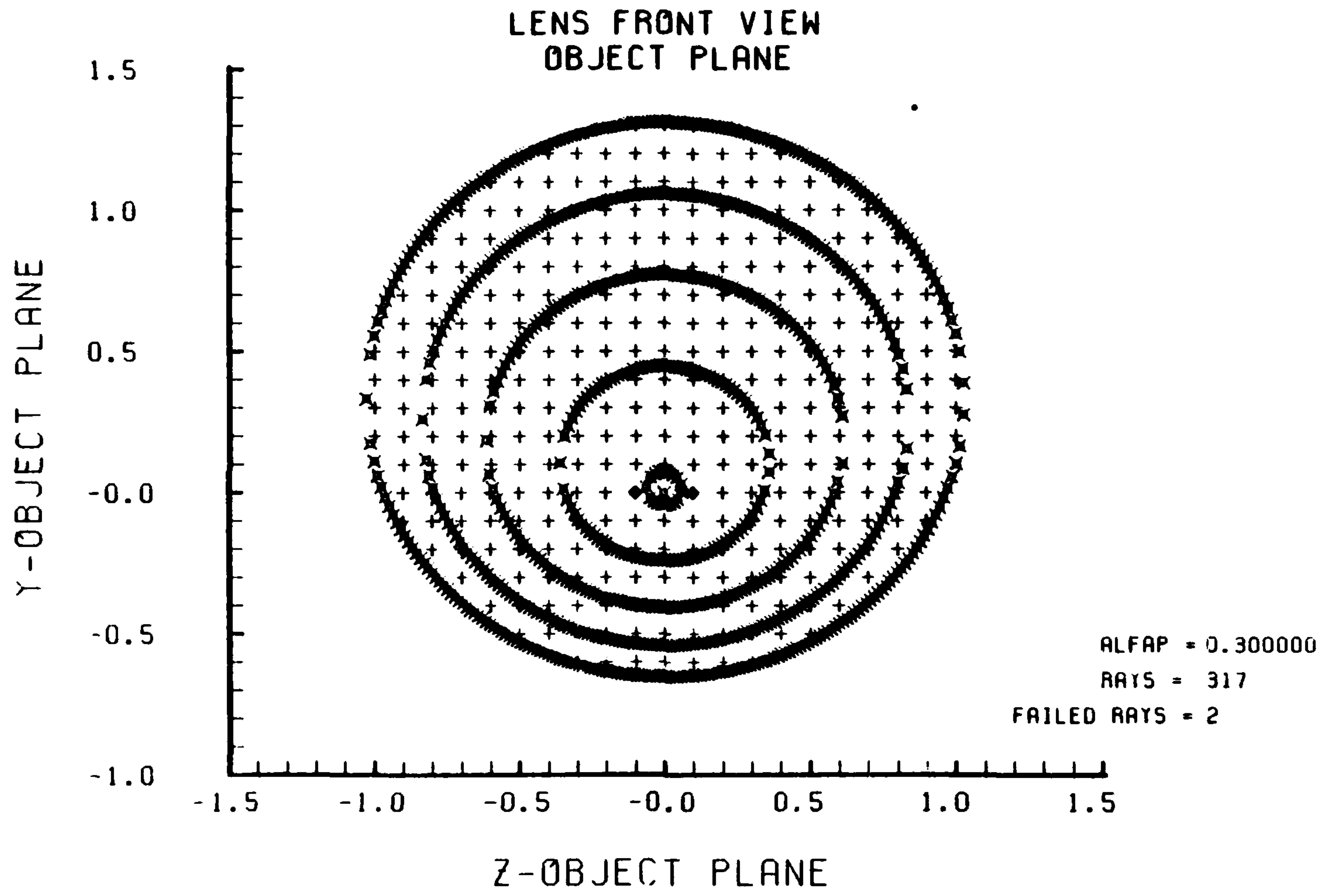

Figure F-106. Grid Plane at $\alpha_p = 0.3$ for Lens of Figure F-105

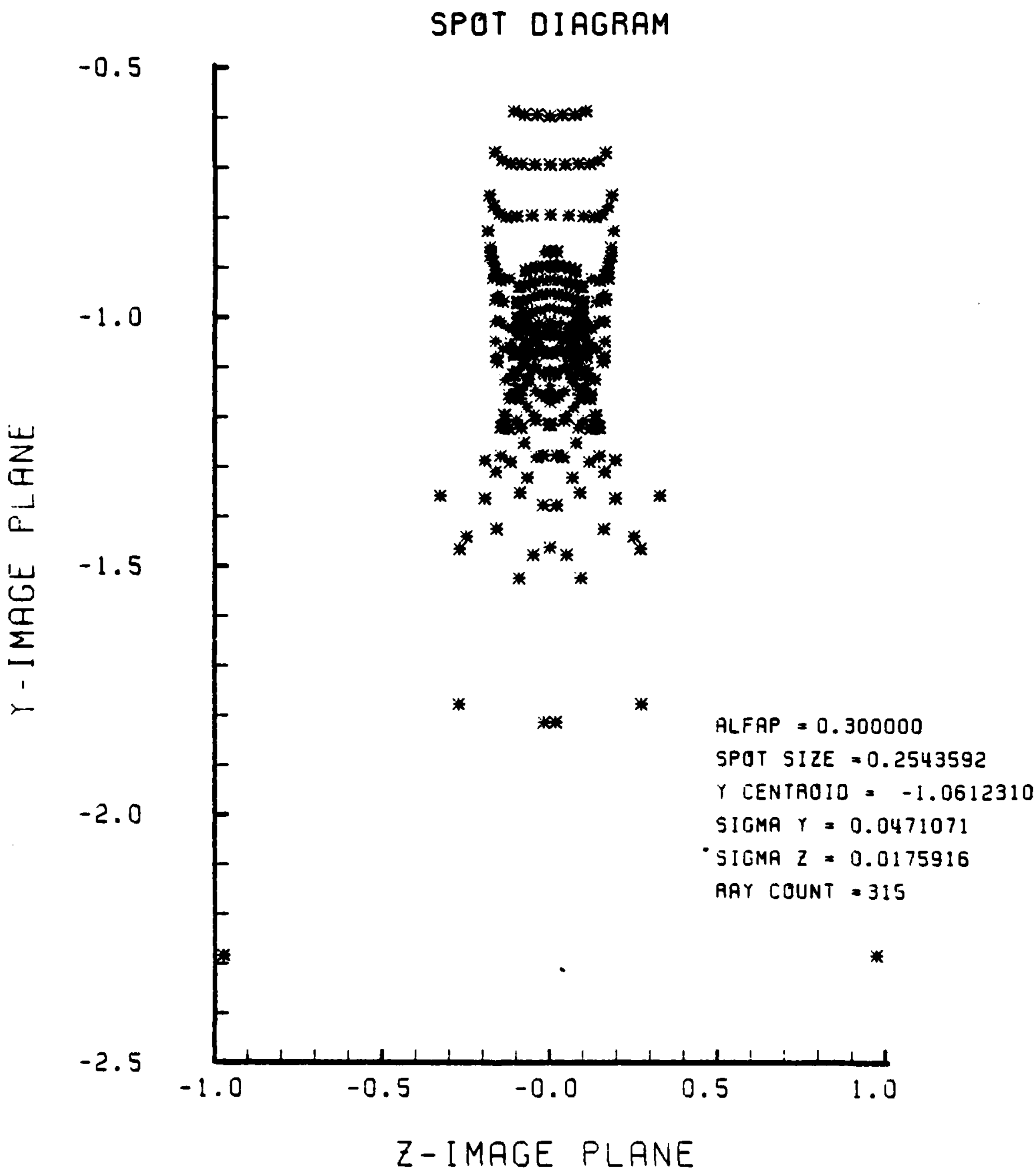

Figure F-107. Spot Diagram for Grid of Figure F-106

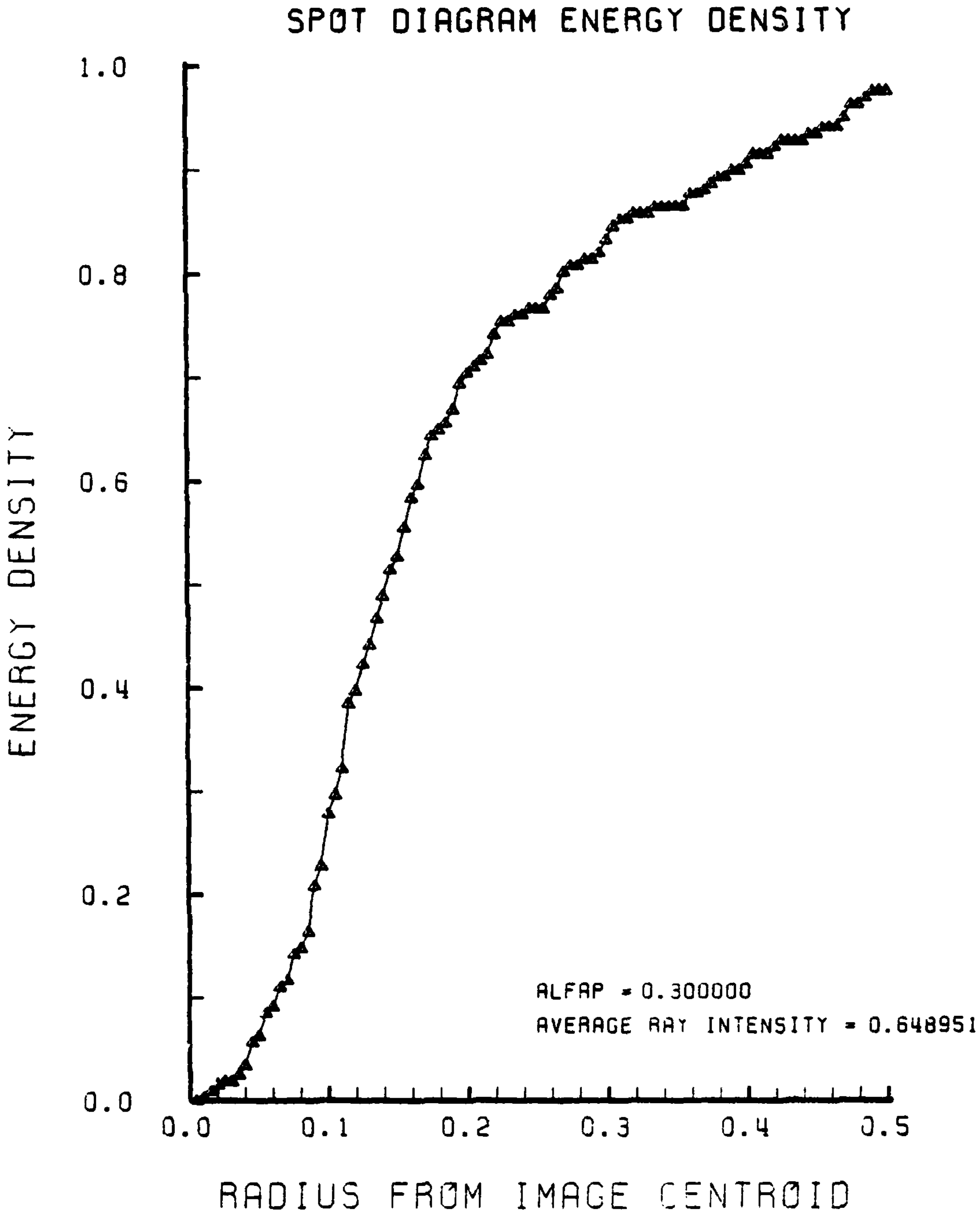

Figure F-108. Encircled Energy of Figure F-107

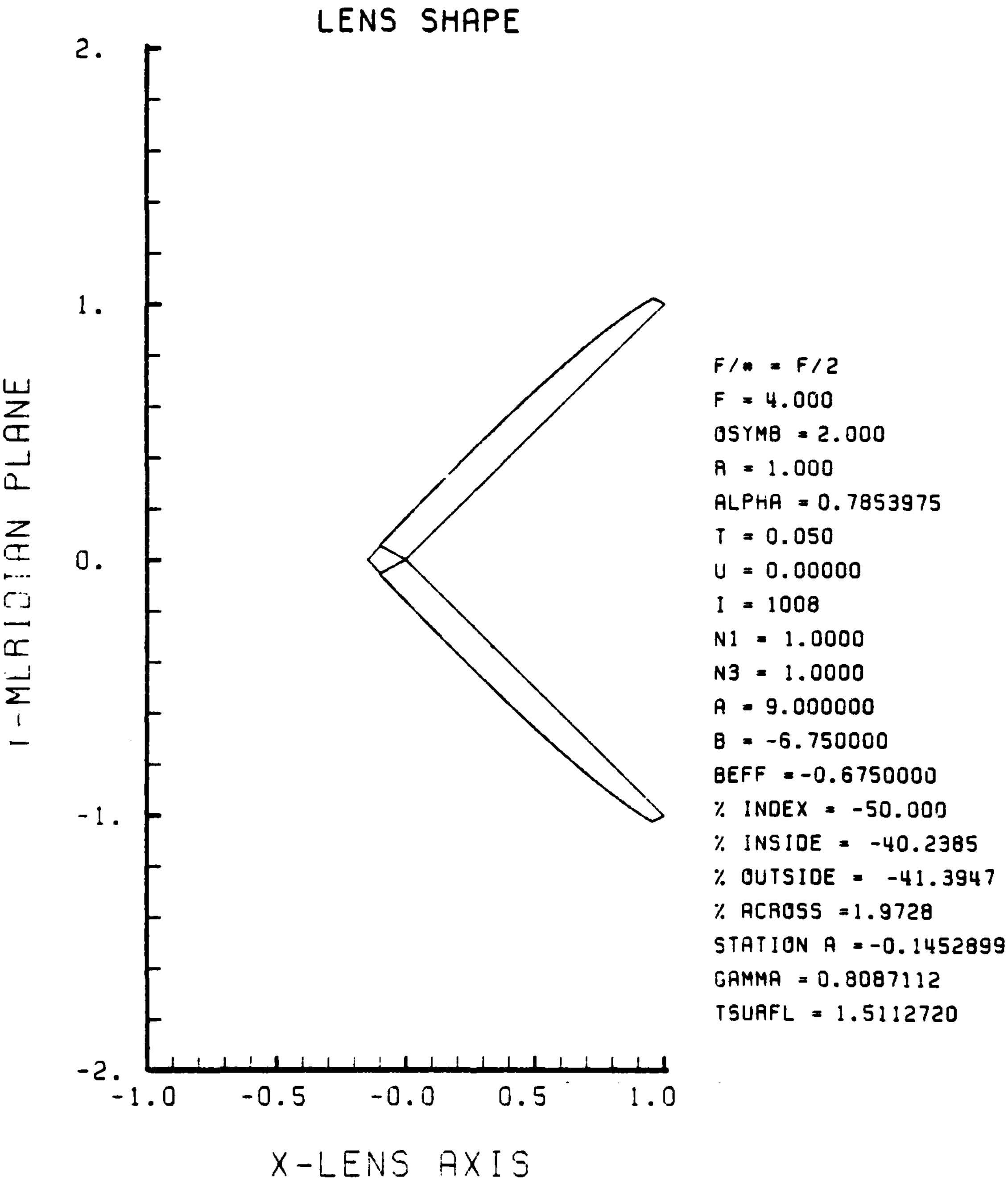

Figure F-109. GRIN Lens Shape at -50%, OB = 2.00, a = 9.00

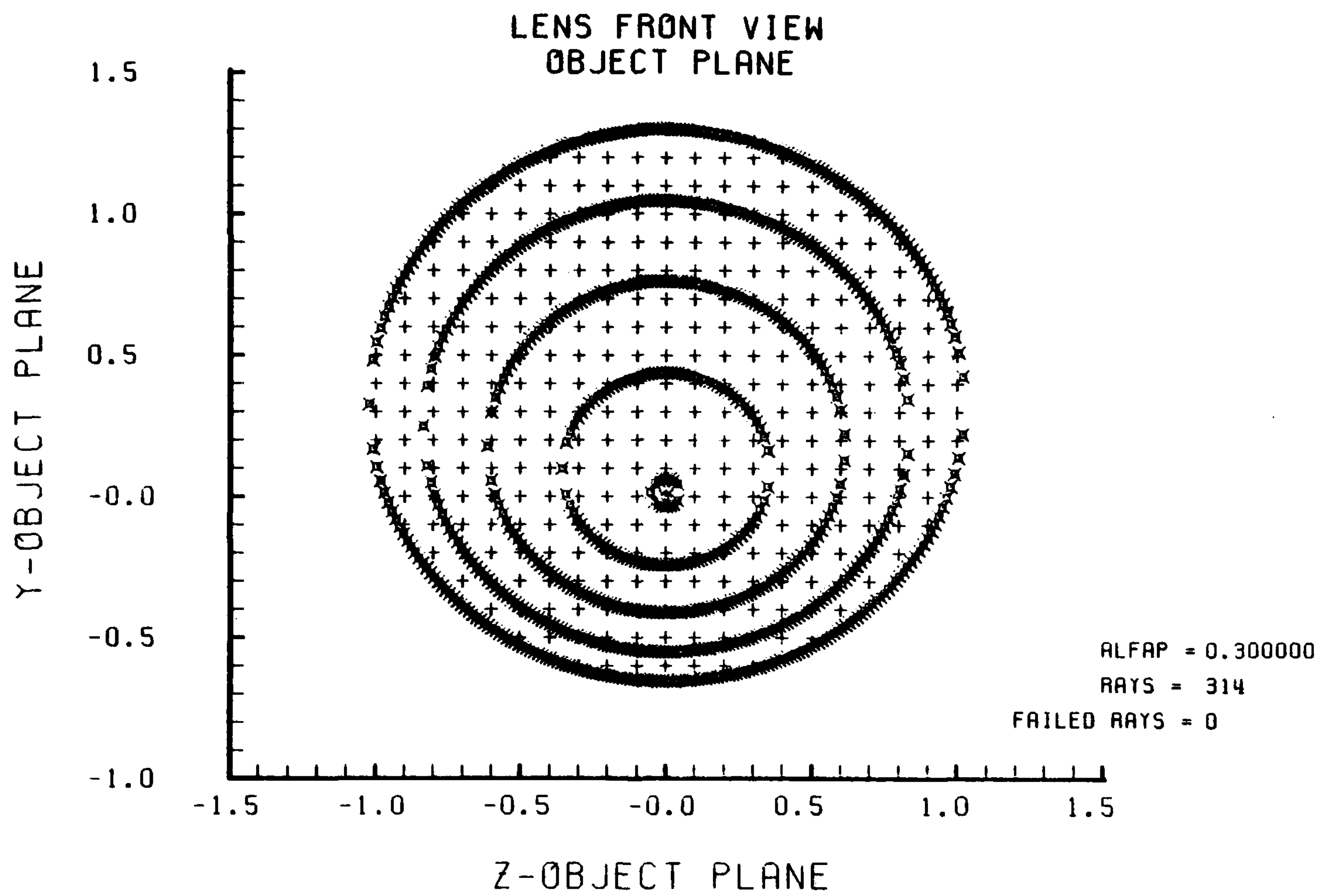

Figure F-110. Grid Plane at $\alpha_p = 0.3$ for Grid of Figure F-109

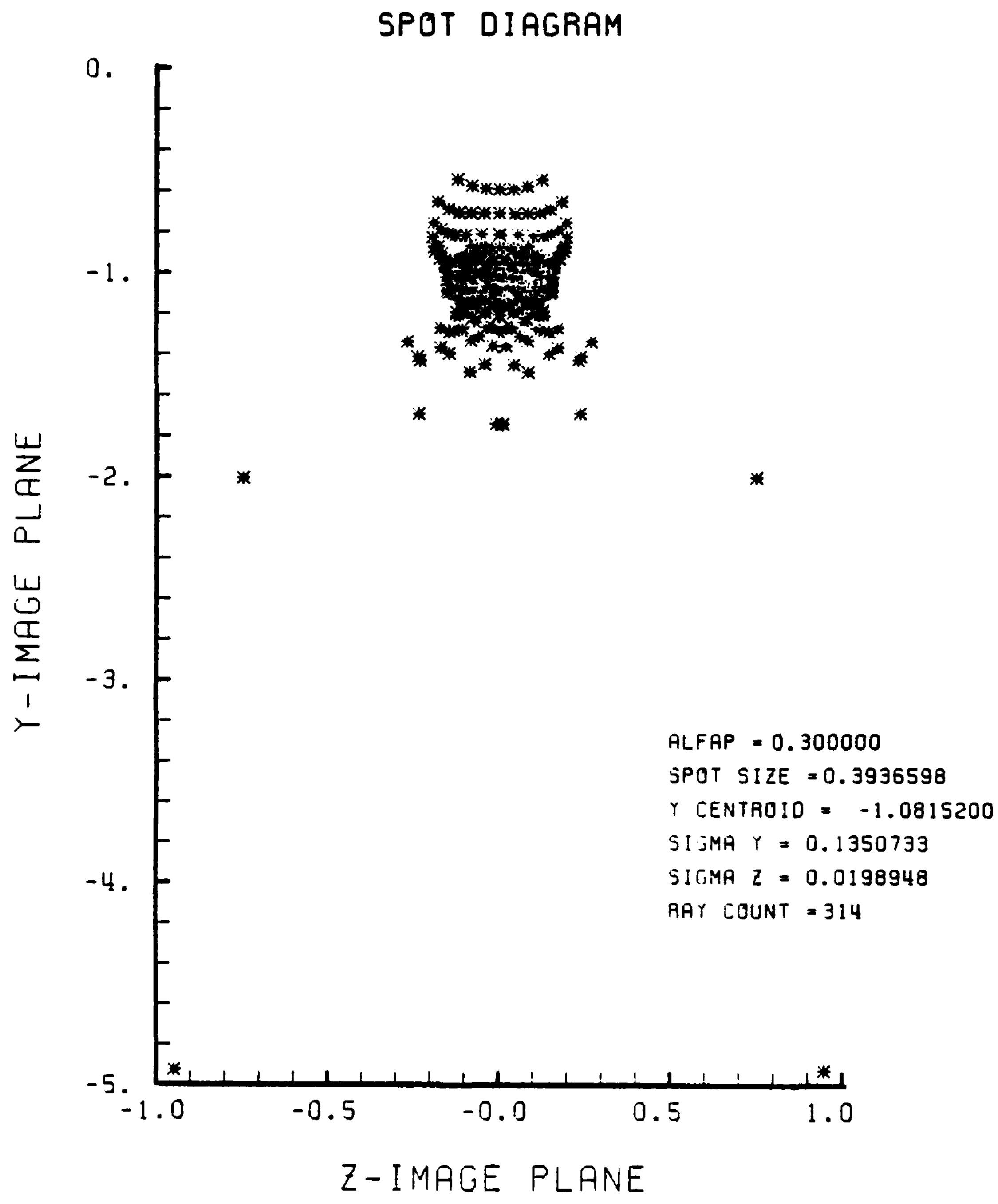

Figure F-111. Spot Diagram for Grid of Figure F-110

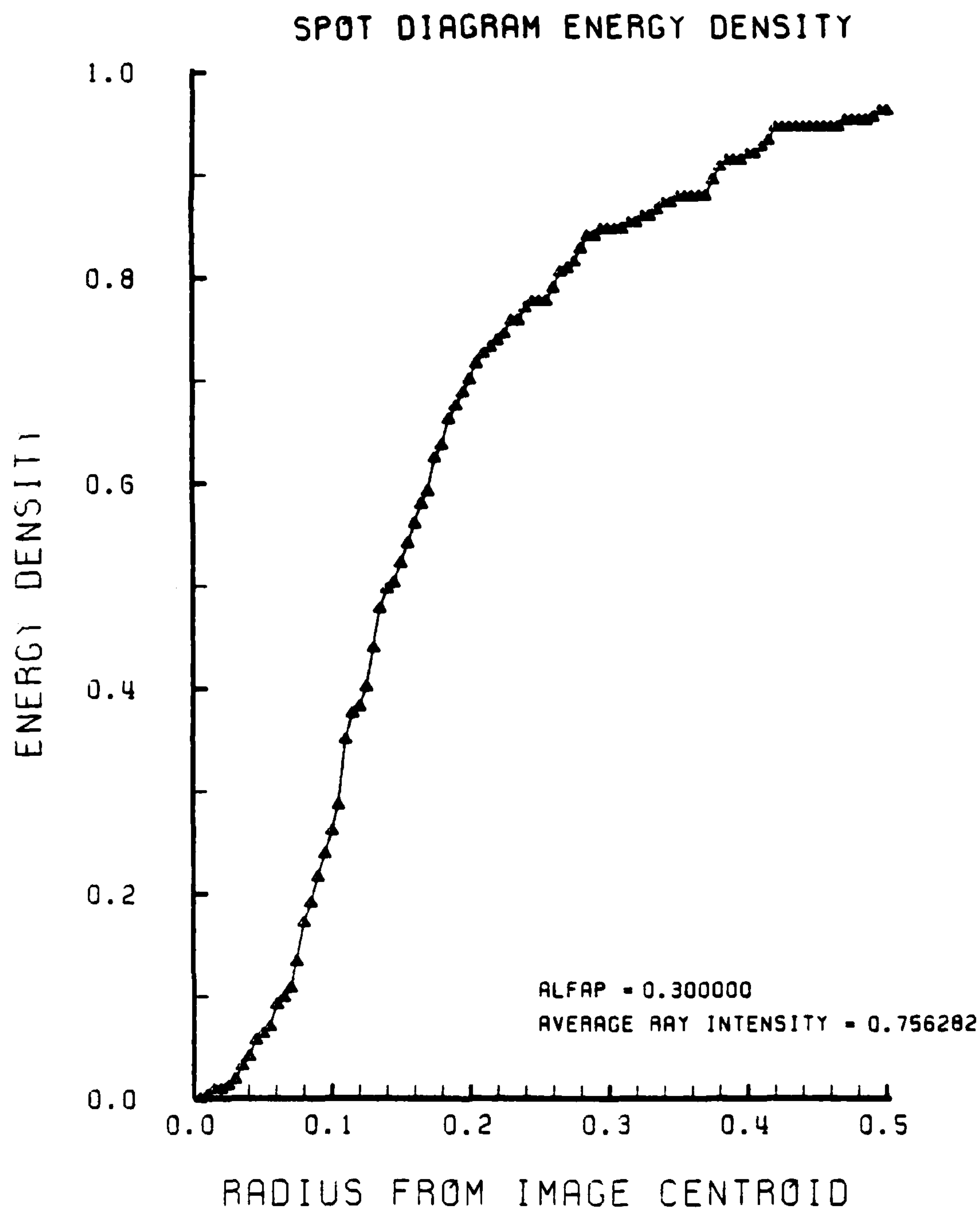

Figure F-112. Encircled Energy of Figure F-111

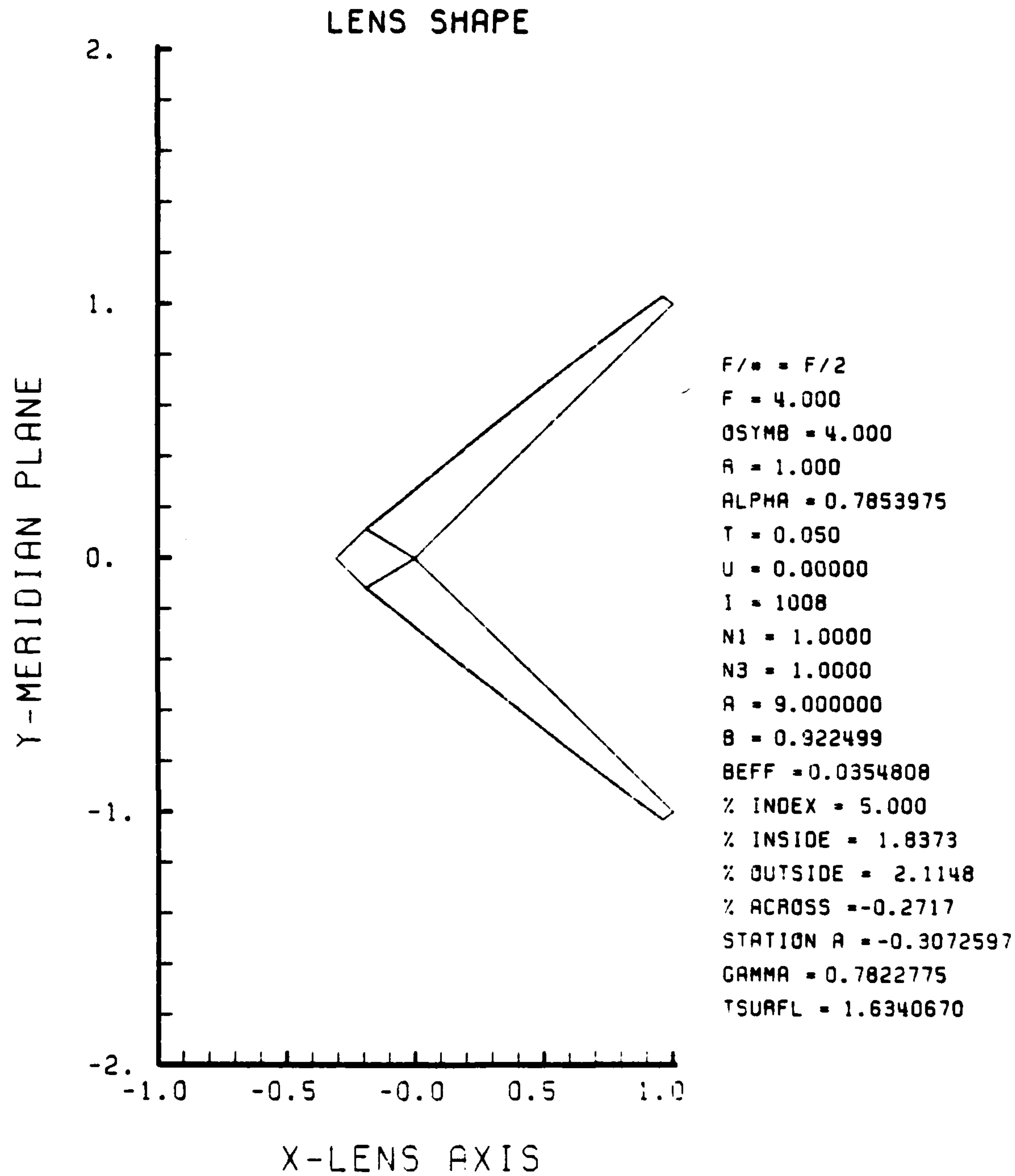

Figure F-113. GRIN Lens Shape at +5%, OB = 4.00, a = 9.00

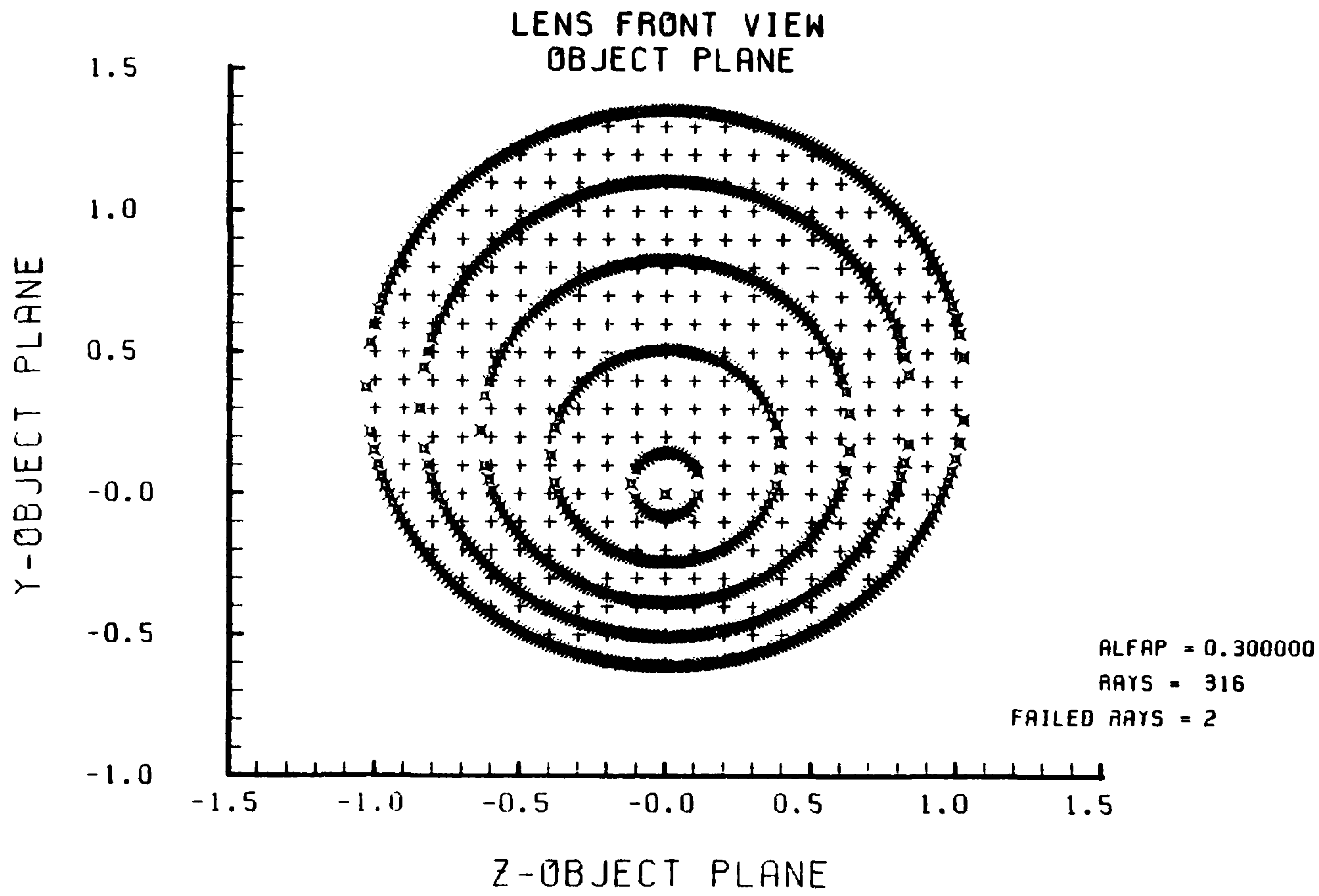

Figure F-114. Grid Plane at α_p = 0.3 for Lens of Figure F-113

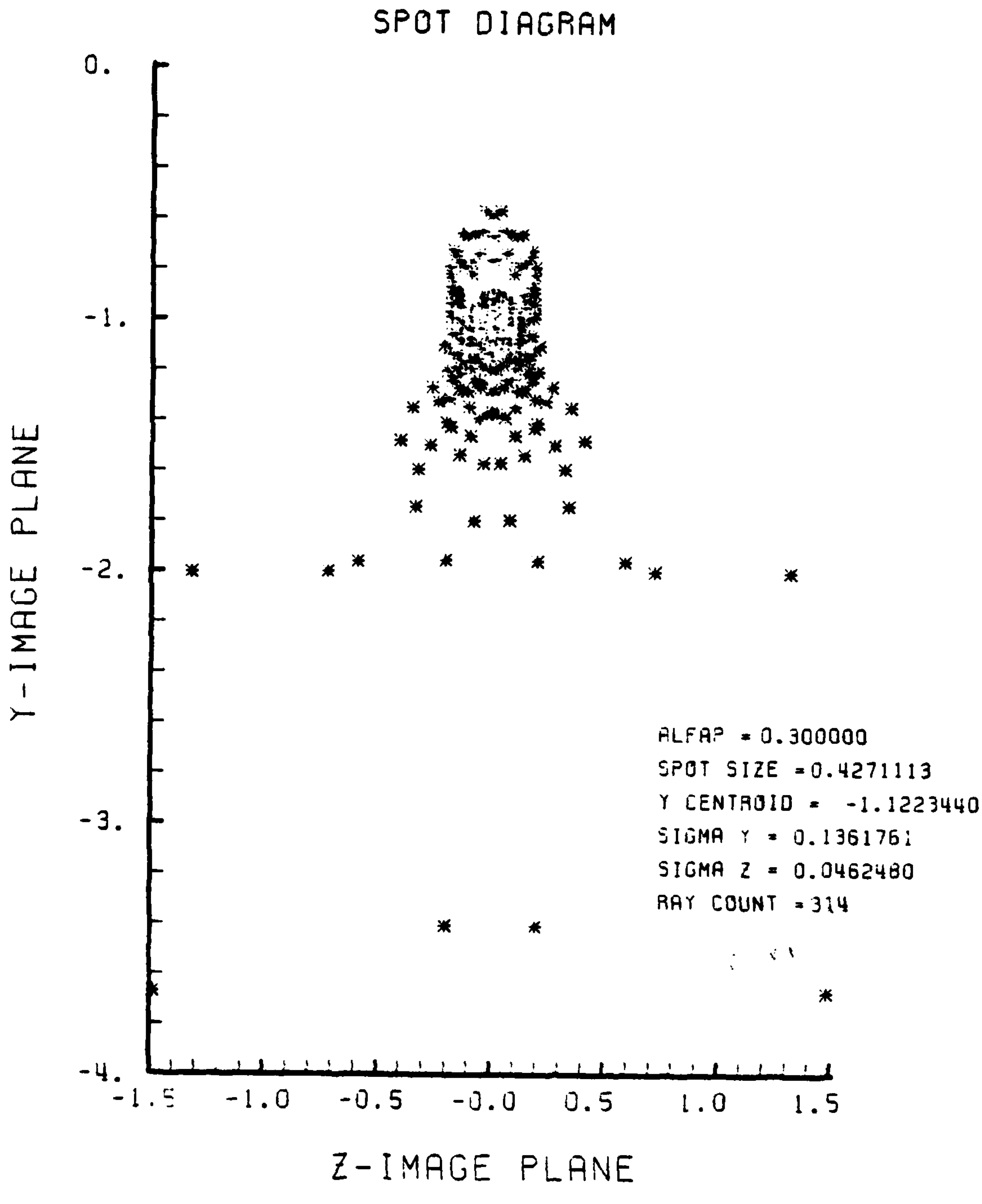

Figure F-115. Spot Diagram for Grid of Figure F-114

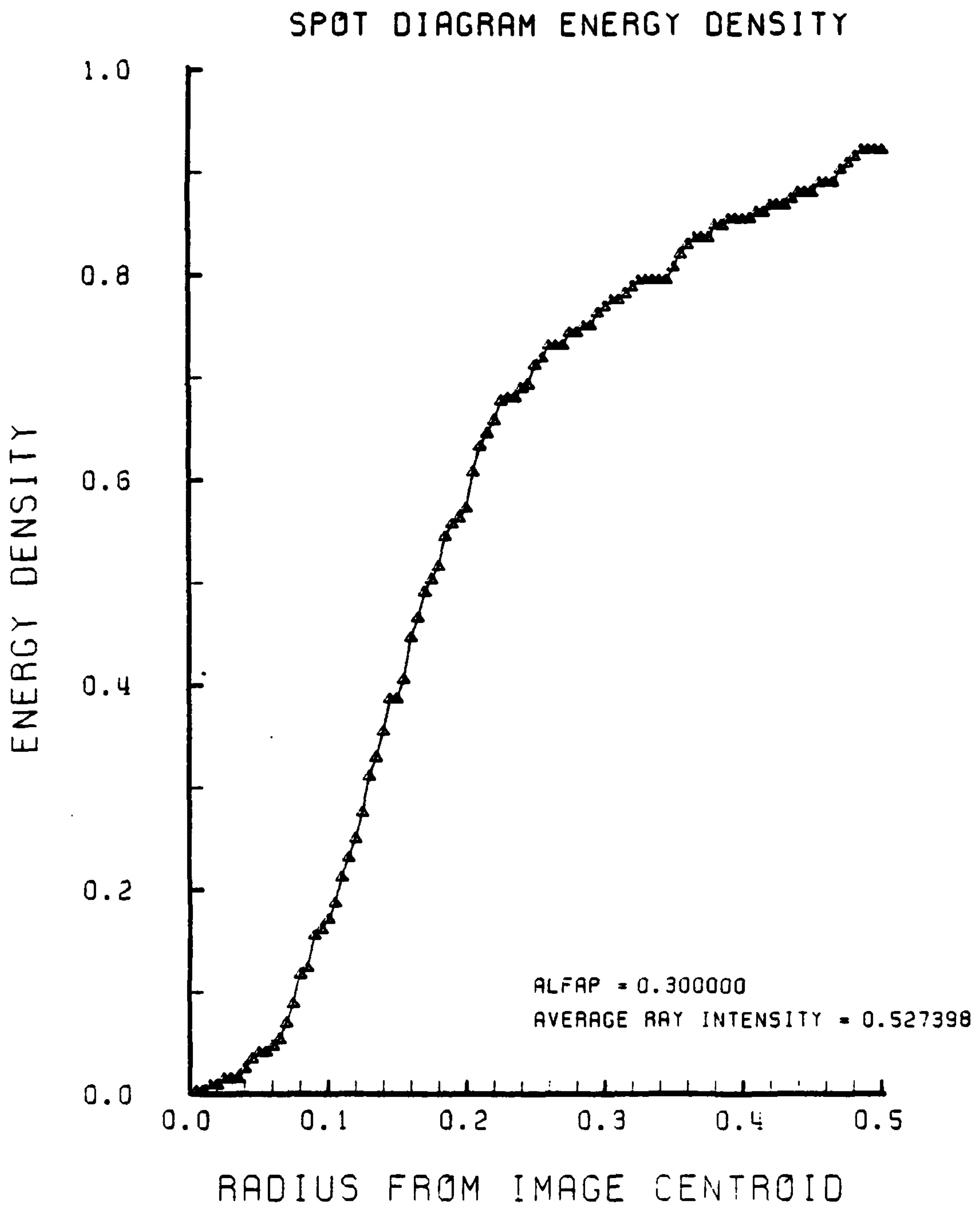

Figure F-116. Encircled Energy of Figure F-115

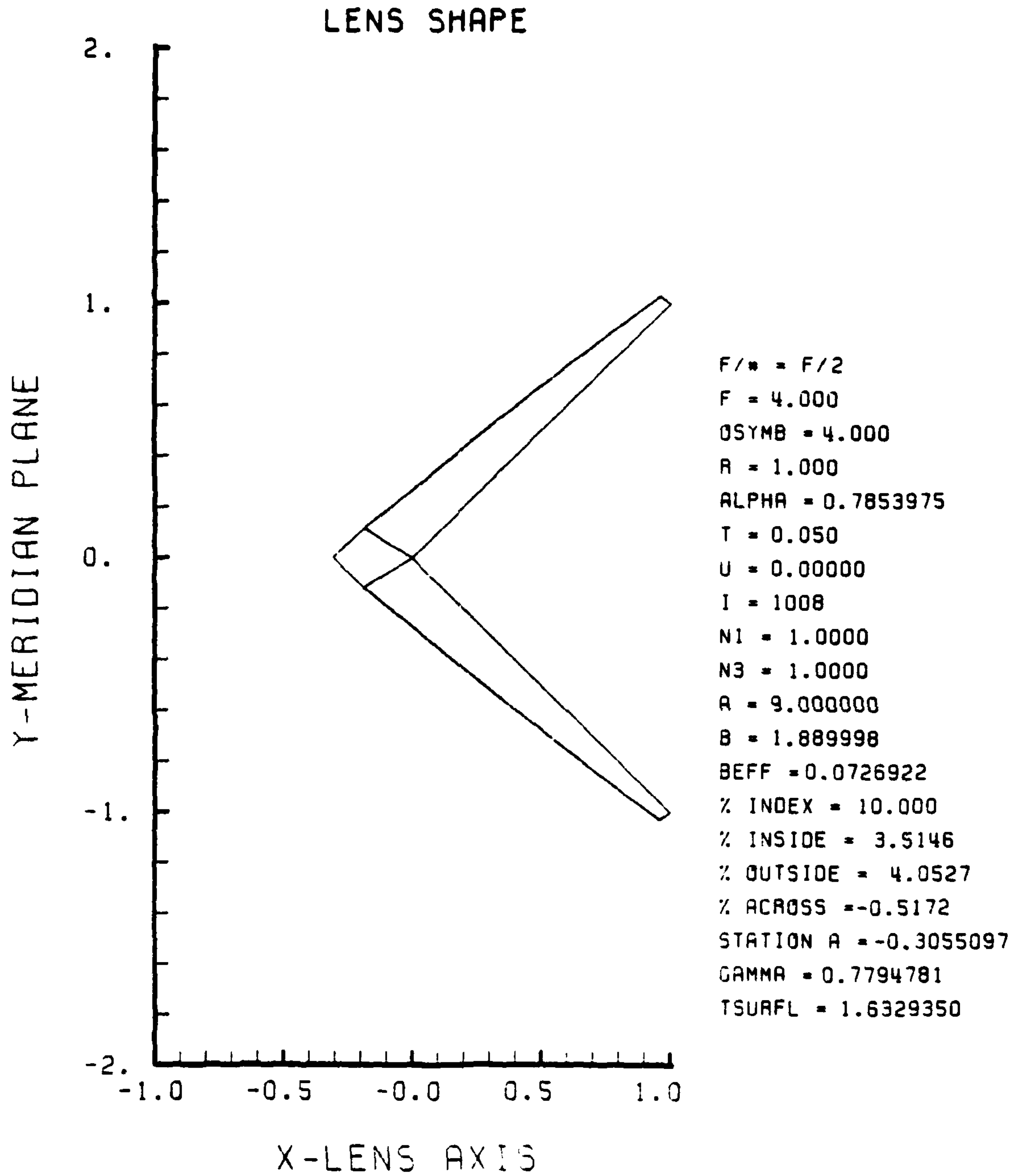

Figure F-117. **GRIN Lens Shape at +10%, OB = 4.00, a = 9.00**

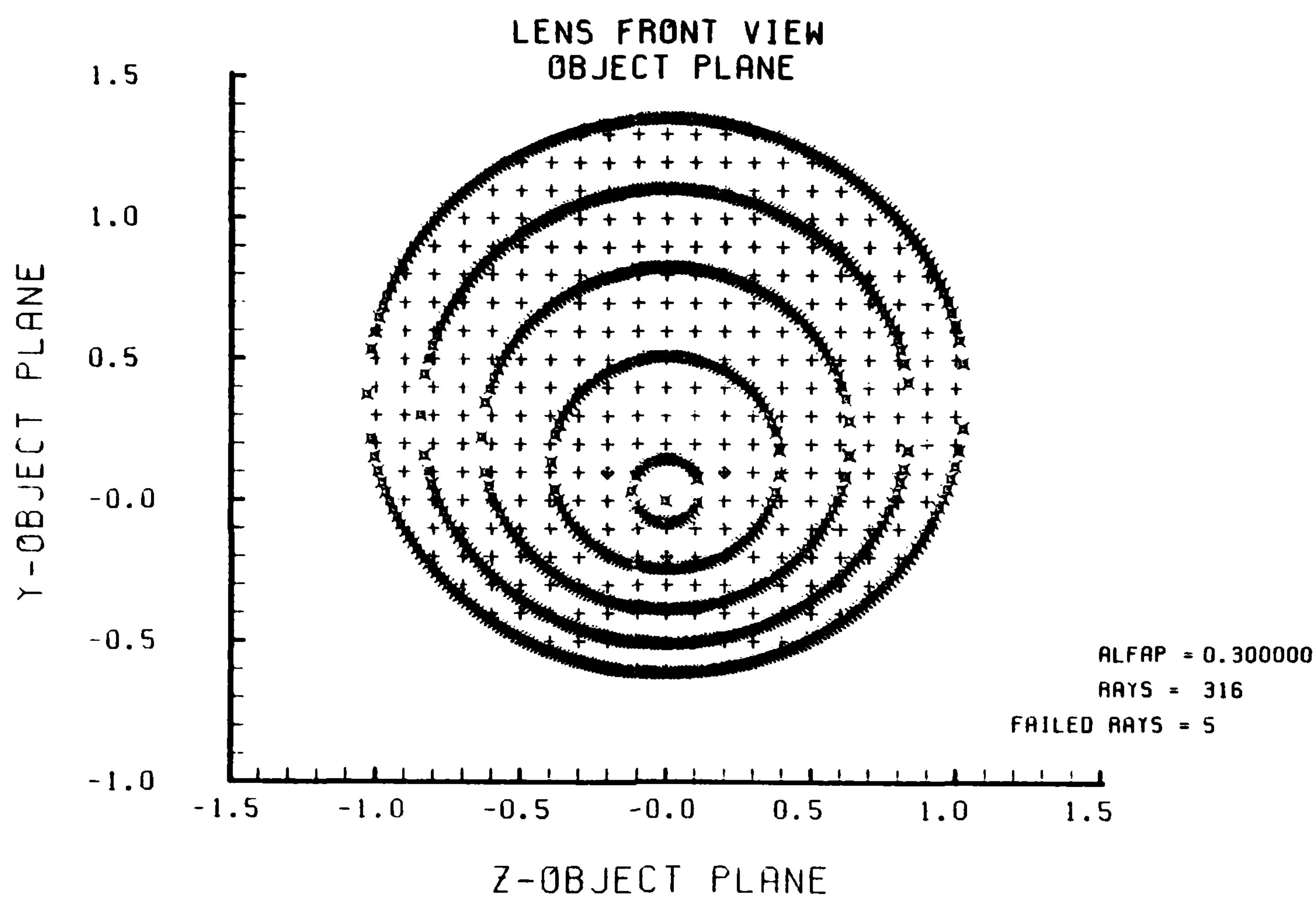

Figure F-118. Grid Plane at $\alpha_p = 0.3$ for Lens of Figure F-117

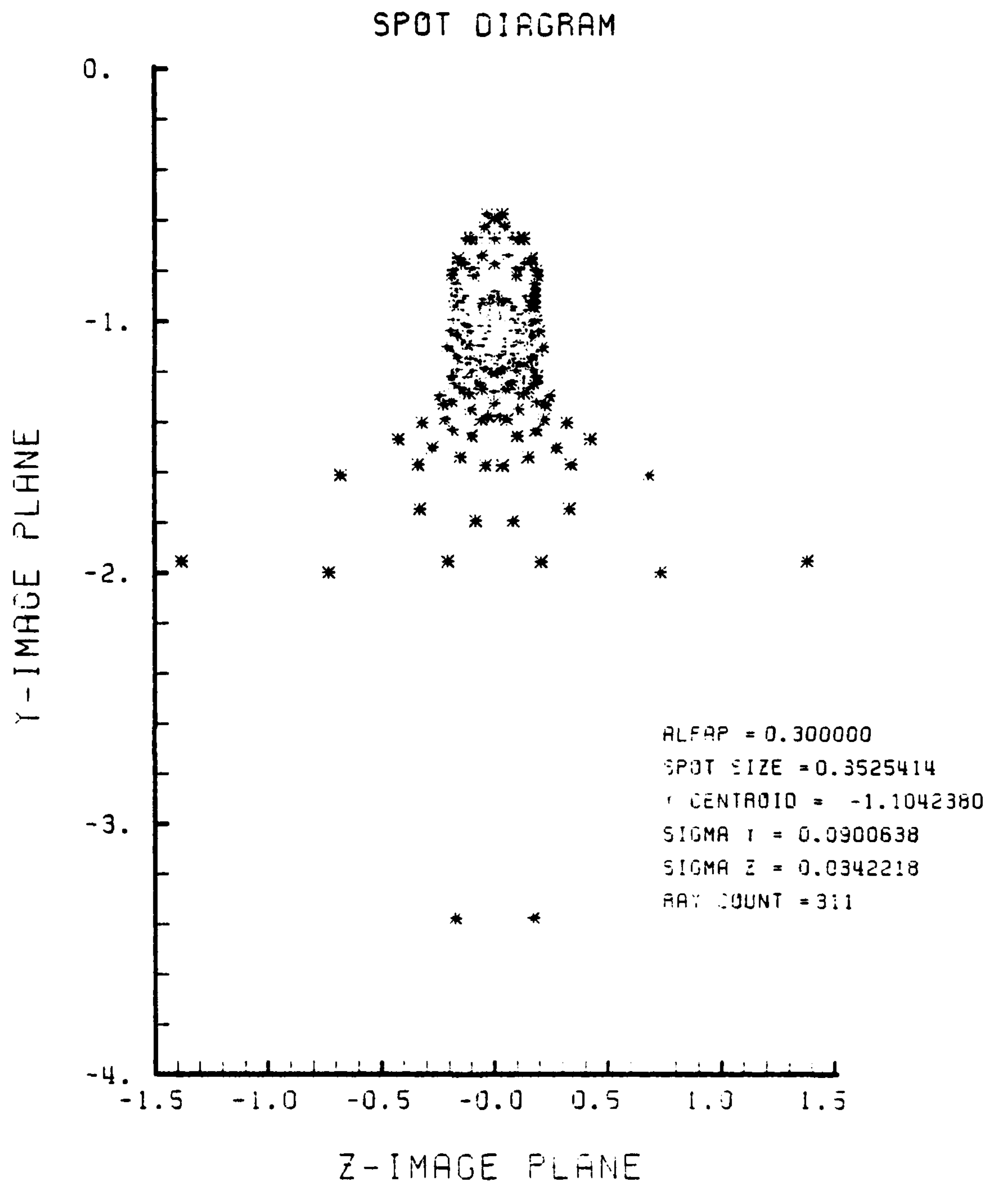

Figure F-119. Spot Diagram for Grid of Figure F-118

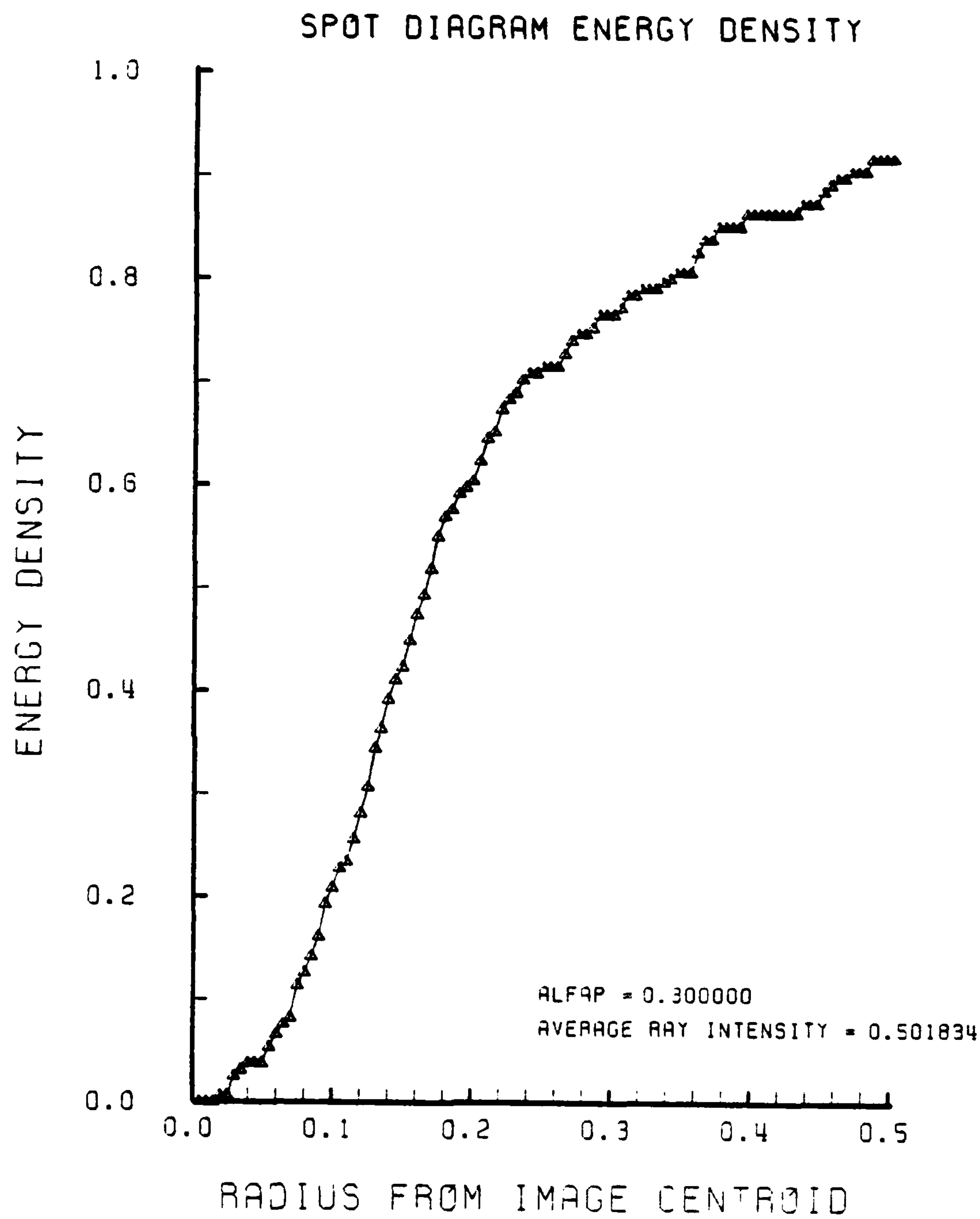

Figure F-120. Encircled Energy of Figure F-119

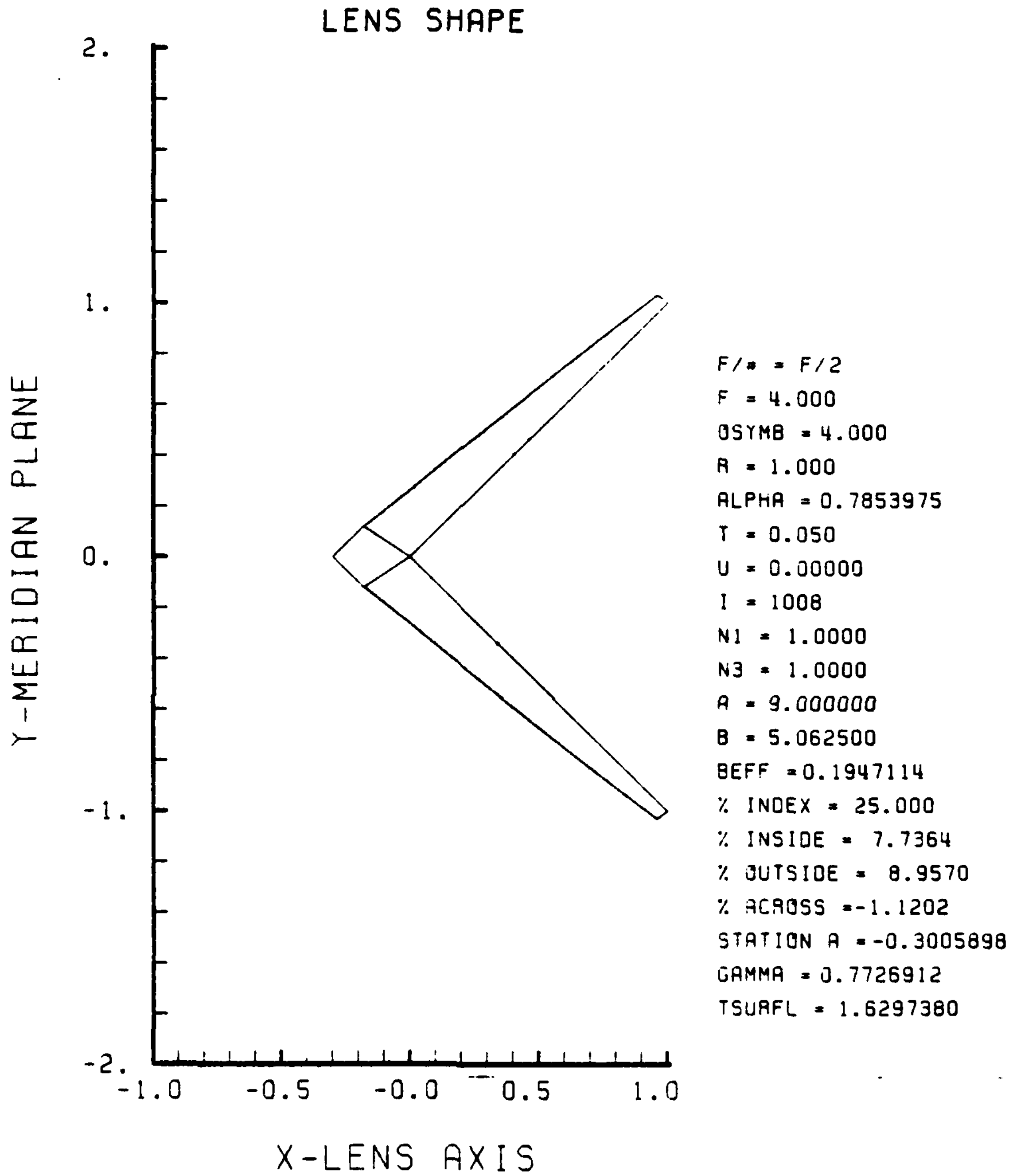

Figure F-121. GRIN Lens Shape at +25%, OB = 4.00, a = 9.00

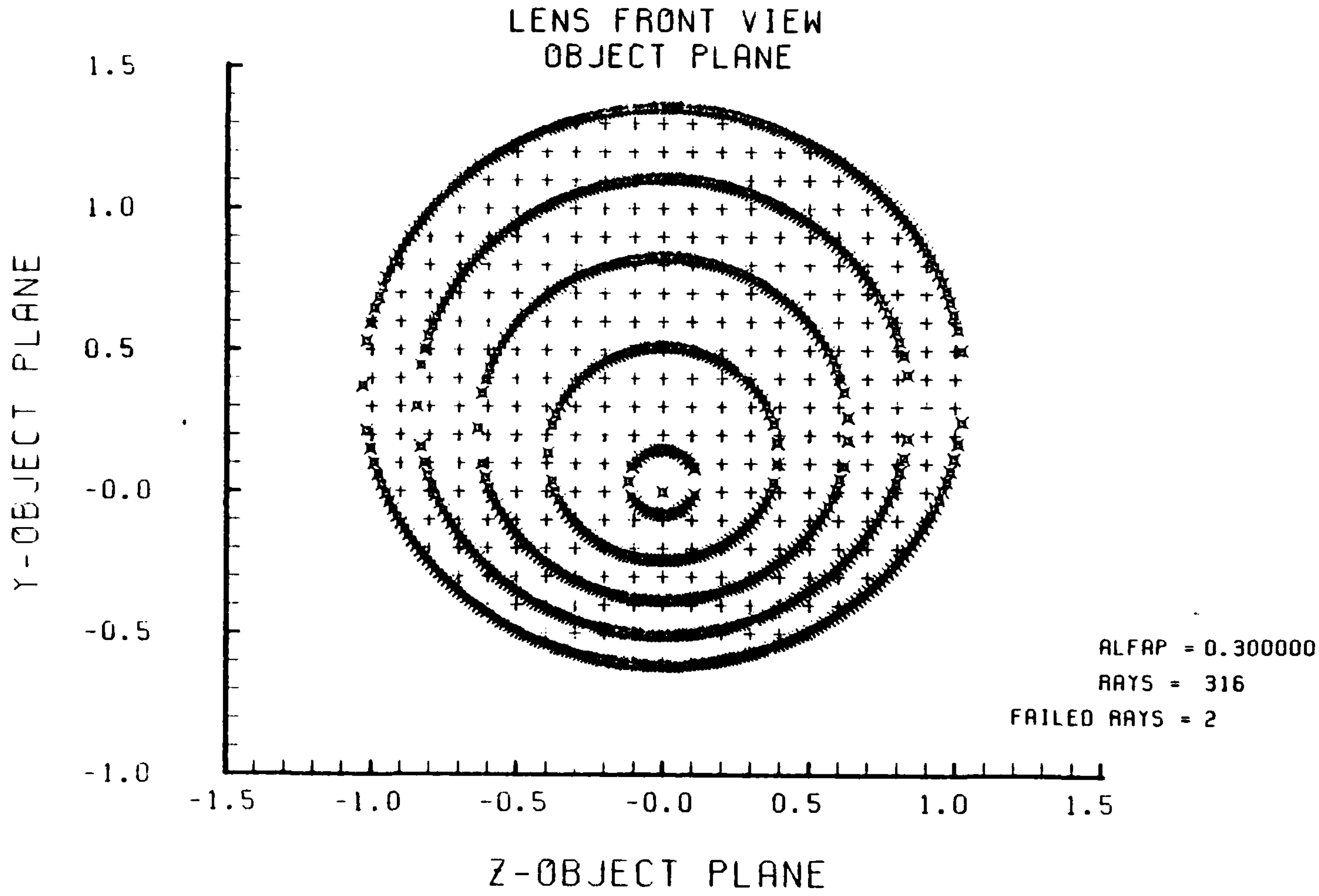

Figure F-122. Grid Plane at α_p = 0.3 for Lens of Figure F-121

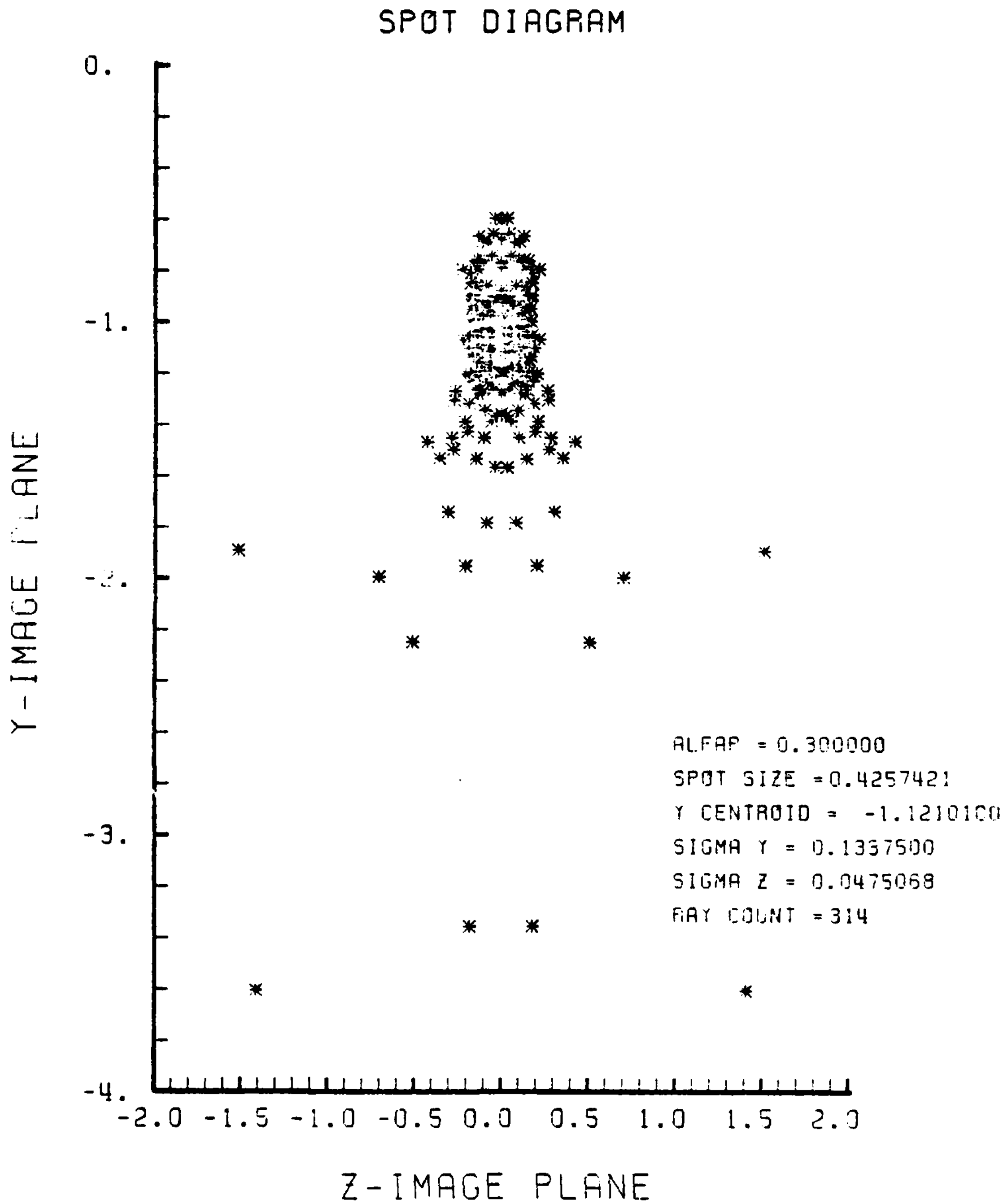

Figure F-123. Spot Diagram for Grid of Figure F-122

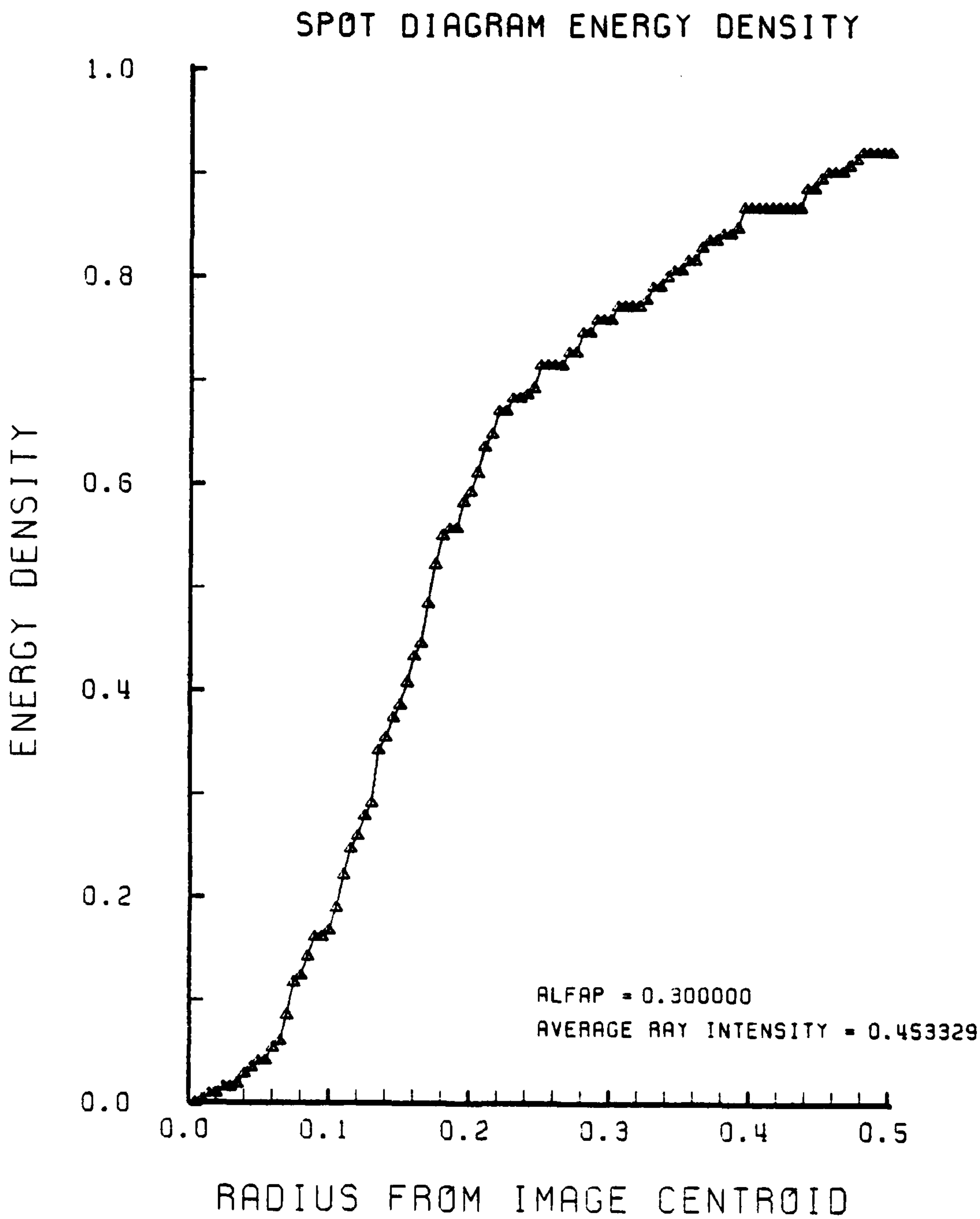

Figure F-124. Encircled Energy of Figure F-123

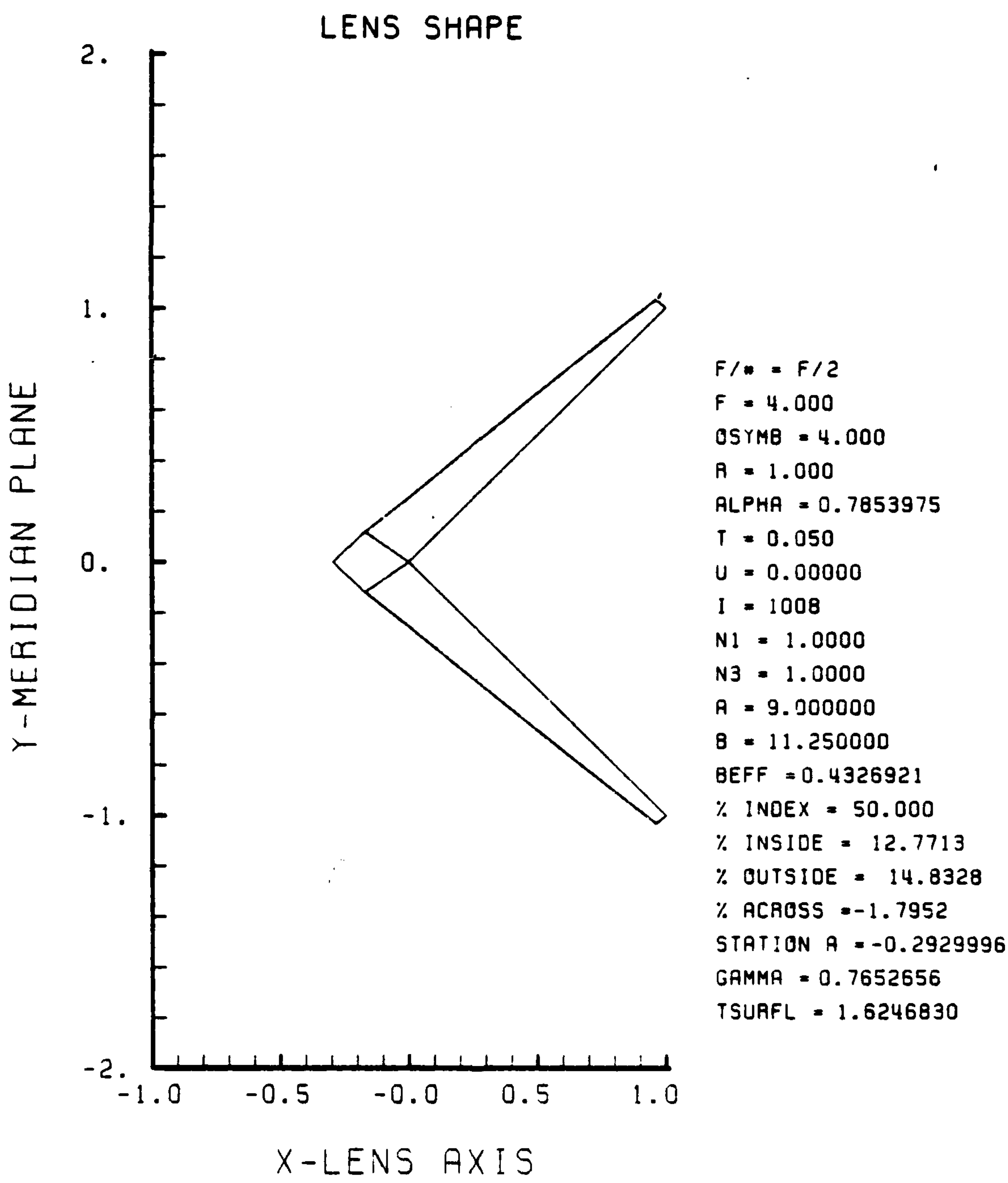

Figure F-125. GRIN Lens Shape at +50%, OB = 4.00, a = 9.00

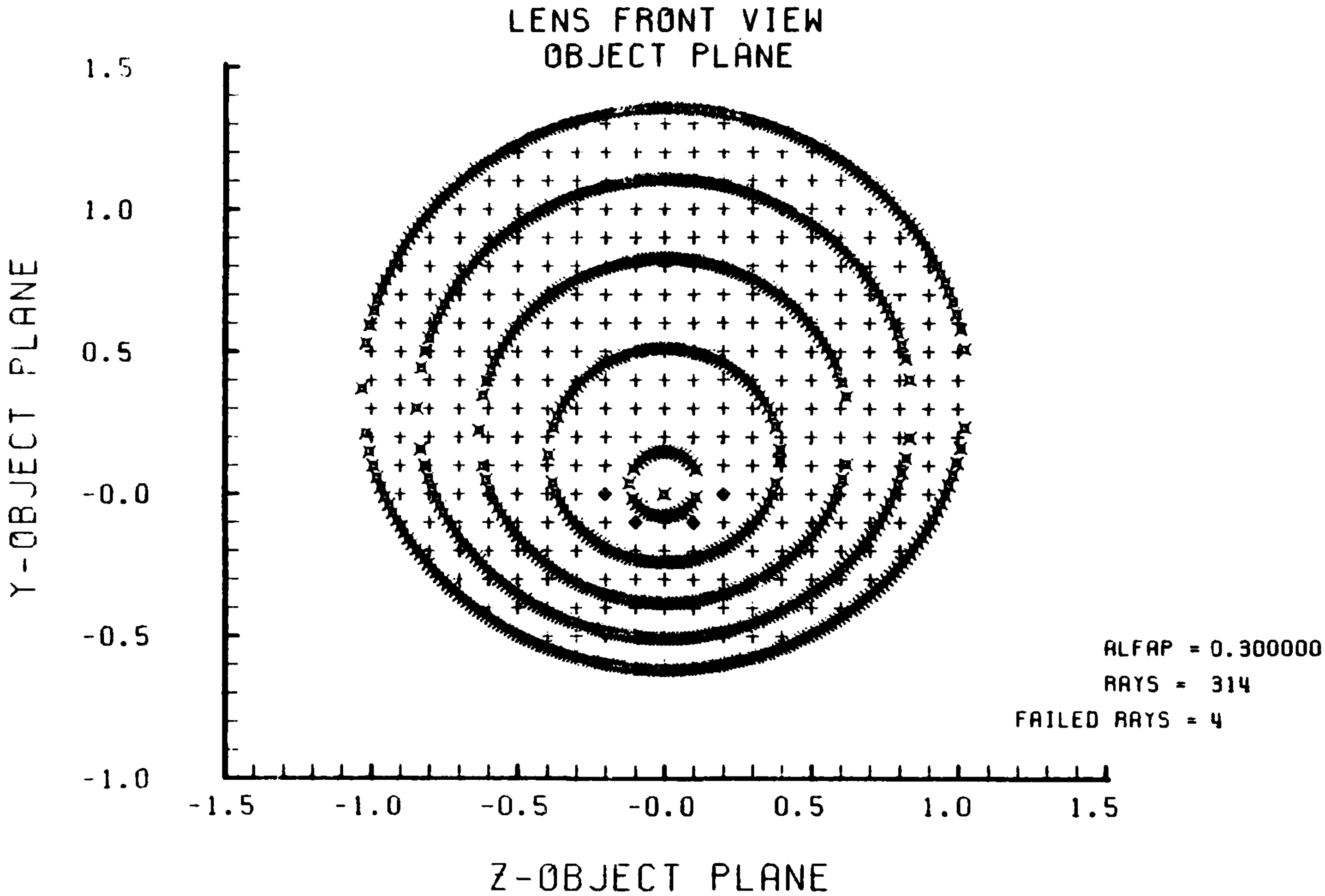

Figure F-126. Grid Plane at α_p = 0.3 for Lens of Figure F-125

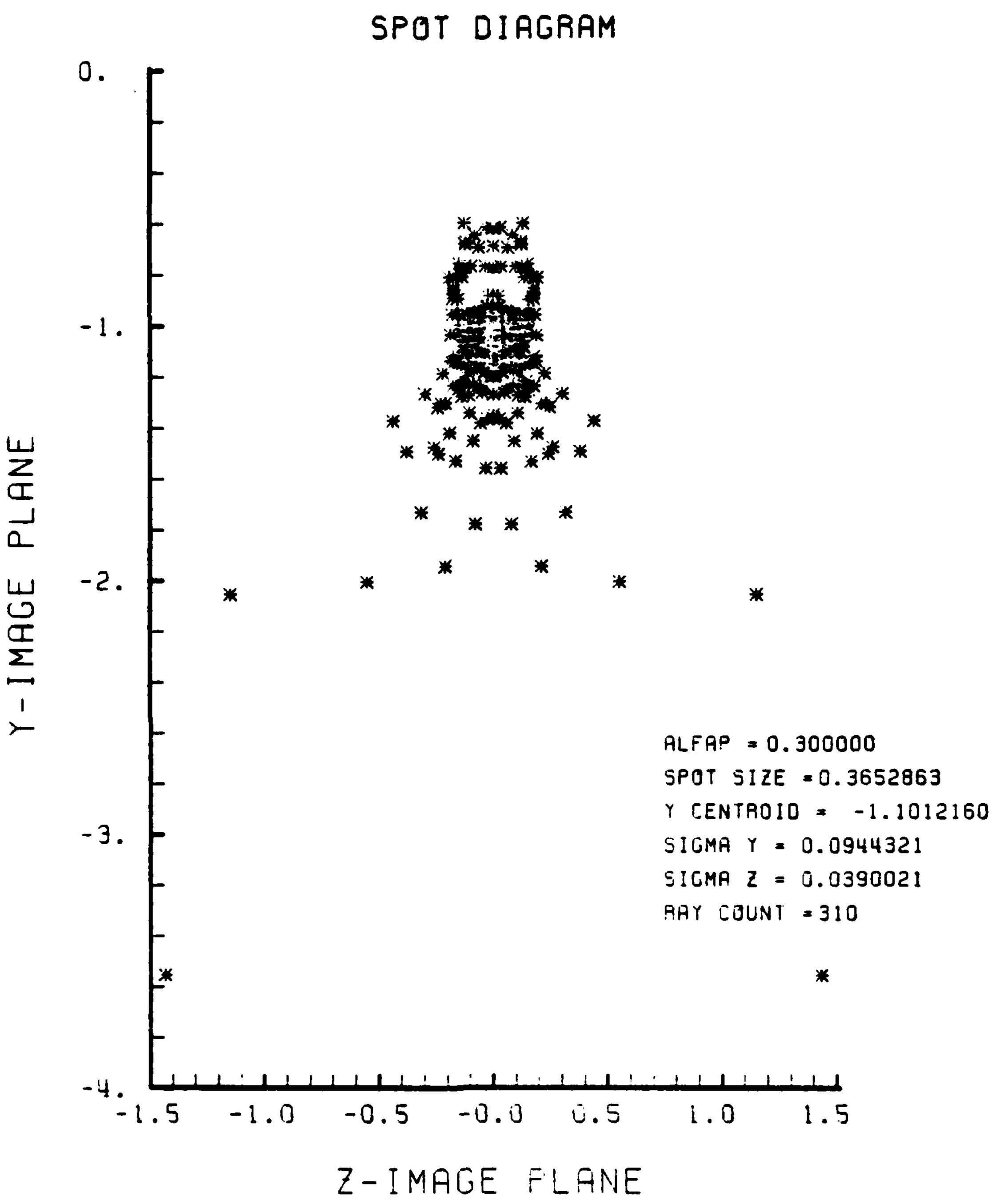

Figure F-127. Spot Diagram for Grid of Figure F-126

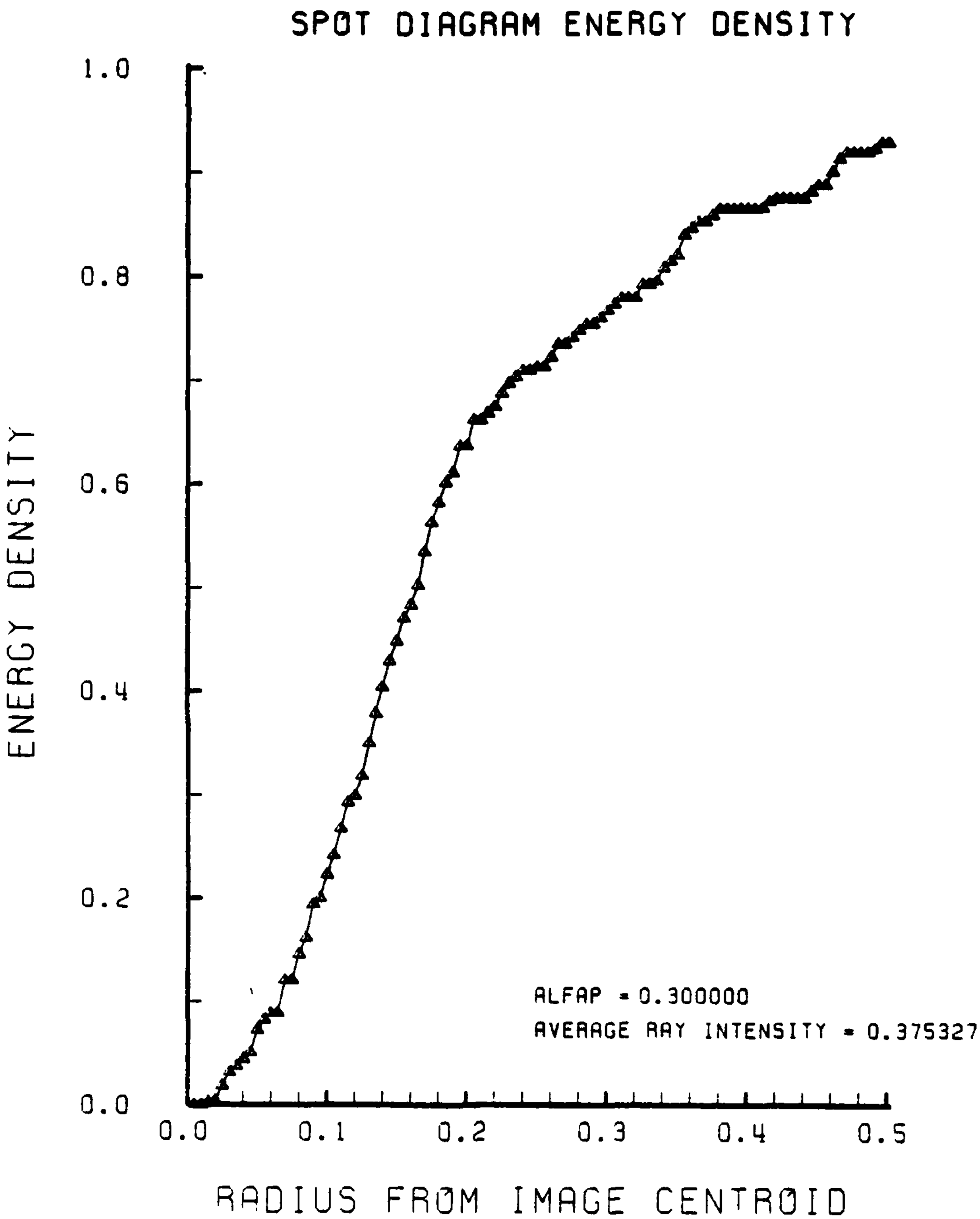

Figure F-128. Encircled Energy of Figure F-127

APPENDIX G

"BEST" GRIN LENS PERFORMANCE PLOTS IN THE F/2 CONFIGURATION

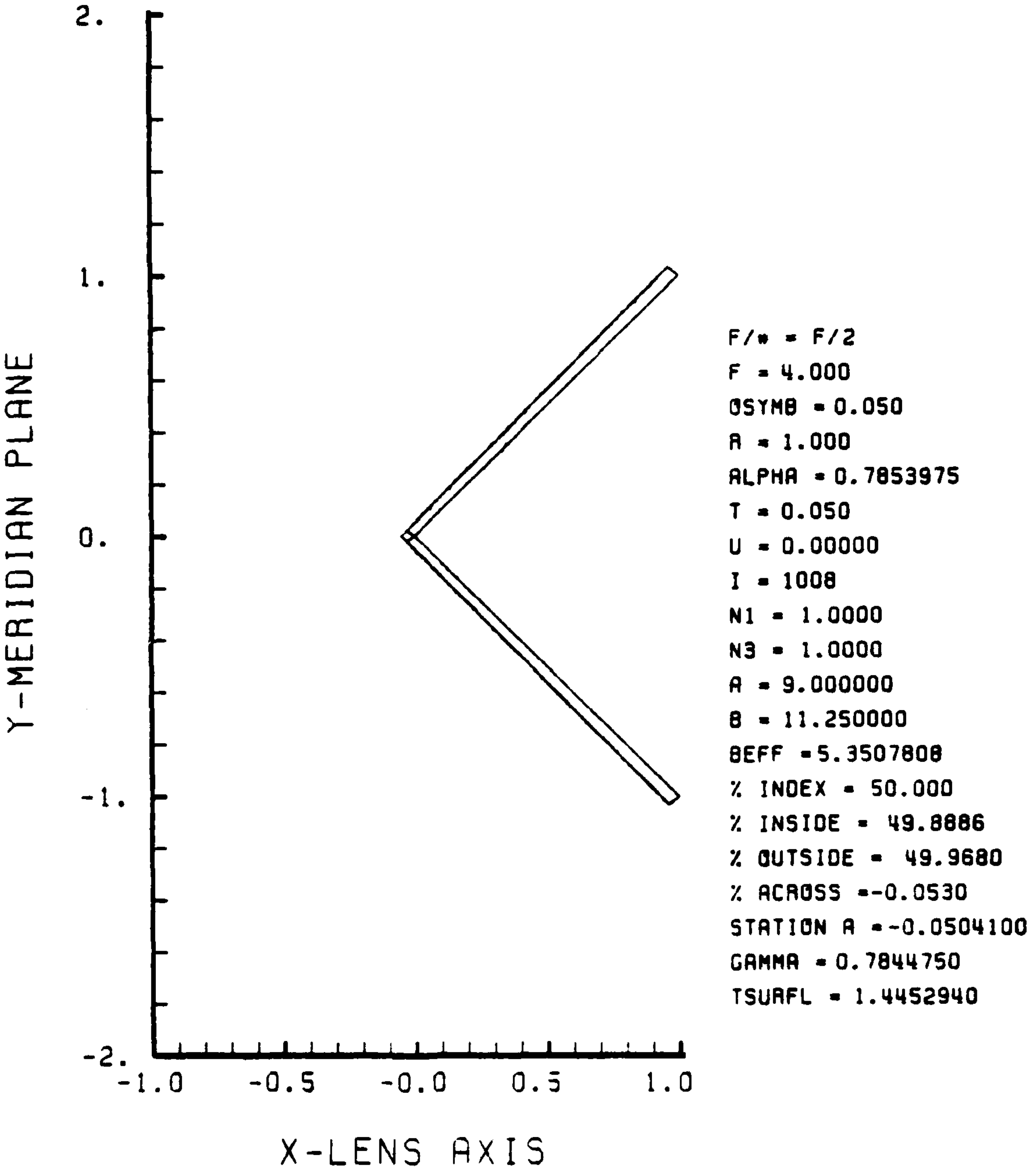

Figure G-1. "Best" GRIN Lens Shape with 50% Gradient, OB = 0.05 and a = 9.00 in the F/2 Configuration

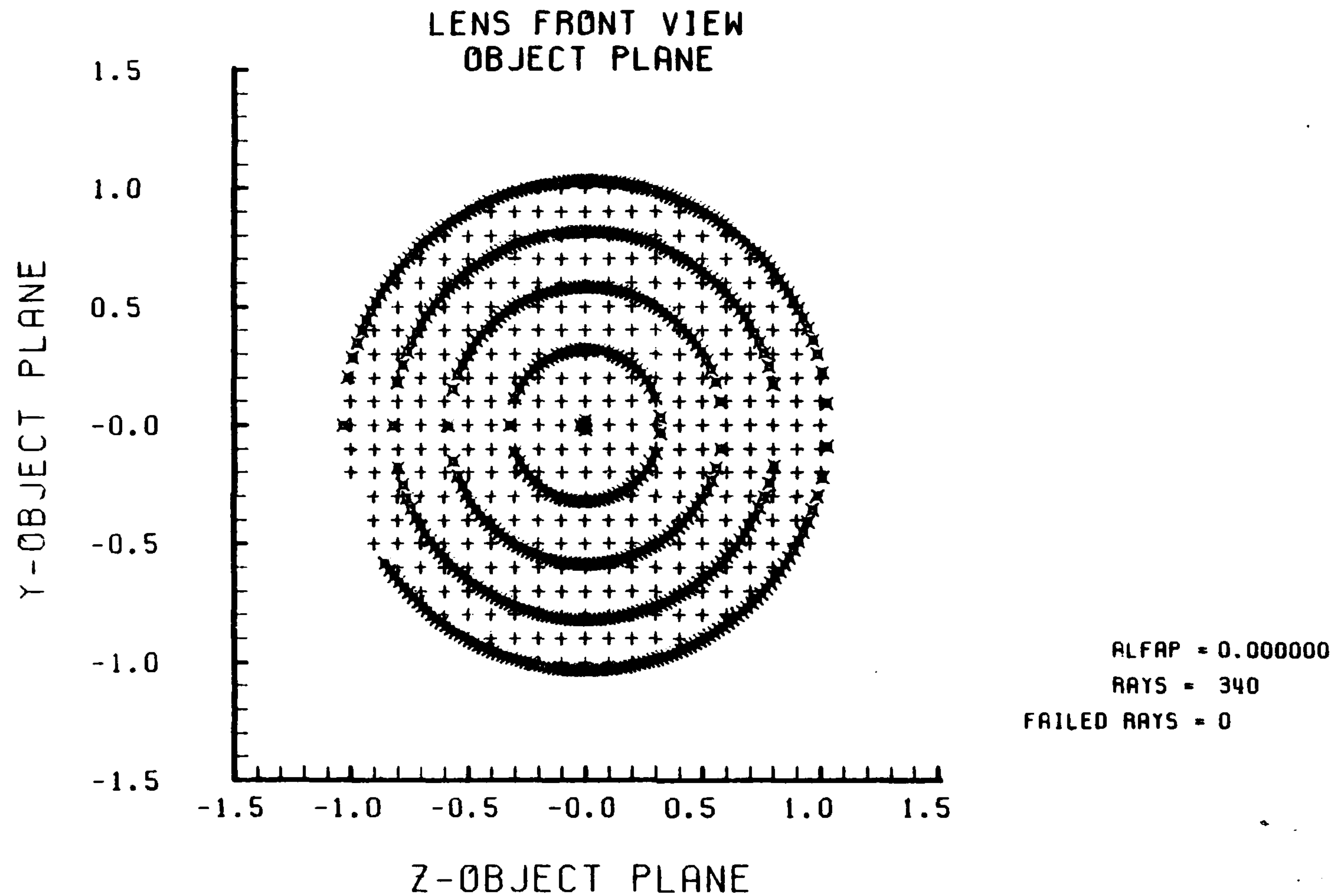

Figure G-2. Grid Plane at α_p = 0.0 for Lens of Figure G-1

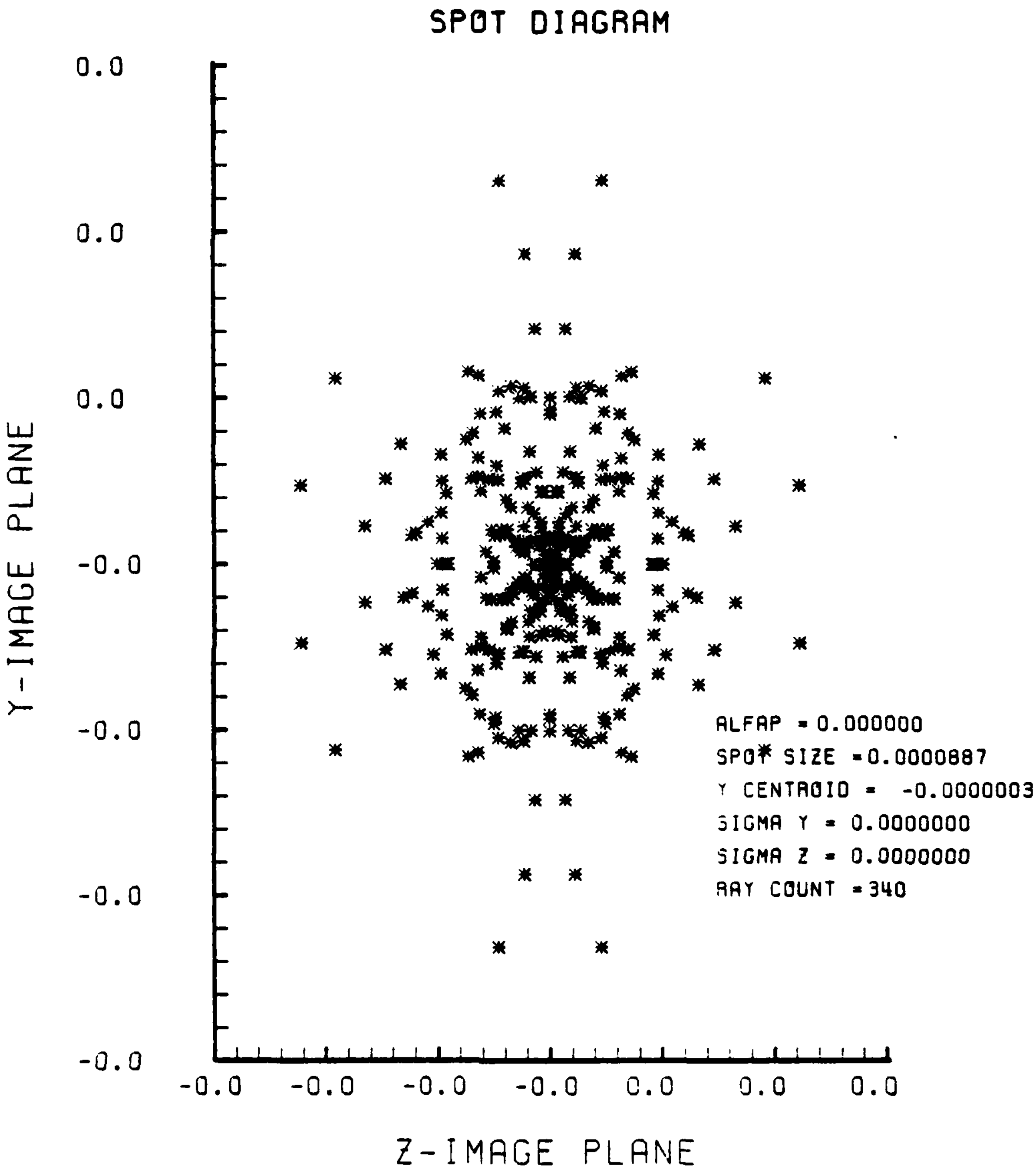

Figure G-3. Spot Diagram for Grid of Figure G-2

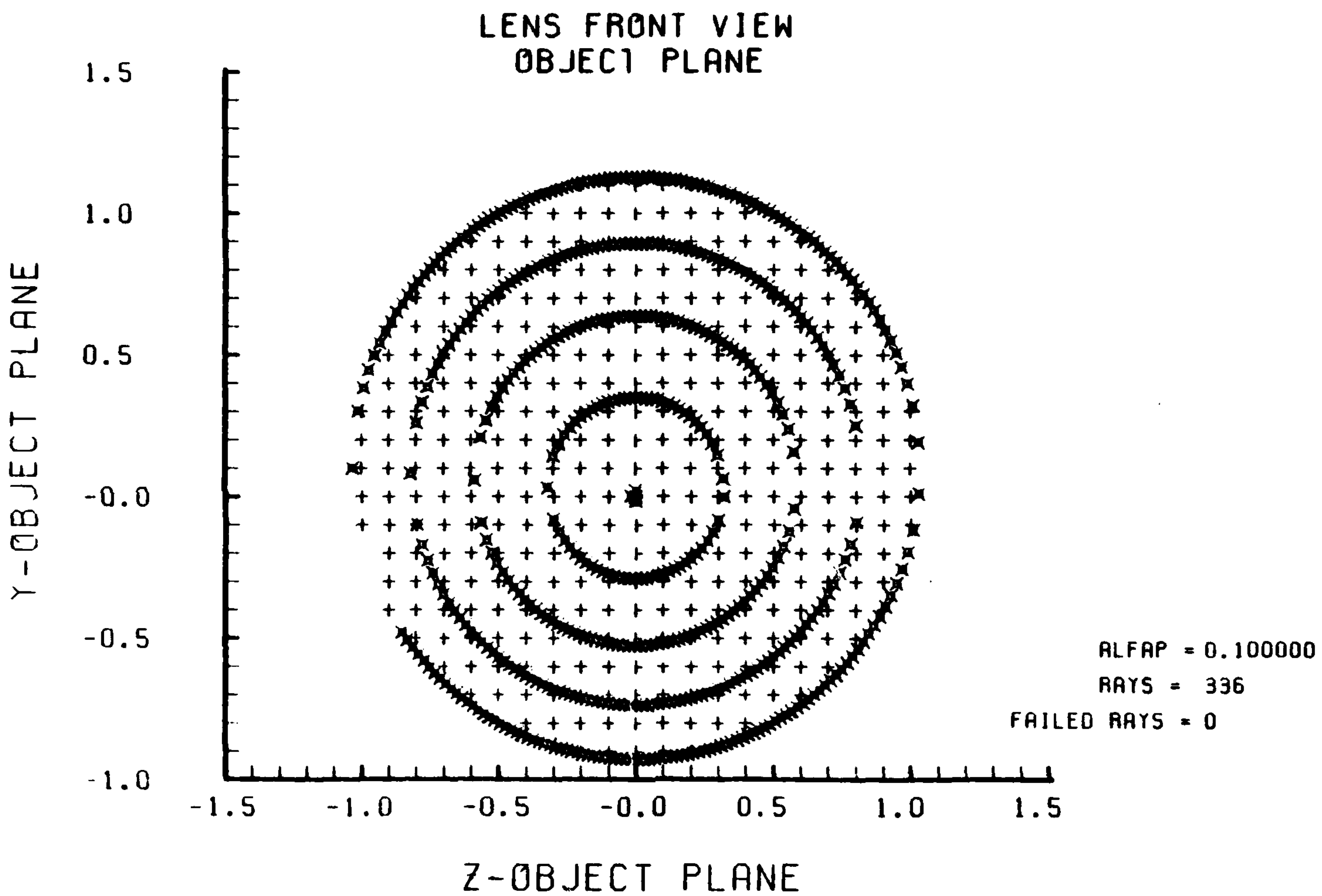

Figure G-4. Grid Plane at α_p = 0.1 for Lens of Figure G-1

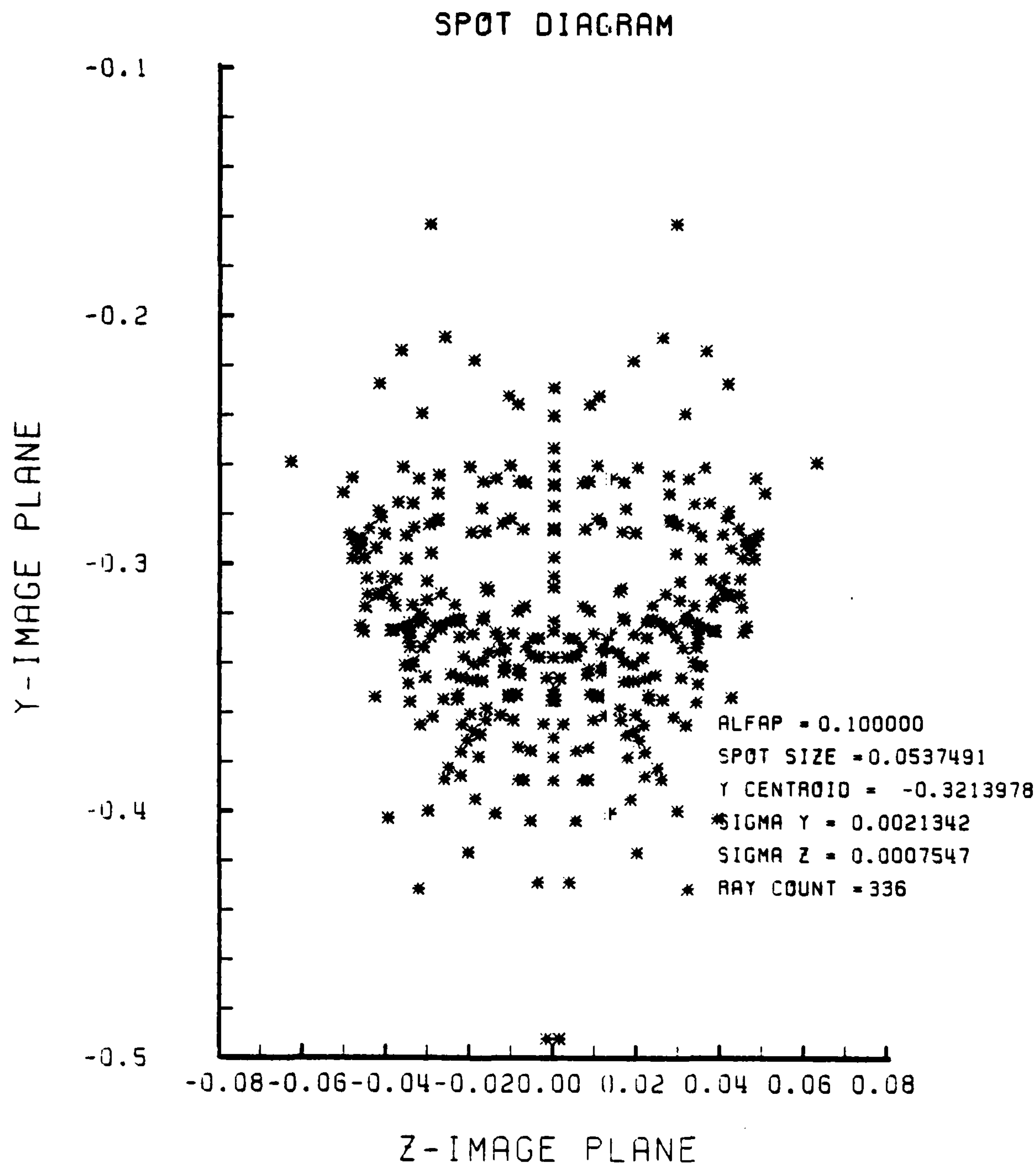

Figure G-5. Spot Diagram for Grid of Figure G-4

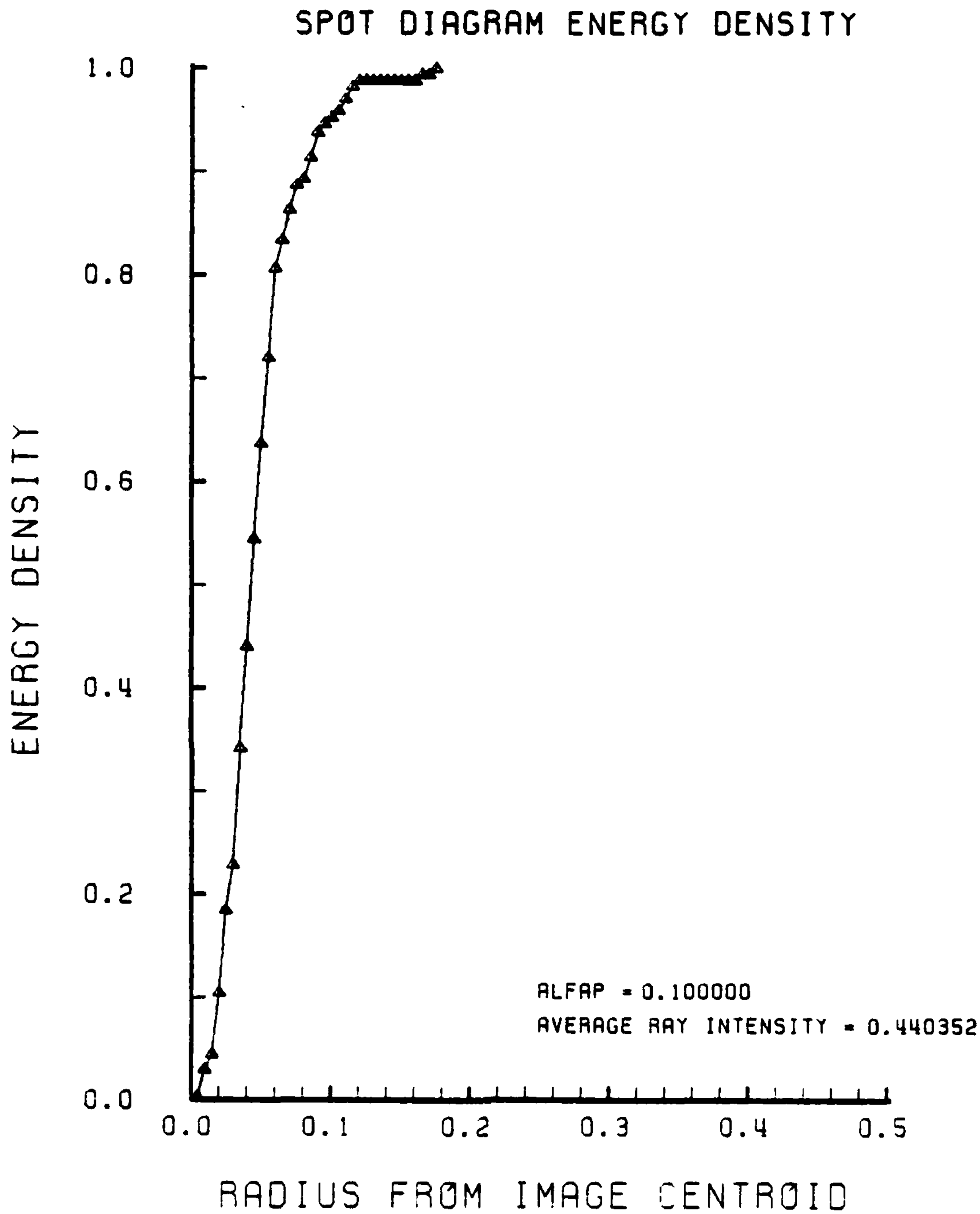

Figure G-6. Encircled Energy of Figure G-5

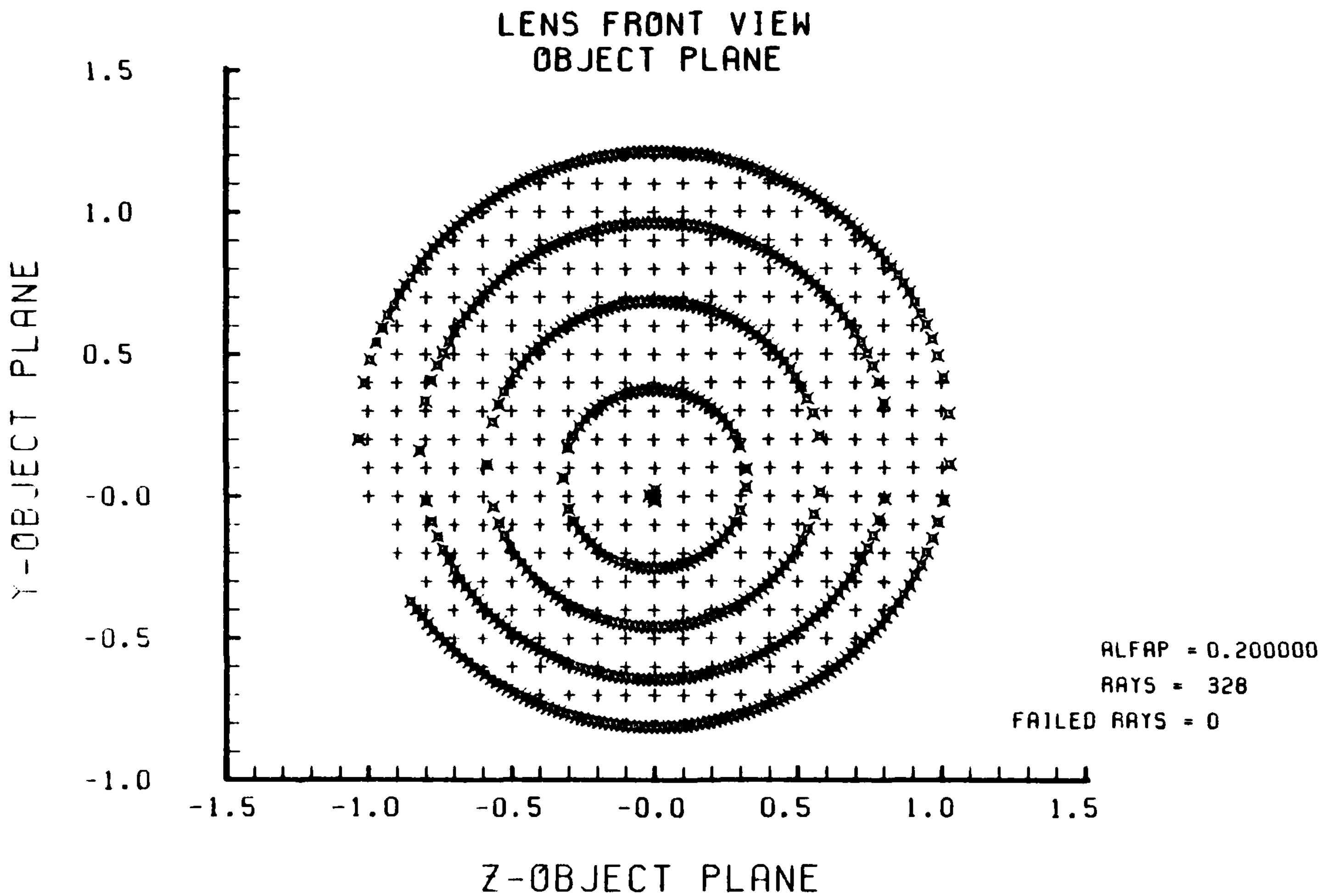

Figure G-7. Grid Plane at $\alpha_p = 0.2$ for Lens of Figure G-1

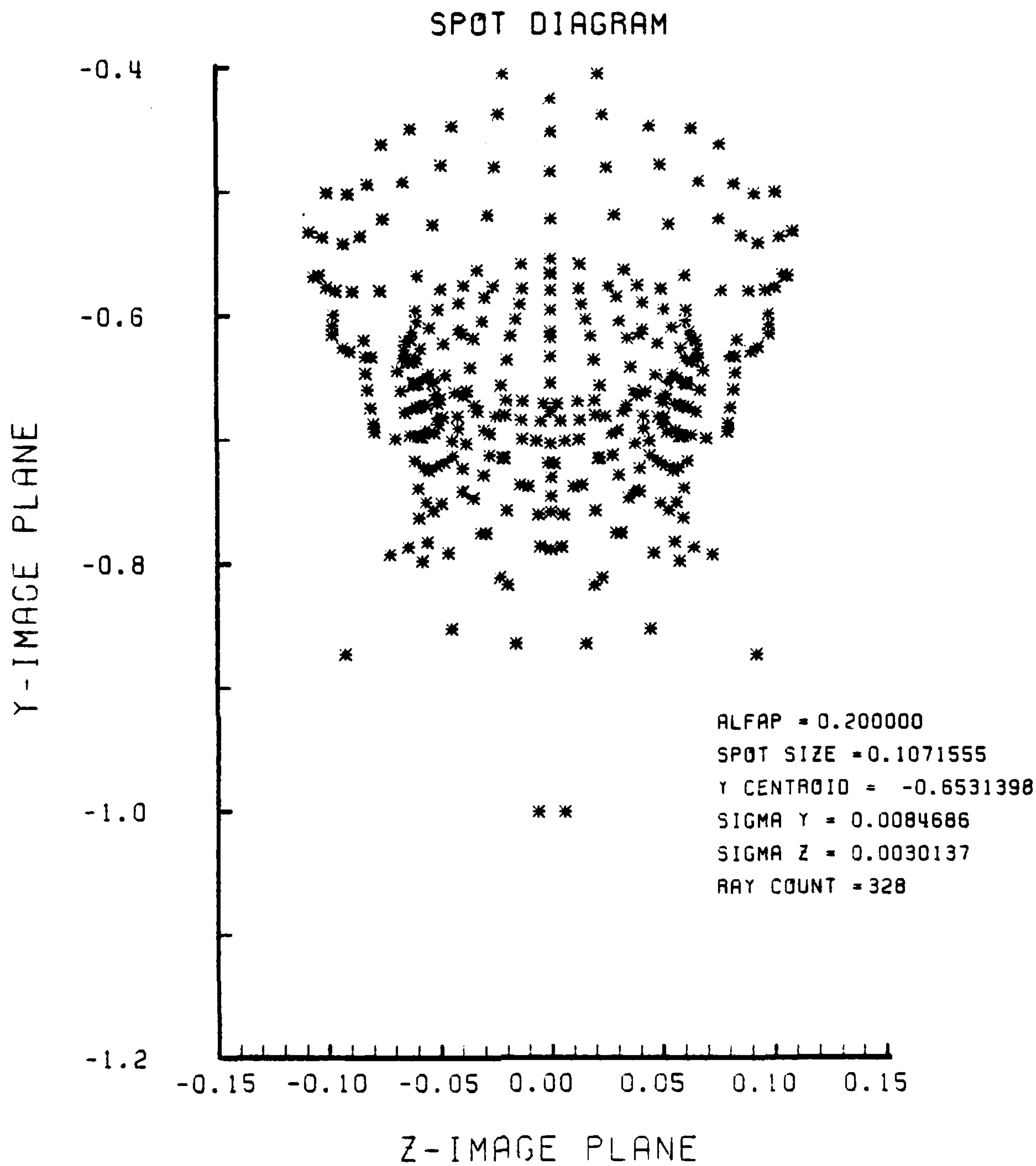

Figure G-8. Spot Diagram for Grid of Figure G-7

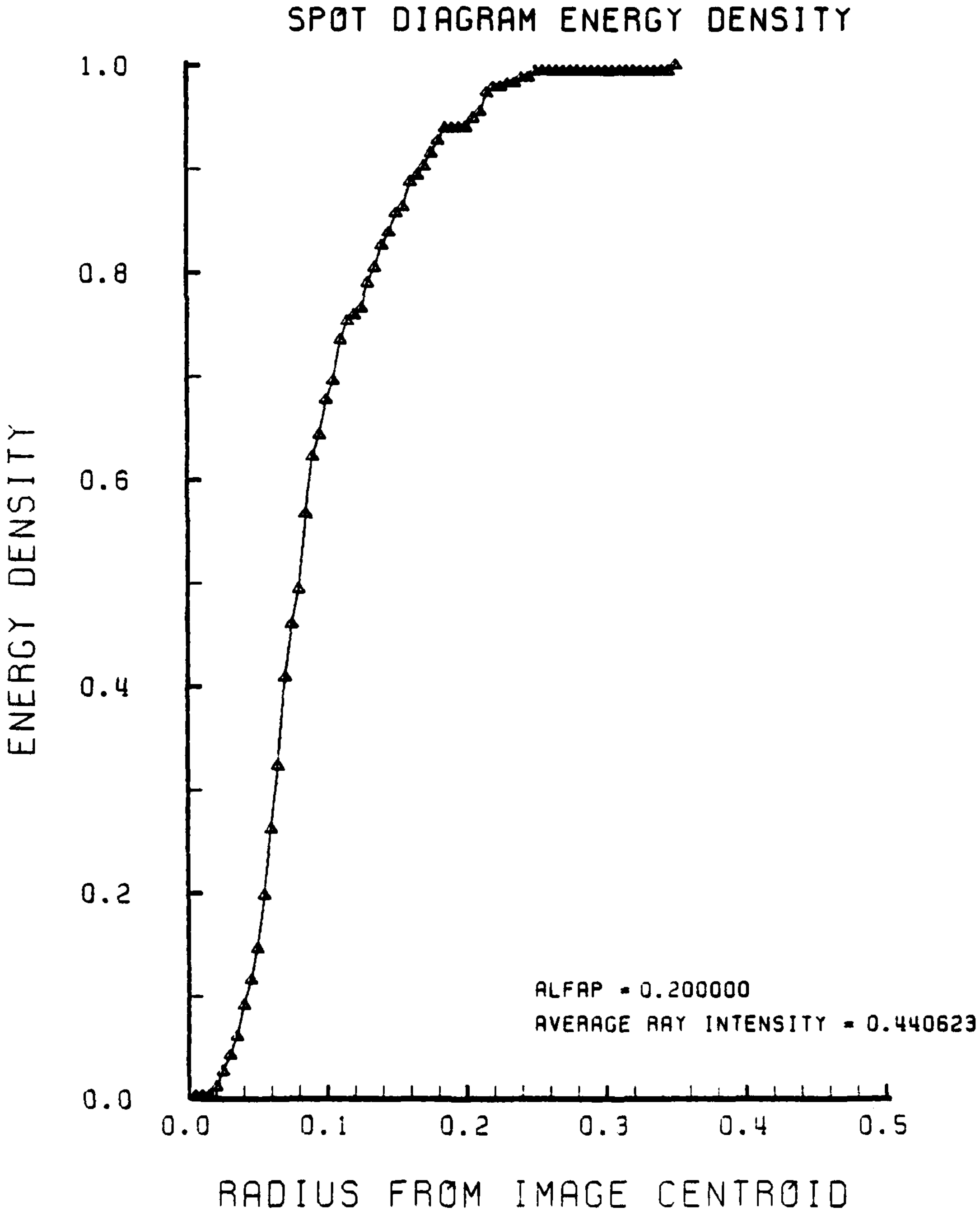

Figure G-9. Encircled Energy of Figure G-8

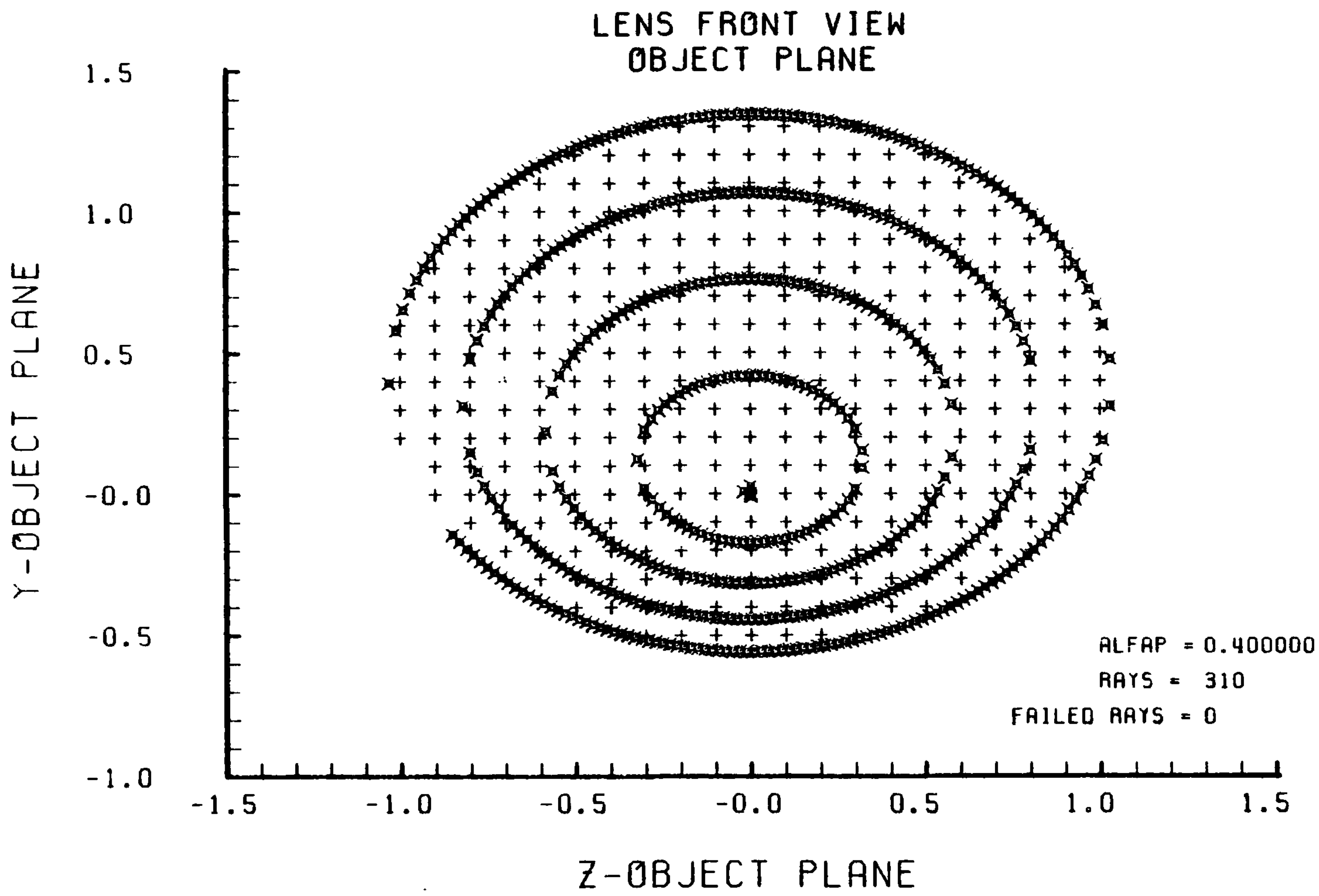

Figure G-10. Grid Plane at $\alpha_p = 0.4$ for Lens of Figure G-1

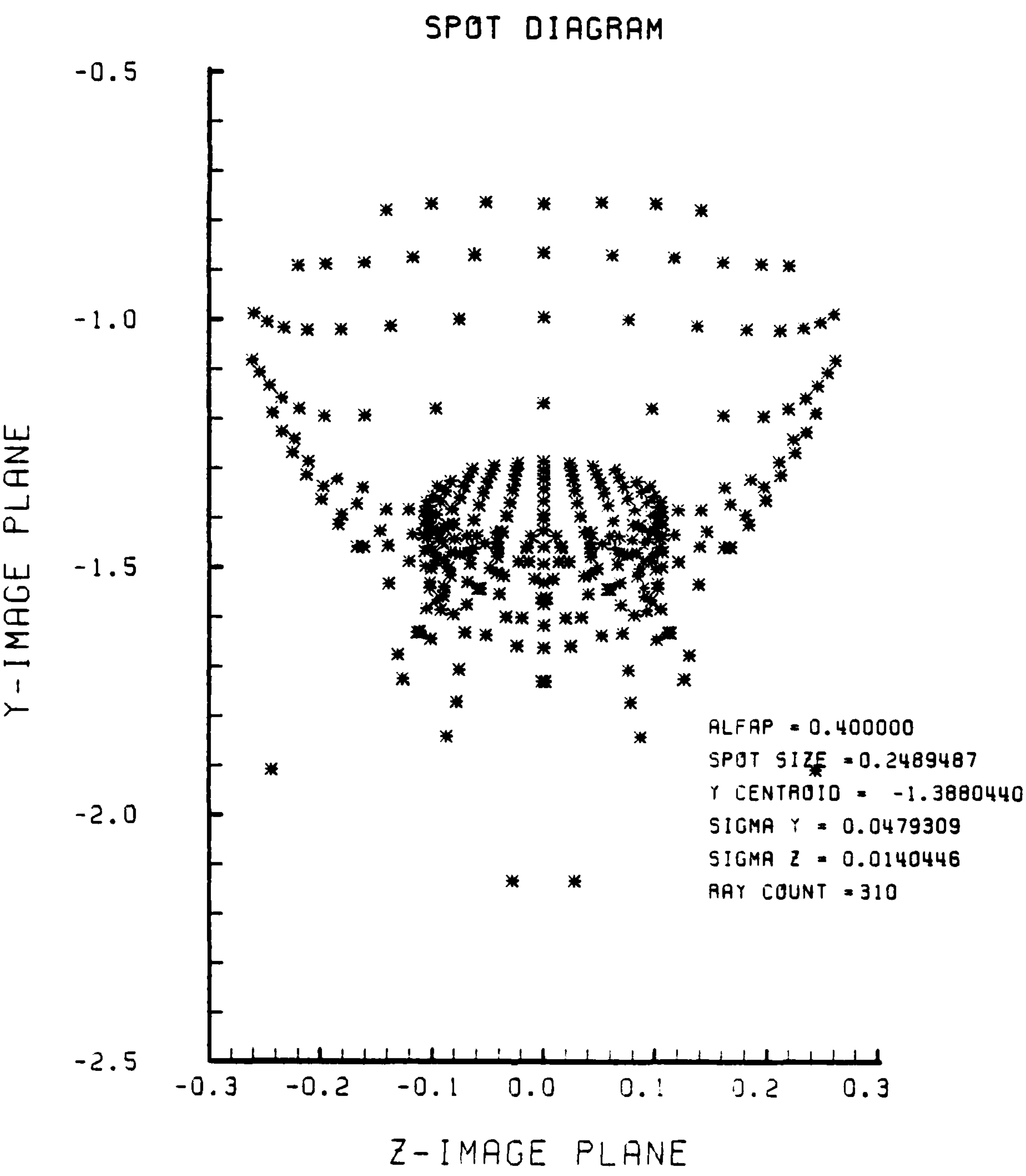

Figure G-11. Spot Diagram for Grid of Figure G-10

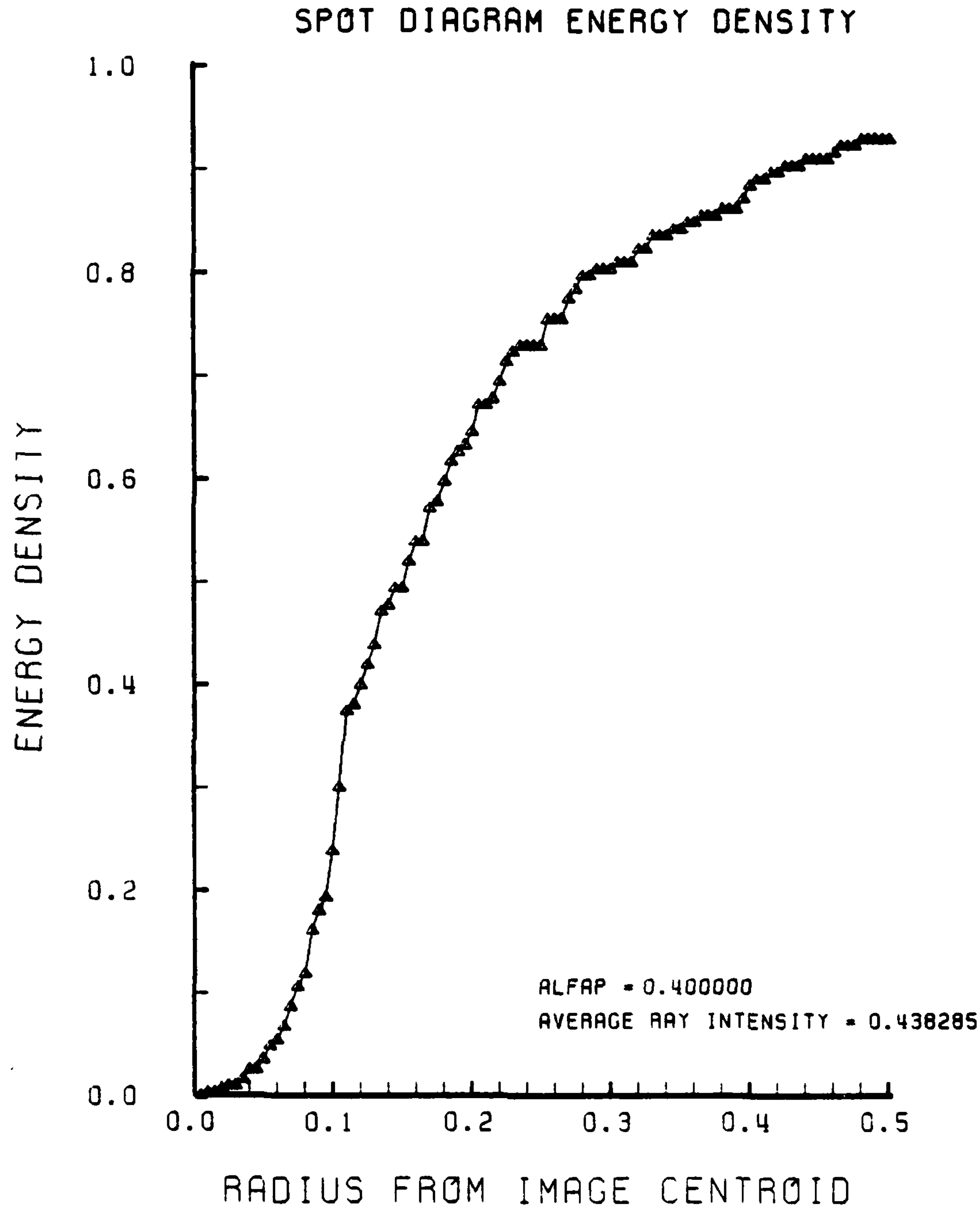

Figure G-12. Encircled Energy of Figure G-11

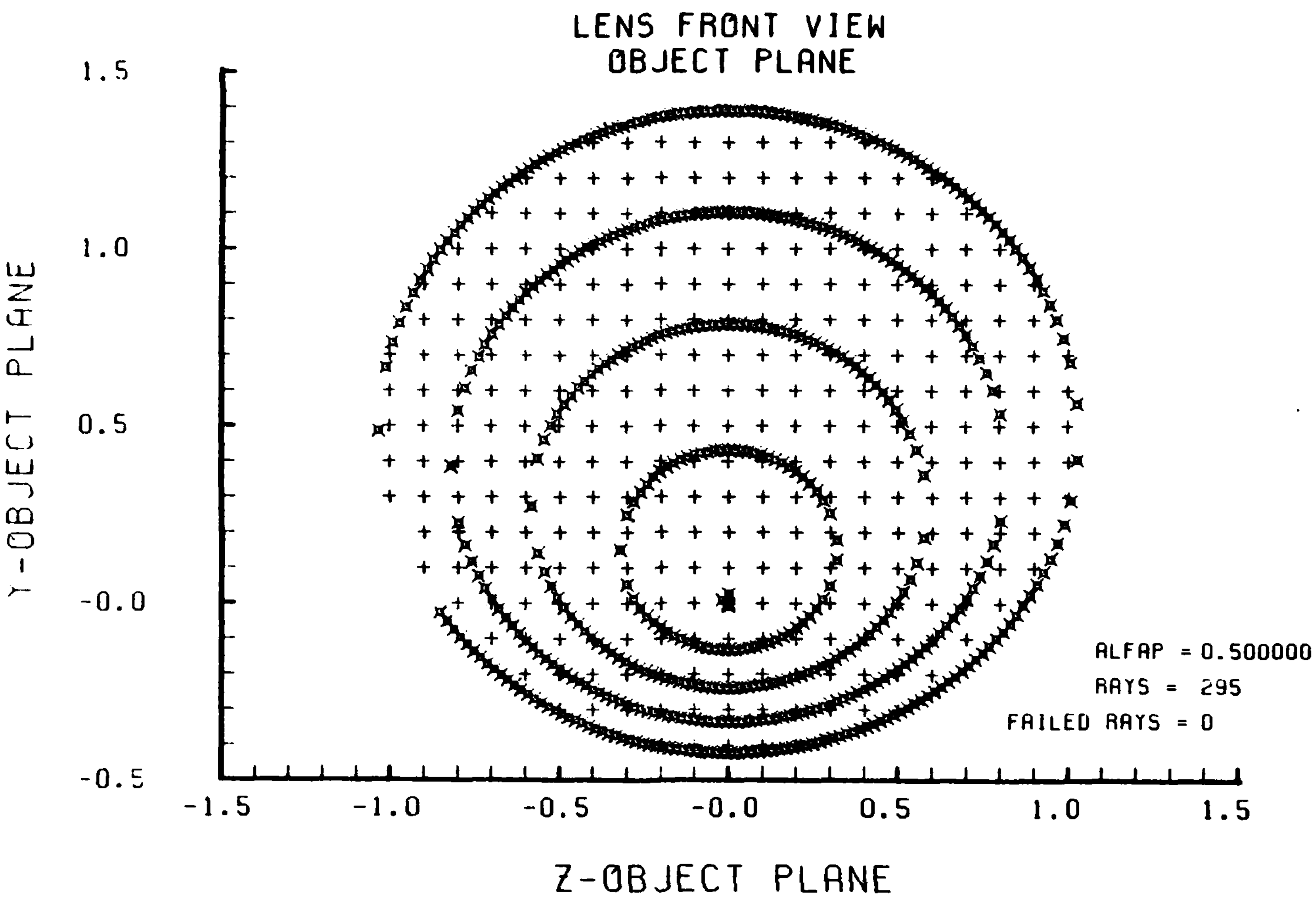

Figure G-13. Grid Plane at $\alpha_p = 0.5$ for Lens of Figure G-1

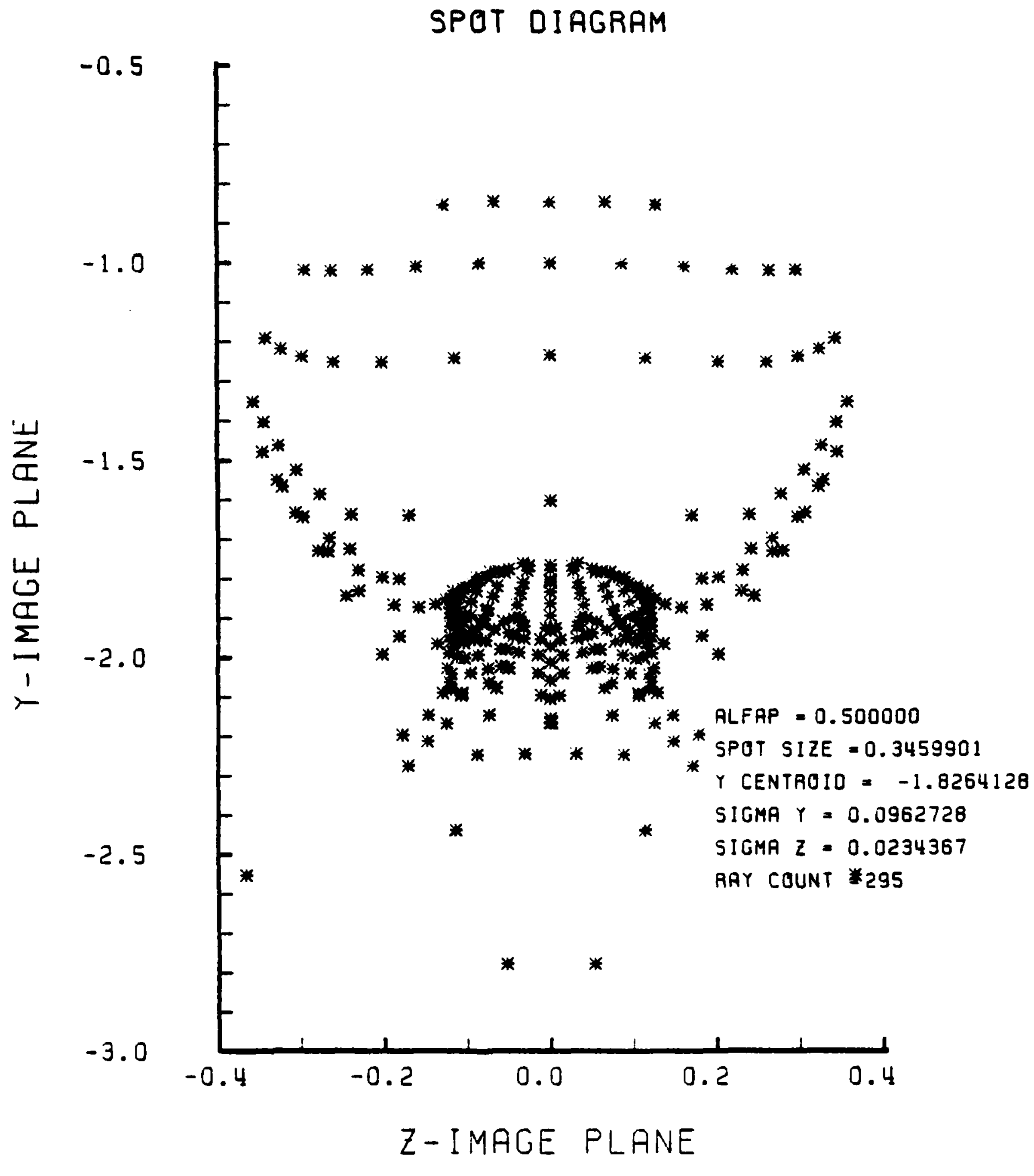

Figure G-14. Spot Diagram for Grid of Figure G-13

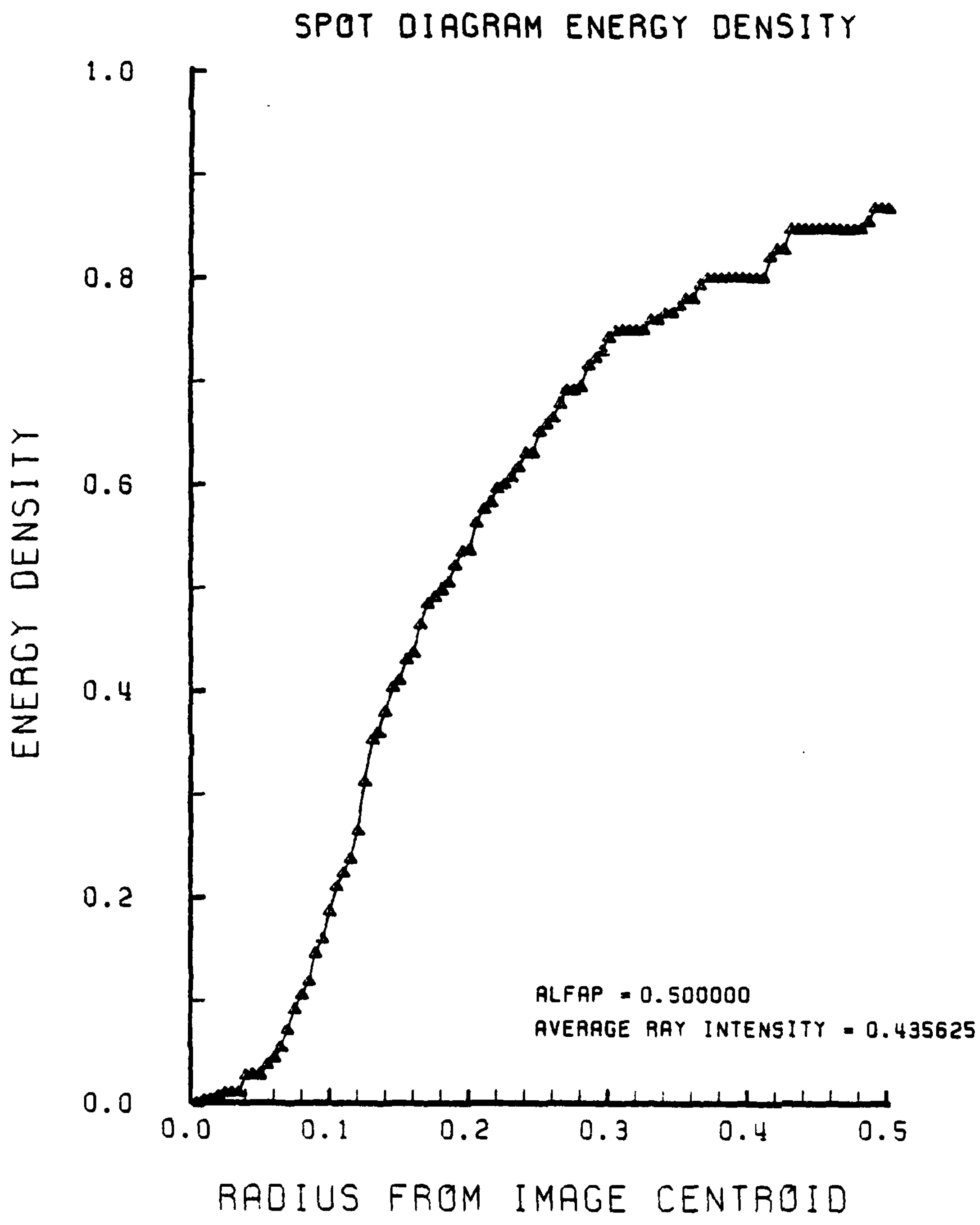

Figure G-15. Encircled Energy of Figure G-14

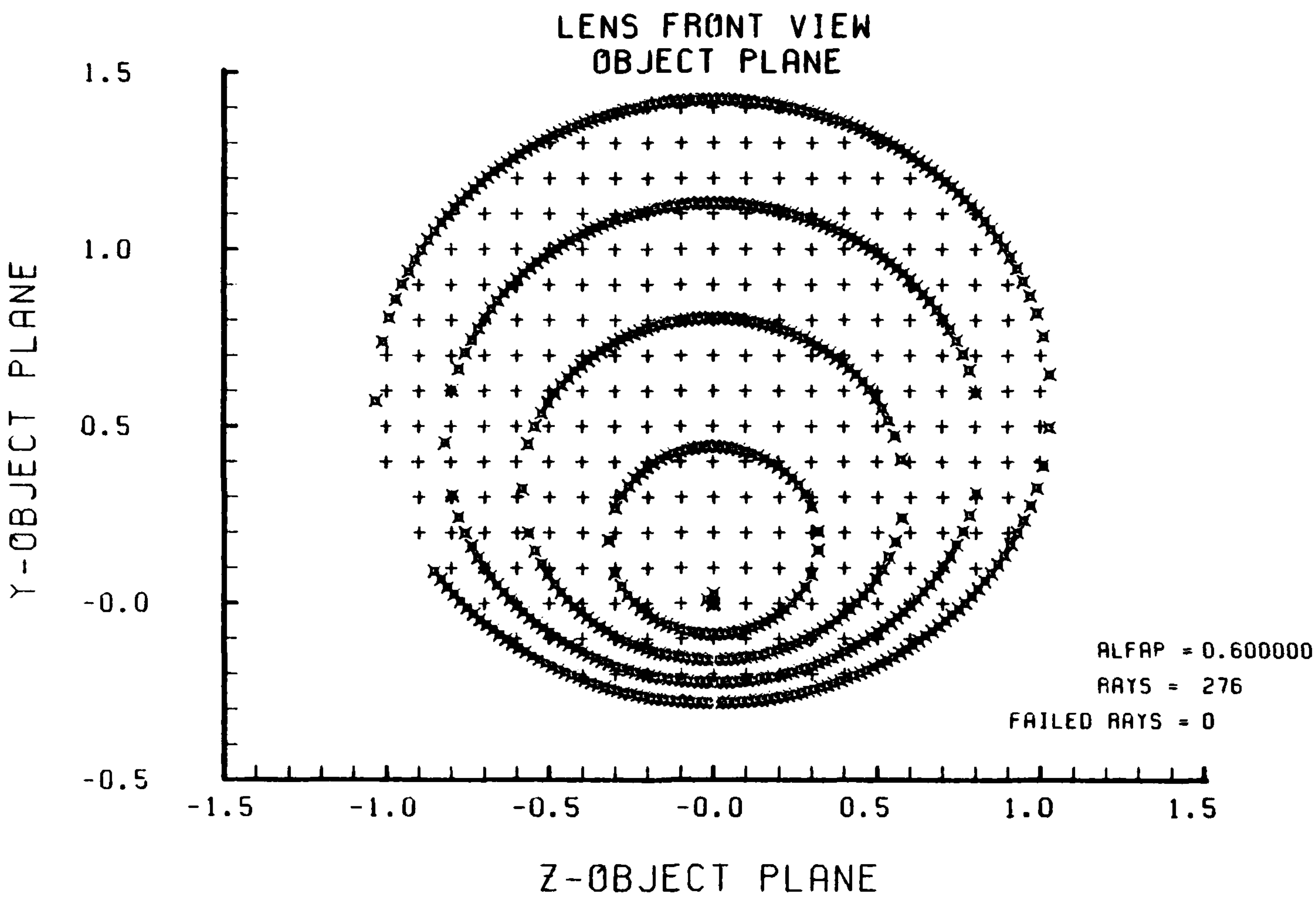

Figure G-16. Grid Plane at $\alpha_p = 0.7$ for Lens of Figure G-1

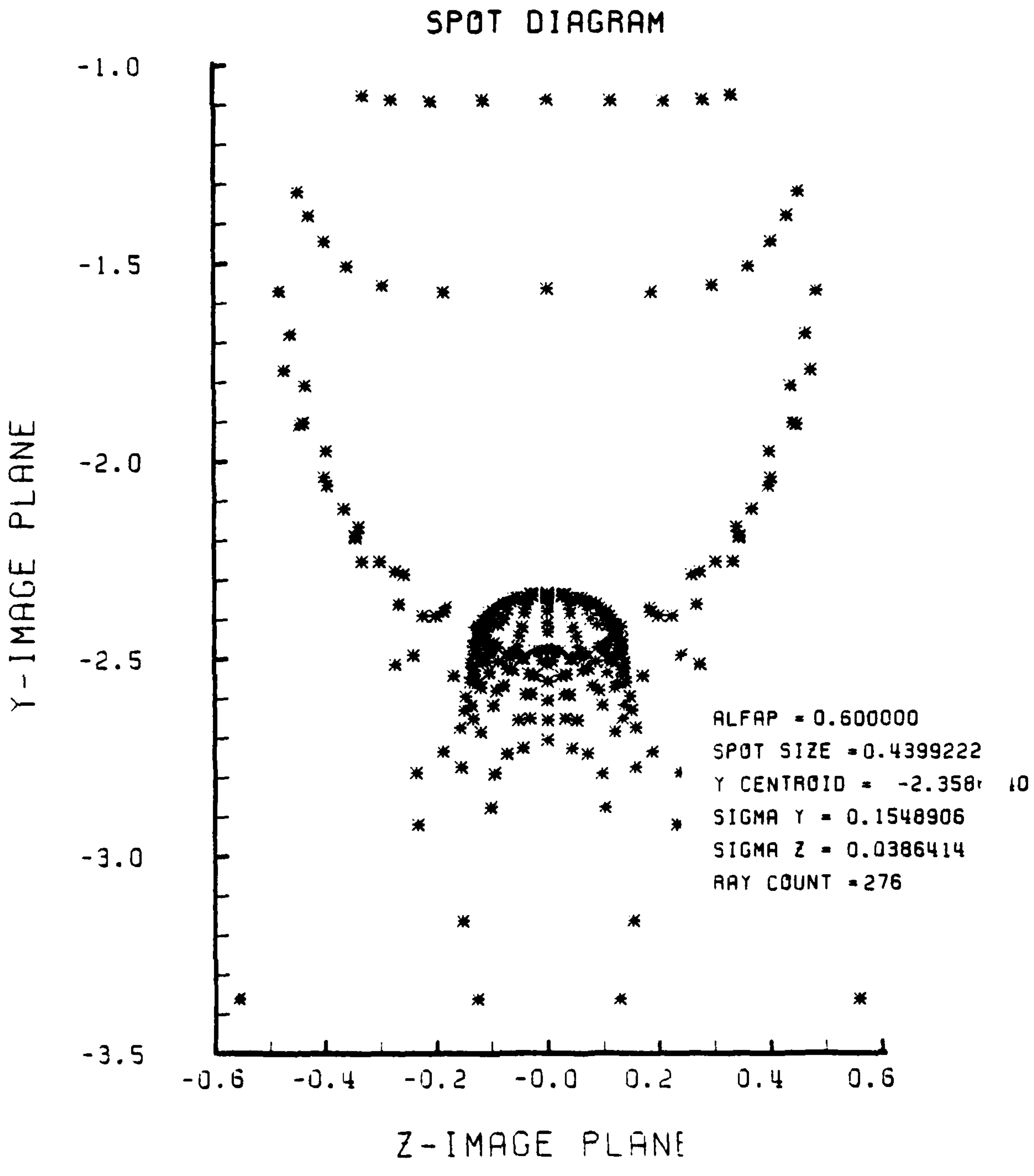

Figure G-17. Spot Diagram for Grid of Figure G-16

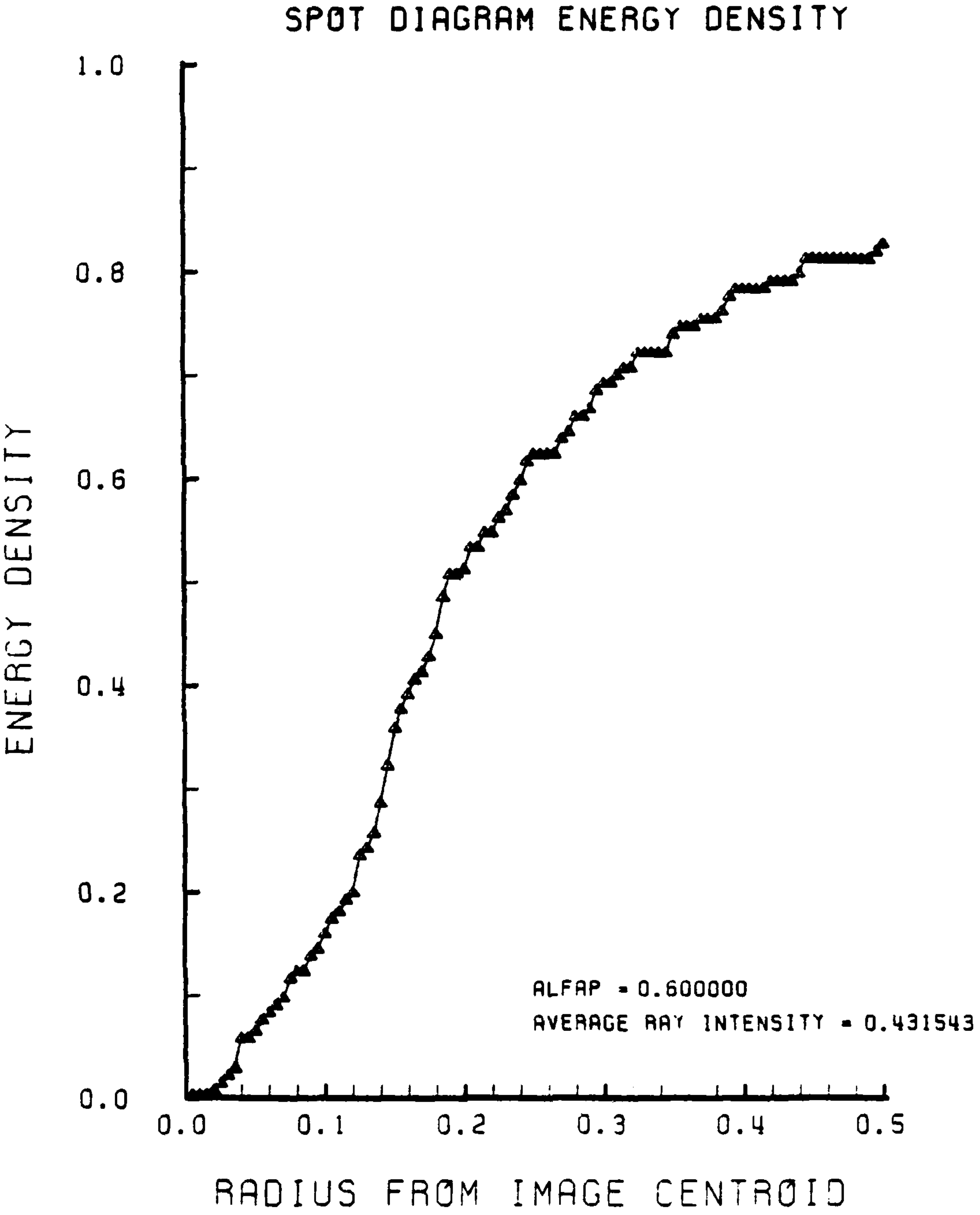

Figure G-18. Encircled Energy of Figure G-17

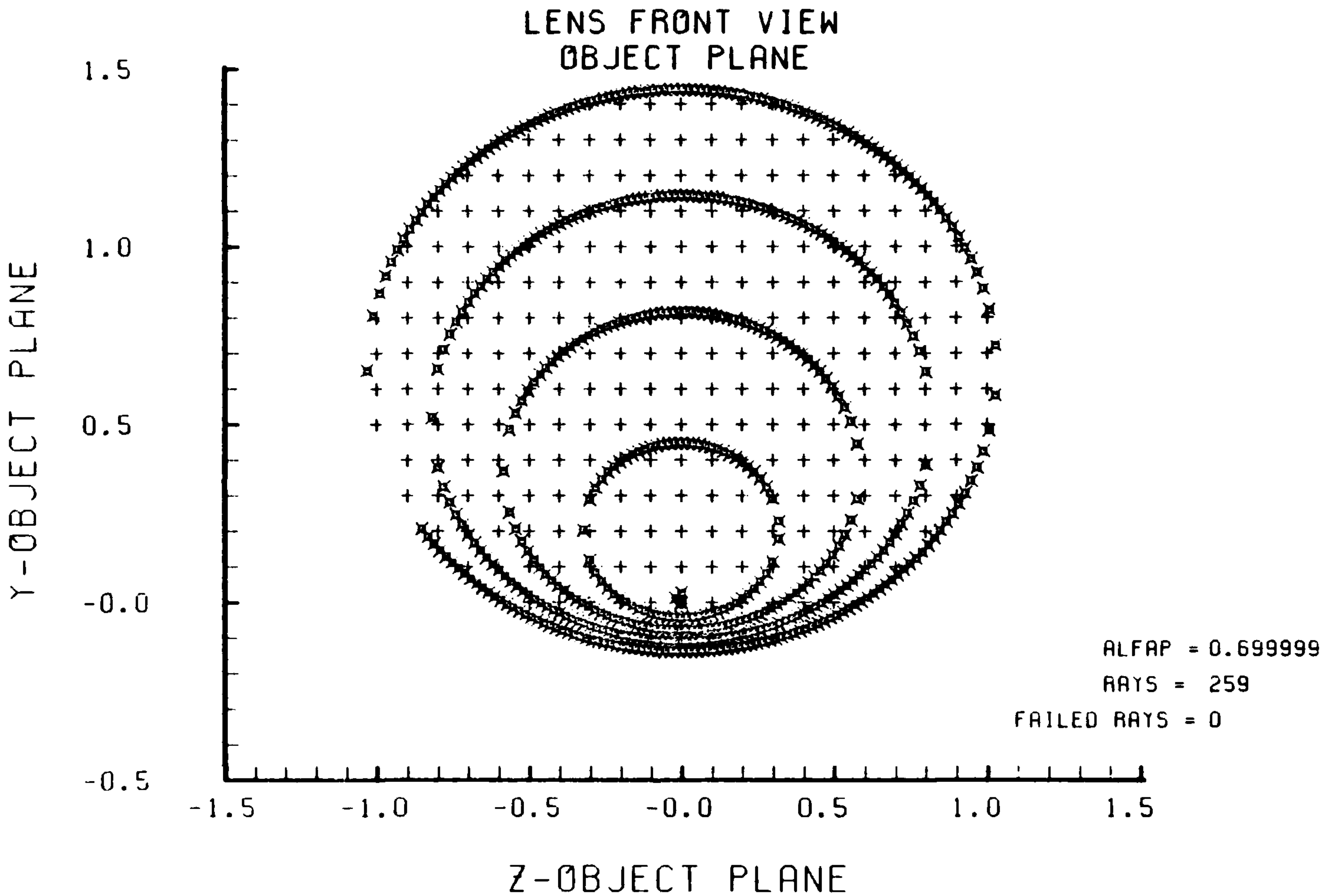

Figure G-19. Grid Plane at $\alpha_p = 0.7$ for Lens of Figure G-1

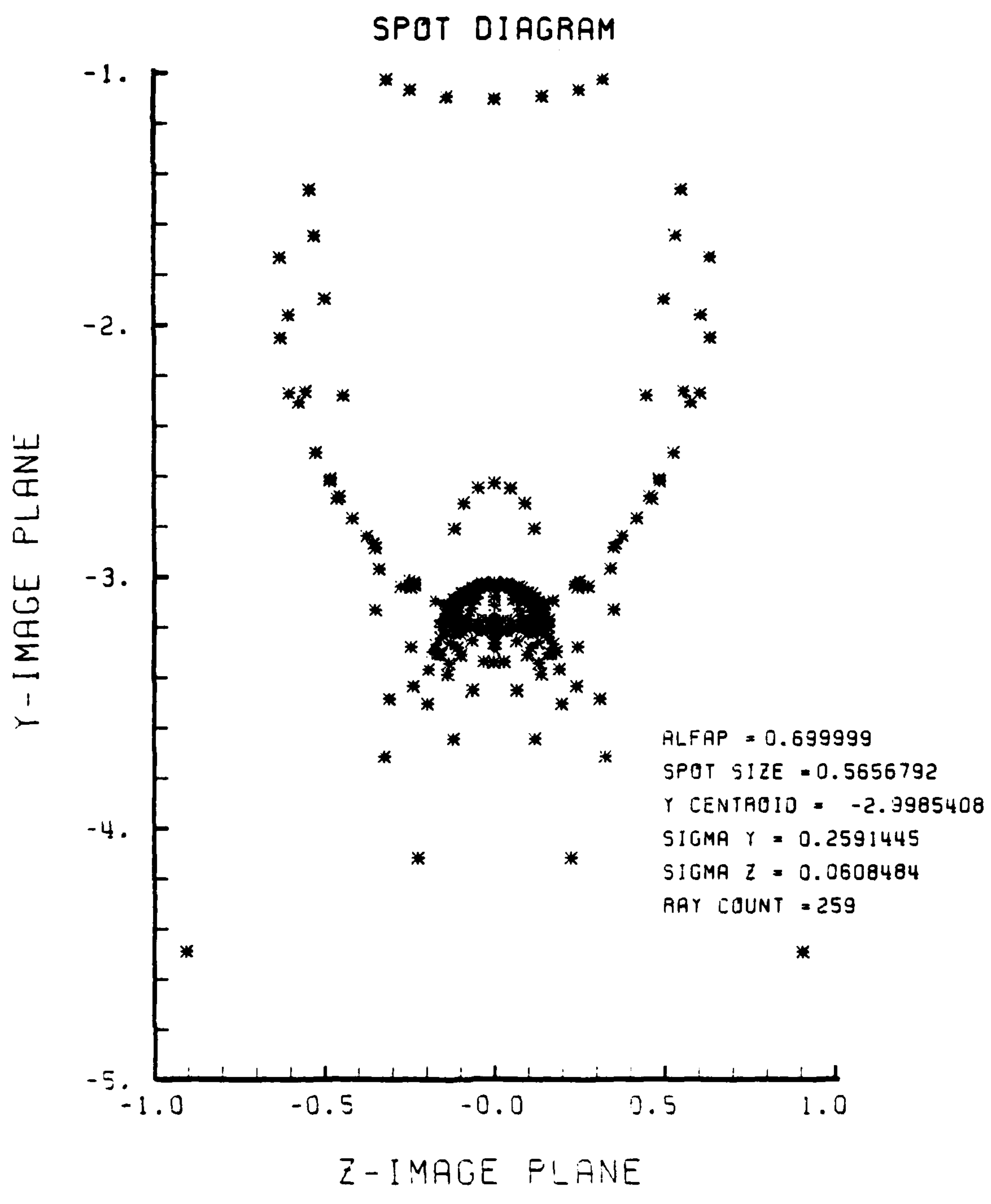

Figure G-20. Spot Diagram for Grid of Figure G-19

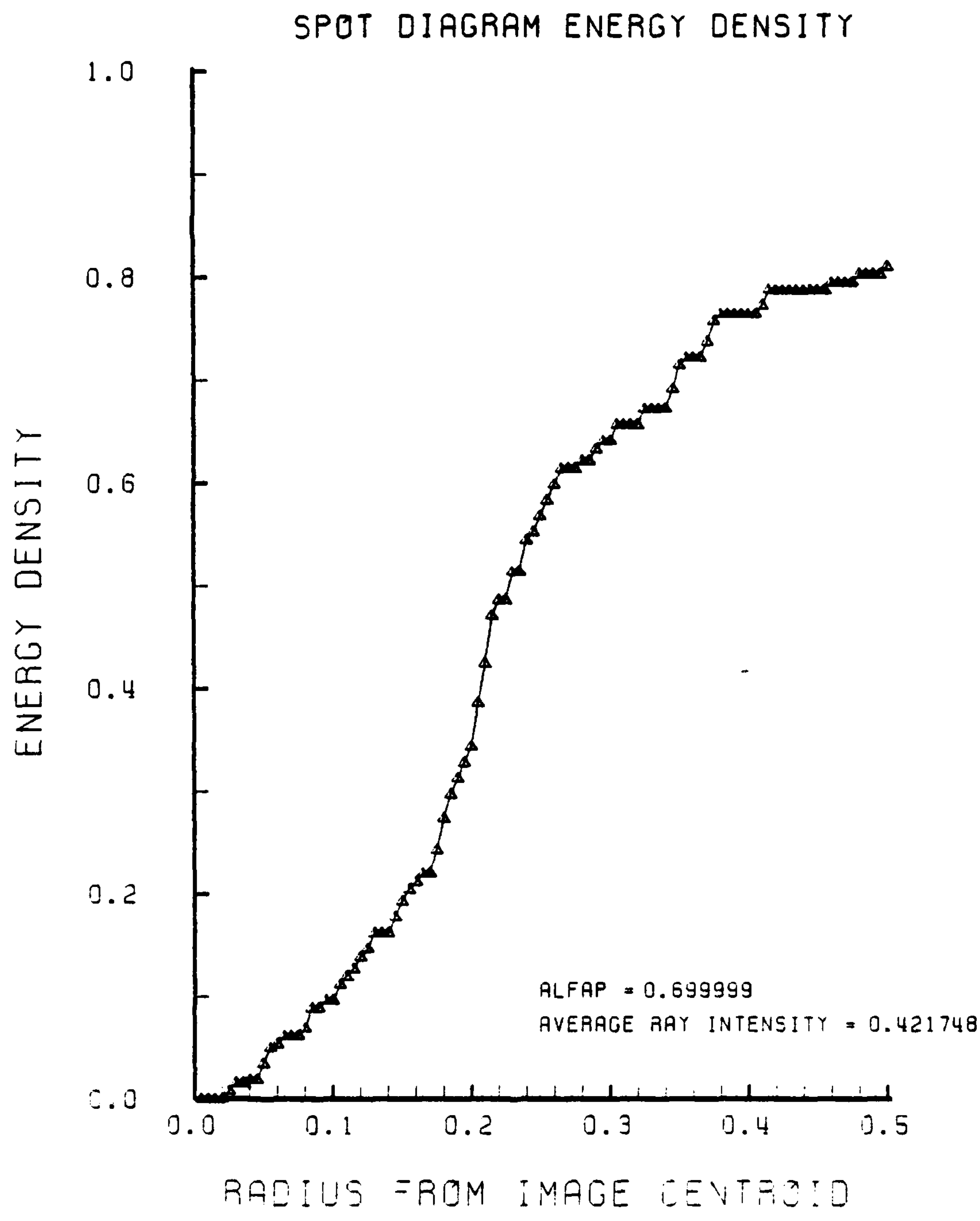

Figure G-21. Encircled Energy of Figure G-20

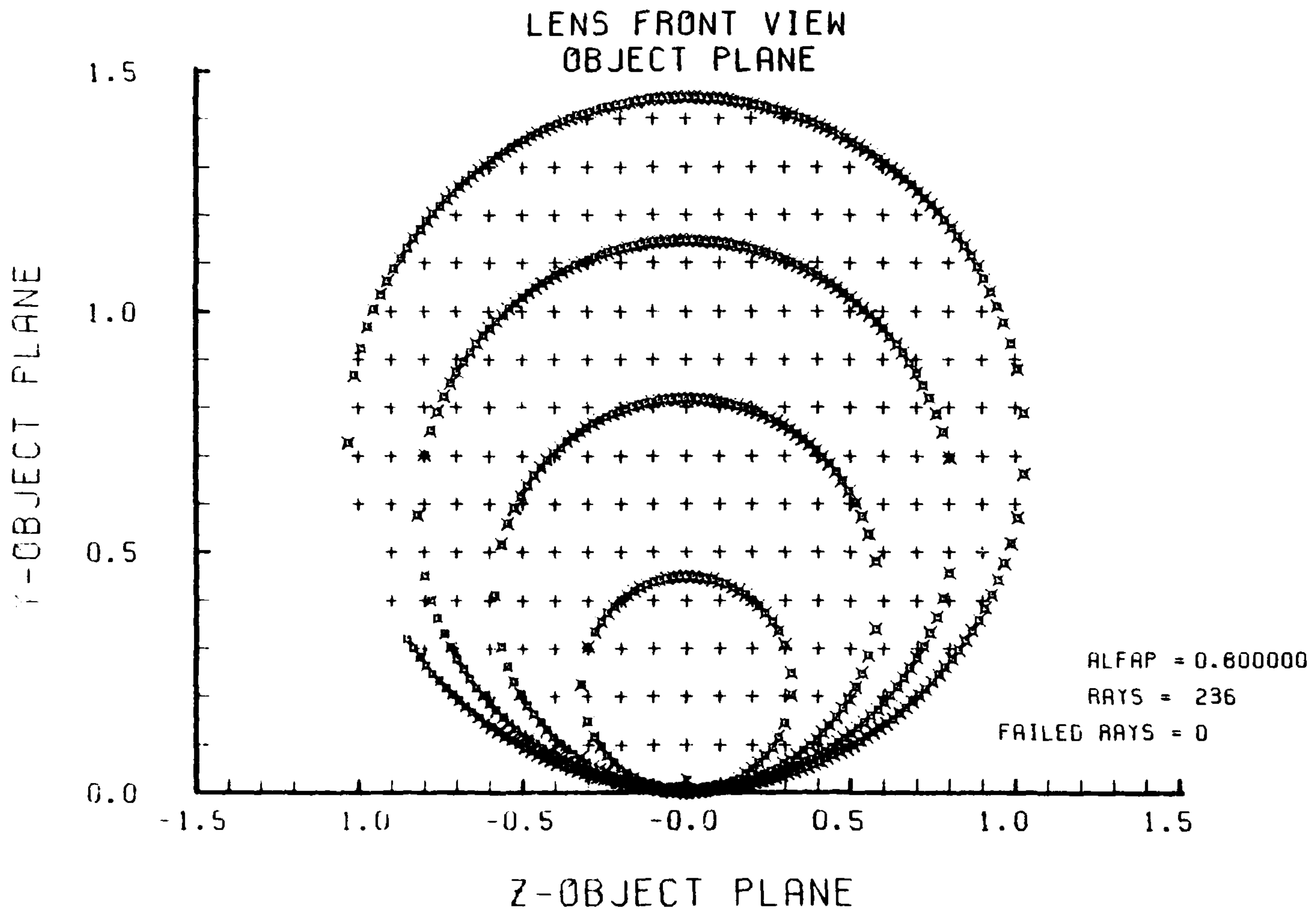

Figure G-22. Grid Plane at α_p = 0.8 for Lens of Figure G-1

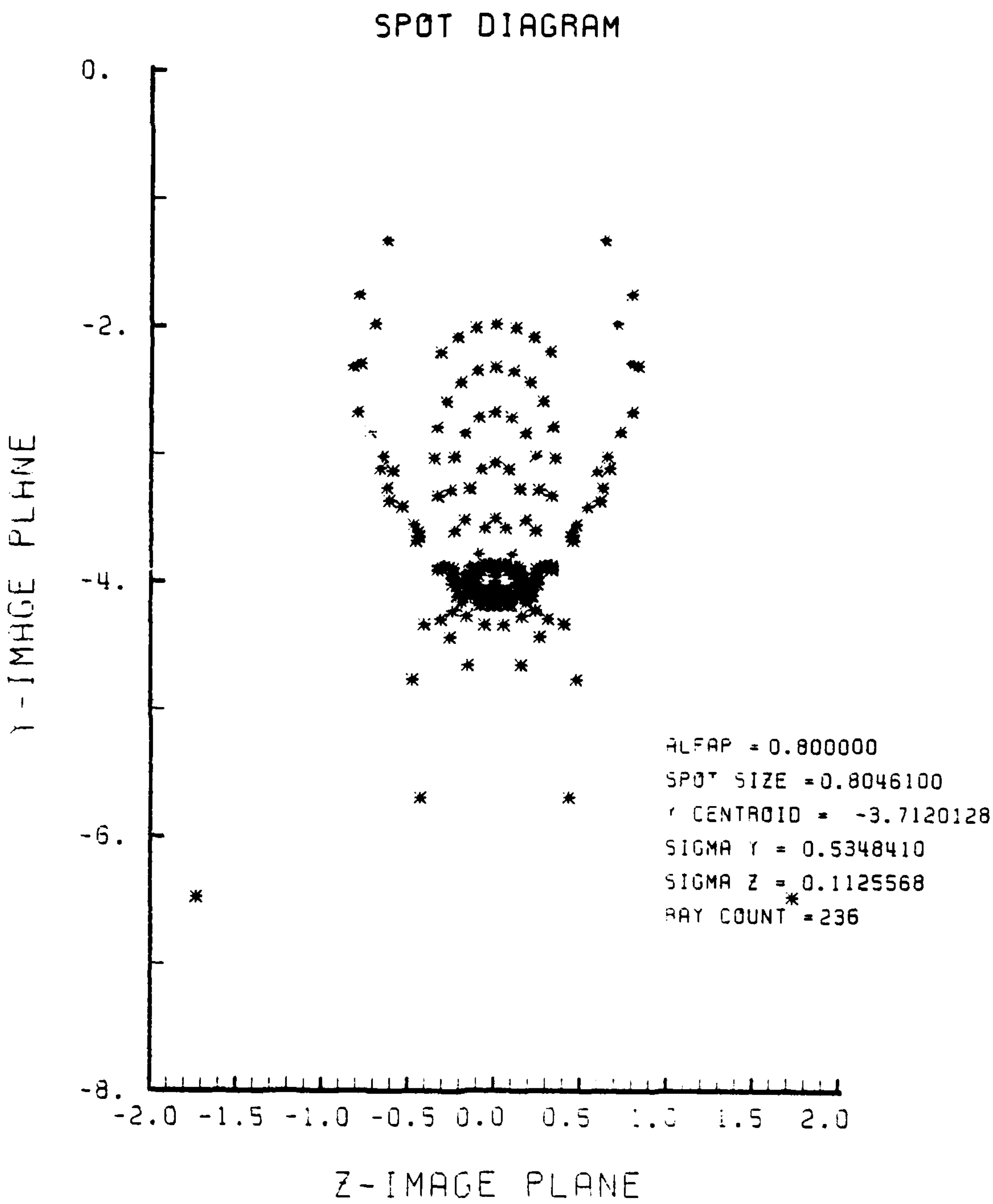

Figure G-23. Spot Diagram for Grid of Figure G-22

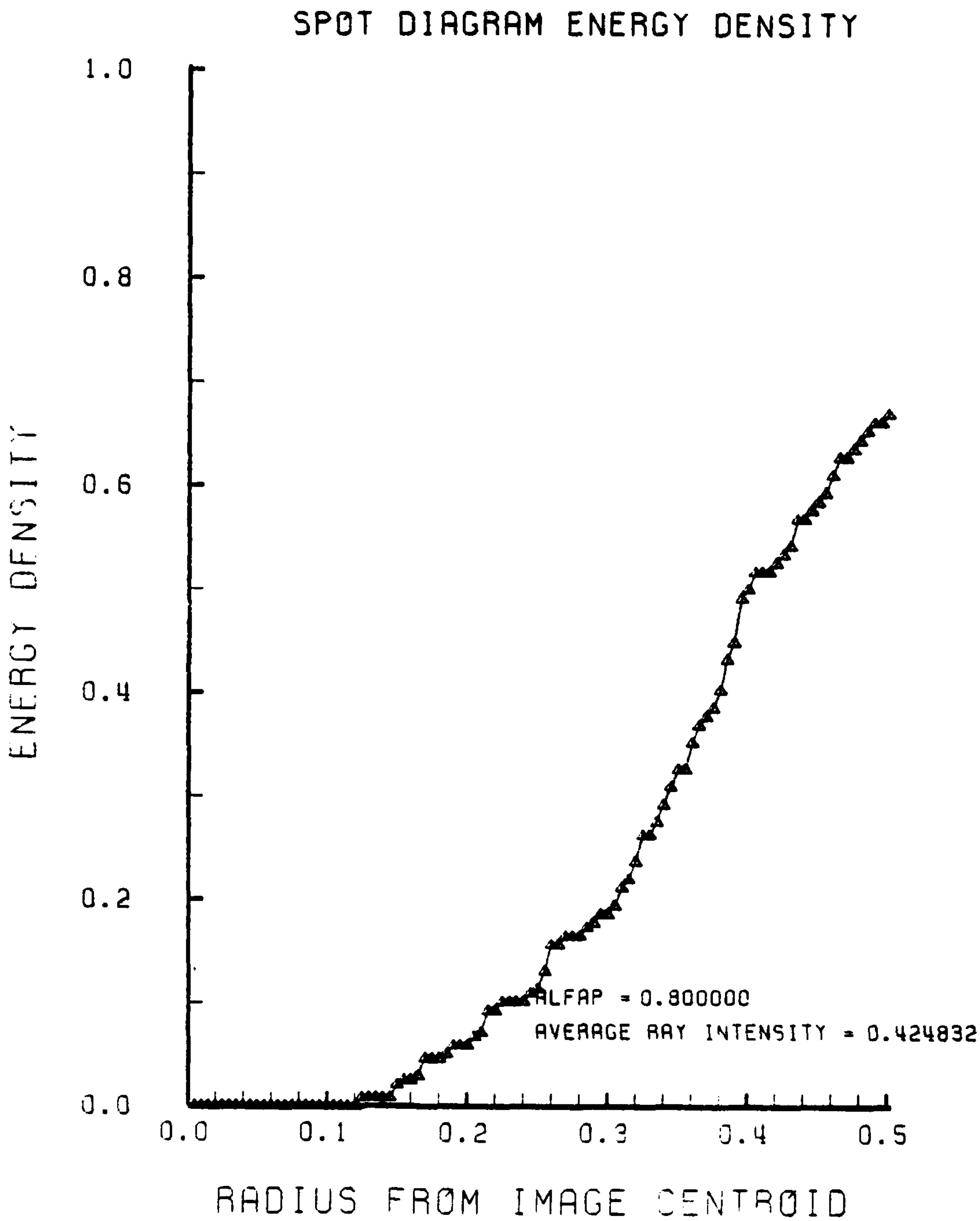

Figure G-24. Encircled Energy of Figure G-23

APPENDIX H

"BEST" GRIN LENS PERFORMANCE PLOTS IN THE F/1 CONFIGURATION

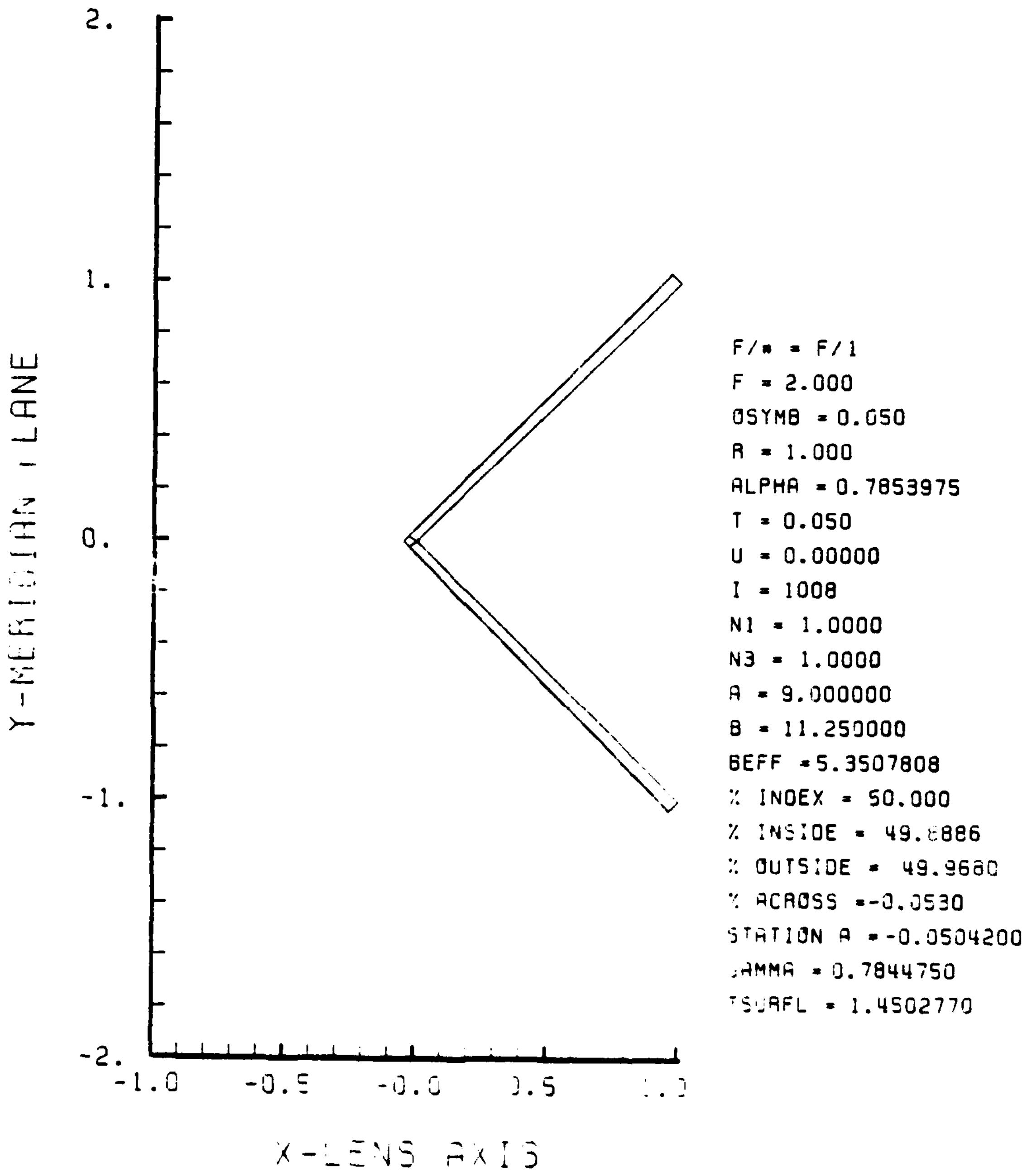

Figure H-1. "Best" GRIN Lens Shape with 50% Gradient, OB = 0.05, and a = 9.00 in the F/1 Configuration

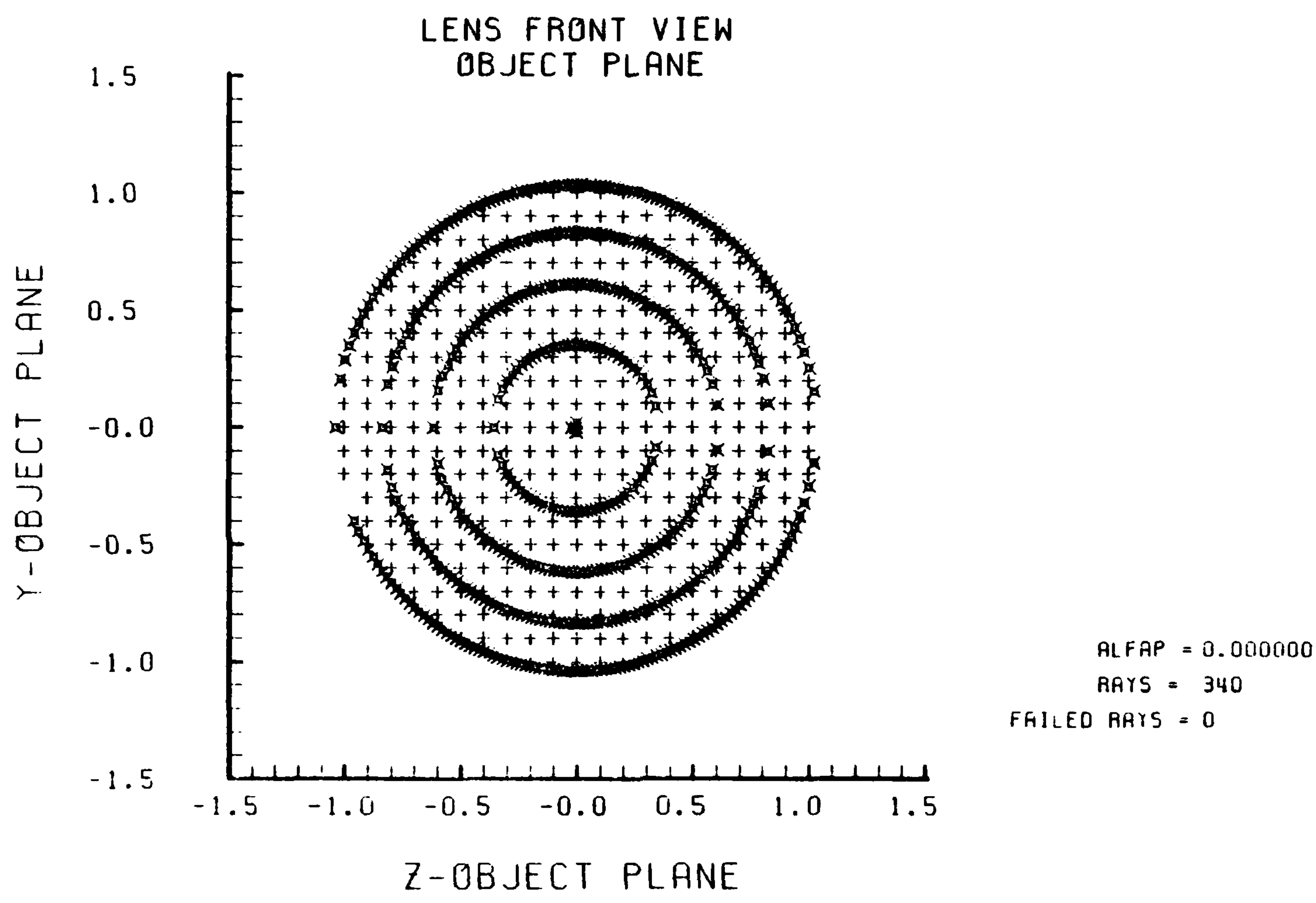

Figure H-2. Grid Plane at α_p = 0.0 for Lens of Figure H-1

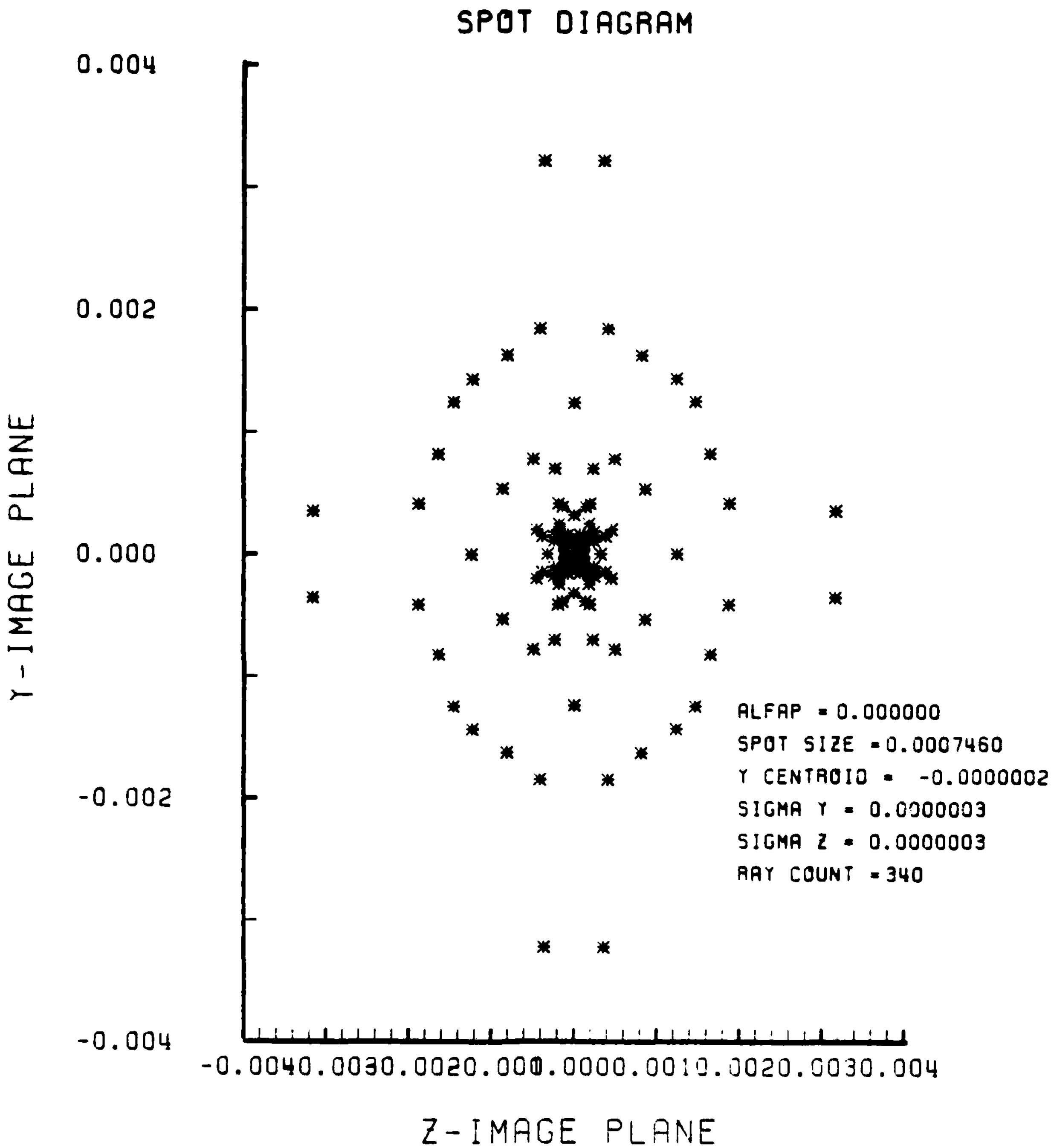

Figure H-3. Spot Diagram for Grid of Figure H-2

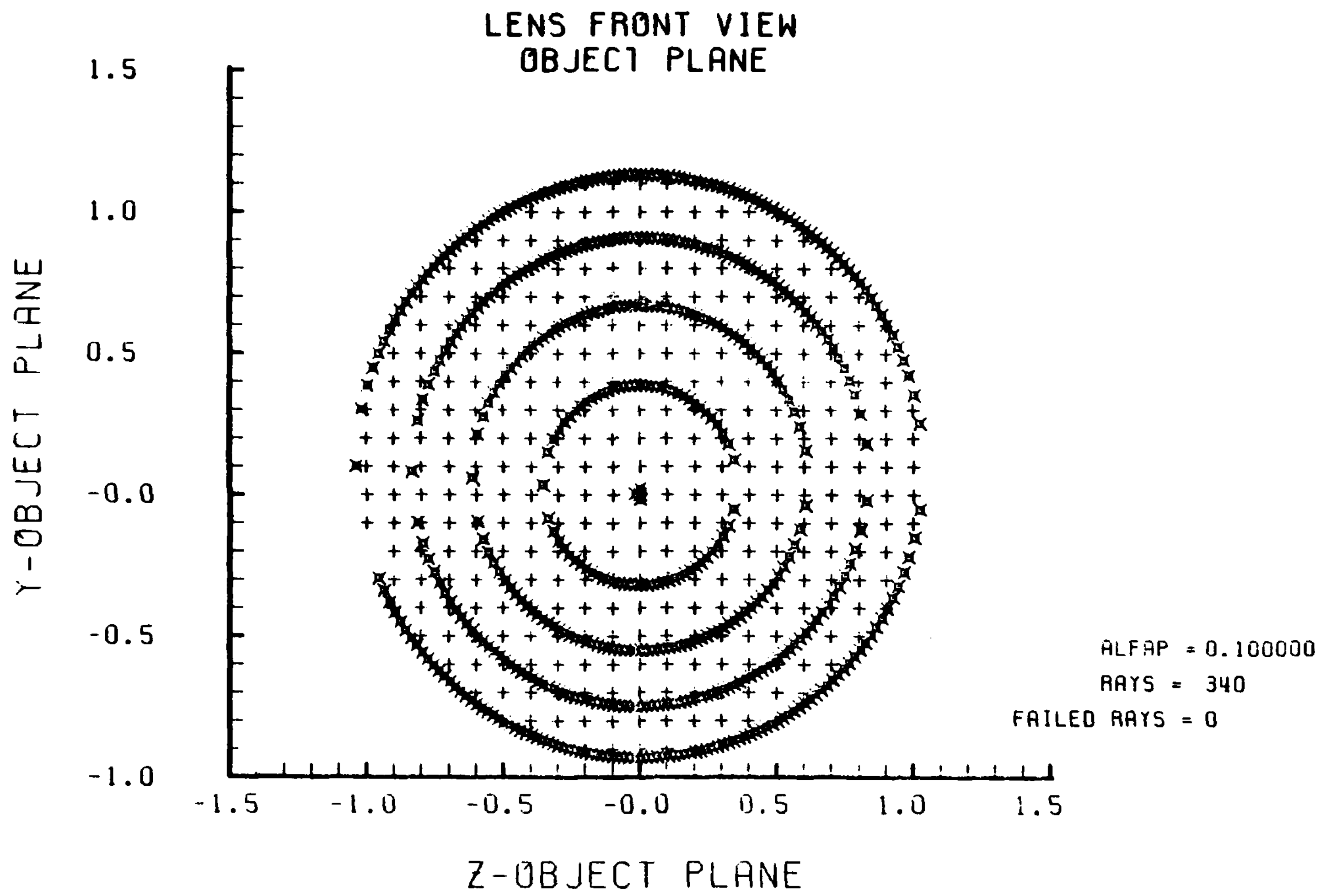

Figure H-4. Grid Plane at α_p = 0.1 for Lens of Figure H-1

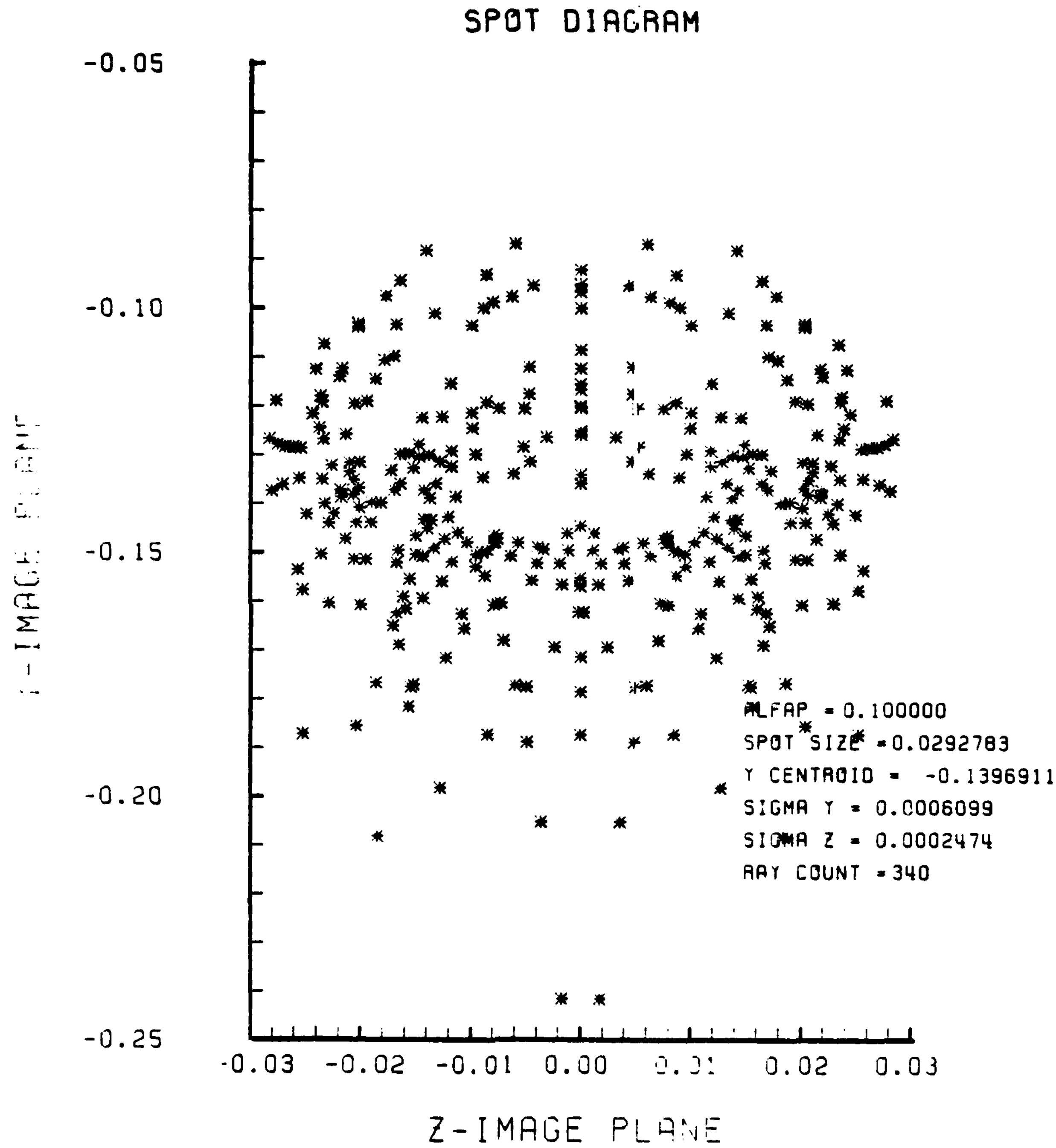

Figure H-5. Spot Diagram for Grid of Figure H-4

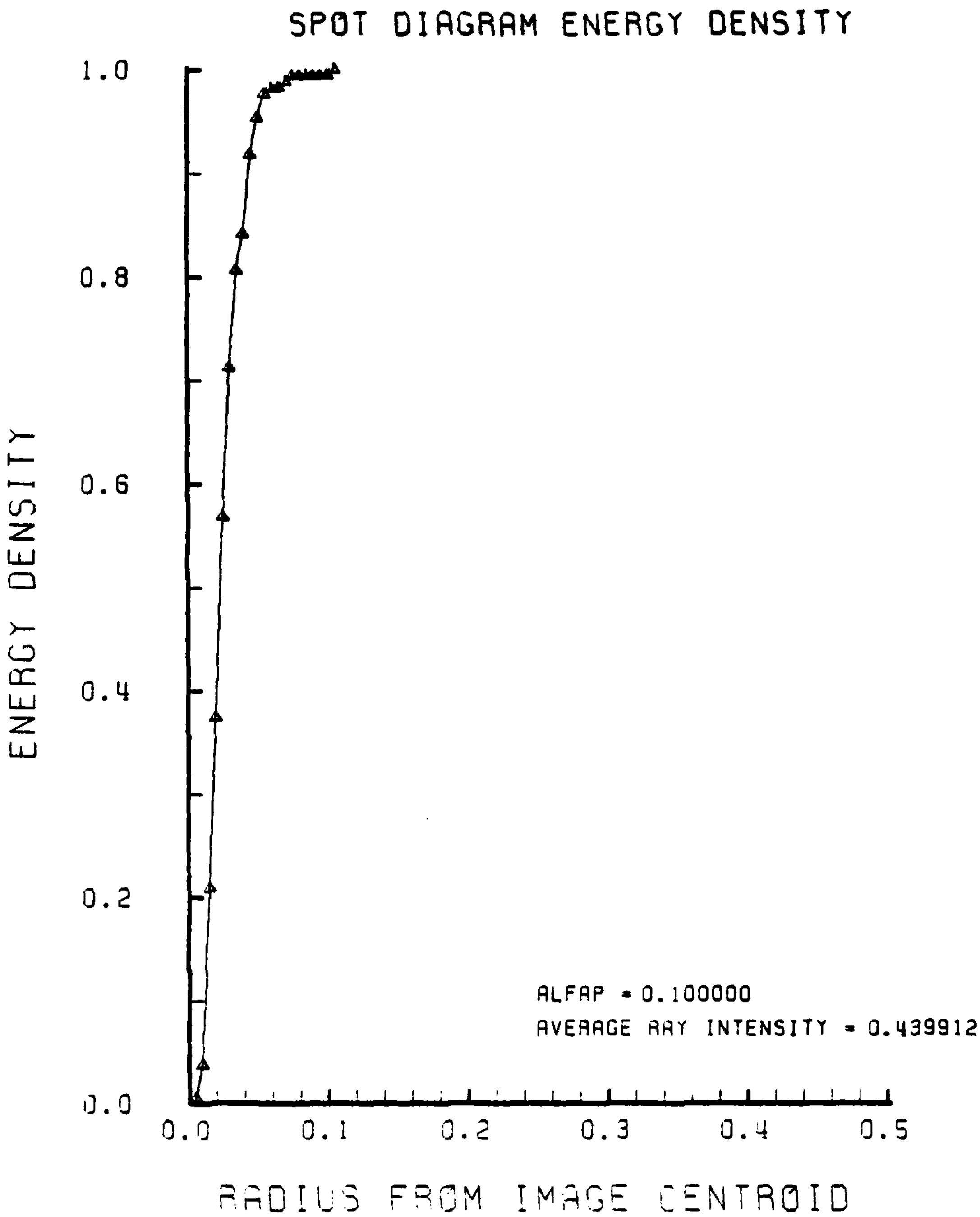

Figure H-6. Encircled Energy of Figure H-5

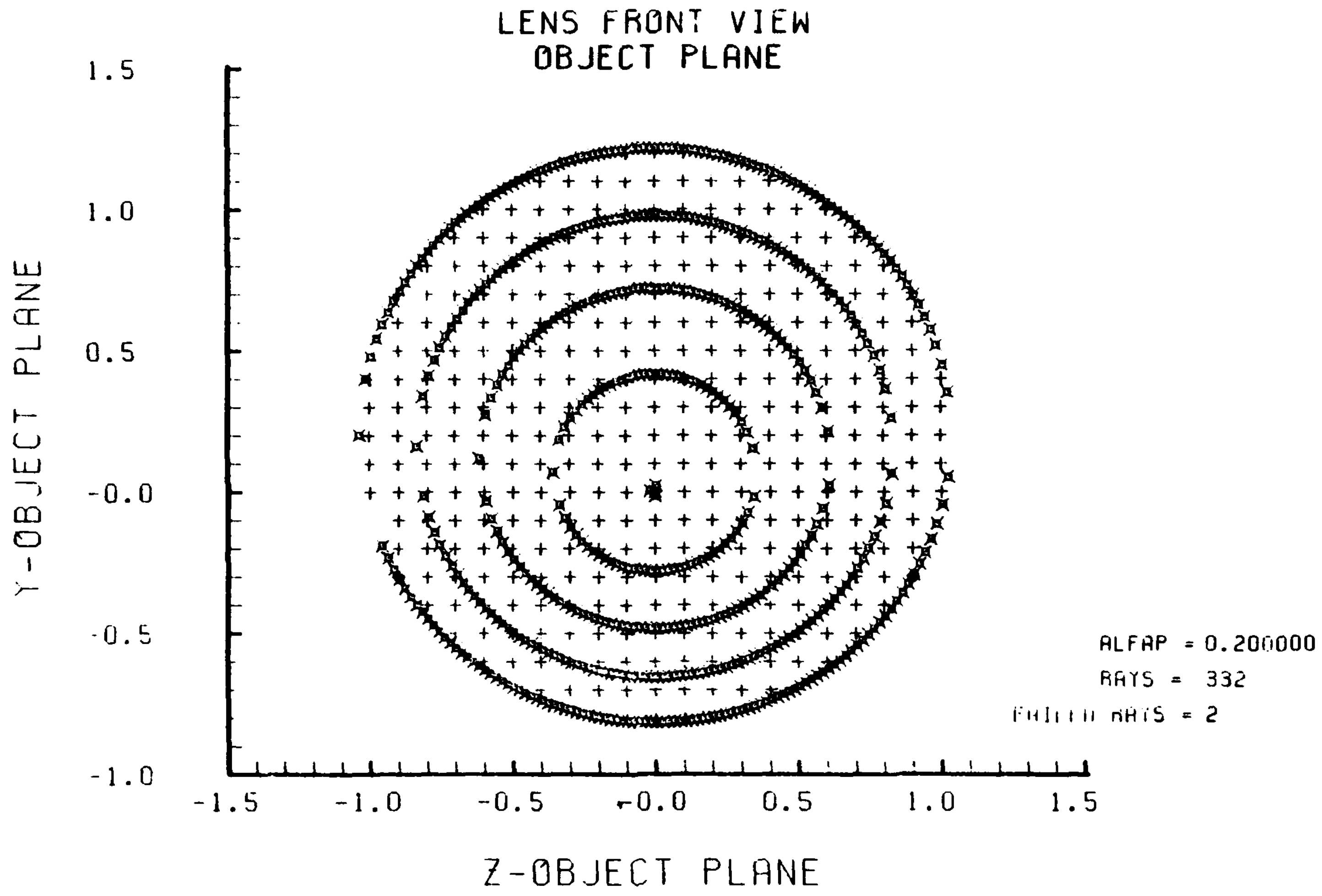

Figure H-7. Grid Plane at $\alpha_p = 0.2$ for Lens of Figure H-1

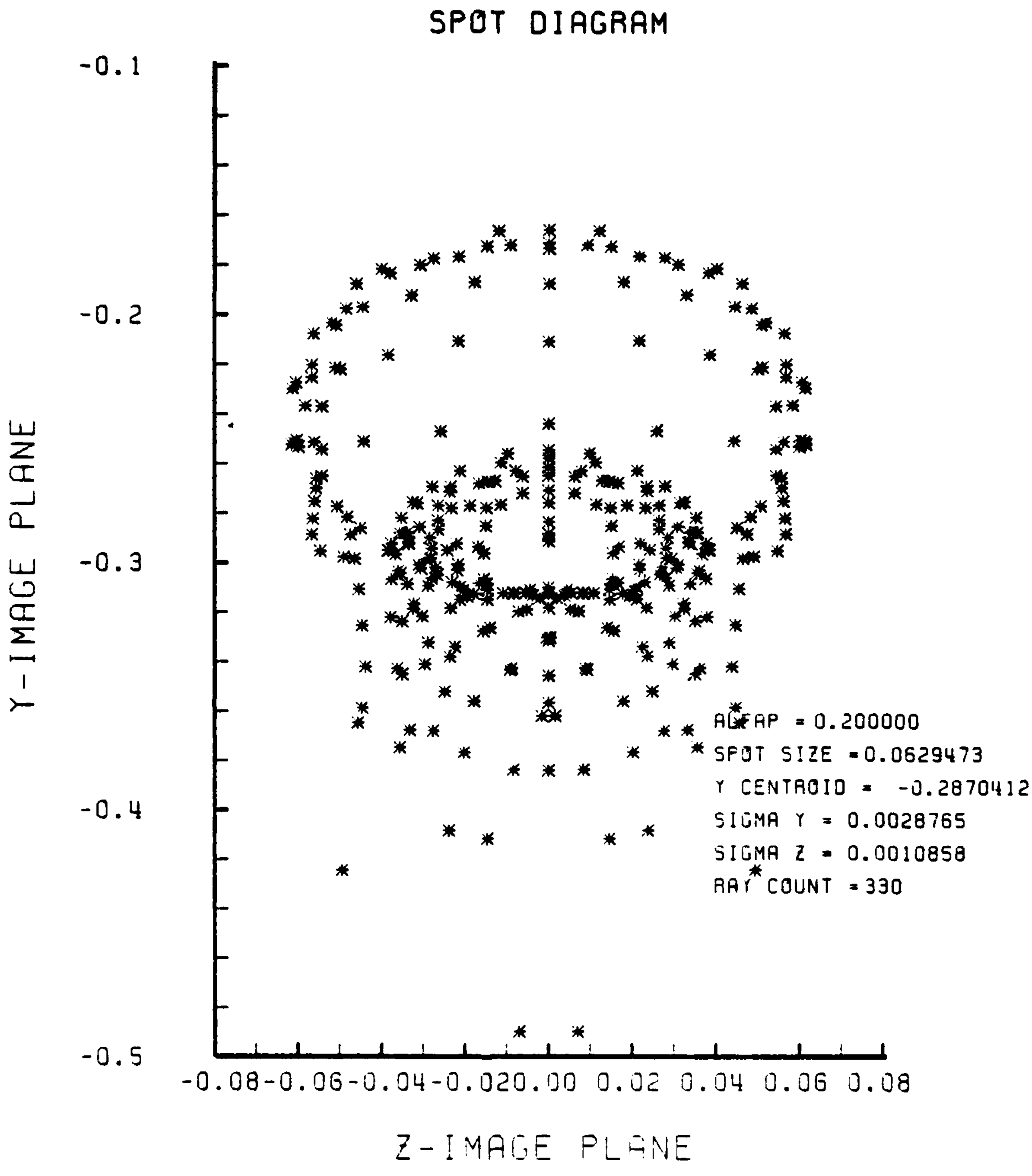

Figure H-8. Spot Diagram for Grid of Figure H-7

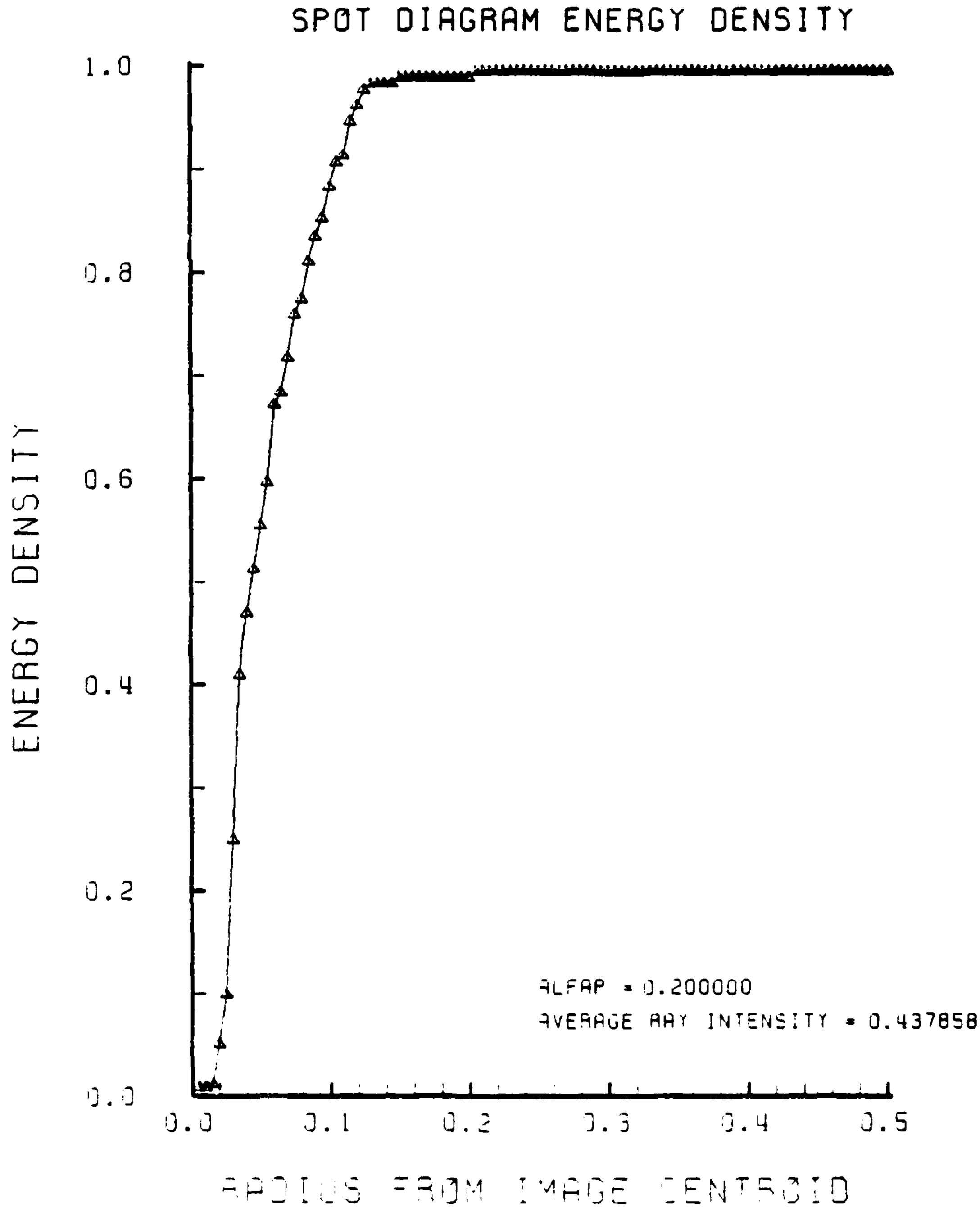

Figure H-9. Encircled Energy of Figure H-8

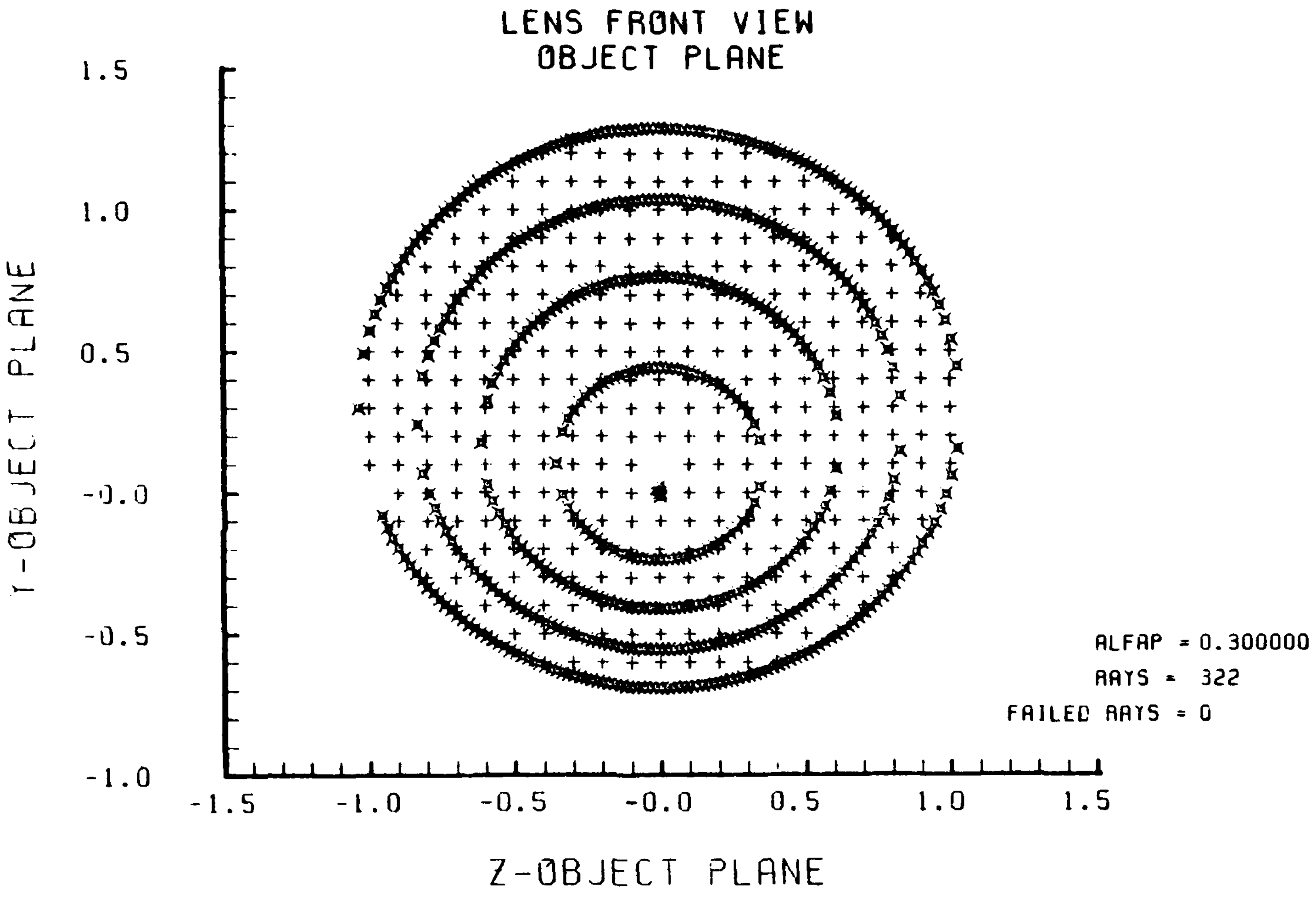

Figure H-10. Grid Plane at $\alpha_p = 0.3$ for Lens of Figure H-1

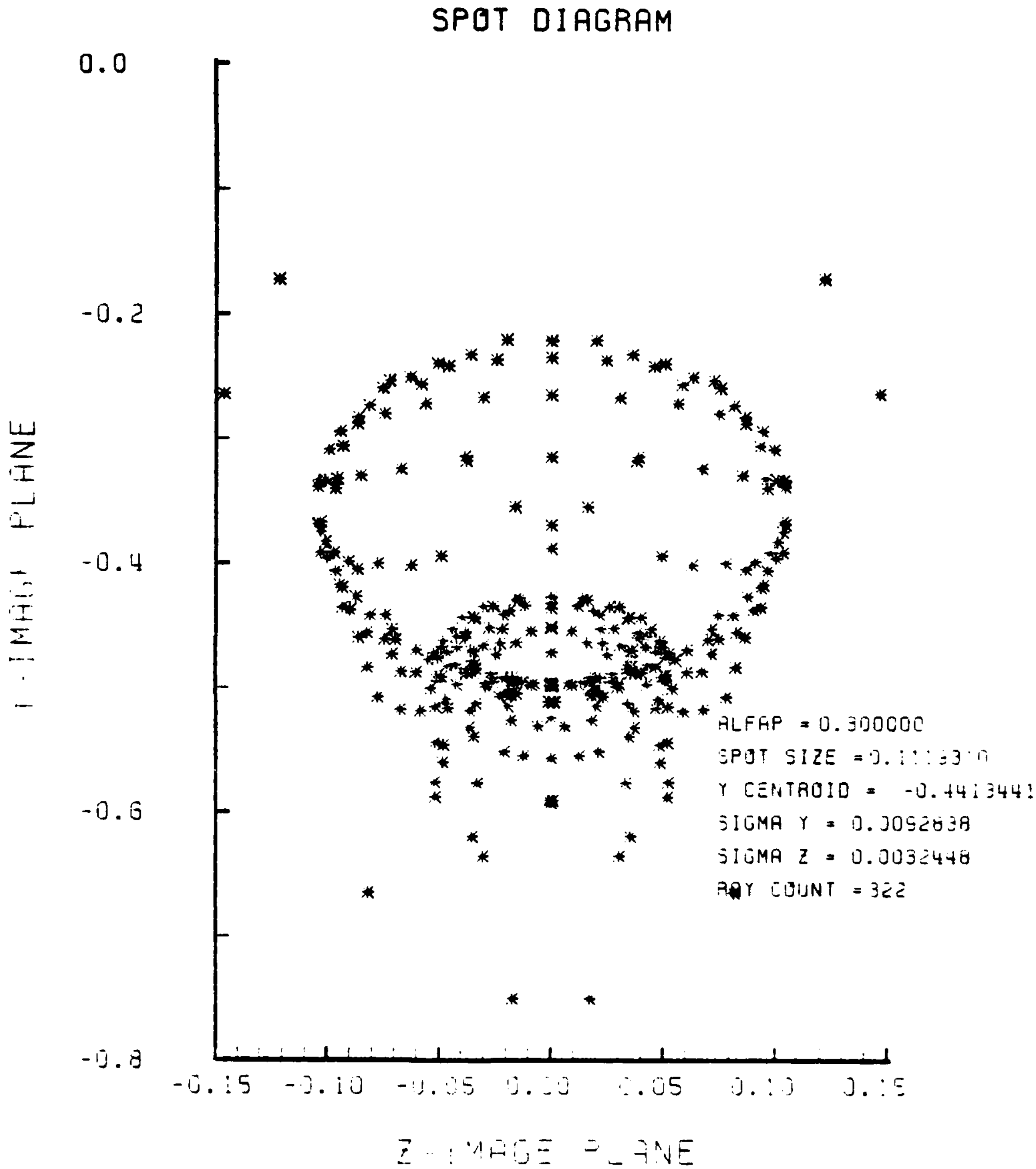

Figure H-11. Spot Diagram for Grid of Figure H-10

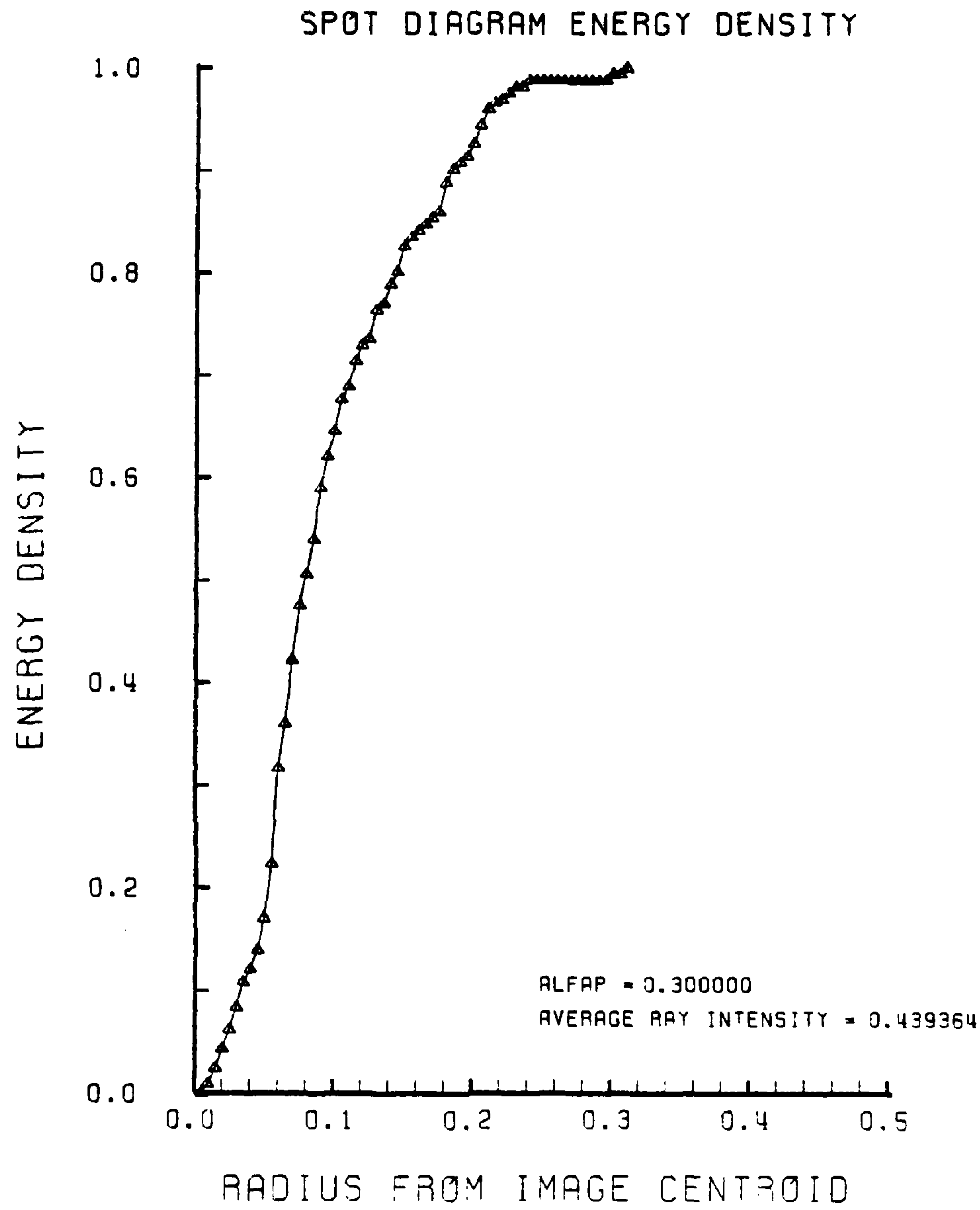

Figure H-12. Encircled Energy of Figure H-11

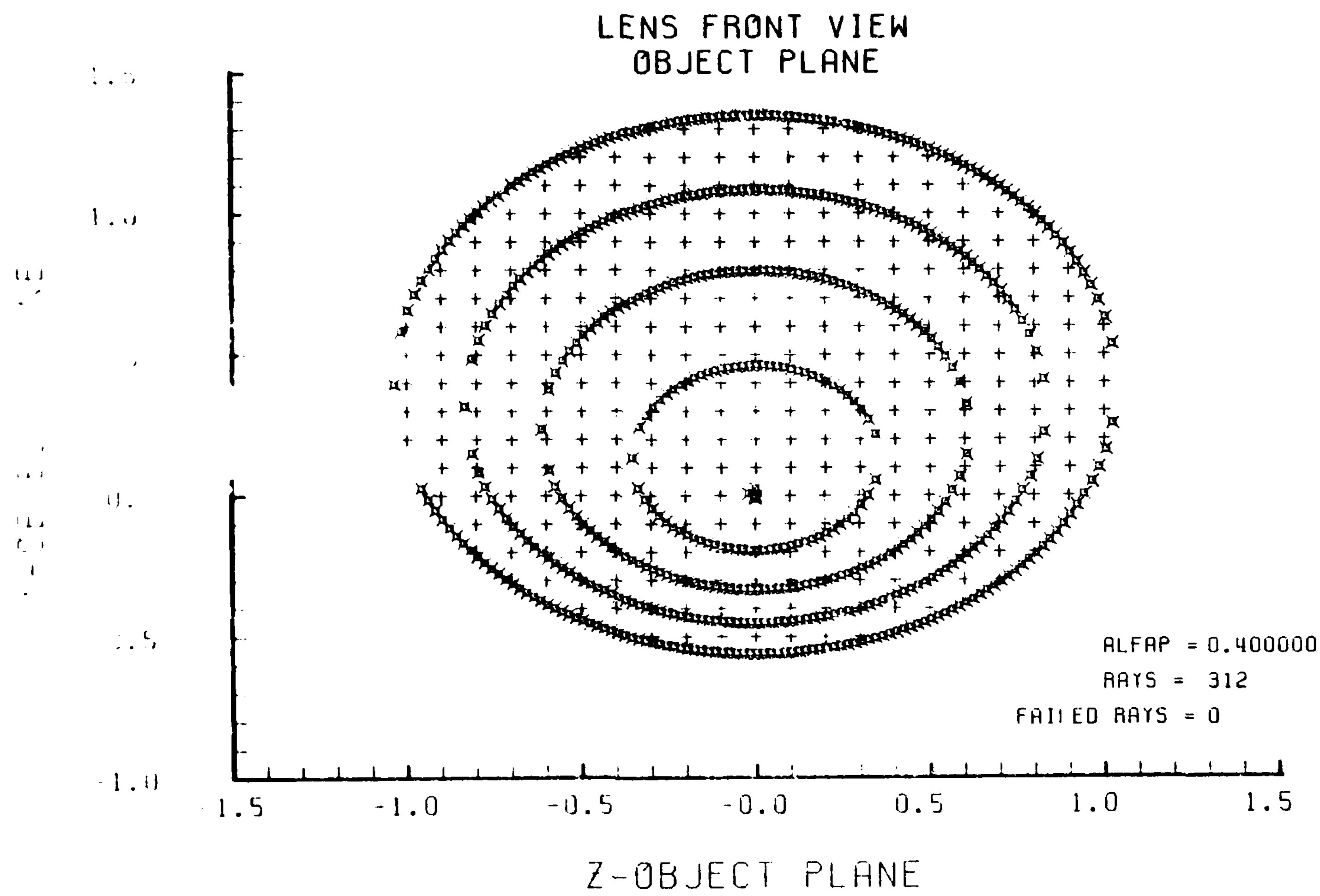

Figure H-13. Grid Plane at $\alpha_p = 0.4$ for Lens of Figure H-1

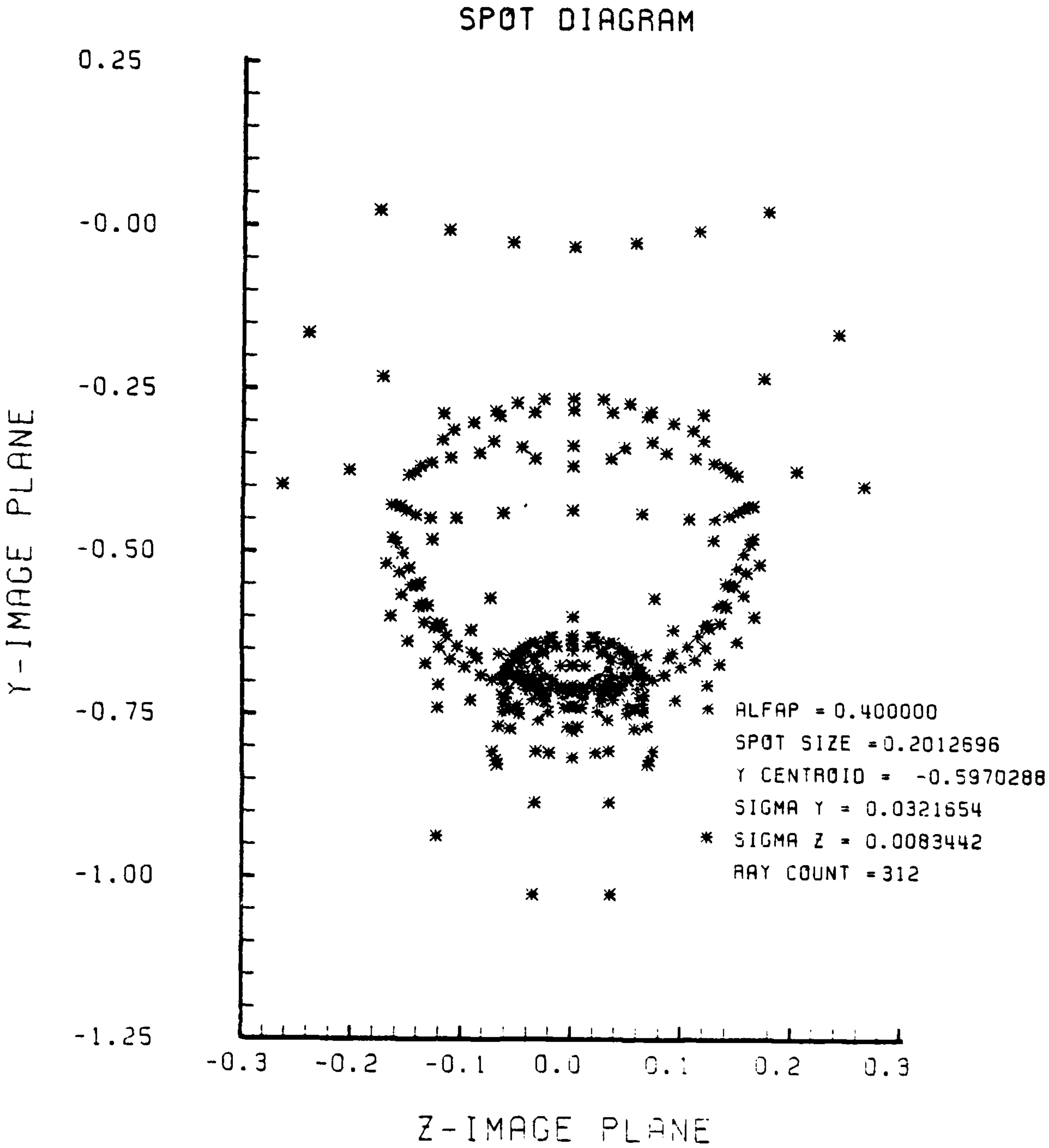

Figure H-14. Spot Diagram for Grid of Figure H-13

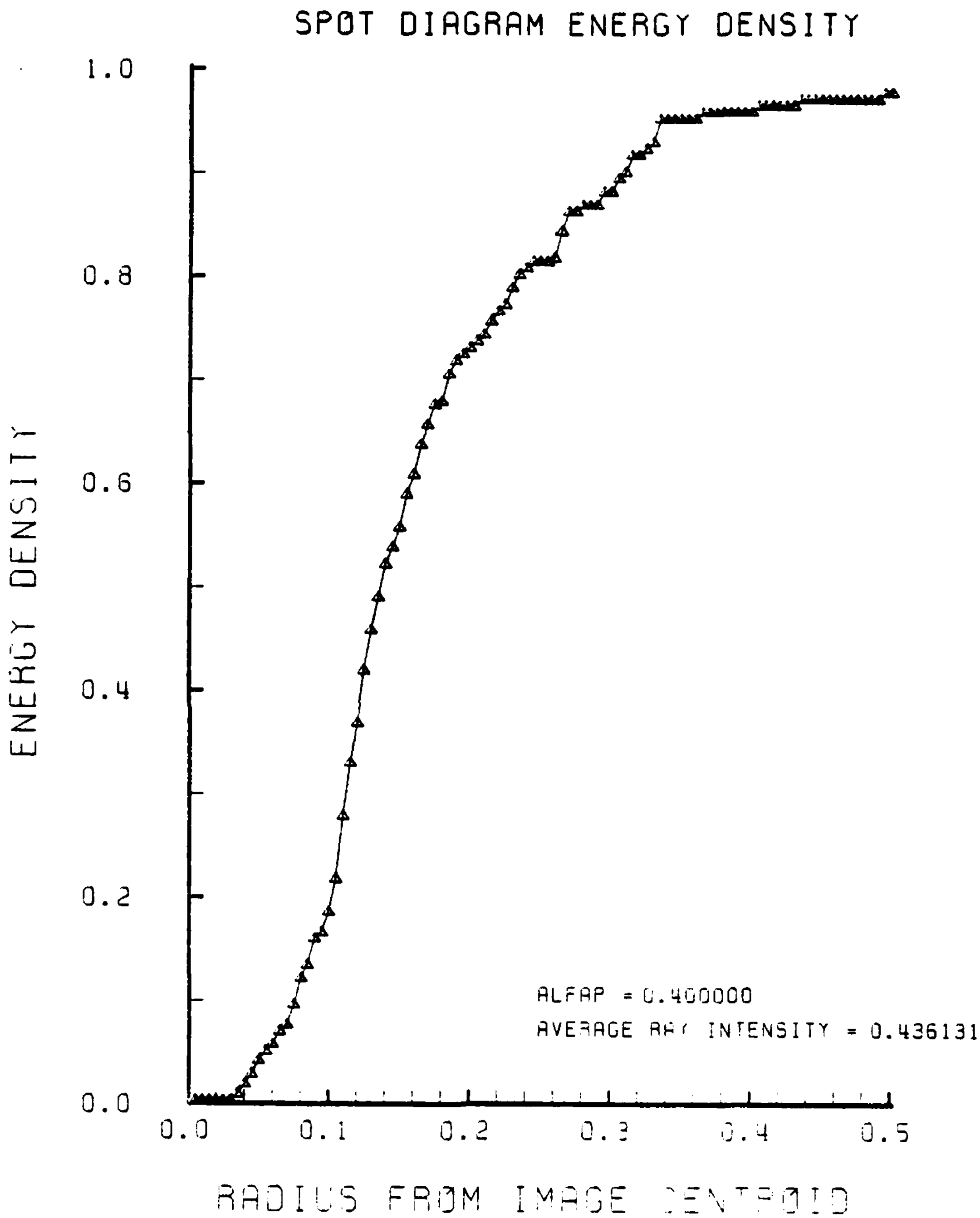

Figure H-15. Encircled Energy of Figure H-14

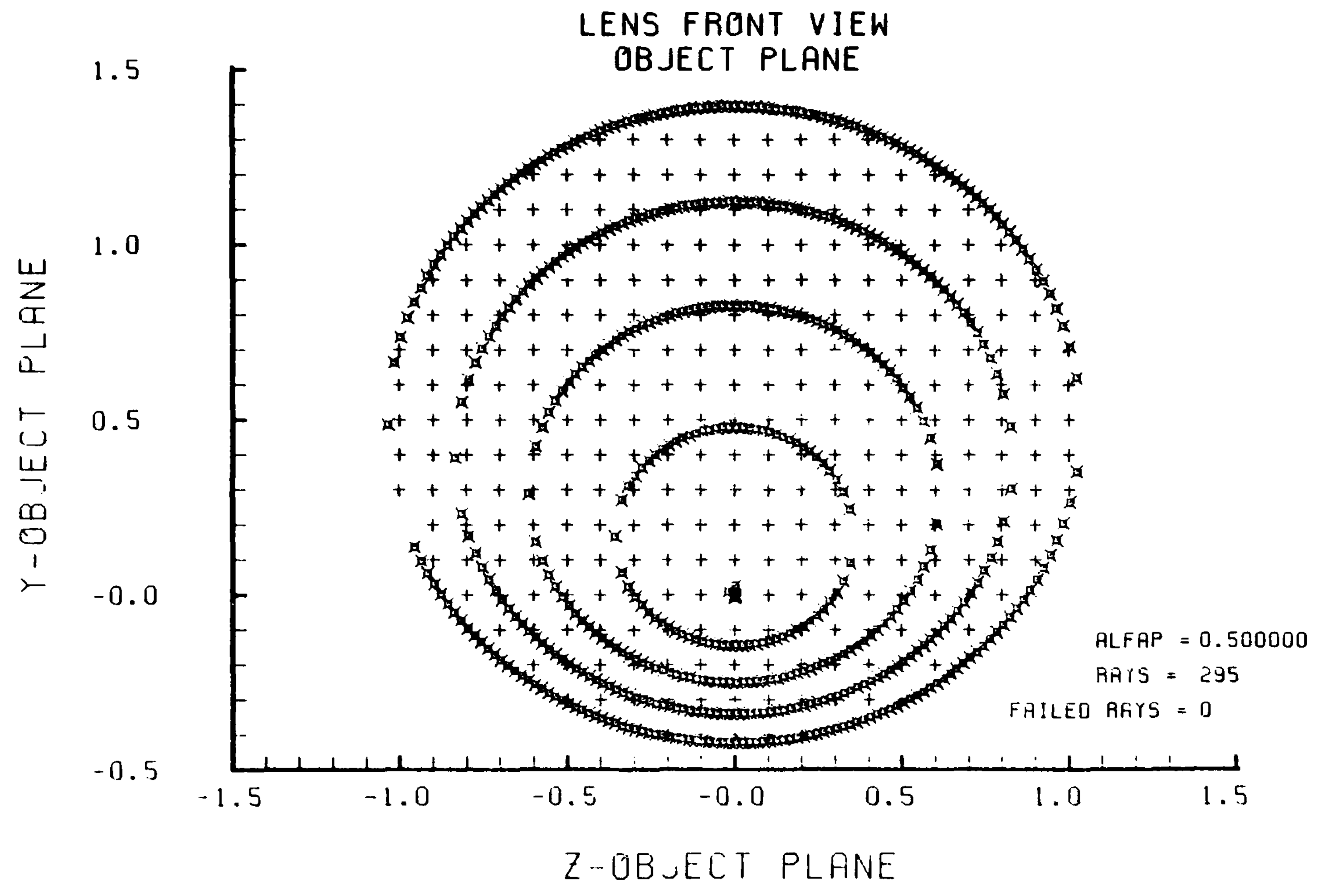

Figure H-16. Grid Plane at $\alpha_p = 0.5$ for Lens of Figure H-1

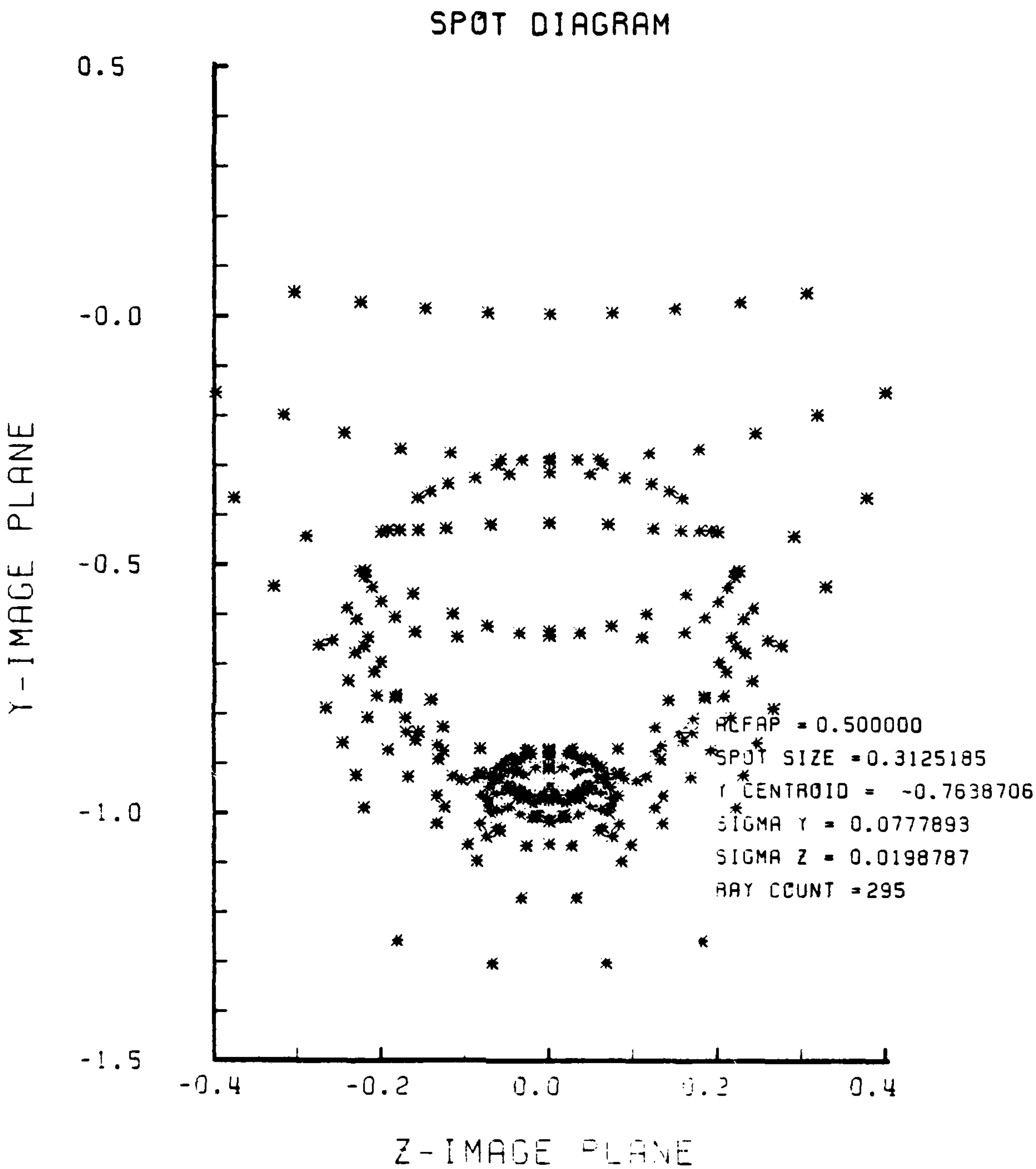

Figure H-17. Spot Diagram for Grid of Figure H-16

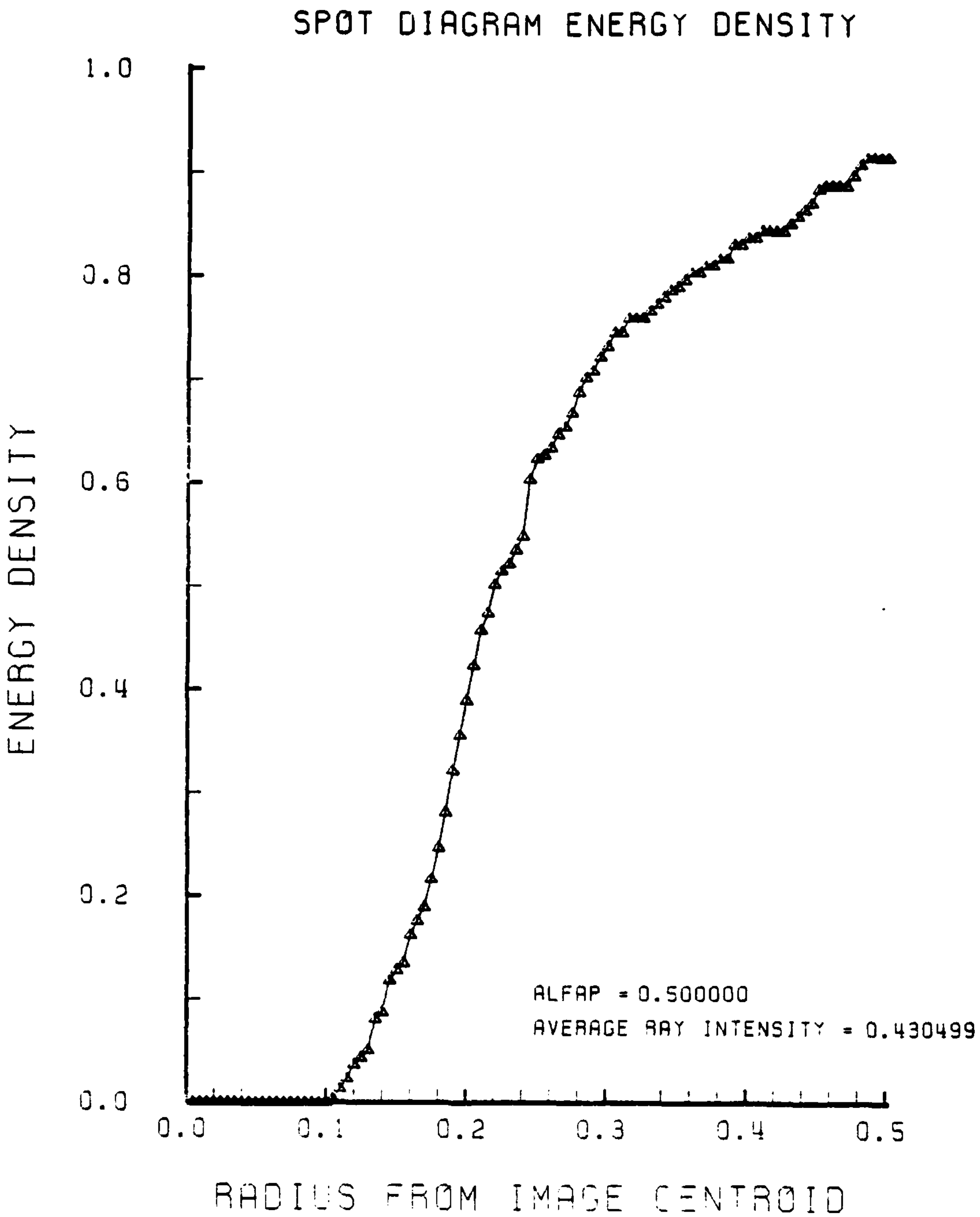

Figure H-18. Encircled Energy of Figure H-17

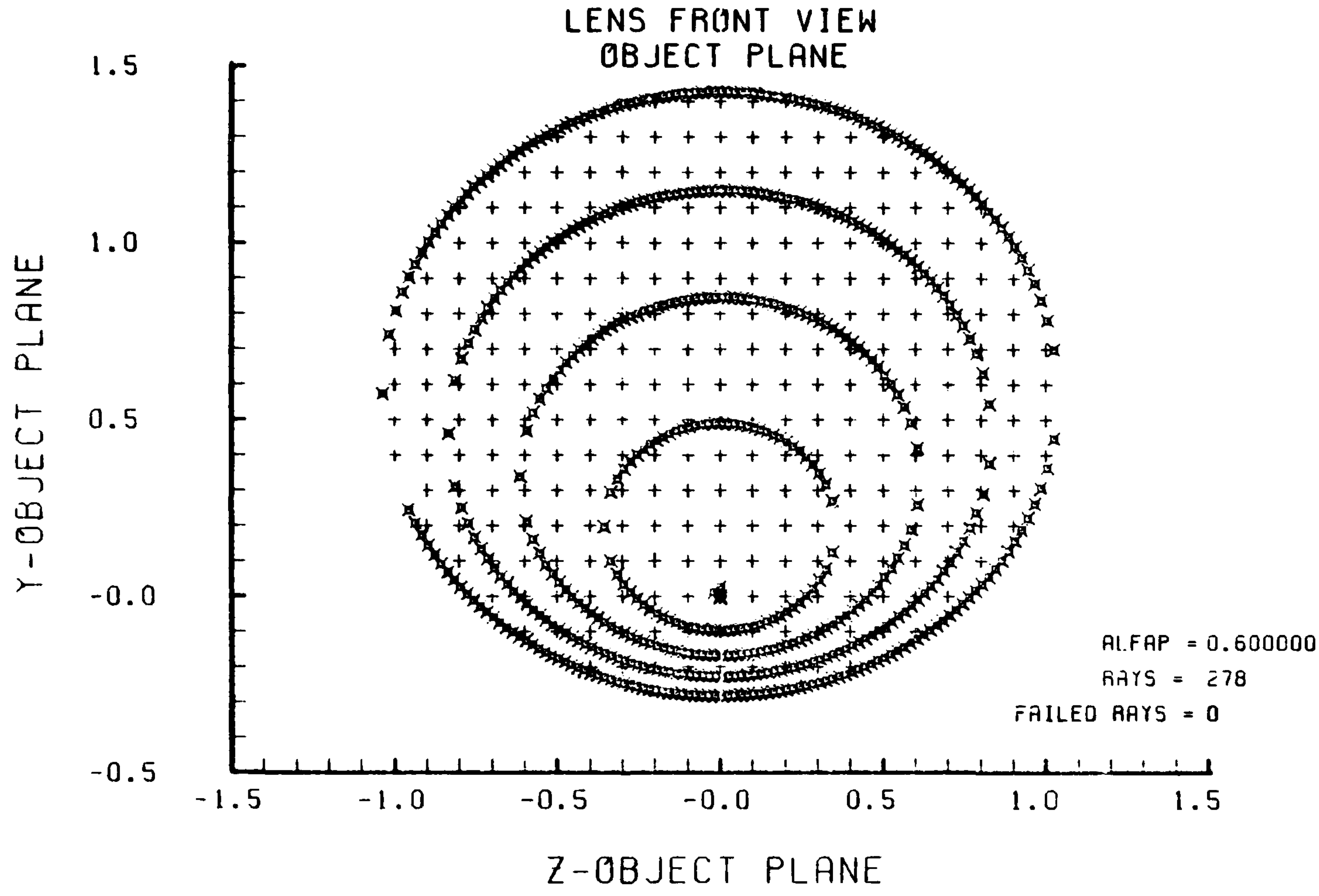

Figure H-19. Grid Plane at $\alpha_p = 0.6$ for Lens of Figure H-1

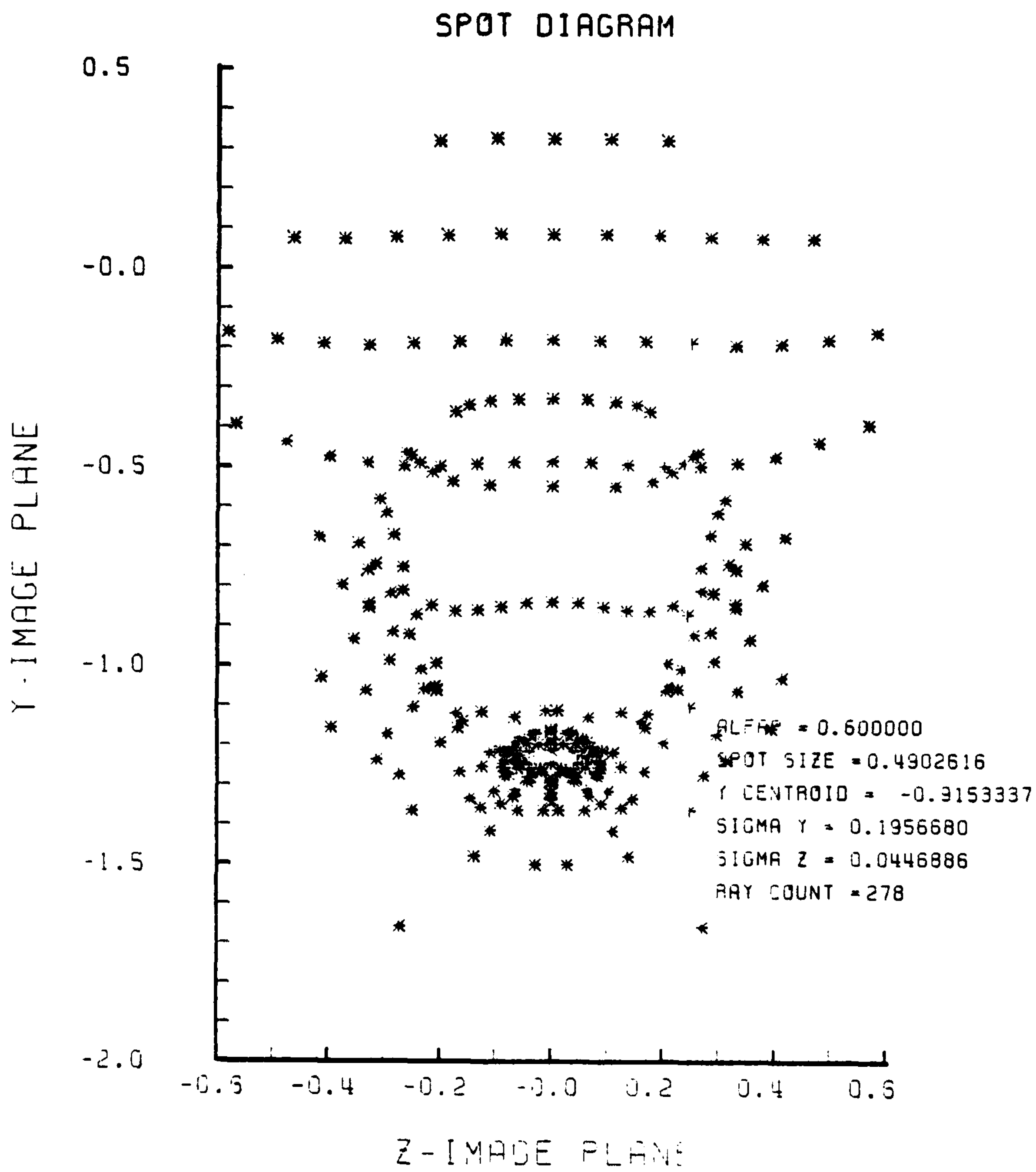

Figure H-20. Spot Diagram for Grid of Figure H-19

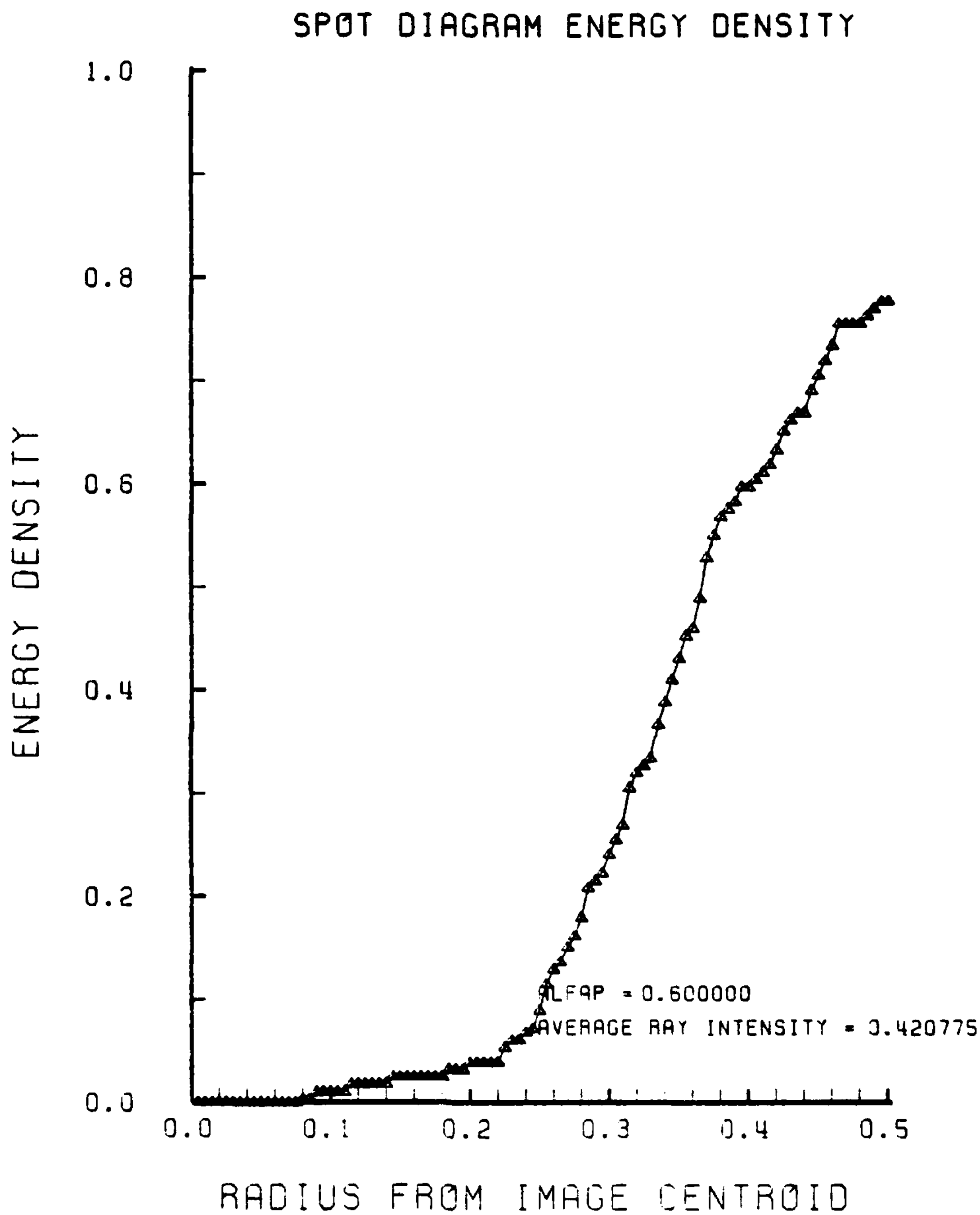

Figure H-21. Encircled Energy of Figure H-20

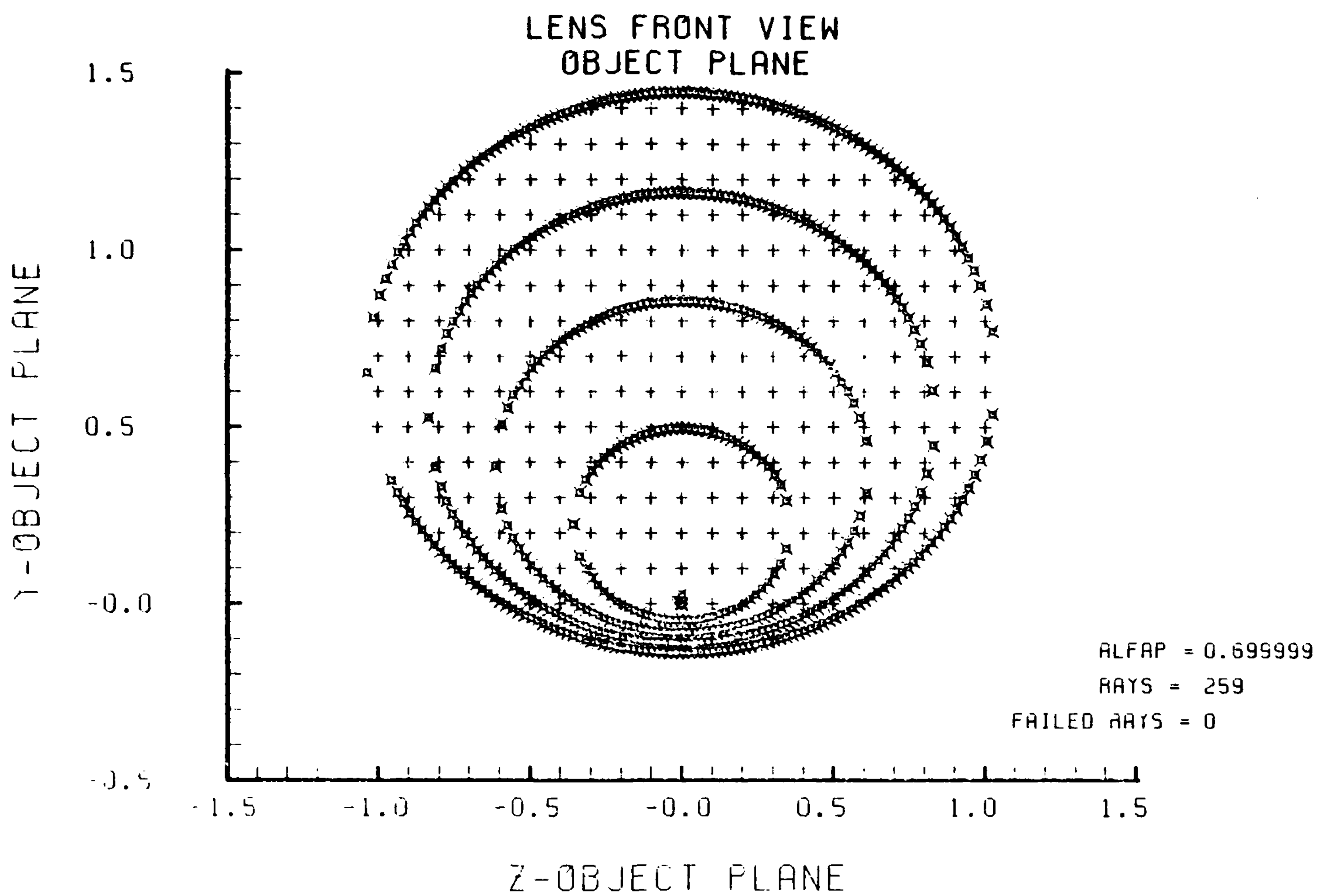

Figure H-22. Grid Plane at α_p = 0.7 for Lens of Figure H-1

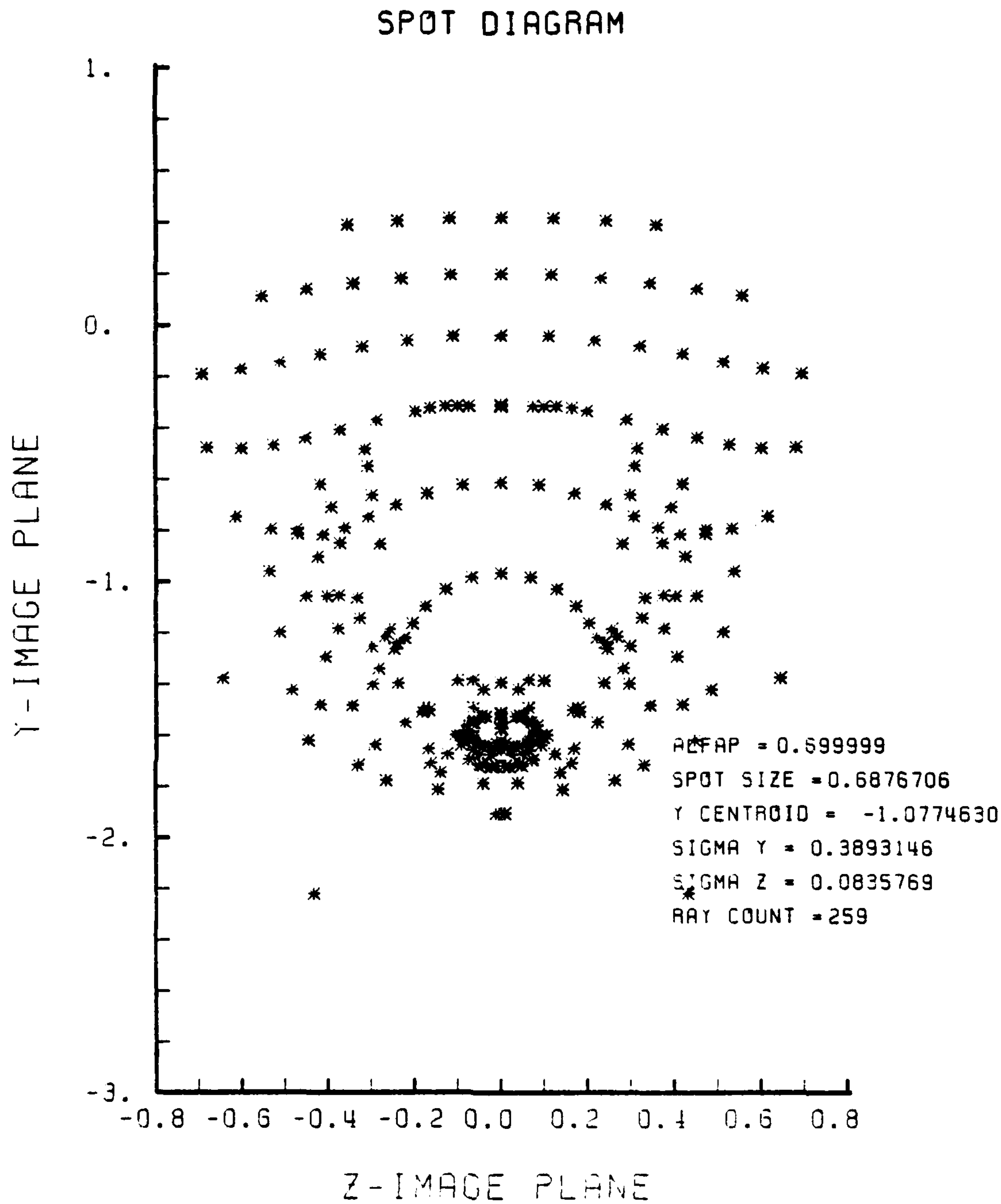

Figure H-23. Spot Diagram for Grid of Figure H-22

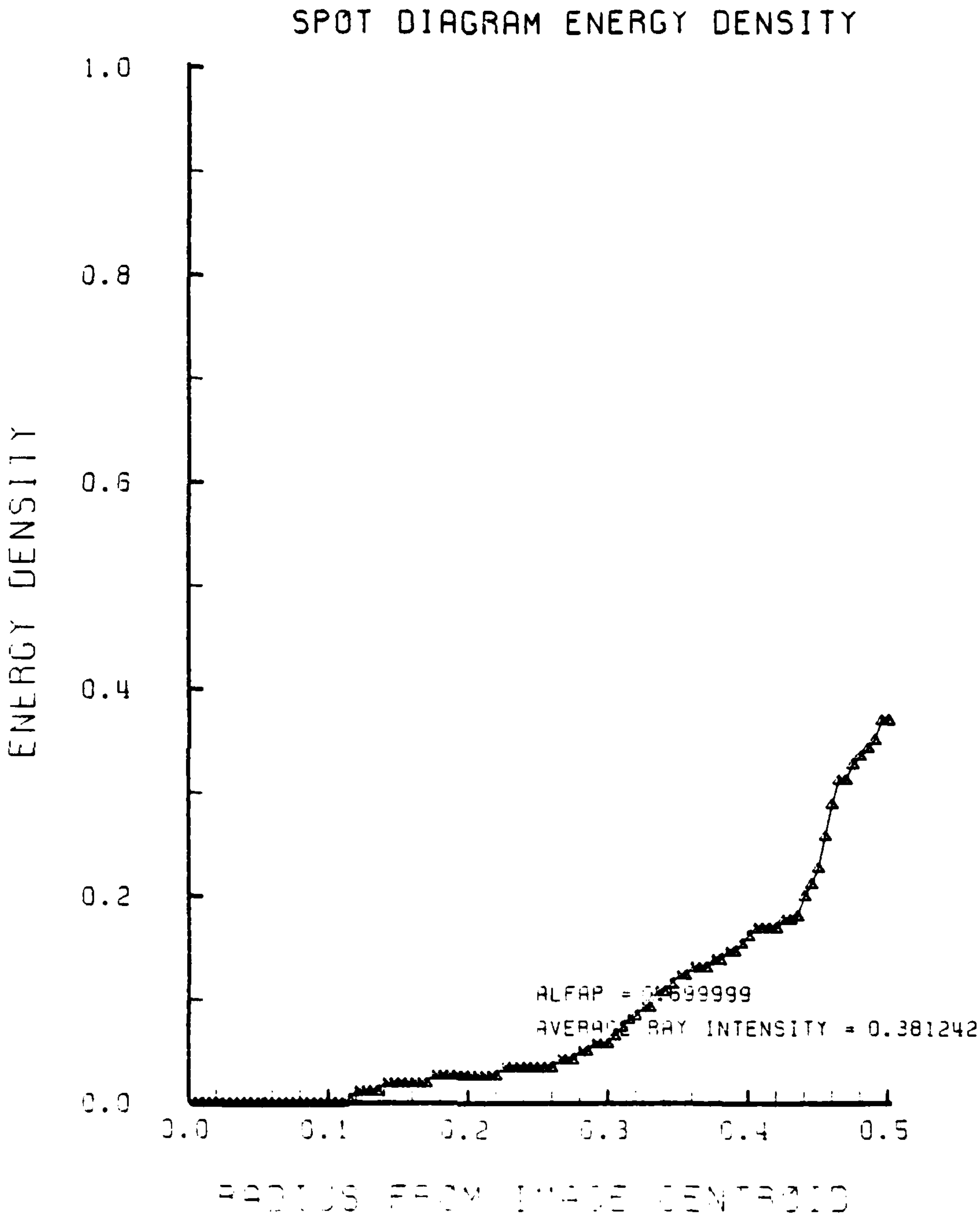

Figure H-24. Encircled Energy of Figure H-23

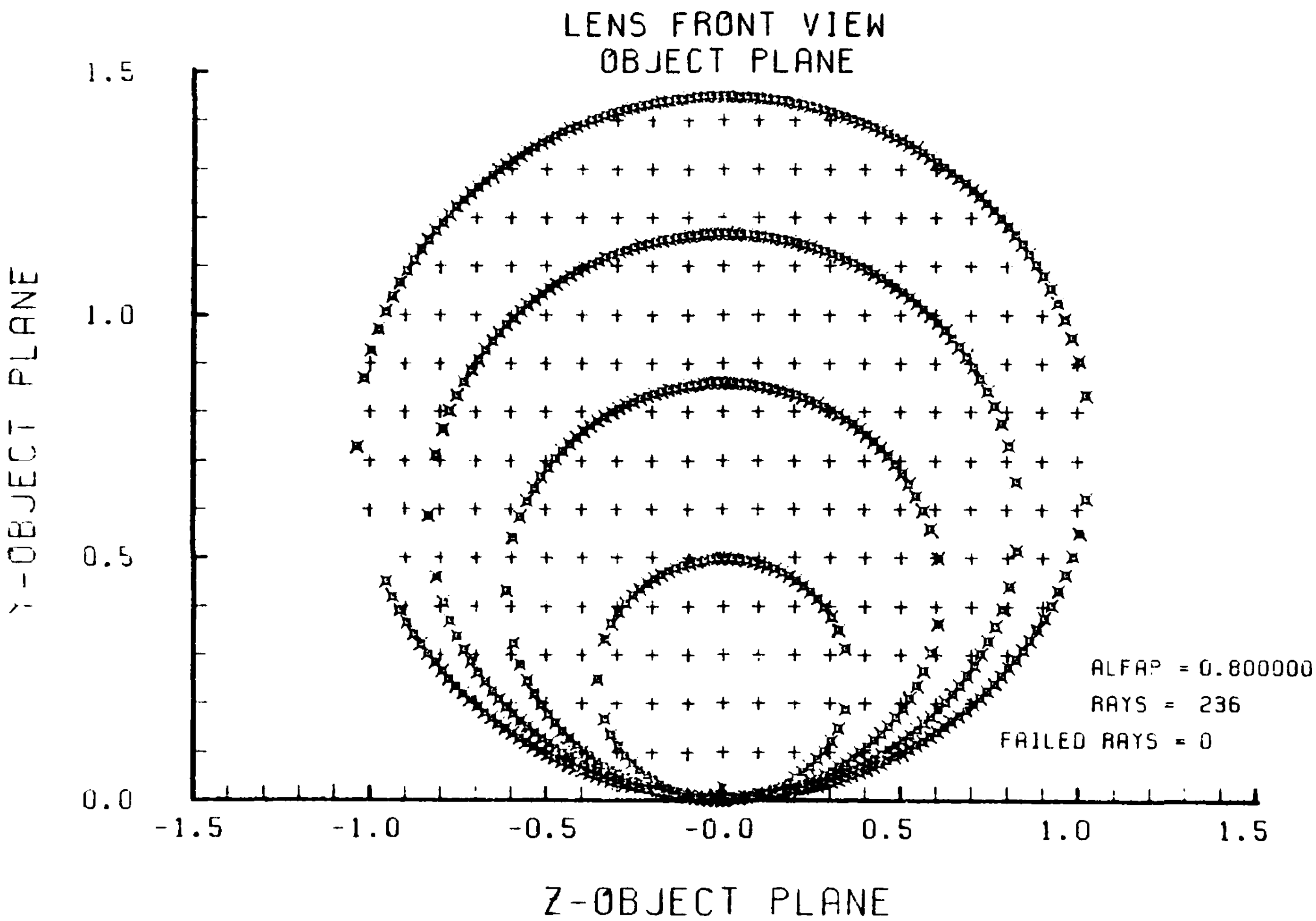

Figure H-25. Grid Plane at $\alpha_p = 0.8$ for Lens of Figure H-1

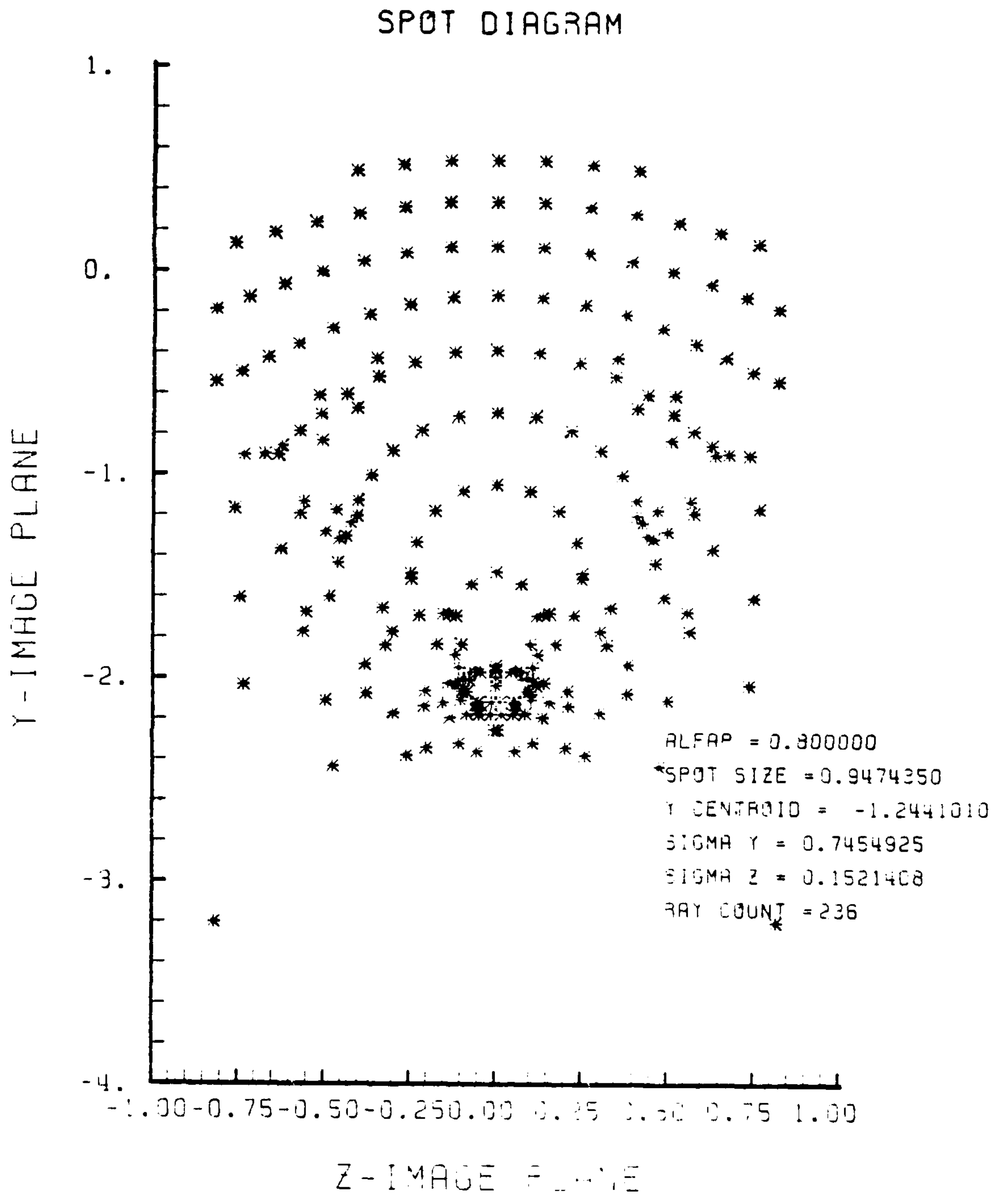

Figure H-26. Spot Diagram for Grid of Figure H-25

AD-A125 167 AERODYNAMICALLY EFFICIENT GRADIENT REFRACTIVE INDEX MISSILE SEEKER LENS(U) NAVAL POSTGRADUATE SCHOOL MONTEREY CA H M CARR OCT 82 NPS67-82-012 6/6

UNCLASSIFIED F/G 16/4 NL

END

FILMED

DTIC

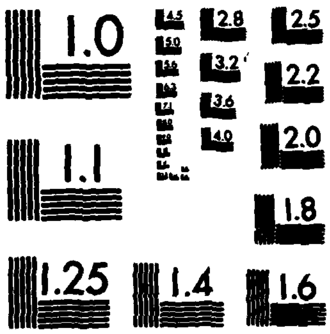

MICROCOPY RESOLUTION TEST CHART
NATIONAL BUREAU OF STANDARDS-1963-A

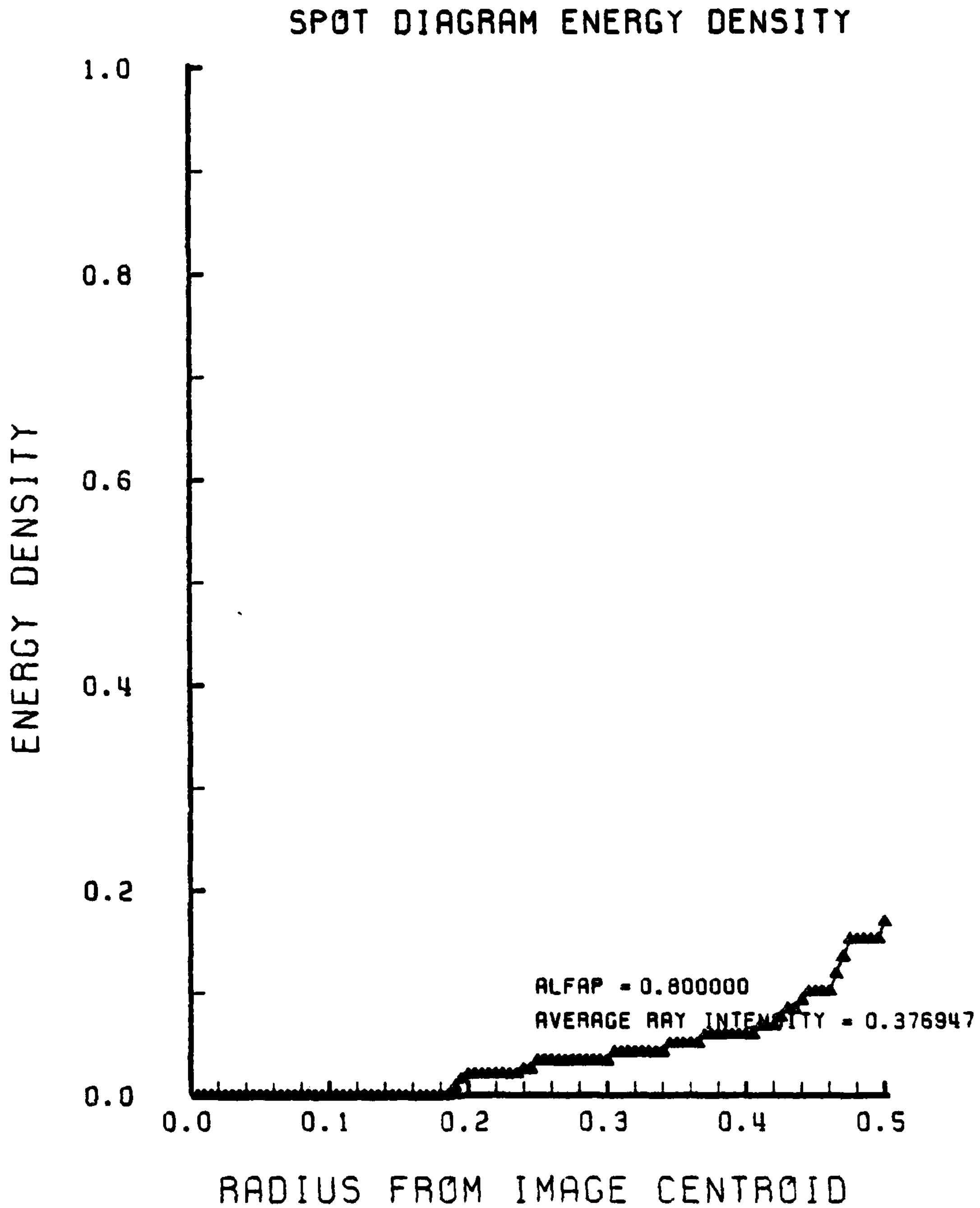

Figure H-27. Encircled Energy of Figure H-26

LIST OF REFERENCES

1. Marchand, Erich W., "Gradient-index imaging optics today", Applied Optics, V. 21, number 6, p. 983, 15 March 1982.

2. Kitano, I., Nishigawa, K., and Momokita, A., "Diffusion behavior of doped polarizable ions in glass during the ion-exchange process", Applied Optics, V. 21, number 6, p. 1017-1020, 15 March 1982.

3. Frazier, Robert L., Exterior Ballastics, Guidance Laws and Optics for a Gun-Launched Missile, M.S. Thesis, Naval Postgraduate School, Monterey, California, December 1980.

4. Terrell, James M., Conical Lens for 5"/54 Gun Launched Missile, M.S. Thesis, Naval Postgraduate School, Monterey, California, June 1981.

5. Amichai, Oded, Sharp Nose Lens Design Using Refractive Index Gradient, Contractor Report, Naval Postgraduate School, Monterey, California, June 1982.

6. Otten, L.J. and Gilbert, K.G., Aero-Optical Phenomena, V. 80, AIAA Progress Series in Astronautics and Aeronautics, 1982.

7. Kingslake, Rudolf, Lens Design Fundamentals, Academic Press, 1978.

8. Hecht, Eugene and Zajac, Alfred, Optics, Addison-Wesley, 1979.

9. Marchand, Erich W., Gradient Index Optics, Academic Press, 1978.

10. Curcio, M.E., "Precision-machined optics for reducing system complexity", Infrared Imaging Systems Technology, Society of Photo-Optical Instrumentation Engineers (SPIE), V. 226, p. 91-97, April 1980.

11. Harney, R.C., "Dual active/passive infrared imaging systems", Infrared Imaging Systems Technology, Society of Photo-Optical Instrumentation Engineers (SPIE), V. 226, p. 74-82, April 1980.

12. Robb, Paul N., "Lens design using optical aberration coefficients", Proceedings of 1980 International Lens Design Conference (OSA), Society of Photo-Optical Instrumentation Engineers (SPIE), V. 237, p. 109-118, 1980.

13. Sharma, Anurog, Kumar, D.A. Vizia, and Ghatak, A.K., "Tracing rays through graded-index media: a new method", Applied Optics, V. 21, number 6, p. 984-987, 15 March 1982.

14. Moore, Duncan T., and Stagaman, Joan M., "Ray tracing in anamorphic gradient-index media", Applied Optics, V. 21, number 6, p. 999-1003, 15 March 1982.

INITIAL DISTRIBUTION LIST

		No. Copies
1.	Defense Technical Information Center Cameron Station Alexandria, Virginia 22314	2
2.	Library, Code 0142 Naval Postgraduate School Monterey, California 93940	2
3.	Department Chairman, Code 67 Department of Aeronautics Naval Postgraduate School Monterey, California 93940	1
4.	Distinguished Professor A. E. Fuhs Code 67Fu Department of Aeronautics Naval Postgraduate School Monterey, California 93940	4
5.	LTC Rene Larriva, USMC Defense Advanced Research Projects Agency 1400 Wilson Blvd. Arlington, Virginia 22209	2
6.	Commander, Naval Sea Systems Command Naval Sea Systems Command Headquarters Attn: Code 62YC Washington, D.C. 20362	1
7.	Mr. Conrad Brandts Naval Surface Weapons Center Dahlgren, Virginia 22448	1
8.	Dr. Fred Billig Applied Physics Lab Johns Hopkins Road Laurel, Maryland 20810	1
9.	Commander, U.S. Army Armament Research and Development Command (ARRAD COM) Attn: Mr. Lou Marino Dover, N.J. 07801	1
10.	Deputy Chief of Staff for Research Development and Studies Headquarters USMC Washington, D.C. 20370	1

11. Commander 1
Development Command
USMC Base
Quantico, Virginia 22134

12. Commander 1
Artillery Development Command
Fort Sill, Oklahoma 73503

13. Captain Herbert M. Carr 3
2100 Raleigh Ave.
Austin, TX 78703

14. Dr. Lloyd Smith 1
Code 3205
Naval Weapons Center
China Lake, California 93555

15. Dr. Harold L. Bennett 1
Code 3272
Naval Weapons Center
China Lake, California 93555

16. Dr. T. G. Bergman 1
Code 3941
Naval Weapons Center
China Lake, California 93555

17. Dr. Oded Amichai 1
Ministry of Defense
P.O.B. 2250
Haifa, ISRAEL

18. Research Administration 1
Code 012A
Naval Postgraduate School
Monterey, California 93940

19. Deputy Under Secretary of the Army 1
for Operations Research
Room 2E261, Pentagon
Washington, D.C. 20310

20. LT James Terrell, USN 1
Code 290
Supervisor of Shipbuilding, Conversion,
and Repair, USN
Pascagoula, MS 39567

END